Transfer dynamics of antibiotic resistance determinants across urban water systems
The free-floating genetic perspective

Calderon Franco, D.

DOI
10.4233/uuid:8b66ead8-eeb3-42f5-a492-238d3febb9b3

Publication date
2023

Document Version
Final published version

Citation (APA)
Calderon Franco, D. (2023). *Transfer dynamics of antibiotic resistance determinants across urban water systems: The free-floating genetic perspective*. [Dissertation (TU Delft), Delft University of Technology]. https://doi.org/10.4233/uuid:8b66ead8-eeb3-42f5-a492-238d3febb9b3

Important note
To cite this publication, please use the final published version (if applicable).
Please check the document version above.

TRANSFER DYNAMICS OF ANTIBIOTIC RESISTANCE DETERMINANTS ACROSS URBAN WATER SYSTEMS

THE FREE-FLOATING GENETIC PERSPECTIVE

David Calderón Franco

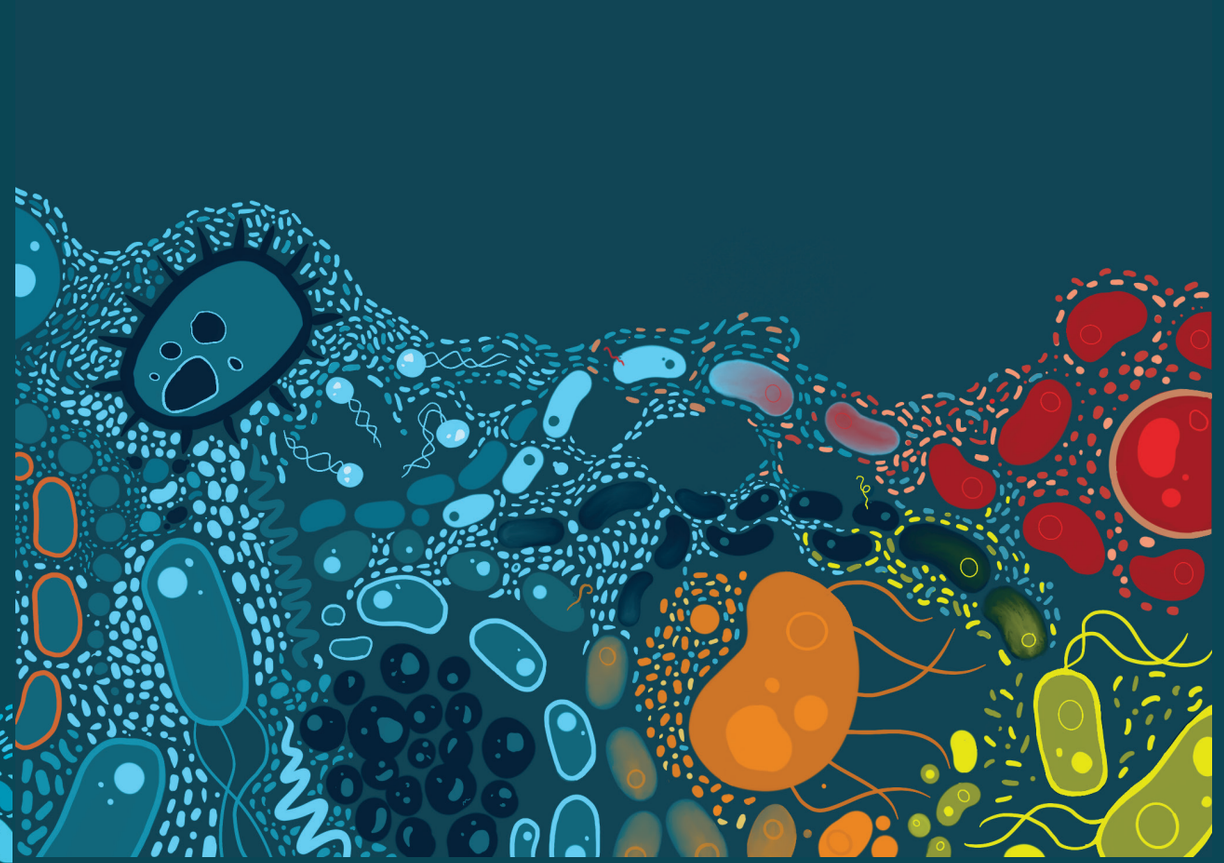

Transfer dynamics of antibiotic resistance determinants across urban water systems

The free-floating genetic perspective

David Calderón Franco

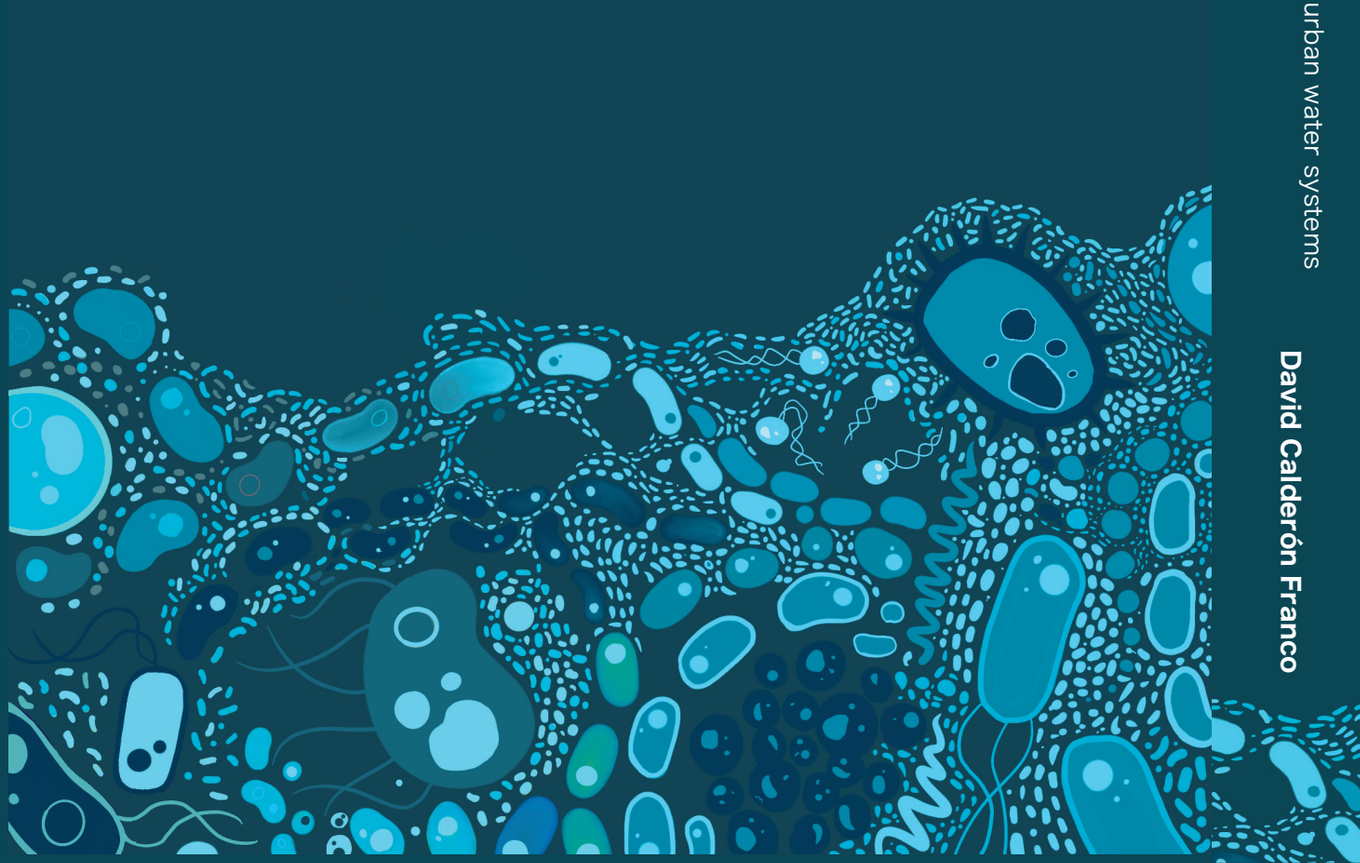

Transfer dynamics of antibiotic resistance determinants across urban water systems

The free-floating genetic perspective

Transfer dynamics of antibiotic resistance determinants across urban water systems

The free-floating genetic perspective

Dissertation

For the purpose of obtaining the degree of doctor
at Delft University of Technology,
by the authority of the Rector Magnificus prof. dr. ir. T.H.J.J. van der Hagen,
Chair of the Board for Doctorates,
to be defended publicly on Friday 17 February 2023 at 10:00 o'clock

by

David CALDERÓN FRANCO

Master of Science in Bioengineering
Institut Químic de Sarrià - Ramon Llull University, Spain

Born in Barcelona, Spain.

This dissertation has been approved by the promotor

promotor: Prof. dr. ir. M.C.M. van Loosdrecht
promotor: Prof. dr. ir. D.G. Weissbrodt
promotor: Dr. T.E.P.M.F. Abeel

Composition of the doctoral committee:

Rector Magnificus,	chairperson
Prof. dr. ir. M.C.M. van Loosdrecht,	Delft University of Technology, promotor
Prof. dr. ir. D.G. Weissbrodt,	Norwegian University of Science and Technology, Norway former Delft University of Technology, promotor
Dr. T.E.P.M.F. Abeel,	Delft University of Technology, promotor
Independent members:	
Prof. dr. H. Schmitt,	Delft University of Technology
Prof. dr. A.M. de Roda Husman,	Utrecht University
Prof. dr. G. van Wezel,	Leiden University
Dr. ir. H. Bürgmann,	The Swiss Federal Institute of Aquatic Science and Technology (Eawag), Switzerland
Reserve member:	
Prof. dr. P.A.S. Daran-Lapujade,	Delft University of Technology, reserve member

This work is part of the research project "Transmission of Antimicrobial Resistance Genes and Engineered DNA from Transgenic Biosystems in Nature" (TARGETBIO) funded by the Biotechnology and Safety Program of the Ministry of Infrastructure and Water Management (grant no. 15812) of the Applied and Engineering Sciences (TTW) Division of the Netherlands Organization for Scientific Research (NWO).

Keywords: Antibiotic Resistance Genes; Mobile Genetic Elements; Metagenomics; Horizontal Gene Transfer; Wastewater
Printed by: Proefschrift specialist
Cover design by: David Calderón Franco.

ISBN 978-94-6384-402-4

An electronic version of this dissertation is available at
https://repository.tudelft.nl/.

Para los que el mundo va despacio
For those who the world goes too slow

Contents

Summary

Antibiotic resistance is one of the biggest threats to global health, food security, and development today, leading to a growing number of difficult-to-treat infections and an economic burden. It can affect anyone of any age and in any country. It is mainly accelerated by the misuse and abuse of antibiotics, poor hygiene, and a lack of sanitation infrastructure.

From the One Health concept, water is the main link connecting all the compartments where antibiotic resistance has primarily developed (human, animal, and natural environments). It carries microorganisms, pharmaceuticals such as antibiotics, floating genetic information in the form of mobile genetic elements (MGEs), and genes conferring antibiotic resistance. It is thought that bacteria found in anthropogenic barriers such as wastewater and drinking water treatment plants could play a role in transferring and disseminating resistant bacteria into the natural environment. However, the mechanisms by which bacteria can exchange via horizontal gene transfer (HGT) to further disseminate antibiotic resistance genes (ARGs) in such compartments are unknown.

Natural transformation is one of the main HGT phenomena by which competent bacteria pull extracellular DNA into their cytoplasm. Still, it remains widely unknown which bacteria can use such a mechanism and under which circumstances. Unraveling the composition of such free-floating extracellular DNA (exDNA) fraction in complex systems such as wastewater is crucial to identify the environmental conditions promoting gene transfer. This thesis aims to understand further the role of exDNA in the transfer and development of antibiotic-resistant bacteria (ARBs) from complex systems.

The status of released DNA from different model microorganisms after different sterilization procedures was evaluated in **Chapter 2**. The results showed that current sterilization methods are effective in microorganism inactivation. However, stable DNA is released from microbial cultures and ends up in sewage streams with genetic information from microorganisms originating from human and animal discharges. In **Chapter 3**, a method using chromatography to isolate and enrich exDNA without causing cell lysis from complex wastewater matrices like influent (9 µg exDNA was obtained out of 1 L), activated sludge (5.6 µg out of 1 L), and treated effluent (4.3 µg out of 1 L) was developed. Thus, this was necessary to profile its genetic composition. Surprisingly, results highlighted that exDNA is mainly comprised of MGEs (65%), posing a risk as the prevalence of MGEs in the extracellular fraction can indirectly promote antibiotic resistance development mainly via natural transformation.

In the two field investigation chapters (**Chapters 4 and 5**), the transfer of ARGs and MGEs and their removal capacity in a full-scale Nereda® reactor removing nutrients with aerobic granular sludge and in chlorine-free drinking water treatment plants were evaluated. These two chapters summarize the journey that antibiotic-resistant bacteria follow toward water sanitation. Resistance determinants decreased their load reaching effluents from wastewater (1.1 log gene copies mL^{-1}) and drinking water treatment plants (2.5 log gene copies mL^{-1}), at least when inside active bacterial cells. It is less clear regarding exDNA since the treatment process involves cell decay and lysis that releases exDNA into the environment.

After profiling the exDNA both in lab-scale and full-scale experiments, the effect of environmental factors such as increasing antibiotic concentrations was evaluated on exDNA transformation in an activated sludge enrichment in **Chapter 6**. We showed the feasibility of distantly-related microorganisms for DNA uptake when strong environmental pressures ($\geq$50 mg L^{-1}) were applied. Thus, it shows that natural transformation under environmental antibiotic concentrations may not be the driving force by which bacteria take up exDNA in complex systems. However, the focus should be on other compartments such as research facilities and pharmaceutical industrial discharges. Finally, strategies to remediate ARGs (intracellular and extracellular) and ARBs from wastewater effluents were evaluated in **Chapter 7**. We showed how byproducts from wastewater and drinking water treatment plants, such as sewage-sludge biochar and iron-oxide coated sands, were effective at removing ARBs and exDNA from effluent waters.

Collectively, this thesis shows that the exDNA fraction from water matrices is an overlooked pool of genetic fragments containing MGEs and ARGs. Thus, these could be used as genetic material to transform competent bacteria and develop ARBs. However, exDNA transformation under environmental antibiotic concentrations is not the main mechanism by which bacteria evolve and adapt in mixed cultures. It is important to highlight that anthropogenic barriers are effective at remediating ARBs, which should redirect the focus from wastewater treatment plants and tackle the antibiotic resistance issue from multiple compartments simultaneously.

Samenvatting

Antibioticaresistentie is een van de grootste bedreigingen voor de volksgezondheid en voedselveiligheid. Het ontwikkelen van resistentie leidt tot een groeiend aantal slecht behandelbare infecties en heeft daarmee een grote impact op de economie. Iedereen, van iedere leeftijd en in ieder land kan benadeeld worden door antibioticaresistentie. De factoren die het ontwikkelen van antibioticaresistentie het meest in de hand werken zijn slecht passend gebruik en misbruik van antibiotica, slechte hygiëne en gebrek aan sanitaire voorzieningen.

Het One Health concept beschrijft dat water de link is tussen de verschillende compartimenten waarbinnen antibioticaresistentie zich heeft ontwikkeld (in mens, dier en natuurlijke milieus). Water bevat en vervoert micro-organismen, farmaceutica zoals antibiotica, wateroplosbare genetische informatie in de vorm van mobiele genetische elementen (MGEs) en genen die antibioticaresistentie verschaffen. Antropogene barrières, zoals afvalwaterzuiveringen en drinkwaterzuiveringen zouden een rol kunnen spelen in het overdragen en verspreiden van resistente bacteriën in het milieu. Echter zijn de mechanismen waarmee bacteriën via horizontale gen-overdracht (HGO) antibiotica-resistentiegenen kunnen verspreiden in de verschillende bovengenoemde compartimenten tot op heden onbekend.

Natuurlijke transformatie is een van de meest voorkomende mechanismen voor horizontale gen-overdracht en houdt in dat competente bacteriën extracellulair DNA het cytoplasma in trekken. Het is echter nog overwegend onbekend welke bacteriën dit kunnen en onder welke omstandigheden dat zo is. Het ontrafelen van de compositie van vrij extracellulair DNA (exDNA) in complexe systemen als de afvalwaterzuivering is cruciaal om de condities waarin gen-overdracht gestimuleerd wordt te begrijpen. Dit proefschrift is heeft het doel om de rol van exDNA in de overdracht en ontwikkeling van antibioticaresistente bacteriën (ARBs) in complexe systemen beter te begrijpen.

De toestand van uitgescheiden DNA uit verschillende modelorganismen na verschillende sterilisatieprocedures is bestudeerd in **Hoofdstuk 2**. De resultaten wijzen uit dat de huidige sterilisatiemethodes effectief zijn voor het inactiveren van micro-organismen. Echter laten de organismen stabiel DNA los. Dit komt terecht afvalwaterstromen met genetische informatie afkomstig van menselijke- en dierlijke uitwerpselen. In **Hoofdstuk 3** is een methode gebaseerd op chromatografie ontwikkeld waarmee exDNA geïsoleerd en geconcentreerd kan worden uit complexe afvalwatermatrices zonder lysis van cellen te veroorzaken. Uit 1 liter inkomend afvalwater werd 9 µg exDNA verkregen, uit 1 liter actief slib 5.6 µg en 4.3 µg uit

gezuiverd effluent. Het isoleren van exDNA uit verschillende afvalwatermatrices was nodig voor het beschrijven van de genetische compositie van exDNA in de verschillende stromen in de afvalwaterzuivering. Verbazingwekkend genoeg blijkt uit deze studie dat exDNA voornamelijk bestaat uit MGEs (65%), wat betekent dat hierdoor een indirect verhoogd risico op het ontwikkelen van antibioticaresistentie via natuurlijke transformatie in de afvalwaterzuiveringstanks bestaat.

In de veldwerkstudies in **Hoofdstuk 4 en 5** werd de overdrachts- en de verwijdercapaciteit van ARGs en MGEs geëvalueerd in actieve Nereda® reactoren waarin nutriënten worden verwijderd met actief korrelslib en in een chloorvrije drinkwaterzuiveringsinstallatie. In deze twee hoofdstukken wordt de reis van antibioticaresistente bacteriën door het sanitaire systeem beschreven. De aanwezigheid van resistentie-indicatoren in actieve bacteriële cellen ging omlaag naarmate het einde van het zuiveringsproces naderde. Er werden 1.1 log gen-kopieën mL^{-1}) gevonden in het effluent van de afvalwaterzuivering en 2.5 log gen-kopieen mL^{-1}) in het effluent van de drinkwaterzuivering. Omdat celsterfte, waardoor exDNA kan ophopen, in beide processen een rol speelt is de rol van exDNA moeilijker te beschrijven.

Na het bestuderen van exDNA in experimenten op lab- en industriële schaal is ook het effect van selectiedruk, zoals verhoogde antibioticaconcentraties, op exDNA-transformatie in een ophopingscultuur van actief slib getest in **Hoofdstuk 6**. We hebben laten zien dat micro-organismen die genetisch ver uit elkaar liggen hetzelfde exDNA kunnen opnemen bij hoge selectiedruk ($\geq$50 mg L^{-1}). De resultaten wijzen uit dat het onwaarschijnlijk is dat natuurlijke transformatie het mechanisme is voor het opnemen van exDNA bij de antibioticaconcentraties die normaliter in complexe systemen gevonden worden. Dit betekent dat de focus verlegd moet worden naar andere compartimenten, zoals afvalwater van onderzoeksinstellingen en de farmaceutische industrie. **Hoofstuk 7** bediscussieert verschillende strategieën voor het verwijderen van ARGs (zowel intra- als extracellulair) en ARBs uit afvalwaterstromen. We hebben beschreven hoe bijproducten van afval- en drinkwaterzuiveringsinstallaties, zoals biokolen en zand gecoat met ijzeroxides, effectief werken in het verwijderen van ARBs en exDNA uit effluents.

Alle onderdelen van dit proefschrift samen laten zien dat de exDNA-fractie van watermatrices een over verzameling genetische fragmenten is die MGE's en ARG's bevatten die op dit moment over het hoofd worden gezien. Deze fragmenten zouden dus kunnen worden gebruikt als genetisch materiaal om competente bacteriën te transformeren en ARB's te ontwikkelen. ExDNA-transformatie is echter niet het belangrijkste mechanisme waardoor bacteriën evolueren en zich aanpassen in gemengde culturen bij antibioticaconcentraties die in complexe systemen aanwezig zijn. Het is belangrijk om te benadrukken dat antropogene barrières effectief zijn bij het saneren van ARB's, wat betekent dat we de focus van afvalwaterzuiveringsinstallaties moeten verleggen naar het bestrijden van antibioticaresistentie vanuit meerdere compartimenten tegelijk.

Resumen

La resistencia a los antibióticos es una de las mayores amenazas para la salud mundial, la seguridad alimentaria y el desarrollo en general. Es la causa del incremento de infecciones difíciles de tratar además de considerarse un gasto económico importante en salud pública. Puede afectar a cualquier persona de cualquier edad y en cualquier país siendo el uso indebido y el abuso de antibióticos, la falta de higiene y la falta de infraestructura sanitaria la causa principal de la aceleración de casos.

Bajo el concepto One Health ("Salud compartida"), el agua es el principal eslabón que conecta todos los compartimentos donde se desarrollan resistencias a los antibióticos (humanos, animales y medio ambiente). El agua transporta microorganismos, productos farmacéuticos como antibióticos, información genética flotante en forma de elementos genéticos móviles (EGMs) y genes que confieren resistencia a los antibióticos. Se cree que las bacterias que se encuentran en dichas barreras antropogénicas, tales como estaciones depuradoras de aguas residuales y potabilizadoras de agua, podrían desempeñar un papel en la transferencia y diseminación de bacterias resistentes en el entorno natural. Sin embargo, se desconocen los mecanismos por los cuales las bacterias pueden intercambiar a través de la transferencia génica horizontal (TGH), diseminando así los genes de resistencia a los antibióticos (GRA) en dichos compartimentos.

La transformación natural es uno de los principales mecanismos de TGH mediante el cual las bacterias competentes captan e introducen el ADN extracelular en su citoplasma. Aún así, se desconoce qué bacterias pueden utilizar dicho mecanismo y bajo qué circunstancias. Desentrañar la composición de dicha fracción de ADN extracelular flotante (exDNA) en sistemas complejos como las aguas residuales es crucial para identificar las condiciones ambientales que promueven la transferencia de genes. Esta tesis tiene como objetivo comprender mejor el papel del exDNA en la transferencia y el desarrollo de bacterias resistentes a los antibióticos (BRA) en sistemas complejos.

El estado del ADN liberado de microorganismos después de ser tratados por diferentes métodos de esterilización fue evaluado en el **Capítulo 2**. Los resultados muestran que los métodos de esterilización actuales son efectivos en la inactivación de microorganismos. Sin embargo, el ADN liberado es estable y puede terminar en corrientes de aguas residuales con información genética de microorganismos procedentes de descargas humanas y animales. En el **Capítulo 3**, se desarolló un método cromatográfico para aislar y enriquecer exDNA sin causar lisis celular con aguas residuales complejas como orígen. Se obtuvo exDNA de influente (9 µg de

exDNA de 1 L), lodos activados (5.6 µg de 1 L), y efluentes (4.3 µg de 1 L) de una planta depuradora de aguas residuales. Esto fue necesario para perfilar su composición genética. Sorprendentemente, los resultados destacaron que el exDNA se compone principalmente de EGMs (65%), lo que representa un riesgo ya que la prevalencia de EGMs en la fracción extracelular puede promover indirectamente el desarrollo de resistencia a los antibióticos, principalmente a través de la transformación natural.

En los dos capítulos de investigación de campo (**Capítulos 4 y 5**), la transferencia de GRAs y EGMs y su capacidad de ser eliminados fueron evaluados en reactores Nereda® a gran escala usando lodos aerobios granulares además de en plantas potabilizadoras de agua sin uso de cloro. Estos dos capítulos resumen la trayectoria que siguen las bacterias resistentes a los antibióticos en el proceso de saneamiento del agua. Los determinantes de resistencia disminuyeron en los efluentes de plantas depuradoras de aguas residuales (1.1 log copias de genes mL^{-1}) y en plantas potabilizadoras (2.5 log copias de genes mL^{-1}), al menos dentro de células bacterianas activas. Hay más debate con el rol del exDNA ya que el proceso de tratamiento implica la descomposición celular y lisis, liberándolo en el medio ambiente.

Después de perfilar el exDNA tanto en experimentos a escala laboratorio como a gran escala, se evaluó el efecto de los factores ambientales, como el aumento de la concentración de antibióticos, en la transformación del exDNA en un cultivo enriquecido a partir de lodos activados en el **Capítulo 6**. Demostramos la viabilidad de la transformación de exADN por parte de microorganismos lejanos entre sí cuando se aplicaron fuertes presiones ambientales ($\geq$50 mg L^{-1}). Por lo tanto, muestra que la transformación natural bajo concentraciones de antibióticos ambientales puede no ser la fuerza impulsora por la cual las bacterias toman exDNA en sistemas complejos. Sin embargo, la atención debe centrarse en otros compartimentos, como instalaciones de investigación y descargas industriales farmacéuticas. Finalmente, las estrategias para remediar los GRAs (intracelulares y extracelulares) y las BRA de los efluentes de aguas residuales se evaluaron en el **Capítulo 7**. Mostramos cómo los subproductos de estaciones depuradoras de aguas residuales y agua potable, como el carbón activo obtenido de lodos activados y arenas recubiertas de óxido de hierro, fueron efectivos para eliminar los BRA y el exADN de los efluentes de aguas residuales.

En resumen, esta tesis muestra que el normalmente ignorado exDNA en muestras de agua contiene una fracción significativa de EGMs y GRAs. Por lo tanto, podrían usarse como material genético en transformación de bacterias competentes, con el consecuente desarrollo de BRAs. Sin embargo, la transformación de exDNA bajo concentraciones ambientales de antibióticos no es el principal mecanismo por el cual las bacterias evolucionan y se adaptan en cultivos mixtos. Es importante resaltar que las barreras antropogénicas son efectivas en remediación de BRAs, lo que debería descentralizar el foco de las plantas depuradoras de aguas residuales y abordar el problema de la resistencia a los antibióticos desde múltiples compartimentos de manera simultánea.

1

Introduction

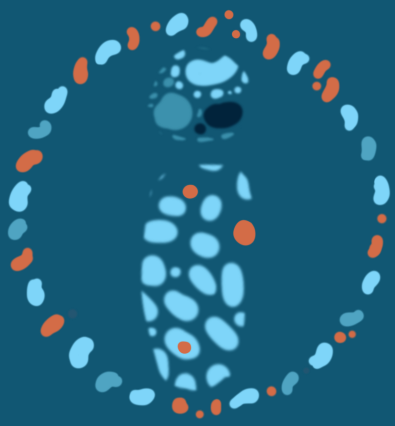

A partial version of this chapter has been published as: Miłobedzka, A., Ferreira, C., Vaz-Moreira, I., Calderón-Franco, D., Gorecki, A., Purkrtova, S., Jan Bartacek, Dziewit, L., Singleton, C.M., Nielsen, P.H., Weissbrodt, D.G., Manaia, C.M., 2022. Monitoring antibiotic resistance genes in wastewater environments: The challenges of filling a gap in the One-Health cycle. J. Hazard. Mater. 424. https://doi.org/10.1016/j.jhazmat.2021.127407

1.1. Antimicrobials, antibiotics, and antibiotic resistance

Antimicrobials are the broad term for substances used to prevent and treat infections in humans, animals, and plants. These include antibiotics, antivirals, antifungals, and antiparasitics. Antibiotics are the specific antimicrobials used for fighting bacterial infections. Antibiotics are responsible for bacterial cell death. They use a wide range of complex processes that start with the physical interaction between the antibiotic (or drug) with the cells and end up triggering alterations in the affected bacterium at the biochemical, molecular, or structural levels [1].

The most common ways by which antibiotic act include the inhibition of **(1)** cell wall synthesis (i.e., beta-lactams), **(2)** DNA synthesis (i.e., quinolones), **(3)** protein synthesis (i.e., aminoglycosides, tetracylcines, macrolides, lincosamide, and streptogramins) generating misfolded proteins that are membrane incorporated facilitating higher antibiotic influx, and **(4)** folic acid synthesis for DNA synthesis (i.e., sulfonamides and trimethoprims) (Figure 1.1). They all have, as a result, slow bacterial growth (bacteriostatic agent) or cell death (bactericidal agent).

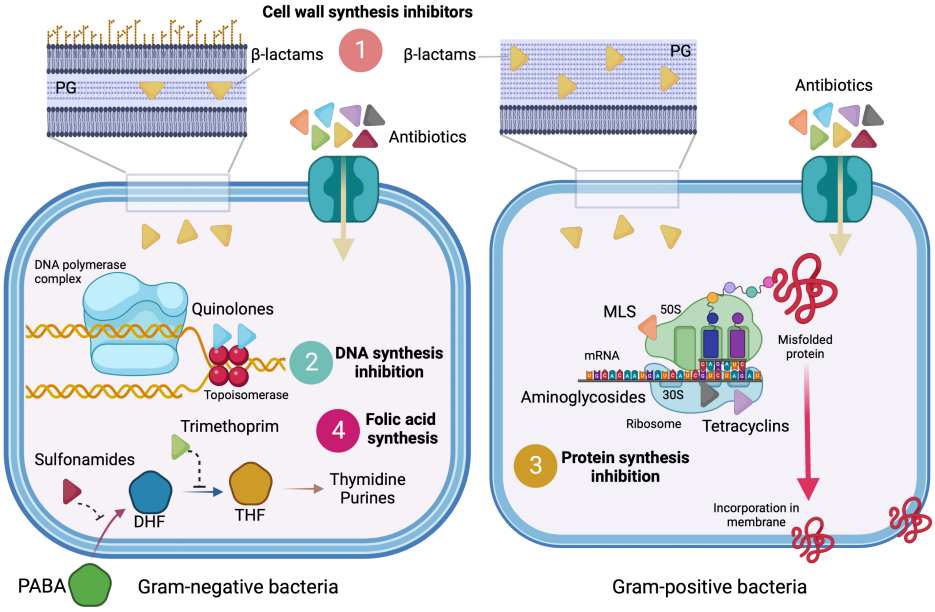

Figure 1.1: Main antibiotic targets in bacterial cells. Gram-positive and Gram-negative bacteria were only displayed for membrane differences visualization. **Notes: PD** = Peptidoglycan; **MLS** = Macrolide, Lincosamide, Streptogramins; **PABA** = p-aminobenzoic acid; **DHF** = dihydrofolic acid; **THF** = tetrahydrofolic acid.

Antibiotics are undoubtedly the most significant medical breakthrough of the 20th century; not only for treating infectious diseases but also for allowing the practice of many modern medical procedures such as cancer treatment, organ transplants, and open-heart surgery [2]. However, the overuse and misuse of large quantities of antibiotics to control infection in healthcare and agriculture, together with improper waste management, lack of sanitation and environmental transmission, have generated the perfect conditions for resistance determinants mobilization in bacterial populations, leading to substantially increased antibiotic resistance and their associated persistent bacteria [3, 4]. This rise in global resistance is accompanied by a failure in antibacterial drug discovery to reach the market. The last original class of antibiotics was discovered in the late 1980s (daptomycin). The main reasons are a lack of profit for pharmaceutical companies and difficulty developing antibiotics against a broad spectrum of pathogens, mainly because of a lack of understanding of drug penetrations and efflux systems in Gram-negative bacteria [3, 5].

The silent pandemic

Humankind has tried very hard to prevent bacterial infections, which has led to an improvement in quality of life. However, bacteria have also been researching, communicating with other bacteria, and rearming their walls and machinery to fight back the presence of antibiotics. They have developed a special research and development program focused only on antibiotic resistance. This is bringing us to what has been described as "silent pandemic": Antimicrobial resistance occurs when disease-causing microbes change over time, meaning that they are harder to treat because they can resist the drug's effects. This means that in the case of bacteria, bacterial infections are more difficult to treat, or in some cases, impossible.

Antibiotic resistance is a tool box that bacteria have acquired through evolution to fight against antibiotics. Antibiotic resistance can arise from mutations in the pre-existing genome of a bacterium or from the uptake of foreign DNA. These tools are encoded in antibiotic resistance genes (ARGs). The main resistance mechanisms that employ these tools (Figure 1.2) are **(1)** uptake inhibition, where specific antibiotics, such as antibiotic C, cannot cross the outer membrane, **(2)** antibiotics extrusion via efflux pumps, and **(3)** target site changes either via allele mutations or via target site protection, and **(4)** direct antibiotic inactivation either via hydrolysis or by modifying the antibiotic structure so it cannot interact anymore [6]. By using these defensive mechanisms, bacteria have succeeded in harming back, to the point that antibiotics are losing their effectiveness.

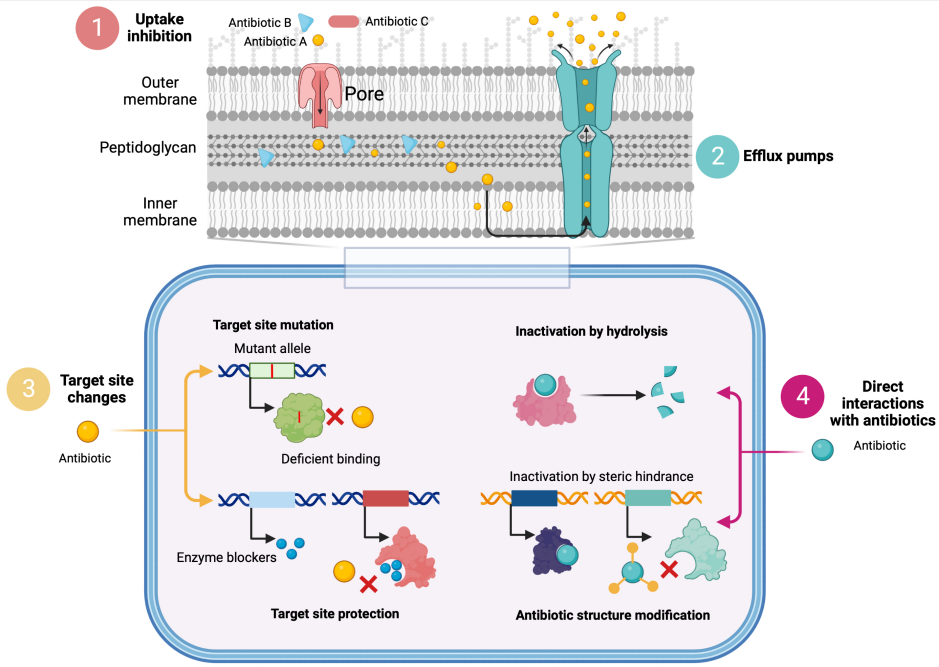

Figure 1.2: Main antibiotic resistance mechanisms used by bacteria.

1.2. One Health and antibiotic resistance as central concern

Antibiotic resistance can jeopardize medical interventions, extend hospitalization due to infections, and affect the patient's quality of life. These led the World Health Organization (WHO) to place antimicrobial resistance (together with viruses, fungi, and protozoa) among the biggest threats to the human [7]. The O'Neil report commissioned by the United Kingdom government [8] alerted authorities worldwide to the antibiotic resistance threat. The report estimated that if nothing is done to invert the current trends, by 2050, antimicrobial resistant infections will cause 10 million deaths per year, i.e., more than mortality induced by cancer or traffic accidents. This will also lead to severe impacts on the Gross Domestic Product (GDP), reaching world costs of up to 100 trillion USD.

Opportunistic antibiotic-resistant bacterial infections are sometimes associated with different co-morbidities, making antibiotic resistance a major threat reported and managed at the clinical level. However, the current knowledge shows the complexity of the ecology of antibiotic resistance, often led by ubiquitous bacteria and genetic elements adapted to travel through, persist and proliferate in a wide array of hosts and habitats. This proposes that antibiotic resistance dissemination must be assessed under the One-Health concept, which refers to "the collaborative

effort of multiple health science professions, together with their related disciplines and institutions – working locally, nationally, and globally – to attain optimal health for people, domestic animals, wildlife, plants, and our environment" [9].

When applied to antibiotic resistance, the One-Health concept recommends that surveillance and control measures are implemented across human, animal, and natural environments, based on the assumption that bacteria and genes can move freely between those three significant compartments (Figure 1.3) [10].

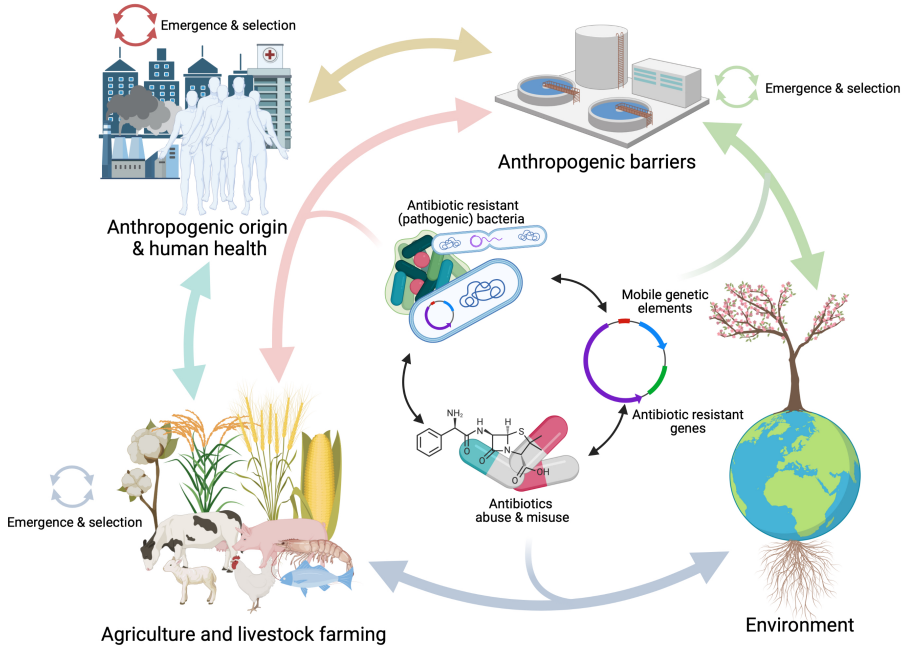

Figure 1.3: One-health diagram showing how genes and bacteria can move across the different compartments.

1.3. Wastewater and drinking water treatment plants as anthropogenic barriers

Water, which in the One-Health context is classified within the environment compartment, is a significant link between humans, animals, and nature. Water is an unconfined path for transporting nutrients, pollutants, micro-, and nanoparticles, and a primary bacterial habitat with a high potential for antibiotic resistance dissemination [11–13]. In the urban water cycle, wastewater represents the liquid emissions from human domestic activities. Urban wastewater treatment plants (UWTPs) are the endpoint of a more or less complex sewer network where wastewater is treated and major contaminants are removed before the return to

the natural environment, resulting in an adequate protection of the environment and human health [14]. However, antibiotic residues, antibiotic-resistant bacteria (ARB), and ARGs, combined with a complex mixture of other contaminants (e.g., pharmaceuticals, hygiene products), are not removed during wastewater treatment, even when tertiary treatment is implemented, and are discharged into the receiving environment [15, 16]. The substantial body of research on environmental chemistry, ecotoxicology and engineering over the last 20 years has led to the reappraisal of regulations and extensions of WWTPs for the removal of micropollutants from wastewater [17].

Drinking water treatment plants (DWTPs) and water distribution systems are the last sanitation point before humans and animals. There is limited knowledge about their role in the development of ARBs, mainly by their low biomass and micropollutant concentrations. However, ARGs and ARBs have been detected in drinking water and tap water [18]. It is unclear whether environmental ARB and ARGs in source water, DWTPs, and drinking water distribution systems significantly impacts human exposure to pathogenic ARB [19].

The widespread occurrence of antibiotic resistance has propelled research in water bodies, wastewater, soils, and wildlife, and shown the need to systematically implement monitoring schemes [20–23].

1.4. Horizontal gene transfer

There are two main ways by which bacteria transfer their genetic information. The first is vertical gene transfer, where genetic information flows from parent cells to offspring cells by binary fission. The second one is HGT, where the genetic flow goes between bacterial genomes not necessarily from the same taxa, enabling them to adapt to changing environmental conditions. This foreign DNA can contain elements that expand the niche of an organism, change its relationship with its host or provide a competitive edge against other organisms within its environment [24].

Calling your friends

Rearming bacteria to fight antibiotics meant they had to communicate and check what other mechanisms their neighbor populations were using. If interested, bacteria had to incorporate these new tools into their weaponry. These new tools are the so-called antibiotic resistance genes (ARGs), and the underlying paths by which they exchange these genes are called horizontal gene transfer (HGT) mechanisms. The chariots to move the information around are called mobile genetic elements (MGEs), including plasmids, transposons, integrons, and insertion sequences.

An example of a competitive trait typically transferred is ARGs within transferrable cassettes inside mobile genetic elements (MGEs). DNA can be mobilized through multiple mechanisms. These are conjugation, transduction, transformation, and

outer membrane vesicle usage, depicted in Figure 1.4.

Conjugation involves the transfer of DNA through conjugative pili. It is the predominant mechanism by which DNA is transferred between bacteria. It needs a cell-to-cell contact [25, 26]. **Transduction** involves bacteriophages infecting bacterial cells, where genetic material is introduced into bacterial genomes [26]. **Transformation** is the uptake and incorporation in the genome or episomally of extracellular DNA originating from cell lysis or active release in the surrounding environment [27]. There are other HGT mechanisms, of which little is known, such as genetic exchange through the **outer membrane vesicles** [28]. A recent study has highlighted a new mechanism in cell wall-deficient bacteria (so called L-forms), where extracellular material (not only DNA) gets engulfed by intracellular vesicles [29].

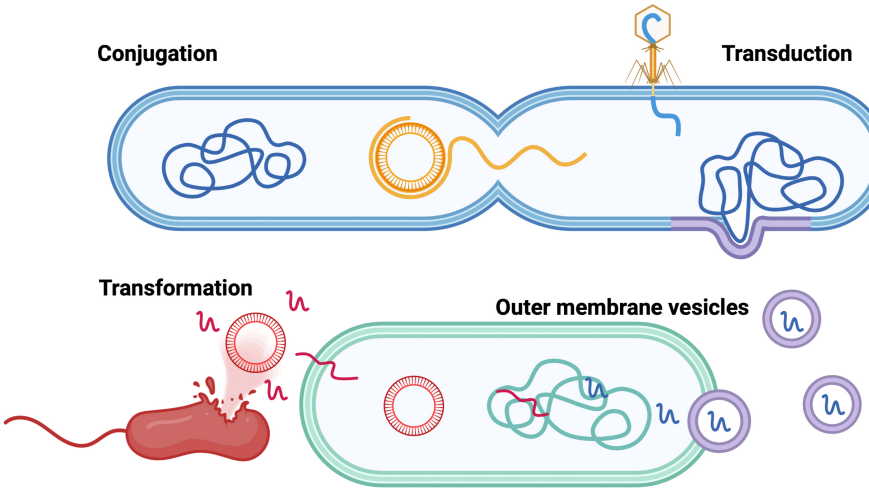

Figure 1.4: Available routes of horizontal gene transfer within natural communities. The schematic shows the different mechanisms of horizontal gene transfer.

1.5. Extracellular DNA, competence state, and natural transformation

Extracellular DNA (exDNA) is the genetic material obtained directly from environmental samples (i.e., soil, sediment, marine water, and wastewater) that are not enclosed in living cells [30]. The origins of this exDNA are diverse and caused by different processes such as the active release of DNA from physiologically active cells, i.e., structural as in biofilm formation [31] or passive release from moribund or dead cells [32].

The utilization of genetically modified organisms in different industries such as pharmaceutical, food, and industrial biotechnology has led to an increasing

concern about the fate of the transgenes and their associated selection markers, such as ARGs. There is a particular concern when these ARGs are embedded inside MGEs such as plasmids containing transposons, integrons, and insertion sequences promoting the mobility of ARGs.

1.5.1. Different ways by which DNA can integrate into bacteria

First discovered in *Streptococcus pneumoniae*, natural bacterial transformation is regarded as a parasexual process involving two partners: exDNA and a recipient cell. The canonical methods rely on cells, which have activated their competence state, where mainly double-stranded DNA (dsDNA) is integrated as single-stranded DNA (ssDNA) as a nutritional resource, and as a source of nucleotides for DNA synthesis or homologous recombination with the host genome. However, recent studies have demonstrated that some bacteria can integrate DNA as dsDNA. These processes enable bacteria to acquire new genetic traits and adapt to changing environmental conditions, promoting – for example – antibiotic resistance. The proteins involved in DNA transformation are known to be expressed in a transient state called competency. The number of species described as natural competent is scarce [33], but this number could be much bigger as most bacteria found in complex systems are not cultivable. Assays measuring genetic transformation are highly sensitive, but they can be done only in species where a selectable genetic marker is available (typically an antibiotic-resistance allele) and fail to discover competence in species where DNA uptake rarely leads to recombination [33]. Fewer species have been directly tested for their ability to take up DNA actively; these assays typically use radiolabelled DNA and, although technically straightforward, are relatively insensitive [34].

1.5.2. Do antibiotics induce competence?

Natural competence is the state by which bacteria actively pull DNA fragments from their environment into their cells. These fragments provide nucleotides, but their high similarity with the chromosome allows them to change the genotype of the cell by homologous recombination.

Competence is not activated by the availability of DNA mainly because environmental DNA is ubiquitous, especially in biofilms. Competence seems to be regulated by other environmental and biochemical cues with some exceptions, such as the constitutive expression in *Neisseria*. The most straightforward system is the one from *Haemophilus influenzae*, where cells respond to a lack of phosphotransferase system (PTS) sugars and purine precursors by inducing the expression of 25 genes from 12 operons under the control of the catabolite regulator cyclic AMP receptor protein and its competence-specific cofactor Sxy [33].

Several antibiotics can exert a positive effect for activating the competence state.

Slager et al. [35] have reported that antibiotics targeting DNA replication in *Streptococcus pneumoniae* caused an increase in the copy number of genes proximal to the origin of replication (oriC), which contains all the genes required for competence initiation nearby. More recently, in the same microorganism, antibiotics such as aztreonam and clavulanic acid induced competence by reshaping quorum sensing, increasing the time window in which cells can take up DNA, potentially accelerating the spread of the antibiotic resistance [36]. However, Sturød et al. [37] have concluded that antibiotics might vary in their effects on competence, ranging from inhibitory to stimulatory effects affecting the transformation outcome. Antibiotics that increase the transformation rate are of particular clinical relevance, as they may alter the bacteria to escape the antibiotic effect.

1.5.3. Canonical natural transformation

Bacteria are thought to share common mechanisms of DNA uptake and processing with some exceptions by using conserved proteins simultaneously expressed during the competence state. *Bacillus subtilis* and *Streptococcus pneuomoniae* transformation systems are the models used to conceptualize this process (Figure 1.5). Genes and proteins nomenclature varies between species, but *B. subtilis* nomenclature can be used as it was the first characterized in detail [38].

Briefly, extracellular dsDNA is the substrate for transformation. One strand is degraded, and the other is internalized single-stranded through the ComEC transmembrane channel. Internalized ssDNA is bound by the transformation-dedicated DprA (DNA processing A) protein, which loads the recombinase RecA onto ssDNA. RecA polymerizes on the ssDNA and promotes a homology search in the host chromosome.

Gram-positive and Gram-negative bacteria rely on highly similar DNA-uptake systems. The only major difference is the requirement for transport across the outer membrane in Gram-negative, which involves the PilQ secreting channel. The competence pseudopilus (ComGC) is used to transport DNA in bacteria from both types of Gram staining. ComEA delivers dsDNA to a protein that generates ssDNA for internalization. The nuclease EndA degrades one DNA strand, enabling the complementary strand import through the ComEC pore. Finally, homologous recombination is initiated in all organisms by ssDNA. Homologous recombinases (such as RecA) require cofactors such as DprA to facilitate the loading onto ssDNA and assist the recombination process for gaining or losing genes as well as DNA damage repair. DNA can end up having other functions such as nutrient source, and used as building blocks.

1.5.4. Alternative transformation systems

A new route for dsDNA transfer in *Escherichia coli* has been described [40]. Via an unidentified channel, exogenous DNA transfers across the outer membrane. The

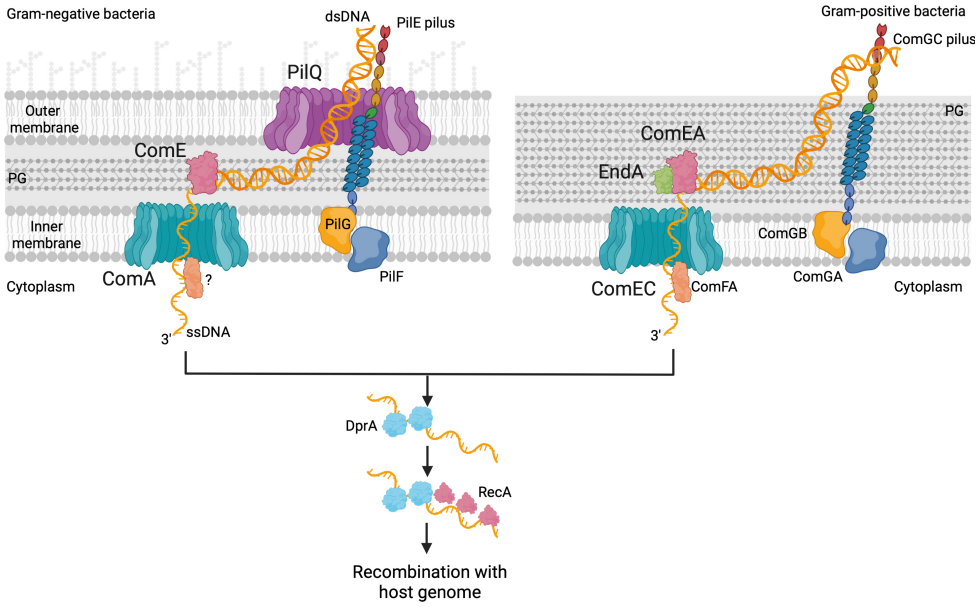

Figure 1.5: Schematic representation of the transformation process in Gram-negative and Gram-positive bacteria. PG = Peptidoglycan. Adapted from Johnston et al. [39]

pore-forming protein OmpA can compete for DNA with the unknown channel. To pass across the inner membrane, the incoming DNA binds the substrate-binding protein YdcS. It is translocated from the periplasm to the cytoplasm via an internal membrane channel formed by YdcV. Whether a plasmid enters *E. coli* as intact circular or linear dsDNA remains unclear. Still, if it enters circular, episomally, it would be crucial to understand in which MGEs the myriad of ARGs are embedded.

1.6. Exploring the environmental resistome

Due to the limited cultivability of environmental bacteria, the screening of ARGs and MGEs directly on DNA extracts is now standard practice. The detection, quantification, and characterization of specific ARB and ARGs in different environmental compartments have been supported by molecular biology methods, like quantitative PCR (qPCR) and metagenomics among several other techniques, in numerous studies [41–44]. qPCR is advantageous for epidemiological studies as it can track a specific ARG through different compartments and establish a proxy for the risk of its transmission from the environment to humans [45–52]. This paradigm change has been strongly influenced by recent advances such as the broader accessibility to molecular techniques, the lowering of sequencing prices, and the establishment of public databases on microbiology (e.g., MiDAS: Field Guide to the Microbes of Activated Sludge and Anaerobic Digesters MiDAS [53]), and resistance data (e.g., Comprehensive Antibiotic Resistance Database (CARD);

[54]), or the refinement and user-friendliness of bioinformatics pipelines.

Although the selection of methods must be driven by the investigation question and monitoring objectives, the proliferation of data from different research groups using different techniques has made comparisons between datasets and studies questionable. This impedes our ability to develop control measures [21]. The scientific community prefers genetic methods based on PCR and DNA sequencing for quantifying ARGs, although other methods are also used (Table **1.1**). In the absence of guidelines to implement standardized methods, each study can only compare its own data, which seriously hampers the potential applications of the immense amount of information generated over the last decade. The results obtained by each method are impacted by user skills, repeatability, reproducibility, and high-throughput vs. fast-throughput constraints and costs.

Table 1.1: Strengths and weaknesses of molecular biology methods that can be used for detecting and quantifying ARGs.

Methods	Strengths	Weaknesses	References
qPCR	Fast, effective, enabling quantification of gene and/or transcript numbers High sensitivity and specificity towards targeted sequences in mixed communities Wide dynamic range for quantification (7-8 log10) Well developed technology Objective and simple interpretation of results Allows analysis of a large number of samples Allows expression analysis (RNA) No post-PCR manipulations minimize the chances for cross-contamination in the laboratory	Biases in the template to product ratios of target sequence Biases increase with increasing numbers of PCR cycles Need of normalization improvements qPCR inhibitors present in environmental matrices Expensive reagents Available only for known ARGs RNA liability compared to DNA requires careful isolation Design of primers and standards can be a constraint	[45, 47, 48, 50–52, 55, 56]
LAMP	Rapid (provide results in less than half an hour) Simple and low-cost effective equipment, no need of thermo-cycler Good and effective detection method for developing countries Both amplification and detection of the target gene are done in a single step It can be visually detected through fluorescence High sensitivity and specificity when one gene is targeted Multiple commercial detection oligonucleotides	More sensitive than qPCR to inhibitors Less versatile than qPCR Design of primers and standards can be a constraint No single amplicon obtaining: banding pattern on a gel Poor sensitivity and specificity for multi-LAMP assays High initial design efforts Large amount of DNA required Cross-hybridizations may happen if not optimized	[57–59]
Whole genome sequencing	Allow individual isolates studies with high precision High sensitivity and specificity High level of detail at gene level (specific allele profiles and single nucleotide polymorphisms)	High costs Time and labor consuming	[60–62]
Metagenomics sequencing	Information on the whole microbial community, at the phylogenetic and functional levels Identifies uncultivable, unknown or emergent microorganisms Allows detection of ARGs in complex samples Provides information on AR prevalence, distribution and routes of transmission Detects simultaneously phage and bacterial DNA Identification of horizontal gene transfer phenomena and novel antibiotic synthesis pathways	High bioinformatics skills Need of continuously updated databases and tools High "noise":multitude of databases, non-relevant ARGs High costs Time and labor consuming Wet-lab and dry-lab standardization and optimization	[43, 61, 63, 64]
Hi-C sequencing	Information on the whole microbial community and how they interact Allows quantification of interactions between all possible pairs of DNA fragments simultaneously Allows linkage of specific plasmids harbouring integrons, transposons and ARGs to bacterial hosts Allows horizontal gene transfer phenomena detection across urban water systems	High bioinformatics skills High costs Time and labor consuming High abundant genomes: clustering artifacts Contig resolution between closely related species: defective links	[65–68]

1.6.1. Amplification-based methods

In general, the primary aims of characterizing the environmental resistome include: (i) quantify ARGs, (ii) assess the diversity of ARGs, and (iii) assess the range of hosts of ARGs. The latter has traditionally been supported by cultivation methods but is now moving to culture-independent approaches. One of the essential characteristics of amplification-based methods like PCR is the possibility of developing a targeted search for specific genetic determinants, such as those reported in human infections, and to amplify the detection signal by multiplication of the genetic templates. qPCR helps determine the abundance of a given genetic element per volume or mass of sample or per total amount of bacteria in a sample, giving an estimate of the density or prevalence of a genetic determinant of antibiotic resistance.

The qPCR approaches are more sensitive than the metagenomics [48]. However, they require higher efforts to cover a wide array of genes or taxonomic markers. Multiplexing qPCR can overcome these limitations with the simultaneous quantification of multiple ARGs and housekeeping genes. Novel PCR solutions, such as digital PCR (dPCR), enable gene monitoring at high throughput. While qPCR relies on a calibration curve and calculation of the number of cycles needed to achieve gene amplification in a sample, in dPCR, gene amplification occurs in thousands of independent compartments (microwell, capillary, oil emulsion, or array). The quantification is based on the estimation of the number of positive and negative reactions [69].

Gene-targeted quantifications in environmental samples using qPCR have been employed for almost two decades [70–73] . However, it is uncertain if these data are comparable: qPCR is susceptible to factors such as the reaction components, master mixes, primers design and choice, the analytical equipment, and the operator, as well as the type of sample (e.g., wastewater, treated wastewater, and river water). qPCR results are also importantly impacted by DNA extractions [74]. Although further studies are needed to assess qPCR data comparability, some inter-laboratory qPCR assays have suggested that the differences may be acceptable to determine patterns or variations [75, 76].

1.6.2. Metagenomics-based methods

Metagenomics is a non-targeted method for exploring the taxonomic and functional genetic diversity in complex environments. The metagenomic analysis permits the determination of the relative abundances of given gene and sequence categories. It allows inferences on the occurrence and proportions of distinct groups in complex microbial communities [77]. The mass of genetic information that can be retrieved from a complex biological sample makes metagenomics one of the most attractive tools for exploring microbial complexities in natural environments. The metagenomics analysis of the environmental resistome has mainly been encouraged by the availability of public databases of ARGs and MGEs. Metagenomics helps identify hundreds of ARGs and MGEs in one sequencing run.

If adequate multivariate numerical and statistical analyses are used, it is possible to explore inferences about the relationship between the resistome and mobilome profiles and the microbiome composition or the overlapping of resistomes in distinct environments [60, 78–81].

However, as with any other method, the analysis of resistomes by metagenomics is not exempt from biases. For instance, the sequencing depth can influence the abundance and diversity of ARGs detected in the dataset [82]. The reads generated for the same sample can vary between sequencing runs. A balance between the number of replicates and the sequencing depth is required to detect statistically significant differences. qPCR permits the estimation of absolute quantification from gene copy number per volume or weight of the sample and relative abundance from gene copy number per *16S rRNA* copy number. In contrast, metagenomics sequence data is expressed in relative abundance since the number of ARGs reads per total number of sequenced reads or *16S rRNA* gene or other housekeeping genes reads such as *rpoB*. Because of its single copy in the genomic DNA, *rpoB* can form an efficient "universal" reference bacterial biomarker to overcome the analytical biases induced by the heterogeneous multiple copies of the *16S rRNA* gene among bacterial genomes [83]. A widespread use of *rpoB* as bacterial genetic marker will request the development of large databases like for the *16S rRNA* gene. Genome-centric metagenomics now enables to bin and assemble genomes of uncultured microorganisms from metagenomes of microbial communities [84]. Public databases get currently populated with metagenome-assembled genomes (MAGs) that will further support genome-based phylogenetic analyses, at the condition that near-complete MAGs of high quality are deposited.

1.6.3. Who carries what in the environmental resistome?

The dissemination of ARGs and the associated risks are strongly influenced by the ecology and physiology of the host bacteria and the mobile genetic elements associated. The assessment of the diversity and abundance of ARGs seems insufficient to uncover the ecology of antibiotic resistance and to unravel how it can be controlled and if there are direct or indirect risks to human health. Investigating co-localization between ARGs and MGEs and the range of specific microbial hosts can contribute to determining the rate of DNA exchange or uptake. However, identifying the hosts of ARGs in different environments is an ambitious goal. Different approaches have been developed: the molecular technique involving emulsion, paired isolation, and concatenation PCR (epicPCR) aims at linking functional genes with phylogenetic markers that permit the identification of the taxon that hosts the targeted gene. It was described as a promising single-cell analysis approach that contours cultivation needs. Still, probably due to the technical complexity versus the obtained outputs, it has so far less been commonly used in literature reports than initially expected [85]. Other techniques to identify hosts of ARGs are 3D proximity-ligation techniques such as Hi-C sequencing, where DNA conformation is used to capture and quantify

interactions between all possible pairs of DNA fragments simultaneously by crosslinking the biomass samples with formaldehyde [66]. It is a very promising technique for is capacity to linkage specific plasmids harboring i.e. integrons and ARGs to specific microorganisms found in complex microbial communities [68].

The growing availability of metagenomes and the consolidation of bioinformatics capabilities and resources has encouraged the recovery of MAGs from distinct environmental compartments. This significantly contributed to expanding the tree of life and improving the current perspective of critical genes or functions held by specific taxa, and investigating the microverse of "microbial dark matter" [86]. One of the exciting applications refers to analyses of ARGs in MAGs. For example, 1083 high-quality MAGs incorporating full-length *16S rRNA* genes were recovered from Danish activated sludge plants [84]. ARG screening of these MAGs revealed 21 MAGs encoding ARGs, representing well-known and abundant wastewater microbes in the Candidatus *Accumulibacter* and the genus *Rhodoferax*. Combining this information with the available functional and eco-physiological characteristics will improve the understanding of the functioning, diversity, and abundance of ARB in activated sludge and wastewater systems in general.

Methods relying on linking the gene, ARG or MGE with bacterial hosts will be determinant to advancing the knowledge in this field. Examples are the in vivo proximity-ligation method Hi-C [68] besides epicPCR, and long-read sequencing.

1.7. Main knowledge gaps

Little to nothing is known about the following research gaps:

- *The integrity of DNA released into the environment towards wastewater treatment after sterilization procedures.* On the One Health basis, water connects multiple critical compartments receiving DNA from different sources. This released DNA may contain ARGs and MGEs and little is known about the state and integrity of DNA in receiving water bodies.
- *The concentration and composition of extracellular free DNA in wastewater samples.* This extracellular free DNA is a difficult fraction to be studied, mainly due to its low concentration in water matrices. Methodologies available are not suitable for its molecular high-resolution analysis.
- *The dynamics of free-floating extracellular DNA in full-scale wastewater treatment plants.* Most surveillance studies monitor the levels and removal of selected ARGs and MGEs in intracellular DNA (iDNA) extracted from WWTP influents and effluents. The role of extracellular free DNA in wastewater and the actual transfer of ARGs in the microbiome of WWTPs and its biofilm samples is mostly overlooked.
- *The dynamics of antibiotic resistant bacteria in chlorine-free drinking-water treatment plants.* The effect biological unit operations and chlorine-free, full-scale DWTPs have on promoting the selection of antibiotic resistant bacteria

has been largely overlooked.

- *The effect of antibiotic concentrations on free-floating extracellular DNA uptake in mixed cultures.* Due to different layers of complexity introduced by natural systems, the quantitative transformation transfer of genetic information in mixed cultures remains unclear.
- *Strategies to remediate free-floating extracellular ARGs and ARBs in wastewater effluents.* Low-cost, easily implementable, and scalable solutions are needed for sanitation across regions, especially in low-income countries where water sanitation is not everywhere in place.

1.8. Research aim and outline of this dissertation

Specifically, the thesis addressed the following main research question:

Research Question

What is the role of extracellular free DNA in spreading antibiotic resistance determinants through aquatic anthropogenic barriers?

This research question was answered across this dissertation in eight chapters and working objectives.

In the introductory **Chapter 1**, a literature review exposing the implications that antibiotic resistance is causing on the One Health basis, the ways that bacteria use to adapt to it, and the available techniques that scientists deploy to monitor antibiotic resistance determinants in the environment are defined.

The role of sterilization procedures from different biological sources on DNA release from microbial cultures was assessed in **Chapter 2**. If anthropogenic barriers receive active extracellular DNA, this could become a pool of resistance determinants ready to be transformed during biological treatments. This would serve as a basis to further identify these DNA fraction's genetic compositions for risk management.

In **Chapter 3**, the development of a chromatographic method to isolate free-floating extracellular DNA from complex water matrixes was done to obtain enough DNA yield for next-generation sequencing analysis. Metagenomics evaluated the extracellular DNA origin, the load in antibiotic resistance genes, and the associated mobile genetic elements.

The method developed in the previous chapter was used as the basis for **Chapter 4**, which analyzes how antibiotic resistance genes and mobile genetic elements transfer through different-sized biomasses (granules and flocs) found at the full-scale aerobic granular sludge wastewater treatment plant. Such DNA fractions were analyzed quantitatively (quantitative PCR) to assess the plant removal capacity and qualitatively (metagenomics) to evaluate which ARGs were embedded inside the MGEs.

Chapter 5 evaluated the effect of the individual stages, including physical-chemical and biological processes, in chlorine-free drinking water treatment plants on developing or removing antibiotic-resistant bacteria. Sanitation processes applied in these plants are the last anthropogenic barriers before drinking water arrives for human and animal consumption, therefore crucial for shaping gut microbiomes.

In **Chapter 6**, the effects of different antibiotic concentrations in chemostats inoculated with activated sludge and a synthetic plasmid with a fluorescent reporter and an antibiotic resistance gene were evaluated. Enrichment cultures were analyzed with proximity-ligation Hi-C sequencing to assess if microorganisms

transformed the specific plasmid and quantify the number of interactions between the host and the plasmid. Natural transformant bacteria are scarce and often unidentified. This chapter tried to quantitatively analyze horizontal gene transfer, specifically transformation events, in complex systems.

In **Chapter 7**, in a sanitation and circular economy approach, we studied the upgrading of by-products from the wastewater and drinking water treatment plants studied in the previous chapters as low-cost adsorbents to remove environmental and free-floating exDNA. We produced sewage-sludge biochar and used iron-oxide-coated sands. The intention is to evaluate the potential of these cheap recycled materials to prevent the release of ARB, ARGs, and MGEs in WWTP effluents into aquatic ecosystems.

Chapter 8 presents a set of conclusions drawn in this thesis. On top of that, it offers an outlook on future research, focusing on the technical applications of tracking gene transfer events and a self-reflection about the limitations in the field. Moreover, a recommendation regarding which stakeholders are needed to move this field forward and avoid the so-called silent pandemic is discussed.

Collectively, these research chapters were essential to better capture the role of genetic information free in aquatic environments toward advancing into the so-necessary quantitative microbial risk assessment on antimicrobial resistance.

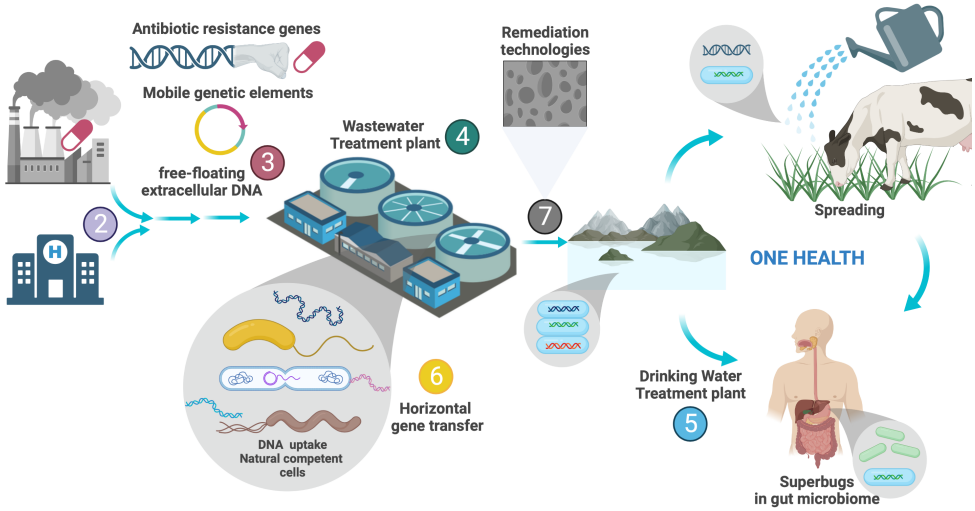

Figure 1.6: Structural overview of this thesis. Chapter numbers correspond to the numbers depicted in this figure.

Bibliography

[1] M. A. Kohanski, D. J. Dwyer, and J. J. Collins. "How antibiotics kill bacteria: From targets to networks". In: *Nature Reviews Microbiology* 8.6 (2010), pp. 423–435. ISSN: 17401526. DOI: 10.1038/nrmicro2333.

[2] M. Hutchings, A. Truman, and B. Wilkinson. "Antibiotics: past, present and future". In: *Current Opinion in Microbiology* 51.Figure 1 (2019), pp. 72–80. ISSN: 18790364. DOI: 10.1016/j.mib.2019.10.008. URL: https://doi.org/10.1016/j.mib.2019.10.008.

[3] E. D. Brown and G. D. Wright. "Antibacterial drug discovery in the resistance era". In: *Nature* 529.7586 (2016), pp. 336–343. ISSN: 14764687. DOI: 10.1038/nature17042.

[4] M. Miethke, M. Pieroni, T. Weber, M. Brönstrup, P. Hammann, L. Halby, P. B. Arimondo, P. Glaser, B. Aigle, H. B. Bode, R. Moreira, Y. Li, A. Luzhetskyy, M. H. Medema, J. L. Pernodet, M. Stadler, J. R. Tormo, O. Genilloud, A. W. Truman, K. J. Weissman, E. Takano, S. Sabatini, E. Stegmann, H. Brötz-Oesterhelt, W. Wohlleben, M. Seemann, M. Empting, A. K. Hirsch, B. Loretz, C. M. Lehr, A. Titz, J. Herrmann, T. Jaeger, S. Alt, T. Hesterkamp, M. Winterhalter, A. Schiefer, K. Pfarr, A. Hoerauf, H. Graz, M. Graz, M. Lindvall, S. Ramurthy, A. Karlén, M. van Dongen, H. Petkovic, A. Keller, F. Peyrane, S. Donadio, L. Fraisse, L. J. Piddock, I. H. Gilbert, H. E. Moser, and R. Müller. "Towards the sustainable discovery and development of new antibiotics". In: *Nature Reviews Chemistry* 5.10 (2021), pp. 726–749. ISSN: 23973358. DOI: 10.1038/s41570-021-00313-1. URL: http://dx.doi.org/10.1038/s41570-021-00313-1.

[5] B. Plackett. "No money for new drugs". In: *Nature Outlook* 586 (2020), pp. 50–52.

[6] J. M. Blair, M. A. Webber, A. J. Baylay, D. O. Ogbolu, and L. J. Piddock. "Molecular mechanisms of antibiotic resistance". In: *Nature Reviews Microbiology* 13.1 (2015), pp. 42–51. ISSN: 17401534. DOI: 10.1038/nrmicro3380.

[7] World Health Organization (WHO). "Global antimicrobial resistance surveillance system". In: *Global Antimicrobial Resistance Surveillance System: Manual for Early Implementation* (2015), p. 36.

[8] J. O'Neill. "Antimicrobial Resistance : Tackling a crisis for the health and wealth of nations." In: December (2014).

[9] W. B. Adisasmito, S. Almuhairi, C. B. Behravesh, P. Bilivogui, S. A. Bukachi, N. Casas, N. Cediel Becerra, D. F. Charron, A. Chaudhary, J. R. Ciacci Zanella, A. A. Cunningham, O. Dar, N. Debnath, B. Dungu, E. Farag, G. F. Gao, D. T. S. Hayman, M. Khaitsa, M. P. G. Koopmans, C. Machalaba, J. S. Mackenzie, W. Markotter, T. C. Mettenleiter, S. Morand, V. Smolenskiy, and L. Zhou. "One Health: A new definition for a sustainable and healthy future". In: *PLOS Pathogens* 18.6 (2022), e1010537. DOI: 10.1371/journal.ppat.1010537.

[10] S. A. McEwen and P. J. Collignon. "Antimicrobial Resistance: A One Health Colloquium". In: *Microbiology Spectrum* 6.2 (2018).

[11] T. T. Do, S. Murphy, and F. Walsh. "Antibiotic Resistance and Wastewater Treatment Process". In: *Antimicrobial Resistance in Wastewater Treatment Processes*. Ed. by P. Keen and R. Fugère. John Wiley & Sons, Inc, 2018, pp. 263–291.

[12] C. M. Manaia, G. Macedo, D. Fatta-Kassinos, and O. C. Nunes. *Antibiotic resistance in urban aquatic environments: can it be controlled?* 2016. DOI: 10.1007/s00253-015-7202-0.

[13] I. Vaz-Moreira, O. C. Nunes, and C. M. Manaia. *Bacterial diversity and antibiotic resistance in water habitats: Searching the links with the human microbiome*. 2014. DOI: 10.1111/1574-6976.12062.

[14] H. Bürgmann, D. Frigon, W. H Gaze, C. M Manaia, A. Pruden, A. C. Singer, B. F Smets, and T. Zhang. "Water and sanitation: an essential battlefront in the war on antimicrobial resistance". In: *FEMS Microbiology Ecology* 94.9 (Sept. 2018), pp. 1–14. ISSN: 1574-6941. DOI: 10.1093/femsec/fiy101.

[15] L. Rizzo, C. Manaia, C. Merlin, T. Schwartz, C. Dagot, M. C. Ploy, I. Michael, and D. Fatta-Kassinos. "Urban wastewater treatment plants as hotspots for antibiotic resistant bacteria and genes spread into the environment: A review". In: *Science of the Total Environment* 447 (2013), pp. 345–360. ISSN: 00489697. DOI: 10.1016/j.scitotenv.2013.01.032. URL: http://dx.doi.org/10.1016/j.scitotenv.2013.01.032.

[16] R. Singh, A. P. Singh, S. Kumar, B. S. Giri, and K. H. Kim. *Antibiotic resistance in major rivers in the world: A systematic review on occurrence, emergence, and management strategies*. 2019. DOI: 10.1016/j.jclepro.2019.06.243.

[17] R. I. Eggen, J. Hollender, A. Joss, M. Schärer, and C. Stamm. "Reducing the discharge of micropollutants in the aquatic environment: The benefits of upgrading wastewater treatment plants". In: *Environmental Science and Technology* 48.14 (2014), pp. 7683–7689. ISSN: 15205851. DOI: 10.1021/es500907n.

[18] M. Sevillano, Z. Dai, S. Calus, Q. M. Bautista-de los Santos, A. M. Eren, P. W. van der Wielen, U. Z. Ijaz, and A. J. Pinto. "Differential prevalence and host-association of antimicrobial resistance traits in disinfected and non-disinfected drinking water systems". In: *Science of the Total Environment* 749 (2020), p. 141451. ISSN: 18791026. DOI: 10.1016/j.scitotenv.2020.141451. URL: https://doi.org/10.1016/j.scitotenv.2020.141451.

[19] E. Sanganyado and W. Gwenzi. "Antibiotic resistance in drinking water systems: Occurrence, removal, and human health risks". In: *Science of the Total Environment* 669 (2019), pp. 785–797. ISSN: 18791026. DOI: 10.1016/j.scitotenv.2019.03.162. URL: https://doi.org/10.1016/j.scitotenv.2019.03.162.

[20] V. Barragan, S. Olivas, P. Keim, and T. Pearson. *Critical knowledge gaps in our understanding of environmental cycling and transmission of Leptospira spp.* 2017. DOI: 10.1128/AEM.01190-17.

[21] T. U. Berendonk, C. M. Manaia, C. Merlin, D. Fatta-Kassinos, E. Cytryn, F. Walsh, H. Bürgmann, H. Sørum, M. Norström, M. N. Pons, N. Kreuzinger, P. Huovinen, S. Stefani, T. Schwartz, V. Kisand, F. Baquero, and J. L. Martinez. "Tackling antibiotic resistance: The environmental framework". In: *Nature Reviews Microbiology* 13.5 (2015), pp. 310–317. ISSN: 17401534. DOI: 10.1038/nrmicro3439.

[22] Food and Agriculture Organization and World Health Organization. *Joint FAO/WHO Expert Meeting in collaboration with OIE on Foodborne Antimicrobial Resistance: Role of the Environment, Crops and Biocides – Meeting report*. 2019. ISBN: 9789251318904.

[23] B. Guerra, J. Fischer, and R. Helmuth. "An emerging public health problem: Acquired carbapenemase-producing microorganisms are present in food-producing animals, their environment, companion animals and wild birds". In: *Veterinary Microbiology* 171.3-4 (2014), pp. 290–297. ISSN: 18732542. DOI: 10.1016/j.vetmic.2014.02.001. URL: http://dx.doi.org/10.1016/j.vetmic.2014.02.001.

[24] I. L. Brito. "Examining horizontal gene transfer in microbial communities". In: *Nature Reviews Microbiology* 19.7 (2021), pp. 442–453. ISSN: 17401534. DOI: 10.1038/s41579-021-00534-7. URL: http://dx.doi.org/10.1038/s41579-021-00534-7.

[25] W. Arber. "Horizontal Gene Transfer among Bacteria and Its Role in Biological Evolution." In: *Life (Basel, Switzerland)* 4.2 (2014), pp. 217–24. ISSN: 2075-1729. DOI: 10.3390/life4020217. URL: www.mdpi.com/journal/life%20http://www.scopus.com/inward/record.url?eid=2-s2.0-84900839965&partnerID=tZOtx3y1.

[26] N. D. Zinder and J. Lederberg. *Genetic exchange in Salmonella*. Tech. rep. 5. 1952, pp. 679–699. URL: https://www.ncbi.nlm.nih.gov/pmc/articles/PMC169409/pdf/jbacter00011-0097.pdf.

[27] M. G. Lorenz and W. Wackernagel. *Bacterial gene transfer by natural genetic transformation in the environment*. Tech. rep. 3. 1994, pp. 563–602. URL: https://www.ncbi.nlm.nih.gov/pmc/articles/PMC372978/pdf/microrev00022-0281.pdf.

[28] S. Fulsundar, K. Harms, G. E. Flaten, P. J. Johnsen, B. A. Chopade, and K. M. Nielsen. "Gene transfer potential of outer membrane vesicles of Acinetobacter baylyi and effects of stress on vesiculation". In: *Applied and Environmental Microbiology* 80.11 (2014), pp. 3469–3483. ISSN: 10985336. DOI: 10.1128/AEM.04248-13.

[29] R. Kapteijn, S. Shitut, D. Ashmann, L. Zhang, M. d. Beer, D. Daviran, R. Roverts, A. Akiva, G. v. Wezel, A. Kros, and D. Claessen. "DNA uptake by cell wall-deficient

bacteria reveals a putative ancient macromolecule uptake mechanism". In: *bioRxiv* (2022), p. 2022.01.27.478057. URL: https://www.biorxiv.org/content/10.1101/2022.01.27.478057v1%0Ahttps://www.biorxiv.org/content/10.1101/2022.01.27.478057v1.abstract.

[30] A. Torti, M. A. Lever, and B. B. Jørgensen. "Origin, dynamics, and implications of extracellular DNA pools in marine sediments". In: *Marine Genomics* 24 (2015), pp. 185–196. ISSN: 18747787. DOI: 10.1016/j.margen.2015.08.007. URL: http://dx.doi.org/10.1016/j.margen.2015.08.007.

[31] D. M. Dominiak, J. L. Nielsen, and P. H. Nielsen. "Extracellular DNA is abundant and important for microcolony strength in mixed microbial biofilms". In: *Environmental Microbiology* 13.3 (2011), pp. 710–721. ISSN: 14622912. DOI: 10.1111/j.1462-2920.2010.02375.x.

[32] K. M. Nielsen, P. J. Johnsen, D. Bensasson, and D. Daffonchio. "Release and persistence of extracellular DNA in the environment". In: *Environmental Biosafety Research* 6.1-2 (2007), pp. 37–53. ISSN: 1635-7922. DOI: 10.1051/ebr:2007031. URL: http://www.ebr-journal.org/10.1051/ebr:2007031.

[33] J. C. Mell and R. J. Redfield. "Natural competence and the evolution of DNA uptake specificity". In: *Journal of Bacteriology* 196.8 (2014), pp. 1471–1483. ISSN: 10985530. DOI: 10.1128/JB.01293-13.

[34] G. Poje and R. J. Redfield. "Transformation of Haemophilus influenzae". In: *Hemophilus influenzae Protocols*. New Jersey: Humana Press, 2002, pp. 57–70. ISBN: 0896039285. DOI: 10.1385/1-59259-321-6:57. URL: http://link.springer.com/10.1385/1-59259-321-6:57.

[35] J. Slager, M. Kjos, L. Attaiech, and J. W. Veening. "Antibiotic-induced replication stress triggers bacterial competence by increasing gene dosage near the origin". In: *Cell* 157.2 (2014), pp. 395–406. ISSN: 10974172. DOI: 10.1016/j.cell.2014.01.068. URL: http://dx.doi.org/10.1016/j.cell.2014.01.068.

[36] A. Domenech, J. Slager, and J. W. Veening. "Antibiotic-Induced Cell Chaining Triggers Pneumococcal Competence by Reshaping Quorum Sensing to Autocrine-Like Signaling". In: *Cell Reports* 25.9 (2018), pp. 2390–2400. ISSN: 22111247. DOI: 10.1016/j.celrep.2018.11.007. URL: https://doi.org/10.1016/j.celrep.2018.11.007.

[37] K. Sturød, G. Salvadori, R. Junges, and F. C. Petersen. "Antibiotics alter the window of competence for natural transformation in streptococci". In: *Molecular Oral Microbiology* 33.5 (2018), pp. 378–387. ISSN: 20411014. DOI: 10.1111/omi.12240.

[38] D. Dubnau. *Genetic competence in Bacillus subtilis*. 1991. DOI: 10.1128/mmbr.55.3.395-424.1991.

[39] C. Johnston, B. Martin, G. Fichant, P. Polard, and J. P. Claverys. "Bacterial transformation: Distribution, shared mechanisms and divergent control". In: *Nature Reviews Microbiology* 12.3 (2014), pp. 181–196. ISSN: 17401526. DOI: 10.1038/nrmicro3199.

[40] D. Sun. "Two different routes for double-stranded DNA transfer in natural and artificial transformation of Escherichia coli". In: *Biochemical and Biophysical Research Communications* 471.1 (2016), pp. 213–218. ISSN: 10902104. DOI: 10.1016/j.bbrc.2016.01.137. URL: http://dx.doi.org/10.1016/j.bbrc.2016.01.137.

[41] S. Gandra, G. Alvarez-Uria, P. Turner, J. Joshi, D. Limmathurotsakul, and H. R. van Doorn. *Antimicrobial resistance surveillance in low-and middle-income countries: Progress and challenges in eight South Asian and Southeast Asian countries*. 2020. DOI: 10.1128/CMR.00048-19.

[42] A. George. *Antimicrobial resistance (AMR) in the food chain: Trade, one health and codex*. 2019. DOI: 10.3390/tropicalmed4010054.

[43] R. S. Hendriksen *et al.* "Global monitoring of antimicrobial resistance based on metagenomics analyses of urban sewage". In: *Nature Communications* 10.1 (2019). ISSN: 20411723. DOI: 10.1038/s41467-019-08853-3.

[44] H. Waseem, S. Jameel, J. Ali, H. S. Ur Rehman, I. Tauseef, U. Farooq, A. Jamal, and M. I. Ali. *Contributions and challenges of high throughput qPCR for determining antimicrobial resistance in the environment: A critical review*. 2019. DOI: 10.3390/molecules24010163.

[45] M. F. Anjum. "Screening methods for the detection of antimicrobial resistance genes present in bacterial isolates and the microbiota". In: *Future Microbiology* 10.3 (2015), pp. 317–320. ISSN: 17460921. DOI: 10.2217/FMB.15.2.

[46] D. M. Bickhart, M. Watson, S. Koren, K. Panke-Buisse, L. M. Cersosimo, M. O. Press, C. P. Van Tassell, J. A. S. Van Kessel, B. J. Haley, S. W. Kim, C. Heiner, G. Suen, K. Bakshy, I. Liachko, S. T. Sullivan, P. R. Myer, J. Ghurye, M. Pop, P. J. Weimer, A. M. Phillippy, and T. P. Smith. "Assignment of virus and antimicrobial resistance genes to microbial hosts in a complex microbial community by combined long-read assembly and proximity ligation". In: *Genome Biology* 20.1 (2019), pp. 1–18. ISSN: 1474760X. DOI: 10.1186/s13059-019-1760-x.

[47] P. Kralik and M. Ricchi. "A basic guide to real time PCR in microbial diagnostics: Definitions, parameters, and everything". In: *Frontiers in Microbiology* 8.FEB (2017), pp. 1–9. ISSN: 1664302X. DOI: 10.3389/fmicb.2017.00108.

[48] C. M. Manaia, J. Rocha, N. Scaccia, R. Marano, E. Radu, F. Biancullo, F. Cerqueira, G. Fortunato, I. C. Iakovides, I. Zammit, I. Kampouris, I. Vaz-Moreira, and O. C. Nunes. "Antibiotic resistance in wastewater treatment plants: Tackling the black box". In: *Environment International* 115.April (2018), pp. 312–324. ISSN: 18736750. DOI: 10.1016/j.envint.2018.03.044. URL: https://doi.org/10.1016/j.envint.2018.03.044.

[49] J. Rocha, T. Fernandes, M. V. Riquelme, N. Zhu, A. Pruden, and C. M. Manaia. "Comparison of culture-and quantitative PCR-based indicators of antibiotic resistance in wastewater, recycled water, and tap water". In: *International Journal of Environmental Research and Public Health* 16.21 (2019). ISSN: 16604601. DOI: 10.3390/ijerph16214217.

[50] C. J. Smith and A. M. Osborn. "Advantages and limitations of quantitative PCR (Q-PCR)-based approaches in microbial ecology". In: *FEMS Microbiology Ecology* 67.1 (2009), pp. 6–20. ISSN: 01686496. DOI: 10.1111/j.1574-6941.2008.00629.x.

[51] D. N. Wang, L. Liu, Z. G. Qiu, Z. Q. Shen, X. Guo, D. Yang, J. Li, W. L. Liu, M. Jin, and J. W. Li. "A new adsorption-elution technique for the concentration of aquatic extracellular antibiotic resistance genes from large volumes of water". In: *Water Research* 92 (2016), pp. 188–198. ISSN: 18792448. DOI: 10.1016/j.watres.2016.01.035.

[52] Y. Yang, B. Li, F. Ju, and T. Zhang. "Exploring variation of antibiotic resistance genes in activated sludge over a four-year period through a metagenomic approach". In: *Environmental Science and Technology* 47.18 (2013), pp. 10197–10205. ISSN: 0013936X. DOI: 10.1021/es4017365. URL: https://pubs.acs.org/sharingguidelines.

[53] M. Nierychlo, K. S. Andersen, Y. Xu, N. Green, C. Jiang, M. Albertsen, M. S. Dueholm, and P. H. Nielsen. "MiDAS 3: An ecosystem-specific reference database, taxonomy and knowledge platform for activated sludge and anaerobic digesters reveals species-level microbiome composition of activated sludge". In: *Water Research* 182 (2020). ISSN: 18792448. DOI: 10.1016/j.watres.2020.115955.

[54] B. P. Alcock, A. R. Raphenya, T. T. Lau, K. K. Tsang, M. Bouchard, A. Edalatmand, W. Huynh, A. L. V. Nguyen, A. A. Cheng, S. Liu, S. Y. Min, A. Miroshnichenko, H. K. Tran, R. E. Werfalli, J. A. Nasir, M. Oloni, D. J. Speicher, A. Florescu, B. Singh, M. Faltyn, A. Hernandez-Koutoucheva, A. N. Sharma, E. Bordeleau, A. C. Pawlowski, H. L. Zubyk, D. Dooley, E. Griffiths, F. Maguire, G. L. Winsor, R. G. Beiko, F. S. Brinkman, W. W. Hsiao, G. V. Domselaar, and A. G. McArthur. "CARD 2020: Antibiotic resistome surveillance with the comprehensive antibiotic resistance database". In: *Nucleic Acids Research* 48.D1 (2020), pp. D517–D525. ISSN: 13624962. DOI: 10.1093/nar/gkz935.

[55] R. Girones, M. A. Ferrús, J. L. Alonso, J. Rodriguez-Manzano, B. Calgua, A. de Abreu Corrêa, A. Hundesa, A. Carratala, and S. Bofill-Mas. "Molecular detection of pathogens in water - The pros and cons of molecular techniques". In: *Water Research* 44.15 (2010), pp. 4325–4339. ISSN: 00431354. DOI: 10.1016/j.watres.2010.06.030.

[56] M. A. Valasek and J. J. Repa. "The power of real-time PCR". In: *American Journal of Physiology - Advances in Physiology Education* 29.3 (2005), pp. 151–159. ISSN: 15221229. DOI: 10.1152/advan.00019.2005.

[57] T. Notomi, H. Okayama, H. Masubuchi, T. Yonekawa, K. Watanabe, N. Amino, and T. Hase. "Loop-mediated isothermal amplification of DNA Tsugunori". In: *Nucleic Acids Research* 28.12 (2000), p. 63. ISSN: 00257818.

[58] P. R. Sahoo, K. Sethy, S. Mohapatra, and D. Panda. "Loop mediated isothermal amplification: An innovative gene amplification technique for animal diseases". In: *Veterinary World* 9.5 (2016), pp. 465–469. ISSN: 22310916. DOI: 10.14202/vetworld.2016.465-469.

[59] L.-l. Zhong, Q. Zhou, S. Ahmed, G. Chen, M. Dai, F. Yang, and Y. Xia. "Multiplex loop-mediated isothermal ampli fi cation (multi-LAMP) assay for rapid detection of mcr-1 to mcr-5 in colistin-resistant bacteria". In: *Infection and Drug Resistance* (2019), pp. 1877–1887.

[60] R. S. Hendriksen, V. Bortolaia, H. Tate, G. H. Tyson, F. M. Aarestrup, and P. F. McDermott. "Using Genomics to Track Global Antimicrobial Resistance". In: *Frontiers in Public Health* 7.September (2019). ISSN: 22962565. DOI: 10.3389/fpubh.2019.00242.

[61] E. A. Oniciuc, E. Likotrafiti, A. Alvarez-Molina, M. Prieto, J. A. Santos, and A. Alvarez-Ordóñez. "The present and future of whole genome sequencing (WGS) and whole metagenome sequencing (WMS) for surveillance of antimicrobial resistant microorganisms and antimicrobial resistance genes across the food chain". In: *Genes* 9.5 (2018), pp. 1–28. ISSN: 20734425. DOI: 10.3390/genes9050268.

[62] S. A. Shelburne, J. Kim, J. M. Munita, P. Sahasrabhojane, R. K. Shields, E. G. Press, X. Li, C. A. Arias, B. Cantarel, Y. Jiang, M. S. Kim, S. L. Aitken, and D. E. Greenberg. "Whole-genome sequencing accurately identifies resistance to extended-spectrum β-lactams for major gram-negative bacterial pathogens". In: *Clinical Infectious Diseases* 65.5 (2017), pp. 738–745. ISSN: 15376591. DOI: 10.1093/cid/cix417.

[63] R. De. "Metagenomics: Aid to combat antimicrobial resistance in diarrhea". In: *Gut Pathogens* 11.1 (2019), pp. 1–9. ISSN: 17574749. DOI: 10.1186/s13099-019-0331-8. URL: https://doi.org/10.1186/s13099-019-0331-8.

[64] J. Pollock, A. Muwonge, M. R. Hutchings, G. Mainda, B. M. Bronsvoort, D. L. Gally, and A. Corbishley. "Resistance to change: AMR gene dynamics on a commercial pig farm with high antimicrobial usage". In: *Scientific Reports* 10.1 (2020), pp. 1–10. ISSN: 20452322. DOI: 10.1038/s41598-020-58659-3.

[65] J. N. Burton, I. Liachko, M. J. Dunham, and J. Shendure. "Species-level deconvolution of metagenome assemblies with Hi-C-based contact probability maps". In: *G3: Genes, Genomes, Genetics* 4.7 (2014), pp. 1339–1346. ISSN: 21601836. DOI: 10.1534/g3.114.011825.

[66] J. Fraser, I. Williamson, W. A. Bickmore, and J. Dostie. "An Overview of Genome Organization and How We Got There: from FISH to Hi-C". In: *Microbiology and Molecular Biology Reviews* 79.3 (2015), pp. 347–372. ISSN: 1092-2172. DOI: 10.1128/mmbr.00006-15.

[67] M. O. Press, A. H. Wiser, Z. N. Kronenberg, K. W. Langford, M. Shakya, C.-c. Lo, K. A. Mueller, S. T. Sullivan, P. S. G. Chain, and I. Liachko. "Hi-C deconvolution of a human gut microbiome yields high-quality draft genomes and reveals plasmid-genome interactions." In: *bioRxiv* (2017), p. 198713. DOI: 10.1101/198713. URL: https://www.biorxiv.org/content/early/2017/10/05/198713.full.pdf+html.

[68] T. Stalder, M. O. Press, S. Sullivan, I. Liachko, and E. M. Top. "Linking the resistome and plasmidome to the microbiome". In: *ISME Journal* (2019), pp. 2437–2446. ISSN: 17517370. DOI: 10.1038/s41396-019-0446-4. URL: http://dx.doi.org/10.1038/s41396-019-0446-4.

[69] J. Kuypers and K. R. Jerome. *Applications of digital PCR for clinical microbiology*. 2017. DOI: 10.1128/JCM.00211-17.

[70] T. Fernandes, I. Vaz-moreira, and C. M. Manaia. "Neighbor urban wastewater treatment plants display distinct profiles of bacterial community and antibiotic resistance genes". In: (2019).

[71] C. Narciso-da-rocha, J. Rocha, I. Vaz-moreira, F. Lira, J. Tamames, I. Henriques, J. Luis, and C. M. Manaia. "Bacterial lineages putatively associated with the dissemination of antibiotic resistance genes in a full-scale urban wastewater treatment plant". In: *Environment International* 118.February (2018), pp. 179–188. ISSN: 0160-4120. DOI: 10.1016/j.envint.2018.05.040.

[72] S. Rodriguez-Mozaz, S. Chamorro, E. Marti, B. Huerta, M. Gros, A. Sànchez-Melsió, C. M. Borrego, D. Barceló, and J. L. Balcázar. "Occurrence of antibiotics and antibiotic resistance genes in hospital and urban wastewaters and their impact on the receiving river". In: *Water Research* 69 (2015), pp. 234–242. ISSN: 18792448. DOI: 10.1016/j.watres.2014.11.021.

[73] T. Schwartz, W. Kohnen, B. Jansen, and U. Obst. "Detection of antibiotic-resistant bacteria and their resistance genes in wastewater, surface water, and drinking water biofilms". In: *FEMS Microbiology Ecology* (2003). ISSN: 01686496. DOI: 10.1016/S0168-6496(02)00444-0.

[74] S. Agrawal, D. G. Weissbrodt, M. Annavajhala, M. M. Jensen, J. M. C. Arroyo, G. Wells, K. Chandran, S. E. Vlaeminck, A. Terada, B. F. Smets, and S. Lackner. "Time to

act–assessing variations in qPCR analyses in biological nitrogen removal with examples from partial nitritation/anammox systems". In: *Water Research* 190 (2021), p. 116604. ISSN: 18792448. DOI: 10.1016/j.watres.2020.116604. URL: https://doi.org/10.1016/j.watres.2020.116604.

[75] J. Rocha, D. Cacace, I. Kampouris, H. Guilloteau, T. Jäger, R. B. Marano, P. Karaolia, C. M. Manaia, C. Merlin, D. Fatta-Kassinos, E. Cytryn, T. U. Berendonk, and T. Schwartz. "Inter-laboratory calibration of quantitative analyses of antibiotic resistance genes". In: *Journal of Environmental Chemical Engineering* 8.1 (Feb. 2020), p. 102214. ISSN: 22133437. DOI: 10.1016/j.jece.2018.02.022.

[76] J. Rocha and C. M. Manaia. "Cell-based internal standard for qPCR determinations of antibiotic resistance indicators in environmental water samples". In: *Ecological Indicators* 113.October 2019 (June 2020), p. 106194. ISSN: 1470160X. DOI: 10.1016/j.ecolind.2020.106194.

[77] Committee on Metagenomics: Challenges and Functional Applications. *The new science of metagenomics. Revealing the secrets of our microbial planet.* Vol. 12. 4. Washington, DC: THE NATIONAL ACADEMIES PRESS, 2007, pp. 378–394. ISBN: 9780309106764. DOI: 10.1088/0957-0233/12/4/303.

[78] Y. Che, Y. Xia, L. Liu, A. D. Li, Y. Yang, and T. Zhang. "Mobile antibiotic resistome in wastewater treatment plants revealed by Nanopore metagenomic sequencing". In: *Microbiome* 7.1 (2019), pp. 1–13. ISSN: 20492618. DOI: 10.1186/s40168-019-0663-0.

[79] A. Karkman, T. A. Johnson, C. Lyra, R. D. Stedtfeld, M. Tamminen, J. M. Tiedje, and M. Virta. "High-throughput quantification of antibiotic resistance genes from an urban wastewater treatment plant". In: *FEMS Microbiology Ecology* 92.3 (2016), pp. 1–7. ISSN: 15746941. DOI: 10.1093/femsec/fiw014.

[80] F. Lira, I. Vaz-Moreira, J. Tamames, C. M. Manaia, and J. L. Martínez. "Metagenomic analysis of an urban resistome before and after wastewater treatment". In: *Scientific Reports* 10.1 (2020). ISSN: 20452322. DOI: 10.1038/s41598-020-65031-y.

[81] C. Munck, M. Albertsen, A. Telke, M. Ellabaan, P. H. Nielsen, and M. O. Sommer. "Limited dissemination of the wastewater treatment plant core resistome". In: *Nature Communications* 6 (2015). ISSN: 20411723. DOI: 10.1038/ncomms9452.

[82] J. Bengtsson-Palme, D. G. Larsson, and E. Kristiansson. "Using metagenomics to investigate human and environmental resistomes". In: *Journal of Antimicrobial Chemotherapy* 72.10 (2017), pp. 2690–2703. ISSN: 14602091. DOI: 10.1093/jac/dkx199.

[83] R. J. Case, Y. Boucher, I. Dahllöf, C. Holmström, W. F. Doolittle, and S. Kjelleberg. "Use of 16S rRNA and rpoB genes as molecular markers for microbial ecology studies". In: *Applied and Environmental Microbiology* 73.1 (2007), pp. 278–288. ISSN: 00992240. DOI: 10.1128/AEM.01177-06.

[84] C. Singleton, F. Petriglieri, J. Kristensen, R. Kirkegaard, T. Michaelsen, M. Andersen, Z. Kondrotaite, S. Karst, M. Dueholm, P. Nielsen, and M. Albertsen. "Connecting structure to function with the recovery of over 1000 high-quality activated sludge metagenome-assembled genomes encoding full-length rRNA genes using long-read sequencing". In: *bioRxiv* (2020). DOI: 10.1101/2020.05.12.088096.

[85] J. Hultman, M. Tamminen, K. Pärnänen, J. Cairns, A. Karkman, and M. Virta. "Host range of antibiotic resistance genes in wastewater treatment plant influent and effluent". In: *FEMS microbiology ecology* 94.4 (2018). ISSN: 15746941. DOI: 10.1093/femsec/fiy038.

[86] T. Zamkovaya, J. S. Foster, V. de Crécy-Lagard, and A. Conesa. "A network approach to elucidate and prioritize microbial dark matter in microbial communities". In: *ISME Journal* 15.1 (2021), pp. 228–244. ISSN: 17517370. DOI: 10.1038/s41396-020-00777-x. URL: http://dx.doi.org/10.1038/s41396-020-00777-x.

2

Anticipating xenogenetic pollution at the source: Impact of sterilizations on DNA release from microbial cultures

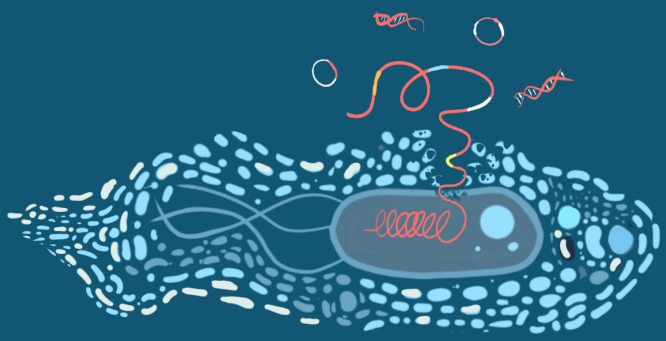

This chapter has been published as: Calderón-Franco, D., Lin, Q., van Loosdrecht, M.C.M., Abbas, B., Weissbrodt, D.G., 2020. Anticipating Xenogenic Pollution at the Source : Impact of Sterilizations on DNA Release From Microbial Cultures. Front. Bioeng. Biotechnol. 8, 1–13. https://doi.org/10.3389/fbioe.2020.00171

ABSTRACT

The dissemination of DNA and xenogenic elements across waterways is under scientific and public spotlight due to new gene-editing tools, such as do-it-yourself (DIY) CRISPR-Cas kits deployable at kitchen table. Over decades, prevention of spread of genetically modified organisms (GMOs), antimicrobial resistances (AMR), and pathogens from transgenic systems has focused on microbial inactivation. However, sterilization methods have not been assessed for DNA release and integrity. Here, we investigated the fate of intracellular DNA from cultures of model prokaryotic (Escherichia coli) and eukaryotic (Saccharomyces cerevisiae) cells that are traditionally used as microbial chassis for genetic modifications. DNA release was tracked during exposure of these cultures to conventional sterilization methods. Autoclaving, disinfection with glutaraldehyde, and microwaving are used to inactivate broths, healthcare equipment, and GMOs produced at kitchen table. DNA fragmentation and PCR-ability were measured on top of cell viability and morphology. Impact of these methods on DNA integrity was verified on a template of free λ DNA. Intense regular autoclaving (121°C, 20 min) resulted in the most severe DNA degradation and lowest household gene amplification capacity: 1.28 ± 0.11, 2.08 ± 0.03, and 4.96 ± 0.28 logs differences to the non-treated controls were measured from E. coli, S. cerevisiae, and λ DNA, respectively. Microwaving exerted strong DNA fragmentation after 100 s of exposure when free λ DNA was in solution (3.23 ± 0.06 logs difference) but a minor effect was observed when DNA was released from E. coli and S. cerevisiae (0.24 ± 0.14 and 1.32 ± 0.02 logs differences with the control, respectively). Glutaraldehyde prevented DNA leakage by preserving cell structures, while DNA integrity was not altered. The results show that current sterilization methods are effective on microorganism inactivation but do not safeguard an aqueous residue exempt of biologically reusable xenogenic material, being regular autoclaving the most severe DNA-affecting method. Reappraisal of sterilization methods is required along with risk assessment on the emission of DNA fragments in urban systems and nature.

Keywords: *Sterilizations; DNA release; Xenogenic pollution; DIY biology; Antimicrobial resistances*

2.1. Introduction

The rapid development of gene-editing tools together with the broad applications of genetically modified organisms (GMOs) have triggered biosafety concern on the hazard composed by the dissemination of unwanted DNA into the environment after sterilization [1].

Concerns have been risen on the emission of xenogenic and mobile genetic elements that may carry antibiotic resistance genes (ARGs) or pathogenicity, and their transport across urban waterways through wastewater treatment plants into nature [2, 3]. Novel CRISPR-Cas technologies propel the engineering of microorganisms out of industry boundary with do-it-yourself (DIY) kits available at kitchen table. Uncontrolled, diffuse emission of GMO materials via domestic waste streams could be a threat.

Current sterilization methods are proven to efficiently inactivate microorganisms. However, a key knowledge gap remains on their impact on DNA and its potential release into industrial, clinical, and domestic sewage. Common methods used to treat industrial broths, healthcare equipment and surfaces, and domestic waste primarily involve autoclaving, glutaraldehyde, and microwaving, respectively. Several studies have shown how DNA present in food products react with different sterilization procedures [4–6]. Treatments such as irradiation and autoclaving affect DNA in meat products or edible seeds by decreasing the total DNA content as well as causing DNA fragmentation, degradation and denaturation [7, 8]. However, the impact highly depends on the cell type, the sterilization method, and the process conditions.

Temperature, pressure, pH, and sterilization times significantly exert effects on DNA quality. For instance, temperatures over 100°C have resulted in significant DNA strand clipping and irreversible loss of secondary structure [5]. Normal autoclaving (121°C between 5 to 20 min) of food and crops did not impeded it to be available for PCR amplification [4, 5, 9].

Microwaving is commonly used in kitchen procedures such as water boiling and food heating [10, 11]. It has been suggested to effectively kill bacteria, yeast, and molds on kitchen sponges [12]. Microwaves at frequencies of 2450 MHz have been used to sterilize soil due to its ability to inhibit nitrification and sulfur oxidations [13–15]. It has also been used in laboratory settings for pharmaceutical glass vials, culture media, or clinical specimens sterilization [16]. The thermal effect mechanism is based on the absorption of microwave heat energy by the cell constituents, which leads to fast vibrations of cell membrane lipids resulting in the emergence of pores [17]. These pores may cause leakage of vital intracellular molecules being able to cause cell death. High temperatures denature cellular biomolecules such as proteins, which may also be a reason of cells lysis [18].

Glutaraldehyde is commonly used in industry, research labs and, more specific, in hospitals as a disinfectant on dental and medical instruments, such as endoscopes, and surfaces. Glutaraldehyde has a wide range of biocidal activity against both

Gram-positive and Gram-negative bacteria, viruses, and spores [19, 20]. It is a strong cross-linker that combines with multiple molecular functions such as amino and sulfhydryl groups [21]. Glutaraldehyde affects cells by binding to nucleic acids and cross-linking enzymes responsible for oxygen uptake, destroying secondary structures and therefore causing disfunction of cytoplasmic molecules and death of cells [22].

Here, the model bacterium *Escherichia coli* and yeast *Saccharomyces cerevisiae* were used as model organisms to test the impact of autoclaving, microwaving, and glutaraldehyde on the release of DNA from microbial cultures of prokaryotes and eukaryotes, respectively. We elucidated the effects of these three dominant sterilization methods on DNA release, fragmentation, degradation, and amplification capacity on top of cellular inactivation, morphology, and integrity. This incepting work provides first insights to foster the management of the emission of xenogenic pollution.

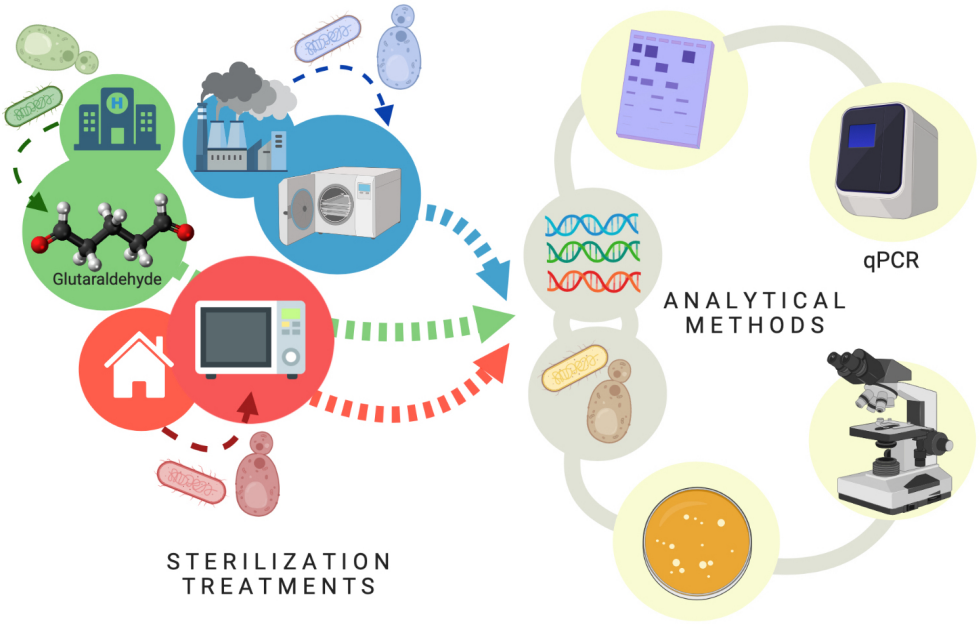

Figure 2.1: Graphical abstract

2.2. Material & Methods

Bacterial and yeast strains and culture preparations

A frozen stock of *Escherichia coli*, DH5α (Cell System Engineering Section, Department of Biotechnology, TU Delft, the Netherlands) was thawed and inoculated into a 300-mL flask containing 200 mL of Luria-Bertani (LB) cultivation broth. This culture was incubated in a rotary shaker for 6 h at 37°C, 200 rpm, where late log phase was reached. A frozen stock of *Saccharomyces cerevisiae*, CEN.PK (Cell System Engineering Section, Department of Biotechnology, TU Delft, the Netherlands) was thawed and inoculated into a 500-mL flask containing 200 mL of yeast extract-peptone-dextrose (YEPD) broth composed of 1% yeast extract, 2% peptone, and 2% glucose/dextrose. This culture was incubated in a rotary shaker for 6 h at 30°C and 200 rpm. Samples of 5 mL at 10^{11} CFU L^{-1} of cell cultures were prepared for further sterilization treatments.

Physical sterilization treatment by microwaving

A microwave oven (Bestron Model ER-M18, 2450 MHz, 230V, 850W) with a rotating table was used. A sealed glass bottle containing 5 mL of each microorganism was placed at the center of the rotating table, 20 cm away from the irradiation source. The microwave was irradiated for a maximum of 30 s within which different time intervals were taken. For each interval time point (0, 5, 10, 12, 14, 16, 18, 20, 25 and 30 s), different sampling tubes were used to ensure that the treatment duration was continuous. Extra exposure times of 40 to 60, 70 and up to 100 s were applied to test for the qPCR-ability of the DNA fragments on top of their release from microbial cells. Microwave was set at maximum power mode in order to avoid its automatic on and off switching. Quality controls were performed with pure 1 ng λ DNA μL^{-1} (Thermo Fisher Scientific Inc., Waltham, MA, USA) by irradiating the sample with microwaves for a maximum of 100 s.

Chemical sterilization treatment by glutaraldehyde

A generic buffer was prepared by mixing 10 g of sodium bicarbonate ($NaHCO_3$) with 90 g of disodium hydrogen phosphate (Na_2HPO_4). This buffer mixture was used to adjust the pH of the glutaraldehyde ($C_5H_8O_2$) solution to an alkaline value of 8.0 which ensures the bactericidal activity of glutaraldehyde (Ballantyne and Jordan, 2001). A 2% (w/w) glutaraldehyde solution (20 g L^{-1}, 0.2 M) was prepared and the final pH of the mixture was set at 8.0. Volumes of 12 mL of microorganism suspensions were collected into 15-mL Falcon tubes and were centrifuged at 6000 x g at 4°C for 15 min. Afterwards, the pellets were resuspended in 12 mL of 1x PBS solution (pH 7.4) and placed in an 18°C water bath for chemical sterilization. Samples were treated with final glutaraldehyde concentrations of 50, 100, 150, 200, 250, and 300 mgL^{-1}. Each cell suspension was tested out for 20 min. After reaction, cells were washed and resuspended in 1xPBS solution. The same procedure was followed for quality controls performed with pure λ DNA at 1 ng μL^{-1}.

Thermal sterilization treatment by autoclaving

Sterilization by autoclaving was tested in an autoclave (SHP Steriltechnik AG, Germany) at 110°C and 121°C and 1.1 atm overpressure. The 5 mL cell suspensions were placed in a 25-mL glass tube inside the autoclave and subjected to sterilization under four different autoclaving default programs (program P1: 110°C, 20 min; P2: 110°C, 30 min; P3: 121°C, 20 min; P4: 121°C, 30 min).

Same procedure was followed for quality controls with pure λ DNA at 1 ng μL^{-1}. All sterilization experiments were done in technical triplicates by treating three individual samples taken from each culture.

Cell survival

After sterilization, samples of *E. coli* were plated on LB agar plates, and samples of *S. cerevisiae* were plated on YEPD agar plates (100 µL). *E. coli* cells were incubated at 37°C for 24 h, and *S. cerevisiae* cells were incubated at 30°C for 24 h. Plates which contained 30 to 300 colonies were considered suitable for cell counting [23]. Experiments were done in technical triplicates.

DNA quantification

After sterilization, 2 mL of each cell sample was centrifuged at 10000 x g, 4°C for 3 min. After the first centrifugation, 2 mL of supernatant was collected. To maximize DNA recovery, the residual pellet was washed with 1 mL 1xPBS solution, centrifuged again, prior collecting 1 mL of supernatant. A total of 3 mL supernatant was obtained from each sample. Supernatants and pellets were separated and stored at -80°C pending DNA analysis.

Intracellular DNA from the pellets was extracted before and after sterilizations with the DNeasy UltraClean Microbial Kit (Qiagen, Germany). The total DNA content of each sample was the combination of the released DNA obtained on the supernatant fraction plus the DNA obtained from the pellet fraction. The amount of DNA released after sterilization was measured from the supernatant by HS dsDNA Qubit assays (Qubit 3.0, Invitrogen, California, USA) according to manufacturer's protocol.

DNA fragmentation

DNA samples were analyzed by gel electrophoresis with agarose at 1% (w/v) (Sigma-Aldrich, Haverhill, United Kingdom) in 1xTAE buffer. DNA was post-stained using SYBR Gold solution (10000x) (Thermo Fisher Scientific, USA) mixed in 1x TAE buffer (AppliChem, Germany) at 1/10K (v/v).

Gels after running were immersed into staining buffer for 40 min and were further checked with fluorescence imaging system (Syngene, UK).

Primers selection for *E. coli* and *S. cerevisiae* and design for λ DNA

Forward and reverse primers were designed to assess the PCR ability of the released DNA fragments after the different sterilization methods used in this study. All primers were purchased from Sigma-Aldrich (Sigma-Aldrich, Haverhill, United Kingdom). The β-glucuronidase (*uidA*) gene is a molecular marker from *E. coli* that was evaluated by using *uidA* forward (5'-TGGTAATTACCGACGAAAACGGC-3') and *uidA* reverse (5'-ACGCGTGGTTACAGTCTTGCG-3') primers [24]. The TATA binding protein-associated factor (*TAF10*) gene from *S. cerevisiae* was evaluated using *TAF10* forward (5'-ATATTCCAGGATCAGGTCTTCCGTAGC-3') and *TAF10* reverse (5'-GTAGTCTTCTCATTCTGTTGATGTTGTTGTTG-3') primers [25]. The selection of the gene fragments is not random. The β-glucuronidase (*uidA*) gene has already been reported to efficiently allow for detection and enumeration of *E. coli* while avoiding false positives [26]. Regarding *S. cerevisiae*, the TATA binding protein-associated factor *TAF10* is a gene, whose expression remains stable independently of growth conditions and strain backgrounds. It makes it a good reference gene for quantitative analysis by qPCR [27]. For λ DNA, an interesting mobile genetic element was found integrated in its genome: the tyrosine recombinase is involved in the mobility of antibiotic resistance gene cassettes on bacterial class 1 integron-integrase gene (*intI1*). The *intI1* gene was therefore assessed by qPCR. This nicely put this study into the context of horizontal gene transfer phenomena and the emerging concern of antibiotic resistant genes emissions and transfer across the water network. The λ bacteriophage genome was obtained from GenBank (Wu, 1972; Entry Number J02459.1). Primers targeting the λ integrase (*intI1*) gene were designed in house using SnapGene (GSL Biotech, www.snapgene.com): λ int forward (5'-GTTACCGGGCAACGAGTTGG-3'), λ int reverse (5'-ATGCCCGAGAAGATGTTGAGC-3') primers.

DNA extraction and quantitative PCR (qPCR) analysis

The quantification of the λ *int* gene, *E. coli uidA* gene, and *S. cerevisiae TAF10* gene in DNA fragments potentially released after sterilization treatments were analyzed by qPCR (QTower 3, Analytica Jena, Germany). For the standard curve construction, genomic DNA from the model organisms *E. coli* and *S. cerevisiae* was isolated using NucleoSpin® Soil (Macherey-Nagel) and Yeast DNA Extraction (Thermo Fisher Scientific Inc., Waltham, MA, USA) kits, respectively. Serial dilutions from 100 ng μL^{-1} down to 10^{-5} ng μL^{-1} were used to generate the standard curve. Validation of the standard curve construction was performed by purchasing 0.3 µg μL^{-1} λ pure DNA (Thermo Fisher Scientific Inc., Waltham, MA, USA). Serial dilution from 1 ng μL^{-1} down to 10^{-8} ng μL^{-1} were used to generate the standard curve. The samples were tested for amplification capacity after sterilization treatments by collecting 1 mL of sterilized culture and centrifugating it at 15000 x g for 5 min. The supernatant containing released DNA was collected and diluted 1:10 in ultrapure water (Sigma-Aldrich, Haverhill,

United Kingdom) prior being used for qPCR analysis. All qPCR reactions were performed in volumes of 20 μL composed of 10 μL of IQ™ SYBR® Green Supermix (Bio-Rad), 0.2 μL of each primer at 50 μM, 8.6 μL ultrapure water (Sigma-Aldrich, Haverhill, United Kingdom) and 1 μL of template DNA. The thermal profile selected for the λ *int* gene consisted of 5 min at 95°C hot-start polymerase activation followed by 40 cycles of DNA dissociation at 95°C for 30 s, primers annealing at 55°C for 30 s fragment elongation at 72°C for 30 s, and terminated by holding at 4°C. The thermal profile selected for the *E. coli uidA* gene gene consisted of 5 min at 95°C hot-start polymerase activation followed by 40 cycles of DNA dissociation at 95°C for 30 s, primers annealing at 57°C for 30 s, fragment elongation at 72°C for 30 s, and terminated by holding at 4°C. The thermal profile selected for the *S. cerevisiae TAF10* gene consisted of 5 min at 95°C hot-start polymerase activation followed by 40 cycles of DNA dissociation at 95°C for 30 s, primers annealing at 55°C for 30 s, fragment elongation at 72°C for 30 s, and terminated by holding at 4°C.

Quality controls

Different quality controls were used across sterilization experiments and measurements.

Controls for DNA release from cells were produced by bead-milling (or also known as bead-beating) of the bacterial and yeast cultures using the DNeasy UltraClean Microbial Kit. Bead-milled positive controls is considered as an easy and straightforward method for induced intracellular DNA release [28] and non-bead-milled negative controls were included in the analyses.

Controls for DNA degradation were performed by subjecting free-floating λ DNA to the same sterilization conditions as the cell cultures. It served as a control as it avoids the effect of cell breakage and other artifacts, and therefore allowed assessing the effect of sterilization on DNA fragmentation and degradation.

Statistical analysis

Statistical analyses were performed with R 3.5.1 (R Foundation for Statistical Computing., 2018) and RStudio (https://www.rstudio.com/). For the analysis and determination of the most effective parameters of the sterilization methods effect on DNA amplification a one-way ANOVA test, that can tolerate skewed or kurtotic distribution data, followed by a post-hoc Tukey's honestly significant difference (HSD) test at the 0.05 probability level were performed. Figures were prepared using GraphPad Prism 6 (GraphPad Software, San Diego, CA, USA). The absorbance (or "optical density", OD) of the culture was corrected for by assessing the effect of the sterilization methods, assuming homogeneous cultures, thus technical triplicates per biological sample were used.

2.3. Results & Discussion

Sterilization methods inactivated over 99% of living bacterial and yeast cells

The microwave effect on cell viability (**Figure** 2.2**a**) showed similar end-points but different profiles for both model prokaryotic and eukaryotic microorganisms. For both *E. coli* and *S. cerevisiae*, the microwaving performance for 15 s was sufficient to reduce the number of cells to nearly 10% of control untreated samples, indicating severe inactivation effect on both microorganisms. Thermal effect is responsible for absorption of microwave energy by cell molecules, producing general heating of the cell [29]. This causes disarrangement of cell membrane and disruption of cell wall structures by destroying the lipopolysaccharides and peptidoglycan of the cell surface. This results in the emergence of pores, cell aggregations, cytoplasmic proteins aggregation, and changes of membrane permeability [17, 30], explaining why biomolecules such as proteins or nucleic acids [15] are detected in the extracellular fraction.

The biocidal effects of the increasing dose of glutaraldehyde were shown on both types of microorganism cells 2.2**b**. *E. coli* and *S. cerevisiae* both displayed significant reduction of cell viabilities compared to their non-treated control samples. When 300 mg L^{-1} glutaraldehyde was applied, both microorganisms decreased to a range between 0.1% to 1% viable cells when compared to control cultures.

The autoclaving treatment was the most effective on both *E. coli* and *S. cerevisiae* (**Table** S.1). All autoclaving programs decreased the number of viable cells below the minimum detection limit of <100 CFU mL^{-1}, thus resulting in nearly zero survivor cells in the autoclaved cell suspension.

Cell lysis and aggregation after autoclaving and microwaving whereas loss of cell transparency is common after all sterilization methods

Phase-contrast microscopy images showed that untreated *E. coli* cells were intact and displayed long rod-shaped structures with smooth surface (**Figure** 2.3, **upper part**). Microwave treatment for 10 s did not affect the overall *E. coli* cell structure as most of the cells maintained their shape (**Figure** S.1). After 25 s, cells showed considerable cell debris as well as non-conventional shapes and cell aggregations. Cell transparency was also fully lost after 15 s, becoming dark non-conventional shaped cells compared to the non-treated cells. Short-term microwave treatment preserved cell structure (**Figure** S.1**e-f**) but displayed cell aggregations. The visible damage of *S. cerevisiae* cells emerged 25 s (Figure S.2**d-f**), where cell wall destruction resulted in the fusion of *S. cerevisiae* cells into a pool of broken cells. Loss of cell transparency was also observed.

E. coli cells displayed severe structural damages under autoclaving treatment as cells no longer preserved the transparent rod-shaped morphology presented in control samples (Figure 2.3, **middle column**). Cells were mostly ruptured into

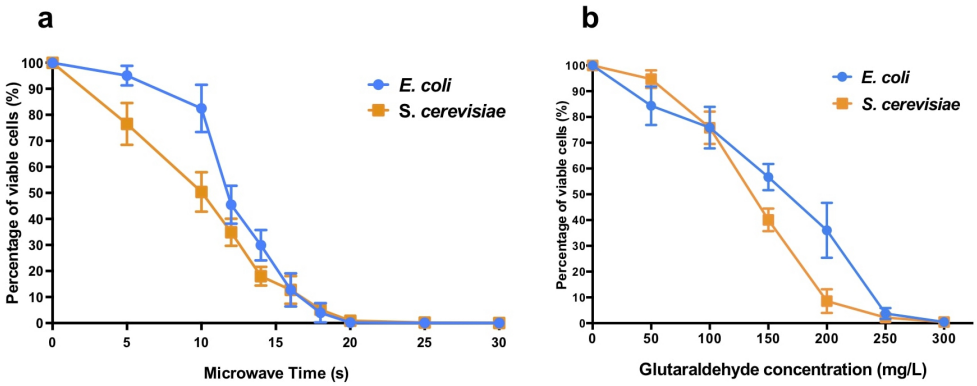

Figure 2.2: Cell viability of *E. coli* and *S. cerevisiae* after **(a)** different microwave exposure times and **(b)** glutaraldehyde concentrations. The percentage of viable cells is calculated against corresponding control sample cells (untreated with microwave and untreated with glutaraldehyde, respectively).

pieces of debris, twisted and shrunk, filled with denatured intracellular molecules (**Figure** S.3). For *S. cerevisiae*, under the first three types of autoclaving programs, cells completely maintained their spherical shape, and hardly any cell debris were observed (**Figure** S.4). Cell metamorphosis occurred under the highest intensity of autoclaving (**Figure** 2.3, **middle column**) where cells lost their clear surface layer and started to perform partial fusions.

The most obvious effect of glutaraldehyde fixation on the morphology of both *E. coli* and *S. cerevisiae* cells (**Figure** 2.3, **right column**) was the change of cell transparency. The intracellular area of *E. coli* cells turned black when fixed with glutaraldehyde and for *S. cerevisiae*, dark spots were present in their cytoplasm. No cell aggregation nor significant cell damage was observed. Cells from both microorganisms still preserved their structural frame even when the highest concentration of glutaraldehyde of 300 mg L^{-1} was applied (Figures S.5 and S.6).

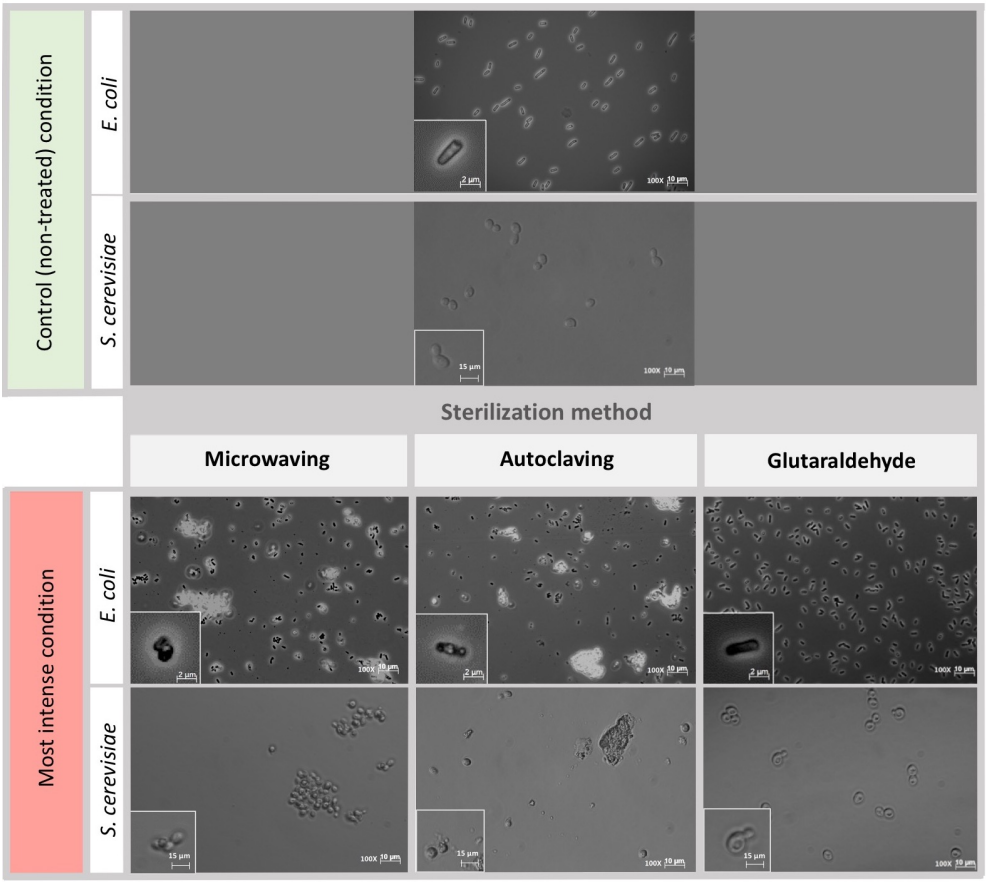

Figure 2.3: Cell morphology of *E. coli* and *S. cerevisiae* before and after being treated with the harshest sterilization method condition. Pictures were taken at 100x magnification. **Upper part**: Control (non-treated) condition: microscopic pictures after overnight. **Down part**: Left column: Microwaving effect. Most intense condition corresponds to 30 s microwaves exposure time. Middle column: Autoclaving effect. Most intense condition corresponds to P4 (121°C – 30 min). Right column: Glutaraldehyde effect. Most intense condition corresponds to 300 mg L^{-1} glutaraldehyde. The morphological structure of single cells at each time point are shown at bottom left of each picture. Same initial control culture was used prior any sterilization treatment.

Significant DNA release observed under microwave and autoclaving sterilizations

The microwave effect on the total DNA released by *E. coli* was observed after 12 s and increased abruptly after 16 s of exposure (**Figure** 2.4**a**). In *S. cerevisiae* cultures, the total DNA released increased constantly from the beginning of the treatment (**Figure** 2.4**a**). Even if *S. cerevisiae* cells released DNA constantly from the start, their cell wall protective ability was higher than the *E. coli* ones: yeasts displayed higher resistance in terms of cell structural collapse and DNA release

into the extracellular media. This links to the microscopic pictures presented in **Figure** 2.3, where after 20 s under the microwaves, the *S. cerevisiae* cells preserved their structure whereas the *E. coli* cells lysed and aggregated (Figures S.1 and S.2). Resistance differences also resulted in a lower percentage of total DNA released from *S. cerevisiae* at maximum exposure (30 s) of microwave sterilization. Nearly 35% of total DNA (73.9 ng μL^{-1}) was released from *S. cerevisiae* cells at 30 s, in contrast to almost 50% (59.1 ng μL^{-1}) from *E. coli* (**Figure** S.7**a-d**).

All types of autoclaving led to considerable amount of DNA released to the medium from both microorganisms (**Figure** 2.4**b**). Different autoclaving programs caused 65% (P1) to nearly 80% (P4) of total DNA leakage from *E. coli* cells while lower amounts of total DNA, 53% (P1) to 65% (P4), were observed on *S. cerevisiae* cultures (**Figure** S.8).

When an increasing amount of glutaraldehyde was applied from 0 to 300 mg L^{-1}, the percentage of total DNA released to extracellular medium (**Figure** 2.4**c**) stayed either steady at 0.6% for *S. cerevisiae* or fluctuating from 0.4 to 0.9% for *E. coli*. Almost all the DNA from both microorganisms remained intracellularly (**Figure** S.7**e-h)**. Glutaraldehyde displays a protective effect against cell lysis [31, 32] and strongly inhibits autolytic and proteolytic processes [33]. This explains why DNA was not released into the extracellular fraction. Glutaraldehyde does perform cross-linking reactions with compounds present in the cell outer layers, thus negatively altering the permeability and transportability of cell membranes [20, 22, 34]. Our observations show that this chemical exposure time (20 min) is enough to inactivate cells and prevent the transport and release of nucleic acids across membranes.

Long microwave exposures and all the autoclave programs showed severe DNA damage

The DNA fragments of the untreated *E. coli* control sample displayed on agarose gel have a size above 10 kb. When cells were treated with increasing duration of microwave, the intracellular DNA bands were less intense and displayed a slight decline gradient of DNA sizes, trailed by smears at different degrees (**Figure** S.9). For *S. cerevisiae* (**Figure** S.9**c-d**), the DNA extracted from untreated cells showed multiple bands of various lengths from approximately 400 bp to over 10 kb. After 25 s of microwaving, no clear bands but smears were displayed on the gels. An exposure of 30 s resulted in elimination of *S. cerevisiae* visible bands in the intracellular fraction (Figure S.9**c**). The fragmentation patterns in *E. coli* matched the measurements of DNA content (**Figure**2.4) for which a significant amount of DNA was released from 18 s onwards (**Figure** S.9**b**). An increasing gradient of the free-floating DNA intensity on the gel from *S. cerevisiae* fitted to the gradual DNA release (**Figure**2.4**a**).

In contrast to microwaving, extracellular and intracellular DNAs from both microorganisms were more highly fragmented and/or degraded when heat and pressure (1.1 atm overpressure) were applied (**Figure**2.4**b**), displaying smears on agarose gels (Figure S.10**a-d**). The highest autoclaving program (121 ^{o}C, 30 min)

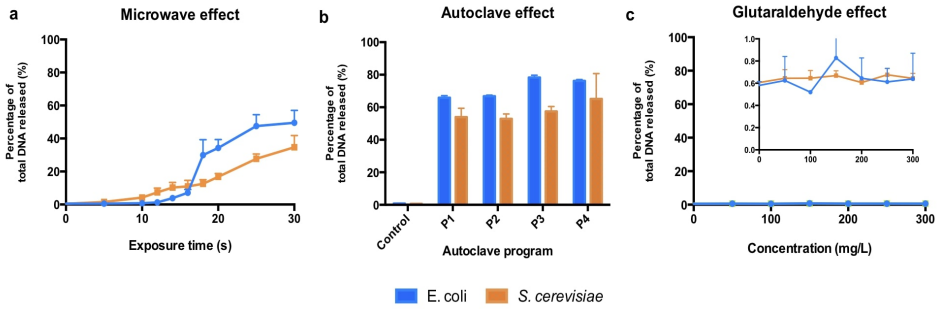

Figure 2.4: Total DNA released from *E. coli* and *S. cerevisiae* treated with **(a)** different microwave exposure times, **(b)** different autoclave programs and **(c)** different glutaraldehyde concentrations. The percentage shows the ratios of the amount of DNA (dsDNA) released in the supernatant against the total amount of DNA (released and remained combined). Autoclave programs: P1 (110°C – 20 min), P2 (110°C – 30 min), P3 (121°C – 20 min) and P4 (121°C – 30 min). Control (non-treated cells). 100% correspond to 59.1 ng μL^{-1} and 73.9 ng μL^{-1} for *E. coli* and *S. cerevisiae*, respectively.

showed the strongest DNA damage and release when compared with controls and other conditions (Figure S.10**a,c**, lanes 5). Even when the harshest autoclaving was applied, intense bands of DNA were still observed on the agarose gels. The degree of intracellular DNA degradation was lower than the released DNA after autoclaving treatment, presumably due to the protection of cells on its cytoplasmic DNA against external damage [1, 35, 36]. A possible reason why *E. coli* shows higher resistance to stress when compared to *S. cerevisiae*, apart from their higher surface to volume ratio, could be its polyunsaturated fatty acids (PUFAs) composition in their membrane: they contribute to cell membrane flexibility. PUFAs level in *S. cerevisiae* membranes are low or inexistent when growing under normal conditions [37, 38] whereas in *E. coli* cells are higher [39].

Intracellular DNA of *E. coli* treated with the highest concentration of glutaraldehyde resulted a smear with high fragment lengths (**Figure** S.11**a**, lane 7). Intracellular genomic DNA on *S. cerevisiae* did not result in the absence of DNA bands but a decrease of the band intensity (**Figure** S.11**c**, lane 7). The extracellular DNA from both types of microorganisms (**Figure** S.11**b,d**) showed similar patterns containing short DNA fragments from <100 bp to >200 bp, same as their corresponding untreated controls. The presence of residual extracellular DNA primarily results from the natural DNA release of microbial cells even before application of glutaraldehyde [40].

Autoclaving was the most effective in compromising PCR-ability

The amplification efficiency of selected genes was assessed after sterilization by qPCR. Differences of log_{10} number of DNA copies per mL between bead-milled control samples (autoclaving and microwaving) or non-bead-milled control samples (glutaraldehyde) and treated samples gave an insight on the DNA integrity after sterilization. For autoclaving and microwaving, log_{10} values close to the control indicated a high number of amplifiable DNA sequences available in the sample. This meant that DNA was not degraded enough and maintained its integrity. For glutaraldehyde, values close to the non-bead-milled samples indicated no DNA release nor an effect on PCR ability. Glutaraldehyde treatment did not release any significant amount of DNA in the supernatant (**Figure** 2.4**c**). For this reason, a non-bead-milled control was added. It was important to know if the amount of DNA released after glutaraldehyde treatment was similar to non-sterilized samples, where culture supernatant was basically assessed by qPCR without being sterilized. This gave an idea about the number of DNA copies available that could have been released by some passive release mechanisms or some basal cells decay during the overnight culture.

Bead-milling was the method of choice to release most of the intracellular DNA and is conventionally used for DNA extractions from microbial samples, but sometimes it is possible that the sterilization experiments showed higher release. It was expected with the mechanical disruption that DNA was released (but potentially not denatured). With the sterilizations here applied, DNA was expected to be released and potentially denatured and thus less PCR-able. Controls are not unique for all the cases: controls were included simultaneously to sterilized samples.

For qPCR analysis, the amplified DNA fragments should not exceed 200-250 bp. This is a relatively short DNA fragment size. It was hypothesized that qPCR measurements will highlight whether the DNA released after sterilization was strongly damaged. A high fragmentation of genomic DNA would result in DNA fragment sizes below 200-250 bp, allowing to see an effect in loss of PCR ability.

In *E. coli* cultures, no effect on PCR ability was observed when DNA was released from cells after microwaving. There were higher initial (5 s) log_{10} differences with the bead-milled control sample (0.77 $\pm$ 0.02) values due to lack of DNA available on the extracellular fraction (6.79 log_{10} gene copies mL^{-1}). DNA was exponentially released after 25 s (7.22 $\pm$ 0.07 log_{10} gene copies mL^{-1}, **Figure** 2.5), and significantly released after 70 s, 7.84 $\pm$ 0.01 log_{10} gene copies mL^{-1}). After 100 s exposure, DNA was released from cells (7.81 $\pm$ 0.08 log_{10} DNA copies) as its number of sequences even got higher than the control values (7.56 $\pm$ 0.01 log_{10} DNA copies) but its PCR ability was not compromised. Regarding autoclaving, a signal was observed even after P3 and P4 programs were applied (**Figure** 2.5**c**): 1.28 $\pm$ 0.11 and 1.16 $\pm$ 0.04 log_{10} gene copies per mL difference with the bead-milled control, respectively. Glutaraldehyde did not have a

significant effect on the PCR ability (**Figure** 2.5**e**) mainly because samples treated with glutaraldehyde did not release DNA (**Figure** 2.4**c**). In this case, the non-bead-milled control contained a relatively high number of gene copies in the supernatant, which anyway corresponded to similar values when different glutaraldehyde concentrations were applied. Overall, the qPCR background was relatively high for both the controls and the samples (**Figure** 2.5**e**). An analysis of variance (ANOVA) on these scores yielded significant variation among autoclaving and microwaving treatments but not glutaraldehyde treatments. When compared with the bead-milled control sample, F= 10245.62 and F=149.09, $p < 0.0001$ were observed for autoclaving and microwaving, respectively. A post-hoc Tukey test showed that all the autoclaving treatments (P1, P2, P3 and P4) and control belonging group differed significantly at $p < .05$ (table not shown) on the PCR-ability of release DNA from E. coli cultures. Regarding microwaving, the Tukey test showed significant ($p < .05$) differences from 60 to 100 s exposure times.

In *S. cerevisiae* cultures, DNA was released in a constant trend when microwaving meaning that lower amounts of DNA were available in the supernatant per time unit. This balance of DNA release seems to be proportional to degradation over time. This was reflected in **Figure** 2.5**b**, where constant values around 1.5 log_{10} differences are observed over time. A decrease of 4.78 ± 0.18 log_{10} DNA copies per mL at 60 s was observed but went up to 5.11 ± 0.2 log_{10} DNA copies per mL at 70 s. After the longest microwaving exposure time of 100 s, the number of amplicons increased (5.4 ± 0.02 log_{10}) indicating no significant effect on DNA integrity (i.e., can be amplified by qPCR). DNA release pattern and PCR ability from *S. cerevisiae* differ drastically from the exponential released observed in *E. coli* cultures (**Figure** 2.5**a**). After autoclaving, qPCR still detected some sequences (1.62 ± 0.15 log_{10} difference) even after the most intensive programs (P4: 121°C, 30 min, **Figure** 2.5**d**). However, P3 (121°C, 20 min) resulted in lower amplifiable DNA sequences (2.08 ± 0.03 log_{10} difference). As observed in *E. coli* cultures, glutaraldehyde did not have a significant effect on DNA PCR ability mainly because samples released non-detectable levels of DNA (**Figure** 2.5**e**). It was observed that DNA found in supernatant after glutaraldehyde treatment was at a similar level to the negative control confirming that DNA was not released and thus, not amplified. An ANOVA on these scores yielded significant variation among autoclaving treatment but not after microwave and glutaraldehyde treatments. When compared with the bead-milled control sample, F=137.77, $p < 0.0001$ were observed for autoclaving. Tukey test showed that all the autoclaving treatments (P1, P2, P3 and P4) and control belonging group differed significantly at $p < .05$ (table not shown) on the PCR-ability of release DNA from *S. cerevisiae* cultures. Regarding microwaving and glutaraldehyde, no significant ($p > .05$) mean differences were observed supporting the low effect of these methods on PCR ability. High temperature in combination with high pressure massively degrades DNA even in a short period of time of 5 min [18].

Some studies have shown that dry autoclaving at 100°C for 10 min has been already

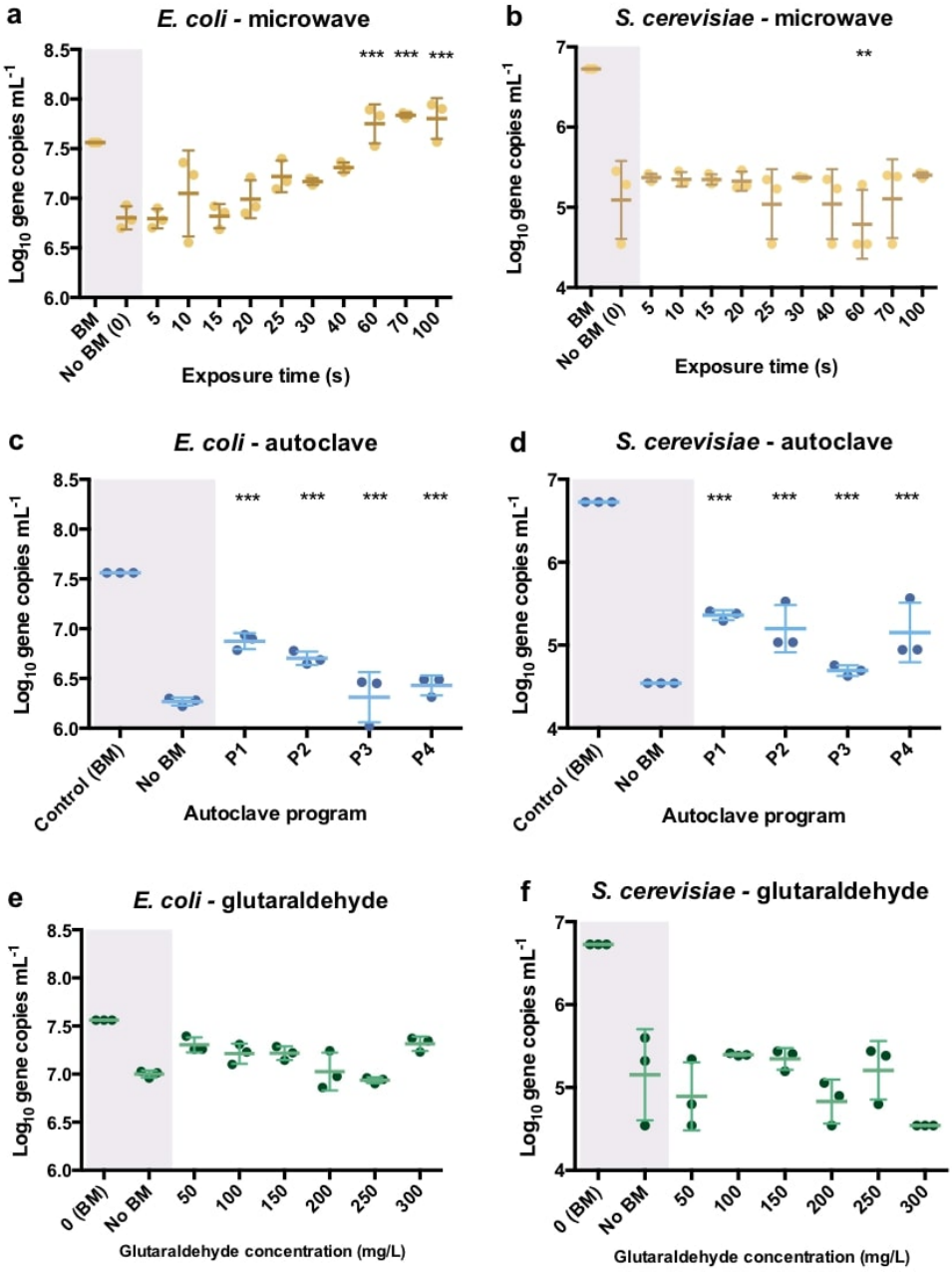

Figure 2.5: qPCR results after the different sterilization methods. Number of DNA copies obtained on supernatant of pure *E. coli* and *S. cerevisiae* cultures after microwave **(a,b)**, autoclave **(c,d)** and glutaraldehyde **(e,f)** treatments. The results are expressed in log_{10} copies per mL. Autoclave programs: P1 (110°C – 20 min), P2 (110°C – 30 min), P3 (121°C – 20 min) and P4 (121°C – 30 min). BM: Bead-Mill treatment. ANOVA followed by post hoc Tukey test, $^{**}p < 0.05$, $^{***}p < 0.005$.

sufficient to result in not amplifiable DNA from soybean [6]. However, genomic DNA amplification has been observed at different autoclaving times (from 10 to 40 min) out of cultures of *Pseudomonas aeruginosa*, *Salmonella Nottingham*, and *Escherichia coli*. Collectively, this suggests a potential risk made by residual genomic DNA after inactivation of microbial cells due to potential horizontal gene transfer phenomena [41]. Little is known on the amplification capacity of free DNA after autoclaving treatment of industrial model organisms, being a source of xenogenic contamination out of industries and laboratories.

DNA fragmentation was experienced with both autoclaving and microwaving. Although fragmented, the DNA pieces could still be amplified to some extent by qPCR. The sterilization exposure time was sufficient to break the cells, to release and fragment the DNA, while not sufficiently long to lead to a DNA residue degraded enough to affect its PCR ability. For autoclaving and microwaving we can postulate the following mechanistic steps in the sterilization process: (i) cells breakage, (ii) DNA release, (iii) DNA fragmentation, (iv) DNA degradation.

Quality test experiments using autoclave and microwave treatments showed faster pure DNA degradation patterns when compared to pure cultures

The different sterilization treatments were tested out in vitro on pure phage λ DNA and analyzed by gel electrophoresis to assess afterwards their effect on free extracellular DNA.

All the autoclaving programs applied on pure λ DNA reflected neither visible bands nor smears on gel electrophoreses, meaning that complete degradations of naked λ DNA occurred (**Figure** 2.6**b**). DNA was not visible for SYBR-Gold staining. In contrast with the DNA treated by autoclaving in vivo (**Figure** S.10), where intracellular DNA migrated slower and displayed higher fragment length than released DNA. The disappearing of λ DNA treated with high temperature and pressure manifested the protection of DNA by cells against damage. Slight increased pressure and temperatures decay the primary structure of double-strand DNA by hydrolyzing its chemical bonds [42]. This significantly affects the DNA stability and causes DNA fragmentation. This is remarkable with free DNA and was confirmed by the autoclaving of pure free λ DNA, where gels did exhibit severe DNA fragmentation (**Figure** 2.6**b**).

An exposure of 30 s to microwaves was not sufficient to cause degradation and fragmentation to free pure λ DNA: the band obtained after treatment (**Figure** 2.6**a**, lane 7) remained identical to the untreated template (**Figure** 2.6**a**, lane 1). At 40 s, the DNA band lost its intensity, resulting in a smear with lower fragment lengths. After 60 s, the band disappeared and completely turned into a smear. In comparison with the results in microbial cultures (**Figure** S.9), the phage λ DNA treated with the same duration of microwaving resulted in slower migrations across the gel than the DNA released from *E. coli* and *S. cerevisiae* cultures. Non-thermal

factors are all of the effects that are not caused by an increase of temperature, especially when low frequencies and intensities are applied [43]. Belayev et al. [44] have shown that radiation-induced DNA breaks could not be repaired after non-thermal microwave exposure. This effect inhibits DNA repair being a plausible cause for cells inactivation. When moving from the cellular to the DNA level, microwaves can destroy DNA by denaturation, degradation, and fragmentation [11, 45].

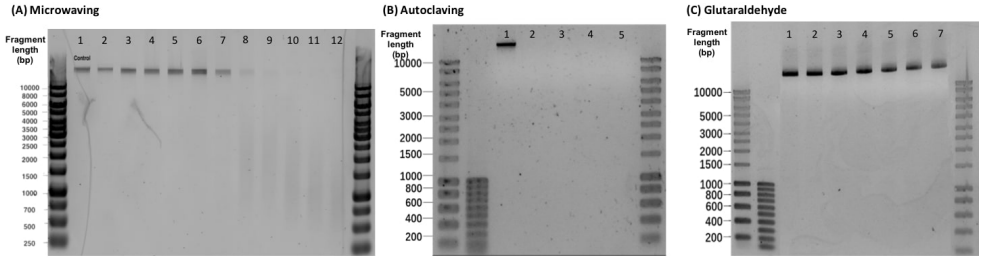

Figure 2.6: Effect of different sterilization methods on λ DNA fragmentation. **(a)** Microwaving. Lanes 1–12 correspond to 0, 5, 10, 15, 20, 25, 30, 40, 50, 60, 70, 100 s microwave exposure time, respectively. **(b)** Autoclaving. Lanes 1–5 correspond to control, P1, P2, P3, and P4, respectively. Autoclave programs: P1 (110°C – 20 min), P2 (110°C – 30 min), P3 (121°C – 20 min) and P4 (121°C – 30 min). **(c)** Glutaraldehyde. Lanes 1–7 correspond to 0,50, 100, 150, 200, 250 and 300 mg L^{-1} glutaraldehyde, respectively.

No DNA degradation nor fragmentation could be observed when increasing glutaraldehyde concentrations (**Figure** 2.6**c**).

Pure λ DNA amplification efficiency decreased under long microwave exposures and all autoclaving programs

The qPCR of the pure bacteriophage λ int gene was used to evaluate the extracellular DNA capacity to be amplified right after the different sterilization methods.

All the autoclave treatments were shown to significantly affect the PCR ability of the λ DNA (**Figure** 2.7**b**) notably when applying program P4 (121 ºC, 30 min) when compared with the non-treated λ DNA control. Differences of 2.56 ± 0.61, 3.04 ± 1.22, 4.75 ± 0.24, 4.96 ± 0.28 logs were observed for P1, P2, P3 and P4 versus the control, respectively. An ANOVA on these scores yielded significant variation among autoclaving treatments when compared with the control, $F = 11.41$, $p < 0.001$. A Tukey test showed that all the autoclaving treatments (P1, P2, P3 and P4) and control belonging group differed significantly at $p < .05$ (table not shown) on the PCR-ability of λ DNA.

It took around 30 to 50 s to detect high concentrations of DNA in the extracellular fraction and around more than 100 s to start seeing a decay in PCR ability. From the combination of experiments with microbial cultures and free-floating λ DNA, exposure time longer than 100 s would be necessary to inactivate cells, release DNA, and fragment it. Otherwise, no effect will be observed on DNA integrity.

Similar results were observed when samples were exposed for over 40 s, 0.5 ± 0.09 logs difference, under microwaves (**Figure** 2.7**a**). Significant variation among microwaving treatments when compared with the control, F= 26.04, p < .0001 was observed. Moreover, a Tukey test showed that exposure times over 60 s, 1.31 ± 0.17 logs difference, differed significantly at p < 0.05 (table not shown). This is supporting the clear band loss after 60 s during gel electrophoresis (**Figure** 2.6**a**). At 100 s, a difference of 3.23 ± 0.06 logs with the untreated control sample was observed.

Under microwave treatment, DNA damage on pure λ DNA was more severe than in DNA released from microbial cells. Although the DNA of E. coli (approximately 4 Mb) and S. cerevisiae (approximately 12.1 Mb) harbors significant differences in the size of their genomes, which are also both larger than the size of λ DNA (48 kb) [46, 47], the main reason mainly resided in the contact time with the sterilization treatments.

The sterilization processes by microwaving and autoclaving conducted on cells were described to involve 4 different steps from cell breakage to DNA release, DNA fragmentation, and DNA degradation. In most of experiments performed on cell cultures, the contact time was not long enough to enable degradation of DNA beyond its release. In the case of the free DNA control, λ DNA was directly exposed from start to the sterilization treatments. λ DNA was therefore longer in contact with the sterilization conditions than the DNA released from cell. This longer exposition led to degradation of λ DNA to some extent.

In addition, when cells are treated with microwaves, temperature in highly concentrated cell suspensions increased faster than in low cell concentration suspensions [30]. Hence, the DNA released from suspensions of *E. coli* and *S. cerevisiae* could end up with a higher temperature compared to the pure λ DNA solution when treated with the same duration of microwave, accelerating DNA degradation. However, even if DNA in suspension could end up with higher temperatures, first it should be released before being nakedly exposed to the

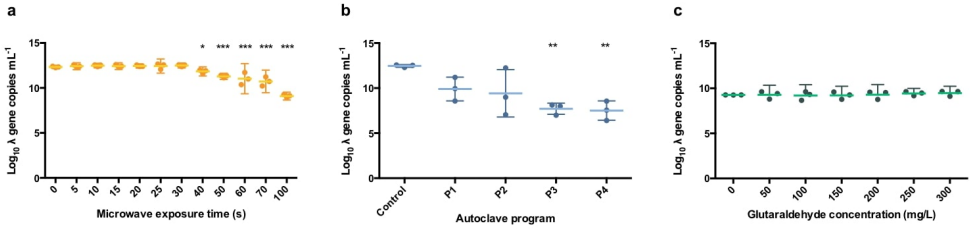

Figure 2.7: Number of int copies from λ DNA available after microwaving **(a)**, autoclaving **(b)** and treating with glutaraldehyde **(c)**. The results are expressed in log_{10} copies per mL. The middle line represents the mean, and the whiskers represent the 95% CI. Autoclave programs: P1 (110°C – 20 min), P2 (110°C – 30 min), P3 (121°C – 20 min) and P4 (121°C – 30 min). Control: non-sterilized samples corresponding to 1 g L^{-1} λ DNA.

environmental conditions of the system.

In our study, a first question targeted whether DNA was released: this was confirmed by Qubit results (**Figure** 2.4**a**) and gel electrophoresis (**Figure** S.9). A second question targeted whether the integrity of DNA was impacted during the treatments, which was checked by qPCR. The summary of the microwave effect on microbial cultures (**Figure** 2.4**a**; **Figure** 2.5**a-b**) and on naked pure DNA (**Figure** 2.6**a**; Figure 2.7**a**) does provide important information for bench-top practice if microwave is the desired method to sterilize your microbial culture. Our results suggest that an exposure time of more than 100 s is needed under our experimental conditions to efficiently inactivate microorganisms and degrade the potentially harmful DNA they may contain. The initial 40-50 s are needed to inactivate/break cells and release the DNA out of the cells, plus another extra time to observe a degradation of the DNA and decay of its PCR ability (i.e., its potential to be biologically re-used and genomically integrated by microorganisms).

In contrast, the glutaraldehyde treatments did not affect the amplification capacity of pure λ DNA (**Figure** 2.7**c**). An ANOVA on these scores did not yield significant variation among the different concentrations of glutaraldehyde when compared with the control ($F= 0.70$, $p > 0.658$), supporting the results obtained from the DNA fragmentation experiments (**Figure** 2.6**b**). No significant effect on amplification ability was observed when a standard incubation time of 20 min was applied. Glutaraldehyde damages DNA [48] and compromises the PCR ability of DNA after some days of incubation only [49]. In clinical procedures, an exposure of 20 min at 20°C in a 2% w/w glutaraldehyde solution is solely used to disinfect medical instruments [50]. We showed that this short incubation time of 20 min was not enough to impact the integrity and PCR ability of DNA. Overall, glutaraldehyde offers an efficient way to disinfect and contain DNA and xenogenic elements inside cells.

2.4. Conclusions

Overall, all common sterilization methods here tested are effective to inactivate microorganisms, highlighting short incubation time of 20 min with glutaraldehyde for its capacity to avoid DNA release. In terms of DNA loss of integrity, autoclave is shown to be the most effective method. However, integrity of released DNA is not completely compromised as shown by qPCR results. This opens a window for improvement in case total extracellular DNA degradation was desired. Alternatives to standard procedures are combination of methods here tested or further steps towards total removal such as ethylene oxide that has been shown to reduce DNA amplification when long exposure times are applied [51]. Fragmented sequences as short as 20 bp haven been shown to be taken up and incorporated into the bacterial DNA, including mammoth DNA [52]. Even if the majority of short residual DNA fragments will be re-metabolized in case they are taken up, there is a probability to be genome integrated generating new diversity [53].

Horizontal gene transfer phenomena from sterilized cultures may exchange all kind of DNA fragments as soon as these enter microbiome hotspots such as wastewater treatment plants [3]. New microbial diversity can be generated through gene transfer, but also undesirable fragments such as ARGs and pathogenic islands could be unfavorably mobilized by microorganisms [54, 55]. This underlies the ubiquity and potentiality of these DNA fragments generated after sterilizations. Further research on the quality and composition of released DNA as well as rates of horizontal gene transfer are necessary to develop risk assessments strategies and to address the impact of the standard sterilization methods on biosafety and environmental and public health.

2.5. Supplementary material

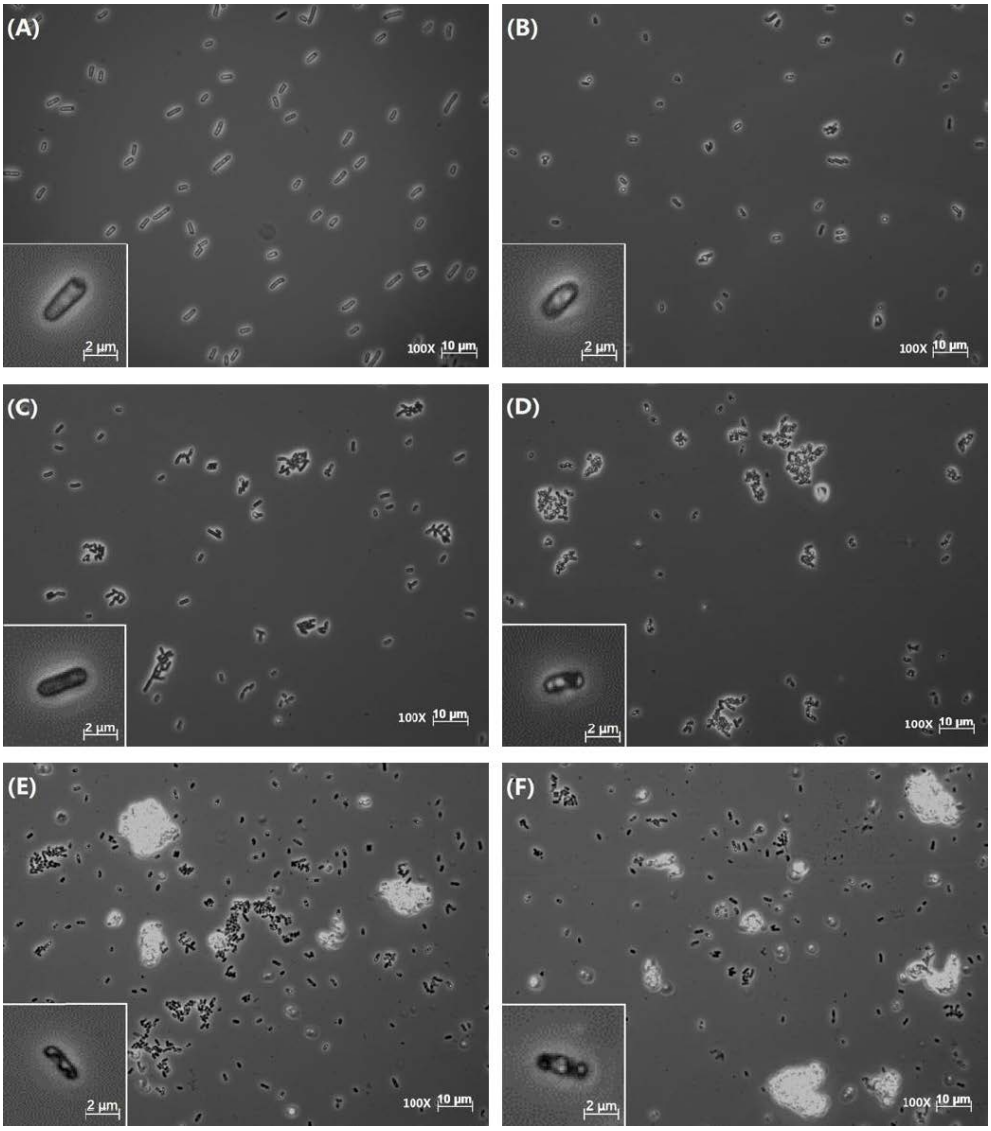

Figure S.1: Microscopic pictures of *E. coli* cells treated with microwave (2450 MHz, 230V, 66 850W) sterilization method at 10 s **(b)**, 15 s **(c)**, 20 s **(d)**, 25 s **(e)**, and 30 s **(f)** in comparison 67 with 0 s untreated control cells **(a)**. The morphological structure of single cells at each time 68 point are shown at bottom left.

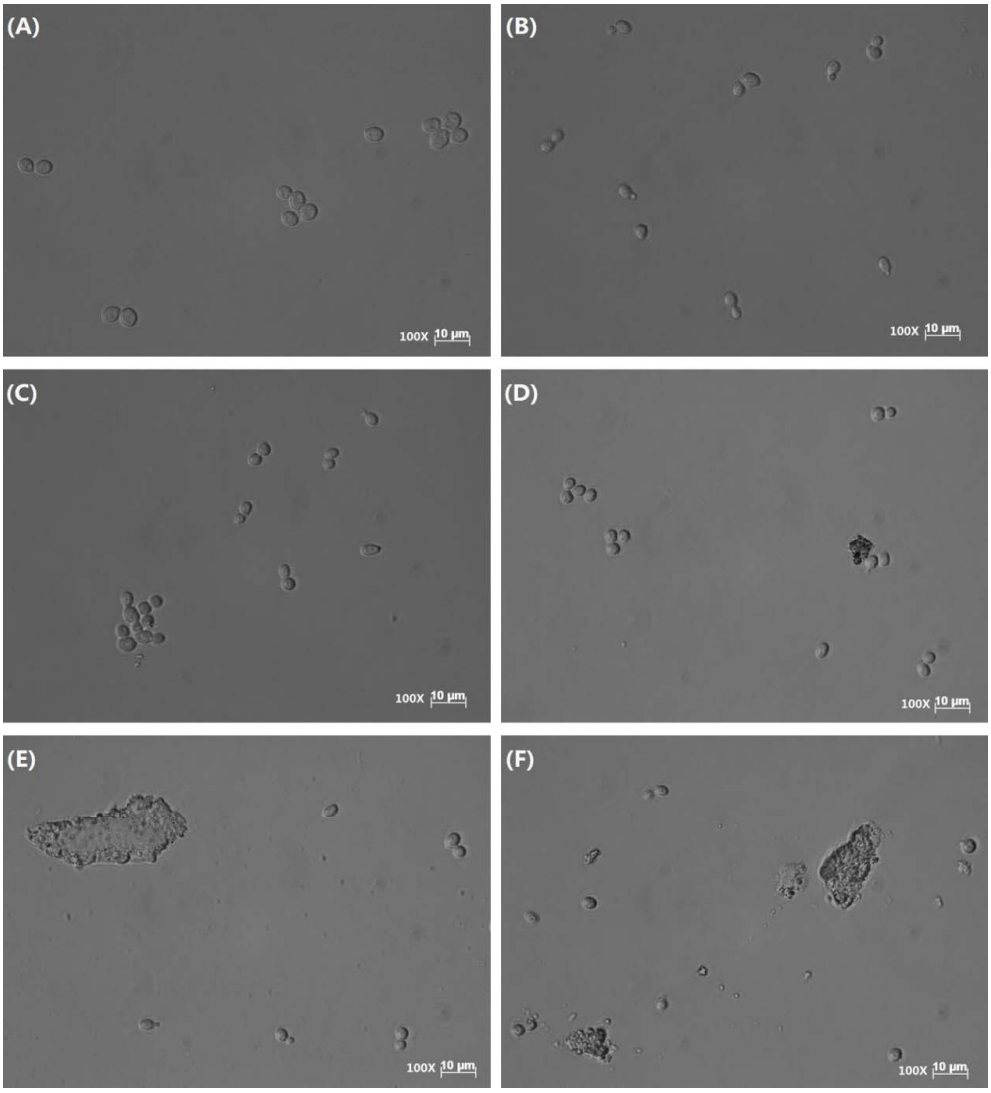

Figure S.2: Microscopic pictures of *S. cerevisiae* cells treated with microwave (2450 MHz, 230V, 66 850W) sterilization method at 10 s **(b)**, 15 s **(c)**, 20 s **(d)**, 25 s **(e)**, and 30 s **(f)** in comparison 67 with 0 s untreated control cells **(a)**.

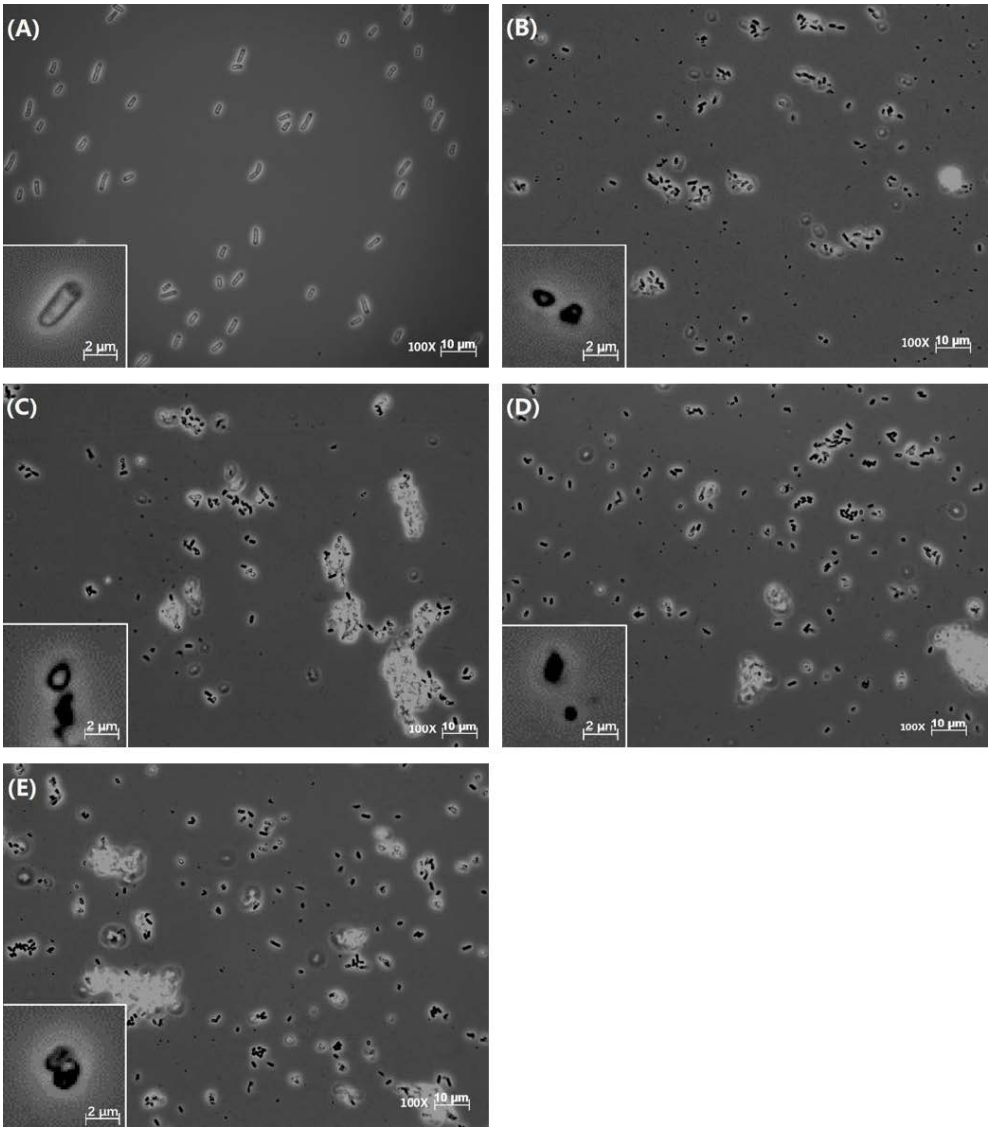

Figure S.3: Microscopic image of *E. coli* cells through different type of autoclaving program. Cells after autoclaving program of 110 °C, 20 min **(b)**, 110 °C, 30 min **(c)**, 121 °C, 20 min **(d)**, 121°C, 30 min **(e)** are in comparison wit untreated control cells **(a)**. The morphological structure of single cells under each types of autoclaving program are shown at bottom left.

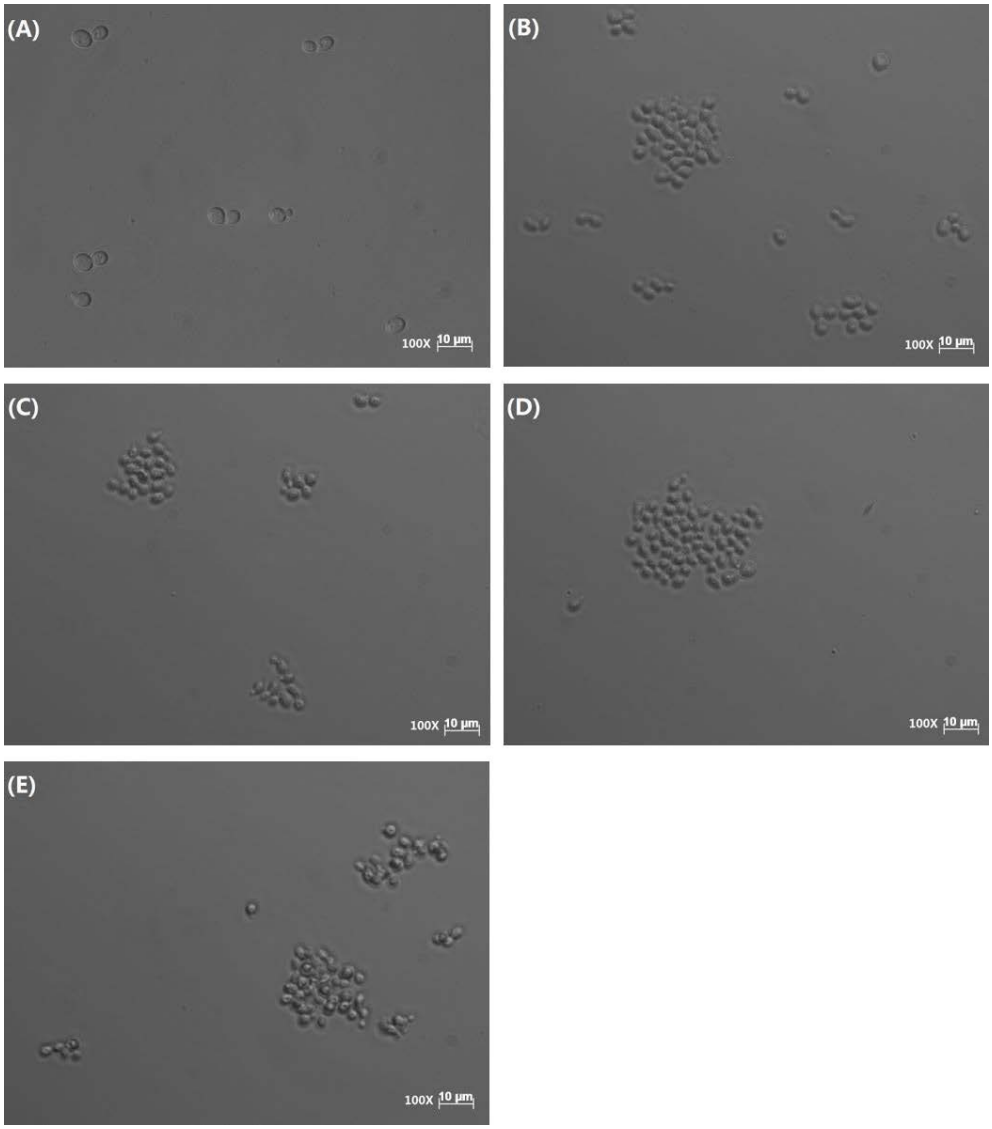

Figure S.4: Microscopic image of *S. cerevisiae* cells through different type of autoclaving program. Cells after autoclaving program of 110 °C, 20 min **(b)**, 110 °C, 30 min **(c)**, 121 °C, 20 min **(d)**, 121°C, 30 min **(e)** are in comparison wit untreated control cells **(a)**. The morphological structure of single cells under each types of autoclaving program are shown at bottom left.

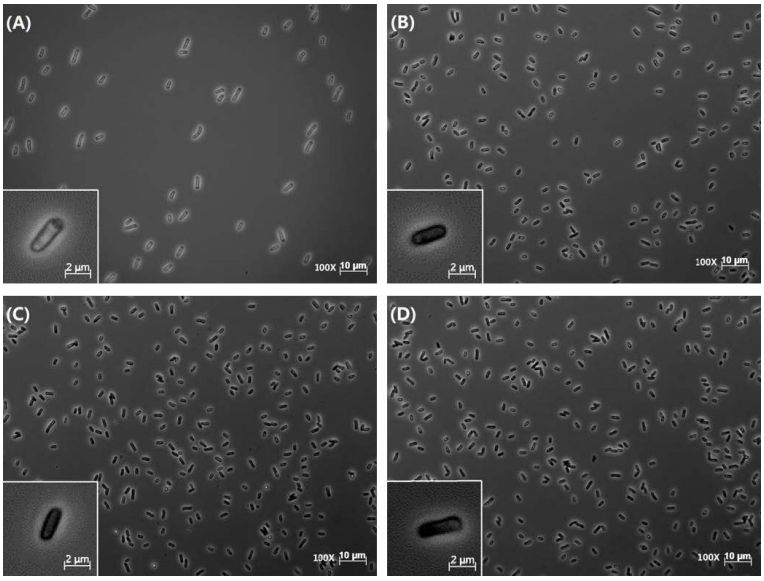

Figure S.5: Microscopic pictures of *E. coli* cells treated with various concentrations of glutaraldehyde after 20 min incubation time. Cells affected by 100 mg L^{-1} **(b)**, 200 mg L^{-1} **(c)**, and 300 mg L^{-1} **(d)** of glutaraldehyde are in comparison with untreated control cells **(a)**. The morphological structure of single cells treated with each dose of glutaraldehyde are shown at bottom left.

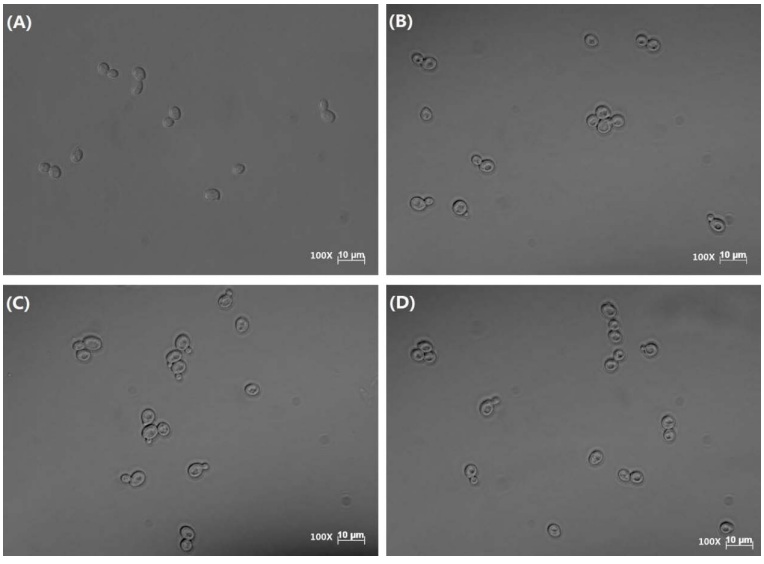

Figure S.6: Microscopic pictures of *S.cerevisiae* cells treated with various concentrations of glutaraldehyde after 20 min incubation time. Cells affected by 100 mg L^{-1} **(b)**, 200 mg L^{-1} **(c)**, and 300 mg L^{-1} **(d)** of glutaraldehyde are in comparison with untreated control cells **(a)**.

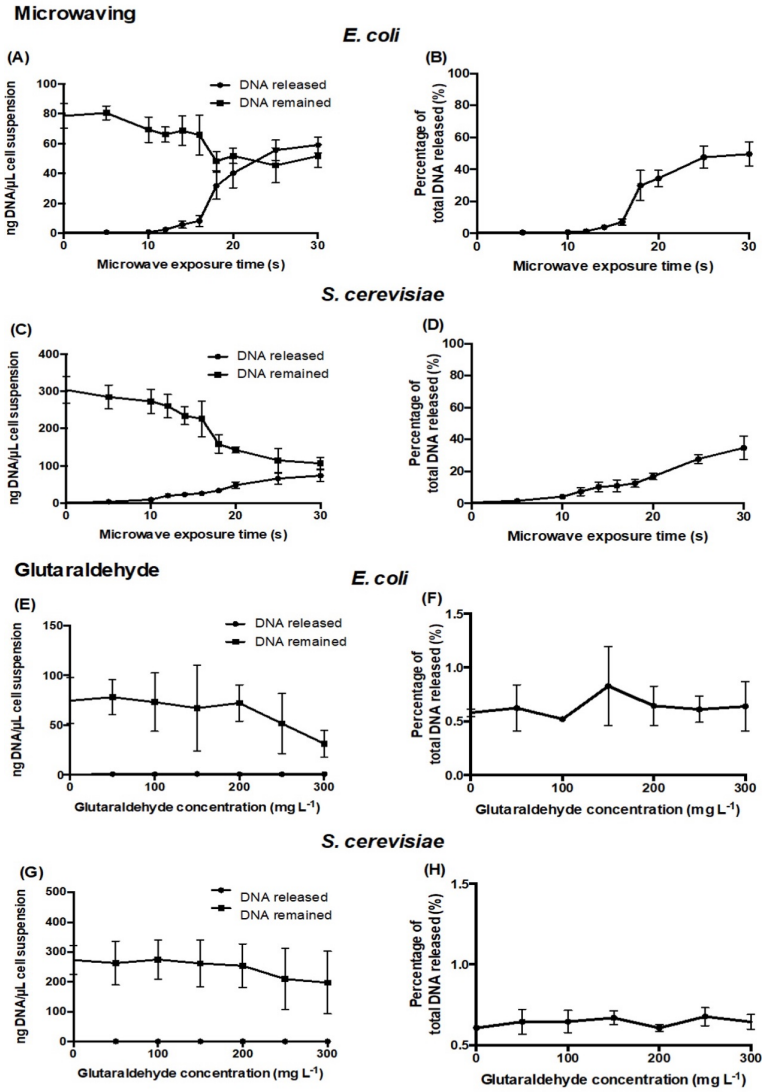

Figure S.7: DNA quantification measurement on the amount of DNA released and remained of *E. coli* **(a)** and *S. cerevisiae* **(c)** treated with different microwave exposure times. DNA released and remained of *E. coli* **(e)** and *S. cerevisiae* **(g)** treated with different glutaraldehyde concentrations. Total DNA released from *E. coli* **(b)** and *S. cerevisiae* **(d)** treated with different microwave exposure times. Total DNA released from *E. coli* **(f)** and *S. cerevisiae* **(h)** treated with different glutaraldehyde concentrations. The percentage shows the ratios of the amount of DNA released in the supernatant against the total amount of DNA (released and remained combined).

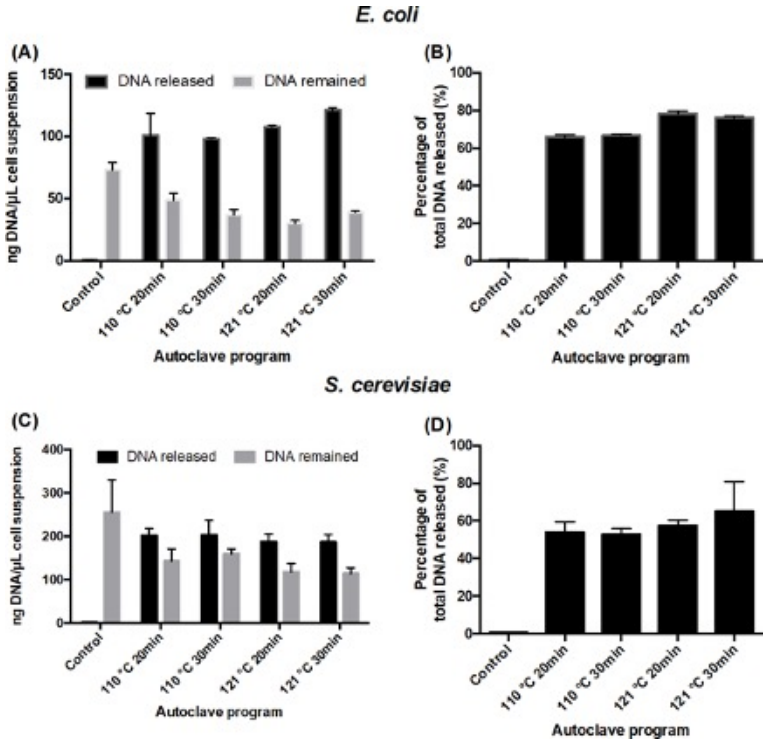

Figure S.8: DNA quantification measurement on the amount of DNA released and remained of *E. coli* **(a)** and *S. cerevisiae* **(c)** treated with four different autoclaving programs. Total DNA released from *E. coli* **(b)** and *S. cerevisiae* **(d)** treated with four different autoclaving programs. The percentage shows the ratios of the amount of DNA released in the supernatant against the total amount of DNA.

Table S.1: *E. coli* and *S. cerevisiae* cell viability after different autoclaving programs. The percentage of viable cells is calculated against corresponding control sample cells (non-autoclaved cells).

	E. coli		*S. cerevisiae*	
Autoclaving program	Cell number Log (CFU)/mL	Viability (%)	Cell number Log (CFU)/mL	Viability (%)
110 °C, 20 min	*NA	*NA	*NA	*NA
110 °C, 30 min	*NA	*NA	*NA	*NA
121 °C, 20 min	*NA	*NA	*NA	*NA
121 °C, 30 min	*NA	*NA	*NA	*NA
121 °C, 30 min	*NA	*NA	*NA	*NA

* NA (not applicable): Cell concentration reduced under the accurate detection limit of 100 CFU $mL{-}1$.

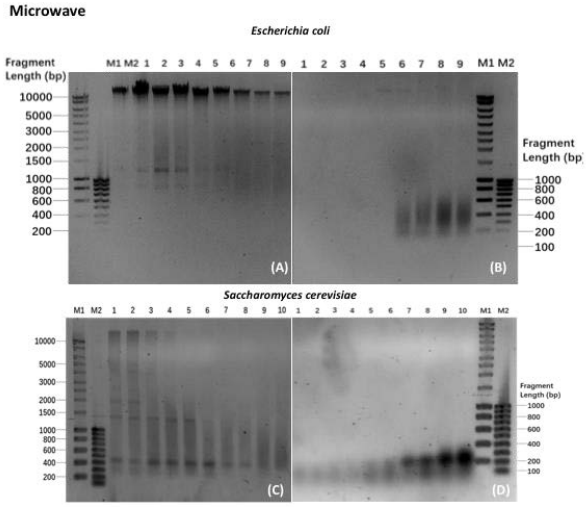

Figure S.9: Electrophoretic gel of *E. coli* intracellular **(a)** and released DNA **(b)** together with *S. cerevisiae* intracellular **(c)** and released DNA **(d)** with increasing microwave exposure times. Lanes 1-10: *S. cerevisiae* intracellular DNA collected at 0, 10, 12, 14, 16, 18, 20, 25, 30, 40 s. Lanes 1-9 *E. coli* intracellular DNA collected at 0, 10, 12, 14, 16, 18, 20, 25, 30, 40 s.

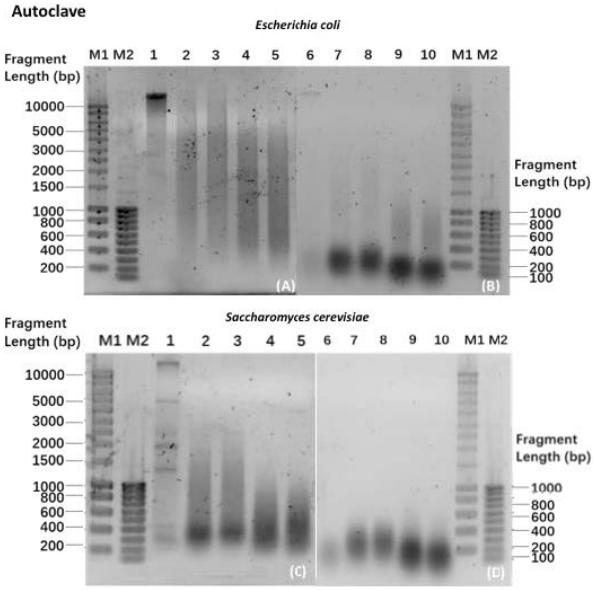

Figure S.10: Electrophoretic gel of *E. coli* intracellular **(a)** and released DNA **(b)** together with *S. cerevisiae* intracellular **(c)** and released DNA **(d)** with different types of autoclaving. Lane 1: control sample intracellular DNA. Lane 2-5: intracellular DNA treated with P1, P2, P3 and P4. Lane 6: control sample released DNA. Lane 7-10: released DNA treated with P1, P2, P3 and P4 autoclaving programs. Autoclave programs: P1 (110 ºC – 20 min), P2 (110 ºC – 30 min), P3 (121 ºC – 20 min) and P4 (121 ºC – 30 min).

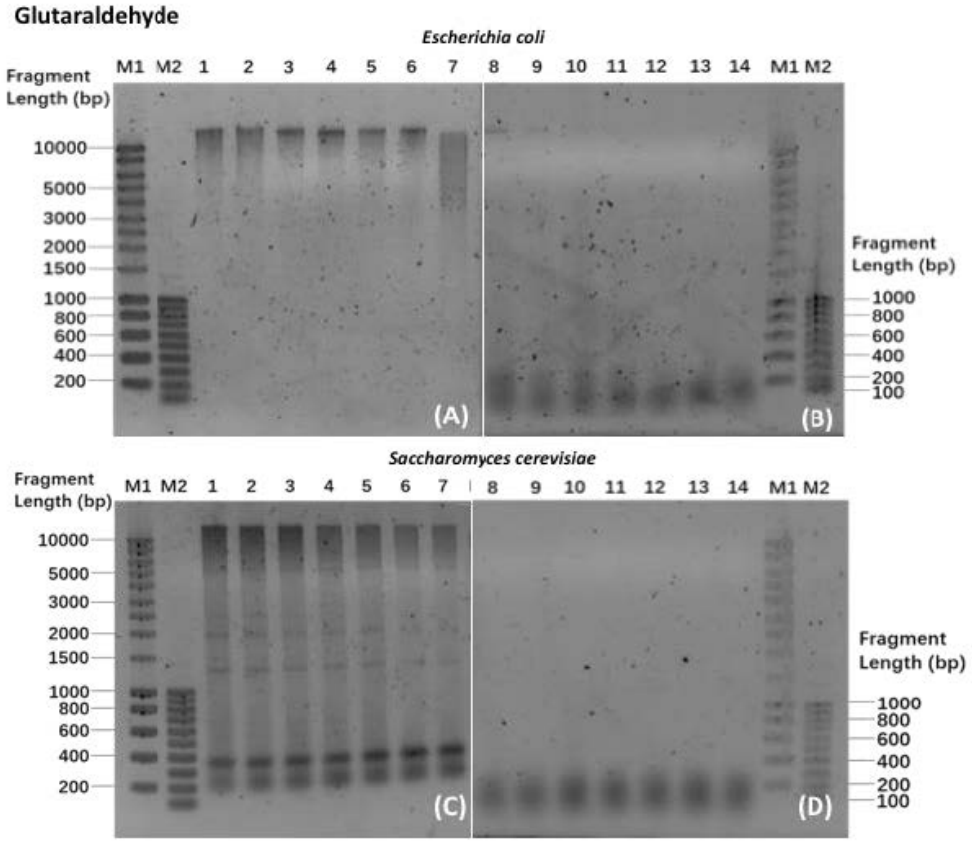

Figure S.11: Electrophoretic gel of *E. coli* intracellular **(a)** and released DNA **(b)** together with *S. cerevisiae* intracellular **(c)** and released DNA **(d)** with increasing concentration of glutaraldehyde. Lanes 1-7: intracellular DNA collected at 0, 5, 100, 150, 150, 200, 300 mg L^{-1} glutaraldehyde. Lanes 8-14: released DNA collected at 0, 50, 100, 150, 200, 300 mg L^{-1} glutaraldehyde.

Bibliography

[1] K. E. Simmon, D. D. Steadman, S. Durkin, A. Baldwin, W. H. Jeffrey, P. Sheridan, R. Horton, and M. S. Shields. "Autoclave method for rapid preparation of bacterial PCR-template DNA". In: *Journal of Microbiological Methods* 56.2 (2004), pp. 143–149. ISSN: 01677012. DOI: 10.1016/j.mimet.2003.10.003.

[2] C. Bouki, D. Venieri, and E. Diamadopoulos. "Detection and fate of antibiotic resistant bacteria in wastewater treatment plants: A review". In: *Ecotoxicology and Environmental Safety* 91 (2013), pp. 1–9. ISSN: 01476513. DOI: 10.1016/j.ecoenv.2013.01.016.

[3] J. H. Miller, J. T. Novak, W. R. Knocke, and A. Pruden. "Survival of antibiotic resistant bacteria and horizontal gene transfer control antibiotic resistance gene content in anaerobic digesters". In: *Frontiers in Microbiology* 7.MAR (2016), pp. 1–11. ISSN: 1664302X. DOI: 10.3389/fmicb.2016.00263.

[4] F. Debode, E. Janssen, and G. Berben. "Physical degradation of genomic DNA of soybean flours does not impair relative quantification of its transgenic content". In: *European Food Research and Technology* 226.1-2 (2007), pp. 273–280. ISSN: 14382377. DOI: 10.1007/s00217-006-0536-1.

[5] N. Gryson. "Effect of food processing on plant DNA degradation and PCR-based GMO analysis: A review". In: *Analytical and Bioanalytical Chemistry* 396.6 (2010), pp. 2003–2022. ISSN: 16182642. DOI: 10.1007/s00216-009-3343-2.

[6] E. Bergerová, Z. Godálová, and P. Siekel. "Combined effects of temperature, pressure and low pH on the amplification of DNA of plant derived foods". In: *Czech Journal of Food Sciences* 29.4 (2011), pp. 337–345. ISSN: 12121800.

[7] J. P. Maity, S. Chakraborty, S. Kar, S. Panja, J. S. Jean, A. C. Samal, A. Chakraborty, and S. C. Santra. "Effects of gamma irradiation on edible seed protein, amino acids and genomic DNA during sterilization". In: *Food Chemistry* 114.4 (2009), pp. 1237–1244. ISSN: 03088146. DOI: 10.1016/j.foodchem.2008.11.001.

[8] M. López-Andreo, M. Aldeguer, I. Guillén, J. A. Gabaldón, and A. Puyet. "Detection and quantification of meat species by qPCR in heat-processed food containing highly fragmented DNA". In: *Food Chemistry* 134.1 (2012), pp. 518–523. ISSN: 03088146. DOI: 10.1016/j.foodchem.2012.02.111.

[9] O. Takeshi, A. Fumihiro, A. Hiroshi, G. Yukihiro, and O. Yoshihiro. "Fragmentation of DNAs of processed foods made from genetically modified soybeans". In: *Japanese Journal of Food Chemistry* 10.3 (2003), pp. 155–160.

[10] S. Y. Kim, E. K. Jo, H. J. Kim, K. Bai, and J. K. Park. "The effects of high-power microwaves on the ultrastructure of Bacillus subtilis". In: *Letters in Applied Microbiology* 47.1 (2008), pp. 35–40. ISSN: 02668254. DOI: 10.1111/j.1472-765X.2008.02384.x.

[11] Y. Fang, J. Hu, S. Xiong, and S. Zhao. "Effect of low-dose microwave radiation on Aspergillus parasiticus". In: *Food Control* 22.7 (2011), pp. 1078–1084. ISSN: 09567135. DOI: 10.1016/j.foodcont.2011.01.004.

[12] M. Sharma, J. Eastridge, and C. Mudd. "Effective household disinfection methods of kitchen sponges". In: *Food Control* 20.3 (2009), pp. 310–313. ISSN: 09567135. DOI: 10.1016/j.foodcont.2008.05.020.

[13] R. S. Ferriss. *Effects of Microwave Oven Treatment on Microorganisms in Soil*. 1984.

[14] J. T. Trevors. "ofMicrobiological Methods Sterilization and inhibition of microbial activity in soil". In: *Journal of Microbiological Methods* 26 (1996), pp. 53–59.

[15] I. S. Woo, I. K. Rhee, and H. D. Park. "Differential damage in bacterial cells by microwave radiation on the basis of cell wall structure". In: *Applied and Environmental Microbiology* 66.5 (2000), pp. 2243–2247. ISSN: 00992240. DOI: 10.1128/AEM.66.5.2243-2247.2000.

[16] F. Akşen, A. Kaya, and N. Akpolat. "Comparision of bactericidal activity of microwave, ultraviolet and disinfectant solutions on some bacterial strains". In: *Biotechnology and Biotechnological Equipment* 18.2 (2004), pp. 122–127. ISSN: 13102818. DOI: 10.1080/13102818.2004.10817098.

[17] S. Jankovic, M. Milosev, and M. Novakovic. "The effects of microwave radiation on microbial cultures". In: *Hospital Pharmacology - International Multidisciplinary Journal* 1.2 (2014), pp. 102–108. ISSN: 2334-9492. DOI: 10.5937/hpimj1402102j.

[18] M. Karni, D. Zidon, P. Polak, Z. Zalevsky, and O. Shefi. "Thermal Degradation of DNA". In: *DNA and Cell Biology* 32.6 (2013), pp. 298–301. ISSN: 1044-5498. DOI: 10.1089/dna.2013.2056.

[19] B. Ballantyne and S. L. Jordan. "Toxicological, medical and industrial hygiene aspects of glutaraldehyde with particular reference to its biocidal use in cold sterilization procedures". In: *Journal of Applied Toxicology* 21.2 (2001), pp. 131–151. ISSN: 0260437X. DOI: 10.1002/jat.741.

[20] S. K. Sehmi, E. Allan, A. J. MacRobert, and I. Parkin. "The bactericidal activity of glutaraldehyde-impregnated polyurethane". In: *MicrobiologyOpen* 5.5 (2016), pp. 891–897. ISSN: 20458827. DOI: 10.1002/mbo3.378.

[21] K. Okuda, I. Urabe, Y. Yamada, and H. Okada. "Reaction of Glutaraldehyde with Amino and Thiol Compounds". In: 2 (1991), pp. 100–105.

[22] T. J. Munton and A. D. Russell. "Effect of glutaraldehyde on cell viability, triphenyltetrazolium reduction, oxygen uptake, and β-galactosidase activity in Escherichia coli". In: *Applied microbiology* 26.4 (1973), pp. 508–511. ISSN: 0003-6919.

[23] D. M. Tomasiewicz, D. K. Hotchkiss, G. W. Reinbold, R. B. Read, and P. A. Hartman. "The Most Suitable Number of Colonies on Plates for Counting". In: *Journal of Food Protection* 43.4 (1979), pp. 282–286. ISSN: 0362-028X. DOI: 10.4315/0362-028x-43.4.282.

[24] T. Shimpoh, Y. Hirata, S. Ihara, N. Suzuki, H. Kinoshita, Y. Hayakawa, Y. Ota, A. Narita, S. Yoshida, A. Yamada, and K. Koike. "Prevalence of pks-positive Escherichia coli in Japanese patients with or without colorectal cancer". In: *Gut Pathogens* 9.1 (2017), pp. 1–8. ISSN: 17574749. DOI: 10.1186/s13099-017-0185-x.

[25] A. E. Masser, G. Kandasamy, J. Mohanakrishnan Kaimal, and C. Andreasson. "Luciferase NanoLuc as a reporter for gene expression and protein levels in Saccharomyces cerevisiae". In: *Yeast* March 2016 (2016), pp. 191–200. DOI: 10.1002/yea.3155.

[26] S. S. Silkie, M. P. Tolcher, and K. L. Nelson. "Reagent decontamination to eliminate false-positives in Escherichia coli qPCR". In: *Journal of Microbiological Methods* 72.3 (2008), pp. 275–282. ISSN: 01677012. DOI: 10.1016/j.mimet.2007.12.011.

[27] M. A. Teste, M. Duquenne, J. M. François, and J. L. Parrou. "Validation of reference genes for quantitative expression analysis by real-time RT-PCR in Saccharomyces cerevisiae". In: *BMC Molecular Biology* 10 (2009), p. 99. ISSN: 14712199. DOI: 10.1186/1471-2199-10-99.

[28] P. Caleb, R. Gabriella, S. Shelby, B. Easparro, J. Atwood, and R. Nash. "Evaluating the Impact of Bead Media Diameter and Material Composition". In: *Omni International, Inc.* 63. 2019, pp. 1–18. DOI: 10.3791/3064.

[29] S. M. Michaelson. "Effects of exposure to microwaves: problems and perspectives". In: *Environmental Health Perspectives* Vol 8.August (1974), pp. 133–155. ISSN: 00916765.

[30] S. W. Zeng, Q. L. Huang, and S. M. Zhao. "Effects of microwave irradiation dose and time on Yeast ZSM-001 growth and cell membrane permeability". In: *Food Control* 46 (2014), pp. 360–367. ISSN: 09567135. DOI: 10.1016/j.foodcont.2014.05.053.

[31] J. Azeredo, V. Lazarova, and R. Oliveira. "Methods to extract the exopolymeric matrix from biofilms: A comparative study". In: *Water Science and Technology* 39.7 (1999), pp. 243–250. ISSN: 02731223. DOI: 10.1016/S0273-1223(99)00174-2.

[32] S. F. D'Souza and K. Z. Marolia. "Stabilization of Micrococcus lysodeikticus cells towards lysis by lysozyme using glutaraldehyde: Application as a novel biospecific ligand for the purification of lysozyme". In: *Biotechnology Techniques* 13.6 (1999), pp. 375–378. ISSN: 0951208X. DOI: 10.1023/A:1008979709047.

[33] M. V. Flores, R. J. Ertola, and C. E. Voget. "Characterization of a glutaraldehyde stabilized yeast cell biocatalyst with β-galactosidase activity". In: *Journal of Fermentation and Bioengineering* 81.6 (1996), pp. 524–529. ISSN: 0922338X. DOI: 10.1016/0922-338X(96)81473-5.

[34] J. Y. Maillard. “Bacterial target sites for biocide action”. In: *Journal of Applied Microbiology Symposium Supplement* 92.1 (2002), pp. 16–27. ISSN: 02674440.

[35] M. J. Espy, J. R. Uhl, L. M. Sloan, J. E. Rosenblatt, F. R. Cockerill, and T. F. Smith. “Detection of vaccinia virus, herpes simplex virus, varicella-zoster virus, and Bacillus anthracis DNA by LightCycler polymerase chain reaction after autoclaving: Implications for biosafety of bioterrorism agents”. In: *Mayo Clinic Proceedings* 77.7 (2002), pp. 624–628. ISSN: 00256196. DOI: 10.4065/77.7.624.

[36] G. Elhafi, C. J. Naylor, C. E. Savage, and R. C. Jones. “Microwave or autoclave treatments destroy the infectivity of infectious bronchitis virus and avian pneumovirus but allow detection by reverse transcriptase-polymerase chain reaction”. In: *Avian Pathology* 33.3 (2004), pp. 303–306. ISSN: 03079457. DOI: 10.1080/0307945042000205874.

[37] S. Kajiwara, A. Shirai, T. Fujii, T. Toguri, K. Nakamura, and K. Ohtaguchi. “Polyunsaturated fatty acid biosynthesis in Saccharomyces cerevisiae: Expression of ethanol tolerance and the FAD2 gene from Arabidopsis thaliana”. In: *Applied and Environmental Microbiology* 62.12 (1996), pp. 4309–4313. ISSN: 00992240.

[38] H. Uemura. “Synthesis and production of unsaturated and polyunsaturated fatty acids in yeast: Current state and perspectives”. In: *Applied Microbiology and Biotechnology* 95.1 (2012), pp. 1–12. ISSN: 01757598. DOI: 10.1007/s00253-012-4105-1.

[39] A. Shokri and G. Larsson. “Characterisation of the Escherichia coli membrane structure and function during fedbatch cultivation”. In: *Microbial Cell Factories* 3 (2004), pp. 1–12. ISSN: 14752859. DOI: 10.1186/1475-2859-3-9.

[40] D. U. Kloos, M. Stratz, A. Guttler, R. J. Steffan, and K. N. Timmis. “Inducible cell lysis system for the study of natural transformation and environmental fate of DNA released by cell death”. In: *Journal of Bacteriology* 176.23 (1994), pp. 7352–7361. ISSN: 00219193. DOI: 10.1128/jb.176.23.7352-7361.1994.

[41] J. M. Yap, C. E. Goldsmith, and J. E. Moore. “Integrity of bacterial genomic DNA after autoclaving: Possible implications for horizontal gene transfer and clinical waste management”. In: *Journal of Hospital Infection* 83.3 (2013), pp. 247–249. ISSN: 01956701. DOI: 10.1016/j.jhin.2012.11.016.

[42] C. I. Masters, C. A. Miles, and B. M. Mackey. “Survival and biological activity of heat damaged DNA”. In: *Letters in Applied Microbiology* 27.5 (1998), pp. 279–282. ISSN: 02668254. DOI: 10.1046/j.1472-765X.1998.00447.x.

[43] I. Belyaev, Y. D. Alipov, V. S. Shcheglov, and V. N. Lystsov. “Resonance Effect of Microwaves on the Genome Conformational State of E. coli Cells”. In: *Zeitschrift fur Naturforschung - Section C Journal of Biosciences* 47.7-8 (1992), pp. 621–627. ISSN: 18657125. DOI: 10.1515/znc-1992-7-822.

[44] I. Belyaev. “Nonthermal biological effects of microwaves: Current knowledge, further perspective, and urgent needs”. In: *Electromagnetic Biology and Medicine* 24.3 (2005), pp. 375–403. ISSN: 15368378. DOI: 10.1080/15368370500381844.

[45] Y. Yang and J. Hang. “Fragmentation of genomic DNA using microwave irradiation”. In: *Journal of Biomolecular Techniques* 24.2 (2013), pp. 98–103. ISSN: 15240215. DOI: 10.7171/jbt.13-2402-005.

[46] F. R. Blattner, G. Plunkett, C. A. Bloch, N. T. Perna, V. Burland, M. Riley, J. Collado-Vides, J. D. Glasner, C. K. Rode, G. F. Mayhew, J. Gregor, N. W. Davis, H. A. Kirkpatrick, M. A. Goeden, D. J. Rose, B. Mau, and Y. Shao. *The complete genome sequence of Escherichia coli K-12*. 1997. DOI: 10.1126/science.277.5331.1453.

[47] S. R. Engel, F. S. Dietrich, D. G. Fisk, G. Binkley, R. Balakrishnan, M. C. Costanzo, S. S. Dwight, B. C. Hitz, K. Karra, R. S. Nash, S. Weng, E. D. Wong, P. Lloyd, M. S. Skrzypek, S. R. Miyasato, M. Simison, and J. M. Cherry. “The Reference Genome Sequence of Saccharomyces cerevisiae : Then and Now”. In: *G3: Genes—Genomes—Genetics* 4.3 (2014), pp. 389–398. DOI: 10.1534/g3.113.008995.

[48] D. Hopwood. “The reactions of glutaraldehyde with nucleic acids”. In: *The Histochemical Journal* 7.3 (1975), pp. 267–276. ISSN: 00182214. DOI: 10.1007/BF01003595.

[49] K. Das, M. R. Fernando, S. Basiaga, S. M. Wigginton, and T. Williams. “Effects of a novel cell stabilizing reagent on DNA amplification by PCR as compared to traditional stabilizing reagents”. In: *Acta Histochemica* 116.1 (2014), pp. 55–60. ISSN: 00651281. DOI: 10.1016/j.acthis.2013.05.002.

[50] S. Park, J. Y. Jang, J. S. Koo, J. B. Park, Y. J. Lim, S. J. Hong, S. W. Kim, and H. J. Chun. "A review of current disinfectants for gastrointestinal endoscopic reprocessing". In: *Clinical Endoscopy* 46.4 (2013), pp. 337–341. ISSN: 22342400. DOI: 10.5946/ce.2013.46.4.337.

[51] K. Shaw, I. Sesardić, N. Bristol, C. Ames, K. Dagnall, C. Ellis, F. Whittaker, and B. Daniel. "Comparison of the effects of sterilisation techniques on subsequent DNA profiling". In: *International Journal of Legal Medicine* 122.1 (2008), pp. 29–33. ISSN: 09379827. DOI: 10.1007/s00414-007-0159-5.

[52] S. Overballe-Petersen, K. Harms, L. A. Orlando, J. V. Moreno Mayar, S. Rasmussen, T. W. Dahl, M. T. Rosing, A. M. Poole, T. Sicheritz-Ponten, S. Brunak, S. Inselmann, J. De Vries, W. Wackernagel, O. G. Pybus, R. Nielsen, P. J. Johnsen, K. M. Nielsen, and E. Willerslev. "Bacterial natural transformation by highly fragmented and damaged DNA". In: *Proceedings of the National Academy of Sciences of the United States of America* 110.49 (2013), pp. 19860–19865. ISSN: 00278424. DOI: 10.1073/pnas.1315278110.

[53] S. Overballe-Petersen and E. Willerslev. "Horizontal transfer of short and degraded DNA has evolutionary implications for microbes and eukaryotic sexual reproduction". In: *BioEssays* 36 (2014), pp. 1005–1010. DOI: 10.1002/bies.201400035.

[54] T. S. Jørgensen, A. S. Kiil, M. A. Hansen, S. J. Sørensen, and L. H. Hansen. "Current strategies for mobilome research". In: *Frontiers in Microbiology* 5.DEC (2014), pp. 1–6. ISSN: 1664302X. DOI: 10.3389/fmicb.2014.00750.

[55] M. Messerer, W. Fischer, and S. Schubert. "Investigation of horizontal gene transfer of pathogenicity islands in Escherichia coli using next-generation sequencing". In: *PLoS ONE* 12.7 (2017), pp. 1–17. ISSN: 19326203. DOI: 10.1371/journal.pone.0179880.

3

Free-floating extracellular DNA: Systematic profiling of mobile genetic elements and antibiotic resistance from wastewater

This chapter has been published as: Calderón-Franco, D., van Loosdrecht, M., Abeel, T., Weissbrodt, D., 2020. Free-floating extracellular DNA: Systematic profiling of mobile genetic elements and antibiotic resistance from wastewater. Water Research. 189, 1–13. https://doi.org/10.1101/2020.05.01.072397

ABSTRACT

The free-floating extracellular DNA (exDNA) fraction of microbial ecosystems harbors antibiotic resistance genes (ARGs) and mobile genetic elements (MGEs). Natural transformation of these xenogenetic elements can generate microbial cells resistant to one or more antibiotics. Isolating and obtaining a high yield of exDNA is challenging due to its low concentration in wastewater environments. Profiling exDNA is crucial to unravel the ecology of free-floating ARGs and MGEs and their contribution to horizontal gene transfer. We developed a method using chromatography to isolate and enrich exDNA without causing cell lysis from complex wastewater matrices like influent (9 μg exDNA out of 1 L), activated sludge (5.6 μg out of 1 L), and treated effluent (4.3 μg out of 1 L). ARGs and MGEs were metagenomically profiled for both the exDNA and intracellular DNA (iDNA) of activated sludge, and quantified by qPCR in effluent water. qPCR revealed that ARGs and MGEs are more abundant in the iDNA fraction while still significant on exDNA (100-1000 gene copies mL^{-1}) in effluent water. The metagenome highlighted that exDNA is mainly composed of MGEs (65%). According to their relatively low abundance in the resistome of exDNA, ARGs uptake by natural transformation is likely not the main transfer mechanism. Although ARGs are not highly abundant in exDNA, the prevalence of MGEs in the exDNA fraction can indirectly promote antibiotic resistance development. The combination of this method with functional metagenomics can help to elucidate the transfer and development of resistances in microbial communities. A systematic profiling of the different DNA fractions will foster microbial risk assessments across water systems, supporting water authorities to delineate measures to safeguard environmental and public health.

Keywords: *Free-floating extracellular DNA; Wastewater; Xenogenetic elements; Antimicrobial resistance; qPCR; Metagenomics*

3.1. Introduction

Xenogenetic pollution has become a global threat to environmental and public health [1]. Risk evaluation due to transmission and proliferation of pathogenic agents, antibiotic resistance genes (ARGs), mobile genetic elements (MGEs), and materials from genetically-modified organisms (GMOs) via waterways and biological systems like wastewater environments are under active examination [2–4]. While ARGs and MGEs are now widely targeted across investigations of sewage, their survey has primarily been made based on the molecular analysis of total DNA extracts from the microbial communities of wastewater. However, besides the intracellular DNA (iDNA), the extracellular DNA (exDNA) that is free-floating in the bulk liquid water phase may carry a substantial amount of ARGs and MGEs of environmental and public health concern. The exDNA fraction has not been studied in detail, even if there are some exceptions in sludge, cattle manure and swine waste samples [5, 6]. Differential isolation and systematic profiling of iDNA and free-floating exDNA is necessary to elucidate the mechanisms of transfer of these mobile DNA contaminants that replicate. exDNA retrieved from environmental samples can be defined as the DNA fraction that is not housed within the envelope of the cell membrane [7]. The acronym "eDNA" is widely intermixed to describe either environmental DNA or extracellular DNA. Environmental DNA does not necessarily discriminate between extracellular and intracellular fractions of nucleic acids. It only means that DNA extracted originates from cells that were present in the investigated ecosystem at the sampling event [8]. We define free-floating exDNA as *"all the DNA components that are neither enclosed inside cells nor adsorbed or aggregated in complex matrices and that are persistently floating in aqueous samples"*. This exDNA fraction can represent a genetic proxy of microbial and cellular diversity among different biogeographical areas [7, 9]. Isolating and analyzing exDNA from environmental samples provides insight into the dynamics, interactions, and evolutionary history of populations of microorganisms and higher organisms that are or have been present in the investigated environment. Moreover, exDNA is abundant and plays an important role as a structural component of microcolonies, stabilizing microbial bioaggregates [10–12], being a key component within the matrix of extracellular polymeric substances (EPS) [10, 13–15]. However, biofilm and flocs have also been suggested as reservoirs for ARG occurrence and dissemination [16, 17]. Active or passive release out of cells are the main sources of exDNA [7, 18]. Whether exDNA is actively or passively released in these biological environments remains unsolved, although some authors provide claims about one or the other hypotheses [19, 20]. Until mechanistic measurements will be made available, strong debate will remain on the 'intention' of cells to release DNA to drive biofilm formation. In this study, exDNA immobilized in the EPS matrix is considered to be likely less available to gene transfer in comparison with free-floating exDNA [21].

The persistence of exDNA in biofilms and of free-floating exDNA (that can also sorb to surfaces) may generate hotspots for horizontal gene transfer (HGT) in

microbial biocoenoses. Natural competence is a widely distributed cellular mechanism harboured by microorganisms in nature to take up molecular resources from their surroundings. Naturally competent microbes may take up free or bound exDNA [18]. Natural transformation is a parasexual mechanism for the exchange of genetic material induced by stress conditions such as nutrient limitations or the presence of antibiotics [22]. Such conditions are found in densely populated cultures such as activated sludge samples. Natural transformation in managed environments does not implicitly result in a threat for human health since it is a mechanism generating diversity and adaptation [23].

However, if ARGs, MGEs, and pathogenic islands can be found in exDNA fractions, the formation of pathogenic bacterial cells resistant to one or more antibiotics – also known as superbugs – could be induced [24]. DNA fragments that have been released by sterilization of microbial cultures using, e.g., industrial and research facility methods does not lose its integrity and capacity to be re-amplified [25], thus making it an undesired source of xenogenetic pollution. The molecular mechanisms generating superbugs and the underlying sources of genetic materials that can prompt it need to be studied. Methods to efficiently isolate, quantify, and metagenomically characterize exDNA templates from complex biological samples are required.

In the last years, a few methods to extract exDNA have been published. Wang *et al.* (2016) have used an aluminum hydroxide column to adsorb aquatic exDNA. Nagler *et al.* (2018) have opted for sequential steps involving enzymatic treatments to extract exDNA from cattle rumen samples. Yuan *et al.* (2019) have integrated magnetic beads in combination with the classic DNA precipitation method involving the surfactant cetyl trimethyl ammonium bromide (CTAB), yielding a relatively good amount of exDNA of 0.2 μg out of 5 mL of wastewater. Silica solid phases similar to commercial silica resin columns have been tested to adsorb and extract exDNA from low-concentration clinical samples [29]. Cell lysis has seldom been investigated (although often debated) across protocols for exDNA extractions. Assessing and preventing cell lysis during exDNA isolations is crucial to obtain confident analytical results from exDNA templates. Moreover, volumes previously used (<100 mL) have hindered a more detailed exDNA characterization by metagenomics due to low isolation yields. Metagenomics can be used for deciphering the distribution, mobility and microbial hosts of ARGs in both DNA fractions from environmental samples such as sludge [6].

A mathematical model that accounts for ARGs sitting on both iDNA and exDNA fractions has been developed to predict the fate and transport of ARGs in receiving waters downstream of WWTPs [30]. An improved quantitative understanding of these processes and of the impact of exDNA on ARG spread and occurrence requires more effective methods to extract exDNA. It will enable a more accurate risk assessment toward more targeted mitigation of antibiotic resistance.

Here, we systematically profiled xenogenetic elements from free-floating exDNA

out of the complex biological environment of wastewater. We highlight for the first time the potential xenogenetic risk associated with free-floating exDNA fragments transported with sewage across urban water systems. We provide an efficient analytical method to investigate it at high resolution.

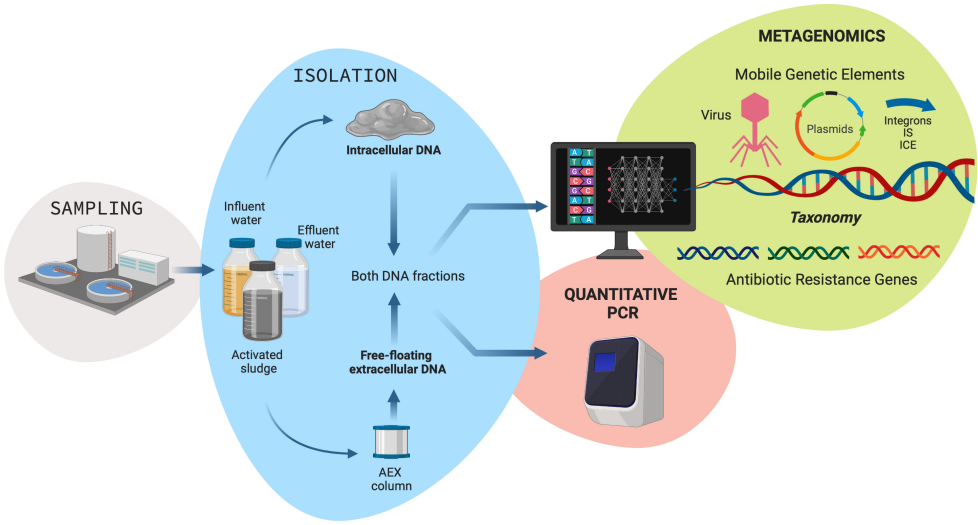

Figure 3.1: Graphical abstract

3.2. Material & Methods

Sampling from the influent, activated sludge tank, and effluent of a wastewater treatment plant

Biological samples were collected from influent wastewater, activated sludge, and effluent water of the urban wastewater treatment plant (WWTP) Harnaschpolder (Waterboard Delfland, The Netherlands) operated for full biological nutrient removal. Grab sampling was used totest the exDNA isolation method on the different wastewater matrices, and to metagenomically characterize and molecularly quantify what ARGs and MGEs sit on which DNA fractions in these matrices, rather than performing a "mass balance" per se. Influent wastewater was collected after primary treatment. Three biological replicates were collected on three different days as grab samples. A total of 1000 mL of influent wastewater was collected per replicate. All samples were processed in a timeframe of less than 2 h prior to DNA extraction.

Six biological replicates of activated sludge were collected in two different sampling campaigns as grab samples from the activated sludge tank. Each campaign consisted of three successive dry days, i.e., without recent rainfall and variations in the hydraulic retention time. The first round of exDNA isolation experiments was performed with three biological replicates of activated sludge. Once the method was successful, we conducted a second campaign for which additional three samples were taken from three different days from the three different biological matrices: influent, activated sludge and effluent. All raw activated sludge samples were stored at 4°C in a timeframe of less than 2h prior to isolations of free-floating exDNA and extractions of iDNA. A total volume of 1000 mL of activated sludge was collected per replicate.

Effluent water was collected at the outlet of the tertiary treatment. Three biological replicates were collected in three different days as grab samples. A total of 1000 mL of treated water per replicate was collected. All samples were processed in a timeframe of less than 2 h prior to DNA extraction.

Isolation of free-floating extracellular DNA from influent, activated sludge and effluent water samples

The workflow used to isolate free-floating exDNA from influent, activated sludge, and effluent samples is sketched in **Figure** 3.2.

Activated sludge was centrifuged at 6000 x g at 4°C for 10 min for removing biomass in order to make the next filtration step easier. Pellet was stored at 4°C for intracellular DNA extraction. The supernatant was used for free-floating DNA isolation.

Influent, activated sludge supernatant, and effluent samples were sequentially filtered through 0.45 and 0.2 μm 47 mm PES membrane filter (Pall Corporation, USA). The membrane filters holding the biomass were stored at 4°C for further

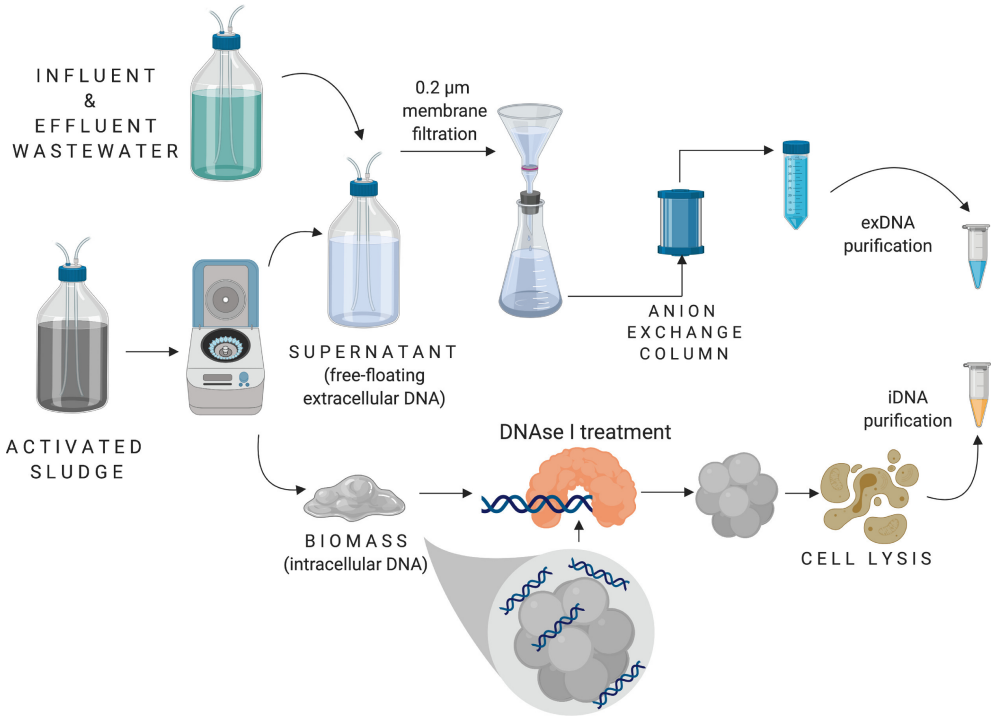

Figure 3.2: Schematic representation of the free-floating exDNA and iDNA isolation method.

intracellular DNA extraction. The filtered samples (1000 mL influent, activated sludge supernatant and influent) were loaded on a positively charged 1-mL diethylaminoethyl cellulose (DEAE) chromatographic column (BIA Separations, Slovenia) using an LC-8A preparative liquid chromatography pump (Shimadzu Corporation, Japan) and 0.76 x 1.6 mm tubing (Thermo Fisher Scientific, USA). This anion-exchange column was preliminarily equilibrated at a flowrate of equilibration buffer of 0.6 mL min^{-1} while maintaining the pressure below the maximum limit of 1.8 MPa. Because of very high porosity, reusability, and flow characteristics (up to 16 mL min^{-1}), this monolithic chromatographic column is an efficient tool to separate or purify large biomolecules such as genomic and viral DNAs [31]. Column preparation and processing were performed according to the manufacturer's instructions.

Buffers and solutions were used to equilibrate, elute, regenerate, clean, and store the column. The equilibration buffer consisted of a mixture at pH 7.2 of 50 mmol L^{-1} Tris and 10 mmol L^{-1} EDTA. The elution buffer was a mixture at pH 7.2 of 50 mmol L^{-1} Tris, 10 mmol L^{-1} EDTA, 1.5 mol L^{-1} NaCl. The regeneration buffer was a mixture at pH 7.2 of 50 mmol L^{-1} Tris, 10 mmol L^{-1} EDTA, 2 mol L^{-1} NaCl. The cleaning solution comprised 1 mol L^{-1} NaOH and 2 mol L^{-1} NaCl. The storage solution consisted of 20% ethanol in ultrapure water (Sigma Aldrich, USA).

The elution of exDNA was tracked over time using an HPLC photodiode array detector (Waters Corporation, USA) recording the UV–VIS absorbance at the absorbance wavelength characteristic of DNA (260 nm).

The eluted exDNA fraction was further treated sequentially with absolute ethanol and a solution of 70% ethanol in ultrapure water (Sigma Aldrich, USA) [32] to precipitate the raw exDNA. The precipitated raw exDNA was incubated with proteinase K (Sigma-Aldrich, UK) at 0.85 g L^{-1} during 2 h in order to digest remaining co-extracted proteins (e.g., DNA-bound proteins). The enzymatic reaction was stopped in a heat block at 50°C for 10 min. The precipitated and protein-digested raw exDNA extract was finally purified using a GeneJET NGS Cleanup Kit (Thermo Scientific, USA). The purified exDNA isolates were stored at -20°C pending molecular analysis.

Extraction of intracellular DNA from biomass separated from activated sludge and effluent water

iDNA was extracted from cells present in activated sludge and effluent water for analytical comparison of xenogenetic elements with exDNA. Biomass was obtained as a pellet by centrifugation (6000 x g at 4 °C for 10 min) of activated sludge and filtration (0.45 and 0.2 μm 47 mm PES membrane filter (Pall Corporation, USA) of effluent water.

An amount of 0.25 g wet weight of activated sludge (3.6 g TSS L^{-1}) was incubated during 1 h with 300 U mL^{-1} of DNase I in order to remove the residual exDNA from the biological sample, before extraction of the iDNA using a NucleoSpin® Soil kit (Macherey-Nagel) according to manufacturer's instructions. The biomass from the effluent water was obtained by filtering a volume of 500 mL of effluent through a 0.22 μm PVDF membrane (Pall corporation, USA). Filters were frozen at -20°C until extraction. The iDNA present on filters was extracted with the Power Water DNeasy kit (Qiagen, NL) following the manufacturer's instructions.

The quality and quantity of the DNA extracts were measured by NanoDrop spectrophotometry (ND-1000, USA) and Qubit® dsDNA assays (Thermo Fisher Scientific, USA), respectively.

Plasmid DNA used as chromatography selectivity control

A bacillus expression pHT01 plasmid (MoBiTec GmbH, Germany) was used as nucleic acid selectivity control for the DEAE anion-exchange column.

Biomass pre-treatment, live-dead staining, and flow cytometry analysis

Flow cytometry combined with live-dead staining was used to check for the prevention of cell lysis across the exDNA isolation workflow. Cells from the

biological samples were disaggregated as a prerequisite for the migration of individual cells in the flow cytometer. Activated sludge samples were diluted at 1:500 in 1x PBS buffer. The diluted sludge samples were mild-sonicated (Branson Sonifier 250, USA) on ice in 3 cycles of 45 s at 40 W. After sonication, samples were diluted at 1:500 in 1x PBS buffer. Right after the second dilution, samples were filtered through a 10 µm syringe filter in order to remove possible residual cell debris and membranes.

The live-dead staining protocol and flow cytometry analyses were based on previous works [33–36]. Two staining dyes were used to track viable cells with SYBR green (Invitrogen, USA) and dead cells with red-fluorescent propidium iodide (PI) (Invitrogen, USA). Two working solutions were prepared from 10000 x SYBR Green and 30 mmol L^{-1} PI dissolved in di-methyl sulfoxide (DMSO) stock solutions.

To obtain the total stained cell count, 10 μL of 10,000x SYBR Green stock solution was diluted in Tris–HCl (pH 8), obtaining a final 100 x SYBR Green working solution. To obtain the viable cell count, a final working solution of 100 x SYBR Green and 6 $\mu mol\ L^{-1}$ PI was used. Working solutions were thoroughly mixed by homogenization using a vortex and stored at -20°C in the dark pending analysis.

Volumes of 5 µL of each of the staining working solutions were added to 495 μL of pre-treated biomass samples. After stains addition, samples were incubated at 37°C for 10 min. After incubation, samples were kept in the dark until flow cytometry measurement.

Flow cytometry measurements were performed in a BD Accuri C6 flow cytometer (BD Biosciences, Belgium) equipped with a 50 mW laser tuned at an excitation wavelength of 488 nm. Fluorescence intensity was collected at emission wavelengths of the green (FL1 = 533 ± 30 nm) and red (FL3 > 670 nm) fluorescence detection channels. Measurements were performed at a flow-rate of 66 mL min^{-1} on 50 μL sample volume with a threshold value of 700 on FL1 to reduce the background detection noise.

Gel electrophoresis on the free-floating extracellular DNA

To analyze the different lengths of exDNA templates, the exDNA samples were analyzed by gel electrophoresis with agarose at 1% (w/v) (Sigma-Aldrich, Haverhill, United Kingdom) in 1xTAE buffer.

Quantitative polymerase chain reaction (qPCR) analysis of selected ARGs and MGEs on exDNA and iDNA from effluent water samples

A panel of genes was selected for qPCR analysis on exDNA and iDNA fractions extracted from effluent water samples. The 16S rRNA gene was selected as a proxy to quantify total bacteria. ARGs and MGEs were selected from a panel used for wastewater samples [2, 37]. Standards for qPCR were generated from ResFinder, a curated database of ARGs. The chosen ARGs targeted: macrolides (multidrug export protein gene *ermB*), sulfonamides (sulfonamide resistance genes *sul1* and *sul2*), fluoroquinolones (quinolone resistance gene *qnrS*) and extended-spectrum β-lactamase (cefotaxime-hydrolyzing β-lactamase bla_{CTXM}) (**Table** S.1). The class I integron-integrase gene *intI1*, known to be responsible for genes mobility [38], was included to assess the presence of MGEs. Standards, primers, and reaction conditions are listed in **Tables** S.2 and S.3 in supplementary material.

Metagenomic profiling of exDNA and iDNA fractions from activated sludge samples

Metagenomics libraries of exDNA and iDNA samples at 50 ng μL^{-1} were sequenced using a MiSeq PE300 benchtop sequencer (Illumina, USA). Library preparation was done with a TruSeq DNA PCR-Free kit (LT Lib PREP KT-ST B PhiX control v3). Datasets of 14 million reads were obtained per sample corresponding to a sequencing depth of 6.5 GB for iDNA and 6.8 GB for exDNA fractions. Raw metagenomic data have been deposited in BioProject under accession number PRJNA632452 and *ID: 632452*. Activated sludge was selected for metagenomics for being a highly diverse sample, from which microbiome, resistome and mobilome differences could be assessed in order to check the applicability of the extraction method.

The quality of the acquired Illumina reads was assessed by FastQC version 0.11.9 with default parameters [39]. Paired-ends reads were trimmed and filtered by Trimmomatic version 0.39 with default parameters [40]. Alignments were performed by BWA-mem version 2 with default parameters [41], generating a SAM file. To filter soft and hard clipped reads, SAM files were filtered by Samclip tool with default parameters, removing undesirable alignments that could generate downstream problems (https://github.com/tseemann/samclip). Centrifuge [42] was applied for taxonomic microbial classification (http://ccb.jhu.edu/software/centrifuge). The MEGARes 2.0 database was used to identify ARGs (http://megares.meglab.org). The metagenomes were searched for signatures of known MGEs, plasmids, prophages, and viruses through ACLAME (http://aclame.ulb.ac.be) [43]. The mobilome was searched for integrative conjugative elements through the ICEberg database (http://db-mml.sjtu.edu.cn/ICEberg/) [44], insertion sequences through ISfinder (https://isfinder.biotoul.fr) [45], and integrons through the INTEGRALL database (https://integrall.bio.ua.pt) [46]. Different databases of ARGs and MGEs of different completeness and curation levels are available in public repositories such

as the aforementioned, while no consensus database is available yet. Follow-up research will lead to a comprehensive database for wastewater environments (REPARES).

Both MEGARes 2.0 and ACLAME were used as references for the alignment of trimmed and filtered metagenomic reads. The output SAM file from the BWA-mem alignment was converted into a BAM file using SAMtools version v1.4 [47] (https://github.com/samtools/samtools). Unmapped reads were removed and secondary alignments ignored in order to get a list of the best hits for further data processing. ARGs and MGEs hits were considered when 2 or more reads per variant were aligned.

Comparative subsystems analysis of the metagenomic data

Unassembled clean reads from the exDNA and iDNA fractions of activated sludge were annotated using the open-access metagenome curation and analysis platform Metagenome Rapid Annotation using Subsystem Technology (MG-RAST) (http://metagenomics.nmpdr.org/) [48]. The subsystem classification MG-RAST ID are available for the free-floating extracellular DNA (mgm4886400.3) and the intracellular DNA (mgm4886611.3).

Statistics

Statistical analyses were performed on all molecular datasets with R 3.5.1 [49] and RStudio. For the analysis of significance on the purification effect on the yield of DNA isolation, a non-parametric Wilcoxon test was performed. For both exDNA and iDNA samples, biological replicates were used from influent water (3 replicates), activated sludge (6 replicates) and effluent water (3 replicates). A parametric two-tailed Student's t-test with statistical significance established at the 95% confidence level ($p<0.05$) was performed to analyze the significance of the differences in ARG and MGE compositions between exDNA and iDNA fractions. For both exDNA and iDNA samples, 3 biological replicates with 3 technical replicates were used from effluent water.

3.3. Results & Discussion

High yields of free-floating exDNA were obtained by anion-exchange chromatography

The column performed with high nucleic acid selectivity for the retention, separation, and spectrophotometric detection (λ = 260 nm) with known concentration of pure pHT01 plasmid of *Bacillus subtilis* as control (**Figure** S.1**a**). A sharp and well-resolved narrow peak was obtained in the chromatographic elution and detection of the plasmid control. The raw non-precipitated exDNA obtained from filtered activated sludge started to elute after 10 min for 35 min (**Figure** S.1**b**). The chromatographic peak maximum was detected at a retention time of 18 min. The concentrated raw free-floating exDNA extract displayed a hydrogel aspect (**Figure** 3.3). Its color related to the source of the exDNA extract, namely dark brown with influent water, yellow with activated sludge, or colorless with effluent water. The explanation could relate to either polyphenols or humic acids. Polyphenols are soluble in water and change to a red coloration when in contact with air [50]. Humic acids are abundant in wastewater and can interact with DNA [51].

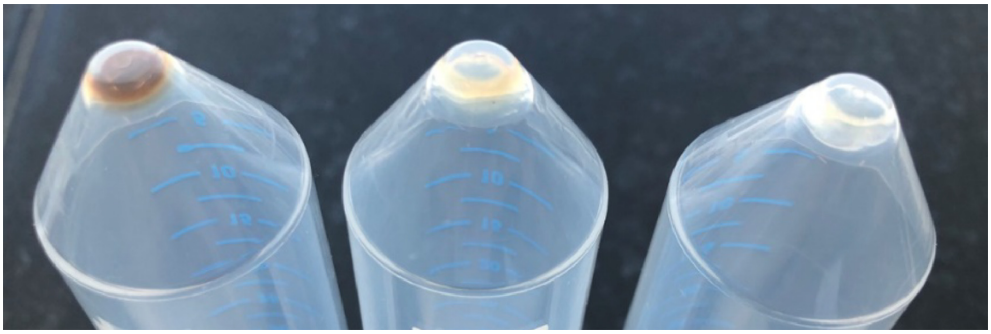

Figure 3.3: Aspects of raw extracts of free-floating exDNA obtained from different wastewater environments. From left to right: **(i)** filtered influent wastewater (brown free-floating exDNA extract due to high presence of humic acids), **(ii)** centrifuged and filtered activated sludge supernatant (yellow extract), and **(iii)** filtered effluent water (colorless extract).

The concentration of humic acids decreases during wastewater treatment [52]. For instance, humic acids adsorb onto activated sludge [53]. They are less abundant in absolute concentration in effluent water [54]. Therefore, we hypothesize that the loss of color in the exDNA extract through the process is due to loss of humic acids that are co-extracted with the exDNA. The diethylaminoethyl cellulose (DEAE) column efficiently isolated and concentrated the free-floating exDNA fraction from large volumes of influent wastewater, activated sludge, and effluent water of the WWTP.

The yields (i.e., mass of DNA isolated in molecular biology after the isolation and purification procedures) of raw and purified (with a commercial DNA purification kit after Proteinase K treatment) free-floating exDNA isolated from influent

wastewater, activated sludge, and effluent water are shown in **Figure** S.2. Yields and concentrations are summarized in **Table** 3.1. The exDNA fraction corresponded to <1% of the total DNA extracted from activated sludge. Only exDNA obtained from activated sludge samples showed significant differences in the yields between raw and purified exDNA ($p<0.05$). There was no significant difference ($p>0.05$) between in yields of raw exDNA obtained from different water quality samples. However, the influent wastewater displayed a significantly ($p<0.05$) higher fraction of purified free-floating exDNA (9'000 ng out of 1000 mL initial sample volume) than activated sludge (5'631 ng out of 1000 mL initial sample volume) and effluent water (4'276 ng out of 1000 mL initial sample volume).

Table 3.1: exDNA yield and concentrations for different water qualities before and after commercial kit purification. The sample volume corresponds to the volume of the initial water sample from which exDNA had been extracted.

Sample	Initial sample volume (mL)	exDNA extract	exDNA yield (µg)	exDNA concentration in initial sample (ng mL^{-1})
	1000	Raw	12.5	12.5
Influent wastewater[a]	1000	Purified	9.0	9.0
	1000	Raw	12.3	12.3
Activated sludge[b]	1000	Purified	5.6	5.6
	1000	Raw	8.6	8.6
Effluent water[c]	1000	Purified	4.3	4.3

[a]Filtered influent wastewater.
[b]Centrifuged and filtered activated sludge supernatant.
[c]Filtered effluent water.

The raw exDNA extracted from influent wastewater and activated sludge supernatant samples yielded higher concentrations (12.5 ± 1.9 ng mL^{-1} and 12.3 ± 1 ng mL^{-1}, respectively) than after purification (9.0 ± 0.7 ng mL^{-1} and 5.6 ± 0.46 ng mL^{-1}), respectively. An average mass loss of 42% through the commercial purification kit was measured. In the method, one commercial kit was used for the purification of the exDNA extracts after digestion with proteinase K. For future works, other commercial kits or classical purification methods might also be assessed for the isolation of free-floating exDNA from low-content water samples.

It is paramount to note that the exDNA yields were substantial for the three biological matrices. The free-floating exDNA extracts fulfilled the minimal quantitative and qualitative requirements (mass $\geq$ 1 μg, concentration $\geq$ 20 ng μL^{-1}, volume $\geq$ 20 μL) required for qPCR and high-throughput metagenomics analyses. Much higher yields were obtained than with other isolation methods tested in parallel in this study or reported in literature: ca. 3-fold higher than with classical CTAB and PCI methods, and up to as high as ca. 2000-fold higher than direct precipitation with isopropanol (**Table** 3.2). Our method and the one of Yuan *et al.* (2019) provide the necessary yield of exDNA recovered from wastewater samples for subsequent molecular analyses.

Table 3.2: Concentrations and yields of free-floating extracellular DNA extracts obtained during this study in comparison to other methods. Legend: cetyl trimethyl ammonium bromide (CTAB), phenol:chloroform:isoamyl alcohol and ethanol (PCI).

Method	Reference	Initial sample volume (mL)	exDNA yield (ng)	exDNA concentration in initial sample (ng mL^1)
AEX column	This study	1'000	12'323	12.3
CTAB, PCI	This study	800	3'630	4.53
Magnetic beads	[28]	5	234	78.0
Vivaspin columns 100 kDa	This study	500	136	0.27
Isopropanol precipitation	This study	50	6.5	0.13
DNA extraction kit	This study	50	ND	ND [a]

[a] ND means not detected.

Mild enzymatic post-treatment with proteinase K is necessary to release exDNA from bound extracellular polymeric proteins found in activated sludge

The free-floating exDNA extracted from activated sludge was characterized by an intense band at the top of the agarose gel. This suggested that exDNA was entrapped in a protein mesh that did not allow it to migrate through the gel (**Figure** 3.4**a**). After mild enzymatic treatment of these residual proteins bound to the exDNAs with proteinase K, it was observed that the purified exDNA templates were able to run through the gel (**Figure** 3.4**b**). These were characterized by a distribution of fragments sizes that ranged from 0.5 kbp to >20 kbp. For comparison, the iDNA that was extracted in parallel using commercial kits exhibited DNA fragments that also ranged from less than 0.5 kbp to >20 kbp. Both DNA fractions displayed similar fragment size distribution.

Assuming that the average size of genes present in bacterial genomes is 1.5 kb long, exDNA was suggested to be large enough to contain multiple ARGs and MGEs [5, 55]. No significant differences in band intensity could be observed between untreated biomass and treated with DNase I prior to intracellular DNA extraction (**Figure** 3.4**b**). This suggests a low exDNA content bound to biomass when DNA is extracted from 0.25 g of activated sludge. The extracted pools of free-floating exDNA fragments were suitable for further molecular analyses since purity (1.76 $\pm$ 0.02) was close to optimal the optimum absorbance ratio A_{260nm}/A_{280nm} of 1.8.

Cell lysis is not induced during the isolation of free-floating exDNA

Cell lysis measurements and control were conducted on the processing of activated sludge since exhibiting the highest microbial density among the wastewater environment samples. Thus, activated sludge was considered as more prone to potential cell lysis and cross-contamination of the free-floating exDNA extract with iDNA residues. Flow cytometry was used to measure the total cells counts after each biomass processing step in the developed protocol (**Figure** 3.5**a**) together with the relative abundances of live/dead cells measured after stainings

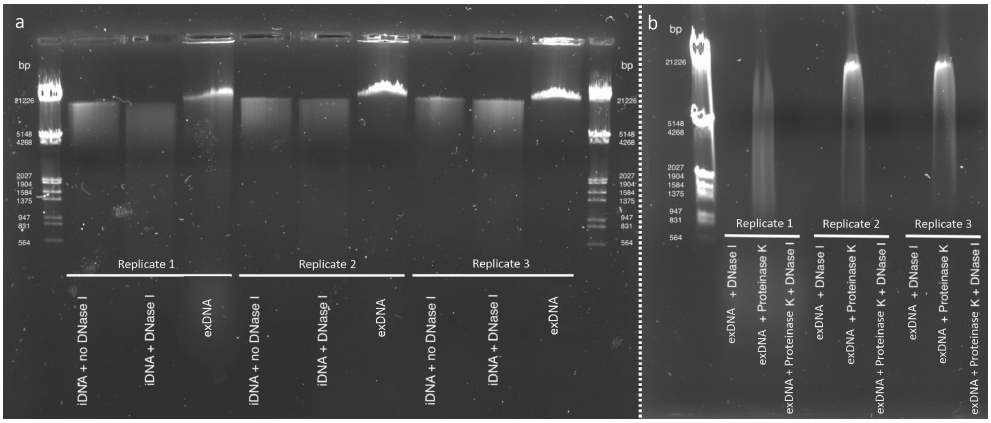

Figure 3.4: The impact of enzymatic post-treatment of raw exDNA extracts with proteinase K to release the exDNA from extracellular protein mesh: **(a)** Agarose gel from three different biological replicates showing the fragment size distributions of intracellular DNA (iDNA) obtained without any pre-treatment, of iDNA obtained after enzymatic pre-treatment of cells with DNase I prior to cell lysis and DNA extraction, and of the raw extract of free-floating extracellular DNA (exDNA) obtained from centrifuged and filtered activated sludge supernatant samples. **(b)** Agarose gel of free-floating exDNA after either pre-treatment of cells with DNase I, post-treatment of exDNA extract with proteinase K, or a combination of both pre- and post-treatments. Values of DNA concentrations after DNAse I treatment are summarized in **Table** S.4.

with SYBR Green and propidium iodide fluorophores, respectively (**Figure** 3.5**b**). After filtration of centrifuged activated sludge supernatant through the 0.45 μm membrane filter, the number of flow cytometry events mL^{-1} was below 10; after second filtration on 0.2 μm, below 1 event. The diluted activated sludge control that consisted of a non-centrifuged and non-filtered activated sludge sample had an average of 1606 events mL^{-1}. Cells retained in the membrane filters were assumed to maintain their robustness and viability [15, 56].

Initial cell viability was preserved and bacterial cells were removed upfront by centrifugation and filtration. Depending on the type of biomasses targeted, even smaller filter pore sizes than 0.2 μm could be used.

Besides high yield, the free-floating exDNA template was therefore of high quality, being deprived of iDNA contamination. The isolation method did not induce cell lysis during the extraction: a cell-free and iDNA-free exDNA fraction was isolated. This quality control ensured that in the exDNA fraction there was no genomic DNA contamination caused by the extraction. Hence, we demonstrated the isolation of free-floating exDNA at high yield and high quality from complex microbial community matrices of activated sludge, across a workflow exempt of cell lysis.

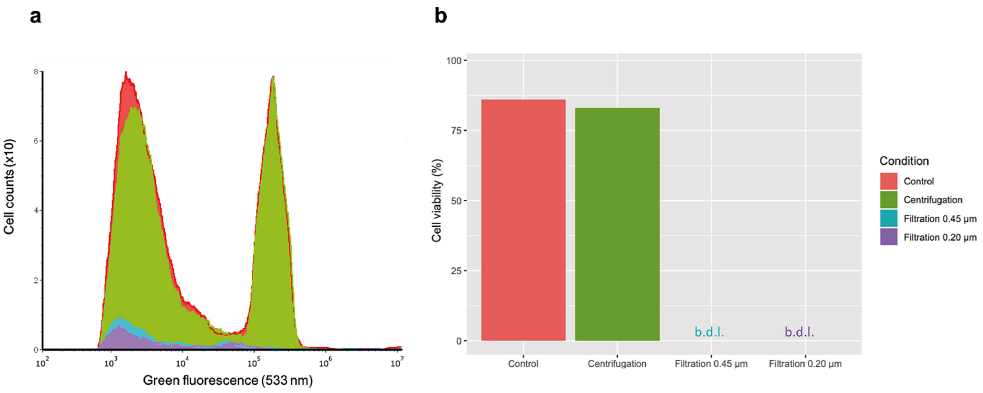

Figure 3.5: (a) Direct comparison of the green fluorescence histograms of activated sludge supernatant water samples with the different protocol extraction steps. Cell counts correspond to the number of events in 50 μL. **(b)** Live/cell staining showing cell viability of samples after the different protocol extraction steps. *Legend*: bdl: below the detection limit (cell lower limit was achieved when both filtrations were applied). An electronic gate on the green (533 nm)/red (670 nm) fluorescence density plot was used to select the signals of cells. Dot-plots can be found in Figure S.3 in supplementary material.

Free-floating exDNA displays lesser ARG copies than iDNA

qPCR results highlighted that molecular analysis of five selected ARGs (*sul1, sul2, ermB, qnrS and* bla_{CTXM}) and one MGE (*intI1*) could be performed from both the iDNA and the free-floating exDNA fractions of wastewater environments, being effluent wastewater in this case (**Figure** 3.6). All genes tested but bla_{CTXM} were detected in both DNA fractions. The free-floating exDNA template harbored a lower number of ARG and MGE copies than iDNA, with a significant difference (Δ) of 0.87 $\pm$ 0.32 log_{10} gene copies (p<0.005) across the gene panel.

At individual gene level, the free-floating exDNA displayed a significantly lower log-based gene copy number of both the bacterial 16S rRNA gene (Δ = 1.2 $\pm$ 0.43 log_{10} gene copies) and the ARGs (Δ) vs. iDNA. Sulfonamides ($\Delta sul1$ = 0.94 $\pm$ 0.33; $\Delta sul2$ = 1.11 $\pm$ 0.32 log_{10} gene copies mL^{-1}) and β-lactamase (Δbla_{CTXM} = 1.92 $\pm$ 0.25 log_{10} gene copies mL^{-1}) ARGs and the integrase type I ($\Delta intI1$ = 1.32 $\pm$ 0.38 log_{10} gene copies mL^{-1}) MGE were significantly lesser in the free-floating exDNA than in the iDNA. Conversely, the macrolides ($\Delta ermB$ = 0.27 $\pm$ 0.24 log_{10} gene copies) and fluoroquinolone ($\Delta qnrS$ <0.1 log_{10} gene copies) ARGs displayed similar copy numbers in both iDNA and exDNA.

Macrolide resistance genes (*ermB*) have been described to be embedded in transposon-like elements such as Tn551, Tn552, Tn4001, or Tn4003 conferring resistance to macrolide-lincosamide-streptogramin B (MLS) [57]. Fluoroquinolone resistance genes have been reported to be plasmid-borne since 1998 [58]. Most of the *qnr* genes have been detected in *Entereobacteriaceae*, with the *qnrS* gene prevalent both in environmental strains [59] and in non-conjugative plasmids

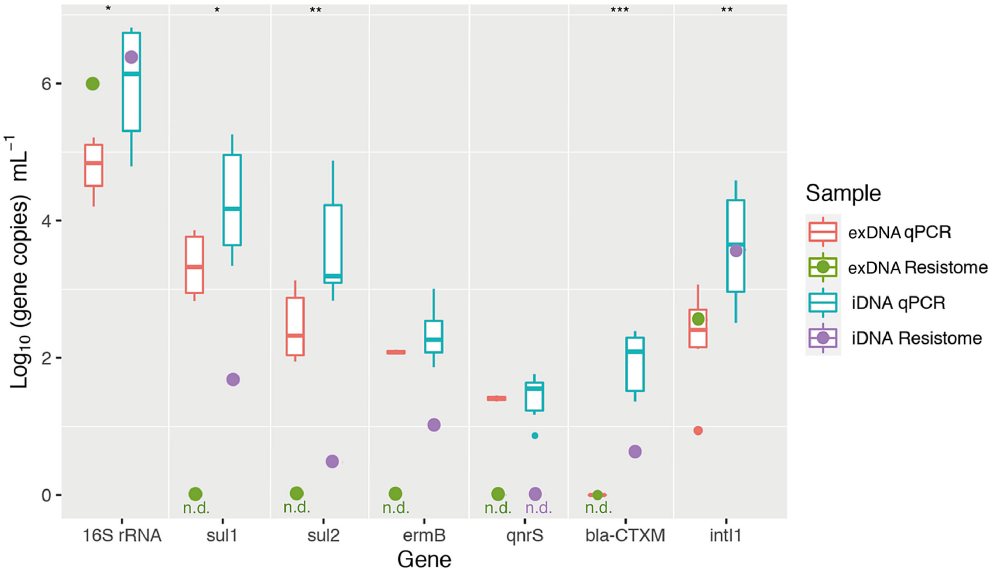

Figure 3.6: Comparison of the qPCR analysis of the selected panel of ARGs and MGEs from the free-floating exDNA and the iDNA fractions of effluent water and of the number of primary aligned metagenomic reads for these genes present in the resistome of exDNA and iDNA of activated sludge. Values are displayed as Log_{10} gene copies mL^{-1} of the 16S rRNA gene, five antibiotic resistance genes (*sul1, sul2, ermB, qnrS and* bla_{CTXM}), and one mobile genetic element (*intI1*). The significance levels of the differences between exDNA and iDNA levels are displayed as $p<0.05$ (*), $p<0.005$ (**), $p<0.0005$ (***). The n.d. labels in the resistome analyses indicate that the primary aligned reads were not detected by metagenomics.

harbouring mob genes allowing their mobilization [60]. These ARGs are commonly found in MGEs forming the principal subsystem component of the exDNA fraction (**Figure** 3.7).

The genes encoding resistance to sulfonamides (*sul1* and *sul2*) were the most abundant ARGs in both iDNA and exDNA fractions from the selected panel. Sulfonamides account within the most systemically used antibiotics in hospitals in The Netherlands [61]. Such a high level of *sul* genes meets with other studies that have measured ARGs from total DNA extracted out of activated sludge biomasses and effluent water [62, 63]. Lower number of ARGs copies have already been observed in the exDNA fraction when compared to the iDNA from sludge using a protocol for extracting exDNA from marine sediments [5, 64].

Here, we made a key contribution to enable the direct comparison of the molecular compositions of the free-floating exDNA and iDNA fractions of wastewater environments, as a relevant milestone within the problematic of ARGs and MGEs in environmental and public health protection. Lower copy numbers measured in the exDNA fraction can arise from different possible causes. It may be considered that DNA fragments of the genes are less released outside cells, thus interrogating whether *sul1/2* and bla_{CTXM} genes are less transferred on plasmids thus less

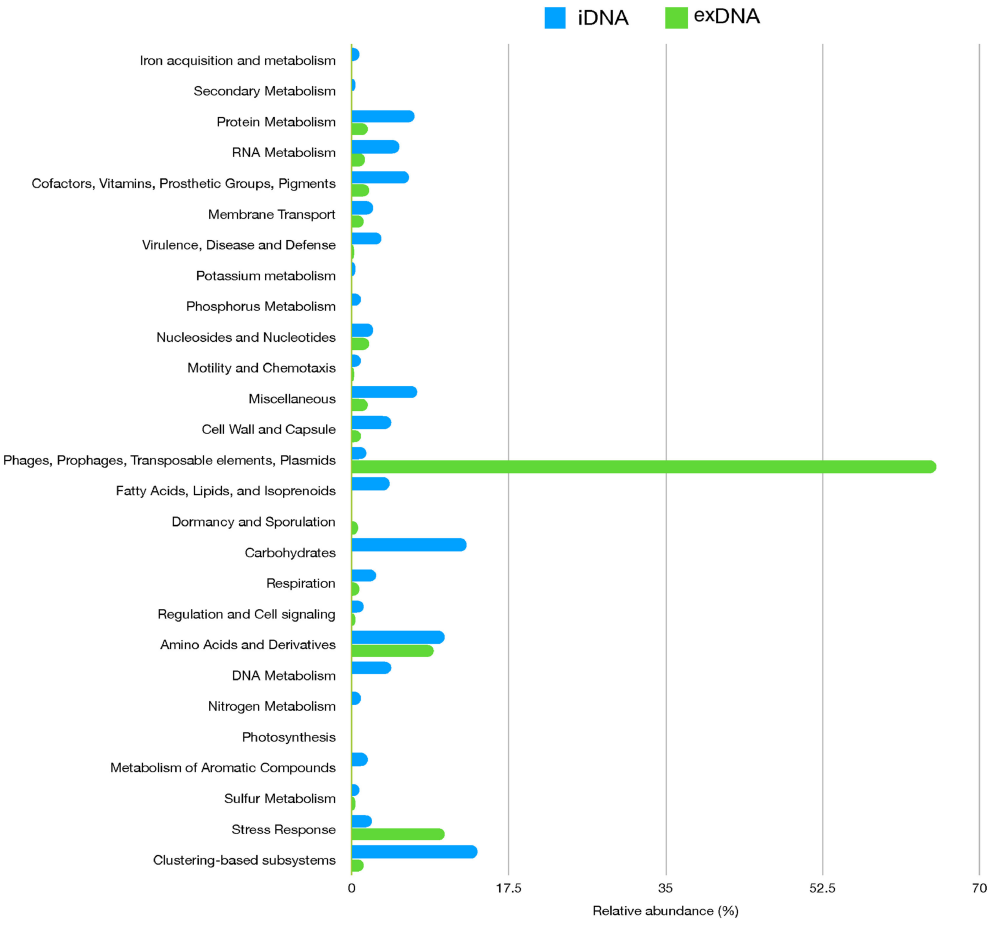

Figure 3.7: Subsystem classification of the functional genes identified from the metagenome of the free-floating extracellular DNA fraction (exDNA, green) fraction and the intracellular DNA (iDNA, blue) fraction using MG-RAST for mapping and computation of relative abundances (%).

mobile. It can also suggest that iDNA, when released because of cell decay or active release mechanisms, may be degraded by nucleases present in both DNA fractions. Another possibility is the degradation of DNA fragments that carried these genes by microorganisms, but DNA degradation by microbes is likely not specific at gene level. All in all, the reason for this difference between compositions of iDNA and free-floating exDNA fractions needs to be investigated in more detail. Our isolation method provides the analytical key to investigate it.

What it is highly remarkable is that ARGs can still be detected in significant amounts (100-1000 gene copies mL^{-1}) in the exDNA fraction that is fully exposed to the environment. Surface water is considered as an indicator for low ARG level and hospitals effluent water as high ARG level. An ARG level of less than 1000

gene copies mL^{-1} is considered low and an ARG level of more than 104 gene copies mL^{-1} is considered high [65, 66]. However, all these indicatory ARG levels are based on analyses of intracellular DNA. Obtaining 100-1000 gene copies mL^{-1} in the free-floating extracellular DNA sample, where DNA is exposed to all kind of nucleases and environmental hazards, would be considered as high. A plausible explanation of why exDNA persists in aqueous environments is that it is clothed with a mesh of extracellular proteins (demonstrated here with the proteinase K post-treatments). Other causes of protection against degradation by nucleases can relate to exDNA being locked within organic and inorganic aggregates, adsorbed onto mineral matrices, or integrated into viral genomes [7].

The qPCR data obtained on the selected panel of ARGs and MGEs measured from effluent water are displayed in **Figure** 3.6 together with the number of primary metagenomic reads retrieved for these genes from the resistome of free-floating exDNA isolated from activated sludge (see next section). Although the two types of analyses cannot be directly compared since made on effluent water and activated sludge, respectively, this comparison was performed to verify if there was a quantitative tendency between DNA fractions followed by both detection methods (qPCR and metagenomics). The resistome dataset showed a lower log_{10} number of ARG reads when compared to qPCR data. This is due to lower sensitivity of metagenomics when compared to PCR-based methods on wastewater samples [67]. The integration of the results presented here with previous studies highlights the need to combine molecular methods for an accurate analysis of ARGs and MGEs in wastewater. Metagenomics provides high resolution on the diversity of genes and their alleles. qPCR provides high sensitivity for the detection of ARGs and MGEs. Strong new insight on the separation and comparison of free-floating exDNA fractions from complex environmental biological samples is therefore provided here.

Genes displayed in **Figure** 3.6 (*sul1, sul2, ermB, qnrS and* bla_{CTXM}) corresponded to less than 2% of the total primary ARGs reads found in the iDNA resistome. From the activated sludge resistome, only the number of reads of the universal *16S rRNA* and ubiquitous *intI1* genes were in line with the ones measured by qPCR in both DNA fractions. When the trend in gene copies per mL was compared, iDNA fractions contained a higher number of primary aligned reads from the selected panel of genes than the exDNA fraction. This was similar to qPCR results. Differences on the comparison results can be explained by the databases used as the resistome analysis fully depends on the databases selected for gene mapping. The resistome analysis was also done with ResFinder (**Table** S.5). Results suggested that using a curated database did not modify the results obtained. ResFinder is also not fully complete as *sul1, sul2, ermB, qnrS* nor bla_{CTXM} genes were not found. ARG sequences that are highly dissimilar to reference sequences deposited in databases cannot be detected, thus not resulting in hits and not appearing in final results [68]. Harmonization of both molecular methods and databases are needed to advance the field.

Metagenomics allowed the comparison of the resistome, mobilome, and microbiome between iDNA and exDNA

The quantity and quality of the exDNA and iDNA templates that were separately retrieved from the complex activated sludge enabled a functional analysis of the different DNA fractions (**Figure** 3.7) and a high-throughput metagenomics analysis of their mobilome, resistome, and microbiome compositions (**Figure** 3.8). The number of reads used for metagenomic analysis are summarized in **Tables** S.6-S.7. The absolute read counts of specific genes were then translated into relative abundances when normalized by the total number of primary aligned reads after samclip filtration per database selected.

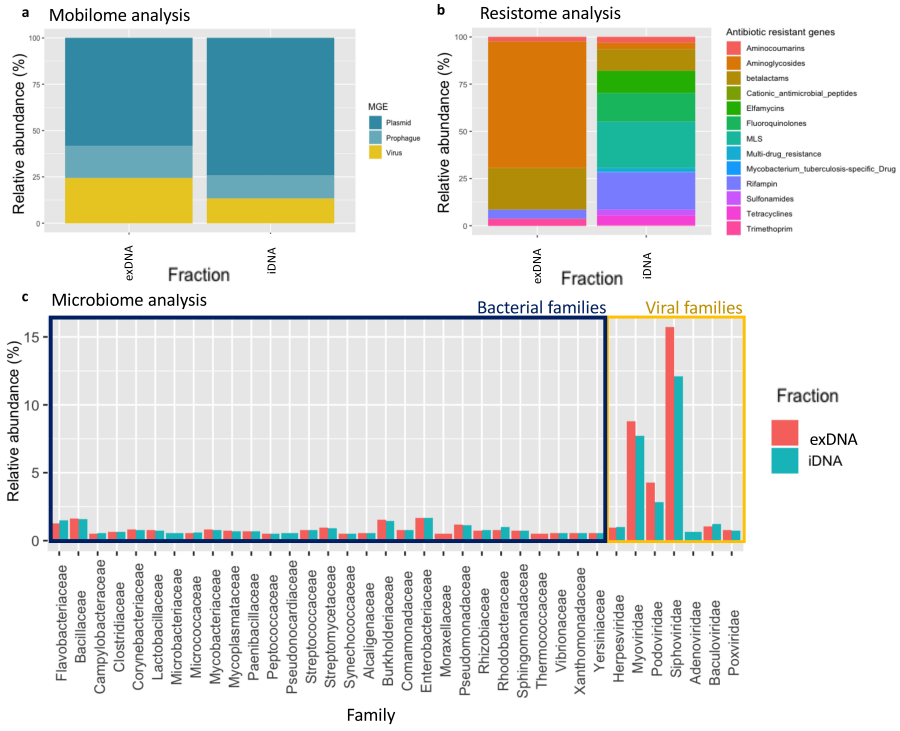

Figure 3.8: Metagenome analysis from exDNA and iDNA fractions obtained from an activated sludge sample **(a)** Mobilome relative abundance. **(b)** Resistome relative abundance. **(c)** Microbiome relative abundance showing bacterial and viral families, whose population composition was >0.5%. Relative abundance (%) states as the ratio between the number of gene target hits divided by the number of total hits from a specific analysis category (mobilome, resistome, or microbiome).

Functional analysis and mobilome profiling of exDNA and iDNA fractions

Figure 3.7 displays the functional assignment (level 1 of subsystem) of metagenomics sequences. From the exDNA and iDNA metagenomes, approximately 40% and 50% of the total predicted proteins with known functions (808'680 and 6'771'570), respectively, matched with the subsystems database on the MG-RAST server [48].

Interestingly, the patterns in the data confirmed that the metagenome of exDNA was predominantly composed of MGEs with phages, prophages, transposable elements and plasmids making 65.1% (526'534 hits) of the sequencing dataset. The same category corresponded to a residual 1.6% (108'713 hits) on the iDNA metagenome. The iDNA fraction showed a heterogeneous distribution, classified mainly by clustering-based subsystems (13.94%, 944'394 hits), carbohydrates (12.8%, 865'220 hits), and amino acids and derivatives (9.13%, 701'175 hits) sublevels, among others. Clustering-based subsystems contain functions such as proteosomes, ribosomes, and recombination-related clusters [69], which are localized in the cytoplasm of microorganisms (i.e., iDNA).

Mobilome results showed that both the free-floating exDNA and the iDNA fractions contained a higher relative abundance of plasmids (58% and 74%, respectively) than viruses and prophages (41% and 26%, respectively) (**Figure** 3.8**a**). In the exDNA fraction, the relative abundance of plasmids was significantly lower than the viruses. This might be explained by extracellular plasmids exposure to and degradation by environmental nucleases. The presence of microorganisms may also enhance the degradation rate of free-floating extracellular DNA plasmids [70]; thus, increasing the relative abundance of viral units in the free-floating extracellular DNA fraction.

MGEs are made of DNA segments that are capable to jump randomly to new locations within a single cell or multiple microorganisms [23]. They include viruses, plasmids, and associated elements such as insertion sequences, transposons, and integrons. Detailed mobilome compositions are summarized in the supplementary material **Table** S.7 and **Figure** S.4 for both free-floating exDNA and iDNA. Integrons, integrative conjugative elements (ICE), and insertion sequences (IS) were analyzed from the exDNA fraction: intI1 (92%) (**Figure** S.4**b**), actinomycete conjugative integrative element (AICE) (35%) and SXT/R391 (30%) (**Figure** S.4**c**), and IS200 (38%) (**Figure** S.4**d**) were the most abundant components in their category, respectively.

Microorganisms use MGEs via HGT as a mechanism to evolve and adapt to new environmental conditions by being subjected to natural selection. Considering that antibiotic concentrations in effluent wastewater and surface waters have increased up to 1 μg L^{-1}in the last years [71], microorganisms can take profit from these mobile genes as an indirect tool to increase their resistance towards antimicrobials. Further research needs to be conducted on the relationship between the MGEs present in the free-floating exDNA fraction of biological systems like wastewater environments and the molecular mechanisms conferring antibiotics resistance.

Overall, the free-floating exDNA was confirmed as a pool of potentially transferrable DNA via HGT mechanisms, since mainly composed of MGEs. These MGEs do not necessarily mobilize ARGs in their structural composition [23] but can contribute to antibiotic resistance acquisition.

Resistome profiling of exDNA and iDNA fractions

We are showing the profile of the resistome of the free-floating exDNA from an activated sludge sample. Resistome results showed more distinct patterns among DNA fractions (Figure 3.8**b**). The free-floating exDNA fraction harbored a total of 12 different ARGs from 5 different antibiotic resistance families. There was a clear relative dominance of aminoglycosides (67%) and β-lactams (22%) resistant genes on the exDNA.

A total of 289 different ARGs from 15 different antibiotic resistance families were found in the iDNA fraction. This matched with the latest work of Jia *et al.* (2020) who detected 297 different genes from 17 different families in water and water filters from a drinking water treatment plant. MLS dominated (24%), followed by rifampin (20%), fluoroquinolones (15.1%), and elfamycins (11.7%) among other resistance genes on the iDNA.

Most of the ARGs are enclosed inside bacterial cells, while some specific types may endure floating or are bound to matrices in activated sludge samples, even if in low quantities. The low amount of ARGs on the free-floating exDNA suggests that natural transformation may not be the main mechanism through which ARG transfer and exchange does occur [5]. However, this smaller amount of extracellular ARGs does not preclude any possibility to be taken up by naturally competent bacteria in complex cultures via transformation processes. It could be discussed whether the occurrence rate is lower in the exDNA fraction because of preferential uptake of exDNA fragments with ARGs.

Microbiome profiling of exDNA and iDNA fractions

Microbiome profiles were more conserved (i.e., both as populations and their relative abundances) between free-floating exDNA and iDNA (**Figure** 3.8**c**). Families found in the extracellular fraction are genomic fragments that at some point have been released from lysed or necropsied cells. These genes are easier to be degraded than plasmid or viral DNA, due to the potential for fragmented double-stranded DNA to be exposed to nucleases. Thus, the exDNA is more likely originating from cell lysis inside the activated sludge rather than immigrating from the influent. Moreover, some studies have suggested that DNA adsorbed to soil or EPS matrices are protected from degradation by environmental nucleases, indicating that genes on plasmid may be better preserved than genomic DNA [9, 73]. In this case, it can be observed that only some specific bacterial and viral families are exclusive from one or another DNA fraction if we consider the 0.5% relative abundance cutoff. Examples are *Microbacteriacae, Pseudonocardiacae*, and

Adenoviridae for the iDNA fraction and *Moraxellaceae* and *Thermococcaceae* for the exDNA (**Figure** 3.8**c**). However, the *Moraxellaceae* family is known as an inductor of activated sludge flocculation [74], being also in the iDNA fraction (0.48%). The same situation was observed with the other bacterial and viral families that were found only in one of the DNA fraction. This meant that no significant differences in populations could be observed at the bacterial family level between the exDNA and iDNA fractions from activated sludge samples. We, therefore, hypothesize that exDNA may originate to some extent from the influent water, but mainly from microbial populations that decayed in the activated sludge tank. Our combined exDNA isolation and characterization method can become an efficient way to track microbial decay phenomena in activated sludge at the population resolution level.

3.4. Conclusions

We aimed to develop a method to isolate and differentially characterize the genetic composition of free-floating exDNA fractions from wastewater. This work led to the following key conclusions:

- The implementation of DEAE chromatography promoted an efficient isolation of free-floating exDNA at high yield and quality from complex matrices of WWTP environments from influent wastewater to activated sludge and effluent water samples.
- qPCR analyses of a panel of selected genes highlighted the presence of ARGs from 1.8 to 3.8 log_{10} copies in the free-floating exDNA fraction. Significant differences were detected between the exDNA and iDNA fractions for the predominant sulfonamides ARGs (*sul1* and *sul2* were 0.93–1.11 log_{10} more abundant in iDNA).
- The metagenomes displayed similar microbiome compositions between exDNA and iDNA fractions, suggesting that a big fraction of free exDNA found in activated sludge may derive from the flocs.
- The mobilomes and resistomes from the exDNA were less rich than on iDNA, but still form a source of MGEs for natural transformation. Interestingly, subsystems classifications showed that the exDNA fraction was mainly composed of MGEs (65.1%). This confirmed the hypothesis that free-floating exDNA is a pool of stable MGEs that can drive HGT and antibiotic resistance.
- Within the field of environmental ecology, free-floating exDNA can serve as a target matrix for biodiversity survey studies. It can help to elucidate the ecological relevance and persistence of pathogenic microorganisms throughout the water sanitation process or to estimate the microbial activity from specific environments [75], among others.

New physical-chemical technologies can be studied for the removal of xenogenetic pollution (specifically ARGs and MGEs) removal from wastewater [76]. High removal of exDNA from effluent water by, e.g., adsorption may allow the discharge of water streams deprived of xenogenetic elements in receiving bodies, thus potentially contributing to reducing the development antibiotic resistant bacteria by transformation processes [1].

Further studies on the conditions promoting HGT in complex biological systems are needed to elucidate the actual natural transformation rate for free-floating exDNA components. Their systematic chromatographic isolation, molecular quantification, and metagenomics profiling will be powerful to generate data useful for xenogenetic risk assessments on ARGs, MGEs, but also residual GMO materials, across urban and natural water systems. It will support measures by water authorities to remove them from wastewater to safeguard environmental and public health.

3.5. Supplementary material

qPCR mix solution and reaction conditions

All ARGs and intI1 qPCR reactions were conducted in 20 µL, including IQTM SYBR green supermix BioRad 1x. Forward and reverse primers, and oligonucleotide probes (when applicable) are summarized in Table S1 and S2. A total of 2 μL of DNA template was added to each reaction, and the reaction volume was completed to 20 μL with DNase/RNase free Water (Sigma Aldrich, UK). All reactions (were performed in a qTOWER3 Real-time PCR machine (Westburg, DE) according to the following PCR cycles: 95ºC for 5 minutes followed by 40 cycles at 95ºC for 15 s and 60ºC for 30 s. The annealing temperature was the same for all the different reactions except for the *sul2* and *sul1* genes. In those cases, the annealing temperatures were 61ºC and 65ºC, respectively.

In order to check the specificity of the reaction, a melting curve was performed from 65 to 95ºC at a temperature gradient of +0.5ºC $(5\ s)^{-1}$. Synthetic DNA fragments (IDT, USA) containing each of the target genes were used as a positive control to create the standard curves. Serial dilutions of gene fragments were performed in sheared salmon sperm DNA 5 µg mL^{-1} (m/v) (Thermofisher, LT) diluted in Tris-EDTA (TE) buffer at pH 8.0. Every sample was analyzed in technical triplicates. Standard curves were included in each PCR plate with at least 6 serial dilutions points and in technical duplicate. An average standard curve based on a standard curve from every run was created for every gene set. Gene concentration values were then calculated from the aforementioned curve.

Table S.1: Genes analyzed by qPCR on exDNA and iDNA fractions obtained from activated sludge and effluent water samples. Genes are classified into three groups of interest: all bacteria (16S rRNA gene), antibiotic resistance genes (ARGs), and mobile genetic element (MGE).

Group	Gene	Function
All bacteria	*16S rRNA*	Proxy to quantify total bacteria
ARGs	*qnrS*	Resistance to quinolone
	sul1	Resistance to sulphonamides
	sul2	Resistance to sulphonamides
	ermB	Resistance to macrolides
	bla_{CTXM}	Resistance to extended spectrum β-lactams
MGE	*intI1*	Integrase of type I interns

Table S.2: *16S rRNA*, ARGs and MGE synthetic DNA fragments ued from ResFinder to generate standard curves for qPCR.

Gene	Sequence
16S rRNA	*ACTCCTACGGGAGGCAGCAGTGGGGAATATTGCACAATGGGCGCAA GCCTGATGCAGCCATGCCGCGTGTATGAAGAAGGCCTTCGGGTTG TAAAGTACTTTCAGCGGGGAGGAAGGGAGTAAAGTTAATACCTTTGCT CATTGACGTTACCCGCAGAAGAAGCACCGGCTAACTCCGTGCCAGCAGCCGCGGTAAT*
qnrS	*GACGTGCTAACTTGCGTGATACGACATTCGTCAACTGCAAGTTCATTGAACAGGGTG ATATCGAAGGCTGCCACTTTGATGTCGCAGATCTTCGTGATGCA AGTTTCCAACAATGCCA*
intI1	*GCCTTGATGTTACCCGAGAGCTTGGCACCCAGCCTGCGCGAGCAGCTGTCGCGTGCA CGGGCATGGTGGCTGAAGGACCAGGCCGAGGGCCGCAGCGGCGTTGCGCTTC CCGACGCCCTTGAGCGGAAGTATCCGCGCGCCGGGCATTCCTGGCCGTGGTTC TGGGTTTTTGCGCAGCACACGCATTCGACCGATC*
sul1	*CGCACCGGAAACATCGCTGCACGTGCTGTCGAACCTTCAAAAGCTGAAGTCGGCGTTGG GGCTTCCGCTATTGGTCTCGGTGTCGCGGAAATCCTTCTTGGGCGCCACCGTTGGC CTTCCTGTAAAGGATCTGGGTCCAGCGAGCCTTGCGGCGGAACTTCA*
sul2	*TGGAGGCCGGTATCTGGCGCCAGACGCAGCCATTGCGCAGGCGCGTAAGCTGATGGCCG AGGGGGCAGATGTGATCGACCTCGGTCCGGCATCCAGCAATCCCGACGCCGCGCCTG TTTCGTCCGACACAGAAATCGCGCGTATCGCGCCGGTGCTGGACGCGCTCAAGGCAGA TGGCATTCCCG*
ermB	*AAAACTTACCCGCCATACCACAGATGTTCCAGATAAATATTGGAAGCTATATACGTAC TTTGTTTCAAAATGG GTCAATCGAGAATATCGTCAACTGTTTACTAAAAATCAGTT TCATCAAGCAATGAAACACGCCAAA*
***bla**$_{CTXM}$*	*CTATGGCACCACCAACGATATCGCGGTGATCTGGCCAAAAGATCGTGCGCCGCTGATTC TGGTCACTTACTTCACCCAGCCTCAACCTAAGGCAGAAAGCCGT*

Table S.3: Primers used for qPCR.

Gene	Forward Primer (5' → 3')	Reverse Primer (5' → 3')
16S rRNA	ACTCCTACGGGAGGCAGCAG	ATTACCGCGGCTGCTGG
qnrS	GACGTGCTAACTTGCGTGAT	TGGCATTGTTGGAAACTTG
intI1	GATCGGTCGAATGCGTGT	GCCTTGATGTTACCCGAGAG
sul1	CGCACCGGAAACATCGCTGCAC	TGAAGTTCCGCCGCAAGGCTCG
sul2	TCCGGTGGAGGCCGGTATCTGG	CGGGAATGCCATCTGCCTTGAG
ermB	AAAACTTACCCGCCATACCA	TTTGGCGTGTTTCATTGCTT
***bla**$_{CTXM}$*	CTATGGCACCACCAACGATA	ACGGCTTTCTGCCTTAGGTT

Table S.4: DNA concentration with and without DNAse I treatment.

Biological replicate	iDNA w/o DNase I (ng/µL)	iDNA with DNase I (ng/µL)	Volume (µL)
1	91.2	67.2	50
2	87.2	58.6	50
3	110	80	50

Table S.5: Number of primary aligned reads when the resistome was analyzed using the curated ResFinder database.

Gene	Primary Aligned Reads
$AADA6_{1\,A}F140629$	6
$APH(3')\text{-}IA_{9\,E}U722351$	1
$APH(4)\text{-}IA_{1\,V}01499$	1
$BLAOXA\text{-}198_{1\,H}Q634775$	1
$BLATEM\text{-}116_{1\,A}Y425988$	1
$BLATEM\text{-}52C_{2\,E}F141186$	1
$DFRA1_{3\,G}U726913$	3

Table S.6: Comparison of the number of sequencing reads identified as ARGs using MEGARes and as MGEs unsing ACLAME from the metagenomic datasets of the free-floating extracellular DNA (exDNA) and intracellular DNA (iDNA) fractions from the activated sludge. The read counts were used to compute relative abundances of ARGs and MGEs in the metagenomes. iDNA was extracted after treatment with DNAse I to remove remaining matrix-bound DNA: the metagenomics reads of the iDNA fraction relate to the intracellular content per se.

Number of sequencing reads from metagenome libraries	**Free-floating exDNA (read count)**	**iDNA (read count)**
Sequencing output		
Number of raw reads out of sequencer	14'127'626	14'788'250
Identification of ARG sequences using MEGARes 2.0[a]		
Number of MEGARes primary aligned reads before samclip [b]	188	9'725
Number of MEGARes primary aligned reads after samclip [b]	82	1'571
Identification of MGE sequences using ACLAME[c]		
Number of ACLAME primary aligned reads before samclip[b]	546'007	1'183'308
Number of ACLAME primary aligned reads after samclip[b]	180'860	315'225

[a] MEGARes is an antimicrobial database for high-throughput sequencing.
[b] Samclip is a bioinformatics tool designed to remove soft and hard clipped alignments.
[c] ACLAME is a database dedicated to the collection and classification of mobile genetic elements (MGEs).

Table S.7: Mobilome number of primary reads after INTEGRALL, ISfinder and ICEberg alignment.

Step	**exDNA**	**iDNA**
Number of INTEGRALL primary aligned	411	4'586
Number of ISfinder primary aligned	140	20'046
Number of ICEberg (ICE) primary aligned	77	9'550

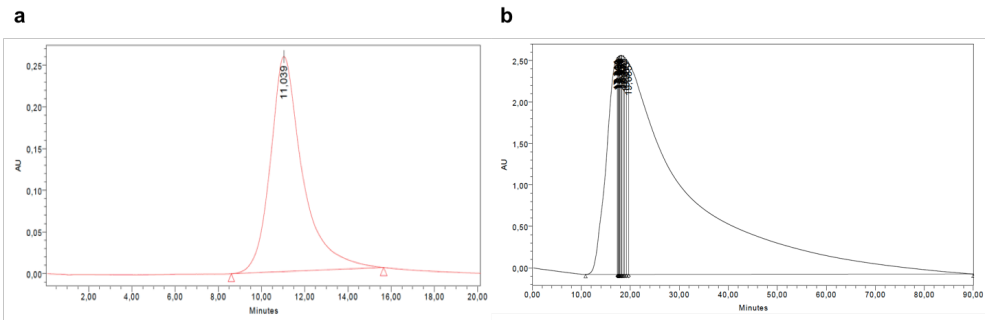

Figure S.1: Control chromatogram (λ=260 nm) with **(a)** solution containing pure plasmid pHT01 (0.73 ng μL^{-1}, 10 mL) **(b)** Raw eDNA from filtered activated sludge water sample (900 mL) chromatogram (λ=260 nm). The DEAE column showed high selectivity and efficiency towards nucleic acids from water samples.

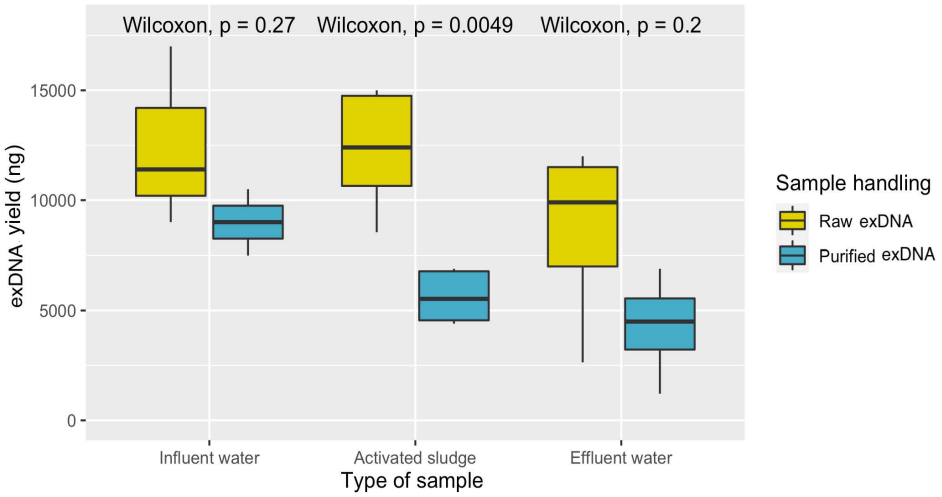

Figure S.2: Effect of purification on exDNA yields depending on different water qualities: influent water, activated sludge and effluent treated water. Raw exDNA refers to exDNA precipitated with ethanol after eluting from the chromatography column. Purified exDNA refers to precipitated exDNA treated with proteinase K and purified through the commercial DNA purification kit. The number of samples per matrix was the following: n(influent water) = 3, n(activated sludge) = 6, n(effluent water) = 3.

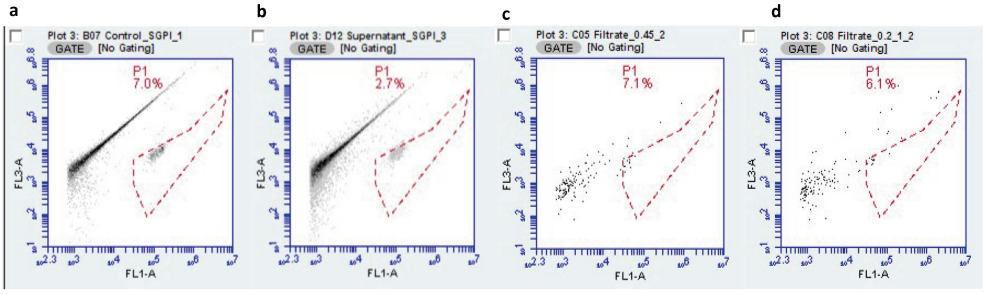

Figure S.3: Dot-plots of fow cytometry data representing **(a)** the control sample, **(b)** supernatant after centrifugation, **(c)** filtrate after 0.45 µm filtration step and **(d)** filtrate after 0.2 μm filtration step. Dot-plots of green fluorescence (FL1; 533 nm), and red fluorescence (FL3;>670 nm) allowed for optimal distinction between the stained microbial cells and instrument noise or sample background. Exactlly the same gates were used for all measurements.

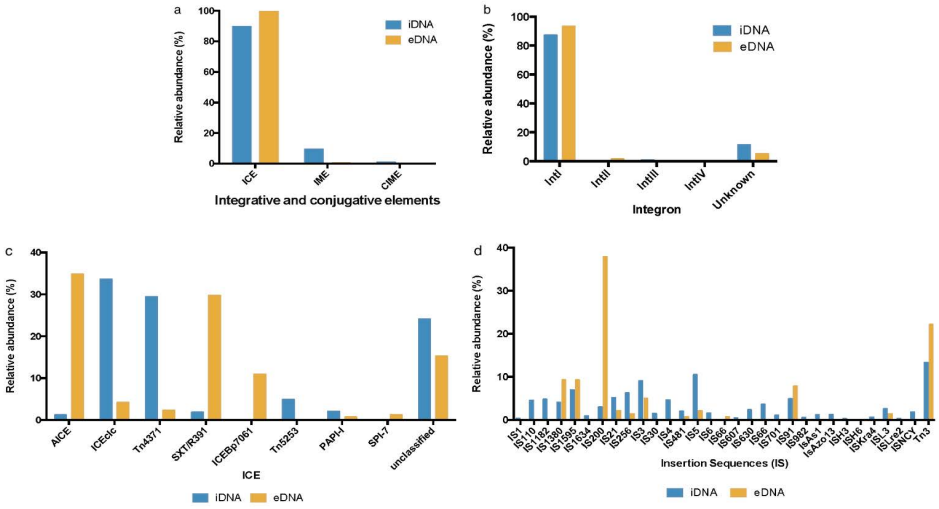

Figure S.4: Mobilome analysis from exDNA and iDNA fractions obtained from an activated sludge sample **(a)** Integrative, conjugative (ICE), mobilizable (IME) and cis-Mobilizable elements (CIME) relative abundance. **(b)** Integrons relative abundance. **(c)** Integrative conjugative elements (ICE) relative abundance and **(d)** insertion sequences relative abundance.

Bibliography

[1] M. R. Gillings, M. Westoby, and T. M. Ghaly. "Pollutants That Replicate: Xenogenetic DNAs". In: *Trends in Microbiology* 26.12 (2018), pp. 975–977. ISSN: 18784380. DOI: 10.1016/j.tim.2018.08.003. URL: http://dx.doi.org/10.1016/j.tim.2018.08.003.

[2] T. U. Berendonk, C. M. Manaia, C. Merlin, D. Fatta-Kassinos, E. Cytryn, F. Walsh, H. Bürgmann, H. Sørum, M. Norström, M. N. Pons, N. Kreuzinger, P. Huovinen, S. Stefani, T. Schwartz, V. Kisand, F. Baquero, and J. L. Martinez. "Tackling antibiotic resistance: The environmental framework". In: *Nature Reviews Microbiology* 13.5 (2015), pp. 310–317. ISSN: 17401534. DOI: 10.1038/nrmicro3439.

[3] H. Bürgmann, D. Frigon, W. H Gaze, C. M Manaia, A. Pruden, A. C. Singer, B. F Smets, and T. Zhang. "Water and sanitation: an essential battlefront in the war on antimicrobial resistance". In: *FEMS Microbiology Ecology* 94.9 (Sept. 2018), pp. 1–14. ISSN: 1574-6941. DOI: 10.1093/femsec/fiy101.

[4] A. Pruden, D. G. Joakim Larsson, A. Amézquita, P. Collignon, K. K. Brandt, D. W. Graham, J. M. Lazorchak, S. Suzuki, P. Silley, J. R. Snape, E. Topp, T. Zhang, and Y. G. Zhu. "Management options for reducing the release of antibiotics and antibiotic resistance genes to the environment". In: *Environmental Health Perspectives* 121.8 (2013), pp. 878–885. ISSN: 00916765. DOI: 10.1289/ehp.1206446.

[5] Y. Zhang, D. D. Snow, D. Parker, Z. Zhou, and X. Li. "Intracellular and extracellular antimicrobial resistance genes in the sludge of livestock waste management structures". In: *Environmental Science and Technology* 47.18 (2013), pp. 10206–10213. ISSN: 0013936X. DOI: 10.1021/es401964s. URL: https://pubs.acs.org/sharingguidelines.

[6] S. Zhou, Y. Zhu, Y. Yan, W. Wang, and Y. Wang. "Deciphering extracellular antibiotic resistance genes (eARGs) in activated sludge by metagenome". In: *Water Research* 161 (2019), pp. 610–620. ISSN: 18792448. DOI: 10.1016/j.watres.2019.06.048. URL: https://doi.org/10.1016/j.watres.2019.06.048.

[7] A. Torti, M. A. Lever, and B. B. Jørgensen. "Origin, dynamics, and implications of extracellular DNA pools in marine sediments". In: *Marine Genomics* 24 (2015), pp. 185–196. ISSN: 18747787. DOI: 10.1016/j.margen.2015.08.007. URL: http://dx.doi.org/10.1016/j.margen.2015.08.007.

[8] P. F. Thomsen and E. Willerslev. "Environmental DNA - An emerging tool in conservation for monitoring past and present biodiversity". In: *Biological Conservation* 183 (2015), pp. 4–18. ISSN: 00063207. DOI: 10.1016/j.biocon.2014.11.019. URL: http://dx.doi.org/10.1016/j.biocon.2014.11.019.

[9] C. Corinaldesi, M. Tangherlini, E. Manea, and A. Dell'Anno. "Extracellular DNA as a genetic recorder of microbial diversity in benthic deep-sea ecosystems". In: *Scientific Reports* 8.1 (2018), pp. 1–9. ISSN: 20452322. DOI: 10.1038/s41598-018-20302-7.

[10] D. M. Dominiak, J. L. Nielsen, and P. H. Nielsen. "Extracellular DNA is abundant and important for microcolony strength in mixed microbial biofilms". In: *Environmental Microbiology* 13.3 (2011), pp. 710–721. ISSN: 14622912. DOI: 10.1111/j.1462-2920.2010.02375.x.

[11] P. Rusanowska, A. Cydzik-Kwiatkowska, and I. Wojnowska-Baryła. "Microbial Origin of Excreted DNA in Particular Fractions of Extracellular Polymers (EPS) in Aerobic Granules". In: *Water, Air, and Soil Pollution* 230.8 (2019). ISSN: 15732932. DOI: 10.1007/s11270-019-4248-0.

[12] D. G. Weissbrodt, T. R. Neu, U. Kuhlicke, Y. Rappaz, and C. Holliger. "Assessment of bacterial and structural dynamics in aerobic granular biofilms". In: *Frontiers in Microbiology* 4.JUL (2013), pp. 1–18. ISSN: 1664302X. DOI: 10.3389/fmicb.2013.00175.

[13] L. Tang, A. Schramm, T. R. Neu, N. P. Revsbech, and R. L. Meyer. "Extracellular DNA in adhesion and biofilm formation of four environmental isolates: A quantitative study". In: *FEMS Microbiology Ecology* 86.3 (2013), pp. 394–403. ISSN: 01686496. DOI: 10.1111/1574-6941.12168.

[14] V. V. Tetz and G. V. Tetz. "Effect of extracellular DNA destruction by DNase I on characteristics of forming biofilms". In: *DNA and Cell Biology* 29.8 (2010), pp. 399–405. ISSN: 10445498. DOI: 10.1089/dna.2009.1011.

[15] J. Wu and C. Xi. "Enzymatic method for extracting extracellular DNA in biofilm matrix". In: *Cold Spring Harbor Protocols* 5.7 (2010). ISSN: 15596095. DOI: 10.1101/pdb.prot5456.

[16] X. p. Guo, Y. Yang, D. p. Lu, Z. s. Niu, J. n. Feng, Y. r. Chen, F. y. Tou, E. Garner, J. Xu, M. Liu, and M. F. Hochella. "Biofilms as a sink for antibiotic resistance genes (ARGs) in the Yangtze Estuary". In: *Water Research* 129 (2018), pp. 277–286. ISSN: 18792448. DOI: 10.1016/j.watres.2017.11.029. URL: https://doi.org/10.1016/j.watres.2017.11.029.

[17] P. He, Y. Zhou, L. Shao, J. Huang, Z. Yang, and F. Lü. "The discrepant mobility of antibiotic resistant genes: Evidence from their spatial distribution in sewage sludge flocs". In: *Science of the Total Environment* 697 (2019), p. 134176. ISSN: 18791026. DOI: 10.1016/j.scitotenv.2019.134176. URL: https://doi.org/10.1016/j.scitotenv.2019.134176.

[18] M. Nagler, H. Insam, G. Pietramellara, and J. Ascher-Jenull. "Extracellular DNA in natural environments: features, relevance and applications". In: *Applied Microbiology and Biotechnology* 102.15 (2018), pp. 6343–6356. ISSN: 14320614. DOI: 10.1007/s00253-018-9120-4.

[19] H. C. Flemming and J. Wingender. "The crucial role of extracellular polymeric substances in biofilms". In: *Nature Reviews Microbiology* 8.9 (2010), pp. 623–633. ISSN: 17401526. DOI: 10.1038/nrmicro2415. URL: http://dx.doi.org/10.1038/nrmicro2415.

[20] R. T. Merod and S. Wuertz. "Extracellular polymeric substance architecture influences natural genetic transformation of Acinetobacter baylyi in biofilms". In: *Applied and Environmental Microbiology* 80.24 (2014), pp. 7752–7757. ISSN: 10985336. DOI: 10.1128/AEM.01984-14.

[21] L. Karygianni, Z. Ren, H. Koo, and T. Thurnheer. "Biofilm Matrixome: Extracellular Components in Structured Microbial Communities". In: *Trends in Microbiology* 28.8 (2020), pp. 668–681. ISSN: 18784380. DOI: 10.1016/j.tim.2020.03.016. URL: https://doi.org/10.1016/j.tim.2020.03.016.

[22] J. P. Claverys, B. Martin, and P. Polard. "The genetic transformation machinery: Composition, localization, and mechanism". In: *FEMS Microbiology Reviews* 33.3 (2009), pp. 643–656. ISSN: 01686445. DOI: 10.1111/j.1574-6976.2009.00164.x.

[23] T. S. Jørgensen, A. S. Kiil, M. A. Hansen, S. J. Sørensen, and L. H. Hansen. "Current strategies for mobilome research". In: *Frontiers in Microbiology* 5.DEC (2014), pp. 1–6. ISSN: 1664302X. DOI: 10.3389/fmicb.2014.00750.

[24] S. Domingues, K. M. Nielsen, and G. J. da Silva. "Various pathways leading to the acquisition of antibiotic resistance by natural transformation". In: *Mobile Genetic Elements* 2.6 (2012), pp. 257–260. ISSN: 2159-256X. DOI: 10.4161/mge.23089.

[25] D. Calderón-Franco, Q. Lin, M. C. M. van Loosdrecht, B. Abbas, and D. G. Weissbrodt. "Anticipating Xenogenic Pollution at the Source : Impact of Sterilizations on DNA Release From Microbial Cultures". In: *Frontiers in Bioengineering and Biotechnology* 8.March (2020), pp. 1–13. DOI: 10.3389/fbioe.2020.00171.

[26] D. N. Wang, L. Liu, Z. G. Qiu, Z. Q. Shen, X. Guo, D. Yang, J. Li, W. L. Liu, M. Jin, and J. W. Li. "A new adsorption-elution technique for the concentration of aquatic extracellular antibiotic resistance genes from large volumes of water". In: *Water Research* 92 (2016), pp. 188–198. ISSN: 18792448. DOI: 10.1016/j.watres.2016.01.035.

[27] M. Nagler, S. M. Podmirseg, G. W. Griffith, H. Insam, and J. Ascher-Jenull. "The use of extracellular DNA as a proxy for specific microbial activity". In: *Applied Microbiology and Biotechnology* 102.6 (2018), pp. 2885–2898. ISSN: 14320614. DOI: 10.1007/s00253-018-8786-y. URL: https://doi.org/10.1007/s00253-018-8786-y.

[28] Q. B. Yuan, Y. M. Huang, W. B. Wu, P. Zuo, N. Hu, Y. Z. Zhou, and P. J. Alvarez. "Redistribution of intracellular and extracellular free & adsorbed antibiotic resistance genes through a wastewater treatment plant by an enhanced extracellular DNA extraction method with magnetic beads". In: *Environment International* 131.April (2019), p. 104986. ISSN:

18736750. DOI: 10.1016/j.envint.2019.104986. URL: https://doi.org/10.1016/j.envint.2019.104986.

[29] C. Katevatis, A. Fan, and C. M. Klapperich. "Low concentration DNA extraction and recovery using a silica solid phase". In: *PLoS ONE* 12.5 (2017), pp. 1–14. ISSN: 19326203. DOI: 10.1371/journal.pone.0176848.

[30] K. Ikuma and C. R. Rehmann. "Importance of extracellular DNA in the fate and transport of antibiotic resistance genes downstream of a wastewater treatment plant". In: *Environmental Engineering Science* 37.2 (2020), pp. 164–168. ISSN: 15579018. DOI: 10.1089/ees.2019.0319.

[31] M. Krajacic, M. Ravnikar, A. Štrancar, and I. Gutiérrez-Aguirre. "Application of monolithic chromatographic supports in virus research". In: *Electrophoresis* 38.22-23 (2017), pp. 2827–2836. ISSN: 15222683. DOI: 10.1002/elps.201700152.

[32] D. Moore and D. Dowhan. "Purification and Concentration of DNA". In: *Current Protocols in Molecular Biology* (2002).

[33] L. Boulos, M. Prévost, B. Barbeau, J. Coallier, and R. Desjardins. "LIVE/DEAD(®) BacLight(TM): Application of a new rapid staining method for direct enumeration of viable and total bacteria in drinking water". In: *Journal of Microbiological Methods* 37.1 (1999), pp. 77–86. ISSN: 01677012. DOI: 10.1016/S0167-7012(99)00048-2.

[34] F. Hammes, M. Berney, Y. Wang, M. Vital, O. Köster, and T. Egli. "Flow-cytometric total bacterial cell counts as a descriptive microbiological parameter for drinking water treatment processes". In: *Water Research* 42.1-2 (2008), pp. 269–277. ISSN: 00431354. DOI: 10.1016/j.watres.2007.07.009.

[35] I. Pinel, M. D.H., J. Vrouwenvelder, and M. Van Loosdrecht. "Bacterial community dynamics and disinfection impact in cooling water systems". In: *Water Research* 172 (2020), p. 115505. ISSN: 00431354. DOI: 10.1016/j.watres.2020.115505. URL: https://linkinghub.elsevier.com/retrieve/pii/S0043135420300415.

[36] E. I. Prest, F. Hammes, S. Kötzsch, M. C. van Loosdrecht, and J. S. Vrouwenvelder. "Monitoring microbiological changes in drinking water systems using a fast and reproducible flow cytometric method". In: *Water Research* 47.19 (2013), pp. 7131–7142. ISSN: 00431354. DOI: 10.1016/j.watres.2013.07.051.

[37] R. Pallares-Vega, H. Blaak, R. van der Plaats, A. M. de Roda Husman, L. Hernandez Leal, M. C. van Loosdrecht, D. G. Weissbrodt, and H. Schmitt. "Determinants of presence and removal of antibiotic resistance genes during WWTP treatment: A cross-sectional study". In: *Water Research* 161 (2019), pp. 319–328. ISSN: 18792448. DOI: 10.1016/j.watres.2019.05.100. URL: https://doi.org/10.1016/j.watres.2019.05.100.

[38] L. Ma, B. Li, X. T. Jiang, Y. L. Wang, Y. Xia, A. D. Li, and T. Zhang. "Catalogue of antibiotic resistome and host-tracking in drinking water deciphered by a large scale survey". In: *Microbiome* 5.1 (2017), p. 154. ISSN: 20492618. DOI: 10.1186/s40168-017-0369-0. URL: https://www.ncbi.nlm.nih.gov/pmc/articles/PMC5704573/pdf/40168_2017_Article_369.pdf.

[39] S. Andrews. *FastQC: a quality control tool for high throughput sequence data.* 2010. URL: http://www.bioinformatics.babraham.ac.uk/projects/fastqc.

[40] A. M. Bolger, M. Lohse, and B. Usadel. "Trimmomatic: A flexible trimmer for Illumina sequence data". In: *Bioinformatics* 30.15 (2014), pp. 2114–2120. ISSN: 14602059. DOI: 10.1093/bioinformatics/btu170.

[41] H. Li. "Aligning sequence reads, clone sequences and assembly contigs with BWA-MEM". In: 00.00 (2013), pp. 1–3. URL: http://arxiv.org/abs/1303.3997.

[42] D. Kim, L. Song, F. P. Breitwieser, and S. L. Salzberg. "Centrifuge: rapid and accurate classifica3on of metagenomic sequences". In: *bioRxiv* 26.12 (2016), p. 054965. ISSN: 1088-9051. DOI: 10.1101/054965. URL: http://www.ncbi.nlm.nih.gov/pubmed/27852649%0Ahttp://www.pubmedcentral.nih.gov/articlerender.fcgi?artid=PMC5131823%0Ahttp://www.biorxiv.org/content/early/2016/05/25/054965.abstract.

[43] R. Leplae, G. Lima-Mendez, and A. Toussaint. "ACLAME: A CLAssification of mobile genetic elements, update 2010". In: *Nucleic Acids Research* 38.SUPPL.1 (2009), pp. 57–61. ISSN: 03051048. DOI: 10.1093/nar/gkp938.

[44] M. Liu, X. Li, Y. Xie, D. Bi, J. Sun, J. Li, C. Tai, Z. Deng, and H. Y. Ou. "ICEberg 2.0: An updated database of bacterial integrative and conjugative elements". In: *Nucleic Acids Research* 47.D1 (2019), pp. D660–D665. ISSN: 13624962. DOI: 10.1093/nar/gky1123.

[45] P. Siguier, J. Filée, and M. Chandler. "Insertion sequences in prokaryotic genomes". In: *Current Opinion in Microbiology* 9.5 (2006), pp. 526–531. ISSN: 13695274. DOI: 10.1016/j.mib.2006.08.005.

[46] A. Moura, M. Soares, C. Pereira, N. Leitão, I. Henriques, and A. Correia. "INTEGRALL: A database and search engine for integrons, integrases and gene cassettes". In: *Bioinformatics* 25.8 (2009), pp. 1096–1098. ISSN: 13674803. DOI: 10.1093/bioinformatics/btp105.

[47] H. Li, B. Handsaker, A. Wysoker, T. Fennell, J. Ruan, N. Homer, G. Marth, G. Abecasis, and R. Durbin. "The Sequence Alignment/Map format and SAMtools". In: *Bioinformatics* 25.16 (2009), pp. 2078–2079. ISSN: 13674803. DOI: 10.1093/bioinformatics/btp352.

[48] F. Meyer, D. Paarmann, M. D'Souza, R. Olson, E. M. Glass, M. Kubal, T. Paczian, A. Rodriguez, R. Stevens, A. Wilke, J. Wilkening, and R. A. Edwards. "The metagenomics RAST server - A public resource for the automatic phylogenetic and functional analysis of metagenomes". In: *BMC Bioinformatics* 9 (2008), pp. 1–8. ISSN: 14712105. DOI: 10.1186/1471-2105-9-386.

[49] R Foundation for Statistical Computing. *R: a Language and Environment for Statistical Computing*. Vol. 2. 2018. ISBN: 3-900051-07-0.

[50] A. Hussain, S. K. Dubey, and V. Kumar. "Kinetic study for aerobic treatment of phenolic wastewater". In: *Water Resources and Industry* 11 (2015), pp. 81–90. ISSN: 22123717. DOI: 10.1016/j.wri.2015.05.002. URL: http://dx.doi.org/10.1016/j.wri.2015.05.002.

[51] K. Saeki, Y. Ihyo, M. Sakai, and T. Kunito. "Strong adsorption of DNA molecules on humic acids". In: *Environmental Chemistry Letters* 9.4 (2011), pp. 505–509. ISSN: 16103653. DOI: 10.1007/s10311-011-0310-x.

[52] N. L. Nemerow and T. A. Doby. "Color Removal in Waste-Water Treatment Plants". In: *Water Environment Federation* 30.9 (1956), pp. 1160–1165.

[53] H. J. Feng, L. F. Hu, Q. Mahmood, Y. Long, and D. S. Shen. "Study on biosorption of humic acid by activated sludge". In: *Biochemical Engineering Journal* 39.3 (2008), pp. 478–485. ISSN: 1369703X. DOI: 10.1016/j.bej.2007.11.004.

[54] H. Ma, H. E. Allen, and Y. Yin. "Characterization of isolated fractions of dissolved organic matter from natural waters and a wastewater effluent". In: *Water Research* 35.4 (2001), pp. 985–996. ISSN: 00431354. DOI: 10.1016/S0043-1354(00)00350-X.

[55] M. DeFlaun, J. Paul, and W. Jeffrey. "Distribution and molecular weight of dissolved DNA in subtropical estuarine and oceanic environments". In: *Marine Ecology Progress Series* 38 (1987), pp. 65–73. ISSN: 0171-8630. DOI: 10.3354/meps038065.

[56] G. B. Tanny, D. Mirelman, and T. Pistole. "Improved Filtration Technique for Concentrating and Harvesting Bacteria". In: *Applied and Environmental Microbiology* 40.2 (1980), pp. 269–273.

[57] S. R. Partridge, S. M. Kwong, N. Firth, and S. O. Jensen. "Mobile Genetic Elements Associated with Antimicrobial Resistance". In: *Clinical Microbiology Reviews* 31.4 (2018), pp. 1–61. ISSN: 0893-8512. DOI: 10.1128/cmr.00088-17.

[58] L. Martínez-martínez, A. Pascual, and G. A. Jacoby. "Quinolone resistance from a transferable plasmid". In: *The Lancet* 351 (1998), pp. 797–799. URL: papers://c5399723-e709-4728-b088-22881cd2bf02/Paper/p99.

[59] T. Guillard, A. Grillon, C. De Champs, C. Cartier, J. Madoux, B. Berçot, A. L. Lebreil, A. Lozniewski, J. Riahi, V. Vernet-Garnier, and E. Cambau. "Mobile insertion cassette elements found in small non-transmissible plasmids in Proteeae may explain qnrD mobilization". In: *PLoS ONE* 9.2 (2014), pp. 1–8. ISSN: 19326203. DOI: 10.1371/journal.pone.0087801.

[60] C. Kehrenberg, K. L. Hopkins, E. J. Threlfall, and S. Schwarz. "Complete nucleotide sequence of a small qnrS1-carrying plasmid from Salmonella enterica subsp. enterica Typhimurium DT193". In: *Journal of Antimicrobial Chemotherapy* 60.4 (2007), p. 903. ISSN: 03057453. DOI: 10.1093/jac/dkm333.

[61] "National Institute for Public Health and the Environment (RIVM)". *NethMap 2019. Consumption of antimicrobial agents and antimicrobial resistance among medically important bacteria in the Netherlands*. Tech. rep. RIVM, 2019. URL: https://www.rivm.nl/bibliotheek/rapporten/2019-0038.pdf.

[62] N. Czekalski, T. Berthold, S. Caucci, A. Egli, and H. Bürgmann. "Increased levels of multiresistant bacteria and resistance genes after wastewater treatment and their

dissemination into Lake Geneva, Switzerland". In: *Frontiers in Microbiology* 3.MAR (2012), pp. 1–18. ISSN: 1664302X. DOI: 10.3389/fmicb.2012.00106.

[63] J. Rocha, T. Fernandes, M. V. Riquelme, N. Zhu, A. Pruden, and C. M. Manaia. "Comparison of culture-and quantitative PCR-based indicators of antibiotic resistance in wastewater, recycled water, and tap water". In: *International Journal of Environmental Research and Public Health* 16.21 (2019). ISSN: 16604601. DOI: 10.3390/ijerph16214217.

[64] C. Corinaldesi, R. Danovaro, D. Anno, and A. D. Anno. "Simultaneous Recovery of Extracellular and Intracellular DNA Suitable for Molecular Studies from Marine Sediments Simultaneous Recovery of Extracellular and Intracellular DNA Suitable for Molecular Studies from Marine Sediments". In: *Society* 71.1 (2005), pp. 46–50. ISSN: 0099-2240. DOI: 10.1128/AEM.71.1.46.

[65] T. H. Le, C. Ng, H. Chen, X. Z. Yi, T. H. Koh, T. M. S. Barkham, Z. Zhou, and K. Y. H. Gin. "Occurrences and characterization of antibiotic-resistant bacteria and genetic determinants of hospital wastewater in a tropical country". In: *Antimicrobial Agents and Chemotherapy* 60.12 (2016), pp. 7449–7456. ISSN: 10986596. DOI: 10.1128/AAC.01556-16.

[66] D. L. Wu, M. Zhang, L. X. He, H. Y. Zou, Y. S. Liu, B. B. Li, Y. Y. Yang, C. Liu, L. Y. He, and G. G. Ying. "Contamination profile of antibiotic resistance genes in ground water in comparison with surface water". In: *Science of the Total Environment* 715 (2020). ISSN: 18791026. DOI: 10.1016/j.scitotenv.2020.136975.

[67] C. M. Manaia, J. Rocha, N. Scaccia, R. Marano, E. Radu, F. Biancullo, F. Cerqueira, G. Fortunato, I. C. Iakovides, I. Zammit, I. Kampouris, I. Vaz-Moreira, and O. C. Nunes. "Antibiotic resistance in wastewater treatment plants: Tackling the black box". In: *Environment International* 115.April (2018), pp. 312–324. ISSN: 18736750. DOI: 10.1016/j.envint.2018.03.044. URL: https://doi.org/10.1016/j.envint.2018.03.044.

[68] M. Willmann and S. Peter. "Translational metagenomics and the human resistome: confronting the menace of the new millennium". In: *Journal of Molecular Medicine* 95.1 (2017), pp. 41–51. ISSN: 14321440. DOI: 10.1007/s00109-016-1478-0. URL: http://dx.doi.org/10.1007/s00109-016-1478-0.

[69] T. O. Delmont, E. Prestat, K. P. Keegan, M. Faubladier, P. Robe, I. M. Clark, E. Pelletier, P. R. Hirsch, F. Meyer, J. A. Gilbert, D. Le Paslier, P. Simonet, and T. M. Vogel. "Structure, fluctuation and magnitude of a natural grassland soil metagenome". In: *ISME Journal* 6.9 (2012), pp. 1677–1687. ISSN: 17517362. DOI: 10.1038/ismej.2011.197. URL: http://dx.doi.org/10.1038/ismej.2011.197.

[70] B. Zhu. "Degradation of plasmid and plant DNA in water microcosms monitored by natural transformation and real-time polymerase chain reaction (PCR)". In: *Water Research* 40.17 (2006), pp. 3231–3238. ISSN: 00431354. DOI: 10.1016/j.watres.2006.06.040.

[71] I. Sanseverino, A. Navarro, R. Loos, and D. Marinov. *State of the Art on the Contribution of Water to Antimicrobial Resistance*. Tech. rep. Joint Research Centre, 2018. DOI: 10.2760/82376. URL: https://publications.jrc.ec.europa.eu/repository/bitstream/JRC114775/amr__jrc_technical__report_final_online_15jan.2019.pdf.

[72] S. Jia, K. Bian, P. Shi, L. Ye, and C.-H. Liu. "Metagenomic profiling of antibiotic resistance genes and their associations with bacterial community during multiple disinfection regimes in a full-scale drinking water treatment plant". In: *Water Research* (Mar. 2020), p. 115721. ISSN: 0043-1354. DOI: 10.1016/J.WATRES.2020.115721. URL: https://www.sciencedirect.com/science/article/abs/pii/S004313542030258X.

[73] R. Grande, M. Di Giulio, L. J. Bessa, E. Di Campli, M. Baffoni, S. Guarnieri, and L. Cellini. "Extracellular DNA in Helicobacter pylori biofilm: A backstairs rumour". In: *Journal of Applied Microbiology* 110.2 (2011), pp. 490–498. ISSN: 13645072. DOI: 10.1111/j.1365-2672.2010.04911.x.

[74] N. M. Shchegolkova, G. S. Krasnov, A. A. Belova, A. A. Dmitriev, S. L. Kharitonov, K. M. Klimina, N. V. Melnikova, and A. V. Kudryavtseva. "Microbial community structure of activated sludge in treatment plants with different wastewater compositions". In: *Frontiers in Microbiology* 7.FEB (2016), pp. 1–15. ISSN: 1664302X. DOI: 10.3389/fmicb.2016.00090.

[75] D. J. Levy-Booth, R. G. Campbell, R. H. Gulden, M. M. Hart, J. R. Powell, J. N. Klironomos, K. P. Pauls, C. J. Swanton, J. T. Trevors, and K. E. Dunfield. "Cycling of extracellular DNA in the soil environment". In: *Soil Biology and Biochemistry* 39.12 (2007), pp. 2977–2991. ISSN: 00380717. DOI: 10.1016/j.soilbio.2007.06.020.

[76] D. Calderón-Franco, S. Apoorva, G. Medema, M. C. van Loosdrecht, and D. G. Weissbrodt. "Upgrading residues from wastewater and drinking water treatment plants as low-cost adsorbents to remove extracellular DNA and microorganisms carrying antibiotic resistance genes from treated effluents". In: *Science of the Total Environment* 778 (2021), p. 146364. ISSN: 18791026. DOI: 10.1016/j.scitotenv.2021.146364.

4

Transfer dynamics of antibiotic resistance determinants in a full-scale granular sludge wastewater treatment plant

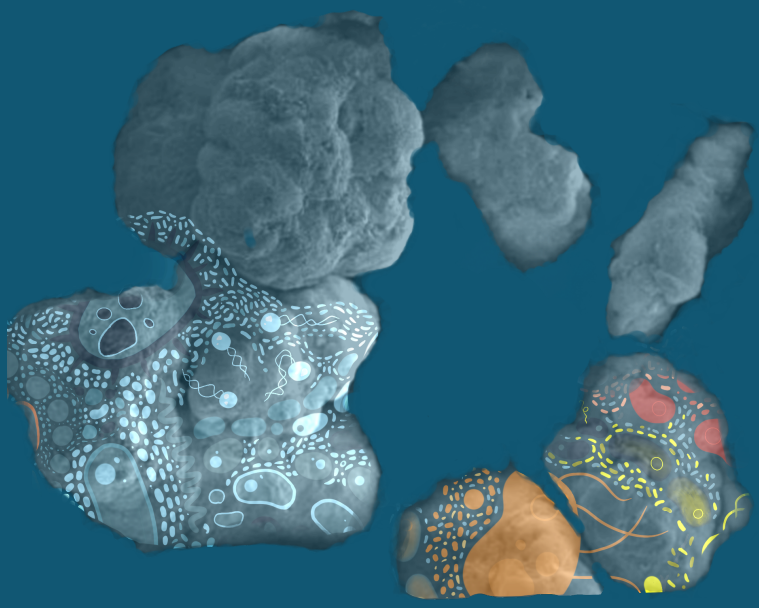

This chapter has been published as: Calderón-Franco, D., Sarelse, R., Christou, S., Pronk, M., van Loosdrecht, M., Abeel, T., Weissbrodt, D., 2022. Metagenomic profiling and transfer dynamics of antibiotic resistance determinants in a full-scale granular sludge wastewater treatment plant. Water Research. 219, 1–12. https://doi.org/10.1016/j.watres.2022.118571

ABSTRACT

In the One Health context, wastewater treatment plants (WWTPs) are central to safeguarding water resources. Nonetheless, many questions remain about their effectiveness in preventing antimicrobial resistance (AMR) dissemination. Most surveillance studies monitor the levels and removal of selected antibiotic resistance genes (ARGs) and mobile genetic elements (MGEs) in intracellular DNA (iDNA) extracted from WWTP influents and effluents. The role of extracellular free DNA (exDNA) in wastewater is mostly overlooked. This study analyzed the transfer of ARGs and MGEs in a full-scale Nereda® reactor removing nutrients with aerobic granular sludge. We tracked the composition and fate of the iDNA and exDNA pools of influent, sludge, and effluent samples. Metagenomics was used to profile the microbiome, resistome, and mobilome signatures of iDNA and exDNA extracts. Selected ARGs and MGEs were analyzed by qPCR. From 2,840 ARGs identified, the genes arr-3 (2%), tetC (1.6%), sul1 (1.5%), oqxB (1.2%), and aph(3")-Ib (1.2%) were the most abundant among all sampling points and bioaggregates. Pseudomonas, Acinetobacter, Aeromonas, Acidovorax, Rhodoferax, and Streptomyces populations were the main potential hosts of ARGs in the sludge. In the effluent, 478 resistance determinants were detected, of which 89% were from exDNA potentially released by cell lysis during aeration in the reactor. MGEs and multiple ARGs were co-localized on the same extracellular genetic contigs. Total intracellular ARGs decreased 3-42% due to wastewater treatment. However, the ermB and sul1 genes increased by 2 and 1 log gene copies mL^{-1}, respectively, in exDNA from influent to effluent. The exDNA fractions need to be considered in AMR surveillance, risk assessment, and mitigation strategies.

Keywords: *Free-floating extracellular DNA; Granular sludge; Antimicrobial resistance; qPCR; Metagenomics*

4.1. Introduction

Drug diseases currently cause at least 700,000 deaths globally per year. This number could increase to 10 million y^{-1} 1 by 2050 across all income regions. Under the most alarming scenario, no action is taken to contain antimicrobial resistance (AMR) [1]. The proliferation of antibiotic-resistant bacteria (ARB) directly correlates with the widespread use of corresponding antibiotics [2]. Medically problematic pathogens that acquire multidrug resistance through misuse of antibiotics are bacteria responsible for tuberculosis, acute respiratory infections, sexually transmitted infections, and bacillary dysentery [3].

Within the One Health context, wastewater treatment plants (WWTPs) should form a barrier between sewage that transports high loads of antibiotics and antibiotic resistance genes (ARGs) emitted by anthropogenic metabolisms and aquatic ecosystems [4]. Microorganisms in WWTPs biological processes are often considered reservoirs of ARGs while also supposed to contribute to mitigating AMR dissemination by degrading antibiotics and AMR determinants. However, current WWTP designs are not optimized to this end.

Currently, AMR surveillance in wastewater is primarily conducted with molecular biology measurements that target the intracellular DNA (iDNA) of ARB. By examining the influent and effluent of 62 Dutch WWTPs by qPCR, Pallares-Vega et al.[5] observed a reduction in the abundance of ARGs and an increase in the relative abundance of resistance plasmids of the incompatibility group 1 (IncP-1). Guo et al.[6] used metagenomics to describe microbiome, mobilome, and resistome patterns from the iDNA pool of a Chinese WWTP, revealing that *Clostridium* and *Nitrosomonas* can carry ARGs during wastewater treatment. Besides identifying the hosts of ARGs in microbial communities of activated sludge at high resolution, it remains primordial to elucidate the mechanisms and mobile genetic elements (MGEs) that transfer AMR determinants in these populations.

In addition to iDNA, extracellular free DNA (exDNA) contains a high proportion of MGEs [7]. Different genetic structures and architectures (plasmids, transposons, insertion sequences, and integrases, among others) transfer ARGs between bacteria, but many questions remain. The analysis of both intracellular ARGs (iARGs) and extracellular ARGs (exARGs) combined with mobilome co-localization analysis has rarely been performed in complex environmental samples such as wastewater biomasses. Such co-localization analysis involves the characterization of the resistome fraction in genomic proximity to horizontal gene transfer (HGT) mediators such as plasmids and other mobile genetic elements [8].

Apart from the presence of exDNA in wastewater, not much is known about the actual transfer of AMR in the microbiome of WWTPs and the underlying effects of biofilms. Dense microbial aggregations can pro- mote the horizontal transfer of antibiotic resistance genes (ARGs) in aquatic environments [9, 10]. Full-scale Nereda® plants that use aerobic granular sludge (AGS) for an integral removal of nutrients [11] harbor a hybrid sludge composed of granules (0.2-3 mm) that have similar properties as biofilms. Therefore, AGS SBRs form interesting microbial

ecosystems to study the fate of AMR. Metagenomic analysis during granulation at pilot scale showed that ARGs enriched in both iDNA and exDNA fractions of AGS during the granule development stage and that integrons played an essential role in carrying exARGs [12].

This study analyzed the transfer dynamics of ARGs and MGEs in a full-scale AGS Nereda® plant. Metagenomic and qPCR analyses were performed on the iDNA and exDNA pools of samples collected from the influent, different sludge fractions and the effluent. To track transfer phenomena, the sludge was sampled over the different SBR phases (end of anaerobic feeding, end of aeration) and sieved for different sized bioaggregates (flocs, small and big granules). The findings highlight the fate of the AMR determinants in a full-scale AGS WWTP and the importance of considering both iDNA and exDNA pools in AMR dissemination studies.

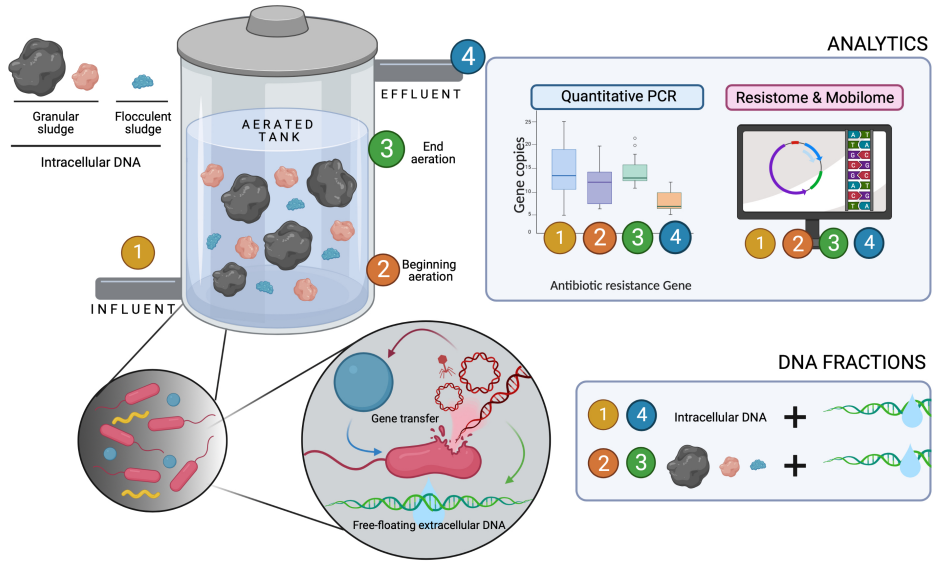

Figure 4.1: Graphical abstract

4.2. Material & Methods

Sampling of a full-scale AGS WWTP

The sampling campaign performed on a Nereda® plant located in Utrecht (52.11215, 5.10813), The Netherlands. Sampling was performed over 3 days (Monday, Wednesday, and Friday) within the same week, under dry weather conditions without significant variations in hydraulic retention time (20 h). Since the sludge retention time was relatively long (30 days in average; >40 days for large granules and <10 days for small granules and flocs) in this installation, the 3 sampling days were considered as biological replicates.

Biological samples were collected every day from pre-settled influent wastewater, from the mixed liquor at the beginning (i.e., after anaerobic feeding of the wastewater) and end of the aeration phase, and from the effluent of the SBR (**Figure** 4.2a). Total volumes of 1 L of influent and 1 L of effluent were collected as a 24-h flow-proportional composite samples. For the other process points, the sludge was sampled from the top of the tank as grab samples of 1 L with a pole container during the daily operations of the SBR. All samples were transported in a cooled container and processed within a time frame of less than 4 h prior to DNA extraction.

The granular sludge samples were sieved in 3 different fractions of bioaggregates (flocs <0.2 mm, small granules of 0.2-1 mm, and large granules >1 mm) according to [13]. The water at the outlet of the sieving unit was used for exDNA isolation. The fractions of exDNA were isolated in a time-frame of less than 4 h after sampling. The sieved fractions of granular sludge were stored at 20°C in a time-frame of less than 4 h after pending isolations of iDNA.

In total, 12 analytes were obtained and sequenced by metagenomics per sampling day, i.e., 36 analytes for the whole campaign. **Table** 4.1 summarizes the set of samples and analytes.

Extractions of exDNA and iDNA analytes

The pools of iDNA and exDNA were differentially isolated for all samples, as recently described by Calderón-Franco et al.[7]. All details can be found in **Supplementary Material**.

Library preparation, sequencing, quality control, assembly, and binning

Selection of analytes

From the set of 36 analytes of exDNA and iDNA obtained over the 3 days, the analytes from the Monday and Friday (i.e., 24 analytes) were selected as duplicates (economic optimum) for metagenomics. These exDNA and iDNA analytes were sent to DNASense (Aalborg, Denmark) for library preparation and sequencing.

Table 4.1: Samples collected from the influent, sludge, and effluent of the SBR during each of the 3 sampling days at WWTP Utrecht. Granular sludge samples were sieved in 3 different fractions of flocs, small granules, and large granules. The pools of intracellular DNA (iDNA) and free-floating extracellular DNA (exDNA) extracted from each sample as analytes for metagenomics are indicated. Two out of the three biological replicates were sequenced for metagenomics analysis, indicated as "-D1" and "-D2" for samples taken on Monday and Friday, respectively.

SBR operation stage sampled	Number of successive days sampled	Type of biological sample and bioaggregate size	DNA pool isolated	Metagenomic samples Identifier	BioSample IDs
				INF-exDNA-D1	SAMN23455551
			exDNA	INF-exDNA-D2	SAMN23455563
				INF-iDNA-D1	SAMN23455550
Influent	3	Global sample	iDNA	INF-iDNA-D2	SAMN23455562
				BA-exDNA-D1	SAMN23455555
		Global sample	exDNA	BA-exDNA-D2	SAMN23455567
				BA-FL-iDNA-D1	SAMN23455554
		Flocs	iDNA	BA-FL-iDNA-D2	SAMN23455566
				BA-SG-iDNA-D1	SAMN23455553
		Small granules	iDNA	BA-SG-iDNA-D2	SAMN23455565
				BA-LG-iDNA-D1	SAMN23455552
Start of aeration	3	Large granules	iDNA	BA-LG-iDNA-D2	SAMN23455564
				EA-exDNA-D1	SAMN23455559
		Global sample	exDNA	EA-exDNA-D2	SAMN23455571
				EA-FL-iDNA-D1	SAMN23455558
		Flocs	iDNA	EA-FL-iDNA-D2	SAMN23455570
				EA-SG-iDNA-D1	SAMN23455557
		Small granules	iDNA	EA-SG-iDNA-D2	SAMN23455569
				EA-LG-iDNA-D1	SAMN23455556
End of aeration	3	Large granules	exDNA	EA-LG-iDNA-D2	SAMN23455568
				EFF-exDNA-D1	SAMN23455561
			exDNA	EFF-exDNA-D2	SAMN23455573
				EFF-iDNA-D1	SAMN23455560
Effluent	3	Global sample	iDNA	EFF-iDNA-D2	SAMN23455572

Preparation of libraries

The DNA was quantified using Qubit (Thermo Fisher Scientific, USA) and fragmented to approximately 550 bp using a Covaris M220 with microTUBE AFA Fiber screw tubes and the settings: Duty Factor 10peak/displayed power 75 W, cycles/burst 200, duration 40 s and temperature 20°C. The fragmented DNA was used for metagenome preparation using the NEB Next Ultra II DNA library preparation kit.

Sequencing of libraries

Libraries were sequenced using the HiSeq sequencer (Illumina, USA) as 2 × 150 bp paired-end reads.

Quality control of sequence reads

After sequencing, a dataset containing 48 paired-end read samples with an average of 16 million reads per sample was obtained. Metagenomics workflow is summarized in **Figure S.1**. The minimum and maximum numbers of quality-filtered, non-duplicated sequencing reads of 150 bp ranged from 12 to 18 million. The quality of the Illumina reads was assessed using FastQC version 0.11.9 with default parameters [14]. Low-quality paired-ends reads were trimmed and filtered by Trimmomatic version 0.39 on paired-end mode [15].

Assembly of sequence reads

The trimmed reads were assembled into contigs using metaSPAdes version 3.14.1 [16] on meta mode on default parameters.

Binning of DNA contigs

Contigs resulting from the sequencing of only the iDNA pools of bioaggregates were binned with MetaBAT version 2.2.15 [17] to reconstruct metagenome-assembled genomes (MAGs) on default parameters. The MAGs were used to analyze secondary metabolite biosynthesis gene clusters.

Generation of the taxonomic database of aerated granular sludge

A database of sequences from MAGs, contigs, and reads specific to the microbial environment of AGS was built to accurately profile the microbiome. The Kraken 2.0 standard database of 9.1 Gbp of genomic sequences [18] was used as a basis. However, because complete genomes of the organisms found in AGS systems were often unavailable in the Kraken 2.0 database, additional genetic fragments specific to some taxa were added to the database. As an example, abundant genera in AGS like *Tetrasphaera*, *Trichococcus* and "*Candidatus* Accumulibacter" were not or poorly annotated in the standard database used in Kraken 2.0. In total, 94,005 sequences of 2,223 unique taxa were added to the Kraken 2.0 standard database.

The taxa of the AGS samples were classified from both short reads and contig sequences by combining the MetaPhlAn3.0 [19], MG-RAST [20] and Kraken 2.0 [18] computational tools for phylogenetic analysis of metagenomics data with their corresponding databases, as well as BLASTn to align contigs of >1500 bp against the MiDAS database of 16S rRNA gene sequences with a cut-off e-value $<10^{-5}$ and sequence identity >97% https://www.midasfieldguide.org/ [21]. A literature study was conducted in which taxa were added to the database if theoretically present above 1% relative abundance but not present in the database.

Kraken 2.0 takes all the sequences added in a selected database and finds k-mers (short genomic substrings specific for certain taxa) for further taxonomic classification.

The reads (full and partial genomes) of the predominant taxa were added to the adapted taxonomic database of AGS, when these lineages were detected above 1% of relative abundance from the metagenomics datasets using one of the previously described classification tool but not present in the Kraken 2.0 database. This was performed on taxonomic levels from phylum to species.

Microbiome profiling of iDNA and exDNA pools obtained from the AGS process

Kraken 2.0 with short-reads as input was selected to profile the microbiome. Classification with Kraken 2.0 was performed on pair-end mode on the quality-controlled short reads, using the newly constructed database.

The taxonomic classification was also performed on contigs >500 bp that were identified to contain ARGs (see 4.2 hereafter), in order to determine potential ARGs hosts.

The taxonomic classification outcomes from Kraken 2.0 were converted into abundance tables using the Pavian visualization tool [22] to explore metagenomics classification datasets. Heatmaps were generated with the R package "pheatmap" [23].

Resistome and mobilome profiling of iDNA and exDNA obtained from the AGS process

ARGs were annotated by aligning the assembled contigs >500 bp to the ResFinder 4.0 resistance gene database using the BLASTn nucleotide alignment tool with a cut-off E-value of $<10^{-5}$ and sequence identity above 90% [24].

MGEs were classified on the same set of contigs >500 bp using BLASTn by aligning them with the same cut-off and sequence identity setpoints to the following databases depending to the types of MGEs. Bacterial insertion sequences were identified by aligning against the ISfinder database [25]. Integrons, integrases, and gene cassettes were identified using the INTEGRALL database [26]. Bacterial integrative and conjugative elements were identified using the ICEBERG database [27].

For all queries, the ARG or MGE identified with the best score (i.e., equal to the sequence identity multiplied by the coverage factor) was selected to annotate the query.

BLASTn was performed with different databases (ResFinder 4.0 for ARGs and ISfinder, INTEGRALL and ICEBERG for MGEs) on the same set of contigs to identify where ARGs and MGEs co-localized. BLASTn was performed with a cut-off E-value of $<10^{-5}$ and sequence identity above 90%. Contigs >500 bp that simultaneously contained hits from the ResFinder 4.0 database and at least one of the different MGE databases were considered to have co-localized.

The contigs that contained both ARGs and MGEs were used as input queries against the NCBI plasmid database in order to know if such contig belonged to a plasmid. A contig was identified as part of a potential plasmid if exclusively aligning with plasmids in the entire NCBI plasmid database with sequence identities >90%.

Functional genetic analysis of iDNA and exDNA pools obtained from the sludge

Prokka version 1.14.5 was used to annotate the assembled contigs >500 bp, with the default databases and parameters on metagenomic mode [28]. K-numbers were assigned to all predicted coding sequences (CDSs) using GhostKoala, after which the KEGG database was used for analyse the functional and AMR pathways [28, 29]. The antibiotics and secondary metabolites analysis shell (antiSMASH, v5.0) tool was used to identify, annotate, and analyze the secondary metabolite biosynthesis gene clusters, such as involved on antibiotics production, in MAGs binned from the iDNA bioaggregate samples [30].

Multidimensional scaling analysis to cluster microbiome and resistome datasets

To identify patterns between the microbiome and resistome, different types of ordination and statistical numerical methods were performed using the R software. The input data was the output of the taxonomic classification from Kraken 2.0 with the adapted database.

Details can be found in **Supplementary Material**. The dimensions of the metagenomics datasets were reduced using Non-metric Multidimensional scaling (NMDS), Principal Coordinates Analysis (PCoA), and t-distributed stochastic neighbor embedding (t-SNE). These methods were applied to the taxonomic data at phylum and genus levels, and to the AMR group data. For all methods, scree-plots, stress-plot, and Shepard-plots were used to visualized the data accurately in two dimensions. t-SNE was applied using the "tsne" package, and a maximum of 2,000 iterations and a perplexity parameter of 5 as input [31]. PCoA, t-SNE, and NMDS were performed on different taxonomic levels and on the resistome data. All dimension reductions yielded similar clustering patterns, giving equivalent results for each sampling point and sample type. PCoA was therefore chosen as representative analysis to characterize the similarities and differences between samples.

Quantitative PCR of selected ARGs

To evaluate the WWTP performance in terms of removing ARGs and MGEs, to examine their presence during the different process steps, and to track their transfer between iDNA and exDNA fractions, a molecular analysis by quantitative polymerase chain reaction (qPCR) was applied to detect a selected panel of genes (**Table** 4.2) from the three biological replicates (Monday, Wednesday, and Friday) of the samples listed in **Table** 4.1.

All iDNA and exDNA analytes isolated from the three-biological sample from the influent, beginning and end of aeration, and effluent of the SBR were used for qPCR. Each analyte was measured in technical duplicates by qPCR.

The 16s rRNA and rpoB reference genes were quantified for the normalization of gene copies to the concentration of bacteria in the iDNA samples.

Based on antibiotics consumption data in the Netherlands [32], ARGs were targeted from the antibiotic groups of β-lactams (*blaCTXM*), macrolides (*ermB*), fluoroquinolones (*qnrs*), sulfonamides (*sul1/sul2*), and tetracyclines (*tetO*). The *intI1* gene encoding the class I integron-integrase was quantified. These integrase class I cassettes are related to ARG mobility, acquisition, and exchange between microorganisms [33]. Primers, thermal cycler conditions, and gBlocks gene fragments used for standards generation and quantification during qPCR are given in **Tables S.1 - S.2**, respectively.

Table 4.2: ARGs and MGE selected for qPCR with their description.

Category	Gene	Description
Bacteria normalization	*16S rRNA*	RNA component of the 30S small subunit of prokaryotic ribosome
	rpoB	Bacterial RNA polymerase subunit β
ARGs	*blaCTXM*	Bla-cefotaxine-hydrolizing -lactamase
	ermB	Erythromycin resistance via methylation of 23S rRNA
	qnrS	Quinolone resistance protein
	sul1	Sulfonamide resistant dihydropteroate synthase
	sul2	Sulfonamide resistant dihydropteroate synthase
	tetO	Tetracycline resistance protein TetO
MGE	*IntI1*	Class 1 integron integrase

4.3. Results & Discussion

Taxonomic composition of exDNA mainly linked to the granular sludge fraction

After taxonomic classification at genus level of the DNA contigs assembled from the metagenomic sequencing reads, principal coordinates analysis (PCoA) and other multidimensional scaling methods were efficient to observe the clustering effects in data related to the specific sample DNA fraction (**Figure 4.2b**).

The influent samples showed a large difference in composition for both the iDNA and exDNA pools. Microbial compositions of sewage can vary over an active week, based on the variety of emission sources and streams in a wastewater catchment area and environmental factors [34].

In the effluent, a lower variability between the two samples was observed for the iDNA fraction. The taxonomic composition of the iDNA of the effluent highly resembled the composition of the iDNA of activated sludge floc fraction in the treatment reactor. On the other hand, the phylogenetic signatures of the exDNA fraction of the effluent showed a larger variation between the samples.

In the wastewater treatment plant microbial cells can lyse, releasing iDNA as exDNA. The exDNA fractions might not persist as "free-floating" during the whole process. It can adhere to particles, get degraded, or taken up via natural transformation in competent cells [35, 36]. However, we mainly studied the free-floating exDNA as we hypothesize it would be the main exDNA fraction being released in the effluents rather than the attached to particles or aggregates.

From the different size fractions of bioaggregates in the sludge, the microbial community compositions of the small (blue in **Figure 4.2b)** and large (red) granules were similar, while the flocs (orange) clustered separately. This is similar as the observations by Ali et al.[13] that the floc fraction is more diverse and contains a large number of bacteria originating from the influent wastewater. Microbial niches establish along gradients of substrates and other dissolved components like oxygen and nitrogen oxides inside bioaggregates [37].

The taxonomic affiliations of the exDNA sequences of the mixed liquor sampled at the end of aeration were similar to those of the iDNA extracted from small and large granules, rather than the flocs. This suggests that exDNA was released from the granules by cell lysis during aeration. Sengar et al.[38] and Toh et al. [39] have shown that dead biomass releases its genetic material into the extracellular environment during the AGS process. In activated sludge, Yuan et al.[40] have identified that the taxa reflected by the iDNA and exDNA fractions are similar, suggesting a correlation between changes in the microbial composition of the activated sludge and in exDNA. Using the same exDNA extraction methodology, we have shown in a previous study that exDNA present in activated sludge mainly originates from decaying microbial populations rather than from transport from the influent [7]. The taxonomic composition of the exDNA fraction in the AGS system was mainly related to the microbiome present in the granular sludge.

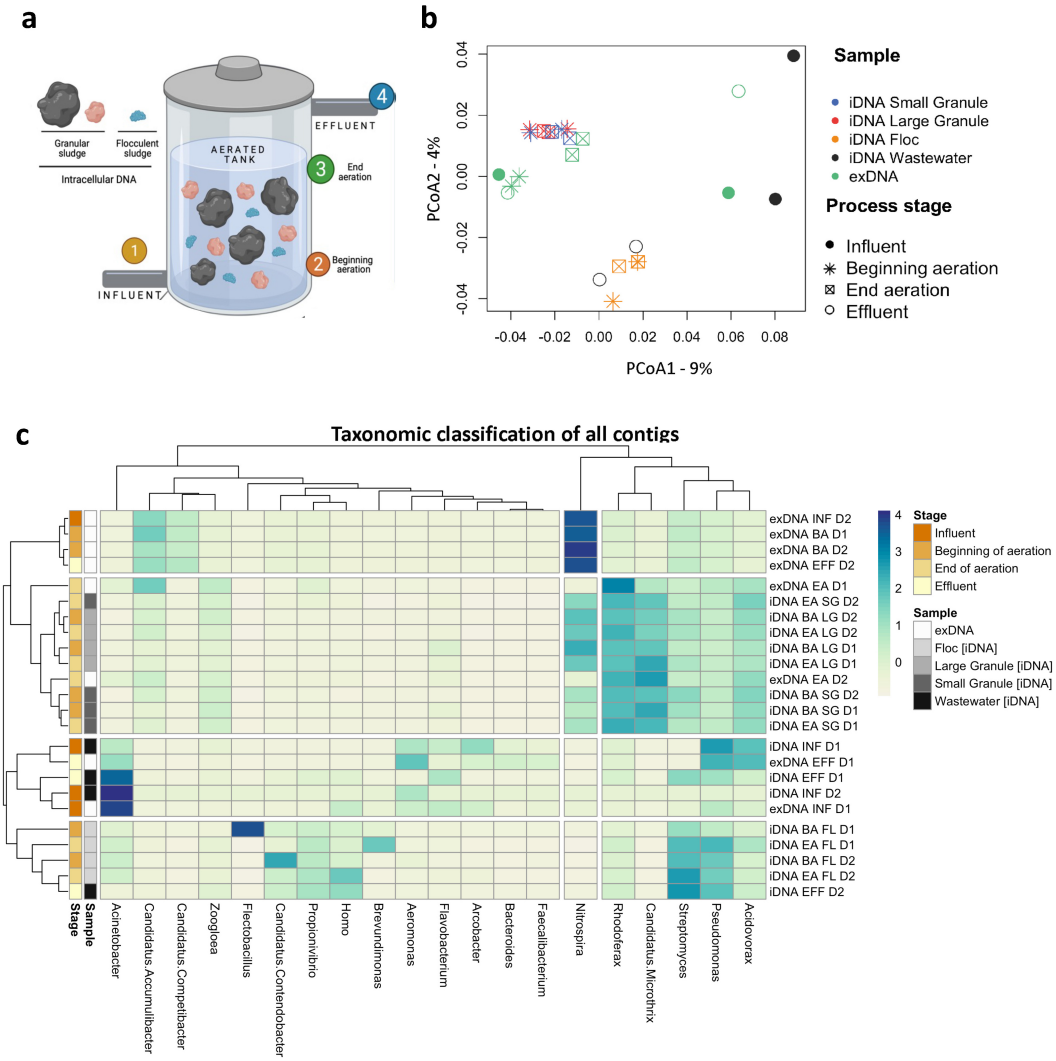

Figure 4.2: **(a)** Schematic representation of an AGS SBR, highlighting biomass metrics and sampling points 1-4. **(b)** PCoA of the absolute microbiome composition at genus-level after normalization and variance stabilization transformation, with Bray-Curtis as distance metric. Colors indicate microbial fractions: iDNA small granule (blue), iDNA large granule (red), iDNA floc (orange), iDNA wastewater (**black**, including influent and effluent samples), and exDNA (green). Symbols indicate stages in WWT operation: Influent (filled circles), beginning of aeration (asterisks), end of aeration (crossed squares), and effluent (empty circles). **(c)** Taxonomic classification at genus-level heatmap. Colors represent the Z-score computed from the relative abundance at genus-level present above 3% in all classified sequences.

AGS microbiome and potential involvement in AMR dissemination

The patterns of relative abundances of genera in the different stages of the AGS process and in the iDNA and exDNA fractions were examined by constructing a heatmap (**Figure 4.2c**) for the clusters observed by PCoA. Using the standard Kraken 2.0 database (NCBI based), 2,548 genera were identified from the whole set of iDNA and exDNA analytes: 57 genera were more abundant than 1% of sequencing read counts, and 15 of those were predominant above 3% in at least one of the samples (**Figure S.2**, ***** symbols). The average annotation rate of the reads was 24.7 ± 3.2 %, i.e., leaving three quarters of the taxonomic information of the reads as to uncover.

To increase the reads annotation rate, a new database of genetic sequences of the AGS microbial environment was constructed. With this database, the average annotation rate was 27.1 ± 3.4 %; 2,679 genera were identified: 55 genera were above 1% relative abundance and 21 were above 3% in at least one of the analytes (**Figure S.2**, ⋄). Although this new annotation rate was only 3% higher than the standard database, important AGS genera were now identified. Metagenomic studies can be hindered by low annotation rates as a consequence of the high fraction of natural microbes that have not been included in the databases. The current development of databases of high-quality MAGs and properly curated databases will help enhance annotation rates in the future [41].

From **Figure 4.2b**, the exDNA taxonomic compositions at the beginning of aeration resembled the exDNA from influent while at the end of aeration from both days closely resembled the iDNA fractions from small and large granules. Flocs displayed a unique profile. While the phylogenic distribution of the effluent exDNA resembled the granule phylogeny, the effluent iDNA resembled the flocs (from both beginning and end of aeration). During the fill/draw operation of the SBR, flocs leave the tank with the selection spill, therefore reducing their retention time in the process [42].

The diversity of abundant populations in the AGS detected by metagenomics is listed in **Figure 4.2c**. Several of these populations are involved in the conversions of C-N-P nutrients in the microbial ecosystem of AGS [37, 43], like "*Ca.* Accumulibacter", *Tetrasphaera*, *Dechloromonas* (C, P), "*Ca.* Competibacter", *Zoogloea, Xanthomonas, Rhodoferax, Pseudomonas, Acidovorax, Comamonas, Rhizobium* (C, N), *Nitrospira* (N), and *Acinetobacter* (C) among others. Some relate to filamentous bulking phenomena like "*Ca.* Microthrix", *Bulkholderia, Nocardioides, Kouleothrix*. Some thrive on metabolites and lysis products from other organisms like *Flavobacterium, Bacteroides*, and *Hydrogenophaga* among many others. The metabolic functions of other organisms in the AGS remains to be uncovered. Less beneficial organisms are *Arcobacter* and *Aeromonas* that are known pathogens. *Arcobacter* crosses WWTPs from influent to effluent without settling properly [44]. The presence in the influent of exDNA affiliating with "*Ca.* Accumulibacter" can relate to the recirculation line coming from the sludge

thickener.

Among the different populations identified from the AGS (**Figure 4.2c**), several are known to carry AMR-related genes. Acidovorax (3.5 ± 0.6%) is a known carrier of β-lactamase resistance plasmids in activated sludge samples [45]. Rhodoferax (3.5 ± 0.5%) has been identified to be of high relative abundance in wastewater effluent, while often identified as a carrier of resistance genes [46].

Nitrospirae (4.1% ± 1.1%) may play a role in AMR dissemination because it is a known host of iARGs and exARGs in WWTPs [36]. Guo et al. [6] used metagenomics to identify "*Candidatus* Accumulibacter" (2.1 ± 0.5%) as a possible carrier of resistance genes over the WWT operation.

Aeromonas was relatively abundant in all our samples (1.88 ± 0.84%). Notably, the three most critical antibiotic-resistant pathogens as designated by the World Health Organization are *Acinetobacter baumannii, Pseudomonas aeruginosa*, and *Enterobacteriaceae* [47]. *Acinetobacter* and *Pseudomonas* were abundant across samples (**Figure 4.2c** and **Figure S.2)**. We suggest that recovering and annotating MAGs for these populations out of AGS biomass could help identify whether they harbour pathogenic traits or not.

Interestingly, the relative abundances of exDNA sequences affiliating with the genera "*Candidatus* Microthrix" (exDNA at beginning of aeration 0.5 ± 0.1% vs. at end of aeration 5.6 ± 2.0%), *Acidovorax* (1.2 ± 0.1% vs. 4.3 ± 0.2%), *Rhodoferax* (1.8 ± 0.2% vs. 7.9 ± 1.3%), and *Zoogloea* (0.8 ± 0.2% vs. 2.6 ± 0.5%) increased over the aeration period.

These filamentous bacteria ("*Ca.* Microthrix") and denitrifiers were abundant >3% in the granule fractions of the SBR but not in flocs. These microbial populations are known to populate AGS used for full biological nutrient removal [37]. The presence of exDNA in the water phase can relate to cell lysis or to "active" release from the cells.

Acinetobacter (iDNA 6.1 ± 2.8%; exDNA 3.4 ± 2.2%), *Flavobacterium* (1.2 ± 0.4%; 1.0 ± 0.5%), and *Pseudomonas* (4.3 ± 0.9%; 4.0 ± 1.1%) secrete DNA in the extracellular environment during growth in liquid media [48].

Collectively, we had identified the main microbial players in thengranular sludge microbiome and the relationship with exDNA fractions and the possible involvement in the dissemination of resistance determinants.

Further mechanistic insights, using well-controlled experiments with systems microbiology methods, are required to identify whether cell decay or active secretion can explain the release of exDNA from microorganisms of the sludge.

A wide range of ARGs are present in the effluent exDNA

The resistome of wastewater systems exhibits a large diversity of ARGs. As many as 2,840 ARGs were identified from all the samples, belonging to 15 antibiotic

subgroups. ARGs affiliating with MLS (Macrolide, Lincosamide, and Streptogramin; n = 910 reads), aminoglycosides (n = 598 reads), sulphonamides (n = 375 reads), β-lactam (n = 330 reads), and tetracycline (n = 233 reads) were the most abundant (**Figure 4.3a**). The resistome profiles matched with Hendriksen et al.[49]:macrolides are the most abundant ARGs in urban sewage in Europe, followed by aminoglycosides and β-lactam.

All samples, including the different types of bioaggregates, and iDNA and exDNA fractions, contained ARGs. The exDNA resistome profiles at beginning and end of aeration resembled the iDNA resistomes of granules. Similar to observations made on taxonomic affiliations of exDNA sequences, exARGs mainly originated from the granules rather than from flocs. In the effluent, exDNA was a combination of fragments coming from the influent iDNA (**Figure 4.3b**) (being in the day 2 part of the bigger dendogram) plus the different bioaggregates.

The 5 most abundant ARGs over all samples were: aminoglycoside *arr-3 gene* (n = 58 reads), tetracycline *tet(C)* (n = 46 reads), sulfonamide *sul1* (n = 44 reads), multidrug efflux pump *oqxB* (n = 34 reads), and aminoglycoside *aph(3")-Ib* (n = 34 reads). Taken together (n = 216 reads), these genes only amount to 7.6% of the total ARGs identified.

This high diversity of resistance genes matches with another metagenomic analysis of activated sludge samples [36]. Of all 478 ARGs identified in the effluent, 89% were carried by exDNA. This can present a risk for AMR dissemination in the environment and for health by natural transformation of exDNA fragments in microorganisms present in receiving water bodies and drinking water resources, especially for the resistance determinants to the last-resource antibiotics such as carbapenem and colistin. The types of exARG and iARG were similar, matching with Zhou et al.[36]. In contrast, using PCR only, Li et al.[12] detected dissimilar compositions of iARGs and exARGs during sludge granulation at pilot scale. Early-stage granulation is a dynamic process involving changing community compositions along the establishment of physicochemical gradients (e.g., increasing anaerobic zones in granules) [38]. This can lead to bacteria decay and DNA release shifts over the process, therefore leading to variations in ARG profiles as well.

Here, mature granules from the full-scale AGS WWTP were used to track the fate of ARGs under pseudo steady-state conditions. Overall, the effluent exDNA is an overlooked DNA fraction that needs to be considered for future risk analysis: it is a highly diverse fraction regarding antibiotic resistance genes.

Gram-negative bacteria are potential carriers of ARGs in the AGS

All contigs >500 bp containing ARGs were taxonomically classified to identify which microorganisms carried and potentially released ARGs (**Figure 4.3b and S.2**). As high as 98% of contigs containing ARGs were annotated with taxonomy.

A contig affiliated to a taxon does not necessarily mean that the read comes from

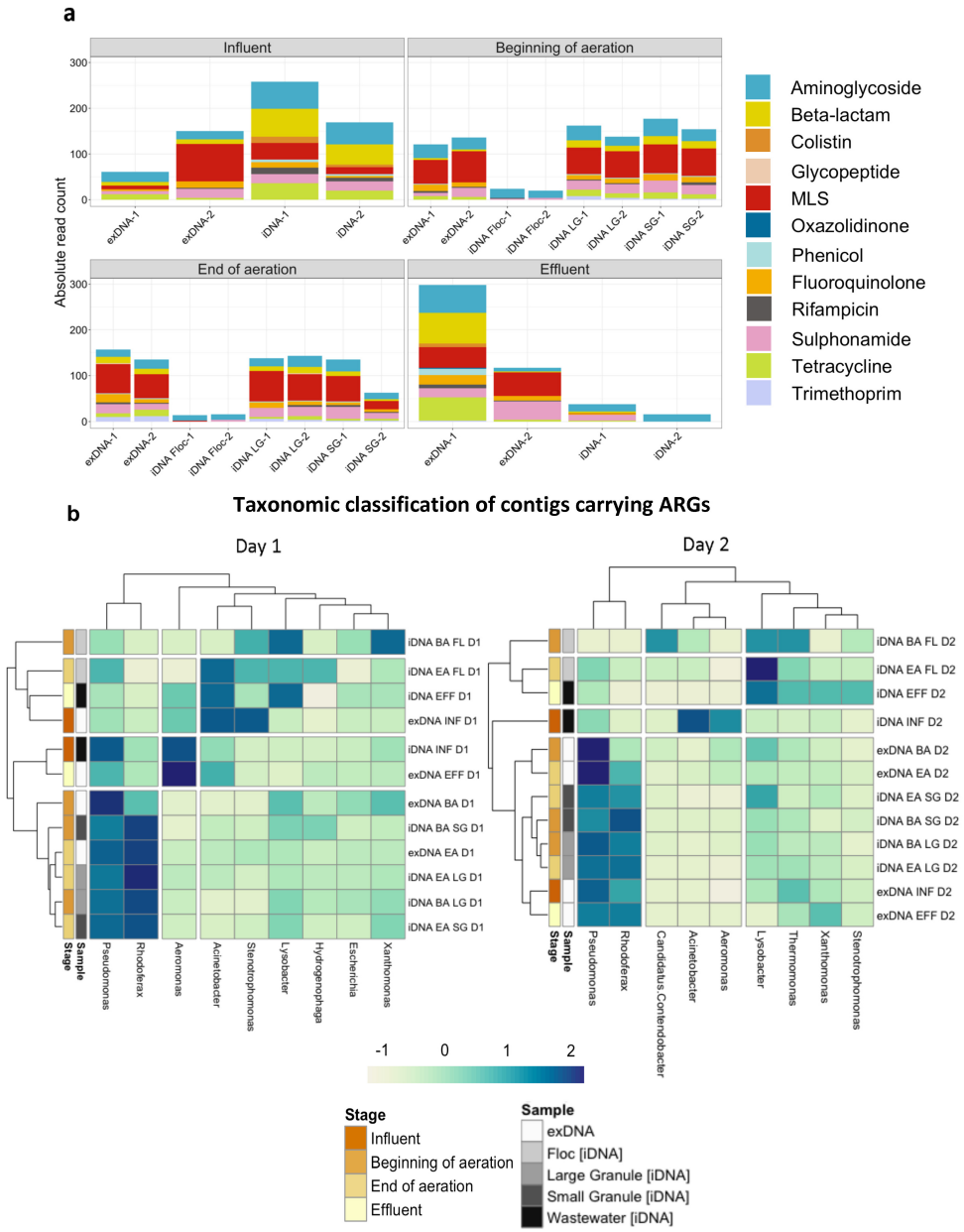

Figure 4.3: (a) Absolute numbers of classified reads of AR-groups. Labels: (F) floccular aggregates, (LG) large granules, (SG) small granules, (-1) first biological replicates, and (-2) second biological replicates. **(b)** Taxonomic classification at genus-level of contigs encoding ARGs heatmap. Colors represent the Z-score computed from the relative abundance at genus-level present above 5% in all classified sequences. Labels: (INF) Influent, (BA) Beginning of the aeration, (EA) End of the aeration, and (EFF) effluent.

that specific organism: different populations can share similar ARG sequences. The contigs containing ARGs over the whole metagenomic dataset of all samples and fractions were affiliated to Gram-negative genera like *Pseudomonas* (8.4 ± 0.7%), *Rhodoferax* (5.6 ± 0.9%), *Acinetobacter* (4.3 ± 1.4%), *Aeromonas* (3.1 ± 1.1%), *Xanthomonas* (3.9 ± 0.9%), and *Acidovorax* (1.9 ± 0.4%) as well as the Grampositive and antibiotic-producing genus *Streptomyces* (1.6 ± 0.4%) (**Figure S.2**).

Pseudomonas and *Rhodoferax* genera's high abundance pattern were similar between the two sampling days (**Figure 4.3b**). iDNA contigs containing ARGs in small and large granules were affiliated at several instances to *Rhodoferax* (10.1 ± 0.4% in granules). Out of the contigs where ARGs were localized, the ARG-containing exDNA affiliated to *Rhodoferax* (beginning of aeration: 2.0 ± 0.5%; end of aeration: 11.0 ± 2.9%). This increase suggests that DNA was released from *Rhodoferax* cells during aeration.

Rhodoferax is abundant in WWTP effluents and often identified as AMR carriers by encoding multiple efflux pumps [46, 50]. ARGs have been identified from MAGs retrieved from activated sludge from Danish WWTPs [41, 51]: *Rhodoferax* was the most abundant population containing multiple ARGs.

The effluent iDNA is mainly composed of microorganisms that go through the process without being removed, from bacteria growing on suspended solids and of microorganisms detached from the AGS bioaggregates. Some microorganisms that entered the AGS plant in high abundance and passed through the WWTP are *Aeromonas* and *Acinetobacter*,especially in day 1. The effluent was enriched by microorganisms coming mainly from floccular sludge such as *Lysobacter* (both days) and *Thermomonas* (day 2) (**Figure 4.3b**). Pathogenic *Arcobacter* crossed WWTPs from influent to effluent (**Figure 4.2c**) but interestingly, no ARG was detected in any of *Arcobacter* contigs. Further research needs to be done to clearly identify which ARGs in which MGEs are inside specific microbial hosts.

Recent analytical advances now allow to identify potential hosts of resistances using Hi-C sequencing [52]: populations of *Aeromonadaceae, Moraxellaceae*, and *Bacteroidetes* were shown to be critical reservoirs of AMR in WWTPs.

The resistome results highlight that AMR determinants released in exDNA during the wastewater operation are importantly linked to Gram-negative bacteria, notably *Rhodoferax*, and to potential pathogenic bacterial genera carrying ARGs in the effluent such as *Pseudomonas* and *Aeromonas*.

MGEs and ARGs often co-localize on contigs recovered from the exDNA of the effluent

Both iDNA and exDNA fractions and all bioaggregates were sources of a diversity of MGEs. The different samples yielded 55,344 different MGEs belonging to bacterial insertion sequences (9,845 reads), integrons, integrases and gene cassettes (20,149 reads), and bacterial integrative conjugative elements (25,350 reads).

When ARGs and MGEs co-localize on the same genetic fragment, there is an increased chance that the fragment can be transferred between bacterial cells. Since MGEs facilitate the transfer, integration, and transposition of genes in genomes, this poses a clear risk for ARG dissemination. From all contigs >500 bp, 312 contigs were identified to contain both ARGs and MGEs (**Table S.10**): their 5 most abundant ARGs were *blaVIM-48* (28), *cmx-1* (28), *sul2* (25), *tetA* (24), and *aadA6* (24). A set of 80 contigs contained multiple ARGs, and of these, 60 also contained MGEs: their 5 most abundant ARGs were all aminoglycoside resistance genes, namely *aph(3")-Ib* (17), *aadA6* (17), *aph(6)-Id* (17), *aadA11* (7), and *aac(3)-Ib* (7).

Multiple co-localization patterns were detected only in the iDNA of granules and in the exDNA of the effluent. For instance, *sul2* and *tetA* were exclusively found in the iDNA from large granules (replicate 2) from the end of the aeration, and in the effluent exDNA fraction (replicate 2). This contig also aligned with ISVsa3, an insertion sequence often found on plasmids [53].

Of the 60 contigs >500bp were multiple ARGs and MGEs colocalized, 3 major groups of contigs are highlighted hereafter because of their abundance in the system or the risk associated with leaving the WWTP in the exDNA of the effluent.

Firstly, as shown in **Table S.10**, 15 contigs were identified both as carriers of two aminoglycoside resistance genes (*aph(3")-Ib* and *aph(6)-Id*), and as part of transposon Tn5393 (**Figure 4.4a**). These contigs were found in all samples across WWT operation for all microbial aggregates and exDNA and iDNA fractions (excluding the flocs). After alignment to the NCBI nucleotide database, the contigs aligned with IncQ plasmids, mostly from populations of *Acinetobacter* and *Pseudomonas* genera, previously identified in our wastewater samples. IncQ plasmids are significant since they are related to the broadest host range of all replicating elements in bacteria [54]. They are known to mobilize via conjugation although natural transformation has also been observed [54–57]. Ellison et al. [58] have proven that double stranded exDNA can directly be captured by natural competent bacteria such as the model organisms *Vibrio cholerae* via retraction of DNA-bound type IV competent pili.

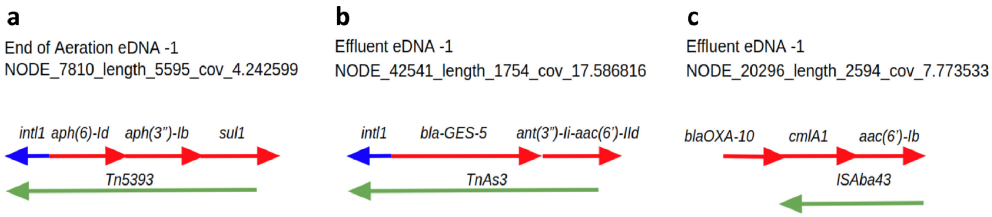

Figure 4.4: Contigs containing both ARGs and MGEs. **(a)** Contig of length 5595 bp, containing the class 1 integron-integrase (intI1), aminoglycoside phosphotransferase *(aph(6-Id)*, also known as *strB*), an aminoglycoside phosphotransferase (*aph(3")-Ib* also known as *strA*), a sulfonamide resistant dihydropteroate synthase (*sul1*), and a fully classified transposon Tn5393. **(b)** Contig of length 1754 bp, containing the class 1 integron-integrase (*intI1*), β-lactamase *bla-GES-5*, integron-encoded aminoglycoside acetyltransferase fusion protein *ant(3")-Ii-aac(6")-IId*, fully classifying as transposon TnAs3. **(c)** Contig of length 2594 bp, containing β-lactamase *blaOXA-10*, a plasmid or transposon-encoded chloramphenicol exporter gene *cmlA1*, an integron-encoded aminoglycoside acetyltransferase *aac(6')-Ib*, and a transposase ISAba43.

Then, 18 contigs aligned with a Tn3 family transposon (TnAs3), normally encoding a β-lactamase gene, a transposase and a resolvase [59] as identified from the exDNA effluent fraction (**Figure 4.4b**). These contigs (identities >95%) aligned exclusively with plasmids from *Escherichia coli*, *Klebsiella pneumoniae*, *Pseudomonas aeruginosa*, *Enterobacter cloacae*, *Enterobacter kobei*, and *Klebsiella oxytoca*. Interestingly, of all pathogens, the World Health Organization stressed that addressing carbapenem-resistance in *Pseudomonas aeruginosa* and *Enterobacteriaceae* should have the highest priority [47].

Finally, another contig of importance found in the exDNA fraction of the effluent carried multiple resistance genes against aminoglycosides (*aac(6')*), β-lactamases (*blaOXA-10*), and phenicols (*cmlA1*) (**Figure 4.4c**). This contig aligned with a 100% sequence identity to a plasmid already annotated from *Aeromonas hydrophila* (pWCX231), carrying 15 different ARGs [60].

The strong presence of mobilized resistance determinants in the extracellular fraction of the AGS WWTP has been also described by Ikuma and Rehmann [61]. Using mathematical modelling, they suggested that, at the WWTP effluent discharge point in a river, the total number count of ARGs was 13 times higher when including exARGs on top of iARGs. Collectively, exARGs in WWTP discharges need to be taken into account for accurate risk assessments of AMR.

Co-localization studies are valuable tools to identify the genetic structures and potential hosts by which resistance determinants are carried and transferred between bacteria. More research needs to be conducted to reconstruct full plasmids from wastewater effluents. This will shed light on the type of plasmids released into the environment, i.e., narrow/broad-range and synthetic/naturally occurring, and on the genetic constructions ARGs are embedded in.

Multiple ARGs often co-localize with MGEs on contigs from all the sampling points: the effluent is one of the predominant pool of MGEs containing ARGs across the

wastewater treatment chain.

No antibiotic-related biosynthetic gene clusters were found in the biomass for the most abundant ARG identified

Functional and pathway analyses were performed on the contigs to identify AMR pathways and on the MAGs to identify potential intrinsic antibiotic production by microorganisms that could promote the development and survival of ARB in AGS systems.

From all the AMR pathways available in the KEGG database [29], we identified the cationic antimicrobial peptide (CAMP) resistance pathway, vancomycin resistance pathway, and β-lactamase resistance pathway, including efflux pumps that actively transport the β-lactam antibiotics out of the cell (RND efflux pumps) (**Figure S.4 - S.6**). Both influent and effluent iDNA and exDNA were sources of genes involved in β-lactam resistance. Most genes involved in these resistance pathways were present in the influent iDNA but not in the influent exDNA. However, in the effluent, both iDNA and exDNA contained resistance pathways genes.

From the antiSMASH analysis of MAGs recovered from small and large granules (no MAGs could be recovered from flocs due to the sequencing depth and short reads used) at the end of aeration, positive hits on non-ribosomal peptide synthetase (NRPS) biosynthetic gene clusters (BGCs) were detected in MAGs of *Nitrospira* and *Janthinobacterium*. NRPS antibiotics include vancomycin, polymyxin, and teixobactin, which are highly effective against multidrug-resistant bacteria [62]. The vancomycin resistance pathway was one of the few reconstructed pathways in the samples analyzed (**Figure S.4**). Terpenes, indoles, T1PKS, and ectoine BGCs were identified as the most recurrent. No aminoglycosides or β-lactams antibiotic BGCs were found in any of the DNA samples.

From the functional analysis of MAGs, we did not recover full antibiotic production pathways from the main populations identified and that relate to the most abundant ARGs present during the process.

AGS treatment is efficient at reducing the load of resistance determinants while some exARGs increased over the WWT operation

To quantify the ARG and ARB occurrence and related removal capacity of the AGS WWTP, a panel of six ARGs and intI1 as MGE were quantified by qPCR. Two normalization methods (using *16S rRNA* and *rpoB* genes) were assessed. Both the ARGs and the MGE were consistently detected across all the AGS process phases and bioaggregates.

The most predominant genes throughout the process were the sulfonamide resistance gene *sul1* and the class 1 integron gene *intI1* (**Figure** 4.5a). These genes were the

most concentrated ones in the effluent with 7.5 (*sul1*) and 7.0 (*intI1*) $\log_{10}$ gene copies mL^{-1} (sum of iDNA and exDNA pools). Genes with the lowest concentration were blaCTXM (2.1),*qnrS* (3.1), and *tetO* (3.2) (same units as above).

Absolute and normalized concentrations of ARGs and MGEs, and iDNA vs. exDNA analysis, are shown in **Figure S.7**. These ARGs concentrations are in agreement with recent studies [5, 7] and comparable to others, especially when considering the variance in sewage and treatment efficiency [63–65].

The absolute concentration of iARGs was significantly higher ($p<0.05$-0.005) than of exARGs across all SBR phases and bioaggreagates (**Figure 4.5a**). The average iDNA/exDNA ratio was 1.9 in the influent and 2.3 in the effluent (**Figure S.7**). We found a significant reduction ($p<0.005$) after treatment for all genes analyzed by qPCR in the iDNA fraction. In contrast, multiple genes such as the bacterial proxy genes *16S rRNA* and *rpoB* as well as the resistance genes ermB (2.1 log_{10} gene copies mL^{-1} higher) and *sul1* (1.0 log_{10} gene copies mL^{-1} higher) increase from the influent to effluent exDNA (**Figure S.9**). Zhang et al. [66] reported an exARGs increase of 0.14-1.99 logs in the biological effluent from a WWTP, reflecting the persistence and low decay rate of exARGs in the discharge water Di Cesare et al. [67] have reported different ARGs patterns of exARGs, iARGs, and integrase MGEs: microbial cell decay and cell lysis can potentially release genetic material extracellularly. Yu et al. [68] confirmed that exARGs were not efficiently removed and were abundant in the final effluents of WWTPs, highlighting again the concern regarding exDNA when considering the control of ARG spreading. The free-floating exDNA is subjected to the fluctuating conditions of the WWTP environment differently than iDNA [12]. Its ability to maintain mobility and be involved in resistance spread needs to be studied in the future. Small granules accumulated higher concentrations of resistance genes (average 0.82 ± 0.31) log_{10} gene copies/ log_{10} *16S rRNA* copies) in their iDNA than big granules (0.62 ± 0.26) or flocs (0.61 ± 0.25) at the end of the aeration. No significant differences were observed between granules at the beginning of the aeration (**Figures 4.5a and S.7**).

It is not clear why small granules accumulated more ARGs during the 9-h aeration process. Flocs and small granules are more susceptible to immigration from the influent/sewage than large granules [13]. The solid retention time (SRT) of small granules is much shorter (7.7 ± 0.5 days) than that of big granules (142.6 ± 14.9 days) [13]. If the influent is enriched with ARB, immigration can explain a faster loading of ARGs in small than large granules. By being more rapidly released out of the tank, small granules can play a role in the release and dissemination of ARGs through WWTP effluent than big granules.

Further studies on ARG distribution across bioaggregates are needed to determine if ARGs are homogeneously distributed across the crosssection of the granules or mainly located at their surface or in one of their layers. Fluorescent in situ hybridization with ARG probes could determine the ARG distribution in granule slices. Such studies will also indicate if transfer between ARGs is more prone to

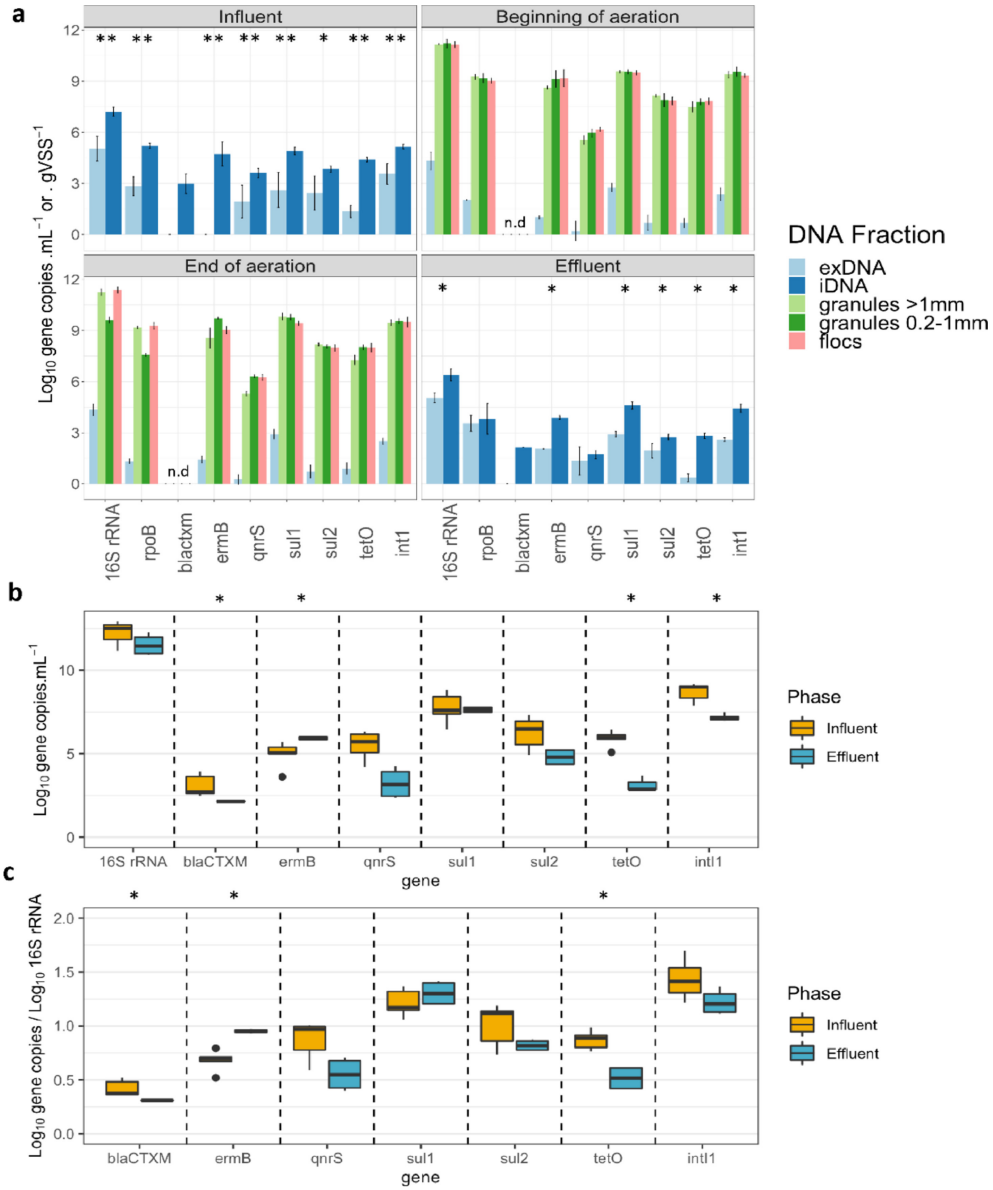

Figure 4.5: (a) Concentration of selected ARGs and int1I across AGS WWT phases. Error bars represent the standard deviation between biological replicates (n=3). The significances of the difference between exDNA and iDNA measurements are indicated by the Wilcoxon test and displayed as p<0.05 (*) and p<0.005 (**). textbf(b) Absolute abundance of ARGs and *intI1* before and after treatment (influent and effluent phase) expressed in log_{10} gene copies mL^{-1}. **(c)** Relative abundance of genes in the influent and effluent expressed as log_{10} gene copies / log_{10} *16S rRNA* copies. The significance of the difference between influent and effluent measurements, as indicated by the Wilcoxon test, is displayed as p<0.05 (*).

happen between or within granules.

Resistance loads in wastewater effluents depend on DNA fraction

Looking at the removal capacity of the full process from influent to effluent, the overall pool of resistance determinants was significantly reduced during WWT (average 1.1 log_{10} gene copies mL^{-1} removal). Some ARGs were still discharged with iDNA inside cells (2-4 log_{10} gene copies g VSS^{-1}) and with exDNA free-floating in water (0.5-3 log_{10} gene copies mL^{-1}) (**Figures 4.5a and S.7**). The majority of the targeted genes decreased after the treatment. From the panel analyzed by qPCR, *intI1*, *blaCTXM*, and *tetO* were significantly ($p<0.05$) removed by 1.3, 1.7, and 2.3 log_{10} gene copies mL^{-1}, respectively.

The AGS process is partially effective at reducing ARGs: Sabri et al. [69] have reported a similar drop for tetracycline resistance gene (*tetW*) in an AGS technology of around 2 log_{10} gene copies mL^{-1}.

Based on the remaining ARGs concentrations in the effluent, an average of 6.3 log_{10} gene copies mL^{-1} were released in total, iDNA plus exDNA (**Figure 4.5b**). Taking hospital discharges as references, this can be considered high (>104 gene copies mL^{-1}) [70]. From **Figure 4.5c**, the normalized values did not significantly enrich bacterial populations carrying ARGs or integrases.

Overall, the AGS WWTP can reduce the amount of ARB but still releases in the environment a significant amount of ARGs enclosed on MGEs of free-floating exDNA. The commonly overlooked exDNA should therefore be considered (together with the iDNA of ARB) as an important factor in the dissemination of resistance determinants in the aquatic environment. Risks associated with exDNA and iDNA fractions discharged in water resources need to be evaluated, with a clear identification of exposures and effects.

4.4. Conclusions

This work led to the following main conclusions:

- *Pseudomonas* and *Rhodoferax* populations were the main potential hosts of antibiotic resistance genes (ARGs) in the biomass. Other potential ARG-carrying populations affiliated with *Acinetobacter*, *Aeromonas*, *Xanthomonas*, *Acidovorax*, *Bacteroidetes*, and *Streptomyces*.
- Several ARGs co-localized with mobile genetic elements (MGEs) on genetic contigs of free-floating extracellular DNA, thus being potentially transferrable to microorganisms. The most abundant ARGs co-localizing with MGEs were the β-lactamases resistance gene *blaVIM-48*, chloramphenicol resistance gene *cmx-1*, sulfonamides resistance gene *sul2*, tetracycline resistance gene *tetA*, and aminoglycoside resistance gene *aadA6*.
- The panel of ARGs and intI1 MGE analyzed by qPCR were detected in all samples.
- The ARG fraction in intracellular DNA decreased with 1.1 log_{10} gene copies mL^{-1} during the process. Conversely, some ARGs located in the exDNA (*ermB*, *sul1* and *sul2*) increased during the process.
- According to metagenomics, exDNA carries ARGs enclosed inside a diversity of MGEs, detected in the WWTP effluent. These can potentially spread AMR in aquatic environments by horizontal gene transfer.

Therefore, studies for the surveillance, risk assessment, and mitigation of AMR in wastewater environments should consider not only iDNA but also exDNA pools.

4.5. Supplementary material

Isolation of intracellular and free-floating extracellular DNA

Filtrations of influents and effluent samples. The total volumes of 1 L of influent and effluent were filtered through 0.22 m polyvinylidene fluoride (PVDF) membranes (Pall Corporation, USA). The filtrates were used to isolate the exDNA. The biomasses retained on membranes were used for iDNA extractions.

Centrifugations and homogenizations of sludge fractions. The sieved sludge fractions were centrifuged at 4,000xG for 10 min before storing at -20°C. The biomass pellets were used for iDNA extraction. The pellets were first treated with DNAse I to remove remaining exDNA fragments, and homogenized with a Potter-Elvehjem pestle (Wheaton, USA).

Isolations of exDNA. The water fractions remaining after sieving were used for exDNA isolation. After filtration through 0.22 µm PVDF membranes, exDNA was loaded for ion-exchange chromatography on a 1-mL, positively charged, diethylaminoethyl cellulose (DEAE) column with 2-µm pore size (BIA Separations, Slovenia). Manufacturer's instructions were followed to condition the column and to process the chromatographic operations. The following buffers and solutions were used to equilibrate, elute, regenerate, clean, and store the DEAE column: (i) equilibration buffer (50 mmol L^{-1} Tris, 10 mmol L^{-1} EDTA at pH 7.2); (ii) elution buffer (50 mmol L^{-1} Tris, 10 mmol L^{-1} EDTA, 1.5 mol L^{-1} NaCl at pH 7.2); (iii) regeneration buffer (50 mmol L^{-1} Tris, 10 mmol L^{-1} EDTA, 2 mol L^{-1} NaCl at pH 7.2); (iv) cleaning solution (1 mol L^{-1} NaOH and 2 mol L^{1} NaCl); (v) storage solution (20% ethanol in ultrapure water). The column was equilibrated using the equilibration buffer at a flowrate of 0.6 mL min^{-1} to maintain the pressure below the maximum limit of 1.8 MPa. After equilibration, the entire volume (1 L) of filtrates containing the exDNA was loaded in the DEAE column using an HPLC pump (Shimadzu Corporation, Japan) at the same flowrate of 0.6 mL min^{-1}. After retention, exDNA was eluted at a flow rate of 1 mL min^{-1} using the elution buffer and tracked over time with an HPLC UV-Vis photodiode array detector (Waters Corporation, USA) recording the UV-light absorption of DNA at 260 nm. The recovered raw exDNA was precipitated from the eluate with ethanol (Moore and Dowhan, 2002). The residual proteins bound to exDNA were digested by 2-h incubation with 0.85 g L^{-1} proteinase K (Sigma-Aldrich, UK) at room temperature. This enzymatic reaction was stopped at 50°C for 10 min in a thermoblock (ThermoMixer, Eppendorf). The protein-digested exDNA was finally purified using GeneJET NGS Cleanup Kit (Thermo Scientific, USA). The purified exDNA isolates were stored at 20°C pending analysis.

Extractions of iDNA. The membranes containing the biomasses filtrated from the influent and effluent samples were directly used for iDNA extraction using PowerWater DNA extraction kit (QIAGEN, The Netherlands) following manufacturer's instructions. For the bioaggregate samples, a mass of 0.25 g of wet weight of homogenized biomass was used to extract iDNA. IDNA extractions were

performed using the DNeasy PowerSoil DNA extraction kit (QIAGEN, The Netherlands) following manufacturer's instructions.

Multidimensional reduction

Dimension reduction is a projection-based method that transforms the data by projecting it onto a set of perpendicular axes. Before dimension reduction, the metagenomic datasets were normalized by dividing the measurements by the corresponding sample size factor using software package "edgeR" [71], and a variance stabilization transformation (VST) was performed using "DESeq2" [72] , respectively. The "vegan" package [73] transformed the stabilized matrices into distance matrices. The Bray-Curtis distance metric was identified as the optimal distance metric for all dimension reduction methods.

Quantitative PCR conditions, primers and standards

Quantitative polymerase chain reaction experiments were performed for the quantification of the genes in Table S1 in the WWTP's DNA samples using the thermal cycler qTOWER3 (Analytica Jena, Germany). Based on the measured cycle threshold values (Ct values), stan¬dard curves were derived, which indicated the efficiency of the reaction and enabled further determination of the genes' concentration. The DNA standards sequences, the standard curves, the reaction results per qPCR. The primers used for each gene and the amplified fragments' lengths are listed in Table S1. The qPCR analysis was performed in a total volume of 20 L using 10 L iQ™ SYBR® Green Supermix1x (BIO-RAD Laboratories; containing dNTPs, iTaq™ DNA Polymerase, MgCl2, SYBR® Green I, enhancers, stabilizers, and passive reference dye fluorescein), 0.2 L of each primer (10 µM), 2 L DNA, and 7.6 L Molecular Biology grade water (Sigma Aldrich, USA). Three technical replicates of each sample were used in all cases to improve accuracy and precision. The thermal cycler's amplification conditions were adjusted according to each gene's properties, and different annealing conditions were applied based on primers' melting temperatures.

Analysis of qPCR results

R version 3.6.3 (R Foundation for Statistical Computing., 2018) was used for visualization and statistical analysis of qPCR data.

A non-parametric Wilcoxon test was performed to determine the significance of the differences detected in the concentrations of genes (log_{10} gene copies VSS^{-1} for iDNA or mL^{-1} for exDNA) between the iDNA and exDNA fractions, and in the absolute and relative abundances of these genes in the influent and effluent (i.e., indicating a removal of the genes due to treatment).

The same Wilcoxon test was used to indicate the significant difference between *rpoB* and *16S rRNA* gene copies for their use as normalization factors in the qPCR results.

Table S.1: Primer sequences used for qPCR amplification in the study and their respective amplification sizes.

Target gene	Primer name	Sequence (5'-3')	Amplicon size (bp)	Reference
16S rRNA	338F	ACTCCTACGGGAGGCAGCAG	146	(Lane, 1991)
	518R	ATTACCGCGGCTGCTGG	146	(Muyzer et al., 1993)
rpoB	rpoB-f-4	CGAACATCGGTCTGATCAACTC	360	(Silkie and Nelson, 2009)
	rpoB-r-2	GTTGCATGTTCGCACCCAT	360	(Silkie and Nelson, 2009)
blaCTXM	CTXM-FW	CTATGGCACCACCAACGATA	103	(Marti and Balcázar, 2013)
	CTXM-RV	ACGGCTTTCTGCCTTAGGTT	103	(Marti and Balcázar, 2013)
ermB	ErmB-F	AAAACTTACCCGCCATACCA	139	(Knapp et al., 2010)
	ErmB-R	TTTGGCGTGTTTCATTGCTT	139	(Knapp et al., 2010)
qnrS	qnrSrtF11	GACGTGCTAACTTGCGTGAT	118	(Marti and Balcázar, 2013)
	qnrSrtR11	TGGCATTGTTGGAAACTTG	118	(Marti and Balcázar, 2013)
sul1	sulI-FW	CGCACCGGAAACATCGCTGCAC	163	(Pei et al., 2006)
	sulI-RV	TGAAGTTCCGCCGCAAGGCTCG	163	(Pei et al., 2006)
sul2	sulII-FW	TCCGGTGGAGGCCGGTATCTGG	191	(Pei et al., 2006)
	sulII-RV	CGGGAATGCCATCTGCCTTGAG	191	(Pei et al., 2006)
tetO	tetO-Fw	ACGGARAGTTTATTGTATACC	171	(Aminov et al., 2001)
	tetO-Rv	TGGCGTATCTATAATGTTGAC	171	(Aminov et al., 2001)
int1	intILC5-fw	GATCGGTCGAATGCGTGT	196	(Barraud et al., 2010)
	intILC1-rv	GCCTTGATGTTACCCGAGAG	196	(Barraud et al., 2010)

Table S.2: The temperature and duration of the annealing phase were different for each gene: *qnrS*, *ermB*, *sul1*, *blaCTXM* – 60ºC, 30 sec; *int1*, *tetO* – 60ºC, 1 min; *sul2* – 61ºC, 1 min; *16S rRNA* – 55ºC, 20 sec; *rpoB* – 55ºC, 30 sec.

Genes	Step	T (ºC)	Time	Genes	Step	T (ºC)	Time
qnrS, sul2, ermB, blaCTXM	1	95	5 min	*16S rRNA, rpoB, tetO, sul1, int1*	1	95	10 min
	2	95	15 sec		2	95	15 sec
	3	Mentioned in description			3	Mentioned in description	
	4	72	30 sec		4	72	10 sec
	5	80	5 sec		5	80	1 sec
	6	80	1 sec		6	95	15 sec
	7	12	59 sec		7	60	1 min
	8	12	1 sec		8	95	15 sec

Statistical significance was established at the 95% confidence level ($p<0.05$). The p-values for the Wilcoxon test are given in **Table S.3-S.4**.

Quantitative PCR statistical results

Table S.3: P-values indicating the statistical significance of the difference between the genes' absolute concentration in the intracellular and the extracellular DNA from influent and the effluent samples.

Gene	Influent	Effluent
16S rRNA	0.005	0.03
blaCTXM	n/a	0.19
ermB	0.003	0.02
qnrs	0.005	0.38
sul1	0.005	0.03
sul2	0.013	0.03
tetO	0.005	0.03
int1	0.005	0.03
rpoB	0.005	0.38

Table S.4: P-values indicating the statistical significance of the differences between the genes' absolute concentration in the different microbial aggregates that constitute the AGS process. LG = Large granules > 1mm, SG = Small granules < 1 mm.

BEGINNING OF AERATION			
Gene	**LG vs SG**	**BG vs flocs**	**SG vs flocs**
16S rRNA	0.030	0.061	0.810
blaCTXM	n/a	n/a	n/a
ermB	1.000	1.000	0.661
qnrs	0.312	0.030	0.194
sul1	0.471	0.885	0.885
sul2	0.665	0.030	1.000
tetO	0.312	0.312	0.665
int1	0.471	0.885	0.665
rpoB	0.381	0.312	0.059
END OF AERATION			
Gene	**LG vs SG**	**BG vs flocs**	**SG vs flocs**
16S rRNA	0.005	0.379	0.005
blaCTXM	n/a	n/a	n/a
ermB	0.028	0.468	0.029
qnrs	0.005	0.005	0.575
sul1	0.936	0.005	0.008
sul2	0.066	0.045	0.936
tetO	0.005	0.013	0.810
int1	0.297	0.936	0.575
rpoB	0.005	0.574	0.005

Metagenomics procedure and quality control

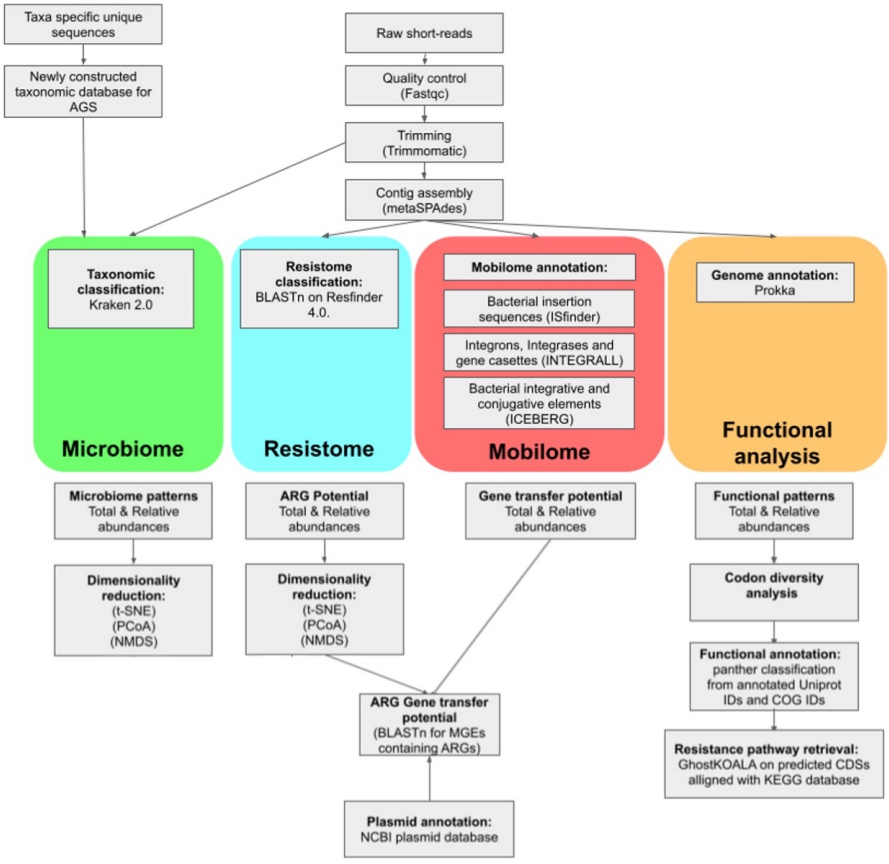

Figure S.1: Schematic representation of the procedures followed for the analysis of the metagenomics dataset.

Taxonomic classification of contigs from all AGS stages and DNA fractions

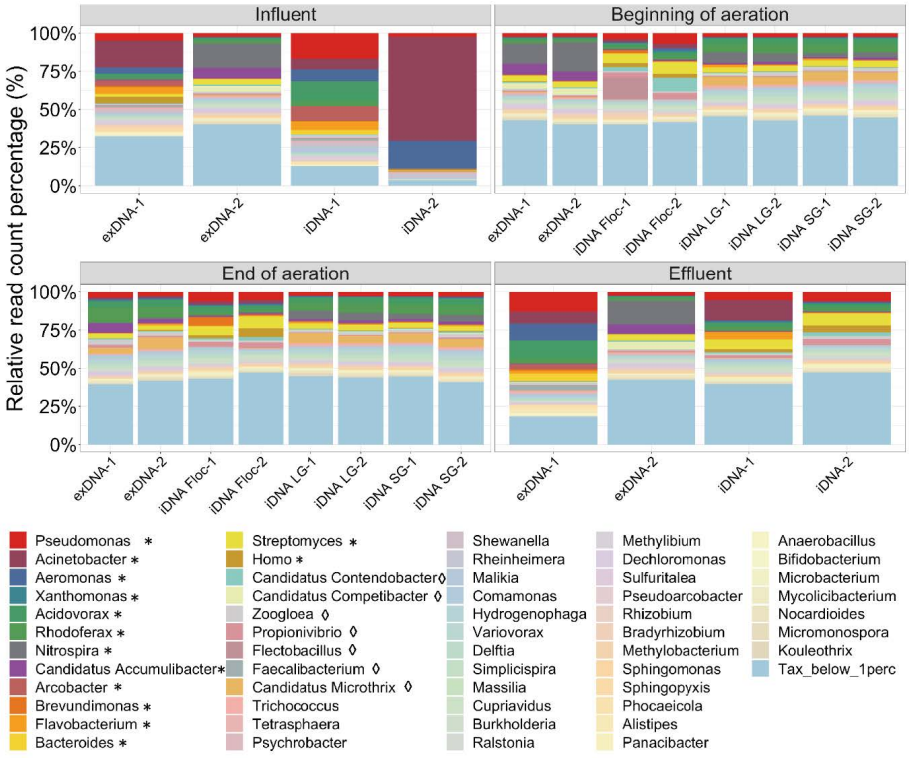

Figure S.2: Taxonomic classification at genus-level of short-reads for different DNA fractions and different microbial aggregate types across four stages of AGS WWT operation. A newly adapted database was used to determine relative abundance (%) of classified reads on genus-level within a sample. Labels: (F) floccular aggregates, (LG) large granules, (SG) small granules, (-1) first biological replicates, and (-2) second biological replicates. Asterisk (*) after genera names indicates genera with >3% relative abundance in at least one of the samples, also with the standard Kraken 2.0 database. Diamond (◇) after genera names indicates genera with >3% relative abundance in at least one of the samples, but not with the standard Kraken 2.0 database. Genera with <1% relative abundance in all samples are labelled as "Tax below 1perc" (light-blue).

Taxonomic classification of ARGs contigs from all AGS stages and DNA fractions

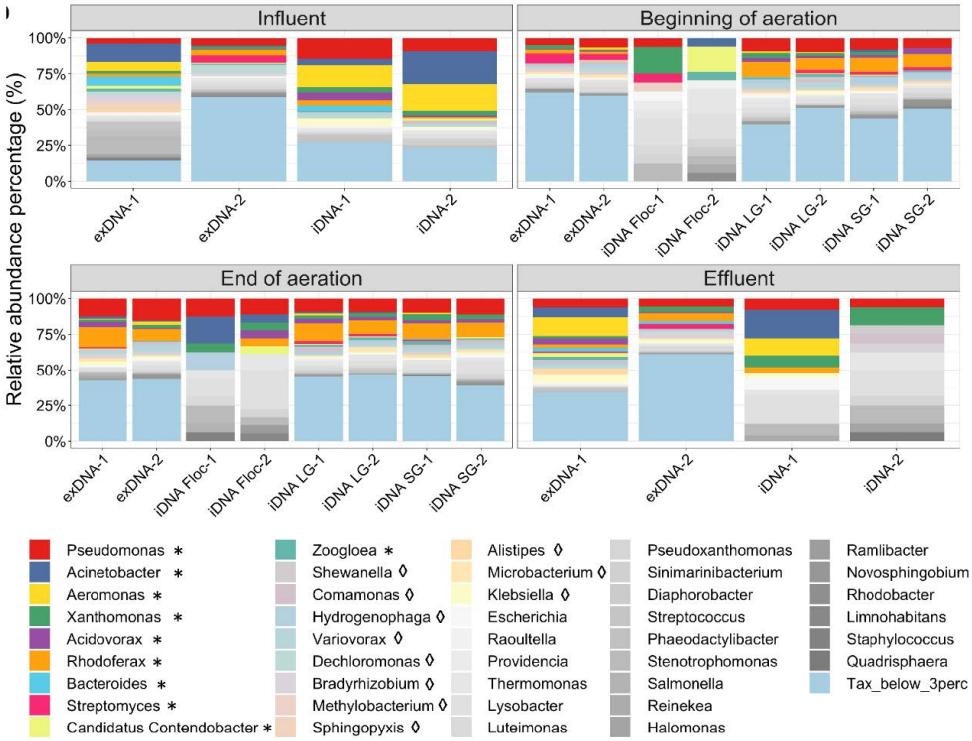

Figure S.3: Relative abundance of contigs containing ARGs across the AGS WWT operation annotated at genus-level using the newly constructed database. Bright colors (*) represent genera above 3% that were already present above 3% relative abundance in the general taxonomic classification **Figure S.2**. Pastel colors (◇) represent genera above 3% that were identified below 3% in the general taxonomic classification. Grey-scale colors represent genera above 3% but identified below 1% in **Figure 4.2c**. Genera with <3% relative abundance in all samples are labelled as "Tax below 3perc" (light-blue).

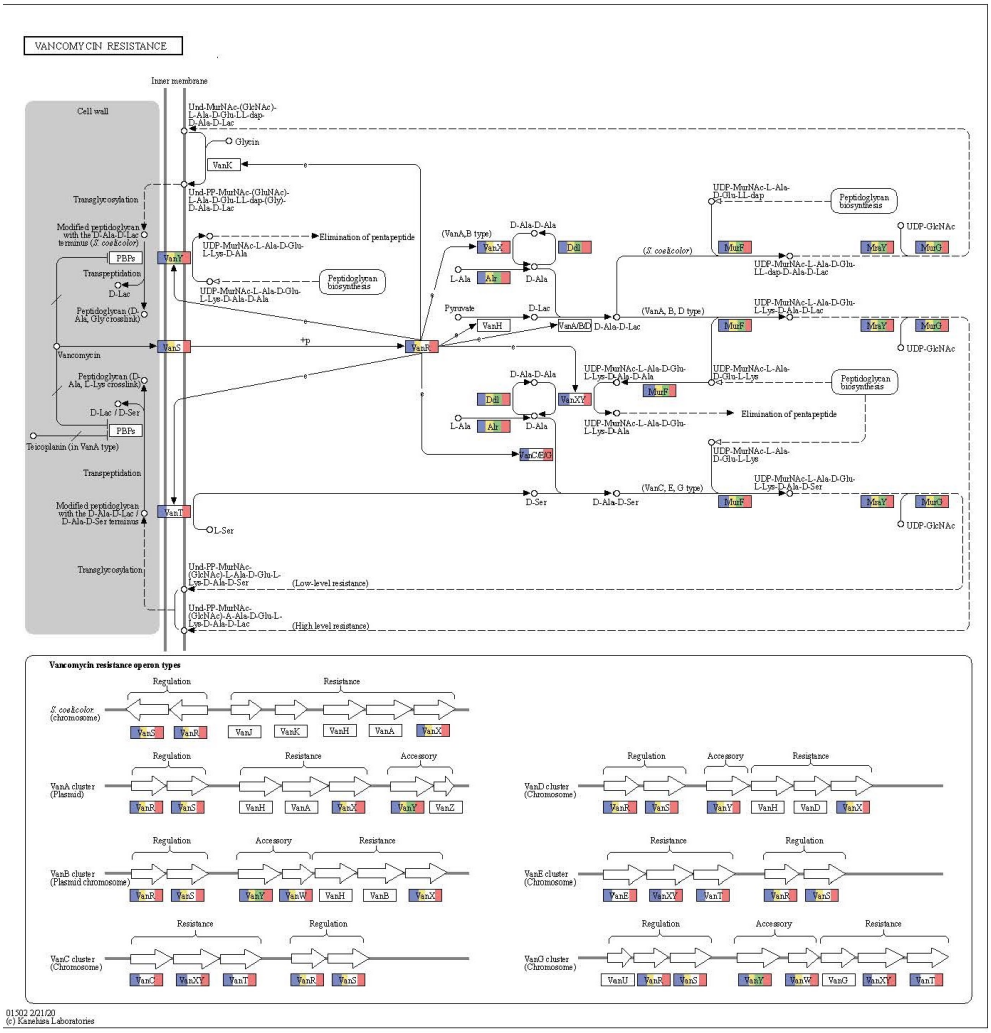

Figure S.4: Vancomycin resistance pathway based on KEGG orthology. Colors indicate the genes that were found to be present in a certain sample: influent iDNA (blue), influent exDNA (yellow), effluent iDNA (green), and effluent exDNA (red).

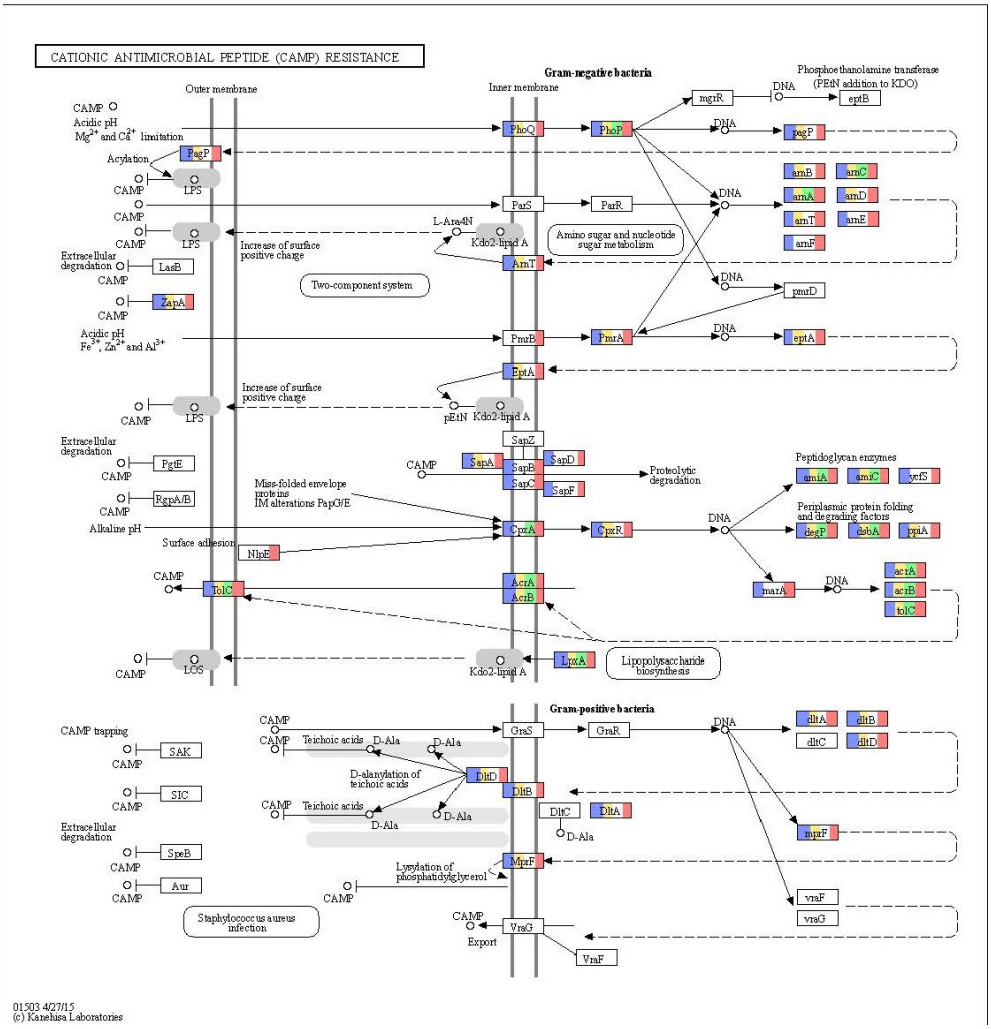

Figure S.5: Cationic antimicrobial peptide (CAMP) resistance pathway based on KEGG orthology. Colors indicate the genes that were found to be present in a certain sample: influent iDNA (blue), influent exDNA (yellow), effluent iDNA (green), and effluent exDNA (red).

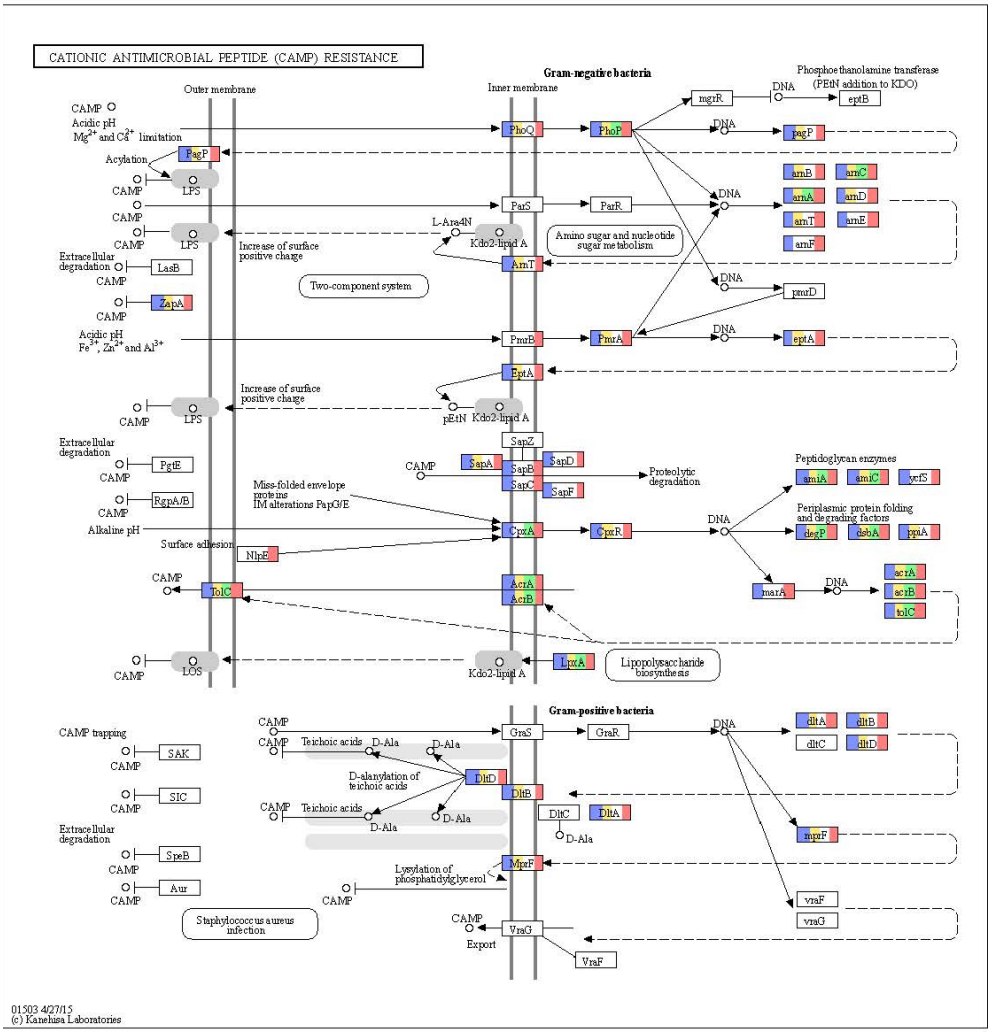

Figure S.6: The β-lactam resistance pathway based on KEGG orthology. Colors indicate the genes that were found to be present in a certain sample: influent iDNA (blue), influent exDNA (yellow), effluent iDNA (green), and effluent exDNA (red).

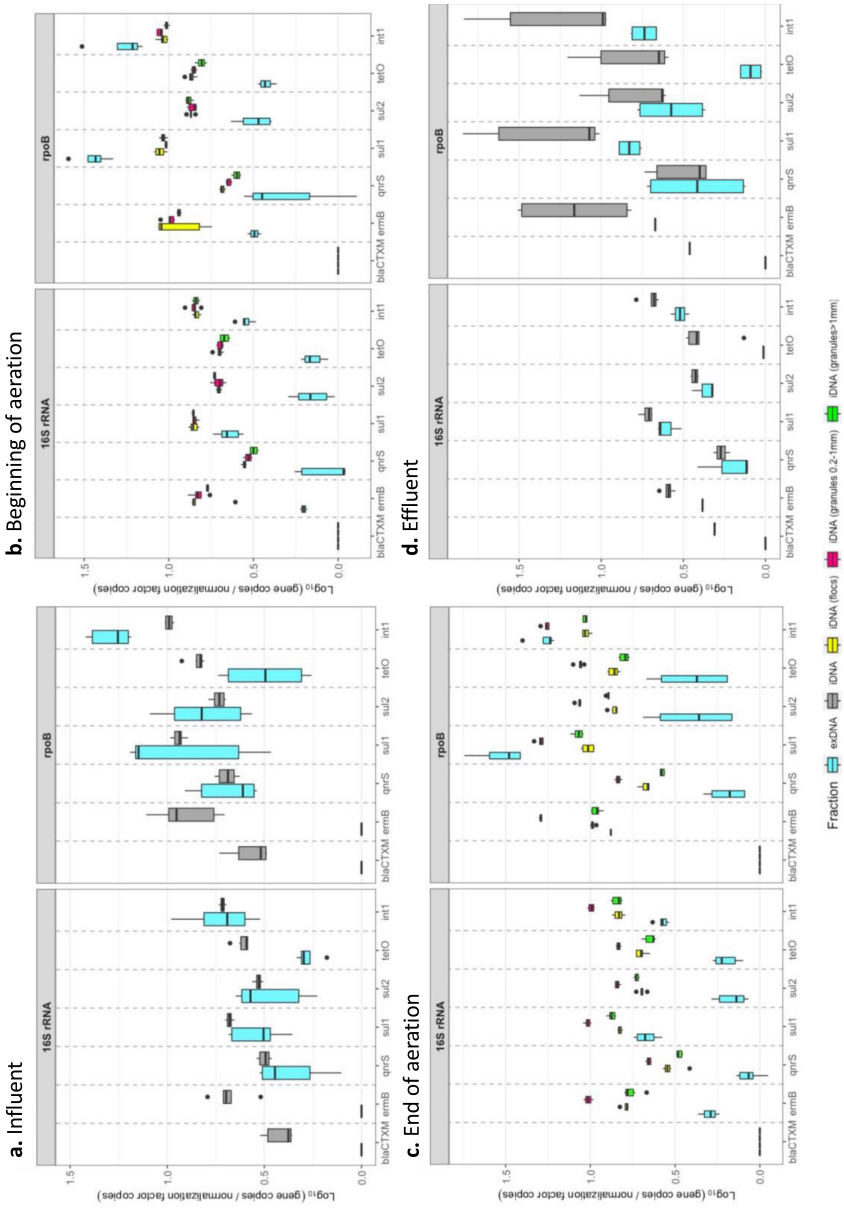

Figure S.7: Relative abundance of gene copies using *16S rRNA* and *rpoB* as a proxy for the concentration of the bacteria. Genes are quantified in terms of log_{10} gene copies / log_{10} *16S rRNA* or *rpoB* gene copies. The four different graphs represent the four AGS WWT steps: **(a)** influent, **(b)** beginning of the aeration, **(c)** end of the aeration, and **(d)** effluent.

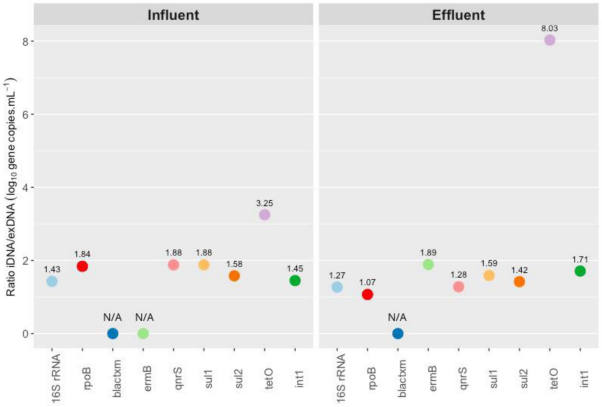

Figure S.8: Ratio of intracellular over extracellular DNA concentration of the genes measured in log_{10} gene copies mL^{-1} for the influent and the effluent phase of the AGS WWT process. Ratios labelled with N/A indicate that the gene was not detected in at least one of the two DNA fractions.

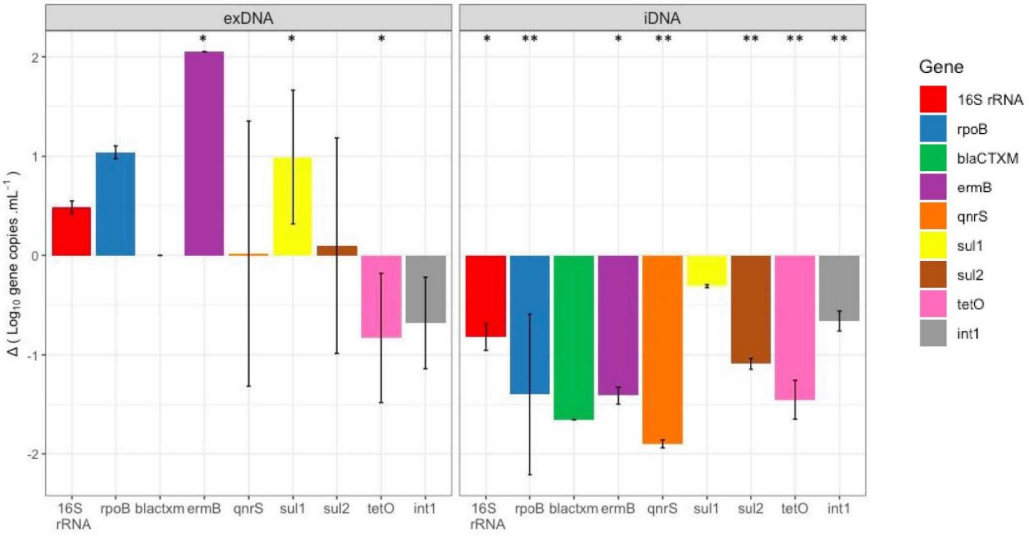

Figure S.9: Effluent minus influent (Δ) in log10 gene copies mL^{-1} for the extracellular (left) and intracellular (right) DNA fraction. The significance of the data, as calculated by the non-parametric Wilcoxon test, is displayed as p<0.05 (* labels) and p<0.005 (** labels).

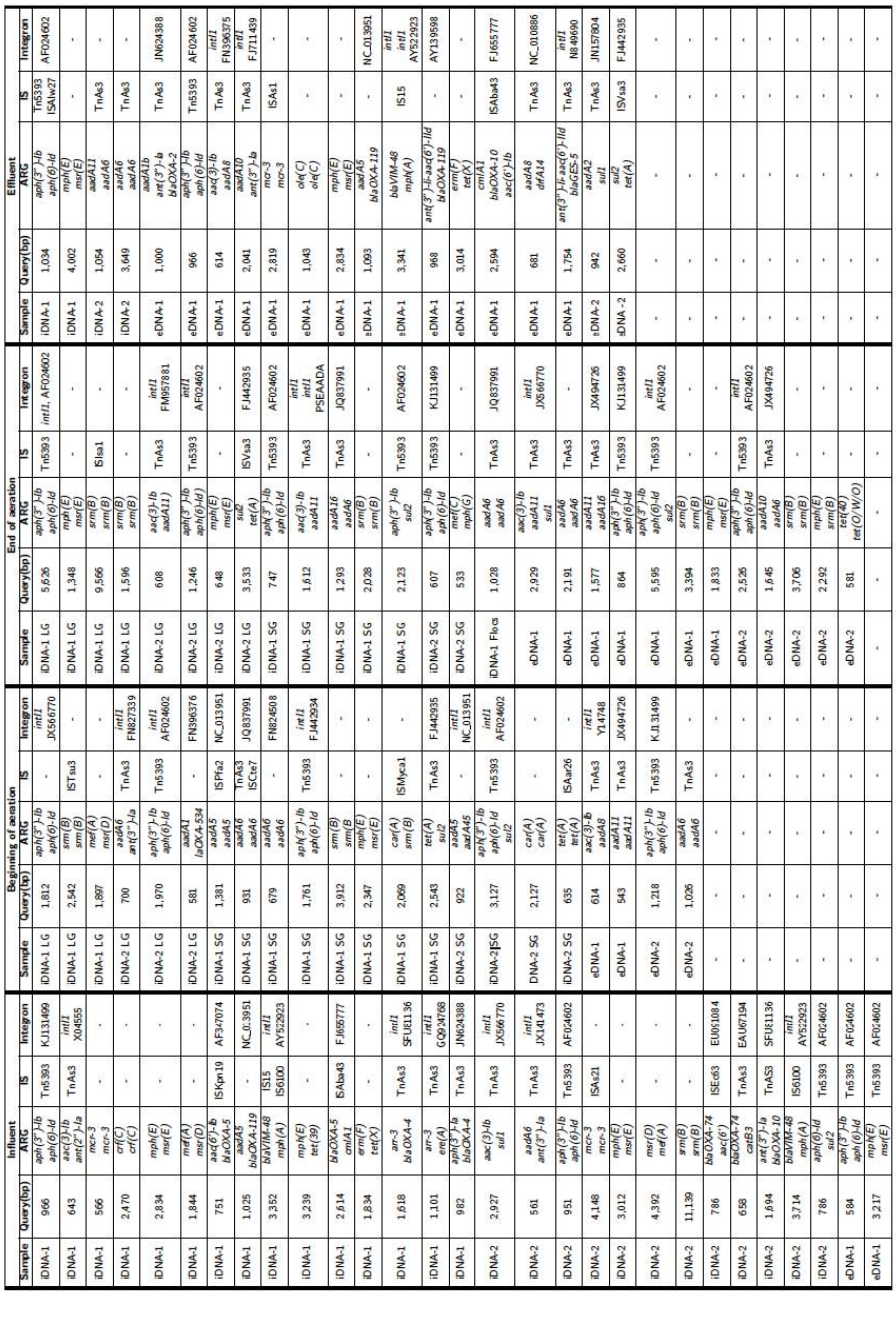

Sample	Query(bp)	Influent ARG	IS	Integron	Sample	Beginning of aeration Query(bp)	ARG	IS	Integron	Sample	End of aeration Query(bp)	ARG	IS	Integron	Sample	Query(bp)	Effluent ARG	IS	Integron
iDNA-1	966	*aph(3'')-Ib aph(6)-Id*	Tn5393	KJ131499	iDNA-1 LG	1,812	*aph(3'')-Ib aph(6)-Id*	-	*intI1* JX566770	iDNA-1 LG	5,626	*aph(3'')-Ib aph(6)-Id*	Tn5393	*intI1*, AF024602	iDNA-1	1,034	*aph(3'')-Ib aph(6)-Id*	Tn5393 ISAlw27	AF024602
iDNA-1	643	*aac(3)-Ib aac(2')-Ia*	TnAs3	*intI1* X04555	iDNA-1 LG	2,542	*sm/(B)*	ISTsa3	-	iDNA-1 LG	1,348	*mph(E) msr(E)*	-	-	iDNA-1	4,002	*mph(E) msr(E)*	-	-
iDNA-1	566	*mcr-3*	-	-	iDNA-1 LG	1,897	*mef(A)*	-	-	iDNA-1 LG	9,566	*sm/(B)*	ISIsa1	-	iDNA-2	1,054	*aadA11*	TnAs3	-
iDNA-1	2,470	*crl(C)*	-	-	iDNA-2 LG	700	*aadA6*	TnAs3	*intI1* FN827339	iDNA-1 LG	1,596	*sm/(B)*	-	-	iDNA-2	3,649	*aadA6*	TnAs3	-
iDNA-1	2,834	*mph(E) msr(E)*	-	-	iDNA-2 LG	1,970	*aph(3'')-Ib aph(6)-Id*	Tn5393	*intI1* AF024602	iDNA-2 LG	608	*aac(3)-Ib aadA11)*	TnAs3	*intI1* FM957881	eDNA-1	1,000	*aadA10 ant(3'')-Ia blaOXA-2*	TnAs3	JN624388
iDNA-1	1,844	*mef(A) msr(D)*	-	-	iDNA-2 LG	581	*aadA1 laOXA-534*	-	FN396376	iDNA-2 LG	1,246	*aph(3'')-Ib aph(6)-Id)*	Tn5393	*intI1* AF024602	eDNA-1	966	*aph(3'')-Ib aph(6)-Id*	Tn5393	AF024602
iDNA-1	751	*aac(6')-Ib blaOXA-5*	ISKpn19	AF347074	iDNA-1 SG	1,381	*aadA5 aadA5*	ISPha2	NC_013951	iDNA-2 LG	648	*mph(E) msr(E)*	-	-	eDNA-1	614	*aac(3)-Ib aadA8*	TnAs3	*intI1* FN396375
iDNA-1	1,025	*aadA5 blaOXA-119*	-	NC_013951	iDNA-1 SG	931	*aadA6 aadA6*	TnAs3 ISCfa7	JQ837991	iDNA-2 LG	3,533	*sul2 tet(A)*	ISVsa3	FJ442935	eDNA-1	2,041	*aadA10 ant(3'')-Ia*	TnAs3	*intI1* FJ711439
iDNA-1	3,352	*blaVIM-48 mph(A)*	ISI15 IS6100	*intI1* AY552923	iDNA-1 SG	679	*aadA6 aadA6*	-	FN824508	iDNA-1 SG	747	*aph(3'')-Ib aph(6)-Id*	Tn5393	AF024602	eDNA-1	2,819	*mcr-3*	ISAs11	-
iDNA-1	3,239	*mph(E) tet(39)*	-	-	iDNA-1 SG	1,761	*aph(3'')-Ib aph(6)-Id*	Tn5393	*intI1* FJ442934	iDNA-1 SG	1,612	*aac(3)-Ib aadA11*	TnAs3	*intI1* PSEAADA	eDNA-1	1,043	*ole(C) ole(C)*	-	-
iDNA-1	2,614	*blaOXA-5 cmlA1*	ISAba43	FJ655777	iDNA-1 SG	3,912	*sm/(B) sm/(B)*	-	-	iDNA-1 SG	1,293	*aadA16 aadA6*	TnAs3	JQ837991	eDNA-1	2,834	*mph(E) msr(E)*	-	-
iDNA-1	1,834	*erm(F) tet(X)*	-	-	iDNA-1 SG	2,347	*mph(E) msr(E)*	-	-	iDNA-1 SG	2,028	*sm/(B) sm/(B)*	-	-	eDNA-1	1,093	*aadA5 blaOXA-119*	-	NC_013951
iDNA-1	1,618	*arr-3 blaOXA-4*	TnAs3	*intI1* SFUE1136	iDNA-1 SG	2,069	*car(A) sm/(B)*	ISMyca1	-	iDNA-1 SG	2,123	*aph(3'')-Ib sul2*	Tn5393	AF024602	iDNA-1	3,341	*blaVIM-48 mph(A)*	IS15	*intI1* AY552923
iDNA-1	1,101	*arr-3 erm(A)*	TnAs3	*intI1* GQ924768	iDNA-1 SG	2,543	*tet(C) tet(C)*	TnAs3	FJ442935	iDNA-2 SG	607	*aph(3'')-Ib aph(6)-Id*	Tn5393	KJ131499	eDNA-1	968	*ant(9'')-Ia-aac(6')-IId blaOXA-119*	-	AY139598
iDNA-1	982	*aph(3'')-Ia blaOXA-4*	TnAs3	JN624388	iDNA-2 SG	922	*aadA45*	-	*intI1* NC_013951	iDNA-2 SG	533	*mef(C) mph(G)*	-	-	eDNA-1	3,014	*erm(F) tet(X)*	-	-
iDNA-2	2,927	*aac(3)-Ib sul1*	TnAs3	*intI1* JX566770	iDNA-2 SG	3,127	*aph(3'')-Ib aph(6)-Id sul2*	Tn5393	*intI1* AF024602	iDNA-1 Fleva	1,028	*aadA6 aadA6*	TnAs3	JQ837991	eDNA-1	2,594	*cmlA1 blaOXA-10 aac(6')-Ib*	ISAba43	FJ655777
iDNA-2	561	*aadA6 ant(3'')-Ia*	TnAs3	*intI1* JX141473	DNA-2 SG	2,127	*car(A) car(A)*	-	-	eDNA-1	2,929	*aac(3)-Ib aadA11 sul1*	TnAs3	*intI1* JX566770	eDNA-1	681	*aadA8 dfrA14*	TnAs3	NC_010886
iDNA-2	951	*aph(3'')-Ib aph(6)-Id*	Tn5393	AF024602	DNA-2 SG	635	*tet(A) tet(A)*	ISAar26	-	eDNA-1	2,191	*aadA6 aadA6*	TnAs3	-	eDNA-1	1,754	*ant(3'')-Ia-aac(6')-IId blaGES-5*	TnAs3	*intI1* N849690
iDNA-2	4,148	*mcr-3 mcr-3*	ISAs21	-	eDNA-1	614	*aac(3)-Ib aadA8*	TnAs3	*intI1* Y14748	eDNA-1	1,577	*aadA11 aadA16*	TnAs3	JX494726	iDNA-2	942	*aadA2 sul1*	TnAs3	JN157804
iDNA-2	3,012	*mph(E) msr(E)*	-	-	eDNA-1	543	*aadA11 aadA11*	TnAs3	JX494726	eDNA-1	864	*aph(3'')-Ib aph(6)-Id*	Tn5393	KJ131499	iDNA -2	2,660	*sul2 tet(A)*	ISVsa3	FJ442935
iDNA-2	4,392	*msr(D) mef(A)*	-	-	eDNA-2	1,218	*aph(3'')-Ib aph(6)-Id*	Tn5393	KJ131499	eDNA-1	5,595	*aph(3'')-Ib aph(6)-Id sul2*	Tn5393	*intI1* AF024602	-	-	-	-	-
iDNA-2	11,139	*sm/(B) sm/(B)*	-	-	eDNA-2	1,026	*aadA6 aadA6*	TnAs3	-	eDNA-1	3,394	*sm/(B) sm/(B)*	-	-	-	-	-	-	-
iDNA-2	786	*blaOXA-74 aac(6')-Ib*	ISEc63	EU001084	-	-	-	-	-	eDNA-1	1,833	*mph(E) msr(E)*	-	-	-	-	-	-	-
iDNA-2	658	*blaOXA-74 catB3*	TnAs3	EAU67194	-	-	-	-	-	eDNA-2	2,526	*aph(3'')-Ib aph(6)-Id*	Tn5393	*intI1* AF024602	-	-	-	-	-
iDNA-2	1,694	*ant(3'')-Ia blaOXA-10*	TnAS3	SFUE1136	-	-	-	-	-	eDNA-2	1,645	*aadA10 aadA6*	TnAs3	JX494726	-	-	-	-	-
iDNA-2	3,714	*blaVIM-48 mph(A)*	IS6100	*intI1* AY552923	-	-	-	-	-	eDNA-2	3,706	*sm/(B) sm/(B)*	-	-	-	-	-	-	-
iDNA-2	786	*aph(6)-Id sul2*	Tn5393	AF024602	-	-	-	-	-	eDNA-2	2,292	*mph(E) sm/(B)*	-	-	-	-	-	-	-
eDNA-1	584	*aph(3'')-Ib sul2*	Tn5393	AF024602	-	-	-	-	-	eDNA-2	581	*tet(40) tet(O/W/O)*	-	-	-	-	-	-	-
eDNA-1	3,217	*mph(E) msr(E)*	Tn5393	AF024602	-	-	-	-	-	-	-	-	-	-	-	-	-	-	-

Figure S.10: Identified contigs containing multiple ARGs. Some also contain MGEs. Annotation of contigs by alignment in ISfinder database is provided in the "Insertion sequence" column with corresponding ISfinder nomenclature. Annotation of contigs by alignment in INTEGRAL database is provided in the "Integron" column with corresponding NCBI accession number.

Bibliography

[1] WHO & UN. *No time to wait: Securing the future from drug-resistant infections report to the secretary-general of the United Nations*. Tech. rep. WHO & UN, 2019. URL: https://www.who.int/antimicrobial-resistance/interagency-coordination-group/IACG_final_report_EN.pdf?ua=1.

[2] J. Davies and D. Davies. "Microbiology and Molecular Biology Reviews Microbiology and Molecular Biology Reviews Origins and Evolution of Antibiotic Resistance". In: *Mol. Biol. Rev. Microbiol. Mol. Biol. Rev* 74.3 (2010), pp. 417–433.

[3] H. O. Ukuhor. *The interrelationships between antimicrobial resistance, COVID-19, past, and future pandemics*. Jan. 2021. DOI: 10.1016/j.jiph.2020.10.018. URL: https://doi.org/10.1016/j.jiph.2020.10.018.

[4] H. Bürgmann, D. Frigon, W. H Gaze, C. M Manaia, A. Pruden, A. C. Singer, B. F Smets, and T. Zhang. "Water and sanitation: an essential battlefront in the war on antimicrobial resistance". In: *FEMS Microbiology Ecology* 94.9 (Sept. 2018), pp. 1–14. ISSN: 1574-6941. DOI: 10.1093/femsec/fiy101.

[5] R. Pallares-Vega, H. Blaak, R. van der Plaats, A. M. de Roda Husman, L. Hernandez Leal, M. C. van Loosdrecht, D. G. Weissbrodt, and H. Schmitt. "Determinants of presence and removal of antibiotic resistance genes during WWTP treatment: A cross-sectional study". In: *Water Research* 161 (2019), pp. 319–328. ISSN: 18792448. DOI: 10.1016/j.watres.2019.05.100. URL: https://doi.org/10.1016/j.watres.2019.05.100.

[6] J. Guo, J. Li, H. Chen, P. L. Bond, and Z. Yuan. "Metagenomic analysis reveals wastewater treatment plants as hotspots of antibiotic resistance genes and mobile genetic elements". In: *Water Research* 123 (Oct. 2017), pp. 468–478. ISSN: 00431354. DOI: 10.1016/j.watres.2017.07.002.

[7] D. Calderón-Franco, M. van Loosdrecht, T. Abeel, and D. Weissbrodt. "Free-floating extracellular DNA: Systematic profiling of mobile genetic elements and antibiotic resistance from wastewater". In: *Water Research* 189.116592 (2021), pp. 1–13. DOI: 10.1101/2020.05.01.072397.

[8] I. B. Slizovskiy, K. Mukherjee, C. J. Dean, C. Boucher, and N. R. Noyes. "Mobilization of Antibiotic Resistance: Are Current Approaches for Colocalizing Resistomes and Mobilomes Useful?" In: *Frontiers in Microbiology* 11.June (2020), pp. 1–20. ISSN: 1664302X. DOI: 10.3389/fmicb.2020.01376.

[9] K. Abe, N. Nomura, and S. Suzuki. *Biofilms: Hot spots of horizontal gene transfer (HGT) in aquatic environments, with a focus on a new HGT mechanism*. 2020. DOI: 10.1093/FEMSEC/FIAA031. URL: https://academic.oup.com/femsec/article/96/5/fiaa031/5766226.

[10] J. S. Madsen, M. Burmølle, L. H. Hansen, and S. J. Sørensen. "The interconnection between biofilm formation and horizontal gene transfer". In: *FEMS Immunology & Medical Microbiology* 65.2 (July 2012), pp. 183–195. ISSN: 0928-8244. DOI: 10.1111/j.1574-695X.2012.00960.x. URL: https://academic.oup.com/femspd/article-lookup/doi/10.1111/j.1574-695X.2012.00960.x.

[11] M. Pronk, M. K. de Kreuk, B. de Bruin, P. Kamminga, R. Kleerebezem, and M. C. van Loosdrecht. "Full scale performance of the aerobic granular sludge process for sewage treatment". In: *Water Research* 84 (2015), pp. 207–217. ISSN: 18792448. DOI: 10.1016/j.watres.2015.07.011. URL: http://dx.doi.org/10.1016/j.watres.2015.07.011.

[12] D. Li, J. Gao, H. Dai, W. Duan, Z. Wang, and Z. Zhou. "Fates of intracellular and extracellular antibiotic resistance genes during a pilot-scale aerobic granular sludge cultivation process". In: *Chemical Engineering Journal* (2020). ISSN: 13858947. DOI: 10.1016/j.cej.2020.127737. URL:

https://reader.elsevier.com/reader/sd/pii/S1385894720338572?token=1246941A70ED9CCF332D30C4300A046A2B248F6625E05A787ED684102E0BF93967D6B5F160C78C8EC3CF5C8575F3originRegion=eu-west-1&originCreation=20210414165816.

[13] M. Ali, Z. Wang, K. W. Salam, A. R. Hari, M. Pronk, M. C. Van Loosdrecht, and P. E. Saikaly. "Importance of species sorting and immigration on the bacterial assembly of different-sized aggregates in a full-scale Aerobic granular sludge plant". In: *Environmental Science and Technology* 53.14 (2019), pp. 8291–8301. ISSN: 15205851. DOI: 10.1021/acs.est.8b07303.

[14] S. Andrews. *FastQC: a quality control tool for high throughput sequence data.* 2010. URL: http://www.bioinformatics.babraham.ac.uk/projects/fastqc.

[15] A. M. Bolger, M. Lohse, and B. Usadel. "Trimmomatic: A flexible trimmer for Illumina sequence data". In: *Bioinformatics* 30.15 (2014), pp. 2114–2120. ISSN: 14602059. DOI: 10.1093/bioinformatics/btu170.

[16] S. Nurk, D. Meleshko, A. Korobeynikov, and P. A. Pevzner. "MetaSPAdes: A new versatile metagenomic assembler". In: *Genome Research* 27.5 (2017), pp. 824–834. ISSN: 15495469. DOI: 10.1101/gr.213959.116.

[17] D. D. Kang, F. Li, E. Kirton, A. Thomas, R. Egan, H. An, and Z. Wang. "MetaBAT 2: An adaptive binning algorithm for robust and efficient genome reconstruction from metagenome assemblies". In: *PeerJ* 2019.7 (2019), pp. 1–13. ISSN: 21678359. DOI: 10.7717/peerj.7359.

[18] D. E. Wood, J. Lu, and B. Langmead. "Improved metagenomic analysis with Kraken 2". In: *Genome Biology* (2019), pp. 1–13. ISSN: 1474-7596. DOI: 10.1101/762302.

[19] D. T. Truong, E. A. Franzosa, T. L. Tickle, M. Scholz, G. Weingart, E. Pasolli, A. Tett, C. Huttenhower, and N. Segata. "MetaPhlAn2 for enhanced metagenomic taxonomic profiling". In: *Nature Methods* 12.10 (2015), pp. 902–903. ISSN: 15487105. DOI: 10.1038/nmeth.3589.

[20] F. Meyer, D. Paarmann, M. D'Souza, R. Olson, E. M. Glass, M. Kubal, T. Paczian, A. Rodriguez, R. Stevens, A. Wilke, J. Wilkening, and R. A. Edwards. "The metagenomics RAST server - A public resource for the automatic phylogenetic and functional analysis of metagenomes". In: *BMC Bioinformatics* 9 (2008), pp. 1–8. ISSN: 14712105. DOI: 10.1186/1471-2105-9-386.

[21] M. Nierychlo, K. S. Andersen, Y. Xu, N. Green, C. Jiang, M. Albertsen, M. S. Dueholm, and P. H. Nielsen. "MiDAS 3: An ecosystem-specific reference database, taxonomy and knowledge platform for activated sludge and anaerobic digesters reveals species-level microbiome composition of activated sludge". In: *Water Research* 182 (2020). ISSN: 18792448. DOI: 10.1016/j.watres.2020.115955.

[22] F. P. Breitwieser and S. L. Salzberg. "Pavian: Interactive analysis of metagenomics data for microbiome studies and pathogen identification". In: *Bioinformatics* 36.4 (2020), pp. 1303–1304. ISSN: 14602059. DOI: 10.1093/bioinformatics/btz715.

[23] R. Kolde. "Package 'pheatmap': pretty heat map". In: (2019), pp. 1–8.

[24] V. Bortolaia, R. S. Kaas, E. Ruppe, M. C. Roberts, S. Schwarz, V. Cattoir, A. Philippon, R. L. Allesoe, A. R. Rebelo, A. F. Florensa, L. Fagelhauer, T. Chakraborty, B. Neumann, G. Werner, J. K. Bender, K. Stingl, M. Nguyen, J. Coppens, B. B. Xavier, S. Malhotra-Kumar, H. Westh, M. Pinholt, M. F. Anjum, N. A. Duggett, I. Kempf, S. Nykäsenoja, S. Olkkola, K. Wieczorek, A. Amaro, L. Clemente, J. Mossong, S. Losch, C. Ragimbeau, O. Lund, and F. M. Aarestrup. "ResFinder 4.0 for predictions of phenotypes from genotypes". In: *Journal of Antimicrobial Chemotherapy* 75.12 (2020). ISSN: 14602091. DOI: 10.1093/jac/dkaa345.

[25] P. Siguier, J. Filée, and M. Chandler. "Insertion sequences in prokaryotic genomes". In: *Current Opinion in Microbiology* 9.5 (2006), pp. 526–531. ISSN: 13695274. DOI: 10.1016/j.mib.2006.08.005.

[26] A. Moura, M. Soares, C. Pereira, N. Leitão, I. Henriques, and A. Correia. "INTEGRALL: A database and search engine for integrons, integrases and gene cassettes". In: *Bioinformatics* 25.8 (2009), pp. 1096–1098. ISSN: 13674803. DOI: 10.1093/bioinformatics/btp105.

[27] M. Liu, X. Li, Y. Xie, D. Bi, J. Sun, J. Li, C. Tai, Z. Deng, and H. Y. Ou. "ICEberg 2.0: An updated database of bacterial integrative and conjugative elements". In: *Nucleic Acids Research* 47.D1 (2019), pp. D660–D665. ISSN: 13624962. DOI: 10.1093/nar/gky1123.

[28] T. Seemann. "Prokka: Rapid prokaryotic genome annotation". In: *Bioinformatics* 30.14 (2014), pp. 2068–2069. ISSN: 14602059. DOI: 10.1093/bioinformatics/btu153.

[29] M. Kanehisa, S. Goto, S. Kawashima, and A. Nakaya. "Thed KEGG databases at GenomeNet". In: *Nucleic Acids Research* 30.1 (2002), pp. 42–46. ISSN: 03051048. DOI: 10.1093/nar/30.1.42.

[30] K. Blin, S. Shaw, A. M. Kloosterman, Z. Charlop-Powers, G. P. van Wezel, M. H. Medema, and T. Weber. "antiSMASH 6.0: improving cluster detection and comparison capabilities". In: *Nucleic Acids Research* 49.May (2021), pp. 29–35. ISSN: 0305-1048. DOI: 10.1093/nar/gkab335.

[31] L. van der Maaten and G. Hinton. "Visualizing Data using t-SNE". In: *Journal of Machine Learning Research* 9 (2008), pp. 2579–2605. ISSN: 15729338. URL: https://www.jmlr.org/papers/volume9/vandermaaten08a/vandermaaten08a.pdf.

[32] RIVM and SWAB. *NethMap 2020*. Tech. rep. 2020. URL: https://www.rivm.nl/publicaties/nethmap-2020-consumption-of-antimicrobial-agents.

[33] L. Ma, A. D. Li, X. L. Yin, and T. Zhang. "The Prevalence of Integrons as the Carrier of Antibiotic Resistance Genes in Natural and Man-Made Environments". In: *Environmental Science and Technology* 51.10 (2017), pp. 5721–5728. ISSN: 15205851. DOI: 10.1021/acs.est.6b05887.

[34] R. Pallares-Vega, L. Hernandez Leal, B. N. Fletcher, E. Vias-Torres, M. C. van Loosdrecht, D. G. Weissbrodt, and H. Schmitt. "Annual dynamics of antimicrobials and resistance determinants in flocculent and aerobic granular sludge treatment systems". In: *Water Research* 190 (2021), p. 116752. ISSN: 18792448. DOI: 10.1016/j.watres.2020.116752. URL: https://doi.org/10.1016/j.watres.2020.116752.

[35] P. Dong, H. Wang, T. Fang, Y. Wang, and Q. Ye. "Assessment of extracellular antibiotic resistance genes (eARGs) in typical environmental samples and the transforming ability of eARG". In: *Environment International* 125.December 2018 (2019), pp. 90–96. ISSN: 18736750. DOI: 10.1016/j.envint.2019.01.050. URL: https://doi.org/10.1016/j.envint.2019.01.050.

[36] S. Zhou, Y. Zhu, Y. Yan, W. Wang, and Y. Wang. "Deciphering extracellular antibiotic resistance genes (eARGs) in activated sludge by metagenome". In: *Water Research* 161 (2019), pp. 610–620. ISSN: 18792448. DOI: 10.1016/j.watres.2019.06.048. URL: https://doi.org/10.1016/j.watres.2019.06.048.

[37] M. K. H. Winkler, C. Meunier, O. Henriet, J. Mahillon, M. E. Suárez-Ojeda, G. Del Moro, M. De Sanctis, C. Di Iaconi, and D. G. Weissbrodt. "An integrative review of granular sludge for the biological removal of nutrients and recalcitrant organic matter from wastewater". In: *Chemical Engineering Journal* 336.July 2017 (2018), pp. 489–502. ISSN: 13858947. DOI: 10.1016/j.cej.2017.12.026. URL: https://doi.org/10.1016/j.cej.2017.12.026.

[38] A. Sengar, F. Basheer, A. Aziz, and I. H. Farooqi. "Aerobic granulation technology: Laboratory studies to full scale practices". In: *Journal of Cleaner Production* 197 (2018), pp. 616–632. ISSN: 09596526. DOI: 10.1016/j.jclepro.2018.06.167. URL: https://doi.org/10.1016/j.jclepro.2018.06.167.

[39] S. K. Toh, J. H. Tay, B. Y. Moy, V. Ivanov, and S. T. Tay. "Size-effect on the physical characteristics of the aerobic granule in a SBR". In: *Applied Microbiology and Biotechnology* 60.6 (2003), pp. 687–695. ISSN: 01757598. DOI: 10.1007/s00253-002-1145-y.

[40] Q. B. Yuan, Y. M. Huang, W. B. Wu, P. Zuo, N. Hu, Y. Z. Zhou, and P. J. Alvarez. "Redistribution of intracellular and extracellular free & adsorbed antibiotic resistance genes through a wastewater treatment plant by an enhanced extracellular DNA extraction method with magnetic beads". In: *Environment International* 131.April (2019), p. 104986. ISSN: 18736750. DOI: 10.1016/j.envint.2019.104986. URL: https://doi.org/10.1016/j.envint.2019.104986.

[41] C. M. Singleton, F. Petriglieri, J. M. Kristensen, R. H. Kirkegaard, T. Y. Michaelsen, M. H. Andersen, Z. Kondrotaite, S. M. Karst, M. S. Dueholm, P. H. Nielsen, and M. Albertsen. "Connecting structure to function with the recovery of over 1000 high-quality metagenome-assembled genomes from activated sludge using long-read sequencing". In: *Nature Communications* 12.1 (2021), pp. 1–13. ISSN: 20411723. DOI: 10.1038/s41467-021-22203-2. URL: http://dx.doi.org/10.1038/s41467-021-22203-2.

[42] H. Guo, J. B. van Lier, and M. de Kreuk. "Digestibility of waste aerobic granular sludge from a full-scale municipal wastewater treatment system". In: *Water Research* 173 (2020),

p. 115617. ISSN: 18792448. DOI: 10.1016/j.watres.2020.115617. URL: https://doi.org/10.1016/j.watres.2020.115617.

[43] D. G. Weissbrodt, N. Shani, and C. Holliger. "Linking bacterial population dynamics and nutrient removal in the granular sludge biofilm ecosystem engineered for wastewater treatment". In: *FEMS Microbiology Ecology* 88.3 (2014), pp. 579–595. ISSN: 15746941. DOI: 10.1111/1574-6941.12326.

[44] J. M. Kristensen, M. Nierychlo, M. Albertsen, and P. H. Nielsen. "Bacteria from the genus arcobacter are abundant in effluent from wastewater treatment plants". In: *Applied and Environmental Microbiology* 86.9 (2020). ISSN: 10985336. DOI: 10.1128/AEM.03044-19.

[45] T. Zhang, X.-X. Zhang, and L. Ye. "Plasmid Metagenome Reveals High Levels of Antibiotic Resistance Genes and Mobile Genetic Elements in Activated Sludge". In: *PLoS ONE* 6.10 (2011), p. 26041. DOI: 10.1371/journal.pone.0026041. URL: www.plosone.org.

[46] C. S. Zhou, J. W. Wu, L. L. Dong, B. F. Liu, D. F. Xing, S. S. Yang, X. K. Wu, Q. Wang, J. N. Fan, L. P. Feng, and G. L. Cao. "Removal of antibiotic resistant bacteria and antibiotic resistance genes in wastewater effluent by UV-activated persulfate". In: *Journal of Hazardous Materials* 388.October 2019 (2020), p. 122070. ISSN: 18733336. DOI: 10.1016/j.jhazmat.2020.122070. URL: https://doi.org/10.1016/j.jhazmat.2020.122070.

[47] E. Tacconelli and N. Magrini. *Global priority list of antibiotic-resistant bacteria to guide research, discovery, and development of new antibiotics.* Tech. rep. 2017, pp. 1–7. URL: https://www.who.int/medicines/publications/WHO-PPL-Short_Summary_25Feb-ET_NM_WHO.pdf.

[48] G. Pietramellara, J. Ascher, F. Borgogni, M. T. Ceccherini, G. Guerri, and P. Nannipieri. "Extracellular DNA in soil and sediment: Fate and ecological relevance". In: *Biology and Fertility of Soils* 45.3 (2009), pp. 219–235. ISSN: 01782762. DOI: 10.1007/s00374-008-0345-8.

[49] R. S. Hendriksen *et al.* "Global monitoring of antimicrobial resistance based on metagenomics analyses of urban sewage". In: *Nature Communications* 10.1 (2019). ISSN: 20411723. DOI: 10.1038/s41467-019-08853-3.

[50] C. Z. Jin, Y. Zhuo, X. Wu, S. R. Ko, T. Li, F. J. Jin, C. Y. Ahn, H. M. Oh, H. G. Lee, and L. Jin. "Genomic and metabolic insights into denitrification, sulfur oxidation, and multidrug efflux pump mechanisms in the bacterium rhodoferax sediminis sp. Nov." In: *Microorganisms* 8.2 (2020), pp. 5–7. ISSN: 20762607. DOI: 10.3390/microorganisms8020262.

[51] A. Miłobedzka, C. Ferreira, I. Vaz-Moreira, D. Calderón-Franco, A. Gorecki, S. Purkrtova, Jan Bartacek, L. Dziewit, C. M. Singleton, P. H. Nielsen, D. G. Weissbrodt, and C. M. Manaia. "Monitoring antibiotic resistance genes in wastewater environments: The challenges of filling a gap in the One-Health cycle". In: *Journal of Hazardous Materials* 424 (2022). ISSN: 18733336. DOI: 10.1016/j.jhazmat.2021.127407.

[52] T. Stalder, M. O. Press, S. Sullivan, I. Liachko, and E. M. Top. "Linking the resistome and plasmidome to the microbiome". In: *ISME Journal* (2019), pp. 2437–2446. ISSN: 17517370. DOI: 10.1038/s41396-019-0446-4. URL: http://dx.doi.org/10.1038/s41396-019-0446-4.

[53] M. A. Toleman and T. R. Walsh. "ISCR Elements Are Key Players in IncA/C Plasmid Evolution". In: *Antimicrobial Agents and Chemotherapy* 54.8 (2010), p. 3534. ISSN: 00664804. DOI: 10.1128/AAC.00383-10.

[54] R. Meyer. "Replication and conjugative mobilization of broad host-range IncQ plasmids". In: *Plasmid* 62.2 (2009), pp. 57–70. ISSN: 0147619X. DOI: 10.1016/j.plasmid.2009.05.001. URL: http://dx.doi.org/10.1016/j.plasmid.2009.05.001.

[55] G. Bönemann, M. Stiens, A. Pühler, and A. Schlüter. "Mobilizable IncQ-related plasmid carrying a new quinolone resistance gene, qnrS2, isolated from the bacterial community of a wastewater treatment plant". In: *Antimicrobial Agents and Chemotherapy* 50.9 (2006), pp. 3075–3080. ISSN: 00664804. DOI: 10.1128/AAC.00378-06.

[56] R. Szczepanowski, I. Krahn, B. Linke, A. Goesmann, A. Pühler, and A. Schlüter. "Antibiotic multiresistance plasmid pRSB101 isolated from a wastewater treatment plant is related to plasmids residing in phytopathogenic bacteria and carries eight different resistance determinants including a multidrug transport system". In: *Microbiology* 150.11 (2004), pp. 3613–3630. ISSN: 13500872. DOI: 10.1099/mic.0.27317-0.

[57] R. Szczepanowski, B. Linke, I. Krahn, K. H. Gartemann, T. Gützkow, W. Eichler, A. Pühler, and A. Schlüter. "Detection of 140 clinically relevant antibiotic-resistance genes

in the plasmid metagenome of wastewater treatment plant bacteria showing reduced susceptibility to selected antibiotics". In: *Microbiology* 155.7 (2009), pp. 2306–2319. ISSN: 13500872. DOI: 10.1099/mic.0.028233-0.

[58] C. K. Ellison, T. N. Dalia, A. Vidal Ceballos, J. C. Y. Wang, N. Biais, Y. V. Brun, and A. B. Dalia. "Retraction of DNA-bound type IV competence pili initiates DNA uptake during natural transformation in Vibrio cholerae". In: *Nature Microbiology* 3.7 (2018), pp. 773–780. ISSN: 20585276. DOI: 10.1038/s41564-018-0174-y. URL: http://dx.doi.org/10.1038/s41564-018-0174-y.

[59] E. Nicolas, M. Lambin, D. Dandoy, C. Galloy, N. Nguyen, C. A. Oger, and B. Hallet. "The Tn3-family of replicative transposons". In: *Mobile DNA III* (2015), pp. 693–726. ISSN: 21650497. DOI: 10.1128/9781555819217.ch32.

[60] O. Nwaiwu and C. C. Aduba. "An in silico analysis of acquired antimicrobial resistance genes in aeromonas plasmids". In: *AIMS Microbiology* 6.1 (2020), pp. 75–91. ISSN: 24711888. DOI: 10.3934/microbiol.2020005.

[61] K. Ikuma and C. R. Rehmann. "Importance of extracellular DNA in the fate and transport of antibiotic resistance genes downstream of a wastewater treatment plant". In: *Environmental Engineering Science* 37.2 (2020), pp. 164–168. ISSN: 15579018. DOI: 10.1089/ees.2019.0319.

[62] Y.-x. Li, Z. Zhong, P. Hou, W.-P. Zhang, and P.-Y. Qian. "Resistance to nonribosomal peptide antibiotics mediated by D-stereospecific peptidases". In: *Nature Chemical Biology* 14.April (2018), pp. 381–387. DOI: https://doi.org/10.1038/s41589-018-0009-4.

[63] J. Alexander, N. Hembach, and T. Schwartz. "Evaluation of antibiotic resistance dissemination by wastewater treatment plant effluents with different catchment areas in Germany". In: *Scientific Reports* 10.1 (2020), pp. 1–9. ISSN: 20452322. DOI: 10.1038/s41598-020-65635-4. URL: http://dx.doi.org/10.1038/s41598-020-65635-4.

[64] J. Lee, J. H. Jeon, J. Shin, H. M. Jang, S. Kim, M. S. Song, and Y. M. Kim. "Quantitative and qualitative changes in antibiotic resistance genes after passing through treatment processes in municipal wastewater treatment plants". In: *Science of the Total Environment* 605-606 (2017), pp. 906–914. ISSN: 18791026. DOI: 10.1016/j.scitotenv.2017.06.250. URL: http://dx.doi.org/10.1016/j.scitotenv.2017.06.250.

[65] J. Wang, L. Chu, L. Wojnárovits, and E. Takács. "Occurrence and fate of antibiotics, antibiotic resistant genes (ARGs) and antibiotic resistant bacteria (ARB) in municipal wastewater treatment plant: An overview". In: *Science of the Total Environment* 744 (2020), p. 140997. ISSN: 18791026. DOI: 10.1016/j.scitotenv.2020.140997. URL: https://doi.org/10.1016/j.scitotenv.2020.140997.

[66] Y. Zhang, A. Li, T. Dai, F. Li, H. Xie, L. Chen, and D. Wen. "Cell-free DNA: A Neglected Source for Antibiotic Resistance Genes Spreading from WWTPs". In: *Environmental Science and Technology* 52.1 (2018), pp. 248–257. ISSN: 15205851. DOI: 10.1021/acs.est.7b04283.

[67] A. Di Cesare, E. M. Eckert, S. D'Urso, R. Bertoni, D. C. Gillan, R. Wattiez, and G. Corno. "Co-occurrence of integrase 1, antibiotic and heavy metal resistance genes in municipal wastewater treatment plants". In: *Water Research* 94 (2016), pp. 208–214. ISSN: 18792448. DOI: 10.1016/j.watres.2016.02.049. URL: http://dx.doi.org/10.1016/j.watres.2016.02.049.

[68] K. Yu, P. Li, Y. He, B. Zhang, Y. Chen, and J. Yang. "Unveiling dynamics of size-dependent antibiotic resistome associated with microbial communities in full-scale wastewater treatment plants". In: *Water Research* 187 (2020). ISSN: 18792448. DOI: 10.1016/j.watres.2020.116450.

[69] N. A. Sabri, S. van Holst, H. Schmitt, B. M. van der Zaan, H. W. Gerritsen, H. H. Rijnaarts, and A. A. Langenhoff. "Fate of antibiotics and antibiotic resistance genes during conventional and additional treatment technologies in wastewater treatment plants". In: *Science of the Total Environment* 741 (2020), p. 140199. ISSN: 18791026. DOI: 10.1016/j.scitotenv.2020.140199. URL: https://doi.org/10.1016/j.scitotenv.2020.140199.

[70] T. H. Le, C. Ng, H. Chen, X. Z. Yi, T. H. Koh, T. M. S. Barkham, Z. Zhou, and K. Y. H. Gin. "Occurrences and characterization of antibiotic-resistant bacteria and genetic determinants of hospital wastewater in a tropical country". In: *Antimicrobial Agents and Chemotherapy* 60.12 (2016), pp. 7449–7456. ISSN: 10986596. DOI: 10.1128/AAC.01556-16.

[71] M. D. Robinson, D. J. McCarthy, and G. K. Smyth. “edgeR: A Bioconductor package for differential expression analysis of digital gene expression data”. In: *Bioinformatics* 26.1 (2009), pp. 139–140. ISSN: 14602059. DOI: 10.1093/bioinformatics/btp616.

[72] M. I. Love, W. Huber, and S. Anders. “Moderated estimation of fold change and dispersion for RNA-seq data with DESeq2”. In: *Genome Biology* 15.12 (2014), pp. 1–21. ISSN: 1474760X. DOI: 10.1186/s13059-014-0550-8.

[73] P. Dixon. “Computer program review VEGAN , a package of R functions for community ecology”. In: *Journal of Vegetation Science* 14.6 (2003), pp. 927–930. URL: http://doi.wiley.com/10.1111/j.1654-1103.2002.tb02049.x.

5

Microbiome, resistome and mobilome of chlorine-free drinking water treatment systems

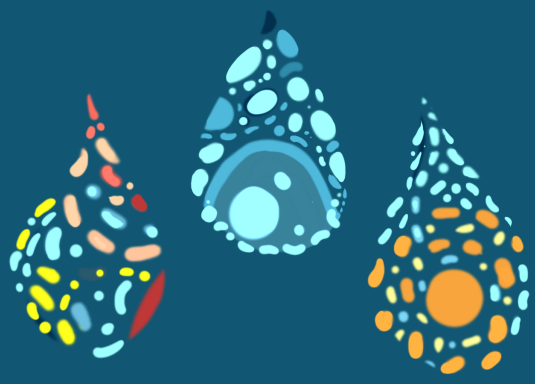

This chapter is submitted: D. Calderon-Franco, F. Corbera-Rubio, M. Cuesta-Sanz, B. Pieterse, D. de Ridder, M.C.M. van Loosdrecht, D. van Halem, M. Laureni and D.G. Weissbrodt. "Microbiome, resistome and mobilome of chlorine-free drinking water treatment systems". In: Water Research (2022)

ABSTRACT

Drinking water treatment plants (DWTPs) are designed to remove physical, chemical, and biological contaminants. However, until recently, the role of DWTPs in minimizing the cycling of antibiotic resistance determinants has got limited attention. In particular, the risk of selecting antibiotic-resistant bacteria (ARB) is largely overlooked in chlorine free DWTPs where biological processes are applied. Here, we combined high throughput quantitative PCR and metagenomics to analyze the abundance and dynamics of microbial communities, antibiotic resistance genes (ARGs), and mobile genetic elements (MGEs) across the treatment trains of two chlorine-free DWTPs involving dune-based and reservoir-based systems. The microbial diversity of the water being treated increased after all biological unit operations, namely rapid and slow sand filtration (SSF), and granular activated carbon filtration. Both DWTPs reduced the concentration of ARGs and MGEs in the water by about 2.5 log gene copies mL^{-1}, despite their relative increase in the disinfection sub-units (SSF in dune-based and UV treatment in reservoir-based DWTPs). The total microbial concentration was also reduced (2.5 log units), and none of the DWTPs were enriched for antibiotic resistant bacteria. Our findings highlight the effectiveness of chlorine-free DWTPs in supplying safe drinking water while reducing the concentration of antibiotic resistance determinants. To the best of our knowledge, this is the first study that monitors the presence and dynamics of antibiotic resistance determinants in chlorine-free DWTPs.

Keywords: *Drinking water treatment plants; Chlorine-free; Antimicrobial resistance; HT-qPCR; Metagenomics*

5.1. Introduction

Access to safe water and sanitation is one key Sustainable Development Goal [1] and objective of the Water Action Decade [2] of the United Nations. Drinking water treatment plants (DWTPs) are used to remove water contaminants and deliver safe water for consumption. The origin and nature of contaminants depends on several factors such as the water source [3], geographical location [4], season [5], and type of anthropogenic activity in the water basin [6]. Contaminants can be divided into physical-chemical (e.g., suspended particles, iron, ammonia, xenobiotic substances) and biological (e.g., pathogens, antimicrobial resistances – AMR) agents [7].

To ensure biological safety in drinking water, microbial (re)growth is usually prevented by the addition of chemical disinfectants such as chlorine [8]. The use of disinfectants generates by-products with mutagenic and carcinogenic effects (Rook, 1976) and selects for antibiotic resistant bacteria (ARB) [9]. A few countries (e.g., The Netherlands, Denmark or Switzerland) ceased their use and rely on strict source-to-consumer production guidelines for drinking water supply [10].

The process configuration of DWTPs is mainly dictated by the water source, either groundwater or surface water. While groundwater is generally microbiologically, surface water may contain pathogenic organisms that must be eliminated [10]. For the chlorine-free production of drinking water from surface water, two main DWTP configurations (dune-based, and reservoir-based) are employed in the Netherlands. Dune-based DWTPs store water under sand dunes and use dune infiltration and rapid sand filtration (RSF) to remove physical-chemical contaminants and slow sand filtration (SSF) to remove microorganisms. Reservoir-based DWTPs store water in open reservoirs and use a treatment train of physical-chemical reactions and RSF to eliminate physical-chemical contaminants and UV disinfection and granular activated carbon (GAC) to remove microorganisms.

In both cases, a large fraction of the treatment consists of bio-based unit operations such as dune infiltration, RSF, SSF or GAC filtration processes that combine biological and physical-chemical processes. In these systems, chemical and biological water contaminants are converted by microbial communities [11, 12] which shape the microbiome of the drinking water that reaches consumers [13]. Therefore, the biological safety of the microbial communities harbored in DWTPs is of utmost importance for public health.

Biofilms are reservoirs of ARB and antibiotic resistance genes (ARGs) [14]. Little is known on the impact of DWTPs on the generation and/or persistence of ARB in drinking water. The selection pressures for ARB development and persistence need to be uncovered as influenced by the very low or non-existent antibiotic concentrations [15], together with the contribution of biofilms present in these biological filters to horizontal gene transfer (HGT) [16].

In contrast to wastewater environments [17–19], few studies focus on the fate and removal of ARGs and ARB in DWTPs. To date, molecular studies of microbial

communities, ARB, and ARGs in DWTPs have been limited by the low biomass concentration present in these systems for DNA extraction, sample collection logistics, and sampling standardization [20]. The results often rely on either lab-scale experiments [21, 22] or specific treatment processes such as biological activated carbon filters (Wan et al., 2021) or tertiary treatments such as chlorine, UV or a combination of them [9, 23]. There is very little information about how biological treatments affect the fate of ARGs and MGEs in full-scale DWTPs from an integral consideration of the treatment chain and from different geographical areas.

Most of the integrative studies that have been reported so far have been carried out in China [24–29], i.e., one of the largest antibiotic-producing and consuming countries world-wide [30]. The studies have used quantitative PCR [24, 26, 29], high-throughput qPCR [27] or sequencing methods like amplicon sequencing and metagenomics [25, 28, 31] to investigate the load and richness of ARGs in full-scale DWTPs. Sevillano et al. [32] have compared the effect of disinfection systems on antimicrobial resistance determinants on tap water samples in DWTPs from The Netherlands, UK and USA, but the effect of the individual process units was overlooked. None of these studies have combined qualitative (metagenomics) and quantitative (HT-qPCR) approaches for their analysis nor focused on the distribution of AMR determinants in chlorine-free DWTPs.

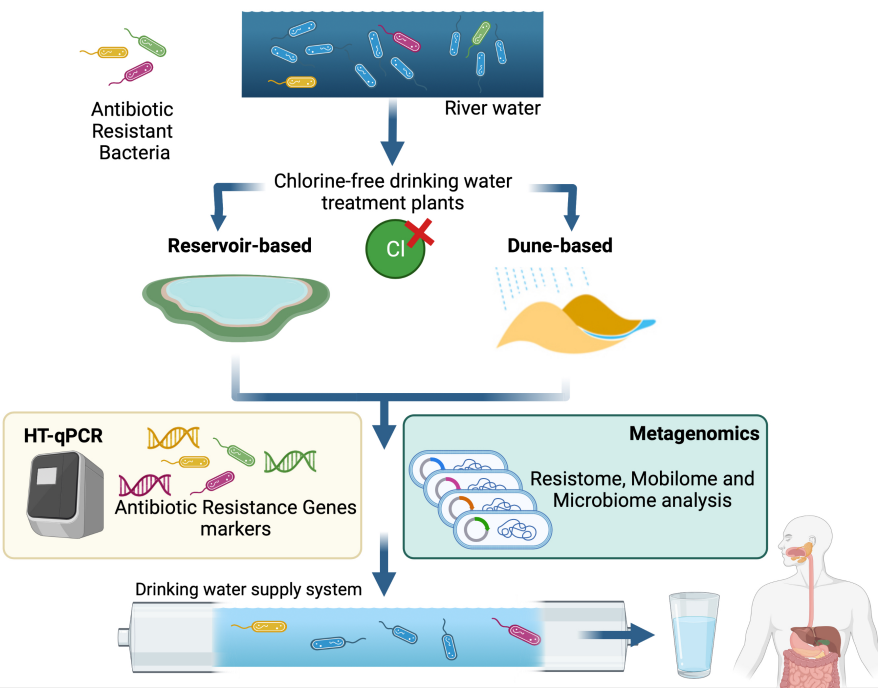

Figure 5.1: Graphical abstract

The dissemination of ARGs throughout an entire DWTP and across process units of treatment chains of low-antibiotic-consuming countries such as The Netherlands was missing. We aimed at quantitatively and qualitatively resolving the role of chlorine-free DWTPs on the spread of ARB and ARGs. We compared the contribution of different methods for water storage, physical-chemical contaminant removal, and disinfection in one dune-based DWTP and one reservoir-based DWTP. Overall, we addressed the fate and diversity of antibiotic resistance determinants in chlorine-free DWTPs.

5.2. Material & Methods

Sampling of two full-scale DWTPs

Water samples were collected from two different chlorine-free DWTPs supplying drinking water to the South Holland and Zeeland provinces in the Netherlands (**Figure 5.2**).

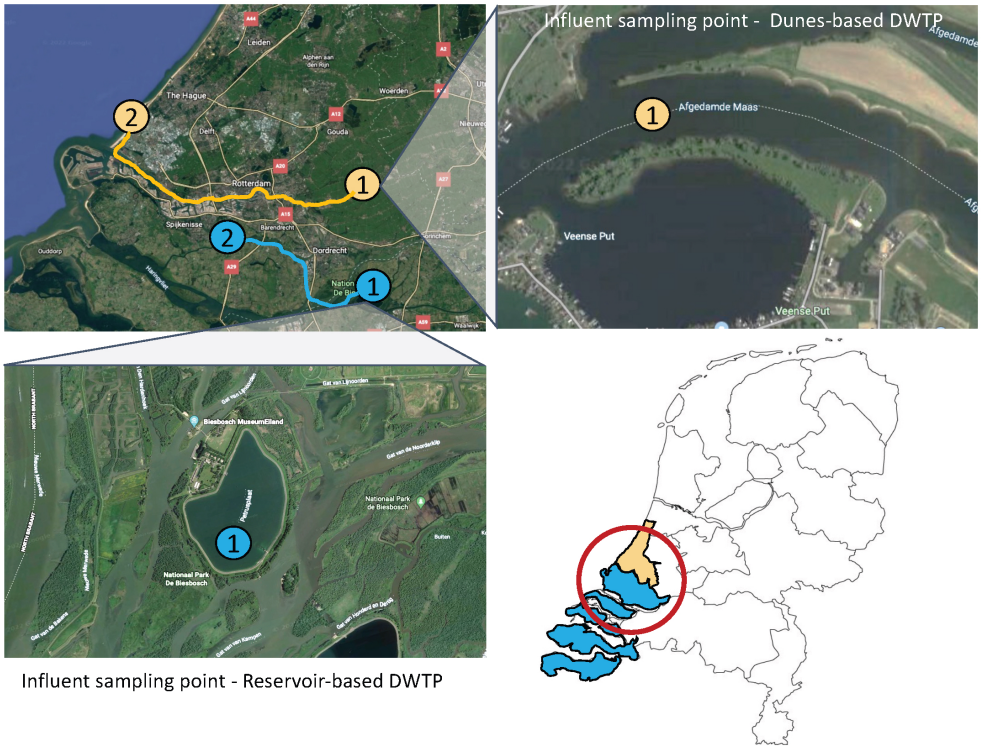

Figure 5.2: Geographic map of sampling sites. Numbering in the figure: (1) represents the river or reservoir from which the influent sample to the DWTP was taken and (2) represents the location of the DWTP.

The first, dune-based DWTP(N 52° 7' 1.9992; E 4° 18' 23.9184) treats surface water from the Meuse River. The second, reservoir-based DWTP (N 51° 48' 44.4132; E 4° 20' 0.2112) processes surface water from the Meuse River (The Netherlands) after storage in a reservoir. Five sampling process stages per DWTP were targeted for water collection across their process stages (**Figure 5.3, Table 5.1**).

The dune-based DWTP samples consisted of: (D1) influent from the Meuse River water (N 51° 55' 41.7288; E 4° 46' 15.7404), (D2) outlet of the first rapid sand filtration, (D3) dune outlet (3 months hydraulic residence time), (D4) outlet of the second rapid sand filtration, and (D5) outlet of the slow sand filtration. The reservoir-based DWTP samples consisted of: (R1) influent of the reservoir from the

Meuse River water (N 51° 45' 39.3228; E 4° 46' 8.6664), (R2) a sample of water after being stored in the reservoir for 3 months, (R3) rapid sand filtration treatment outlet, (R4) UV treatment outlet, and (R5) GAC outlet. Water quality parameters were provided by the DWTPs (**Figure S.2**). The volume of each water sample depended on the expected biomass concentration at each stage, based on author's experience and knowledge of DWTP personnel.

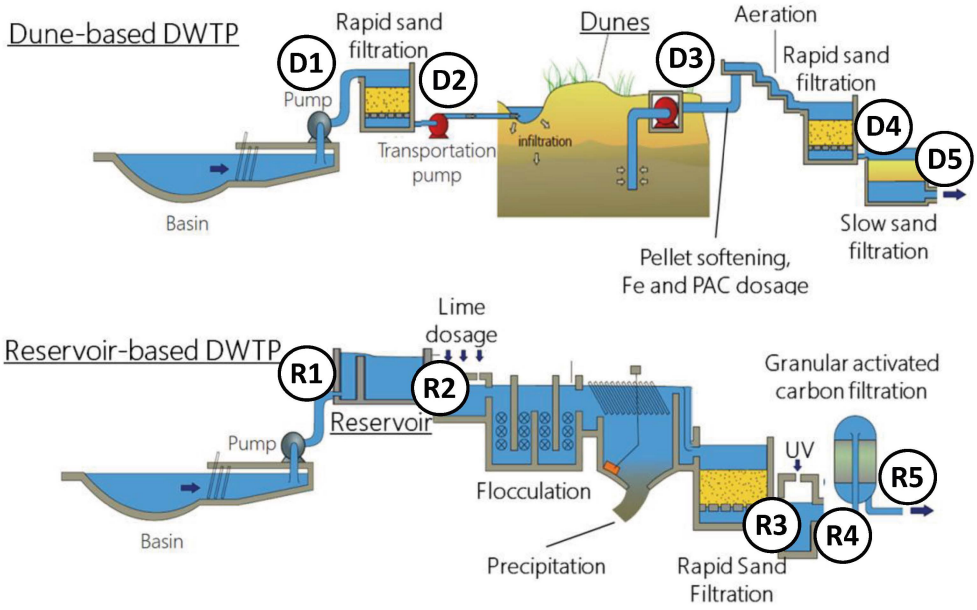

Figure 5.3: Schemes of the dune-based and reservoir-based drinking water treatment processes (DWTPs). The dunes and the reservoir are the storage water steps (underlined). The dune-based DWTP consists of a first rapid sand filtration (RSF1) of the Meuse River water followed by infiltration and storage in dunes (HRT = 3 months). Subsequently, the dune water is processed by pellet softening to regulate hardness, and iron (Fe) and powdered activated carbon (PAC) are dosed to improve the performance of the second rapid sand filtration (RSF2). Finally, the water is disinfected via slow sand filtration (SSF). In the reservoir-based DWTP, the Meuse River water is stored in a reservoir (HRT = 3 months) followed by lime dosage to regulate hardness, flocculation, precipitation and rapid sand filtration to reduce turbidity, and disinfection with UV and taste and odor correction with granular activated carbon (GAC). The overall hydraulic residence times of the waters across the treatment chains amount to circa 3 months in both processes. Sampling points are represented by numbers D1-D5 for the dune-based DWTP (*top*) and R1-R5 for the reservoir-based DWTP (*bottom*). Figure adapted from van Halem and Rietveld [33].

Table 5.1: Water samples collected from the different stages of the dune-based and reservoir-based DWTPs processing surface water from the Meuse River and Meuse River, respectively, in the Netherlands. The metadata for the molecular biology analyses are given.

DWTP system	Sample collection date	Sample description	Water volume extracted (L)	DNA extract quality (A_{260}/A_{280}, ±0.1)	DNA concentration in extract (ng/µL)	Metagenomic analyte identifier
Dune-based	2020-10-26	Meuse River influent	5.8	1.8	71	INF-DB-DWTP
	2020-10-26	RSF1 outlet	9	1.8	27	RSF1-DB-DWTP
	2020-11-30	After dune infiltration	1200	1.8	30	DUNE-DB-DWTP
	2020-12-14	RSF2 outlet	1200	1.8	15.5	RSF2-DB-DWTP
	2020-12-16	SSF outlet	1200	1.8	98	SSF-DB-DWTP
Reservoir-based	2020-12-19	Meuse river influent	1.5	1.8	34	INF-RB-DWTP
	2021-02-24	Reservoir outlet	1.5	1.8	10	RES-RB-DWTP
	2021-03-02	Before UV	100	1.8	11	BefUV-RB-DWTP
	2021-03-03	After UV	100	1.8	22	AftUV-RB-DWTP
	2021-03-05	GAC outlet	210	1.8	11	GAC-RB-DWTP

DNA extraction

Each water sample was immediately filtered on the DWTP site through a 0.22 µm polyethersulfone membrane via vacuum filtration. The membrane containing the biological retentate was folded was introduced into the DNA extraction tubes. Total DNA was extracted using the DNeasy PowerWater DNA extraction kit (Qiagen, The Netherlands) following the manufacturers' instructions. DNA qualities of the extracts were measured as absorbance ratio at 260 and 280 nm using a NanoDrop spectrophotometer. DNA concentrations were measured with a Qubit4 fluorometer (Thermo Fisher Scientific, USA). The DNA quality and concentration obtained for each sample is given in **Table 5.1**.

Library preparation, sequencing, quality control and assembly

Preparation of metagenome libraries

The DNA analytes were sent to Novogene (Cambridge, United Kingdom) for metagenome library preparation and sequencing. A total amount of 1 µg DNA per sample was used as input material for the preparation of libraries that were generated using the NEBNext® Ultra™ DNA Library Prep Kit for Illumina (NEB, USA) following manufacturer's instructions; index codes were added to attribute sequences to each sample. In short, the DNA sample was fragmented by sonication into fragment sizes of 350 bp; the DNA fragments were end-polished, A-tailed, and ligated with the full-length adaptor for Illumina sequencing with further PCR amplification to add the sequence adapters; the PCR products were purified on AMPure XP magnetic beads (Beckman Coulter, USA).

Sequencing of libraries

The library preparations were sequenced with an Illumina HiSEQ PE150 system. Ten raw sequencing files with 150 bp paired-reads were obtained, with an average of 5.6 Gb per sample (41 million reads). More details are given in **Table S.8**.

Quality control of sequenced reads

The quality of the sequenced raw reads was assessed by FastQC (version 0.11.7) with default parameters [34] and visualized with MultiQC (version 1.0) (**Figure S.1**). Low-quality paired-end reads were trimmed and filtered by Trimmomatic version 0.39 on paired-end mode [35].

Assembly of sequence reads

Clean reads were assembled into contigs using MetaSPAdes (version 3.13.0) with a contig length between 300 and 2000 bp [36]. The number of contigs obtained was 37,744.2 on average. All together, they had a total length of 180,840 kb, on average (**Table S.8**).

Microbiome profiling obtained from dune and reservoir-based DWTPs

Taxonomic classification of raw-reads was performed to profile the microbiome from each sample using standard Kraken 2.0 (version 2) database (uses all complete bacterial, archeal, and viral genomes in NCBI Refseq database) with default parameters (Wood et al., 2019). Raw reads, divided into k-mers (substrings of length k contained within a biological sequence, determined by Kraken 2.0), were matched with NCBI database. The absolute abundance of each taxonomic group was indicated as the number of k-mers that aligned to a specific taxonomic group. The relative abundance is the normalization to the total number of k-mers aligned in each sample.

Species richness (S) was measured as the number of different species detected in the raw datasets. The Shannon (H') diversity index was calculated with the following equation:

$$H' = -\sum_{i=1}^{S} p_i \cdot ln\ p_i \tag{5.1}$$

where p_i represents the relative abundance of species i with respect to the total amount of species (S). Microbial community distance estimation was calculated using MinHash in Mash v2.3. [37] with "-k" 18, the minimum value required for distance estimation.

Resistome and mobilome profiling of DNA analytes obtained from both DWTPs

ARGs were annotated by aligning the assembled contigs >500 bp to the ResFinder 4.0 resistance gene database using the BLASTn (version 2.6.0) nucleotide alignment tool with a cut-off E-value $< 10^{-5}$ and sequence identity above 90% [38]. The richness of ARGs was defined as the number of different detected ARGs.

The mobilome was analyzed on the same set of contigs >500 bp using BLASTn (version 2.6.0) with the following specific databases of MGEs with sequence identity >95% and an e-value $< 10^{-20}$. The presence of plasmids was studied with the PLSDB database [39]. Integrons were detected with the INTEGRALL database [40]. The ISfinder database was used to identify bacterial insertion sequences [41]. The ICEberg database (version May 2, 2018) detected bacterial integrative and conjugative elements [42]. For all queries, the ARG or MGE identified with the best score was selected to annotate the query.

Co-occurrence (or co-localization) of MGEs and ARGs within the same contig was identified. It was checked with the BLASTn outputs if a contig contained both ARGs and MGEs. Contigs >500 bp that simultaneously contained hits from the ResFinder 4.0 database and at least one of the different MGE databases were considered to have co-localized. Afterwards, a specific Kraken 2.0 taxonomic analysis was performed with these contigs to identify the potential microbial host that might carry the co-localized ARG and MGE.

Functional analysis of antibiotic-producing microorganisms in water samples

A functional analysis of the metagenomes was performed to detect antibiotic synthesis pathways within microorganisms present in the microbial communities of the water samples. The assembled contigs were transcribed to coding sequences using Prokka (version 1.14.5) with default parameters [43]. Output files were introduced in GhostKOALA (version 2.2.) to assign protein functionality in the Kyoto Encyclopaedia of Genes and Genomes (KEGG) sequence library of "genus_prokaryotes" + "family_eukaryotes" (version 97.0). The mapping onto the KEGG pathway map was performed to obtain the antibiotic-resistance metabolic profile of the metagenome.

High-throughput quantitative PCR analysis

Aliquots of the DNA extracts were sent in parallel to Resistomap (Helsinki, Finland) for high-throughput quantitative PCR (HT-qPCR) in order to detect and quantify the presence and abundance of 295 genes. These genes belonged to ARGs (238 genes), MGEs (51), and pathogens (6). A concentration of 2 ng DNA μL^{-1} in a reaction volume of 0.05 µL was used to obtain the number of gene copies of the different biomarkers. HT-qPCR results were corrected (detailed explanation in

supplementary material) to obtain the number of gene copies existing per volume of filtered water from the DWTPs sampling points.

The gene abundance results were expressed in different ways. The absolute abundance of ARGs and MGEs was calculated as number of gene copies per mL of filtered water as done in Xu et al. [27]. The absolute abundances of ARGs and MGEs sorted by antibiotic class and MGE type were averaged over all genetic components belonging to each group. The relative abundance of ARGs and MGEs was calculated based on the ARG or MGE copies per number of *16S rRNA* gene copies. Abundance values were logarithmically transformed for comprehensive data calculation and visualization.

Statistics and data visualization

Graphs were made with RStudio (version 1.3.1093). Microbiome absolute and relative abundances were calculated by Pavian [44]. Linear correlations between absolute abundances of ARGs and MGEs were analyzed using Pearson correlation coefficient ("ggpubr" R package) at value < 0.05. Pearson correlations between ARGs and each specific type of MGE (plasmid, insertion sequence, integron and transposon) were also calculated. This gives a first-hint proxy for examining the co-localisation of ARGs and MGEs.

5.3. Results

Microbial community composition

Richness and alpha diversity of the water metagenomes

The metagenomes of the microbial communities present at the different sampling points across the dune-based and reservoir-based DWTPs were sequenced to obtain first their taxonomic profiles. DNA extracted from 10 water samples was sequenced, resulting in 41 ± 5 million paired-end reads per sample (**Table S.8**). All sequenced samples had high-quality rates (quality rate per sequence base >30; Q = -10 x log_{10}(P), where P is the probability that a base call is erroneous) (**Figure S.1**). An average of 24.6 ± 6.5% of the raw reads were taxonomically classified. Similar as for wastewater environments, annotation limitations are linked to the still incomplete databases available.

The alpha diversity of the water microbiomes was assessed using richness and Shannon index (**Figure 5.4a**). The first measures the number of different populations (at genus level) in the community, and the latter accounts for the number, relative abundance, and evenness of species [45]. Richness was stable throughout both DWTPs, ranging between 7027 and 7959 different classified species detected from the water metagenomes (**Figure 5.4**). The richness of the influent of the reservoir-based DWTP was 7% higher than the dune-based DWTP influent water. Rapid sand filtration (RSF1 and RSF2), slow sand filtration (SSF), and granular activated carbon (GAC) increased the number of species by 2%, 3.5%, 1%, and 5%, respectively. On the contrary, dune infiltration, reservoir, and UV disinfection decreased it by 4.5%, 3%, and 8%, respectively. The Shannon H' diversity index ranged between 4.9 and 7.7 across all samples (i.e., equivalent to 134 to 2208 virtual equiabundant populations). In the dune-based DWTP, it gradually increased from 5.3 to 7.7 throughout the plant. Equal H' diversity values were found in the influent (6.7) and effluent (6.6) of the reservoir-based DWTP despite its oscillating trend.

The distances between the microbial community compositions were calculated using the MinHash dimensionality-reduction technique in Mash (**Figure 5.4b**). Higher distance indicates larger dissimilarity between the microbial community at each sampling point and the influent. The dissimilarity significantly increased after every step in both DWTPs (p-value < 0.05, expect for After Reservoir where p-value $= 0.09$). Overall, the differences in microbial community compositions across the process chain of the dune-based DWTP were higher than in reservoir-based DWTP.

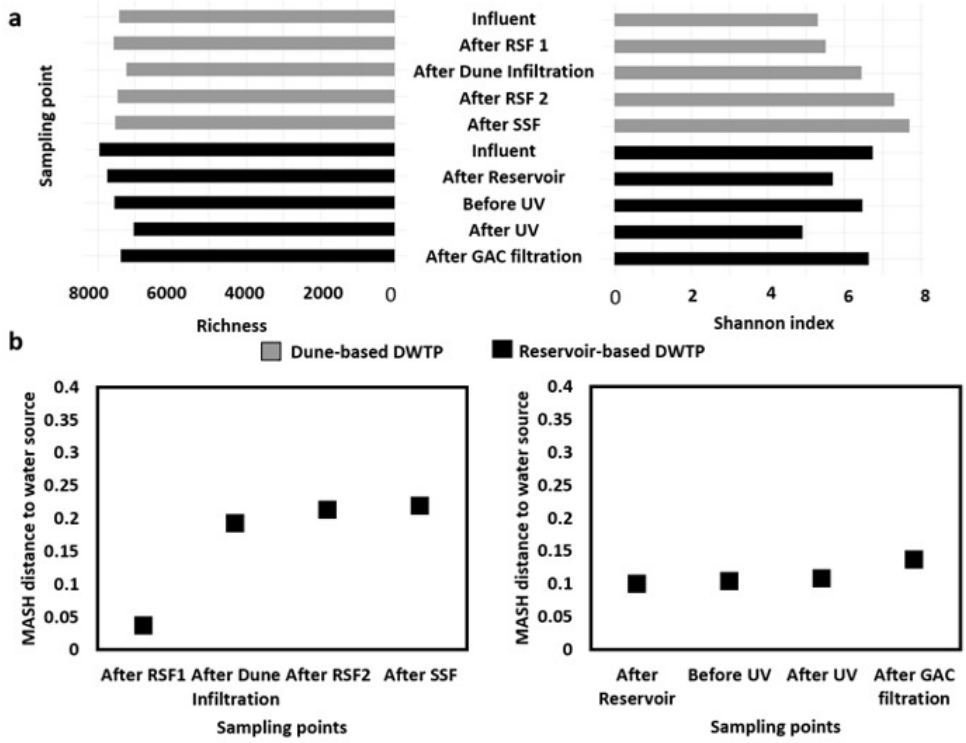

Figure 5.4: a Richness and Shannon diversity indices (x-axes) of the taxonomically classified metagenomics datasets of the waters sampled at the different locations (y-axes) within the dune-based and reservoir-based DWTP chains. **b** Microbial community distance estimation with MinHash between each sampling point and the influent (p-value < 0.05). RSF: rapid sand filtration; SSF: slow sand filtration; GAC: granular activated carbon filtration.

Taxonomic classification of microbial communities

The relative abundance of the detected prokaryotic populations across the DWTPs at phylum and genus levels are shown in **Figure 5.5**. The river influent water of both DWTPs had similar compositions in terms of predominant populations present. At phylum level, *Proteobacteria* (68.1 ± 5.5% in dune-based DWTP *vs.* 76.9 ± 10.2% in reservoir-based DWTP), *Actinobacteria* (17.1 ± 6.5% *vs.* 11.9 ± 5.6%) and *Bacteroidetes* (6.2 ± 3.8% *vs.* 4.9 ± 2.6%) dominated the microbial communities of both DWTPs. No major changes were observed throughout the treatment processes, except for the steady increase in relative abundance of *Firmicutes* from 1.1% to 4.5% across the dune-based DWTP. At genus level, the freshwater genera *Limnohabitans* (24.6% *vs.* 6.4%), "*Candidatus* Planktophila" (8.2% *vs.* 7.5%), and *Flavobacterium* (6.8% *vs.* 6.1%) were the main populations detected in both river waters.

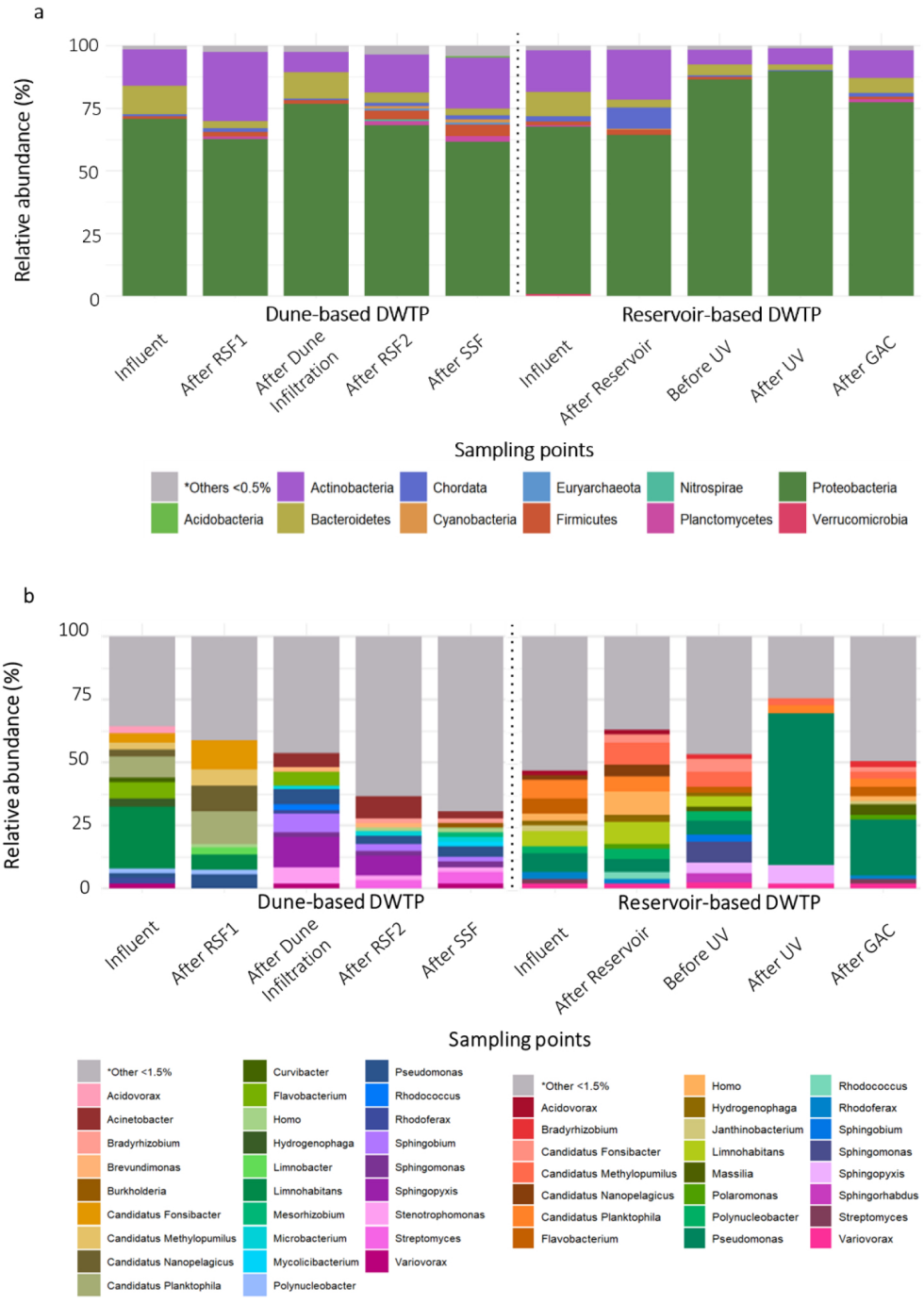

Figure 5.5: Microbial community composition at phylum **(a)** and genus **(b)** level of dune-based and reservoir-based DWTPs, as measured by metagenomics. Relative abundance of classified genera (Y-axis) is represented in the different sampling points (X-axis). Genera with less than 1.5% abundance in all samples was grouped as others.

Their relative abundance decreased throughout the DWTP processes. The main difference between the two DWTPs was the presence of *Pseudomonas* in reservoir-based DWTP (7.6% relative abundance).

In the dune-based DWTP, every sand filter decreased the relative abundance of members of the phylum *Bacteroidetes* (**Figure S.2**) and its most abundant genus *Flavobacterium*. This population decreased from 6.8% to 0.8% in RSF1, from 5.4% to 1% in RSF2, and from 1% to 0.2% in SSF. In contrast, no other genus systematically increased after all sand filtration steps. The most notorious changes were the increase in relative abundance of *Pseudomonas* (3.5%) and *Acinetobacter* (0.9%) in RSF1 and *Streptomyces* (4.5%) in SSF. Overall, the water infiltration in dunes had the highest impact on the microbial community composition: (i) it substantially decreased the relative abundance of genera that where abundant in the influent, namely *Limnohabitans* (from 6.1 to 0.2%) and of "*Ca.* Planktophila" (from 12.8 to <0.1%); and (ii) increased the relative abundances of other genera like *Sphingophyxis* (from 0.1 to 12.1%) and *Sphingobium* (from 0.2 to 12.7%).

Unlike dune infiltration in the dune-based DWTP, the water storage step in the reservoir-based DWTP did not drastically modify the microbial community of the water. The most notorious change is the decrease of *Flavobacterium* from 6.1 to 0.8%. In this DWTP, the most significant change took place in the disinfection step, UV disinfection. The relative abundance of *Pseudomonas* increased from 7.6 to 60%, and *Sphingopyxis* raised from 4.0 to 7.5%. Concomitantly, the presence of the other genera decreased. In the following unit operation, GAC filtration, the relative abundance of *Pseudomonas* decreased to 22.1%, whilst that of other genera such as *Massilia* (3.7%), *Polaromonas* (1.3%) and *Flavobacterium* (2.4%) increased.

Interestingly, we found several microbes in the effluent water absent in the influent. Most of them appeared after dune infiltration, SSF, and GAC filtration. Beyond microorganisms, viruses of the families *Siphoviridae* and *Myoviridae* and genus *Jiaoyazivirus* also displayed such a trend.

Pathogenic bacteria decreased across both chlorine-free drinking water treatment plants

HT-qPCR was used to detect the presence of *Acinetobacter baumannii*, *Pseudomonas aeruginosa* and *Enterobacteriaeae*, the three most critical antibiotic-resistant pathogenic bacteria as designated by the World Health Organization [46]. Overall, the absolute abundance of the pathogenic bacteria detected by qPCR was low ($< 10^6$ gene copies mL^{-1}) and further reduced along the two DWTPs **Figure 5.6**. *Acinetobacter baumanii*, *Pseudomonas aeruginosa*, and *Enterococci* were detected (10^2 genes copies mL^{-1}), while *Klebsiella pneumoniae*, *Campylobacter*, and *Staphylococci* were not. *A. baumanii* was detected across both plants. *P. aeruginosa* was recalcitrant across the treatment chain of the dune-based DWTP, but was not detected after UV disinfection in the reservoir-based DWTP. Interestingly, *Enterococci* was found only after RSF1 in the dune-based DWTP.

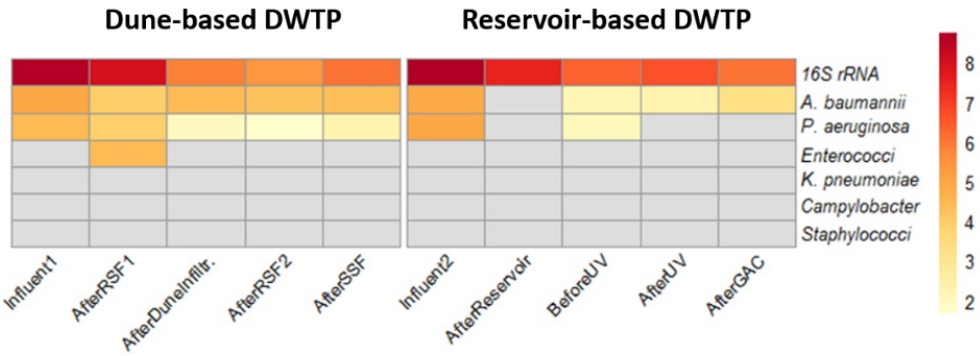

Figure 5.6: Heatmap of absolute gene abundances (number of gene copies mL^{-1}) of 6 pathogenic microorganisms in dune-based and reservoir-based DWTPs, displayed in logarithmic scale. Y-axis represents the abundance of the pathogens in the different sampling points of both DWTPs. In X-axis the *16S rRNA* absolute abundance is provided. RSF: rapid sand filtration; SSF: slow sand filtration; GAC: granular activated carbon filtration.

Gram-negative bacteria as potential carriers of ARGs in DWTPs

The resistance determinants from the two DWTPs exhibited a large diversity of ARGs, highlighted by both qualitative (metagenomics) and quantitative (HT-qPCR) analyses.

The resistome richness ranged from 3 to 20 different ARGs detected per sample. In total, 34 different ARGs were detected in the water of the dune-based DWTP and 58 in the water of the reservoir-based DWTP (**Figure 5.7**). The most abundant ARGs related to resistance against macrolides (MLSB, 57 different ARGs), followed by beta-lactams (13), aminoglycosides (10), quinolones (7), sulfonamide (2), tetracycline (2), and trimethoprim (1). Some ARGs were recalcitrant across the DWTPs: notably, the $msr(D)\_2\_AF27302$ gene conferring macrolide resistance remained in the treated water of the reservoir-based DWTP. In the dune-based DWTP, the dune infiltration step was most prominently increasing the diversity of ARGs. In the reservoir-based DWTP, the rapid sand filtration (before UV step) and the GAC filtration introduced the highest variability in the resistome profile.

We attempted to link ARG contigs to potential microbial origins by assigning taxonomies to contigs carrying ARGs. The results of this analysis at genus level are given in **Figure S.3**. Generally, contigs containing ARGs mainly affiliated with *Limnohabitants* in the influent water samples of both DWTPs. Other genera included *Paracoccus* and "*Ca.* Fonsibacter" in reservoir-based DWTP and *Polynucleobacter*, *Acidovorax*, *Hydrogenophaga* and "*Ca.* Fonsibacter" in dunes-based DWTP. Most of these populations but "*Ca.* Fonsibacter" decreased across the treatment chain in reservoir-based DWTP, while "*Ca.* Fonsibacter" and *Limnohabitans* persisted within the dune-based DWTP.

In the reservoir-based DWTP, the last GAC filtration step mostly increased the number of hosts carrying ARGs. This promoted the release of bacteria potentially carrying ARGs such as *Pseudomonas*, *Kaistella*, *Microbacterium*, *Cellulosimicrobium*, *Caulobacter*, *Methylobacterium*, *Rhodoplanes*, *Messorzhibium* and *Rhodoferax*, among others. In the dune-based DWTP, the dune infiltration step introduced the potential hosts carrying ARGs in the sanitation process. *Acinetobacter*, *Rhodoferax* and *Pseudomonas* were the microbial genera that persisted throughout the whole process after infiltration in the dune.

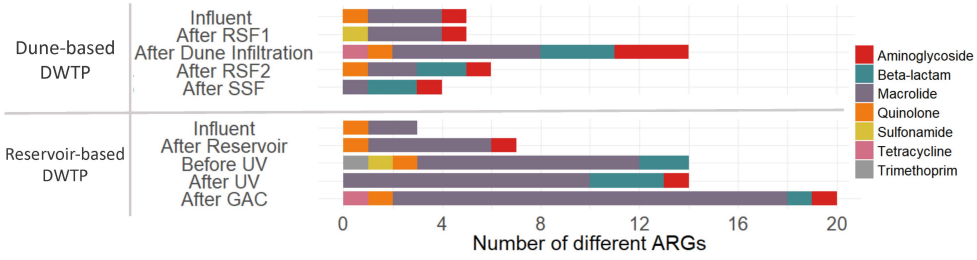

Figure 5.7: Resistome profile of dune-based and reservoir-based DWTP microbiome sorted by antibiotic class. The number of the different ARGs sorted per antibiotic class is represented in the different sampling points. The dotted line discriminates the results coming from each of the analyzed DWTP.

DWTPs are efficient at decreasing the loads of ARGs and MGEs in the treated water

HT-qPCR was used to assess the ARG and MGE removal efficiencies from both DWTPs by quantifying the number of gene copies per volume of filtered water in each sampling point. The absolute concentration of ARGs decreased along the treatment chains down to 2.2 log gene copies mL^{-1} (dune-based DWTP) and 2.6 log gene copies mL^{-1} (reservoir-based DWTP) (**Figure 5.8a**). MGEs decreased by 2.7 log gene copies mL^{-1} (dune-based DWTP) and 2.6 log gene copies mL^{-1} (reservoir-based DWTP) (**Figure 5.8b**). Similarly, the bacterial proxy *16S rRNA* gene decreased by 2.5 (dune-based DWTP) and 2.6 (reservoir-based DWTP) log gene copies mL^{-1}.

The influent water samples from both DWTPs contained similar ARG load: 6.4 ± 0.9 (dune-based DWTP) and 6.8 ± 0.9 (reservoir-based DWTP) log ARG copies mL^{-1}. Across the dune-based DWTP (**Figure 5.8a**), the load of ARGs evolved from 6.0 ± 0.9 (after first rapid sand filtration) to 3.9 ± 0.9 (after dune infiltration), 3.5 ± 0.9 (after second rapid sand filtration), and 4.2 ± 0.9 (after last slow sand filtration) log ARG copies mL^{-1}. In the reservoir-based DWTP, the ARG load evolved from 5.7 ± 0.7 (after 3 months in reservoir) to 4.5 ± 0.9 (before UV treatment), 4.8 ± 0.8 (after UV treatment), and 4.2 ± 0.9 (after GAC filtration) log ARG copies mL^{-1}.

The MGEs load in dune-based DWTP was 7.1 ± 1.2 log MGE copies mL^{-1} in the

influent, 6.2 ± 1.1 log MGE copies mL^{-1} after RSF1 step, 4.2 ± 1.1 log MGE copies mL^{-1} after the dune infiltration, 3.7 ± 1.1 log MGE copies mL^{-1} after the RSF2 and 4.5 ± 1.1 log MGE copies mL^{-1} after the last SSF step. In the reservoir-based DWTP case, the MGE load in the influent was 7.1 ± 1.1 log MGE copies mL^{-1}, followed by 6.0 ± 0.9 log MGE copies mL^{-1} after the 3 months' time in the reservoir, 4.8 ± 1.2 log ARG copies mL^{-1} before UV treatment, 4.9 ± 1.1 log MGE copies mL^{-1} after UV treatment and 4.4 ± 1.2 log ARG copies mL^{-1} after GAC filtration (**Figure 5.8b**).

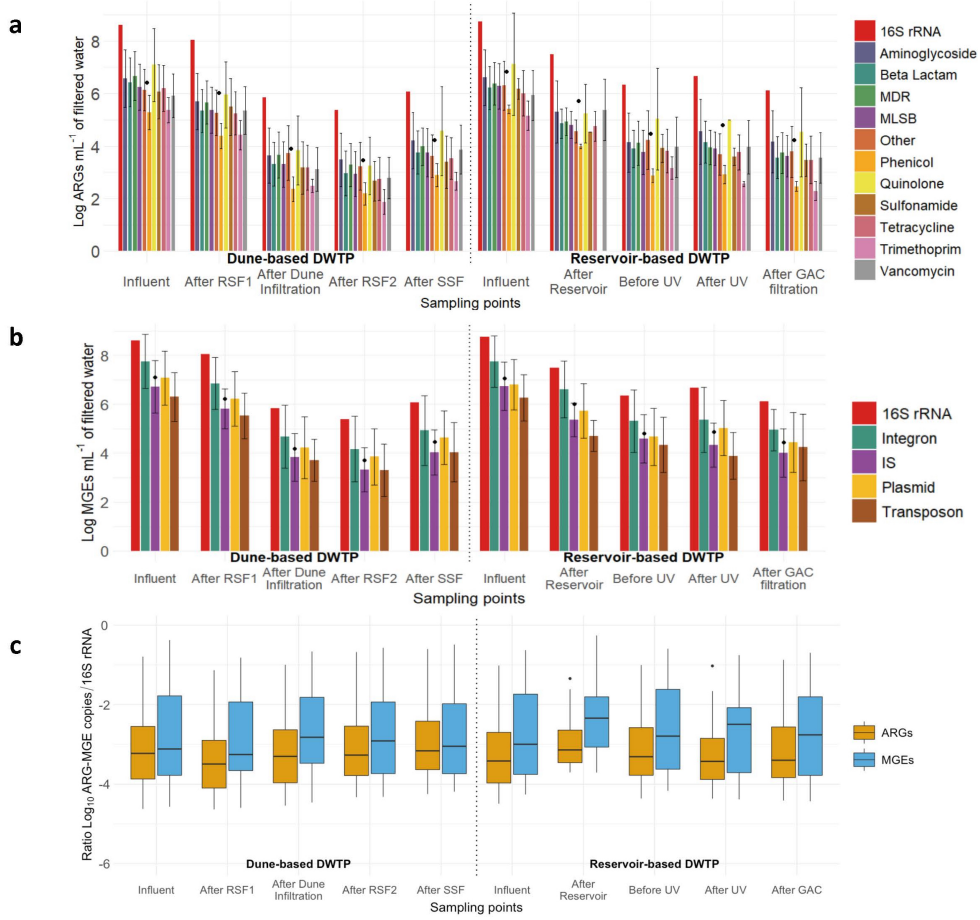

Figure 5.8: (a) Absolute abundance of difference ARGs mL^{-1} (sorted by antibiotic class) from both DWTPs. Values are represented on a logarithmic scale. Black dots indicate the average ARGs abundance per sampling point **(b)** Absolute abundance of difference MGEs mL^{-1} (sorted by antibiotic class) from both DWTPs. Values are represented on a logarithmic scale. Black dots indicate the average ARGs abundance per sampling point. **(c)** The ratio of ARGs or MGEs */16S rRNA* in both DWTPs. Each boxplot represents (from top to bottom) maximum, upper quartile, median, lower quartile, and minimum values. Note: RSF: rapid sand filtration; SSF: slow sand filtration; GAC: granular activated carbon.

Some process stages increased the load of ARGs and MGEs, such as the slow sand filtration in the dune-based DWTP (an increase of 22% in ARGs and 20% in MGEs) and the UV treatment in the reservoir-based DWTP (an increase of 7% in ARGs and 2% in MGEs). However, the decrease in the concentration of ARGs and MGEs was progressive across both DWTPs.

Several ARGs persisted across both DWTPs. The *aadA7* (aminoglycoside resistance; 6.0 ± 1.2 log gene copies mL^{-1}), *mexF* (multi-drug resistance; 5.6 ± 1.2) and *fox5* (beta-lactam resistance; and 5.5 ± 1.3 log gene copies mL^{-1}) genes were the 3 most abundant ARGs in both DWTPs (**Figure S.4**). Other ARGs were not present in the influent but appeared across the DWTPs such as *blaTEM*, *blaPAO* and *vanWG*. From the 238 ARGs tested, 72 (i.e., 30%) were not detected in any sampling point.

Regarding MGEs, the integron genes were the most abundant in both DWTPs (5.8 ± 1.7 log gene copies mL^{-1}): the *intI1_1* (integron), *repA* (plasmid), *intI3* (integron) and *Tn5403* (transposon) genes were the most abundant (**Figure S.5**). The conjugative plasmid sequences such as *IncP_oriT* and *trbC* as well as promiscuous plasmid *IncQ_oriT* gene sequences were also abundant.

Despite the absolute reduction in ARGs and MGEs, the ratios of ARGs and MGEs to the *16S rRNA* gene remained stable throughout both DWTPs (**Figure 5.8c**). This indicates that the DWTP process did not enrich for bacterial populations carrying ARGs or MGEs.

ARGs and MGEs co-localized on contigs of DWTP metagenomes

When ARGs and MGEs co-localize on the same genetic fragment, there is an increased chance that the fragment can be transferred between bacterial cells. Since facilitating the transfer, conjugation, integration and transposition of genes in genomes, MGE can pose a risk for the dissemination of ARGs. Sets of 7 (dune-based DWTP) and 12 (reservoir-based DWTP) events of co-localization of ARGs and MGEs were detected on contigs retrieved from the sequenced metagenomes. Co-localizations were detected in all sampling points from both DWTPs, except for the influent of the reservoir-based DWTP. The ARGs involved coded for mainly aminoglycosides and beta-lactams resistance.

For instance, the *ant(3")-Ia* gene is an aminoglycoside resistant gene broadly described in *Klebsiella pneumoniae*. This persistent ARG was annotated from the metagenome of the dune-based DWTP influent and in the outlets of the RSF1, reservoir, UV and GAC units. This ARG was embedded in plasmids, integrons and bacterial integrative conjugative elements (ICEs), affiliating with *Polynucleobacter* and *Pseudomonas* genera. The *blaVIM* ARG against last-resource beta-lactamases (carbapenem antibiotics) was embedded in plasmid, between insertion sequences, and also in conjugative elements in different stages of the process: in the reservoir-based DWTP, it taxonomically affiliated with *Sphingobium* and

Sphingomonas before UV, and with *Pseudomonas* after UV and GAC.

Other ARGs only appeared once. The *sul2* and *blaOXA-287* genes appeared after RSF1 and dune infiltration, respectively, both affiliating with *Acinetobacter*. The *sul2* gene was carried by plasmid, integrons, as well as bacterial integrative and conjugative elements. The *blaOXA-287* gene was carried by a plasmid. The *sul1* gene appeared before UV, linked to *Sphingobium*. The *blaTEM-181* gene after UV linked to *Bacillus*. Both *sul1* and *blaTEM-181* genes were potentially carried by plasmids, integrons, and bacterial integrative and conjugative elements. The *srm(B)* gene after GAC was already assigned in *Rhodoferax*. The *mef(C)* and *mph(G)* genes appeared after GAC as well, with *Kaistella* as the potential host. These 2 ARGs were detected on the same contig (*NODE*_16870), which implied the possible existence of a plasmid co-containing multiple resistance genes.

5.4. Discussion

Operational units shape the structure of the drinking water microbiome

In order to study the impact of each unit operation on the dynamics of the water microbiome, we applied shotgun metagenomics on water samples collected along the treatment train of two chlorine-free DWTPs, namely a dune-based and a reservoir-based plant. The alpha diversities of both effluents, calculated as H' Shannon diversity indices, were varied from 4.9 to 7.7 (average 6.3 ± 0.8). These values are comparable to other chlorine-free DWTPs (4.37 ± 0.1 – 6.02 ± 0.4; [47], and significantly higher than the ones in plants with chemical disinfection (ca. 2 – 4) [48–50]. Noticeably, the alpha diversity increased after every biological filter (RSF1, RSF2, SSF, and GAC filtration), a likely consequence of direct seeding from biofilm detachment [51, 52].

Proteobacteria, *Actinobacteria*, and *Bacteroidetes* were the most abundant phyla in both DWTPs. This matched with previous observations [26, 53, 54], and with the presence of *Actinobacteria* and *Bacteroidetes* in freshwater ecosystems [55, 56]. Interestingly, the microbial community after the first operational unit of both DWTPs, namely RSF in dune-based DWTP and reservoir in reservoir-based DWTP, was similar to the influent. However, the similarity decreased in the downstream stages of the DWTPs (**Figure 5.4b**). This aligned with the observations of Pinto et al. [13], who highlighted that even though the source water seeds the drinking water microbiome, the unit operations shape the structure of the effluent microbial community.

The conditions within biological sand filters have different impacts on microorganisms fitness [57], yet Webster Fierer [58] postulated that changes in community composition before and after lab-scale biological sand filters are largely predictable. In this line, we found higher abundances of *Actinobacteria* the RSF and SSF effluents as compared to their influents in the dune-based DWTP (**Figure 5.5a**), in analogy to the high *Actinobacteria* abundance in bench-scale sand filters [59]. In contrast, the relative abundance of *Bacteroidetes* decreased after every biological sand filtration unit, similar to earlier reports [60, 61]. Another example are the common freshwater bacteria *Limnohabitans*, "*Ca.* Planktophila", "*Ca.* Nanopelagicus" and *Rhodoluna* [55, 62, 63], abundant in the water influent but almost absent in the DWTPs effluents. Overall, our findings showcase common patterns in the effect of biological operational units unit on the water microbiome dynamics of full-scale DWTP, paving the way to predict and modulate the microbial community in the drinking water effluent.

Chlorine-free DWTPs remove antibiotic resistance determinants

To the best of our knowledge, this is the first study in which the fate of ARG and ARB is monitored throughout the treatment train of chlorine-free DWTPs. Both

DWTPs effectively reduced the concentration of ARGs by ca. 2.5 log gene copies mL^{-1}. These removals are comparable to the highest reported in chlorine-amended DWTPs, between <0.1 log ARG copies mL^{-1} [26, 29] and 2.4 log ARG copies mL^{-1} [24]. Moreover, the total ARG concentration in the water effluent of both chlorine-free DWTPs was ca. 4 log ARG copies mL^{-1}, similar to what Hu et al. [24] found in a chlorine-amended DWTPs. Overall, both chlorine-free DWTP proved at least as effective as chlorine-amended DWTP at reducing ARGs. Additionally, the decrase in ARGs and MGEs concentration was linearly correlated with that of 16S rRNA (**Figure 5.8a, S.6**), proving that none of the biological unit operations in chlorine-free DWTPs selected for ARB, i.e. the ARB/16S ratio did not increase.

The water storage steps yielded the highest ARG and ARB removal in both plants (2.1 and 1.6 ARG copies mL^{-1} in dune- and reservoir-based DWTPs, respectively), likely due to biomass decay and plasmid degradation due to the high hydraulic retention times and low nutrient availability in these systems [64–66]. Likewise, RSFs reduced the ARG and ARB concentration by decreasing biomass concentration, as previously reported [24, 26, 29]. Unexpectedly, GAC filtration also decreased the concentration of ARGs (**Figure 5.8a**), in contrast to previous studies describing GAC filtration as the critical step where resistance determinants increase [26, 28, 67]. However, the decrease in ARGs concentration in this study contrasted with the increase in ARG richness (**Figure 5.7**), which suggests that the microbiome in the GAC effluent is seeded by the GAC biofilm.

The final treatment step before discharge to the environment is disinfection, which is intended to suppress or inactivate harmful microorganisms and prevent the regrowth of opportunistic bacteria [68]. However, the SSF (0.75 log gene copies mL^{-1}) and UV treatments (0.32 log gene copies mL^{-1}) in this study increased the concentration ARGs (**Figure 5.8a-b**). The fate of ARG in SSF has not been directly studied before. However, Xu et al. [59] showed that SSF hardly decreases the concentration of antibiotics in water, and Ciric [69] reported that while their SSF removed most of the microorganisms, those in the effluent were more prone to resistance to antibiotics. In the case of UV treatment, previous studies proved its efficacy for cell reduction (plate counting) but not for ARGs removal [21, 70]. Gram-negative bacteria, and specifically *Pseudomonas*, tolerate UV by efficient repair mechanisms, high growth rates, or the use of low-molecular-weight organic carbon (generated by UV illumination) as an energy source [71]. This can explain the drastic rise in relative abundance of *Pseudomonas*, a common multi-drug resistant bacteria in drinking water systems [26], and the quantitative increase in the 16S rRNA gene marker after UV disinfection **Figure 5.8a**). Nevertheless, despite the intermediate increase of ARGs, MGEs, and pathogenic bacteria after disinfection, DWTPs successfully reduced their effluent concentration **Figure 5.6, 5.8**, S.7).

5.4.1. Clinical implications of gene transfer in chlorine-free DWTPs

In concert with wastewater treatment plants (WWTPs), DWTPs are the ultimate barriers preventing the spread of waterborne diseases, and the release of antibiotics, ARB, and ARGs into water systems [18, 72]. One crucial aspect is the presence of ARGs against last-resort antibiotics such as carbapenems or colistin. Carbapenem resistance genes like *blaIMP* or *blaVIM* (class B beta-lactamases resistant genes) have been described in pathogenic bacteria such as *Pseudomonas*, *Acinetobacter*, or *Enterobacteriaceae* [73, 74]. Carbapenem is a beta-lactam antibiotic with a broad antimicrobial spectrum and administered as a last resort for treating drug-resistant bacterial infections. However, the number of carbapenem-resistant bacteria has steadily increased [75], and represents a primary concern in drinking water. *blaIMP* genes were rarely detected along both DWTPs. However, *blaVIM* was detected along the dune-based DWTP and in the effluent (after GAC treatment) of the reservoir-based DWTP (**Figure S.4)**. The taxonomic annotation of the contigs containing *blaVIM* genes revealed their potential co-localization with multiple plasmids affiliating with *Sphingobium* in the dune-based DWTP, and with *Sphingobium* (plant pathogen) and *Pseudomonas* in the reservoir-based DWTP after GAC filtration. The carbapenem-resistant *Pseudomonas* is accounted by WHO within the list of critical priority pathogens for which new antibiotics are required [46]. Colistin resistance genes, such as *mcr1* variants, were also highly abundant in both the dune-based and the reservoir-based DWTPs. However, this is not unique to chlorine-free DWTPs as multiple last-resort ARGs have also been identified in conventional DWTP (with chlorine use) as well as in tap water [76]. Importantly, the *mcr1* gene load decreased significantly along the water treatment trains and neither co-localized with any MGE nor affiliated with any pathogenic bacteria. Further research should underpin the regrowth capacity of such pathogens in chlorine-free DWTP effluents.

5.5. Conclusion

In this work, we characterized for the very first time the abundance and dynamics of microbial communities, antibiotic resistance genes (ARGs), and mobile genetic elements (MGEs) across the treatment trains of two chlorine-free drinking water treatment plants. The in depth analysis of the metagenomes and resistomes led to the following main conclusions:

- Chlorine-free DWTPs do not select for antibiotic resistant bacteria, as supported by the linear correlated between ARGs and MGEs, and the 16S rRNA concentrations.
- The measured reduction in ARGs concentration by ca. 2.5 log gene copies mL^{-1} in both chlorine-free DWTPs is comparable to the highest removals reported so far for chlorine-amended DWTPs.
- Water storage systems alone reduced the abundance of the 16S rRNA gene, ARGs, and MGEs by ca. 1.6 log gene copies mL^{-1}, and dune infiltration achieved the highest removal.
- Despite a ca. 2.5 log 16S rRNA gene copies mL^{-1} reduction, the effluent microbial diversity increased likely due to the seeding from the biofilms actively growing in the rapid and slow sand filters, and the granular activated carbon ones.
- Despite the overall ARG decrease in the DWTP, disinfection (slow sand filtration and UV radiation) internally increased the concentration of ARGs, MGEs, and 16S rRNA genes by ca. 0.5 log gene copies mL^{-1}, yet with no impact on overall reduction.

Overall, our findings confirm the effectiveness of chlorine-free DWTPs in providing safe drinking water and reducing the load of antibiotic resistance determinants, offering the Water Authorities the possibility to establish centralized risk management around these specific treatment steps.

5.6. Supplementary material

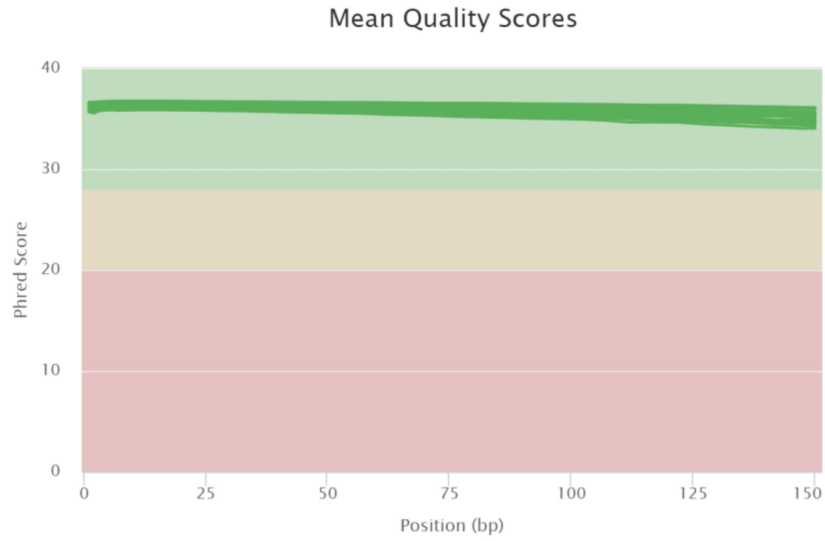

Figure S.1: Mean FastQC quality score for the 10 samples sequenced from dune- and reservoir-based DWTPs. Y-axis represents the mean quality score (Phred) obtained by FastQC and X-axis represents the specific position in the read in basepairs (bp).

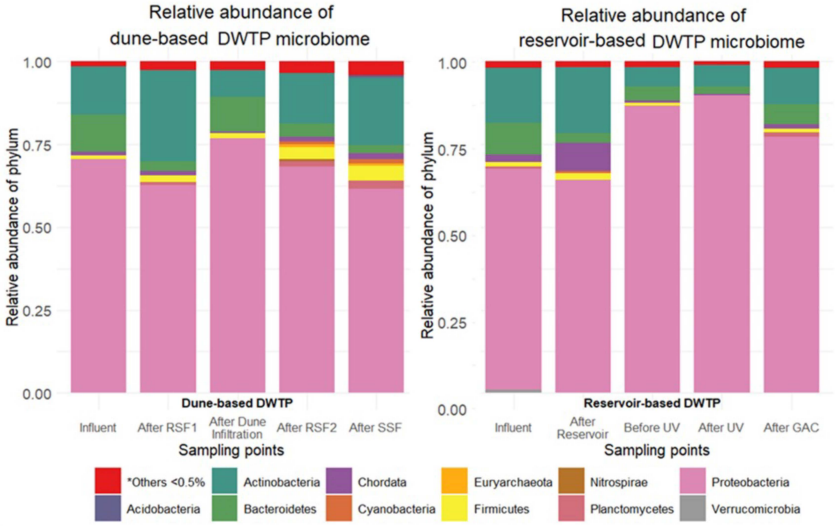

Figure S.2: Microbial community composition at phylum level of dune-based and reservoir-based DWTPs. Relative abundance of the classified phyla (Y-axis) is represented in the different sampling points (X-axis). Phyla with less than 0.5% abundance in all samples was grouped as others.

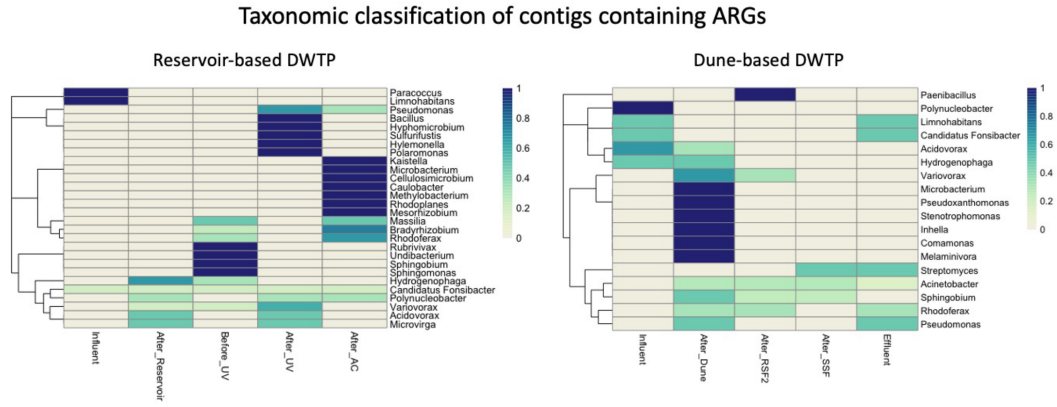

Figure S.3: Taxonomic classification at genus-level of contigs encoding ARGs heatmap. Colors represent the relative abundance at genus level in all classified sequences. Labels: (UV) Ultraviolet, (AC) Granular activated carbon, (RSF2) Second Rapid Sand Filtration, (SSF) Slow Sand Filtration.

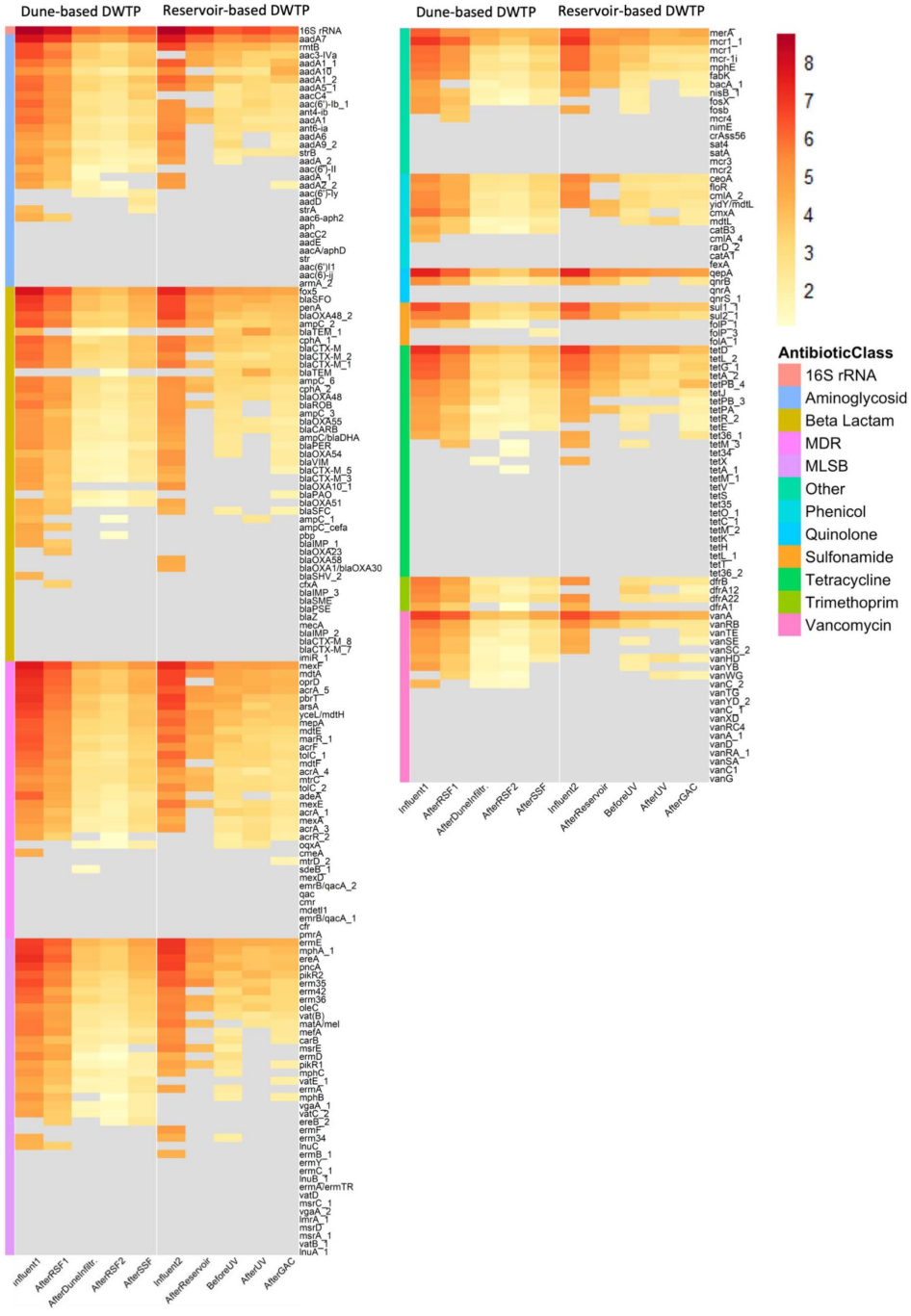

Figure S.4: Heatmap of absolute abundance from the 238 ARGs mL^{-1} tested from both dune-based and reservoir-based DWTPs. The absolute abundance of antibiotic is sorted per antibiotic class in logarithmic scale.

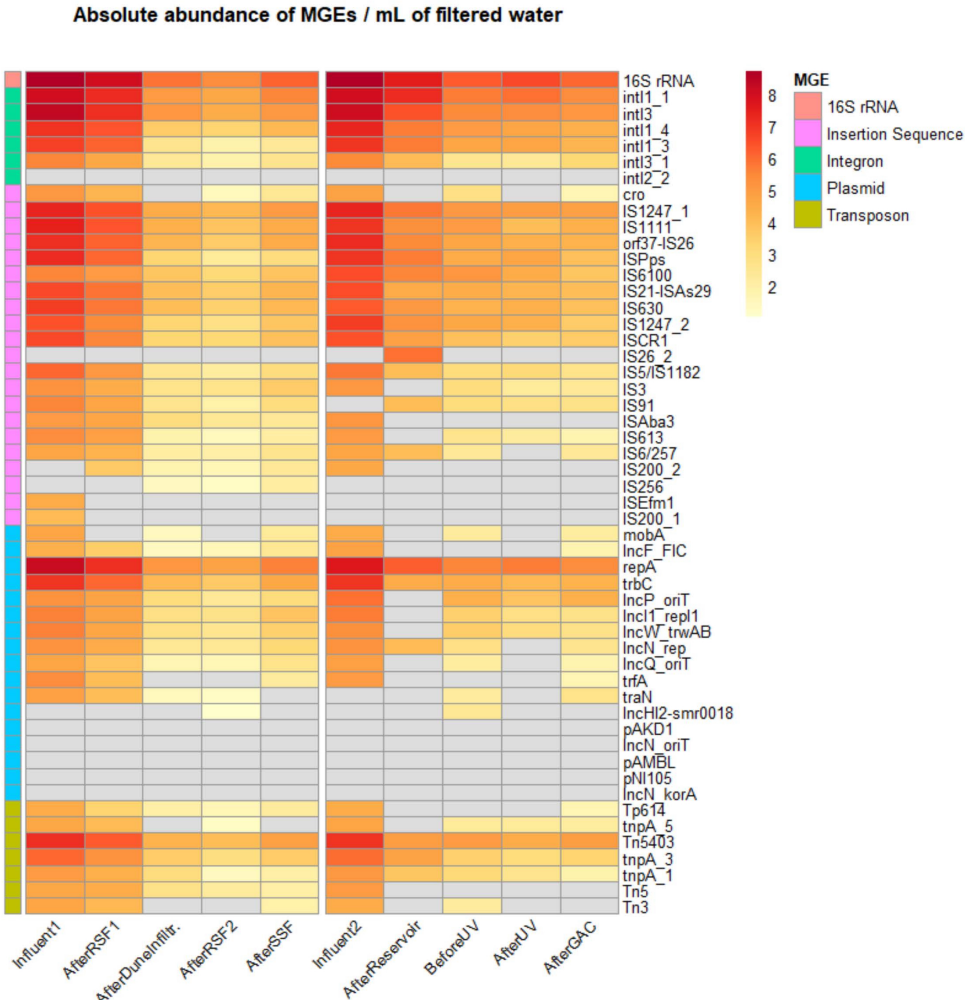

Figure S.5: Heatmap of absolute abundance from the MGEs mL^{-1} tested from both dune-based and reservoir-based DWTPs. The absolute abundance of antibiotic is sorted per MGE type in logarithmic scale.

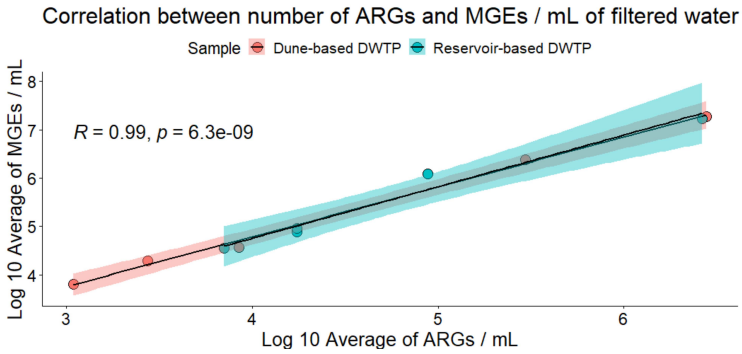

Figure S.6: Correlation between absolute abundance of ARGs and MGEs mL^{-1} of filtered water in dune-based and reservoir-based DWTPs. Both axes are displayed in logarithmic scale.

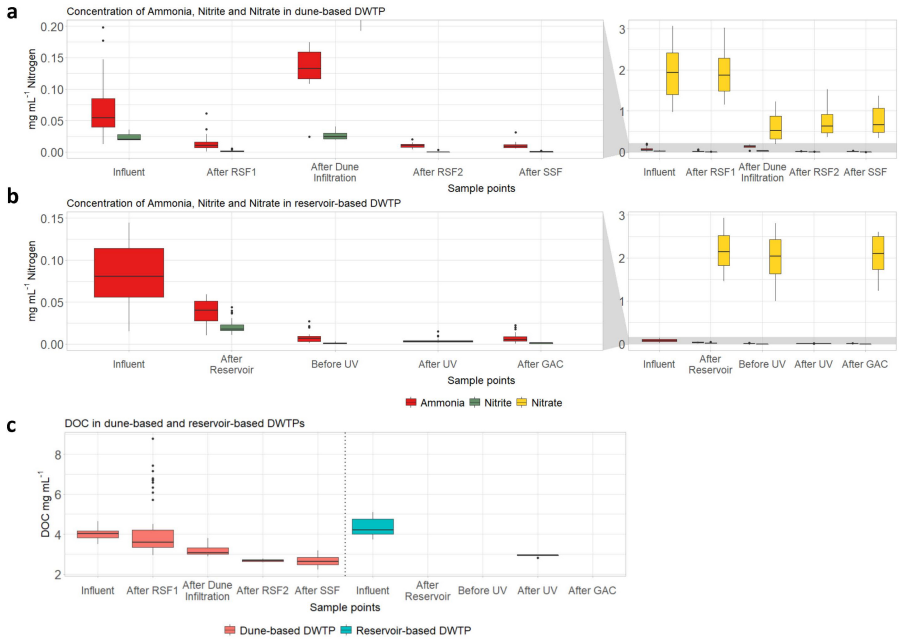

Figure S.7: (a) Concentration of ammonia, nitrite and nitrate (mg N mL^{-1}) in dune-based DWTP, including a zoom in ammonia and nitrite concentration. **(b)** Concentration of ammonia, nitrite and nitrate (mg N mL^{-1}) in reservoir-based DWTP, including a zoom in ammonia and nitrite concentration. **(c)** Concentration of dissolved organic carbon (DOC) (mg L^{-1}) in dune-based and reservoir-based DWTPs. Values were provided by the DWTPs.

Sample		Number of raw-reads	Classified reads (%)	Microbial reads (%)	Bacterial reads (%)	Number of contigs	Contig total lenght (bp)
Dune-based	Influent	36,828,825	30.6	30.3	30.1	41,275	194,379,902
DWTP	After RSF1	43,005,601	26.5	25.8	25.8	37,898	176,143,661
	After Dune Infiltr.	34,987,700	27.8	27.4	27.4	33,582	188,288,835
	After RSF2	36,028,713	15.3	14.8	14.8	19,105	75,981,959
	After SSF	52,785,449	13.3	12.8	12.8	42,138	173,427,678
Reservoir-based	Influent	40,702,369	23.6	23.0	22.8	26,006	116,777,904
DWTP	After Reserv.	39,477,566	21.8	19.9	19.5	34,613	159,087,190
	Before UV	40,235,273	24.9	24.7	24.6	44,602	235,503,423
	After UV	40,202,383	34.7	34.5	34.3	37,436	197,642,846
	After GAC	41,826,898	27.5	27.2	26.9	60,787	291,165,178

Figure S.8: Number of raw reads obtained per sample in dune- and reservoir-based DWTPs, specifying the percentages of classified reads, microbial and bacterial percentage (in relation with the percentage of classified reads), number of assembled contigs, and total average length (bp) of assembled contigs per sample. RSF: rapid sand filtration. SSF: slow sand filtration. GAC: granular activated carbon. DWTP: Drinking water treatment plant.

Bibliography

[1] United Nations. *Sustainable Development Goals*. 2015.

[2] United Nations. *Water Action Decade*. 2018.

[3] L. Yu, J. Rozemeijer, B. M. Van Breukelen, M. Ouboter, C. Van Der Vlugt, and H. P. Broers. "Groundwater impacts on surface water quality and nutrient loads in lowland polder catchments: Monitoring the greater Amsterdam area". In: *Hydrology and Earth System Sciences* 22.1 (2018), pp. 487–508. ISSN: 16077938. DOI: 10.5194/hess-22-487-2018.

[4] UNEP - United Nations Environment Programme. *A Snapshot of the World ' s Water Quality : Towards a global assessment*. 2016, p. 162. ISBN: 9789280735550.

[5] E. Kumpel, A. Cock-Esteb, M. Duret, O. D. Waal, and R. Khush. "Seasonal variation in drinking and domestic water sources and quality in port harcourt, Nigeria". In: *American Journal of Tropical Medicine and Hygiene* 96.2 (2017), pp. 437–445. ISSN: 00029637. DOI: 10.4269/ajtmh.16-0175.

[6] N. Khatri and S. Tyagi. "Influences of natural and anthropogenic factors on surface and groundwater quality in rural and urban areas". In: *Frontiers in Life Science* 8.1 (2015), pp. 23–39. ISSN: 21553777. DOI: 10.1080/21553769.2014.933716. URL: https://doi.org/10.1080/21553769.2014.933716.

[7] United States Environmental Protection Agency. *Types of Drinking Water Contaminants*. 2021.

[8] D. L. Sedlak and U. Von Gunten. *The chlorine dilemma*. Jan. 2011. DOI: 10.1126/science.1196397.

[9] P. Shi, S. Jia, X. X. Zhang, T. Zhang, S. Cheng, and A. Li. "Metagenomic insights into chlorination effects on microbial antibiotic resistance in drinking water". In: *Water Research* 47.1 (2013), pp. 111–120. ISSN: 18792448. DOI: 10.1016/j.watres.2012.09.046. URL: http://dx.doi.org/10.1016/j.watres.2012.09.046.

[10] P. W. Smeets, G. J. Medema, and J. C. Van Dijk. "The Dutch secret: How to provide safe drinking water without chlorine in the Netherlands". In: *Drinking Water Engineering and Science* 2.1 (2009), pp. 1–14. ISSN: 19969465. DOI: 10.5194/dwes-2-1-2009.

[11] P. Mouchet. "From conventional to biological removal of iron and manganese in France". In: *Journal / American Water Works Association* 84.4 (1992), pp. 158–167. ISSN: 0003150X. DOI: 10.1002/j.1551-8833.1992.tb07342.x.

[12] A. G. Tekerlekopoulou, S. Pavlou, and D. V. Vayenas. "Removal of ammonium, iron and manganese from potable water in biofiltration units: A review". In: *Journal of Chemical Technology and Biotechnology* 88.5 (2013), pp. 751–773. ISSN: 02682575. DOI: 10.1002/jctb.4031.

[13] A. J. Pinto, C. Xi, and L. Raskin. "Bacterial community structure in the drinking water microbiome is governed by filtration processes". In: *Environmental Science and Technology* 46.16 (Aug. 2012), pp. 8851–8859. ISSN: 0013936X. DOI: 10.1021/ES302042T/SUPPL{_}FILE/ES302042T{_}SI{_}001.PDF.

[14] J. L. Balcázar, J. Subirats, and C. M. Borrego. "The role of biofilms as environmental reservoirs of antibiotic resistance". In: *Frontiers in Microbiology* 6.OCT (2015), p. 1216. ISSN: 1664302X. DOI: 10.3389/FMICB.2015.01216/BIBTEX.

[15] P. E. Stackelberg, E. T. Furlong, M. T. Meyer, S. D. Zaugg, A. K. Henderson, and D. B. Reissman. "Persistence of pharmaceutical compounds and other organic wastewater contaminants in a conventional drinking-water-treatment plant". In: *Science of the Total Environment* 329.1-3 (2004), pp. 99–113. ISSN: 00489697. DOI: 10.1016/j.scitotenv.2004.03.015.

[16] A. Farkas, A. Butiuc-Keul, D. Ciatarâş, C. Neamţu, C. Crăciunaş, D. Podar, and M. Drăgan-Bularda. "Microbiological contamination and resistance genes in biofilms occurring during the drinking water treatment process". In: *Science of the Total Environment* 443 (2013), pp. 932–938. ISSN: 00489697. DOI: 10.1016/j.scitotenv.2012.11.068.

[17] D. Calderón-Franco, R. Sarelse, S. Christou, M. Pronk, M. C. M. van Loosdrecht, T. Abeel, and D. G. Weissbrodt. "Metagenomic profiling and transfer dynamics of antibiotic resistance determinants in a full-scale granular sludge wastewater treatment plant". In: *Water Research* (2022). DOI: 10.1016/j.watres.2022.118571.

[18] A. Miłobedzka, C. Ferreira, I. Vaz-Moreira, D. Calderón-Franco, A. Gorecki, S. Purkrtova, Jan Bartacek, L. Dziewit, C. M. Singleton, P. H. Nielsen, D. G. Weissbrodt, and C. M. Manaia. "Monitoring antibiotic resistance genes in wastewater environments: The challenges of filling a gap in the One-Health cycle". In: *Journal of Hazardous Materials* 424 (2022). ISSN: 18733336. DOI: 10.1016/j.jhazmat.2021.127407.

[19] R. Pallares-Vega, H. Blaak, R. van der Plaats, A. M. de Roda Husman, L. Hernandez Leal, M. C. van Loosdrecht, D. G. Weissbrodt, and H. Schmitt. "Determinants of presence and removal of antibiotic resistance genes during WWTP treatment: A cross-sectional study". In: *Water Research* 161 (2019), pp. 319–328. ISSN: 18792448. DOI: 10.1016/j.watres.2019.05.100. URL: https://doi.org/10.1016/j.watres.2019.05.100.

[20] L. Ma, B. Li, X. T. Jiang, Y. L. Wang, Y. Xia, A. D. Li, and T. Zhang. "Catalogue of antibiotic resistome and host-tracking in drinking water deciphered by a large scale survey". In: *Microbiome* 5.1 (2017), p. 154. ISSN: 20492618. DOI: 10.1186/s40168-017-0369-0. URL: https://www.ncbi.nlm.nih.gov/pmc/articles/PMC5704573/pdf/40168_2017_Article_369.pdf.

[21] C. Stange, J. P. Sidhu, S. Toze, and A. Tiehm. "Comparative removal of antibiotic resistance genes during chlorination, ozonation, and UV treatment". In: *International Journal of Hygiene and Environmental Health* 222.3 (2019), pp. 541–548. ISSN: 1618131X. DOI: 10.1016/j.ijheh.2019.02.002. URL: https://doi.org/10.1016/j.ijheh.2019.02.002.

[22] K. Wan, M. Zhang, C. Ye, W. Lin, L. Guo, S. Chen, and X. Yu. "Organic carbon: An overlooked factor that determines the antibiotic resistome in drinking water sand filter biofilm". In: *Environment International* 125.October 2018 (2019), pp. 117–124. ISSN: 18736750. DOI: 10.1016/j.envint.2019.01.054. URL: https://doi.org/10.1016/j.envint.2019.01.054.

[23] R. Destiani and M. R. Templeton. "Chlorination and ultraviolet disinfection of antibiotic-resistant bacteria and antibiotic resistance genes in drinking water". In: *AIMS Environmental Science* 6.3 (2019), pp. 222–241. ISSN: 23720352. DOI: 10.3934/environsci.2019.3.222.

[24] Y. Hu, T. Zhang, L. Jiang, Y. Luo, S. Yao, D. Zhang, K. Lin, and C. Cui. "Occurrence and reduction of antibiotic resistance genes in conventional and advanced drinking water treatment processes". In: *Science of the Total Environment* 669.130 (2019), pp. 777–784. ISSN: 18791026. DOI: 10.1016/j.scitotenv.2019.03.143. URL: https://doi.org/10.1016/j.scitotenv.2019.03.143.

[25] S. Jia, K. Bian, P. Shi, L. Ye, and C.-H. Liu. "Metagenomic profiling of antibiotic resistance genes and their associations with bacterial community during multiple disinfection regimes in a full-scale drinking water treatment plant". In: *Water Research* (Mar. 2020), p. 115721. ISSN: 0043-1354. DOI: 10.1016/J.WATRES.2020.115721. URL: https://www.sciencedirect.com/science/article/abs/pii/S004313542030258X.

[26] H. C. Su, Y. S. Liu, C. G. Pan, J. Chen, L. Y. He, and G. G. Ying. "Persistence of antibiotic resistance genes and bacterial community changes in drinking water treatment system: From drinking water source to tap water". In: *Science of the Total Environment* 616-617 (2018), pp. 453–461. ISSN: 18791026. DOI: 10.1016/j.scitotenv.2017.10.318. URL: https://doi.org/10.1016/j.scitotenv.2017.10.318.

[27] L. Xu, W. Ouyang, Y. Qian, C. Su, J. Su, and H. Chen. "High-throughput profiling of antibiotic resistance genes in drinking water treatment plants and distribution systems". In: *Environmental Pollution* 213 (2016), pp. 119–126. ISSN: 18736424. DOI: 10.1016/j.envpol.2016.02.013. URL: http://dx.doi.org/10.1016/j.envpol.2016.02.013.

[28] H. Zhang, H. He, S. Chen, T. Huang, K. Lu, Z. Zhang, R. Wang, X. Zhang, and H. Li. "Abundance of antibiotic resistance genes and their association with bacterial communities

in activated sludge of wastewater treatment plants: Geographical distribution and network analysis". In: *Journal of Environmental Sciences (China)* 82 (2019), pp. 24–38. ISSN: 18787320. DOI: 10.1016/j.jes.2019.02.023.

[29] S. Zhang, W. Lin, and X. Yu. "Effects of full-scale advanced water treatment on antibiotic resistance genes in the Yangtze Delta area in China". In: *FEMS Microbiology Ecology* 92.5 (2016), pp. 1–9. ISSN: 15746941. DOI: 10.1093/femsec/fiw065.

[30] Z. Huang, W. Zhao, T. Xu, B. Zheng, and D. Yin. "Occurrence and distribution of antibiotic resistance genes in the water and sediments of Qingcaosha Reservoir, Shanghai, China". In: *Environmental Sciences Europe* 31.1 (2019). ISSN: 21904715. DOI: 10.1186/s12302-019-0265-2. URL: https://doi.org/10.1186/s12302-019-0265-2.

[31] S. Jia, P. Shi, Q. Hu, B. Li, T. Zhang, and X. X. Zhang. "Bacterial Community Shift Drives Antibiotic Resistance Promotion during Drinking Water Chlorination". In: *Environmental Science and Technology* 49.20 (2015), pp. 12271–12279. ISSN: 15205851. DOI: 10.1021/acs.est.5b03521.

[32] M. Sevillano, Z. Dai, S. Calus, Q. M. Bautista-de los Santos, A. M. Eren, P. W. van der Wielen, U. Z. Ijaz, and A. J. Pinto. "Differential prevalence and host-association of antimicrobial resistance traits in disinfected and non-disinfected drinking water systems". In: *Science of the Total Environment* 749 (2020), p. 141451. ISSN: 18791026. DOI: 10.1016/j.scitotenv.2020.141451. URL: https://doi.org/10.1016/j.scitotenv.2020.141451.

[33] D. van Halem and L. Rietveld. *Introduction to Drinking Water Treatment*. 2014. URL: https://online-learning.tudelft.nl/courses/introduction-to-drinking-water-treatment/.

[34] S. Andrews. *FastQC: a quality control tool for high throughput sequence data*. 2010. URL: http://www.bioinformatics.babraham.ac.uk/projects/fastqc.

[35] A. M. Bolger, M. Lohse, and B. Usadel. "Trimmomatic: A flexible trimmer for Illumina sequence data". In: *Bioinformatics* 30.15 (2014), pp. 2114–2120. ISSN: 14602059. DOI: 10.1093/bioinformatics/btu170.

[36] S. Nurk, D. Meleshko, A. Korobeynikov, and P. A. Pevzner. "MetaSPAdes: A new versatile metagenomic assembler". In: *Genome Research* 27.5 (2017), pp. 824–834. ISSN: 15495469. DOI: 10.1101/gr.213959.116.

[37] B. D. Ondov, T. J. Treangen, P. Melsted, A. B. Mallonee, N. H. Bergman, S. Koren, and A. M. Phillippy. "Mash: Fast genome and metagenome distance estimation using MinHash". In: *Genome Biology* 17.1 (2016), pp. 1–14. ISSN: 1474760X. DOI: 10.1186/s13059-016-0997-x. URL: http://dx.doi.org/10.1186/s13059-016-0997-x.

[38] V. Bortolaia, R. S. Kaas, E. Ruppe, M. C. Roberts, S. Schwarz, V. Cattoir, A. Philippon, R. L. Allesoe, A. R. Rebelo, A. F. Florensa, L. Fagelhauer, T. Chakraborty, B. Neumann, G. Werner, J. K. Bender, K. Stingl, M. Nguyen, J. Coppens, B. B. Xavier, S. Malhotra-Kumar, H. Westh, M. Pinholt, M. F. Anjum, N. A. Duggett, I. Kempf, S. Nykäsenoja, S. Olkkola, K. Wieczorek, A. Amaro, L. Clemente, J. Mossong, S. Losch, C. Ragimbeau, O. Lund, and F. M. Aarestrup. "ResFinder 4.0 for predictions of phenotypes from genotypes". In: *Journal of Antimicrobial Chemotherapy* 75.12 (2020). ISSN: 14602091. DOI: 10.1093/jac/dkaa345.

[39] V. Galata, T. Fehlmann, C. Backes, and A. Keller. "PLSDB: A resource of complete bacterial plasmids". In: *Nucleic Acids Research* 47.D1 (2019), pp. D195–D202. ISSN: 13624962. DOI: 10.1093/nar/gky1050.

[40] A. Moura, M. Soares, C. Pereira, N. Leitão, I. Henriques, and A. Correia. "INTEGRALL: A database and search engine for integrons, integrases and gene cassettes". In: *Bioinformatics* 25.8 (2009), pp. 1096–1098. ISSN: 13674803. DOI: 10.1093/bioinformatics/btp105.

[41] P. Siguier, J. Filée, and M. Chandler. "Insertion sequences in prokaryotic genomes". In: *Current Opinion in Microbiology* 9.5 (2006), pp. 526–531. ISSN: 13695274. DOI: 10.1016/j.mib.2006.08.005.

[42] M. Liu, X. Li, Y. Xie, D. Bi, J. Sun, J. Li, C. Tai, Z. Deng, and H. Y. Ou. "ICEberg 2.0: An updated database of bacterial integrative and conjugative elements". In: *Nucleic Acids Research* 47.D1 (2019), pp. D660–D665. ISSN: 13624962. DOI: 10.1093/nar/gky1123.

[43] T. Seemann. "Prokka: Rapid prokaryotic genome annotation". In: *Bioinformatics* 30.14 (2014), pp. 2068–2069. ISSN: 14602059. DOI: 10.1093/bioinformatics/btu153.

[44] F. P. Breitwieser and S. L. Salzberg. "Pavian: Interactive analysis of metagenomics data for microbiome studies and pathogen identification". In: *Bioinformatics* 36.4 (2020), pp. 1303–1304. ISSN: 14602059. DOI: 10.1093/bioinformatics/btz715.

[45] T. C. Hill, K. A. Walsh, J. A. Harris, and B. F. Moffett. "Using ecological diversity measures with bacterial communities". In: *FEMS Microbiology Ecology* 43.1 (2003), pp. 1–11. ISSN: 01686496. DOI: 10.1016/S0168-6496(02)00449-X.

[46] E. Tacconelli and N. Magrini. *Global priority list of antibiotic-resistant bacteria to guide research, discovery, and development of new antibiotics*. Tech. rep. 2017, pp. 1–7. URL: https://www.who.int/medicines/publications/WHO-PPL-Short_Summary_25Feb-ET_NM_WHO.pdf.

[47] A. Palomo, S. Jane Fowler, A. Gülay, S. Rasmussen, T. Sicheritz-Ponten, and B. F. Smets. "Metagenomic analysis of rapid gravity sand filter microbial communities suggests novel physiology of Nitrospira spp." In: *ISME Journal* 10.11 (2016), pp. 2569–2581. ISSN: 17517370. DOI: 10.1038/ismej.2016.63.

[48] A. Tiwari, A. M. Hokajärvi, J. S. Domingo, M. Elk, B. Jayaprakash, H. Ryu, S. Siponen, A. Vepsäläinen, A. Kauppinen, O. Puurunen, A. Artimo, N. Perkola, T. Huttula, I. T. Miettinen, and T. Pitkänen. "Bacterial diversity and predicted enzymatic function in a multipurpose surface water system – from wastewater effluent discharges to drinking water production". In: *Environmental Microbiomes* 16.1 (2021), pp. 1–17. ISSN: 25246372. DOI: 10.1186/s40793-021-00379-w.

[49] M. B. Waak, R. M. Hozalski, C. Hallé, and T. M. Lapara. "Comparison of the microbiomes of two drinking water distribution systems - With and without residual chloramine disinfection". In: *Microbiome* 7.1 (June 2019). ISSN: 20492618. DOI: 10.1186/s40168-019-0707-5. URL: https://pubmed-ncbi-nlm-nih-gov.tudelft.idm.oclc.org/31174608/.

[50] Z. Dai, M. C. Sevillano-Rivera, S. T. Calus, Q. Melina Bautista-de los Santos, A. Murat Eren, P. W. van der Wielen, U. Z. Ijaz, and A. J. Pinto. "Disinfection exhibits systematic impacts on the drinking water microbiome". In: *bioRxiv* (2019), pp. 1–19. ISSN: 2692-8205. DOI: 10.1101/828970.

[51] S. Velten, M. Boller, O. Köster, J. Helbing, H. U. Weilenmann, and F. Hammes. "Development of biomass in a drinking water granular active carbon (GAC) filter". In: *Water Research* 45.19 (2011), pp. 6347–6354. ISSN: 18792448. DOI: 10.1016/j.watres.2011.09.017.

[52] K. Lautenschlager, C. Hwang, F. Ling, W. T. Liu, N. Boon, O. Köster, T. Egli, and F. Hammes. "Abundance and composition of indigenous bacterial communities in a multi-step biofiltration-based drinking water treatment plant". In: *Water Research* 62 (Oct. 2014), pp. 40–52. ISSN: 18792448. DOI: 10.1016/J.WATRES.2014.05.035.

[53] W. Lin, Z. Yu, H. Zhang, and I. P. Thompson. "Diversity and dynamics of microbial communities at each step of treatment plant for potable water generation". In: *Water Research* 52 (2014), pp. 218–230. ISSN: 18792448. DOI: 10.1016/j.watres.2013.10.071.

[54] S. Oh, F. Hammes, and W. T. Liu. "Metagenomic characterization of biofilter microbial communities in a full-scale drinking water treatment plant". In: *Water Research* 128 (2017), pp. 278–285. ISSN: 18792448. DOI: 10.1016/j.watres.2017.10.054.

[55] S. M. Neuenschwander, R. Ghai, J. Pernthaler, and M. M. Salcher. "Microdiversification in genome-streamlined ubiquitous freshwater Actinobacteria". In: *ISME Journal* 12.1 (Oct. 2018), pp. 185–198. ISSN: 17517370. DOI: 10.1038/ismej.2017.156. URL: https://www.nature.com/articles/ismej2017156.

[56] F. Warnecke, R. Amann, and J. Pernthaler. "Actinobacterial 16S rRNA genes from freshwater habitats cluster in four distinct lineages". In: *Environmental Microbiology* 6.3 (Mar. 2004), pp. 242–253. ISSN: 1462-2920. DOI: 10.1111/J.1462-2920.2004.00561.X. URL: https://onlinelibrary.wiley.com/doi/full/10.1111/j.1462-2920.2004.00561.x%20https://onlinelibrary.wiley.com/doi/abs/10.1111/j.1462-2920.2004.00561.x%20https://sfamjournals.onlinelibrary.wiley.com/doi/10.1111/j.1462-2920.2004.00561.x.

[57] W. Hu, J. Liang, F. Ju, Q. Wang, R. Liu, Y. Bai, H. Liu, and J. Qu. "Metagenomics Unravels Differential Microbiome Composition and Metabolic Potential in Rapid Sand Filters

Purifying Surface Water Versus Groundwater". In: *Environmental science & technology* 54.8 (2020), pp. 5197–5206. ISSN: 15205851. DOI: 10.1021/acs.est.9b07143.

[58] T. M. Webster and N. Fierer. "Microbial Dynamics of Biosand Filters and Contributions of the Microbial Food Web to Effective Treatment of Wastewater-Impacted Water Sources". In: *Applied and environmental microbiology* 85.17 (Sept. 2019). ISSN: 1098-5336. DOI: 10.1128/AEM.01142-19. URL: https://pubmed-ncbi-nlm-nih-gov.tudelft.idm.oclc.org/31227556/.

[59] L. Xu, L. C. Campos, M. Canales, and L. Ciric. "Drinking water biofiltration: Behaviour of antibiotic resistance genes and the association with bacterial community". In: *Water Research* 182 (2020), p. 115954. ISSN: 18792448. DOI: 10.1016/j.watres.2020.115954. URL: https://doi.org/10.1016/j.watres.2020.115954.

[60] N. Mukherjee, D. Bartelli, C. Patra, B. V. Chauhan, S. E. Dowd, and P. Banerjee. "Microbial diversity of source and point-of-use water in rural Haiti - A pyrosequencing-based metagenomic survey". In: *PLoS ONE* 11.12 (Dec. 2016), e0167353. ISSN: 19326203. DOI: 10.1371/journal.pone.0167353. URL: https://journals.plos.org/plosone/article?id=10.1371/journal.pone.0167353.

[61] K. R. Pfannes, K. M. Langenbach, G. Pilloni, T. Stührmann, K. Euringer, T. Lueders, T. R. Neu, J. A. Müller, M. Kästner, and R. U. Meckenstock. "Selective elimination of bacterial faecal indicators in the Schmutzdecke of slow sand filtration columns". In: *Applied Microbiology and Biotechnology* 99.23 (2015), pp. 10323–10332. ISSN: 14320614. DOI: 10.1007/s00253-015-6882-9.

[62] M. W. Hahn. "Rhodoluna". In: *Bergey's Manual of Systematics of Archaea and Bacteria*. Vol. 52. 2016, pp. 1–9. ISBN: 9781118960608. DOI: 10.1002/9781118960608.gbm01312.

[63] V. Kasalický, J. Jezbera, M. W. Hahn, and K. Šimek. "The Diversity of the Limnohabitans Genus, an Important Group of Freshwater Bacterioplankton, by Characterization of 35 Isolated Strains". In: *PLoS ONE* 8.3 (2013). ISSN: 19326203. DOI: 10.1371/journal.pone.0058209.

[64] M. Amarasiri, D. Sano, and S. Suzuki. "Understanding human health risks caused by antibiotic resistant bacteria (ARB) and antibiotic resistance genes (ARG) in water environments: Current knowledge and questions to be answered". In: *Critical Reviews in Environmental Science and Technology* 50.19 (2020), pp. 2016–2059. ISSN: 15476537. DOI: 10.1080/10643389.2019.1692611. URL: https://doi.org/10.1080/10643389.2019.1692611.

[65] R. P. Griffiths, C. L. Moyer, B. A. Caldwell, C. Ye, and R. Y. Morita. "Long-term starvation-induced loss of antibiotic resistance in bacteria". In: *Microbial Ecology* 19.3 (1990), pp. 251–257. ISSN: 00953628. DOI: 10.1007/BF02017169.

[66] T. Zhang, K. Lv, Q. Lu, L. Wang, and X. Liu. "Removal of antibiotic-resistant genes during drinking water treatment: A review". In: *Journal of Environmental Sciences (China)* 104 (2021), pp. 415–429. ISSN: 18787320. DOI: 10.1016/j.jes.2020.12.023. URL: https://doi.org/10.1016/j.jes.2020.12.023.

[67] K. Wan, L. Guo, C. Ye, J. Zhu, M. Zhang, and X. Yu. "Accumulation of antibiotic resistance genes in full-scale drinking water biological activated carbon (BAC) filters during backwash cycles". In: *Water Research* 190 (2021), p. 116744. ISSN: 18792448. DOI: 10.1016/j.watres.2020.116744. URL: https://doi.org/10.1016/j.watres.2020.116744.

[68] National Research Council (US) Safe Drinking Water Committee. "Drinking Water and Health". In: *Drinking Water and Health: Volume 2.* Vol. 2. 6. National Academies Press (US), 1980, pp. 955–956. ISBN: 0309554063. DOI: 10.1111/j.1752-1688.1984.tb04810.x. URL: https://www.ncbi.nlm.nih.gov/books/NBK234590/.

[69] L. Ciric. *ARE VICTORIAN WATER TREATMENT TECHNOLOGIES FIT FOR THE AMR ERA?* 2022. URL: https://microbiologysociety.org/our-work/75th-anniversary-a-sustainable-future/antimicrobial-resistance-amr/antimicrobial-resistance-amr-case-studies/victorian-water-treatment-technologies-amr.html.

[70] H. Chen and M. Zhang. "Effects of Advanced Treatment Systems on the Removal of Antibiotic Resistance Genes in Wastewater Treatment Plants from Hangzhou, China". In: *Environmental Science & Technology* (2013), p. 130711162357003. ISSN: 0013-936X. DOI: 10.1021/es401091y. URL: http://www.ncbi.nlm.nih.gov/%20http://pubs.acs.org/doi/abs/10.1021/es401091y.

[71] X. Cheng, H. M. Delanka-Pedige, S. P. Munasinghe-Arachchige, I. S. Abeysiriwardana-Arachchige, G. B. Smith, N. Nirmalakhandan, and Y. Zhang. "Removal of antibiotic resistance genes in an algal-based wastewater treatment system employing Galdieria sulphuraria: A comparative study". In: *Science of the Total Environment* 711 (2020), p. 134435. ISSN: 18791026. DOI: 10.1016/j.scitotenv.2019.134435. URL: https://doi.org/10.1016/j.scitotenv.2019.134435.

[72] P. J. Collignon and S. A. McEwen. "One health-its importance in helping to better control antimicrobial resistance". In: *Tropical Medicine and Infectious Disease* 4.1 (2019). ISSN: 24146366. DOI: 10.3390/tropicalmed4010022.

[73] P. Nordmann, L. Dortet, and L. Poirel. "Carbapenem resistance in Enterobacteriaceae: Here is the storm!" In: *Trends in Molecular Medicine* 18.5 (2012), pp. 263–272. ISSN: 14714914. DOI: 10.1016/j.molmed.2012.03.003. URL: http://dx.doi.org/10.1016/j.molmed.2012.03.003.

[74] M. Shanthi Amudhan, U. Sekar, A. Kamalanathan, and S. Balaraman. "blaIMP and blaVIM mediated carbapenem resistance in pseudomonas and acinetobacter species in India". In: *Journal of Infection in Developing Countries* 6.11 (2012), pp. 757–762. ISSN: 20366590. DOI: 10.3855/jidc.2268.

[75] WHO. *Guidelines for the prevention and control of carbapenem-resistant Enterobacteriaceae, Acinetobacter baumannii and Pseudomonas aeruginosa in health care facilities*. Tech. rep. World Health Organization, 2017, p. 74. URL: https://apps.who.int/iris/handle/10665/259462.

[76] M. F. Dias, G. da Rocha Fernandes, M. Cristina de Paiva, A. Christina de Matos Salim, A. B. Santos, and A. M. Amaral Nascimento. "Exploring the resistome, virulome and microbiome of drinking water in environmental and clinical settings". In: *Water Research* 174 (2020), p. 115630. ISSN: 18792448. DOI: 10.1016/j.watres.2020.115630. URL: https://doi.org/10.1016/j.watres.2020.115630.

6

Catch me if you can: Capturing extracellular DNA transformation in mixed cultures via Hi-C sequencing

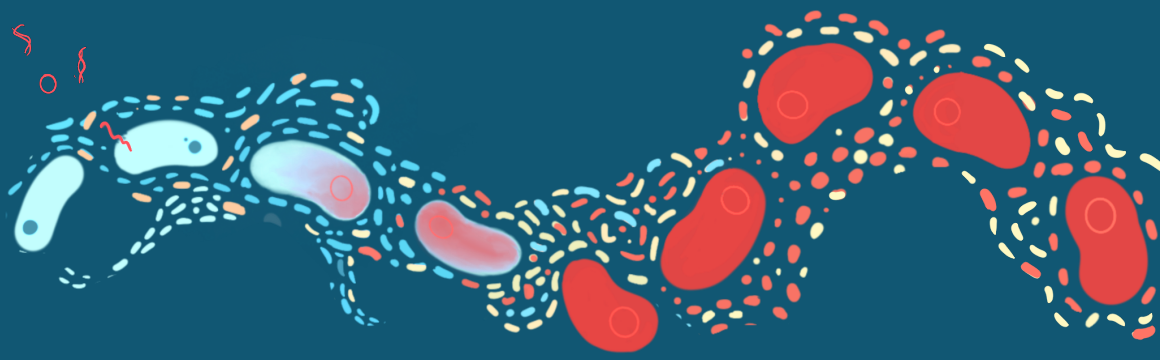

This chapter has been deposited as preprint: Calderón-Franco, D., van Loosdrecht, M.C.M., Abeel, T., Weissbrodt, D., 2021. Catch me if you can: Capturing extracellular DNA transformation in mixed cultures via Hi-C sequencing. bioRxiv. https://doi.org/10.1101/2022.09.16.508255

ABSTRACT

Environmental microorganisms evolve constantly under various stressors using different adaptive mechanisms, including horizontal gene transfer. Microorganisms benefit from transferring genetic information that code for antibiotic resistance via mobile genetic elements. Due to the complexity of natural microbial ecosystems, quantitative data on the transfer of genetic information in microbial communities remain unclear. Two chemostats (one control and one test) were inoculated with activated sludge, fed with synthetic wastewater, and operated for 45 days to study the transformation capacity of a rolling-circle plasmid encoding GFP and kanamycin resistance genes, at increasing concentrations of kanamycin (0.01, 2.5, 50, and 100 mg L^{-1}). The plasmid DNA was spiked daily in the test chemostat. The evolution of the microbial community composition was analyzed by 16S rRNA gene amplicon sequencing and metagenomics, and the presence of the plasmid by quantitative PCR. We used Hi-C sequencing to identify natural transformant microorganisms with low (2.5 mg L^{-1}) and high (50 mg L^{-1}) concentrations of kanamycin. Biomass formation in the presence of kanamycin was higher with the plasmid. Hence, the antibiotic exerted the main pressure on microbial selection, while the plasmid helped these populations better resist the antibiotic treatment and grow. The kanamycin resistance gene increased in both reactors. When higher antibiotic concentrations were applied, the GFP/16S ratio was increased, highlighting plasmids accumulation in the test reactor over time. The plasmid transformed mainly inside populations of Bosea sp., Runella spp., and Microbacterium sp.. This study made one step forward by demonstrating that microorganisms in enrichments can acquire exogenous synthetic plasmids by transformation.

Keywords: *Hi-C sequencing; Transformation; Mixed culture; Free-floating extracellular DNA*

6.1. Introduction

Bacterial antimicrobial resistance (AMR) has emerged as one of the greatest public health threats of the 21^{st} century. It is estimated that by 2050, 10 million lives a year will be at risk due to the rise of drug-resistant infections by antibiotic resistance bacteria (ARB) if no mitigation efforts are engaged [1]. From the One Health context, water from places where antibiotics are highly used, such as healthcare services, agriculture, farming, households, and urban discharges, coincides collectively at wastewater treatment plants (WWTPs). This forms a broth cocktail where drugs and antimicrobial agents meet bacteria in a complex sludge.

Microorganisms in natural and man-made systems constantly evolve under environmental stressors using horizontal gene transfer (HGT) processes, such as conjugation, transduction, or transformation. Microbes benefit from transferring genetic information that code for antibiotic resistance via mobile genetic elements (MGEs) like plasmids, integrons, transposons, and conjugative and integrative elements. The quantitative elucidation of genetic information transfer by transformation in mixed microbial cultures, the environmental conditions that trigger microbial competence (seasonal changes, lack of nutrients, or antibiotic concentrations, among others), and the resistant microbial hosts, carriers, and vectors of these MGEs remain vastly unclear [2].

Recently, we highlighted that the extracellular free DNA (exDNA) in wastewater is a rich pool of MGEs (65%; 5-9 µg exDNA L^{-1}) [3] that can co-localize ARGs [4]. Quantifying DNA uptake from the environment by natural transformation is of key interest [5] since it can pose a risk for the development of ARB in wastewater environments and their discharge into nature and aquatic reservoirs.

Natural transformation is the process by which bacteria can actively take up and integrate exDNA, providing a source of genetic diversity [6]. Naturally competent bacteria actively pull DNA fragments from their environment into their cells [7]. The effects of DNA uptake depend on the nutritional needs of the cells (bacteria can use exDNA as a nutrient source [8]), the presence of DNA damage, the ability of incoming DNA to recombine with chromosomal DNA, and the effects of this recombination on fitness (beneficial traits such as ARGs). Experimental demonstrations of natural competence are limited to only a few dozen species scattered across the bacterial tree and examined in pure cultures [9, 10]. Assays measuring genetic transformation are highly sensitive, but they can be done only in species that harbor a selectable genetic marker (typically an antibiotic resistance gene) and that are cultivable. Such methods fail to discover competence in complex microbial communities as present in wastewater environments, where DNA uptake rarely leads to recombination or episomal integration. The conditions that induce transformation have equally not been elucidated. Thus, one species may be mistakenly described as lacking competence since only non-competent isolates have been tested. Unraveling natural competence and transformation within microbiomes is crucial.

Most studies have so far tried to quantify gene transfer via conjugation [11–13] or transformation [14–16], either *in vitro* or *in vivo*. These approaches help quantify HGT rates under controlled conditions on bench (in vitro) and HGT occurrence in defined synthetic consortia using engineered or well-characterized strains cultivated as biofilms (*in vivo*). However, these methods cannot uncover direct analysis of naturally occurring HGT phenomena in microbial communities (*in situ*).

Despite disadvantages associated with studying HGT directly in microbial communities, such as extensive data requirements, the challenge of drawing direct cause and effect relationships between MGEs and their transfer rates [2], it is to our understanding the best approach to answer the question of who carries, transfers and can uptake ARGs in complex systems via natural transformation. Some studies have attempted to link the resistome, plasmidome, and viruses via Hi-C sequencing to the microbiome of wastewater [17] or rumen samples [18], highlighting the wide microbial diversity able to transfer genetic fragments.

Here, we studied the transformation of an exogenous synthetic rolling-circle plasmid encoding GFP and kanamycin resistance genes in an enrichment from activated sludge mixed culture fed with synthetic wastewater in chemostats exposed to increasing concentrations of kanamycin (0.01, 2.5, 50, and 100 mg L^{-1}). Plasmid DNA was spiked daily in the test chemostat, while the control culture was only exposed to the antibiotic. Microbial community compositions were evaluated by *16S rRNA* gene amplicon sequencing and metagenomics, and the presence of the plasmid was analyzed by quantitative PCR. Natural transformant microorganisms were analyzed by Hi-C sequencing under steady-state conditions with 2.5 and 50 mg L^{-1} of kanamycin. We observed the natural transformation of bacteria with a synthetic plasmid coding for antibiotic resistance, in an activated sludge mixed culture.

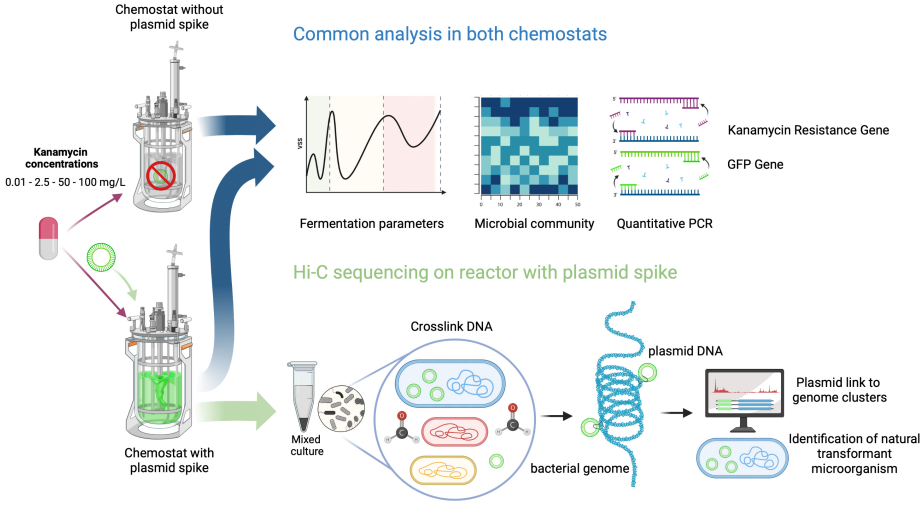

Figure 6.1: Graphical abstract

6.2. Material & Methods

Mixed-culture bioreactor systems and operation

Chemostats

A control chemostat and a test chemostat (both of 1 L total volume and 0.7 L working volume) were operated identically in parallel, under axenic conditions (close environment), aerobically, at room temperature (23 ± 2 °C), fed with a complex synthetic wastewater at a hydraulic retention time (HRT) of 1 day (i.e., flowrate of 1 L d^{-1} or 0.695 mL min^{-1}, and dilution rate of 1 d^{-1} or 0.0417 h^{-1}), and mixed at 600 rpm by mechanical stirring. The dissolved oxygen concentration was controlled with a mass flow controller (Brooks, USA), delivering a flowrate of 0.7 L air min^{-1}. Both chemostats were equipped with oxygen sensors (AppliSens, Poland), thermometers, and pH probes (Mettler Toledo, USA). pH was maintained at 7.0 ± 0.5 by addition of HCl or NaOH at 1 mol L^{-1} each. All samples were taken in sterility using a tube welder (Tekyard, USA). The off-gas from the reactor was filtered-sterilized before release. The effluent was collected in a closed vessel and always autoclaved before discarding. A schematic representation of the equipment is provided in **Figure 6.2**.

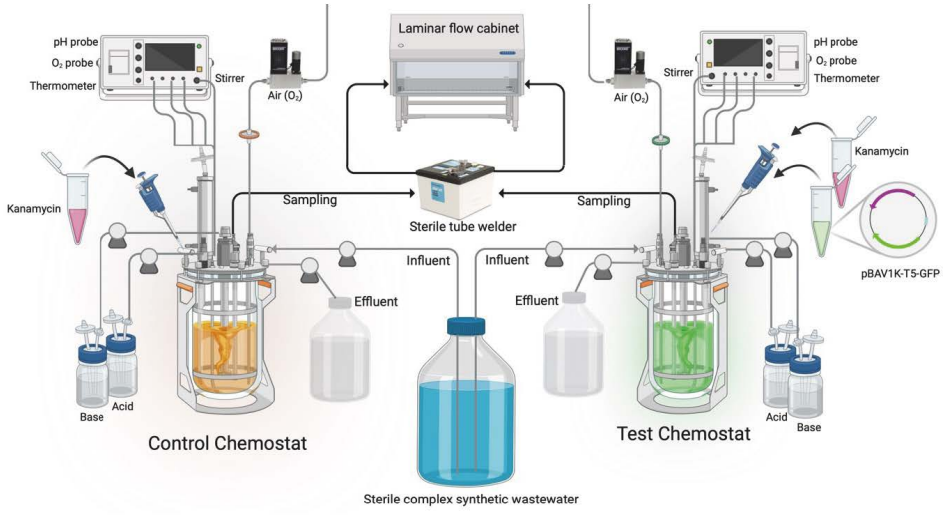

Figure 6.2: Schematic representation of the set containing two continuously stirred bioreactors (chemostats): the control chemostat, where only kanamycin was spiked, and the test chemostat, where kanamycin and the test plasmid (pBAV1K-T5-GFP) were daily spiked. This experimental setting was embedded in a biosafety level II laboratory, where samples had to be extracted via a sterile tube welder and handled under sterility in a laminar flow cabinet.

Inoculum

The reactors were inoculated at a low initial concentration of biomass of 0.043 g VSS L^{-1}, by seeding 10 mL of activated sludge (3 g VSS L^{-1}) collected from WWTP Amsterdam-West (The Netherlands), which is operated for complete biological nutrient removal. The inoculated biomass was equilibrated to the chemostat operation in both reactors over 5 HRTs in the absence of antibiotics.

Antibiotic supply

After acclimation, the reactors were run for 46 days under increasing concentrations of the model antibiotic kanamycin (Thermo Fisher Scientific, USA) from 0.01 to 2.5, 50, and 100 mg L^{-1}. Antibiotic loadings were changed after maintaining each condition over 8-10 HRTs. Kanamycin was spiked daily in both chemostats simultaneously (**Figure S.1**).

Plasmid spikes

In the test reactor only, the rolling circle plasmid pBAV1K-T5-GFP containing genes coding for resistance to kanamycin and a green-fluorescent protein (GFP) as a reporter gene [18] was spiked daily (5 µg L^{-1}) for 37 days. The Monarch Plasmid Miniprep Kit (New England BioLabs, USA) was used to isolate plasmid DNA. This plasmid backbone has already been used for natural transformation in inter-species studies [14]. The plasmid was not spiked over the additional last 10 days of the experiment, to assess if the plasmid would remain accumulated in the mixed culture or washed out due to the continuous operation. The spikes of antibiotics and plasmid were injected through sterile luer connections.

Complex synthetic wastewater composition

A complex synthetic wastewater was prepared according to [19] and previously applied for conjugative experiments [11], to obtain a controlled composition mimicking real wastewater. The detailed influent composition is shown in **Table S.1** and **Table S.2**.

Briefly, this medium was composed of 1/3 volatile fatty acids (1/6 acetate + 1/6 propionate), 1/3 soluble and fermentable substrates (1/6 glucose, 1/6 amino acids), and 2 particulate substrates (1/6 peptone, 1/6 starch) in equal equivalents of chemical oxygen demand (COD).

Amino acids were composed of L-alanine, L-arginine, L-aspartic acid, L-glutamic acid, L-leucine, L-proline, and glycine in COD equivalents. Particulate substrates were peptone from casein, digested with trypsin (Carl Roth, Germany), and starch made from wheat (Merck Sigma, Germany).

Nitrogen was supplied as a combination of soluble ammonium chloride and nitrogen from the aforementioned amino acids and peptone. Phosphorus was composed of soluble orthophosphate.

Analytical methods for the measurements of substrates and biomass concentrations Chemical analyses of the liquid phase

The mixed liquor of the chemostats was sampled as volumes of 11 mL from the effluent in triplicates at a sample frequency every 2 days. 1 mL was centrifuged at 6000 x g 1 min and supernatants filtered through 0.2 µm PVDF membrane filters (Pall, USA), and the filtrates were used for chemical analyses of the liquid phase. Acetate, propionate, and glucose concentrations were measured using a high-performance liquid chromatograph (HPLC; Vanquish™ System, Thermo Fisher Scientific, USA) using an Aminex HPX-87H column (BioRad, USA) maintained at 59°C and coupled to an ultraviolet detector at 210 nm (Waters, USA) and a refractive index detector (Waters, USA). A solution of phosphoric acid at 1.5 mmol L^{-1} was used as eluent. Total nitrogen (5-40 mg L^{-1} TN range) and phosphate (0.5-5.0 mg L^{-1} PO^{3-}-P) were measured with colorimetric-spectrophotometric cuvette tests (Hach-Lange, USA).

Biomass analyses

The concentrations of total suspended solids (TSS) and volatile suspended solids (VSS) of the mixed liquors were analyzed according to Standard Methods [20]. The other 10 mL obtained from the mixed liquor every two days for chemical analyses were used for TSS and VSS measurements.

Preliminary control of plasmid transformation in pure cultures

Escherichia coli K12 and *Bacillus subtilis* str. 168 were used as preliminary controls to verify that the plasmid could transform and express in Gram-negative and Gram-positive microorganisms. *E. coli* cells were electroporated, and *B. subtilis* was transformed with a starvation-induced method [21] with the plasmid and plated in Luria-Bertani (LB) medium with kanamycin (50 mg L^{-1}) to select for positive transformants. Details on electroporation and starvation-induced transformation can be found in **Supplementary Material 6.6**. Microscopic bright field and fluorescent pictures of positively transformed *E. coli* and *B. subtilis* can be found in **Figure S.2**.

Quantitative PCR analysis of kanamycin resistance and GFP marker genes

All qPCR reactions were conducted in 20 µL, including IQ™ SYBR green supermix BioRad 1x. The sets of forward and reverse primers used to amplify the green fluorescent protein (GFP) gene and the kanamycin resistance (*kanR*) gene were retrieved from [18] and summarized in **Tables 6.1 and S.3**. A volume of 2 µL of DNA template was added to each reaction, and the reaction volume was completed to 20 µL with DNase/RNase free Water (Sigma Aldrich, UK). All reactions were

performed in a qTOWER3 Real-time PCR machine (Westburg, DE) according to the following PCR cycles: 95°C for 5 min followed by 40 cycles at 95°C for 15 s and 60°C for 30 s.

Table 6.1: Primers used for qPCR analyses

Gene	Primer forward (5' → 3')	Primer reverse (5' → 3')
16S rRNA	ACTCCTACGGGAGGCAGCAG	ATTACCGCGGCTGCTGG
GFP	TTCAATGCTTTTCCCGTTATCC	CGTCTTGTAGTTCCCGTCATC
kanR	CACTTACTTTGCCATCTTTCAC	CGCTTAGCCGAATTGGATTAC

To check the specificity of the reaction, a melting curve was performed from 65 to 95°C at a temperature gradient of +0.5°C (5 s)$^{-1}$. Synthetic DNA fragments (IDT, USA) containing each target gene were used as a positive control to create the standard curves. Serial dilutions of gene fragments were performed in sheared salmon sperm DNA at 5 µg mL^{-1} (m/v) (Thermofisher, LT) diluted in Tris-EDTA (TE) buffer at pH 8.0. Every sample was analyzed in technical triplicates. Standard curves were included in each PCR plate with at least six serial dilution points and technical duplicates. An average standard curve based on a standard curve from every run was created for every gene set. Gene concentration values were then calculated from the standard curve mentioned above.

Microbial populations dynamics by *16SrRNA* gene amplicon sequencing

Changes in compositions of the microbial communities of the two chemostats during antibiotic regime shifts were analyzed by amplicon sequencing. Volumes of 5 mL of mixed liquors were taken at the end of each antibiotic concentration period (i.e., at steady states) in 15 mL Falcon tubes. Cell pellets were obtained by centrifugation at 6000 x g during 1 min. DNA was extracted from the samples' cell pellets using the PowerSoil microbial extraction kit (Qiagen Inc., Germany), following manufacturer's instructions. The DNA content of the extracts was quantified using a Qubit 4 (Thermo Fisher Scientific, United States). The DNA extracts were preserved at 20°C pending amplicon sequencing analyses.

The DNA extracts were sent to Novogene Ldt (Novogene, Hong Kong) for the V3-V4 *16SrRNA* gene hypervariable regions (position 341-806) on a MiSeq desktop sequencing platform (Illumina, San Diego, USA). The raw sequencing reads were processed by Novogene Ltd and quality filtered using the QIIME software [22]. Chimeric sequences were removed using UCHIME [23], and sequences with 97% identity were assigned to the same operational taxonomic units (OTUs) using UPARSE [24]. Each OTU was taxonomically annotated using the Mothur software against the SSU rRNA database of the SILVA Database [25]. The heatmap of relative abundances was generated using the R package "ampvis2" v2.7.31 [26].

Microbiome profiling by metagenomics

The same biomass samples selected for Hi-C metagenomics sequencing (collected at 2.5 and 50 mg Kan L^{-1}; see §6.2 below) were sequenced in parallel by conventional metagenomics to profile their microbiomes at high resolution. Samples were submitted to and sequenced by Phase Genomics (USA). Both the shotgun library and the Hi-C library were sequenced on the same platform. The details are given in section §6.2.

Classification with Kraken 2.0 [27] was performed on pair-end mode on the quality-controlled short reads, using the Microbial Database for Activated Sludge (MiDAS) [28]. The taxonomic classification outcomes from Kraken 2.0 were converted into a BIOM file using the kraken-biom [29] tool to explore metagenomics classification datasets via the "MicrobiotaProcess" package v1.6.6. in R [30].

Microbiome profiling by metagenomics

Hi-C libraries were prepared as explained in [31] and summarized in **Figure 6.3**.

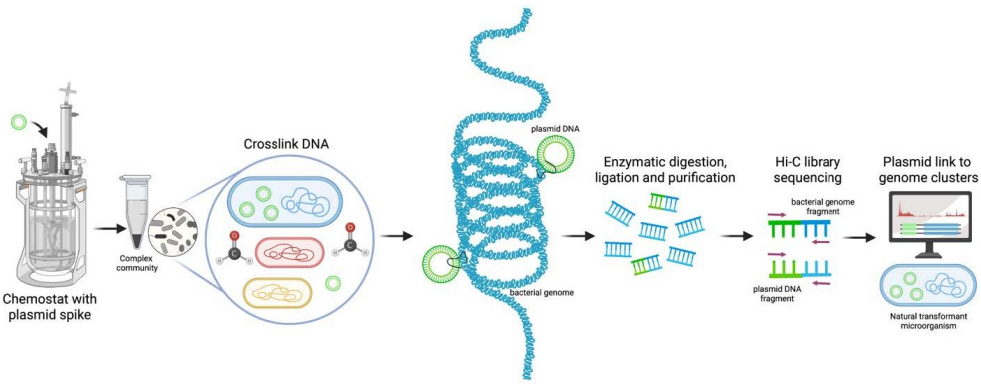

Figure 6.3: Schematic representation of the Hi-C deconvolution process in which the microbial community at a particular time point is crosslinked with formaldehyde before cell lysis, linking plasmids to bacterial genomes. DNA extract is digested enzymatically, biotinylated, ligated, and purified. To generate the Hi-C library, the resultant fraction is sequenced and used to create Hi-C links used to deconvolute contigs into genome clusters, including chromosomes and plasmids.

Biomass sampling

Biomass samples were collected as volumes of 10 mL of mixed liquor at the end of the antibiotic treatment periods at 2.5, and 50 mg Kan L^{-1} from the test reactor spiked with the plasmid and transferred on ice. The biomass was aliquoted in two 1.5 mL Eppendorf. One sample was used for Hi-C library generation, while the other was used for standard metagenomic library preparation.

Biomass sample conditioning for Hi-C analysis

A volume of 1.5 mL of the collected biomass sample was resuspended using 13.5 mL of solution of a commercial 1% formaldehyde-phosphate-buffered saline (F-PBS) (Alfa Aesar - Thermo Fischer Scientific, USA) in a 15 mL Falcon tube under biosafety level II conditions. Formaldehyde was used to generate covalent links between spatially adjacent genetic segments (**Figure 6.3**). The resuspended sample was incubated at room temperature for 30 min with periodic mixing (every 5 min) before adding glycine at a final concentration of 1 g/100 mL to quench the reaction and further incubating the mixture at room temperature for 15 min with periodic mixing. The last step involved a series of three spin down (6000 x g, 1 min) and rinses with PBS of the pellet. Briefly, the sample was spun down for 2 min at 6000 x g, rinsed with PBS, and spun down again (5 min at 6000 x g) before removing the supernatant. The final pellet was kept frozen at 20 °C.

Hi-C library preparation and sequencing

Hi-C libraries were prepared with the Phase Genomics ProxiMeta Hi-C v4.0 Kit using the manufacturer-provided protocol [32]. Briefly, the intracellular DNA pool (comprising the genomic DNA and the accessory genome, i.e., MGEs) of the microbial cells present in each of the two selected samples were crosslinked using the formaldehyde solution. These pre-treated biomass samples were submitted to Phase Genomics for library preparation and sequencing. Cells were bead-beated to release the cross-linked DNA. The released cross-linked DNA was digested using the Sau3AI and MlucI restriction enzymes simultaneously, and proximity ligated with biotinylated nucleotides to create chimeric molecules composed of fragments from different regions of genomes and plasmids that were physically proximal in vivo. Proximity ligated DNA molecules were pulled down with streptavidin beads and processed into an Illumina-compatible sequencing library. Separately, using an aliquot of the original samples, DNA was extracted with a ZYMObiomics DNA miniprep kit (Zymo Research, USA) and a metagenomic shotgun library was prepared using ProxiMeta library preparation reagents.

Sequencing was performed on an Illumina NovaSeq generating PE150 read pairs for both the shotgun libraries and the Hi-C libraries obtained from the aliquots of each of the two biomasses collected at 2.5 and 50 mg Kan L^{-1}. Hi-C and shotgun metagenomic sequencing files were uploaded to the Phase Genomics cloud-based bioinformatics platform for subsequent analysis.

Processing of shotgun metagenomics and Hi-C metagenomics datasets

Quality control of sequenced reads

After sequencing, datasets containing 4 paired-end read samples with an average of 78M reads for the Hi-C samples, and 160M reads for the non-crosslinked samples (i.e., shotgun) were obtained. The quality of the Illumina reads was assessed using

FastQC version 0.11.9 with default parameters [33]. Shotgun reads were filtered and trimmed for quality and normalized using fastp v0.19.6 [34].

Assembly of shotgun sequence reads

The trimmed reads were assembled into contigs using MEGAHIT v1.2.9 [35] for the resistome analysis. The trimmed reads were assembled into contigs using metaSPAdes version 3.14.1 [36] on meta mode on default parameters for following discordant reads analysis (to quantify interactions plasmid:bacteria). We used these two assemblers to verify which one resulted in positive results for plasmid-host detection (only metaSPAdes displayed positive results).

Processing of the Hi-C reads

Each set of Hi-C reads was mapped to the metagenomic assemblies to generate a SAM file containing the information of the assembly and the Hi-C links. Mapping was done using the Burrows-Wheeler alignment tool BWA-MEM v0.7.17-r1188 [37]. During mapping with BWA-MEM, read pairing and mate-pair rescue functions were disabled and primary alignments were forced to be aligned with the lowest read coordinate (5' end) (options: -5SP) [38]. SAMBLASTER v0.1.26 [39] was used to flag PCR duplicates, which were later excluded from the analysis. Alignments were then filtered with samtools v1.13 [40] using the -F 2304 filtering flag to remove non-primary and secondary alignments.

Deconvolution of the Hi-C data for aminoglycoside resistome analysis

Metagenome deconvolution was performed with ProxiMeta [41, 42], creating putative genome and genome fragment clusters (**Figure S.13-S.14**). Clusters (also known as metagenome-assembled genomes or MAGs) were assessed for quality using CheckM v1.1.10 [43] (>90% completeness, <10% contamination) and assigned preliminary taxonomic classifications with Mash v2.3 [44]. NCBI plasmid database was used to identify which contigs had plasmid or genomic DNA as the origin, and NCBI AMRFinderPlus software (v3.10.5) [45] was used to annotate aminoglycoside resistance genes using the NCBI AMRFinder database. AMR genes and plasmids were annotated on all contigs in the assembly. Hi-C signal was used to associated plasmids with their hosts. Thus, if a plasmid was associated with a host and had an AMR gene, the event was annotated as an AMR gene conveyed to the host via a plasmid. If an AMR gene was found on a binned contig that was not annotated as a plasmid, it was classified as an AMR gene originating from genomic DNA [46]. The taxonomic trees were generated with "ggtree" package v3.2.1 in R [47].

Plasmid transformation events detection from Hi-C data using discordant-reads analysis

Both ProxiMeta platform and bin3C v0.1.1. [38] tool were used for the generation of clusters to look for pBAV1K-T5-gfp integration. These available methods were not sensitive enough for detecting Hi-C links by identifying plasmid-contig (host) events. We therefore implemented a discordant reads analysis to quantify the interactions obtained from crosslinking the DNA pool between two genetic sequences that are not necessarily consecutive in the bacterial genome and accessory genome, within cells of the mixed cultures. A detailed explanation of the discordant read analysis, workflow, and visualization of transformation events can be found in **Supplementary Material 6.6**.

6.3. Results

Plasmid spike had a beneficial effect on biomass growth under acute antibiotic treatment

The biomass in both chemostats grew at a growth rate (μ) of 0.042 h^{-1} (i.e., equal to the dilution rate applied) under environmental antibiotic concentrations (0.01-2.5 mg Kan L^{-1}) (**Figure 6.4**). When higher antibiotic pressures were applied (50 – 100 mg Kan L^{-1}), a significantly higher biomass formed (max Δ150 mg VSS L^{-1}) when the plasmid was spiked in the broth. Uptake of plasmid DNA and the kanamycin resistance gene expression can confer a better resistance to higher antibiotic concentrations. Interestingly, the control reactor treated with a high concentration of kanamycin of 50 mg L^{-1} displayed an abrupt decrease in culture viability compared to the test reactor amended both with the antibiotic and the plasmid. The highest antibiotic concentration (100 mg L^{-1}) was eventually selected for biomass able to grow in the control reactor. Details on operation performances are given in **Figure S.3**.

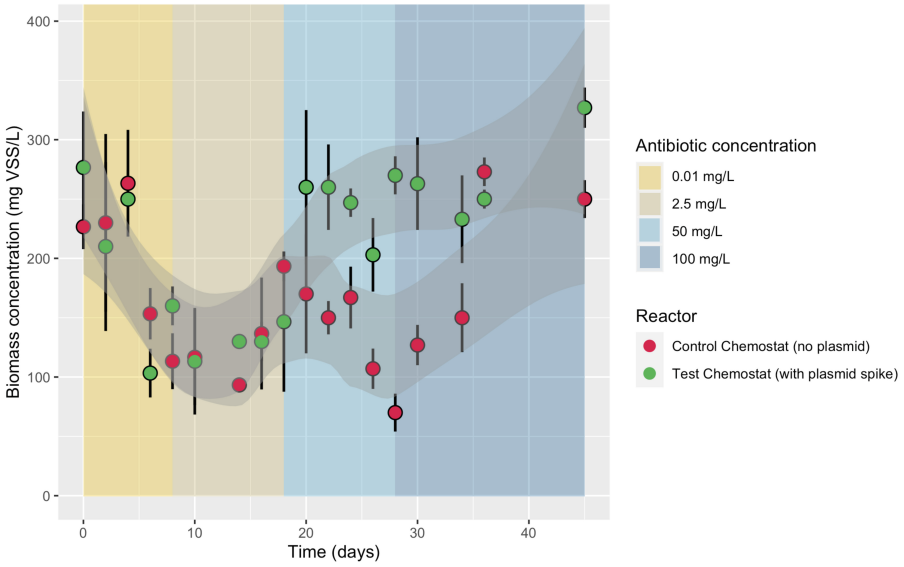

Figure 6.4: Daily-averaged values for volatile suspended solids (VSS) from both reactor control and reactor with free-floating plasmid over the whole operation time the experiment was conducted (45 days). Kanamycin concentrations are displayed as background-colored sections: 0.01 mg L^{-1}, 2.5 mg L^{-1}, 50 mg L^{-1}, 100 mg L^{-1}.

Microbial community compositions under increasing antibiotic pressure

Microbial population composition (**Figure 6.5a**) was analyzed by *16S rRNA* gene amplicon sequencing from both the control (RC) and test (RT) reactors at the end

of each period of increasing kanamycin loading. After inoculation, the reactors were acclimatized for 10 days to chemostat operation prior to antibiotic supply and plasmid spikes (day 0 is the moment of the start of antibiotic addition). The same predominant bacterial populations were enriched in both reactors. Rather than the plasmid spikes, the antibiotic supply exerted the strongest selection pressures on the microbial communities. There was a decrease in diversity with increased antibiotic dosage as it enriched for 5-6 families of *Spirosomaceae*, *Comamonadaceae*, *Rhodocyclaceae*, *Rhizobiaceae*, *Microbacteriaceae*, and *Chitinophagaceae*.

The ratios of *GFP* and *kanR* over *16S rRNA* strongly increased in the test system under high antibiotic concentration. Therefore, biomass samples were collected from the test reactor during the stationary periods at 2.5 (day 18; Test Reactor Day 18, i.e., sample RT.D18) and 50 (day 28; RT.D28) mg L^{-1} of kanamycin and sequenced for metagenomics and Hi-C analyses to uncover the resistome, mobilome, and transformation events in the mixed culture. The metagenome of these two samples RT.D18 (2.5 mg Kan L^{-1}) and RT.D28 (50 mg Kan L^{-1}), shared 90.6% of reads that mainly affiliated with *Microbacterium*, *Bosea*, *Ensifer*, *Zoogloea*, and *Streptomyces* genera (**Figure 6.5b-c**).

The list of MAGs recovered by aligning Hi-C reads against the shotgun assembly, and their quality, both RT.D18 and RT.D28, can be found in **Figure S.13** and **Figure S.14**, respectively.

The spiked plasmid accumulated in the system at high antibiotic concentrations

The kanamycin resistance gene was quantified by qPCR during the whole operation of both the control and test reactors (**Figure 6.6**). A kanamycin-resistant enrichment culture developed with the increasing antibiotic dosage in both reactors. The kanamycin gene was obtained by the microorganisms either via natural transformation from the spiked plasmid pBAV1K-T5-GFP or endogenously present in the activated sludge inoculum.

The spiked plasmid integrated the kanamycin resistance gene and a GFP gene. qPCR was also performed on the GFP gene. The GFP gene was detected in the test reactor spiked with the plasmid but not in the control reactor (**Figure 6.6,upper panel**). Hence, the plasmid was exclusively present in the test reactor. Reporter GFP fluorescence measurements could not be used as validation due to the sample complexity or lack of expression.

Higher antibiotic concentrations resulted in an enrichment of the ratio of GFP to *16S rRNA* genes (GFP/16S ratio) present in the test mixed culture from 3.5 to 1.5 log gene copies (*GFP* and *kanR*, respectively)/*16S rRNA* (**Figure 6.6**). Plasmid accumulation occurred either by uptake by bacteria and replication during growth or adsorbed to extracellular polymeric substances (EPS)[48]. After 18 days of exposure to the highest kanamycin concentration of 100 mg L^{-1}, no plasmid was spiked in the test culture for additional 8 days.

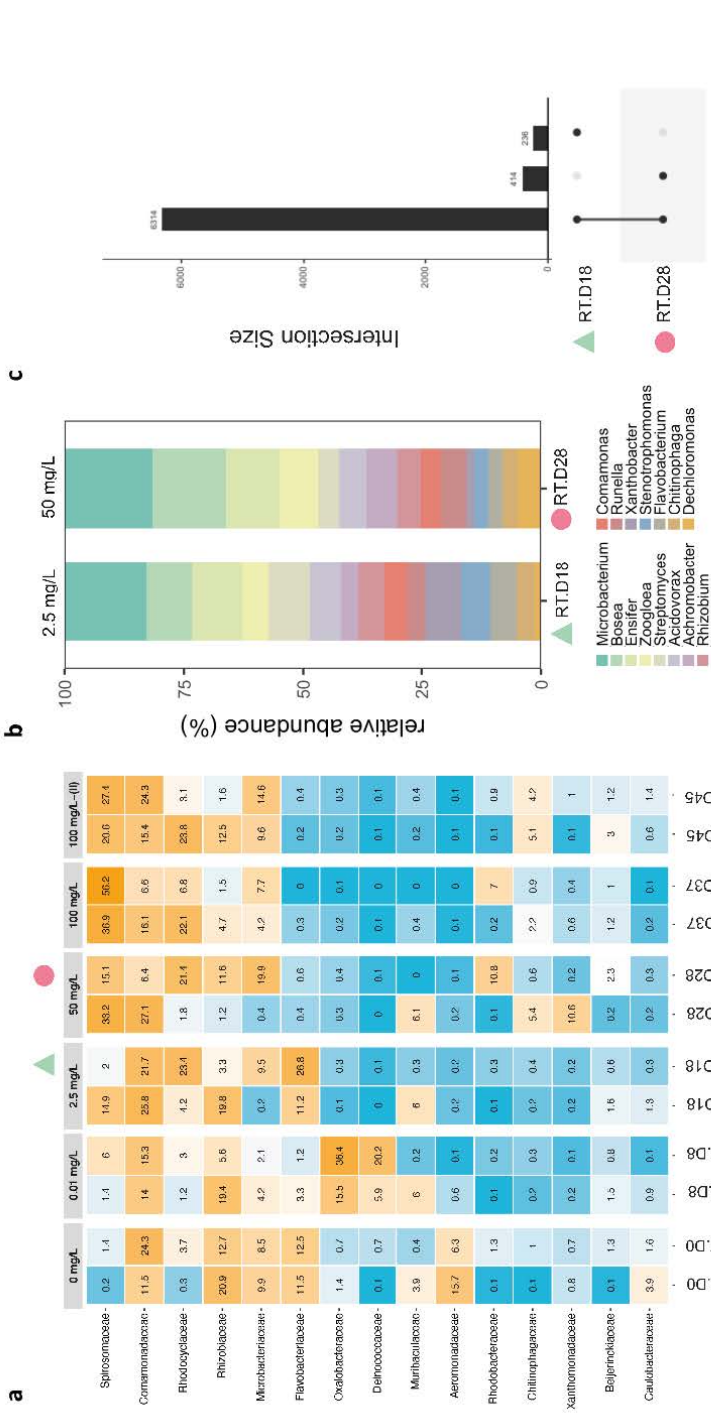

Figure 6.5: (a) Heatmaps from 16SrRNA amplicon sequencing showing bacterial family compositions across the operation in both chemostats grouped per kanamycin concentration (0 mg L^{-1}, 0.01 mg L^{-1}, 2.5 mg L^{-1}, 50 mg L^{-1}, 100 mg L^{-1} with spiked plasmid and 100 mg L^{-1} –(II) without spiked plasmid). The different color intensities represent the relative bacterial family abundance in each population. **Note: RC** = Reactor Control without spiked plasmid. **RT** = Reactor Test with spiked plasmid. (Triangle: Day 18 – 2.5 mg L^{-1} and Circle: Day 28 – 50 mg L^{-1}) represent the samples from the reactor test that were also sent to analyze for Hi-C sequencing. **(b)** Microbiome analysis from the samples sent for Hi-C sequencing at the genus level. **(c)** UpSet plot showing microbiome intersections between day 18 and day 28 from the test reactor.

The resulting GFP/16S ratio did not decrease substantially, supporting the hypothesis that the plasmid had been integrated into the mixed culture's microbial population.

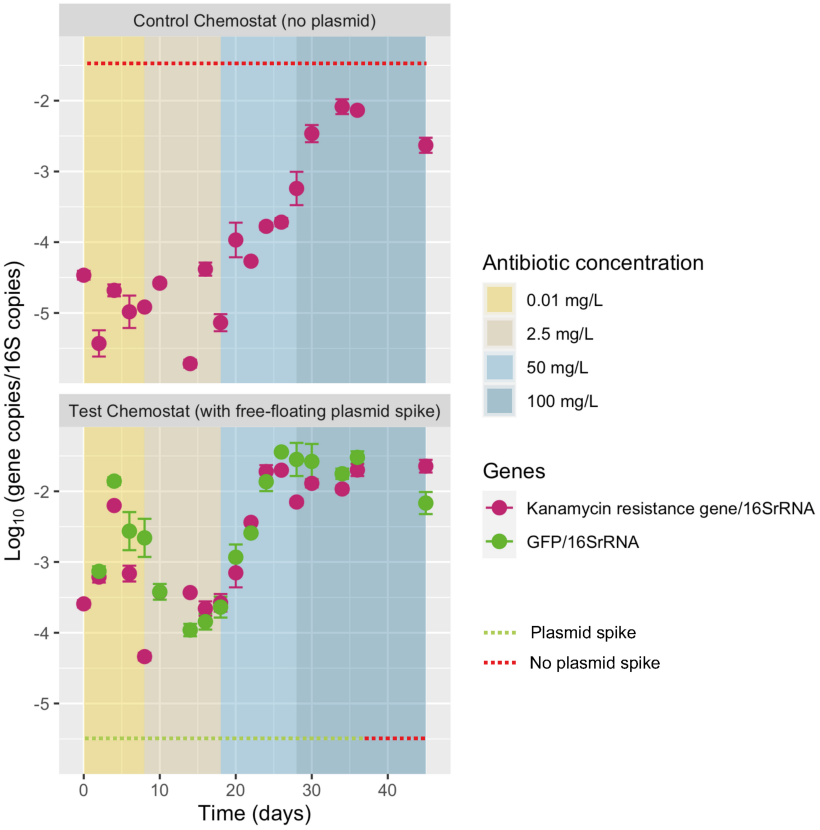

Figure 6.6: Relative abundance of green fluorescent protein (GFP) gene and Kanamycin resistance gene from plasmid pBAV1K-T5-GFP relative to *16S rRNA* gene in every sampling point. Only data from the reactor with free-floating plasmid displayed as non-detected values were detected for reactor control. Kanamycin concentrations are displayed on colored-background sections: 0.01 mg L^{-1}, 2.5 mg L^{-1}, 50 mg L^{-1}, 100 mg L^{-1}. The plasmid was not spiked anymore in the test reactor (after day 36).

Increasing kanamycin concentrations promoted plasmid mobility and aminoglycoside resistance genes Hi-C interactions

The impact of increasing concentrations of kanamycin (aminoglycoside antibiotic family) was not only investigated for the abundance of the kanamycin resistance gene spiked with the synthetic plasmid, but also for the broader presence of aminoglycoside resistance genes of genomic or natural plasmid origins, and their

association in bacterial hosts (**Figure 6.7**).

The higher kanamycin concentration (50 vs. 2.5 mg L^{-1}) doubled the number of bacterial hosts genomic sequences' interacting with aminoglycoside resistance genes (3 vs 7 bacterial hosts). The maximum number of Hi-C interactions between genomic sequences and aminoglycoside resistance genes (expressed as gene:bacterial host) in the mixed culture also doubled: *ant(2")-Ia*:*Zoogloea sp.* (29 Hi-C interactions kb^{-1}; **Figure 6.7a**) vs. *aac(6')-Ib*:*Microbacterium sp.* (59 Hi-C interactions kb^{-1}; **Figure 6.7b**). Thus, more bacterial hosts contained genes coding for aminoglycoside hydrolyzing enzymes and more copies of these genes (that can occur both on the genomic DNA and on naturally occurring plasmids) were detected under high antibiotic pressure.

There was a shift in the origin of the resistance genes: genomic or plasmid DNA. The low kanamycin concentration (2.5 mg L^{-1}) selected mainly for *Zoogloea sp.* which harbored multiple aminoglycoside resistance genes integrated into its genome. Higher concentrations of kanamycin promoted mobility of aminoglycoside resistance genes encoded in plasmids. We detected multiple aminoglycoside resistance genes encoded in plasmids. Some of genes detected in plasmids were found in multiple bacteria such as the aminoglycoside 3'-phosphotransferase gene *(aph(3")-Ib)* in *Zoogloea sp.*, *Acidovorax sp.*, and *Rhodobacter sp.* (**Figure 6.7b**).

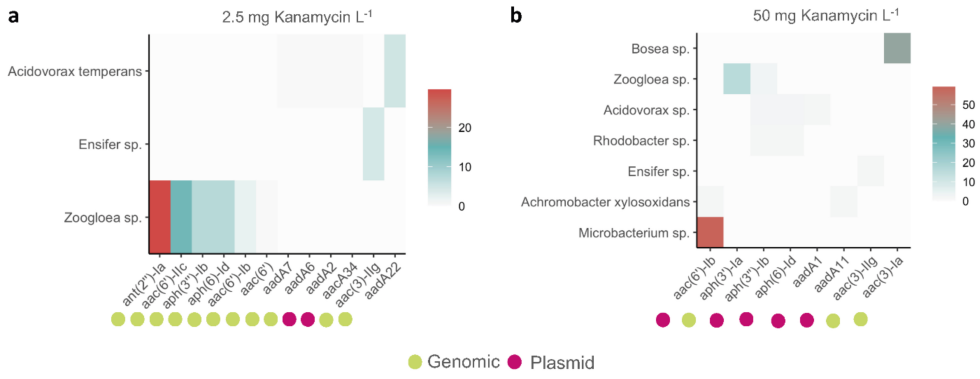

Figure 6.7: The number of Hi-C interactions between aminoglycoside resistance genes and bacterial hosts when **(a)** 2.5 mg Kanamycin L^{-1} and **(b)** 50 mg Kanamycin L^{-1} were applied to the test chemostat. Contigs containing aminoglycoside resistance genes were classified to determine their origin: genomic or plasmid DNA. Colors represent the number of Hi-C interactions normalized by the contig length (kb). Neighbor-joining trees of the different aminoglycoside resistance genes and their alignment can be found in **Figure S.4**.

Discordant reads analysis allowed the quantification of spiked plasmid transformation in bacterial species

Hi-C sequencing results show how difficult it is to capture a transformation event when a specific plasmid is spiked in a mixed culture. Bioinformatic tools available for the analysis of Hi-C libraries, such as bin3c [38] or commercial ProxiMeta

platform [49], were not suited to identify transformation events of one specific plasmid considering the complex diversity of plasmids and other MGEs present in the samples. Therefore, we performed a discordant reads analysis of the aligned Hi-C reads against the shotgun metagenome assembly. The discordant reads analysis quantifies the interactions obtained from crosslinking the DNA pool between two genetic sequences that are not necessarily consecutive in the genome of a bacterial population present in the mixed culture.

Synthetic constructs consisting of the plasmid sequence, the non-coding spacer DNA, and the metagenome contigs with higher Hi-C links with plasmid contigs were generated to verify the transformation of the spiked plasmid inside bacteria and its integration into their genome or its episomal presence in their cytoplasm (**Figure 6.8a**, **Figure S.6**). Hi-C metagenomes were sequenced at antibiotic pressures of 2.5 mg L^{-1} (sample RT.D18) and 50 mg L^{-1} (RT.D28) of kanamycin. No plasmid sequence was retrieved from the raw reads and the assembly of sample RT.D18. At this time point, the plasmid was either present at a very low concentration (which corresponds to the lowest plasmid/16S ratio detected by qPCR; **Figure 6.5**), but metagenomics was not sensitive enough to detect it.

Conversely, the assembly RT.D28 remarkably harbored multiple contigs containing genetic information from the spiked plasmid. This highlights that synthetic plasmids can end up inside microbial populations of an activated sludge mixed culture through transformation. The genomic DNAs of the Gram-negative *Bosea sp.*, *Runella spp.*, *Gemmobacter sp.*, *Zoogloea sp.*, and of the Gram-positive *Microbacterium sp.* were cross-linked with genetic fragments coming from the spiked plasmid (**Figure 6.8b**). *Runella slythiformis* contigs displayed the highest frequency of Hi-C links (102), followed by *Microbacterium oxydans* (90) (**Figure 6.8b**). *Bosea sp.* had the highest number of Hi-C links per kb of contig sequence length (5.1 Hi-C links kb^{-1}), followed by *Runella spp.* (2.2 Hi-C links kb^{-1}) (**Figure 6.8c**). Genus associated to the previous bacteria had a relative fold increase of 2-4 times when compared the microbiome from 2.5 and 50 mg Kan L^{-1}. *Microbacterium* increased from 5.4 mg VSS L^{-1} to 14.6 mg VSS L^{-1}; *Bosea* increased from 3 mg VSS L^{-1} to 12.4 mg VSS L^{-1}; *Runella* increased from 1.6 mg L^{-1} to 3.3 mg L^{-1}; *Zoogloea* increased from 1.74 mg VSS L^{-1} to 6.6 mg VSS L^{-1}.

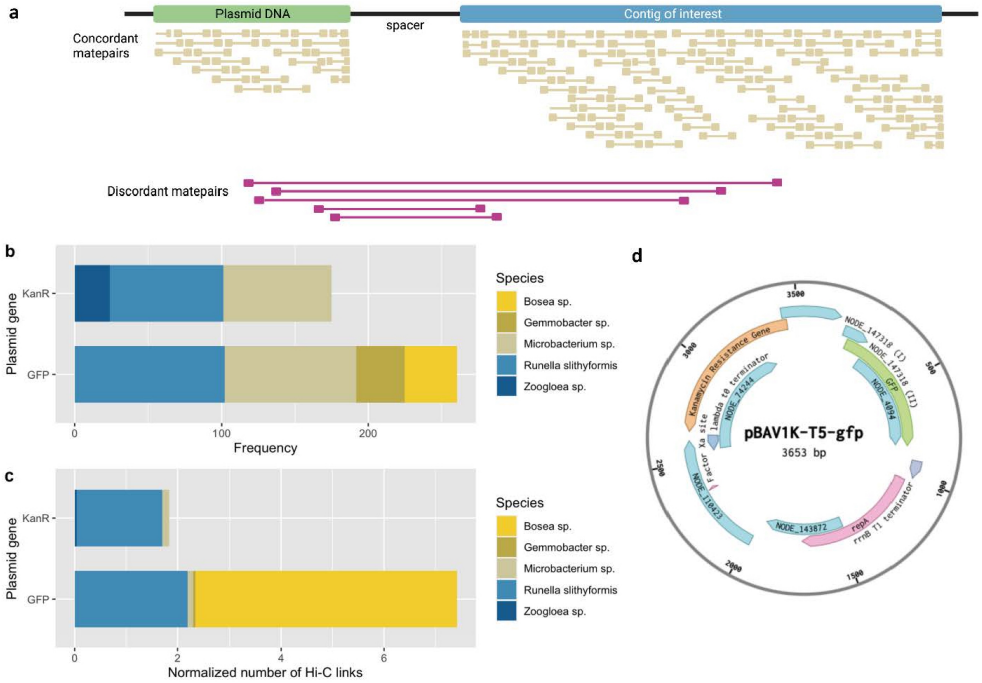

Figure 6.8: (a) Schematic representation of the discordant read analysis performed on contigs interacting with plasmid contigs, where synthetic constructs were generated to quantify the number of interactions from the Hi-C library alignment. **(b-c)** Taxonomic assignment of contigs that were linked to contigs harboring the information of the spiked pBAV1K-T5-GFP plasmid by frequency and by a normalized number of Hi-C links (events divided by the length of the interacting contig). **(d)** Plasmid map containing the contigs used for the discordant read analysis. The *kanR* information in **a-b** is a combination of the number of interactions between the Kanamycin Resistance Gene with the NODE_74244 and NODE_147318 (I). Likewise, the *GFP* information is a combination of the number of interactions between the GFP gene with the NODE_147318 (II) and NODE_4094.

Only contigs interacting with the kanamycin resistance gene (*kanR*) or the *GFP* gene were used to quantify Hi-C links (**Figure 6.8d**). This also informs that microorganisms from different classes, such as *Alphaproteobacteria*, *Actinobacteria*, *Bacteroidetes*, and *Betaproteobacteria*, were transformed in the mixed culture with this rolling-circle plasmid (**Figure S.7**). Visualization examples of cross-linking events with full plasmid are given in Figures S9-S12. They strongly confirmed that *Bosea sp.* and *Runella spp.* took up the plasmid from the environment (**Figure S.7** and **Figure S.8**). Interactions visualization was less clear for the other microbial populations with detected Hi-C links.

These results show that (synthetic) plasmids can transform into different microorganisms of multiple classes in activated sludge mixed cultures when enough selection pressures (high antibiotic concentrations) are introduced into the system.

6.4. Discussion

The growth of the activated sludge biomass under high antibiotic concentrations was promoted by plasmid accumulation

The microbial enrichment culture was able to adapt and substantially grow under high antibiotic concentrations (50 mg Kan L^{-1}) concomitantly to plasmid accumulation in the test reactor (**Figures 6.4-6.5**). At high antibiotic loading, the biomass grew with higher yields in the test reactor than in the control reactor, which was not spiked with the plasmid.

Microorganisms transformed and selected at high concentrations of kanamycin could improve their fitness and resist antibiotic treatment. The plasmid kanamycin resistance gene confers resistance against the antibiotic, allowing bacterial cells to withstand and grow under high kanamycin concentrations. The kanamycin resistance gene was detected in the test reactor spiked with the plasmid designed with *kanR* and in the control reactor that did not receive the plasmid. The qPCR results showed that microorganisms with kanamycin resistance genes were already in the activated sludge inoculum collected at the full-scale WWTP. Genes coding for resistances to aminoglycosides (such as kanamycin) have been identified in the influents, sludges, and effluents of WWTPs [50–52].

The most abundant aminoglycoside resistance genes in the system were *aac(6')-Ib*, *aph(3')-Ia*, *aph(3")-Ib*, *aph(6)-Id*, and *aac(3)-Ia* (**Figures 6.7**). These genes encode the most prevalent aminoglycoside modifying enzymes conferring resistance to tobramycin, amikacin, and kanamycin. These genes were more abundant under laboratory-selection antibiotic concentration (50 mg L^{-1}), helping bacteria like *Microbacterium sp.*, *Bosea sp.*, and *Zoogloea sp.* to resist this condition. *aph(3)-Ib*, and *aph(6)-Id* have been described, complete or in part, within plasmids, integrative conjugative elements, and chromosomal genomic islands [53, 54]. As a consequence of the dissemination of this DNA fragment, the *aph(6)-Id* and *aph(3)-Ib* genes are found in both Gram-positive and Gram-negative organisms [55].

The presence of exDNA and an antibiotic can promote the structural integrity of biofilms [56], hence facilitating bioaggregation and biomass development in the reactor. Microorganisms in the test reactor aggregated easier than in the control reactor (**Figure S.12**). Corno et al. [57] have observed that antibiotics (levofloxacin, tetracycline, and imipenem) can increase the cellular clustering as microcolonies and bioaggregates by 3% (at low antibiotic loading) to 20-25% (at high antibiotic loading) in artificial lake water bacterial communities studied in chemostats. According to Das et al. [58], adding exogenous DNA in pure cultures increases bacterial adhesion and broth viscosity. This was facilitated with an amendment of Ca^{2+} through acid-base interactions and cationic bridges.

Biomass growth under high antibiotic concentrations mainly resulted from the presence of resistant bacteria already in the inoculum rather than a consequence of

transformation. The qPCR showed that the plasmid remained in the test chemostat even after 8 days (i.e., after 8 HRTs, 12 number of generations) after stopping its spiking (**Figures 6.5**). The plasmids remained either transformed inside the predominant bacterial populations selected or adsorbed to EPS. Proximity-ligation Hi-C sequencing was used to quantify the interactions between the pool of genomic and mobile DNA molecules in the same cell within the microbial community, as discussed hereafter.

Microbial community and ecological dynamics of plasmid transfer

It is known from pure cultures of *Streptococcus pneumoniae* and *Legionella pneumophila*, that the exposure to aminoglycoside and fluoroquinolone antibiotics induces their genetic transformability (i.e., competence state) as a result of genotoxic stress [59–61].

Kanamycin promotes competence by inducing decoding errors during translation into aminoacids. It inhibits protein synthesis by binding to the A site of *16S rRNA* in the 30S ribosomal subunit and generates misfolded proteins that activate the serine protease HtrA. This triggers a cascade of reactions involving interactions between competence-stimulating proteins (ComC, ComAB, CSP, and others) that eventually launches the competence state [59, 62].

In this study, microorganisms from different classes (**Figure S.6**) displayed plasmid-host interactions. *Alphaproteobacteria*, *Betaproteobacteria*, *Bacteroidetes*, and *Actinobacteria* contain one or more species that are naturally competent [7]. Experimental demonstrations of natural competence have so far been limited to only a few dozen of species scattered across the bacteria tree and investigated in pure cultures. Such culture-based assays are only conducted with species where a selectable genetic marker is available and cannot help discover competence in uncharacterized populations present in microbial communities that generally do not grow on agar plates [7]. Our approach combining mixed-culture biotechnology and Hi-C metagenomics sequencing successfully uncovered transformability in a microbial community of activated sludge. Further research on competence genes expression and proteome analysis would elucidate the mechanisms by which bacteria have taken up exDNA.

Most of the identified transformed bacteria were Gram-negative (*Bosea sp.*, *Runella sp.*, *Gemmobacter sp.*, and activated sludge floc former *Zoogloea sp.*) and one Gram-positive (*Microbacterium sp.*). Gram-negative bacteria comprise an outer membrane that protects them against the antibiotic and makes them more challenging to kill. Gram-positive ones have a thick peptidoglycan layer that absorbs antibiotics and detergents easier, leading to faster cell death and slower development of resistance [63]. We recently showed that most microorganisms co-localizing MGEs and ARGs in a full-scale WWTP were Gram-negative [4].

A diverse microbial community like activated sludge is composed of many

potential hosts that encompass a diversity of mechanisms to maintain and transfer plasmids, including donor-mediated conjugation once the plasmid is transformed [64]. Conjugative plasmid transfer spreads ARGs even in the absence of antibiotic pressure, as reported from investigations of the gut microbiota [65]. Here, as displayed in **Figure 6.7**, at high antibiotic pressures, there were more hosts containing aminoglycoside resistance genes located in plasmids. Tracking the temporal dynamics of plasmids uptake via transformation together with the more recurrent microbial hosts and spreaders is an important outcome for evaluating the risks associated with the transformation of exogenous (synthetic) MGEs, on top of conjugative events. With this study, we provide the tools to achieve such target in complex microbial communities.

Limitations and alternatives of Hi-C sequencing for detecting transformation events

When building MAGs from microbial communities, microdiversity within a genus or species can challenge the taxonomic affiliation resolution, such as observed for the closely related *Runella spp.*. Besides a taxonomic classification problem, binning can also be affected in such situation. When multiple populations of a single genus are present in a microbial community, parts of a contig can derive from one strain while other parts from other strains can coassemble [38].

Detecting specific fractions of the spiked plasmid interacting with genome clusters (or MAGs) of populations from the mixed culture was challenging. First, commercial and publicly available bioinformatics platforms (ProxiMeta) and computational tools (bin3c) were not sensitive enough to track individual transfer events, while very useful for general resistome and plasmidome to host linkage. Second, only 17.9% of the contigs of the metagenome assembly could be sorted into MAGs (**Figure S.13-S.14**). This leaves 82.1% of the genetic information unanalyzed, potentially containing information about the plasmid-host. Therefore, manual data curation involving all discordant reads analysis and cluster linkage was done. Discordant read analysis was advantageous to compare all contigs of the metagenome interacting with contigs affiliating with the spiked plasmid sequence, bypassing the binning limitation.

epicPCR (emulsion, paired isolation, and concatenation PCR) is an alternative method to Hi-C sequencing for recovering linked phylogenetic and functional genetic information from millions of cells in a single analysis [66]. epicPCR is limited by the requirement of prior knowledge of sequences of the target genes before performing the qPCR and by the biases introduced by amplifying the *16S rRNA* gene [67, 68]. To increase sensitivity, combining Hi-C sequencing and epicPCR would be interesting for identifying transformation events in mixed cultures and identifying new potential natural competent bacterial species.

Natural transformation and rolling-circle plasmids as models

In this transformation experiment of the mixed culture, we used the rolling-circle replication (RCR) plasmid pBAV1K-T5-GFP. This plasmid is a suitable model plasmid for studying natural transformation in microbial communities through its capacity to replicate in both Gram-positive and Gram-negative microorganisms [18]. RCR is one of the simplest mechanisms adopted by some plasmids, which relies on a sequence-specific cleavage. This generates a nick in the double-strand origin of one of the parental DNA strands by an initiator Rep protein (3'-OH end), allowing DNA polymerases to initiate the leading strand replications [69] and circumventing the primer RNA synthesis used in the canonical theta replication.

There are multiple ways by which the spiked plasmid could be incorporated into the genomes of the competent bacteria of the activated sludge. The canonical way is via double-stranded exDNA uptake through the outer membrane, the periplasm, and internalized as single-stranded DNA through the inner membrane (in Gram-negative). In Gram-positive, the exDNA must cross a thick peptidoglycan layer [70]. Methylation plays a protective role in bacteria for avoiding exogenous DNA influx from bacteriophages [71, 72]. The plasmid DNA spiked in the test chemostat was produced in an *E. coli* strain with its dam/dcm methylases activated. However, DNA is usually single-stranded inside the cytoplasm in natural transformation and thus not a target for most restriction enzymes [7].

Double-stranded plasmid DNA could also be transformed via σ^S regulation through ABC transporters [73]. In natural transformation in *E. coli*, dsDNA passes across the outer membrane through an unknown pore. This way, dsDNA could transform and not be genome integrated but maintained episomally. This research focused on the possibility of exDNA being integrated into the genome. However, from the microbial ecology point of view, more research should be done on how bacteria exchange genetic information in samples from complex systems to understand microbial evolution.

Outlook

Overall, among the three main mechanisms of HGT, transformation rarely occurs between bacterial species to transfer drug resistance genes [74] when compared to more efficient processes such as conjugation, since conjugative plasmids account for half of all plasmids, and these can be broad host range [13, 64, 75]. Antibiotic concentrations in the environment range typically from 0.01 µg L^{-1} in the sea to 0.1 µg L^{-1} in rivers, 1 µg L^{-1} in treated municipal sewage, 10 µg L^{-1} in untreated municipal sewage, and up to 100-10'000 µg L^{-1} found in untreated hospital effluents and industrially polluted surface water [76]. Here, transformation was detected under high antibiotic concentration (>50 mg L^{-1}), i.e., resembling highly concentrated antibiotic streams or antibiotic administration in the gut and polluted industrial waters. Such antibiotic level was used to detect a clear microbial community response from the experimental noise. The consequences of

single transformation events may be vast [76], potentially inducing a severe medical issue by developing the so-called "superbugs" or bacteria resistant to two or more antibiotics. The following research should focus on the environmental conditions (nutrient limitation, temperature shifts, linear vs. plasmid DNA, methylation patterns, among others) that trigger competence, exDNA uptake, and exchange within microbial communities.

6.5. Conclusions

We identified that microorganisms in a mixed culture enriched from activated sludge could take up and get transformed by synthetic plasmids present in their wastewater environment, provided a selection pressure is present, like a high antibiotic concentration. The result of this work involving quantitative mixed-culture biotechnology and Hi-C sequencing led to the following additional main conclusions:

- The spike of plasmid DNA helped the biomass adapt and to have a higher yield under high antibiotic concentrations (> 50 mg L^{-1}).
- The plasmid DNA accumulated in the test chemostat even when its spiking was stopped for 8 days, by either uptake inside bacterial cells and/or adsorbed to the EPS.
- High kanamycin concentrations (50-100 mg L^{-1}) promoted the mobility of aminoglycoside resistance genes among bacterial hosts.
- Environmental antibiotic concentrations (2.5 mg L^{-1}) did not induce detectable transformation events, while lab-selection concentrations (50 mg L^{-1}) did.
- The main hosts containing the spiked synthetic plasmid pBAV1K-T5-GFP in the activated sludge were the Gram-negative bacteria *Bosea sp.* and *Runella sp.* (accompanied by *Gemmobacter sp.* and the well-known activated sludge floc former *Zoogloea sp.*), and the Gram-positive *Microbacterium sp.*.

The outcomes are important for not only the science but also the mitigation of the transfer of antibiotic resistance and foreign genetic elements emitted in wastewater catchment areas, especially in regions without wastewater treatment infrastructure or where industrial wastewater is not treated.

Data availability

Metagenome sequencing and amplicon sequencing data were deposited in the NCBI database with the BioProject ID: PRJNA868937.

6.6. Supplementary material

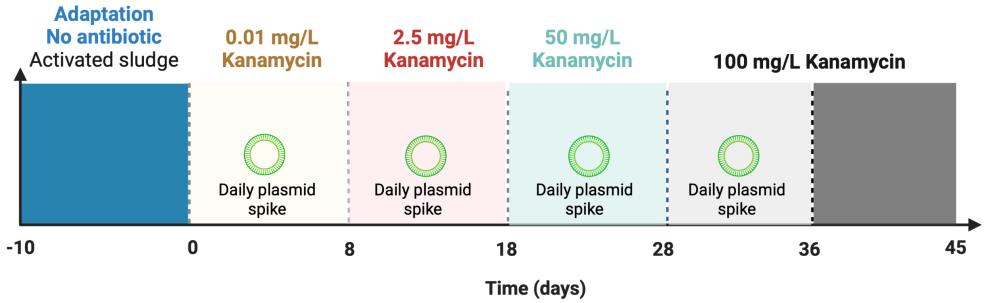

Figure S.1: Schematic representation of the operation over time in the test reactor. The control reactor was operated equally but without plasmid addition.

Table S.1: Recipe of influent complex synthetic wastewater receiving reactors test and control. The recipes provide C, N and P for the wastewater preparation. The recipe was prepared in 20-fold concentration to provide total COD and TN concentrations of 600 mg COD L^{-1} and 52 mg TN L^{-1}, respectively.

Component	Complex synthetic WW Concentration [g L^{-1}]
NaAcetate*3H_2O	4.3
NaPropionate	1.6
$(NH_4)Cl$	1.1
$CaCl_2$* H_2O	0.35
$MgSO_4$	0.33
KCl	0.66
Glucose	1.9
Starch	1.4
Peptone	1.6
Alanine	0.27
Arginine	0.26
Aspartic Acid	0.40
Glutamic Acid	0.29
Glycine	0.45
Leucine	0.16
Proline	0.19
K_2HPO_4	0.23
KH_2PO_4	0.23

Table S.2: Composition of trace element solution, after preparation pH is adapted to 6 using KOH (30% v/v).

Component	Formula	Concentration [g L^{-1}]
EDTA disodium salt dihydrate	$C_{10}H_{14}N_2Na_2O_8$ * $2H_2O$	16.22
Zinc II sulfate	$ZnSO_4$ * $7H_2O$	0.44
Manganese II Chloride	$MnCl_2$ * $6H_2O$	1.01
Ammonium Iron II	$(NH_4)_2Fe(SO_4)_2$* $6H_2O$	7.05
Ammonium Molybdate	$(NH_4)_6Mo_7O_{24}$* $4H_2O$	0.33
Copper II Sulfate	$CuSO_4$* $5H_2O$	0.31
Cobalt II Chloride	$CoCl_2$* $6H_2O$	0.32

Table S.3: *16S rRNA*, *GFP* and *KanR* synthetic DNA fragments used to generate standard curves for qPCR.

Gene	Sequence
16S rRNA	ACTCCTACGGGAGGCAGCAGTGGGGAATATTGCACAATGGGCGCAAGCCTGATGCAGCCATGCCGCGTGTATGAAG AAGGCCTTCGGGTTGTAAAGTACTTTCAGCGGGGAGGAAGGGAGTAAAGTTAATACCTTTGCTCATTGACGTTACCC GCAGAAGAAGCACCGGCTAACTCCGTGCCAGCAGCCGCGGTAAT
GFP	TTCAATGCTTTTCCCGTTATCCGGATCATATGAAACGGTATGACTTTTTCAAGAGTGCCATGCCCGAAGGTTATGTACA GGAACGCACTATATCTTTCAAAGATGACGGGAACTACAAGACG
KanR (aph(3')-IIIa)	CACTTACTTTGCCATCTTTCACAAAGATGTTGCTGTCTCCCAGGTCGCCGTGGGAAAAGACAAGTTCCTCTTCGGGCT TTTCCGTCTTTAAAAAATCATACAGCTCGCGCGGATCTTTAAATGGAGTGTCTTCTTCCCAGTTTTCGCAATCCACATC GGCCAGATCGTTATTCAGTAAGTAATCCAATTCGGCTAAGCG

Pure culture laboratory transformation

Transformation of *E. coli* K12 by electroporation

Electroporation was performed by preparing electrocompetent *E. coli* K12 cells by inoculating *E. coli* K12 in LB medium overnight at 37°C 180 rpm. 100 mL of fresh LB medium was prepared in 500 mL shake flask and the culture grown overnight was added to a final OD_{600} of 0.02 and further incubated at 37°C 200 rpm until it reached OD_{600} 0.5-1.0. Cells were collected at 2000 x g at 4C for 15 min. Cells were washed three times using 10% of the original culture volume with precooled filter sterile 10% glycerol. 50 µL of washed cells and 1 ng of pBAV1K-T5-gfp were transferred to prechilled Gene Pulser®/Micropulser™ electroporation cuvettes (Bio-Rad). After 2 min of incubation on ice, an electrical pulse of 12.5 kV cm^{-1} was added, resulting in a time constant of 4.3 to 4.5 ms. Immediately after the pulse delivery, 1 mL of prewarmed LB medium was added to cells. After incubation at 37°C for 45 min, the cells were plated on LB agar plates containing 50 µg mL^{-1} kanamycin for selection of transformed cells containing pBAV1K-T5-gfp overnight at 37°C.

Transformation of *B. subtilis* by starvation-induced competence

Transformation of *B. subtilis* str 168 was carried out following a published protocol [21]. Cultures of *B. subtilis* 168 were grown overnight at 37°C, 225 rpm. In a freshly prepared pre-warmed 15 mL SM1, 1 mL of the overnight culture was transferred and diluted to a final OD_{600} of 0.4-0.6 and incubated at 37°C 225 rpm for 5 hours.

Once the culture reached the stationary phase (OD_{600} of 2.0-2.8), equal volume of pre-warmed SM2 was added and incubated for 90 min at 37°C for 2h. 500 µL of cell culture was combined with 5 µL (100-500 ng) plasmid DNA and incubated for 30 min at 37°C at 180 rpm. 300 µL of LB was added and further incubated for 30 min at 37°C, 180 rpm. 100 µL of cells were plated onto LB agar plates containing 50 µg mL^{-1} of kanamycin and grown overnight at 37°C.

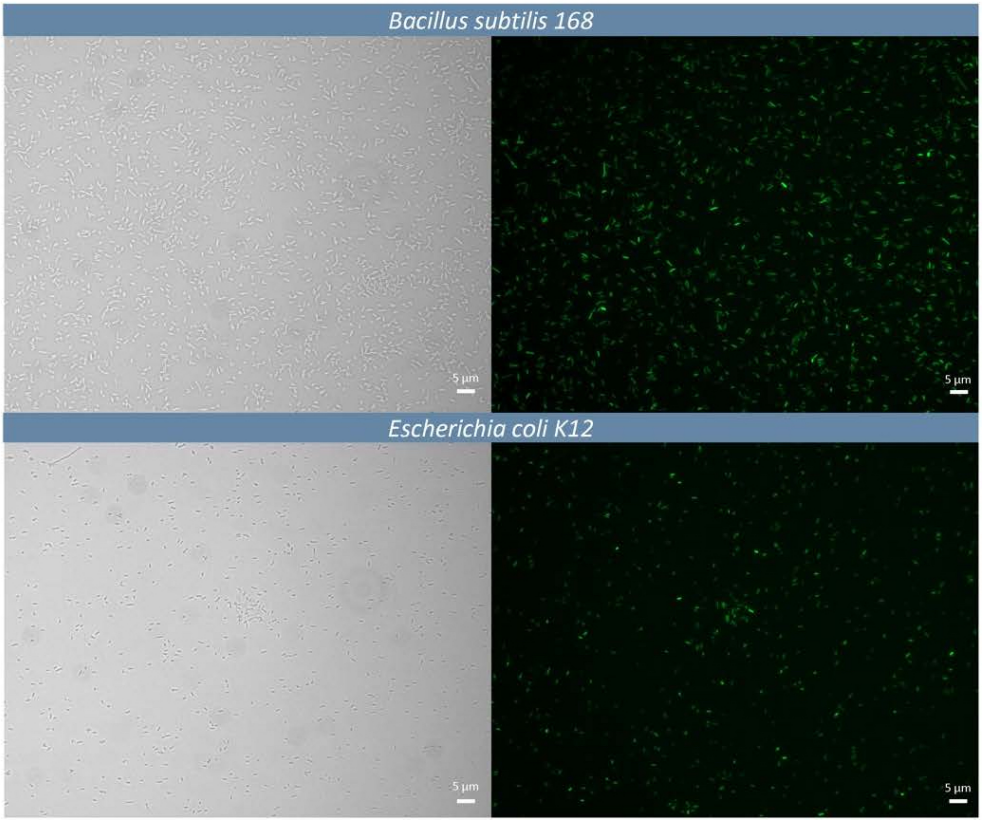

Figure S.2: Microscopic pictures of gram-positive *Bacillus subtilis* 168 (**upper panel**) and gram-negative *Escherichia coli* K12 (**bottom panel**) under bright field (**left figures**) and under fluorescent microscopy (**right figures**) as a consequence of GFP expression.

Chemostat operation parameters

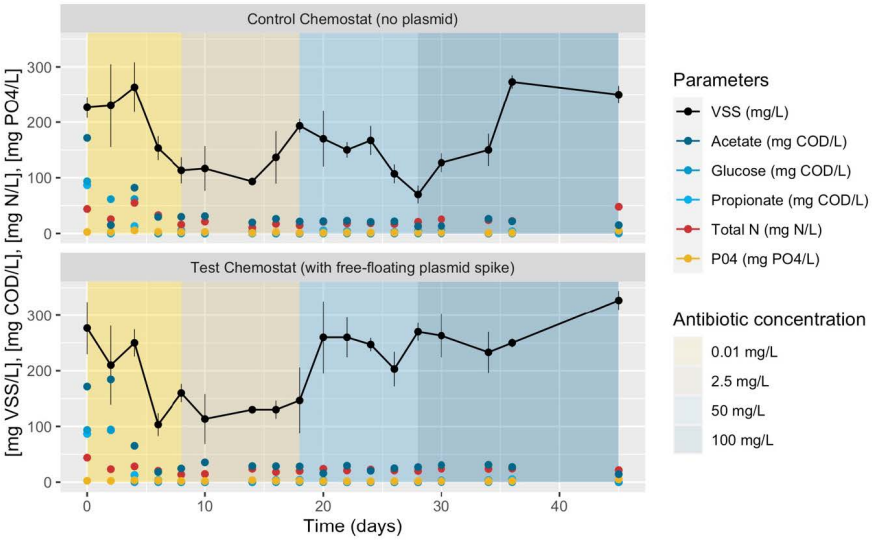

Figure S.3: Daily-averaged values for volatile suspended solids (VSS), volatile fatty acids (VFAs), glucose, total nitrogen and phosphate from both reactor control and reactor with free-floating plasmid over the whole operation time the experiment was conducted (45 days). Kanamycin concentrations are displayed as background-colored sections: 0.01 mg L^{-1}, 2.5 mg L^{-1}, 50 mg L^{-1}, 100 mg L^{-1}.

Aminoglycoside resistance genes alignment tree

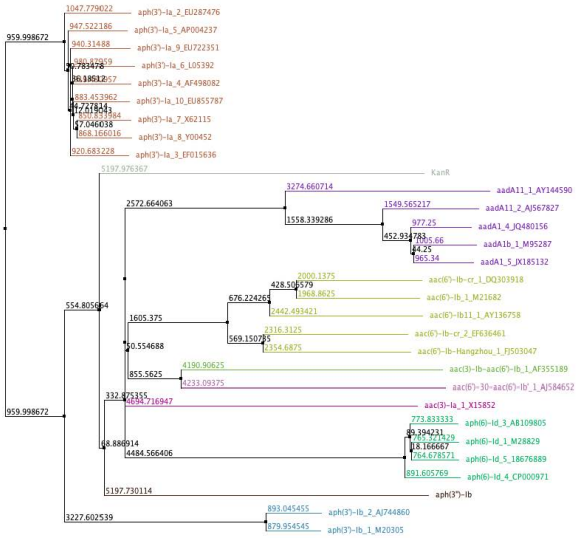

Figure S.4: Neighbor-joining tree, calculated from the input alignment, is being used to cluster sequences in the main alignment window. The input alignment consisted of the aminoglycoside resistance genes (and variants) found inside bacterial hosts in **Figure 6.7**.

6

Discordant read analyis of individual events

Discordant read analysis workflow

The first thing to identify discordantly mapped reads was to determine where the plasmid contigs were by BLASTn (e-value 1^{-20}, coverage 90%) using the genes from the pBAV1K-T5-GFP as query and the assembly as database. From the results, a list containing all the plasmid contigs is created that will be used afterwards. Then, we need to obtain a file from the sam file from aligning the Hi-C reads against the assembly, where paired-end reads are aligned in different contigs. For this end, awk was used to generate a bam file by extracting mate reads mapped on different contigs using the expression: $awk\,'(\$3! = \$7\ \&\&\ \$7 = \text{"}\ =\ \text{"})$.

```
awk '($3!=$7 && $7!="=")' hic_assembly.sam > hic_disc_map.sam
```

```
samtools view -S -h -b hic_disc_map.sam > hic_disc.bam
```

Then, we sort the result by name:

```
samtools sort -n hic_disc.bam > hic_disc_sort.bam
```

Then, we select the entries only containing discordant reads where the contigs containing the information of the plasmid are involved:

```
samtools view hic_disc_sort.bam |fgrep -w -f list_of_plasmid_contigs.txt >
    hic_disc_plasmid_contigs.txt
```

Where the list_of_plasmid_contigs.txt are the contigs coming as a result of the BLASTn contigs vs. plasmid nt database.

To extract the sequences from, for example the contigs 40904_length_1225 (corresponding to GFP):

```
grep "NODE_40904_length_1225_cov_3.529915" hic_disc_plasmid_contigs.txt|
    awk '{ print $3,$7,$10 }'
```

This will give us the results in three columns of which 2 nodes interact and the sequence. For example, to extract the reads where contigs aligned in GFP from the alignment:

```
grep "NODE_40904_length_1225_cov_3.529915\|NODE_147318_length_512_cov_3
    .949672" hic_disc_plasmid_contigs.bam| awk '{ print $3,$7,$10 }' >
    GFP_contigs_disc.txt
```

From this file, the NODES (or contigs) containing information from the other parts of the plasmid (not KanR nor GFP genes) were removed in order to avoid quantification of other plasmids that may share genetic information (*repA*, *rrnBT1* terminator and lambda_t0_terminator). Now, a list of contigs containing GFP interacting with multiple other contigs is generated. Then, duplicate contigs were removed in a different file and used to quantify how many times a specific event happened, from which a frequency table could be retrieved and plotted:

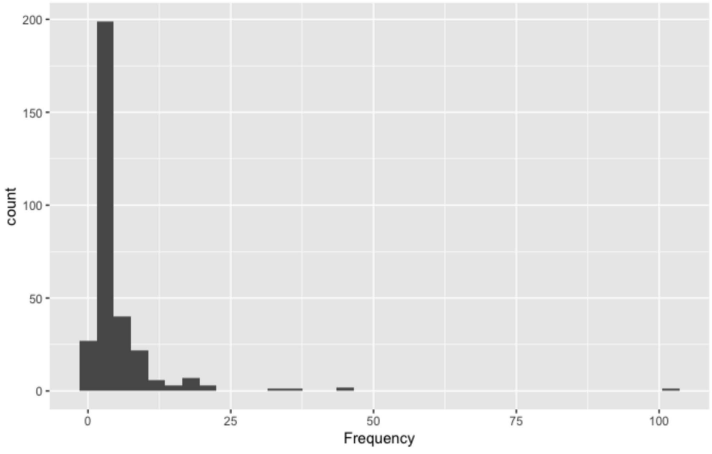

Figure S.5: Frequency graph showing the number of interactions between contigs from microbial clusters and contigs containing the GFP gene information.

We see there are plenty of contigs whose interactions with our reads are higher than 3 (the first column). Those contigs with high frequency (more than 40 interactions) were selected for the next steps.

To further verify that what we have found is correct, a visual analysis of the alignment regions was done. It could be that there are artefacts due to the PCR amplification of the libraries (Hi-C library) so in order to verify if the interactions observed come from real cross-link interaction plasmid-chromosome or if they come due to the PCR artifact, we will create concatenated files and re-align the Hi-C reads against these concatenated files prior visualization. Synthetic constructs consisting of the plasmid sequence, non-coding spacer DNA (1500 bp), and the contigs with higher Hi-C links with plasmid contigs were generated.

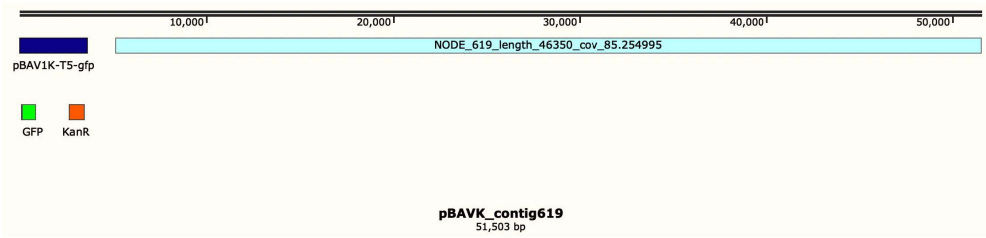

Figure S.6: Synthetic construct generated containing the sequence of the spiked pBAV1K-T5-GFP plasmid, spacer DNA and the NODE_619 for further visualizing the interactions

Synthetic constructs were aligned with Hi-C forward and reverse reads by bwa-mem v0.7.17-r1188 [37] generating a SAM file, that was converted into a BAM file and then sorted (-n) and indexed with samtools view v1.13 [40]. The resulted file was visualized in IGV.

Taxonomic tree

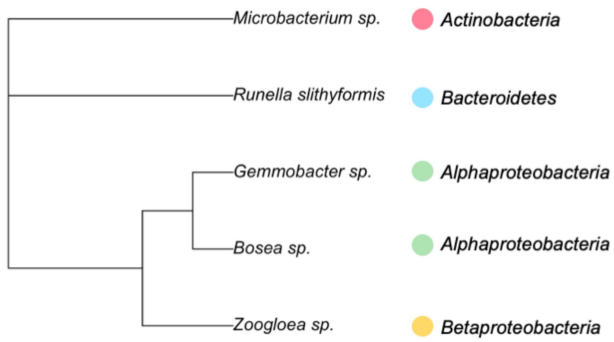

Figure S.7: Phylogenetic tree of the microorganisms that displayed Hi-C links between their genome clusters and plasmid contigs from the analysis of the discordant reads.

Discordant reads analysis visualization in IGV

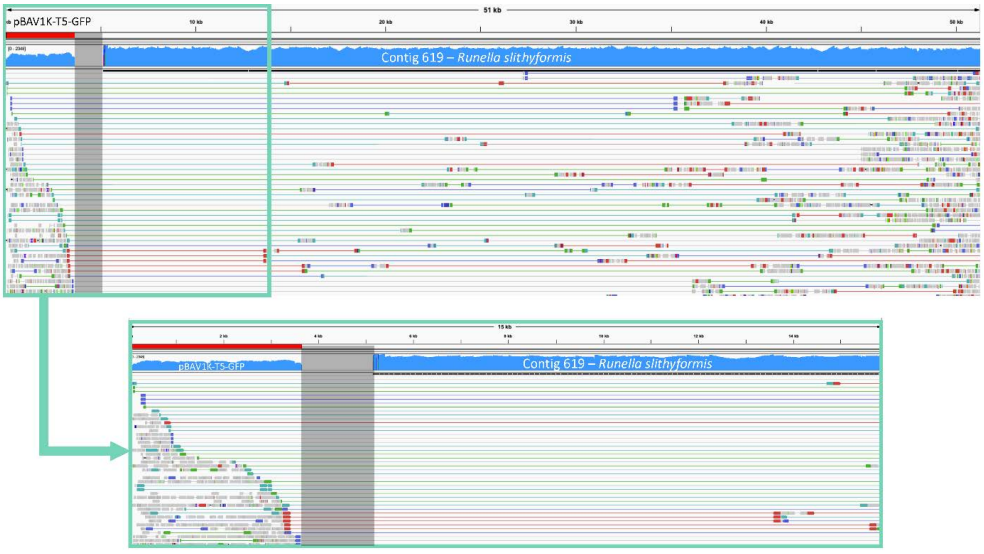

Figure S.8: Discordant read analysis of contig 619 belonging to the Runella slythiformis cluster with the plasmid pBAV1K-T5-GFP.

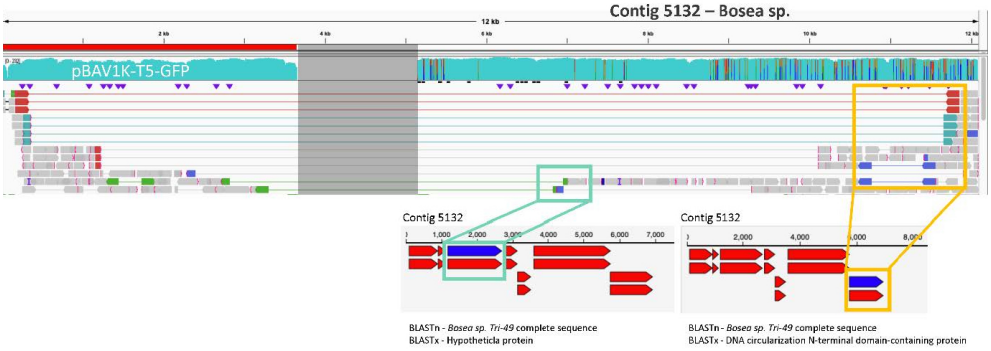

Figure S.9: Discordant read analysis of contig 5132 belonging to the *Bosea sp.* cluster with the plasmid pBAV1K-T5-GFP. Information of the coding genes where the interaction happened is provided.

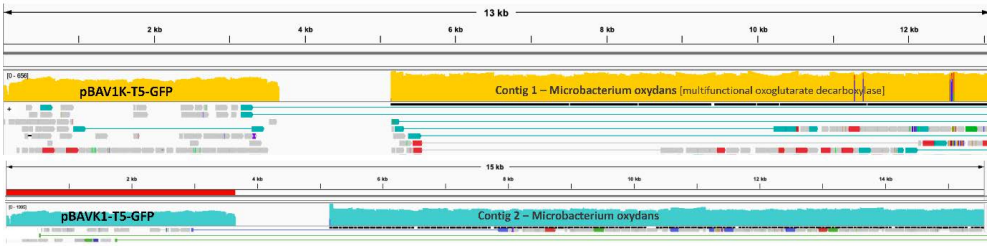

Figure S.10: Discordant read analysis of contig 1 and 2 belonging to the *Microbacterium oxydans* cluster with the plasmid pBAV1K-T5-GFP. Information of the coding genes where the interaction happened is provided.

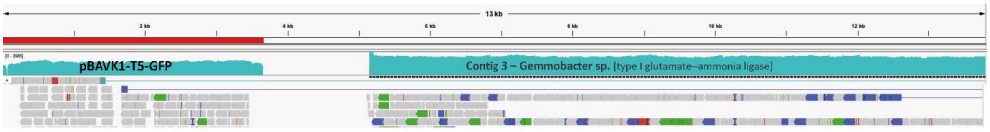

Figure S.11: Discordant read analysis of contig 1 and 2 belonging to the *Gemmobacter sp.* cluster with the plasmid pBAV1K-T5-GFP. Information of the coding genes where the interaction happened is provided.

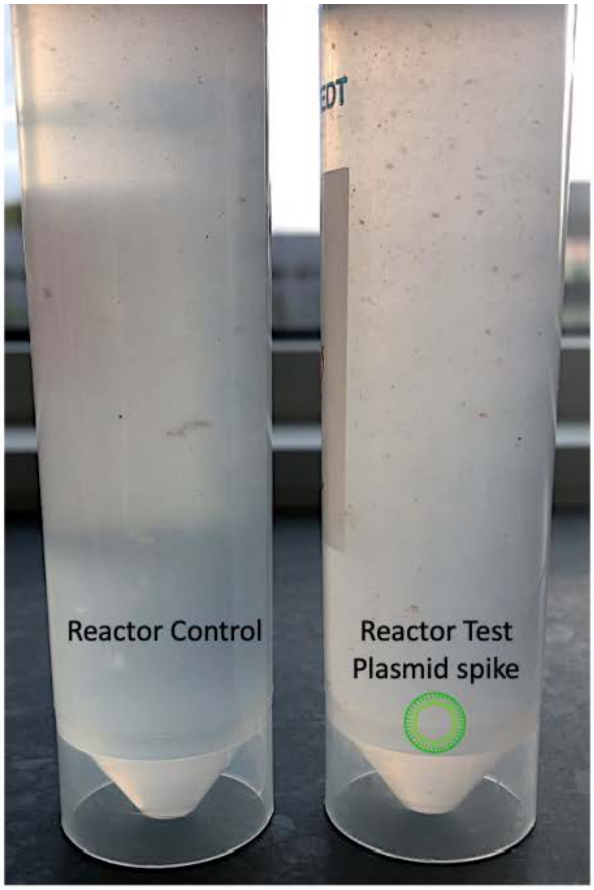

Figure S.12: Macroscopic morphological visualization of the microbial communities growing in the chemostats. Left tube: Reactor Control (no plasmid spike). Right tube: Reactor test (with free-floating extracellular plasmid addition).

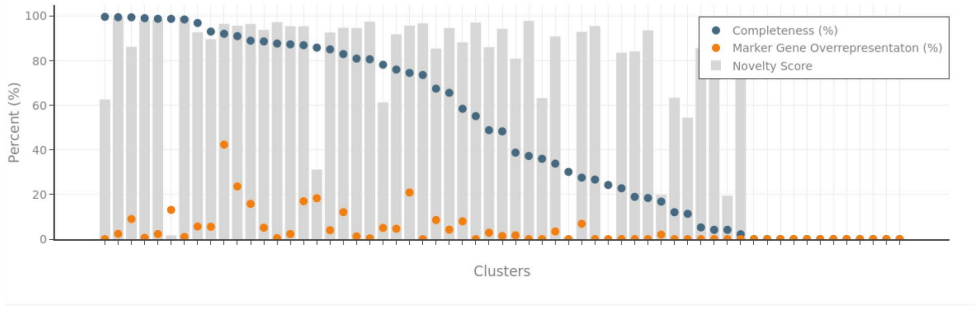

Novel Genome
>70% Complete, <10% MGO*
>90 Novelty Score

Known Genome
>70% Complete, <10% MGO*
<90 Novelty Score

*Marker Gene Overrepresentation

Cluster ID	Top Reference	Complete (%)	MGO (%)	Novelty Score	Abundance[1]	Contig N50	Genome Size	Num Contigs	GC (%)
bin_2	Runella_limosa_DSM_17973	99.70	0.00	62.65	2.90	43,996	7,771,803	199	44.61
bin_14	*p__Bacteroidetes (UID2605)*	99.52	2.38	99.20	7.73	127,206	5,093,898	75	40.45
bin_9	*f__Flavobacteriaceae (UID2817)*	99.49	9.02	86.29	11.36	238,082	5,949,895	109	33.43
bin_5	*o__Cytophagales (UID2937)*	99.09	0.61	98.00	0.92	128,085	6,862,534	91	37.23
bin_1	*o__Cytophagales (UID2936)*	98.81	2.28	98.39	2.05	29,937	8,548,977	603	43.21
bin_4	Hoeflea_sp._108	98.79	13.11	1.67	0.88	10,412	6,909,078	392	63.48
bin_17	*p__Bacteroidetes (UID2591)*	98.52	0.99	99.59	1.58	368,963	4,456,241	34	36.34
bin_12	*o__Burkholderiales (UID4000)*	96.93	5.68	92.78	0.41	182,538	5,347,012	119	67.61
bin_16	*f__Comamonadaceae (UID4119)*	93.08	5.55	89.68	0.16	22,757	4,511,481	137	64.80
bin_3	*f__Rhodocyclaceae (UID3972)*	92.10	42.38	96.57	9.60	3,531	7,267,562	1427	63.66
bin_7	*o__Burkholderiales (UID4000)*	91.03	23.64	95.68	12.81	6,168	6,667,466	1438	67.55
bin_11	*f__Rhodocyclaceae (UID3972)*	89.00	15.82	96.45	2.37	6,129	5,647,604	1053	65.59
bin_22	*o__Burkholderiales (UID4000)*	88.68	5.12	93.83	0.25	11,942	3,795,858	309	64.63
bin_37	*o__Flavobacteriales (UID2815)*	87.72	0.49	97.29	0.03	10,266	2,174,373	259	36.85
bin_27	*o__Actinomycetales (UID1593)*	87.36	2.30	95.50	0.01	55,877	3,100,479	40	67.96
bin_8	*f__Rhodocyclaceae (UID3972)*	86.97	17.01	95.48	4.33	1,391	6,133,532	1187	63.89
bin_15	Acidovorax_temperans	85.89	18.36	31.20	5.53	1,951	4,694,831	657	63.36
bin_29	*o__Actinomycetales (UID1572)*	85.10	4.00	92.69	0.03	144,780	3,060,212	76	64.47
bin_18	*c__Alphaproteobacteria (UID3422)*	82.99	12.12	94.80	0.76	65,826	4,403,640	544	68.90
bin_20	*o__Rhodospirillales (UID3754)*	80.97	1.24	94.68	0.15	4,803	4,029,922	560	69.58
bin_36	*o__Flavobacteriales (UID2815)*	80.66	0.32	97.54	0.02	19,980	2,315,328	66	32.07
bin_10	Acidovorax_sp._CF316	78.20	5.05	61.32	0.18	27,841	5,727,210	213	67.45
bin_35	*o__Actinomycetales (UID1572)*	76.05	4.68	91.85	0.02	53,286	2,459,558	67	64.65
bin_6	*k__Bacteria (UID203)*	74.55	20.92	95.78	9.64	2,732	6,778,553	1338	65.14
bin_23	*p__Bacteroidetes (UID2605)*	73.61	0.00	96.78	0.12	17,571	3,794,460	646	35.76
bin_19	*o__Rhizobiales (UID3642)*	67.49	8.58	85.46	0.05	5,127	4,314,977	640	66.26
bin_24	*c__Alphaproteobacteria (UID3422)*	65.63	4.25	94.63	0.55	7,012	3,727,892	568	68.36
bin_25	*o__Rhizobiales (UID3654)*	58.46	7.99	88.24	0.07	72,124	3,689,705	124	66.76
bin_28	*k__Bacteria (UID203)*	55.17	0.00	97.13	0.05	4,667	3,069,256	495	39.04
bin_26	*f__Flavobacteriaceae (UID2817)*	48.87	2.89	86.06	0.90	9,469	3,657,836	618	33.45
bin_31	*o__Burkholderiales (UID4000)*	48.34	1.40	94.33	0.07	2,589	2,753,277	714	69.15
bin_13	*k__Bacteria (UID203)*	38.79	1.72	80.92	1.06	5,488	5,142,251	869	33.51
bin_44	*k__Bacteria (UID203)*	37.30	0.00	97.87	0.07	10,942	1,151,601	199	39.81
bin_33	*k__Bacteria (UID203)*	36.03	0.00	63.24	0.07	9,348	2,540,106	344	54.37
bin_21	*k__Bacteria (UID203)*	33.86	3.45	90.88	4.68	1,627	4,000,668	1151	67.75
bin_42	Agrobacterium_tumefaciens_F2	30.17	0.00	0.78	0.02	7,644	1,545,968	252	59.37
bin_34	*k__Bacteria (UID203)*	27.59	6.90	92.95	0.04	61,622	2,473,330	77	66.60
bin_38	*k__Bacteria (UID203)*	26.72	0.00	95.58	0.08	7,031	1,970,861	421	64.98
bin_32	Raoultella_ornithinolytica_B6	24.29	0.00	0.00	0.04	9,283	2,545,647	431	57.44
bin_41	*k__Bacteria (UID203)*	22.81	0.00	83.58	0.01	48,002	1,602,368	38	70.29
bin_39	*k__Bacteria (UID203)*	18.97	0.00	84.17	1.41	2,363	1,967,573	577	66.71

Figure S.13: Microbial genomes (bins) recovered from the reactor test, day 18 (2.5 mg Kan L^{-1}) sorted by highest completeness and lowest contamination.

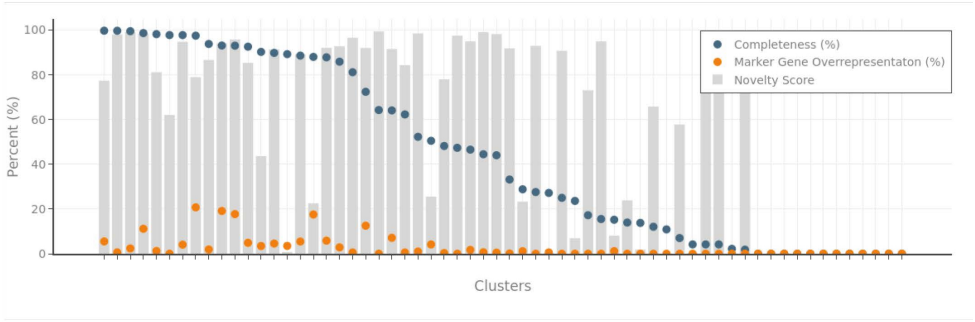

Cluster ID	Top Reference	Complete (%)	MGO (%)	Novelty Score	Abundance[1]	Contig N50	Genome Size	Num Contigs	GC (%)
bin_6	Agrobacterium_sp._ATCC_31749	99.72	5.51	77.36	3.65	144,799	6,284,760	116	59.46
bin_4	*o__Cytophagales (UID2937)*	99.70	0.61	98.01	22.25	310,079	6,944,486	87	37.27
bin_11	*p__Bacteroidetes (UID2605)*	99.52	2.38	99.20	13.27	385,339	5,084,495	76	40.44
bin_1	*o__Cytophagales (UID2936)*	98.66	11.16	98.39	9.62	12,286	10,272,115	1527	43.18
bin_20	Brevundimonas_diminuta_ATCC_11568	98.19	1.24	81.13	0.19	33,846	3,168,438	176	67.61
bin_2	Runella_limosa_DSM_17973	97.77	0.00	62.04	6.48	43,693	7,678,854	323	44.64
bin_8	*o__Rhodospirillales (UID3754)*	97.76	4.06	94.79	1.92	67,605	5,789,486	130	69.73
bin_5	Acidovorax_sp._KKS102	97.50	20.75	78.93	3.49	32,713	6,353,331	227	65.51
bin_12	*f__Flavobacteriaceae (UID2817)*	93.80	1.92	86.65	0.11	20,925	5,073,278	492	33.15
bin_10	*k__Bacteria (UID203)*	93.10	19.12	94.12	2.35	21,288	5,325,121	216	66.80
bin_7	*f__Rhodocyclaceae (UID3972)*	93.02	17.72	95.77	5.86	59,265	6,024,086	253	65.30
bin_22	*o__Actinomycetales (UID1593)*	92.58	4.89	85.33	0.10	81,706	3,048,264	48	70.93
bin_3	Achromobacter_xylosoxidans_A8	90.25	3.46	43.63	0.15	19,788	7,028,286	214	65.84
bin_14	*o__Rhizobiales (UID3642)*	89.80	4.56	91.38	0.15	73,964	4,611,394	108	66.68
bin_9	Hoeflea_sp._108	89.25	3.51	0.63	0.47	66,187	5,599,793	205	63.58
bin_18	*o__Actinomycetales (UID1593)*	88.59	5.47	89.18	0.17	20,534	3,930,038	173	70.12
bin_17	Microbacterium_sp._UCD_TDU	88.01	17.55	22.49	4.41	50,905	3,961,613	50	68.23
bin_24	*o__Actinomycetales (UID1572)*	87.82	5.85	92.05	0.20	101,799	2,899,507	111	64.58
bin_13	*o__Rhizobiales (UID3642)*	85.87	2.85	92.75	0.15	11,783	4,852,037	644	67.13
bin_15	*f__Rhodobacteraceae (UID3340)*	81.16	0.58	96.59	0.60	350,886	4,273,269	83	65.18
bin_19	*k__Bacteria (UID203)*	72.41	12.54	91.97	10.19	159,490	3,400,595	53	65.88
bin_38	*k__Bacteria (UID1453)*	64.25	0.00	99.38	0.53	521,336	979,873	5	48.37
bin_16	*o__Rhizobiales (UID3654)*	64.09	7.13	91.54	1.16	4,308	4,261,460	347	66.29
bin_27	*f__Comamonadaceae (UID4119)*	62.29	0.57	84.32	0.02	26,312	2,319,992	128	66.38
bin_30	*p__Bacteroidetes (UID2591)*	52.29	0.99	98.48	0.18	7,480	2,041,725	390	47.95
bin_25	Ensifer_sp._ZNC0028	50.50	4.15	25.54	0.06	4,514	2,764,972	623	62.84
bin_21	*o__Rhizobiales (UID3642)*	48.18	0.32	78.01	0.16	4,779	3,106,073	296	66.16
bin_31	*k__Bacteria (UID203)*	47.37	0.00	97.49	0.01	140,777	1,804,229	33	60.76
bin_34	*k__Bacteria (UID203)*	46.55	1.72	94.94	2.43	552,907	1,611,961	5	66.23
bin_41	*k__Bacteria (UID3060)*	44.48	0.67	99.10	0.10	2,235	851,433	247	44.19
bin_23	*p__Bacteroidetes (UID2591)*	44.04	0.50	98.20	0.49	5,992	2,992,407	471	40.71
bin_35	*o__Rhizobiales (UID3654)*	33.18	0.10	91.82	0.04	14,209	1,308,997	113	66.62
bin_26	Acidovorax_temperans	28.82	1.14	23.29	0.33	3,148	2,653,104	404	61.89
bin_32	*k__Bacteria (UID203)*	27.59	0.00	92.95	0.03	6,447	1,779,459	445	68.93
bin_40	Leucobacter_sp._PH1c	27.19	0.58	0.09	0.00	69,766	918,698	17	71.51
bin_29	*k__Bacteria (UID203)*	25.00	0.00	90.74	0.65	17,448	2,207,530	151	66.10
bin_28	Kaistia_adipata_DSM_17808	23.62	0.00	6.93	0.06	20,687	2,256,027	144	67.20
bin_46	*k__Bacteria (UID203)*	17.24	0.00	73.08	0.01	9,466	461,638	42	66.85
bin_47	*k__Bacteria (UID203)*	15.52	0.00	94.94	0.28	230,294	439,700	2	65.23
bin_44	*o__Actinomycetales (UID1572)*	15.20	1.17	8.06	0.87	223,544	730,995	3	68.06
bin_33	*k__Bacteria (UID203)*	13.95	0.00	23.86	0.02	13,908	1,657,430	244	66.22

Figure S.14: Microbial genomes (bins) recovered from the reactor test, day 28 (50 mg Kan L^{-1}) sorted by highest completeness and lowest contamination.

Bibliography

[1] J. O'Neill. "Antimicrobial Resistance : Tackling a crisis for the health and wealth of nations." In: December (2014).

[2] J. Moralez, K. Szenkiel, K. Hamilton, A. Pruden, and A. J. Lopatkin. "Quantitative analysis of horizontal gene transfer in complex systems". In: *Current Opinion in Microbiology* 62 (2021), pp. 103–109. ISSN: 18790364. DOI: 10.1016/j.mib.2021.05.001. URL: https://doi.org/10.1016/j.mib.2021.05.001.

[3] D. Calderón-Franco, M. van Loosdrecht, T. Abeel, and D. Weissbrodt. "Free-floating extracellular DNA: Systematic profiling of mobile genetic elements and antibiotic resistance from wastewater". In: *Water Research* 189.116592 (2021), pp. 1–13. DOI: 10.1101/2020.05.01.072397.

[4] D. Calderón-Franco, R. Sarelse, S. Christou, M. Pronk, M. C. M. van Loosdrecht, T. Abeel, and D. G. Weissbrodt. "Metagenomic profiling and transfer dynamics of antibiotic resistance determinants in a full-scale granular sludge wastewater treatment plant". In: *Water Research* (2022). DOI: 10.1016/j.watres.2022.118571.

[5] K. Ikuma and C. R. Rehmann. "Importance of extracellular DNA in the fate and transport of antibiotic resistance genes downstream of a wastewater treatment plant". In: *Environmental Engineering Science* 37.2 (2020), pp. 164–168. ISSN: 15579018. DOI: 10.1089/ees.2019.0319.

[6] E. A. Lin, X. S. Zhang, S. M. Levine, S. R. Gill, D. Falush, and M. J. Blaser. "Natural transformation of helicobacter pylori involves the integration of short DNA fragments interrupted by gaps of variable size". In: *PLoS Pathogens* 5.3 (2009), pp. 1–11. ISSN: 15537366. DOI: 10.1371/journal.ppat.1000337.

[7] J. C. Mell and R. J. Redfield. "Natural competence and the evolution of DNA uptake specificity". In: *Journal of Bacteriology* 196.8 (2014), pp. 1471–1483. ISSN: 10985530. DOI: 10.1128/JB.01293-13.

[8] G. Pietramellara, J. Ascher, F. Borgogni, M. T. Ceccherini, G. Guerri, and P. Nannipieri. "Extracellular DNA in soil and sediment: Fate and ecological relevance". In: *Biology and Fertility of Soils* 45.3 (2009), pp. 219–235. ISSN: 01782762. DOI: 10.1007/s00374-008-0345-8.

[9] L. S. Håvarstein. "Bacterial gene transfer by natural genetic transformation". In: *APMIS, Supplement* 106.84 (1998), pp. 43–46. ISSN: 0903465X. DOI: 10.1111/j.1600-0463.1998.tb05647.x.

[10] M. G. Lorenz and W. Wackernagel. *Bacterial gene transfer by natural genetic transformation in the environment.* Tech. rep. 3. 1994, pp. 563–602. URL: https://www.ncbi.nlm.nih.gov/pmc/articles/PMC372978/pdf/microrev00022-0281.pdf.

[11] R. Pallares-Vega, G. Macedo, M. S. Brouwer, L. Hernandez Leal, P. van der Maas, M. C. van Loosdrecht, D. G. Weissbrodt, D. Heederik, D. Mevius, and H. Schmitt. "Temperature and Nutrient Limitations Decrease Transfer of Conjugative IncP-1 Plasmid pKJK5 to Wild Escherichia coli Strains". In: *Frontiers in Microbiology* 12.July (2021). ISSN: 1664302X. DOI: 10.3389/fmicb.2021.656250.

[12] D. Pérez-Mendoza and F. de la Cruz. "Escherichia coli genes affecting recipient ability in plasmid conjugation: Are there any?" In: *BMC Genomics* 10 (2009), pp. 1–14. ISSN: 14712164. DOI: 10.1186/1471-2164-10-71.

[13] A. J. Lopatkin, S. Huang, R. P. Smith, J. K. Srimani, T. A. Sysoeva, S. Bewick, D. K. Karig, and L. You. "Antibiotics as a selective driver for conjugation dynamics". In: *Nature Microbiology* 1.6 (2016), pp. 1–8. ISSN: 20585276. DOI: 10.1038/nmicrobiol.2016.44. URL: http://dx.doi.org/10.1038/nmicrobiol.2016.44.

[14] R. M. Cooper, L. Tsimring, and J. Hasty. "Inter-species population dynamics enhance microbial horizontal gene transfer and spread of antibiotic resistance". In: *eLife* 6.Cdc (2017), pp. 1–26. ISSN: 2050084X. DOI: 10.7554/eLife.25950.

[15] A. Domenech, A. R. Brochado, V. Sender, K. Hentrich, B. Henriques-Normark, A. Typas, and J. W. Veening. "Proton Motive Force Disruptors Block Bacterial Competence and Horizontal Gene Transfer". In: *Cell Host and Microbe* 27.4 (2020), pp. 544–555. ISSN: 19346069. DOI: 10.1016/j.chom.2020.02.002. URL: https://doi.org/10.1016/j.chom.2020.02.002.

[16] L. Nordgård, T. Nguyen, T. Midtvedt, Y. Benno, T. Traavik, and K. M. Nielsen. "Lack of detectable DNA uptake by bacterial gut isolates grown in vitro and by Acinetobacter baylyi colonizing rodents in vivo". In: *Environmental Biosafety Research* 6.1-2 (2007), pp. 149–160. ISSN: 16357922. DOI: 10.1051/ebr:2007029.

[17] T. Stalder, M. O. Press, S. Sullivan, I. Liachko, and E. M. Top. "Linking the resistome and plasmidome to the microbiome". In: *ISME Journal* (2019), pp. 2437–2446. ISSN: 17517370. DOI: 10.1038/s41396-019-0446-4. URL: http://dx.doi.org/10.1038/s41396-019-0446-4.

[18] A. V. Bryksin and I. Matsumura. "Rational design of a plasmid origin that replicates efficiently in both gram-positive and gram-negative bacteria". In: *PLoS ONE* 5.10 (2010). ISSN: 19326203. DOI: 10.1371/journal.pone.0013244.

[19] M. Layer, A. Adler, E. Reynaert, A. Hernandez, M. Pagni, E. Morgenroth, C. Holliger, and N. Derlon. "Organic substrate diffusibility governs microbial community composition, nutrient removal performance and kinetics of granulation of aerobic granular sludge". In: *Water Research X* 4 (2019), p. 100033. ISSN: 25899147. DOI: 10.1016/j.wroa.2019.100033. URL: https://doi.org/10.1016/j.wroa.2019.100033.

[20] A.P.H.A. *Standard methods for the examination of water and wastewater: 21st ed. A*. 21st ed. Vol. 37. 05. Washington, DC, 2005, pp. 37–2792. DOI: 10.5860/choice.37-2792.

[21] P. R. Bennallack, S. R. Burt, M. J. Heder, R. A. Robison, and J. S. Griffitts. "Characterization of a novel plasmid-borne thiopeptide gene cluster in Staphylococcus epidermidis strain 115". In: *Journal of Bacteriology* 196.24 (2014), pp. 4344–4350. ISSN: 10985530. DOI: 10.1128/JB.02243-14.

[22] J. G. Caporaso, J. Kuczynski, J. Stombaugh, K. Bittinger, F. D. Bushman, E. K. Costello, N. Fierer, A. G. Peña, J. K. Goodrich, J. I. Gordon, G. A. Huttley, S. T. Kelley, D. Knights, J. E. Koenig, R. E. Ley, C. A. Lozupone, D. Mcdonald, B. D. Muegge, M. Pirrung, J. Reeder, J. R. Sevinsky, P. J. Turnbaugh, W. A. Walters, J. Widmann, T. Yatsunenko, J. Zaneveld, and R. Knight. "correspondence QIIME allows analysis of high- throughput community sequencing data Intensity normalization improves color calling in SOLiD sequencing". In: *Nature Publishing Group* 7.5 (2010), pp. 335–336. ISSN: 15487091. DOI: 10.1038/nmeth0510-335. URL: http://dx.doi.org/10.1038/nmeth0510-335.

[23] R. C. Edgar, B. J. Haas, J. C. Clemente, C. Quince, and R. Knight. "UCHIME improves sensitivity and speed of chimera detection". In: *Bioinformatics* 27.16 (2011), pp. 2194–2200. ISSN: 14602059. DOI: 10.1093/bioinformatics/btr381.

[24] R. C. Edgar. "UPARSE: Highly accurate OTU sequences from microbial amplicon reads". In: *Nature Methods* 10.10 (2013), pp. 996–998. ISSN: 15487091. DOI: 10.1038/nmeth.2604.

[25] C. Quast, E. Pruesse, P. Yilmaz, J. Gerken, T. Schweer, P. Yarza, J. Peplies, and F. O. Glöckner. "The SILVA ribosomal RNA gene database project: Improved data processing and web-based tools". In: *Nucleic Acids Research* 41.D1 (2013), pp. 590–596. ISSN: 03051048. DOI: 10.1093/nar/gks1219.

[26] K. Andersen, R. Kirkegaard, S. Karst, and M. Albertsen. "ampvis2: An R package to analyse and visualise 16S rRNA amplicon data". In: *bioRxiv* (2018), pp. 10–11. DOI: 10.1101/299537.

[27] D. E. Wood, J. Lu, and B. Langmead. "Improved metagenomic analysis with Kraken 2". In: *Genome Biology* (2019), pp. 1–13. ISSN: 1474-7596. DOI: 10.1101/762302.

[28] M. Nierychlo, K. S. Andersen, Y. Xu, N. Green, C. Jiang, M. Albertsen, M. S. Dueholm, and P. H. Nielsen. "MiDAS 3: An ecosystem-specific reference database, taxonomy and knowledge platform for activated sludge and anaerobic digesters reveals species-level microbiome composition of activated sludge". In: *Water Research* 182 (2020). ISSN: 18792448. DOI: 10.1016/j.watres.2020.115955.

[29] S. Dabdoub. *kraken-biom: Enabling interoperative format conversion for Kraken results (Version 1.2) [Software]*. 2016. URL: https://github.com/smdabdoub/kraken-biom.

[30] S. Xu, Z. Li, W. Tang, Z. Dai, L. Zhou, T. Feng, M. Chen, S. Liu, X. Fu, T. Wu, E. Hu, and G. Yu. "MicrobiotaProcess: A comprehensive R package for managing and analyzing microbiome and other ecological data within the tidy framework". In: *Research Square* (2022). URL: https://doi.org/10.21203/rs.3.rs-1284357/v1.

[31] J. N. Burton, I. Liachko, M. J. Dunham, and J. Shendure. "Species-level deconvolution of metagenome assemblies with Hi-C-based contact probability maps". In: *G3: Genes, Genomes, Genetics* 4.7 (2014), pp. 1339–1346. ISSN: 21601836. DOI: 10.1534/g3.114.011825.

[32] E. Lieberman-Aiden, N. L. Van Berkum, L. Williams, M. Imakaev, T. Ragoczy, A. Telling, I. Amit, B. R. Lajoie, P. J. Sabo, M. O. Dorschner, R. Sandstrom, B. Bernstein, M. A. Bender, M. Groudine, A. Gnirke, J. Stamatoyannopoulos, L. A. Mirny, E. S. Lander, and J. Dekker. "Comprehensive mapping of long-range interactions reveals folding principles of the human genome". In: *Science* 326.5950 (2009), pp. 289–293. ISSN: 00368075. DOI: 10.1126/science.1181369.

[33] S. Andrews. *FastQC: a quality control tool for high throughput sequence data.* 2010. URL: http://www.bioinformatics.babraham.ac.uk/projects/fastqc.

[34] S. Chen, Y. Zhou, Y. Chen, and J. Gu. "Fastp: An ultra-fast all-in-one FASTQ preprocessor". In: *Bioinformatics* 34.17 (2018), pp. i884–i890. ISSN: 14602059. DOI: 10.1093/bioinformatics/bty560.

[35] D. Li, C. M. Liu, R. Luo, K. Sadakane, and T. W. Lam. "MEGAHIT: An ultra-fast single-node solution for large and complex metagenomics assembly via succinct de Bruijn graph". In: *Bioinformatics* 31.10 (2015), pp. 1674–1676. ISSN: 14602059. DOI: 10.1093/bioinformatics/btv033.

[36] S. Nurk, D. Meleshko, A. Korobeynikov, and P. A. Pevzner. "MetaSPAdes: A new versatile metagenomic assembler". In: *Genome Research* 27.5 (2017), pp. 824–834. ISSN: 15495469. DOI: 10.1101/gr.213959.116.

[37] H. Li. "Aligning sequence reads, clone sequences and assembly contigs with BWA-MEM". In: 00.00 (2013), pp. 1–3. URL: http://arxiv.org/abs/1303.3997.

[38] M. Z. Demaere and A. E. Darling. "Bin3C: Exploiting Hi-C sequencing data to accurately resolve metagenome-assembled genomes". In: *Genome Biology* 20.1 (2019), pp. 1–16. ISSN: 1474760X. DOI: 10.1186/s13059-019-1643-1.

[39] G. G. Faust and I. M. Hall. "SAMBLASTER: Fast duplicate marking and structural variant read extraction". In: *Bioinformatics* 30.17 (2014), pp. 2503–2505. ISSN: 14602059. DOI: 10.1093/bioinformatics/btu314.

[40] H. Li, B. Handsaker, A. Wysoker, T. Fennell, J. Ruan, N. Homer, G. Marth, G. Abecasis, and R. Durbin. "The Sequence Alignment/Map format and SAMtools". In: *Bioinformatics* 25.16 (2009), pp. 2078–2079. ISSN: 13674803. DOI: 10.1093/bioinformatics/btp352.

[41] M. O. Press, A. H. Wiser, Z. N. Kronenberg, K. W. Langford, M. Shakya, C.-c. Lo, K. A. Mueller, S. T. Sullivan, P. S. G. Chain, and I. Liachko. "Hi-C deconvolution of a human gut microbiome yields high-quality draft genomes and reveals plasmid-genome interactions." In: *bioRxiv* (2017), p. 198713. DOI: 10.1101/198713. URL: https://www.biorxiv.org/content/early/2017/10/05/198713.full.pdf+html.

[42] R. D. Stewart, M. D. Auffret, A. Warr, A. H. Wiser, M. O. Press, K. W. Langford, I. Liachko, T. J. Snelling, R. J. Dewhurst, A. W. Walker, R. Roehe, and M. Watson. "Assembly of 913 microbial genomes from metagenomic sequencing of the cow rumen". In: *Nature Communications* 9.1 (2018), pp. 1–11. ISSN: 20411723. DOI: 10.1038/s41467-018-03317-6. URL: http://dx.doi.org/10.1038/s41467-018-03317-6.

[43] D. H. Parks, M. Imelfort, C. T. Skennerton, P. Hugenholtz, and G. W. Tyson. "CheckM: Assessing the quality of microbial genomes recovered from isolates, single cells, and metagenomes". In: *Genome Research* 25.7 (2015), pp. 1043–1055. ISSN: 15495469. DOI: 10.1101/gr.186072.114.

[44] B. D. Ondov, T. J. Treangen, P. Melsted, A. B. Mallonee, N. H. Bergman, S. Koren, and A. M. Phillippy. "Mash: Fast genome and metagenome distance estimation using MinHash". In: *Genome Biology* 17.1 (2016), pp. 1–14. ISSN: 1474760X. DOI: 10.1186/s13059-016-0997-x. URL: http://dx.doi.org/10.1186/s13059-016-0997-x.

[45] M. Feldgarden, V. Brover, N. Gonzalez-Escalona, J. G. Frye, J. Haendiges, D. H. Haft, M. Hoffmann, J. B. Pettengill, A. B. Prasad, G. E. Tillman, G. H. Tyson, and W. Klimke.

"AMRFinderPlus and the Reference Gene Catalog facilitate examination of the genomic links among antimicrobial resistance, stress response, and virulence". In: *Scientific Reports* 11.1 (2021), pp. 1–9. ISSN: 20452322. DOI: 10.1038/s41598-021-91456-0. URL: https://doi.org/10.1038/s41598-021-91456-0.

[46] A. Oladeinde, Z. Abdo, B. Zwirzitz, R. Woyda, S. M. Lakin, M. O. Press, N. A. Cox, J. C. Thomas IV, T. Looft, M. J. Rothrock, G. Zock, J. P. Lawrence, D. Cudnik, C. Ritz, S. E. Aggrey, I. Liachko, J. R. Grove, and C. Wiersma. "Litter Commensal Bacteria Can Limit the Horizontal Gene Transfer of Antimicrobial Resistance to Salmonella in Chickens". In: *Applied and Environmental Microbiology* 88.9 (2022). ISSN: 10985336. DOI: 10.1128/aem.02517-21.

[47] G. Yu. "Using ggtree to Visualize Data on Tree-Like Structures". In: *Current Protocols in Bioinformatics* 69.1 (2020), pp. 1–18. ISSN: 1934340X. DOI: 10.1002/cpbi.96.

[48] T. Das, S. Sehar, and M. Manefield. "The roles of extracellular DNA in the structural integrity of extracellular polymeric substance and bacterial biofilm development". In: *Environmental Microbiology Reports* 5.6 (2013), pp. 778–786. ISSN: 17582229. DOI: 10.1111/1758-2229.12085.

[49] PhaseGenomics. "Capture a complete picture of complex microbial communities , including the moving parts". In: (2020).

[50] K. M. M. Pärnänen, C. Narciso-da-Rocha, D. Kneis, T. U. Berendonk, D. Cacace, T. T. Do, C. Elpers, D. Fatta-Kassinos, I. Henriques, T. Jaeger, A. Karkman, J. L. Martinez, S. G. Michael, I. Michael-Kordatou, K. O'Sullivan, S. Rodriguez-Mozaz, T. Schwartz, H. Sheng, H. Sørum, R. D. Stedtfeld, J. M. Tiedje, S. V. D. Giustina, F. Walsh, I. Vaz-Moreira, M. Virta, and C. M. Manaia. "Antibiotic resistance in European wastewater treatment plants mirrors the pattern of clinical antibiotic resistance prevalence". In: *Science Advances* 5.3 (Mar. 2019), eaau9124. ISSN: 2375-2548. DOI: 10.1126/sciadv.aau9124.

[51] K. Yoo, H. Yoo, J. Lee, E. J. Choi, and J. Park. "Exploring the antibiotic resistome in activated sludge and anaerobic digestion sludge in an urban wastewater treatment plant via metagenomic analysis". In: *Journal of Microbiology* 58.2 (2020), pp. 123–130. ISSN: 19763794. DOI: 10.1007/s12275-020-9309-y.

[52] M. Petrovich, B. Chu, D. Wright, J. Griffin, M. Elfeki, B. T. Murphy, R. Poretsky, and G. Wells. "Antibiotic resistance genes show enhanced mobilization through suspended growth and biofilm-based wastewater treatment processes". In: *FEMS Microbiology Ecology* 94.5 (2018), pp. 1–11. ISSN: 15746941. DOI: 10.1093/femsec/fiy041.

[53] M. Daly, L. Villa, C. Pezzella, S. Fanning, and A. Carattoli. "Comparison of multidrug resistance gene regions between two geographically unrelated Salmonella serotypes". In: *Journal of Antimicrobial Chemotherapy* 55.4 (2005), pp. 558–561. ISSN: 03057453. DOI: 10.1093/jac/dki015.

[54] L. Gordon, A. Cloeckaert, B. Doublet, S. Schwarz, A. Bouju-albert, J. P. Ganière, H. Le bris, A. Le flèche-matéos, and E. Giraud. "Complete sequence of the floR-carrying multiresistance plasmid pAB5S9 from freshwater Aeromonas bestiarum". In: *Journal of Antimicrobial Chemotherapy* 62.1 (2008), pp. 65–71. ISSN: 03057453. DOI: 10.1093/jac/dkn166.

[55] M. S. Ramirez and M. E. Tolmasky. "Aminoglycoside modifying enzymes". In: *Drug Resistance Updates* 13.6 (2010), pp. 151–171. ISSN: 13687646. DOI: 10.1016/j.drup.2010.08.003. URL: http://dx.doi.org/10.1016/j.drup.2010.08.003.

[56] L. Tang, A. Schramm, T. R. Neu, N. P. Revsbech, and R. L. Meyer. "Extracellular DNA in adhesion and biofilm formation of four environmental isolates: A quantitative study". In: *FEMS Microbiology Ecology* 86.3 (2013), pp. 394–403. ISSN: 01686496. DOI: 10.1111/1574-6941.12168.

[57] G. Corno, M. Coci, M. Giardina, S. Plechuk, F. Campanile, and S. Stefani. "Antibiotics promote aggregation within aquatic bacterial communities". In: *Frontiers in Microbiology* 5.JULY (2014), pp. 1–9. ISSN: 1664302X. DOI: 10.3389/fmicb.2014.00297.

[58] T. Das, S. Sehar, L. Koop, Y. K. Wong, S. Ahmed, K. S. Siddiqui, and M. Manefield. "Influence of calcium in extracellular DNA mediated bacterial aggregation and biofilm formation". In: *PLoS ONE* 9.3 (2014), pp. 1–11. ISSN: 19326203. DOI: 10.1371/journal.pone.0091935.

[59] J. Slager, M. Kjos, L. Attaiech, and J. W. Veening. "Antibiotic-induced replication stress triggers bacterial competence by increasing gene dosage near the origin". In: *Cell* 157.2

(2014), pp. 395–406. ISSN: 10974172. DOI: 10.1016/j.cell.2014.01.068. URL: http://dx.doi.org/10.1016/j.cell.2014.01.068.

[60] M. Prudhomme, L. Attaiech, G. Sanchez, B. Martin, and J.-P. Claverys. "Antibiotic Stress Induces Genetic Transformability in the Human Pathogen Streptococcus pneumoniae". In: *Science* 313.5783 (2006), pp. 89–92. ISSN: 02787407. DOI: 10.1029/2002tc001374.

[61] X. Charpentier, E. Kay, D. Schneider, and H. A. Shuman. "Antibiotics and UV radiation induce competence for natural transformation in Legionella pneumophila". In: *Journal of Bacteriology* 193.5 (2011), pp. 1114–1121. ISSN: 00219193. DOI: 10.1128/JB.01146-10. URL: https://www.ncbi.nlm.nih.gov/pmc/articles/PMC3067580/pdf/1146-10.pdf.

[62] K. E. Stevens, D. Chang, E. E. Zwack, and M. E. Sebert. "Competence in streptococcus pneumoniae is regulated by the rate of ribosomal decoding errors". In: *mBio* 2.5 (2011). ISSN: 21507511. DOI: 10.1128/mBio.00071-11.

[63] B. Jubeh, Z. Breijyeh, and R. Karaman. "Resistance of gram-positive bacteria to current antibacterial agents and overcoming approaches". In: *Molecules* 25.12 (2020). ISSN: 14203049. DOI: 10.3390/molecules25122888.

[64] M. J. Bottery. "Ecological dynamics of plasmid transfer and persistence in microbial communities". In: *Current Opinion in Microbiology* 68 (2022), p. 102152. ISSN: 18790364. DOI: 10.1016/j.mib.2022.102152. URL: https://doi.org/10.1016/j.mib.2022.102152.

[65] H. Gumpert, J. Z. Kubicek-Sutherland, A. Porse, N. Karami, C. Munck, M. Linkevicius, I. Adlerberth, A. E. Wold, D. I. Andersson, and M. O. Sommer. "Transfer and persistence of a multi-drug resistance plasmid in situ of the infant gut microbiota in the absence of antibiotic treatment". In: *Frontiers in Microbiology* 8.SEP (2017), pp. 1–10. ISSN: 1664302X. DOI: 10.3389/fmicb.2017.01852.

[66] S. J. Spencer, M. V. Tamminen, S. P. Preheim, M. T. Guo, A. W. Briggs, I. L. Brito, D. A Weitz, L. K. Pitkänen, F. Vigneault, M. P. Virta, and E. J. Alm. "Massively parallel sequencing of single cells by epicPCR links functional genes with phylogenetic markers". In: *ISME Journal* 10.2 (2016). ISSN: 17517370. DOI: 10.1038/ismej.2015.124.

[67] J. Hultman, M. Tamminen, K. Pärnänen, J. Cairns, A. Karkman, and M. Virta. "Host range of antibiotic resistance genes in wastewater treatment plant influent and effluent". In: *FEMS microbiology ecology* 94.4 (2018). ISSN: 15746941. DOI: 10.1093/femsec/fiy038.

[68] J. Florenza, M. Tamminen, and S. Bertilsson. "Uncovering microbial inter-domain interactions in complex communities". In: *Philosophical Transactions of the Royal Society B: Biological Sciences* 374.1786 (2019). ISSN: 14712970. DOI: 10.1098/rstb.2019.0087.

[69] J. Ruiz-Masó, C. Machón, L. Bordanaba-Ruiseco, M. Espinosa, M. Coll, and G. Del Solar. "Plasmid Rolling-Circle Replication". In: *American Society for Microbiology Press* (2015), pp. 1–23. DOI: 10.1128/microbiolspec.PLAS-0035-2014.f1.

[70] C. Johnston, B. Martin, G. Fichant, P. Polard, and J. P. Claverys. "Bacterial transformation: Distribution, shared mechanisms and divergent control". In: *Nature Reviews Microbiology* 12.3 (2014), pp. 181–196. ISSN: 17401526. DOI: 10.1038/nrmicro3199.

[71] S. E. Luria and M. L. Human. "A nonhereditary, host-induced variation of bacterial viruses." In: *Journal of bacteriology* 64.4 (1952), pp. 557–569. ISSN: 00219193. DOI: 10.1128/jb.64.4.557-569.1952.

[72] G. Bertani and J. J. Weigle. "Host controlled variation in bacterial viruses." In: *Journal of bacteriology* 65.2 (1953), pp. 113–121. ISSN: 00219193. DOI: 10.1128/jb.65.2.113-121.1953.

[73] D. Sun. "Two different routes for double-stranded DNA transfer in natural and artificial transformation of Escherichia coli". In: *Biochemical and Biophysical Research Communications* 471.1 (2016), pp. 213–218. ISSN: 10902104. DOI: 10.1016/j.bbrc.2016.01.137. URL: http://dx.doi.org/10.1016/j.bbrc.2016.01.137.

[74] S. Kunhikannan, C. J. Thomas, A. E. Franks, S. Mahadevaiah, S. Kumar, and S. Petrovski. "Environmental hotspots for antibiotic resistance genes". In: *MicrobiologyOpen* 10.3 (2021), pp. 1–11. ISSN: 20458827. DOI: 10.1002/mbo3.1197.

[75] J. B. Alderliesten, S. J. Duxbury, M. P. Zwart, J. A. G. De Visser, A. Stegeman, and E. A. Fischer. "Effect of donor-recipient relatedness on the plasmid conjugation frequency: A meta-analysis". In: *BMC Microbiology* 20.1 (2020), pp. 1–10. ISSN: 14712180. DOI: 10.1186/s12866-020-01825-4.

[76] D. G. Larsson and C. F. Flach. “Antibiotic resistance in the environment”. In: *Nature Reviews Microbiology* 20.5 (2022), pp. 257–269. ISSN: 17401534. DOI: 10.1038/s41579-021-00649-x.

7

Upgrading residues from WWTP and DWTP as adsorbents to remove extracellular DNA and ARB from treated effluents

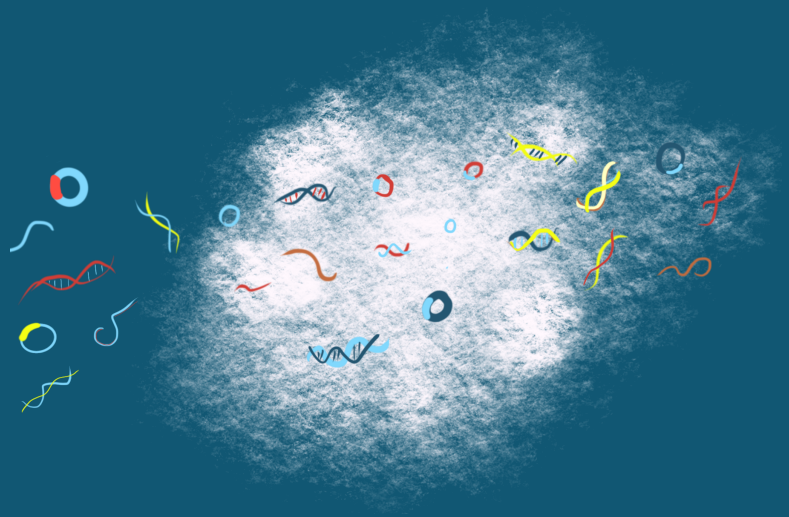

This chapter has been published as: Calderón-Franco, D., Seeram, A., Medema, G., van Loosdrecht, M., Weissbrodt, D., 2021. Upgrading residues from wastewater and drinking water treatment plants as low-cost adsorbents to remove extracellular DNA and microorganisms carrying antibiotic resistance genes from treated effluents. Science of The Total Environment. 778, 1–14. https://doi.org/10.1016/j.scitotenv.2021.146364

ABSTRACT

Wastewater treatment is challenged by the continuous emergence of chemical and biological contaminants. Disinfection, advanced oxidation, and activated carbon technologies are accessible in high-income countries to suppress them. Low-cost, easily implementable, and scalable solutions are needed for sanitation across regions. We studied the properties of low-cost absorbents recycled from drinking water and wastewater treatment plant residues to remove environmental DNA and xenogenetic elements from used water. Materials characteristics and DNA adsorption properties of used iron-oxide-coated sands and of sewage-sludge biochar obtained by pyrolysis of surplus activated sludge were examined in bench-scale batch and up-flow column systems. Adsorption profiles followed Freundlich isotherms, suggesting a multilayer adsorption of nucleic acids on these materials. Sewage-sludge biochar exhibited high DNA adsorption capacity (1 mg g^1) and long saturation breakthrough times compared to iron-oxide-coated sand (0.2 mg g1). Selected antibiotic resistance genes and mobile genetic elements present on the free-floating extracellular DNA fraction and on the total environmental DNA (i.e., both extra/intracellular) were removed at 85% and 97% by sewage-sludge biochar and at 54% and 66% by iron-oxide-coated sand, respectively. Sewage-sludge biochar is attractive as low-cost adsorbent to minimize the spread of antimicrobial resistances to the aquatic environment while strengthening the role of sewage treatment plants as resource recovery factories.

Keywords: *Xenogenetic elements; Sewage-sludge biochar; Iron-oxide-coated sand; Adsorption; Wastewater; Free-floating extracellular DNA*

7.1. Introduction

According to the UNICEF [1], about 785 million people do not have access to potable water world-wide. Population growth and expanded living standards severely affect water resources availability [2]. New and alternate solutions to provide clean water are needed, such as wastewater reuse. The main problem with reclaiming wastewater is the final effluent quality. Sustainable Development Goals (SDG 6.3) targets high water quality by reducing the use of hazardous materials and increasing the proportion of treated water, thus stimulating recycling and safe reuse.

Wastewater treatment plants (WWTPs) are central to recycle used water to aquatic ecosystems. Located at the end of the sewer pipe, they face the full cocktail of pollutants emitted in the catchment area. WWTPs have been designed step-wise to remove pathogens, solids, organic matter, and nutrients like phosphorus and nitrogen. They are not designed to treat a number of persistent xenobiotic compounds, which are often discharged with the effluent [3]. Only a few countries have adopted water quality criteria to legislate the emissions and removal of micropollutants from wastewater, and their ecological impacts [4, 5]. Both chemical and biological contaminants continuously emerge and rise concerns. New technical measures need to be developed to suppress xenobiotic compounds and xenogenetic elements.

Because of the microbial diversity of activated sludge, WWTPs are often hypothesized as hotspots for the horizontal gene transfer and proliferation of antimicrobial resistance (AMR) [6, 7]. Rather than WWTPs per se, the whole set of emission sources in a catchment area needs to be considered at the root of AMR. The continuous release of antibiotics and other chemical and biological pollutants like heavy metals, antibiotic resistant bacteria (ARB), and antibiotic resistance genes (ARGs) in wastewater generates a selective pressure for AMR development and propagation in engineered and natural aquatic ecosystems. AMRs threaten the environmental, animal and human health, by the generation and spread of antibiotic-resistant pathogens across water bodies, soil, and food chain [8, 9]. The overuse and misuse of antibiotics affect the medical effectiveness in combating pathogenic organisms [10, 11].

In contrast to chemicals, AMRs are biological pollutants that replicate [12]. ARB are generated by horizontal transfer of ARGs and mobile genetic elements (MGEs) by and between microorganisms [13]. MGEs form the main component (65%) of extracellular DNA (exDNA) fragments that free-float in wastewater [14, 15]. Stress conditions and complex microbial communities may enhance the transformation of microorganisms by these xenogenetic elements [16, 17].

A recent study of a set of six representative ARGs across more than 60 Dutch WWTPs has highlighted that WWTPs do not amplify the release of these intracellular ARGs [18]. ARGs and MGEs, such as the class I Integron-integrase gene (*intI1*), have been reduced on average of a 1.76 log unit from influents to effluents. However, 106 ARG copies are still present per liter of WWTP effluent.

In a rough estimate, this corresponds to ca. $3–6 \cdot 10^{14}$ ARG copies emitted per day or $1–2 \cdot 10^{17}$ ARG copies emitted per year discharged in the outlet of large WWTPs of 1–4 million person-equivalents. The ARG content in the free-floating extracellular DNA fraction still remains unchecked and overlooked. Quantitative questions arise from water authorities on what level of ARGs can lead to a significant risk for environmental and human health. ARGs persist in river and lakes some kilometers away from the effluent discharge point [19]. While the exposure of environmental, animal and human bodies to ARB and ARGs released from WWTP catchment areas into receiving waters has still to be addressed in order to address the risk, solutions to abate their loads are needed according to precautionary and/or prevention principles.

Tertiary treatments like effluent disinfection using UV or chlorination do not suppress the release of ARGs in the environment: these genes can still be detected in disinfected effluents [20]. Disinfection can inactivate or select for ARB [21–23], while the genes can remain and can be released as free-floating exDNA by cell lysis. Most studies on the fate of AMRs [24] did not consider exDNA. The concentrations of free-floating exDNA measured from different wastewater samples (influent, activated sludge, and effluent) ranged between 2.6 and 12.5 µg L^1 [15]. This exDNA fraction can persist several months or even years in marine and soil matrices [25, 26]. It can attach to suspended particles, sand, clay and humic acids (HAs). However, sorption of exDNA on natural particles does not prevent its mobility and ability to transform into natural competent bacteria [27].

Different advanced technologies can remove ARB and ARGs from wastewater effluents. Process principles can go from solid-liquid separation in membrane bioreactors [28, 29] to coagulation [30, 31], disinfection and advanced oxidation via chlorination, ozonation, UV or UV-activated persulfate [32, 33], besides algal-based wastewater treatment systems [34] among others. The aforementioned physical-chemical methods however employ non-renewable materials or require consistent variations on the WWTP operation processes. These technological designs are mostly accessible in high-income countries. Simple, low-cost, implementable, and scalable solutions are needed for delivering safe sanitation world-wide according to local contexts.

In the water circular economy, upgrading resources recovered from the water cycle [35] can be an efficient solution to remove AMR determinants. Sewage-sludge biochar produced by pyrolysis of surplus activated sludge is an interesting recycled resource for soil amendment to immobilize heavy metals (Cd, Cu, Ni, Pb or As) and prevent environmental risk of such chemicals [36]. Besides implementation of biochar soil, manure and solid waste management, implementation of sewage-sludge biochar for wastewater treatment is limited [37]. Biochar from different sources has lately been studied for DNA and exDNA adsorption under different settings [38–41]. For instance, Fang et al. [38] used local wood chip, wheat straw and peanut shell for biochar production to study adsorption and degradation by nucleases of extracellular DNA. Similar approach was followed by Fu et al. [39], who used maize straw to produce magnetic biochar to remove

extracellular antibiotic resistance genes in aquatic environments. Zhou et al. [41] and Ngigi et al. [40] have proven that the addition of biochar from chicken manure and mushroom residues or pig manure does mitigate the accumulation and spread of ARGs during composting and storage.

Iron-oxide-coated sand are used to remove metals (As, Ni, and Zn) in drinking water treatment plants (WTP). Nucleic acids harbor phosphate-based polyanionic sites that can bind to iron or other multivalent cations. Therefore, DNA may exhibit ionic interactions with positively-charged materials like iron-oxide-coated sand [42, 43].

In a sanitation and circular economy approach, we studied the upgrading of by-products of wastewater and drinking WTPs as low-cost adsorbents to remove environmental and free-floating exDNA. Sewage-sludge biochar prepared by pyrolysis of dewatered sewage sludge and used iron-oxide-coated sands were reclaimed for their adsorption characteristics and capacity to remove ARGs and MGEs as well as ARB from secondary wastewater effluents. We characterized the adsorbents by X-ray fluorescence spectrophotometry, Mössbauer spectroscopy, and scanning electron microscopy. We measured the DNA adsorption isotherms of the adsorbents and breakthrough curves of both free-floating exDNA and total environmental DNA (i.e., microorganisms and exDNA) from batch to up-flow fixed-bed column systems. Our results help delineate the potential of these cheap recycled materials to prevent the release of ARB, ARGs and MGEs in WWTP effluents into aquatic ecosystems.

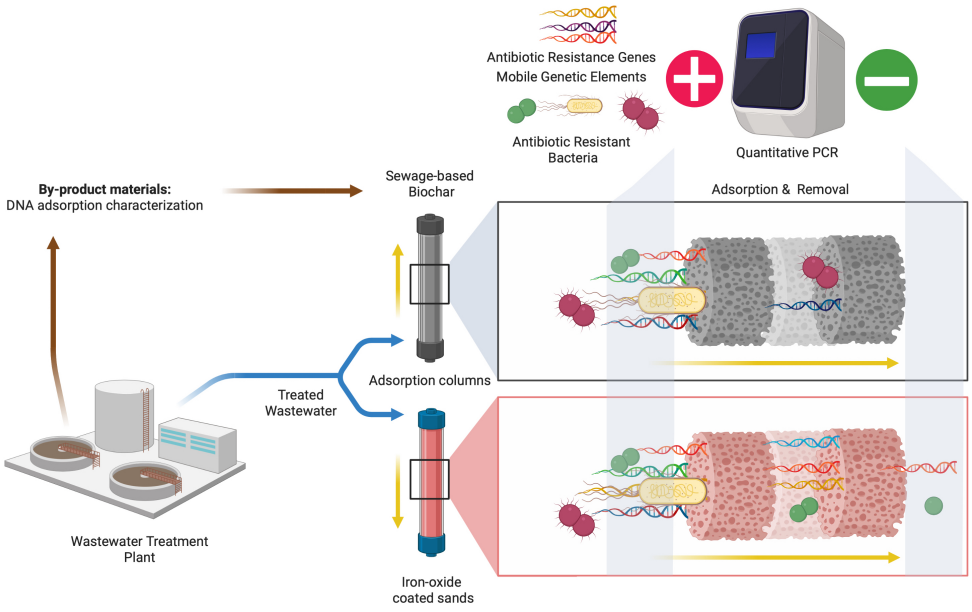

Figure 7.1: Graphical abstract

7.2. Material & Methods

Preparation of sewage-sludge biochar by pyrolysis of dewatered activated sludge and collection of iron-oxide-coated sand

Dewatered sewage sludge was collected from the urban WWTP Harnaschpolder (Waterboard Delfland, The Netherlands) to produce sewage-sludge biochar. The dewatered sewage sludge samples were brought to the lab within 1 h and stored at 4°C pending analyses and pyrolysis. Before pyrolysis, the sewage sludge was characterized by moisture content and volatile matter. The moisture content was performed at 11 ± 1°C and volatile matter at 500 ± 50°C until constant weight was achieved. Sewage-sludge biochar was produced following Agrafioti et al. [36]. Dewatered sludge was heated in a muffle furnace at 600°C under a controlled flow of nitrogen. The temperature increase rate was kept at 17°C min^{-1}. The samples were kept for 30 min residence time. Oxygen-free conditions were maintained by supplying nitrogen at a rate of 200 mL min^{-1}. The cooled samples were then crushed and sieved at 150 µm pore size. Biochar generation by pyrolysis was done in triplicates at one selected temperature (600°C). The methodology for analyzing the properties of the raw material used for the production of biochar was followed according to Agrafioti et al. [36]. The sewage-sludge biochar production yield was determined as the ratio of the produced dry mass of sewage-sludge biochar (after pyrolysis) to the dry mass of sewage-sludge (before pyrolysis). The sewage-sludge biochar was stored at room temperature pending experiments.

An amount of 2 kg of used iron-oxide-coated sand (1–4 mm) was reclaimed from the sand-filtration unit of AquaMinerals B.V., a water sanitation company giving a second life to the resources from drinking WTPs in The Netherlands. Iron-oxide-coated sands received were crushed and sieved at 600 µm, and stored at room temperature for further experiments.

Other sorbents were tested as comparison basis, namely powdered activated carbon (PAC), granular activated carbon (GAC), and mineral wool.

Sampling of effluent water from WWTP

Effluent water was collected from WWTP Harnaschpolder operated for full biological nutrient removal. Effluent water was collected at the outlet of its tertiary treatment. Sample triplicates were collected on three different days. A volume of 1 L of treated water was collected per replicate. All samples were processed in a timeframe of less than 4 h after collection.

Physical-chemical analyses of the adsorbents

Chemical compositions of the adsorbents

The inorganic chemical composition of sewage-sludge biochar was characterized using an Axios Max wavelength dispersive X-ray fluorescence (WD-XRF)

spectrophotometer (Malvern-Panalytical, The Netherlands). The data was evaluated with SuperQ5.0i/Omnian software. Carbon (C), oxygen (O) and nitrogen (N) could not be measured by WD-XRF spectrophotometry. The elemental composition of carbon (C), oxygen (O), hydrogen (H), nitrogen (N) and sulphur (S) from sewage-sludge biochar and of iron (Fe) and silica (Si) from iron-oxide-coated sand were analyzed by elemental analysis (Mikrolab Kolbe, Germany).

Surface area and pore size of the adsorbents

The surface area and pore size of the adsorbents were calculated using a nitrogen gas adsorption analyser (Micrometrics Gemini VII 2390 Surface area analyser, USA). Before analysis, 5 g of the by-product materials were previously degassed under vacuum at 150°C (under N2 flow) during 1 h to eliminate moisture and gasses. A mass of 0.5 g of the by-product materials was introduced in the test tube with liquid nitrogen. N2 isotherms were measured at -196°C. Surface area was calculated according to the Brunauer-Emmett-Teller (BET) method [44], which incorporates a multilayer coverage. The Barret-Joyner-Halenda (BJH) method was used to determine the pore size using Kelvin equation of pore filling, where a cylindrical pore geometry was assumed [45].

Valence state of iron-oxide-coated sands

The valence state of iron (Fe) in iron-oxide-coated sand was determined by Mössbauer Spectroscopy to retrieve its oxidation state. Mössbauer spectra were recorded at 300 K with a conventional constant-acceleration spectrometer, and at 4.2 K (liquid helium cryostat) with a sinusoidal velocity spectrometer, using a ^{57}Co (Rh) source. A velocity calibration curve was performed using an α-Fe foil at room temperature.

Surface observation of adsorbents by scanning electron microscopy

The surface observation of sewage-sludge biochar and iron-oxide-coated sand was analyzed using a scanning electron microscope (SEM; model JSM-6010LA, Jeol Ltd., Japan) at magnifications of 5'000-10'000× and acceleration voltages of 5–15 keV.

DNA standard solutions and chemicals used for adsorption experiments

Solutions of UltraPure™ Salmon sperm DNA (Thermo Fisher Scientific, USA) were used as standards for free-floating exDNA in order to characterize DNA adsorption phenomena in batch and column regimes, before testing the removal of total environmental DNA from WWTP effluent. Salmon sperm DNA is double stranded, and sheared to an average size of 2000 bp. The purity of DNA was

assessed by UV light absorbance at 260 and 280 nm (A260/280 > 1.8) (BioTek, Gen5 plate reader, USA).

The chemicals and other reagents were obtained from Sigma Aldrich (USA). In order to assess the effect of different ions and humic acids on DNA adsorption, stock solutions of 1 mol L^{-1} of salts (NaCl, $CaCl_2$ $2H_2O$, $MgCl_2$ $6H_2O$) and 800 mg L^{-1} of humic acids (CAS No. 1415-93-6) were prepared in ultrapure water (Sigma Aldrich, UK).

DNA adsorption in batches

Preliminary screening of adsorbents

The adsorption efficacies of sewage-sludge biochar and iron-oxide-coated sand were compared to those of powdered activated carbon (PAC), granular activated carbon (GAC), and mineral wool as reference materials. Adsorption efficacies were preliminarily tested in triplicate experiments conducted in 2-mL sterile Eppendorf tubes with 40 mg of tested adsorbent material and 1 mL of working solutions of salmon sperm DNA at initial concentrations of 0, 20, 40, 60, 80, 100, 120 and 140 µg DNA mL^1 in either ultrapure water, tap water, and filtered (0.2 µm) WWTP effluent water. The Eppendorf tubes were mixed continuously at 180 rpm on an orbital shaker at 25°C until equilibrium. The mixture was then centrifuged at 13000 × g for 20 min prior to measuring the DNA concentration from the supernatant (BioTek, Gen5 plate reader, USA).

DNA adsorption equilibria of sewage-based biochar and iron-oxide-coated sand

To find the equilibrium time required for DNA adsorption onto sewage-based biochar and iron-oxide-coated sand, batch experiments were conducted in apothecary glass bottles of 25 mL, with a working solution of 5 mL of salmon sperm DNA at an initial concentrations of 100 µg DNA mL^{-1} in ultrapure water, tap water, and filtered effluent water. The mass of sewage-sludge biochar or iron-oxide-coated sand adsorbents was added in increasing amounts from 0 to 100 mg adsorbent mL^{-1} in separate bottles. Each experiment was performed in triplicates. The bottles were agitated continuously at 180 rpm on an orbital shaker at 25°C for 24 h. Liquid volumes of 0.5 mL were sampled every 1 h from the batches and centrifuged at 13000 × g for 20 min.

Effect of pH, ionic strength and humic acids content on DNA adsorption

To evaluate the influence of pH on DNA adsorption, experiments were run at pH 5, 7 and 9 in 10 mmol L^{-1} Tris-HCl buffer with initial DNA concentrations of 20 and 100 µg DNA mL^{-1}. The interaction effects of cation species on DNA adsorption was studied at initial DNA concentration of 100 µg DNA mL^{-1} in the presence of 0–60 mmol L^{-1} Na^+ (as NaCl), Mg^{2+} (as $MgCl_2$), and Ca^{2+} (as $CaCl_2$) at pH

7. Competition with organic matter on DNA adsorption was investigated at pH 7 in the presence of humic acids (HAs) at 0–100 mg HAs L^{-1} to represent natural organic matter. In all experiments, pH was maintained constant in Tris-HCl buffer.

Quantifying the DNA adsorbed on sewage-sludge biochar and iron-oxide-coated sand

The residual DNA concentration in the supernatants was measured in 96-well UV flat-bottom plates (Greiner UV Star 96, Germany) by UV spectrophotometry at 260 nm (BioTek, Gen5 plate reader, USA). The DNA concentration after incubation with HAs was measured with Qubit® dsDNA assays (Thermo Fisher Scientific, USA) [46]. The amount of DNA adsorbed onto the adsorbent at equilibrium was calculated using Eq. 7.1.

$$\text{DNA adsorbed}\left(\frac{\mu gDNA}{mgAdsorbent}\right) = \frac{[DNA]_0\left(\frac{\mu g}{mLwater}\right) - [DNA]_{final}\left(\frac{\mu g}{mLwater}\right)}{Adsorbent(mg)} \cdot Volume(mL) \quad (7.1)$$

Modelling DNA adsorption isotherms and efficiency

Both Langmuir and Freundlich isotherm models were applied to describe the DNA adsorption from the solution onto the adsorbents.

The Langmuir isotherm model (Eq. 7.2) describes the adsorption of adsorbate molecules (DNA in this case) by assuming behavior as an ideal gas under isothermal conditions. Adsorption is supposed to happen onto homogeneous solid surfaces that exhibit one adsorption site.

$$q_e = \frac{q_{max} K_L C_e}{1 + K_L C_e} \quad (7.2)$$

where qe (mg adsorbate g^{-1} adsorbent) is the amount of adsorbate adsorbed, C_e (mg adsorbate L^{-1}) is the equilibrium adsorbate concentration, qmax (mg adsorbate g^{-1} adsorbent) is the maximum monolayer adsorption capacity, and K_L (L mg^{-1} adsorbate) is the Langmuir empirical constant related to the heat of adsorption. K_L represents the adsorption affinity of the adsorbate onto the adsorbent.

The Freundlich isotherm model (Eq. 7.3) is an empirical relation between the concentration of a solute on the surface of an adsorbent (by-products) and the concentration of the solute in the liquid at its interface. The Langmuir model assumes only a monomolecular layer on the surface at maximum coverage (i.e., no stacking of adsorbed molecules). The Freundlich isotherm does not account for this restriction.

$$q_e = K_L C_e^{\frac{1}{n}} \quad (7.3)$$

where q_e (mg adsorbate g^{-1} adsorbent) is the amount of solute adsorbed, Ce (mg adsorbate L^{-1}) is the equilibrium adsorbate concentration, K_F (mg adsorbate g^1 adsorbent) is the Freundlich constant related to the adsorption capacity, and n (-) is the heterogeneity factor and adsorption favorability.

DNA adsorption in up-flow packed-bed column

Characteristics of the columns packed with sewage-sludge biochar and iron-oxide-coated sand

Continuous up-flow adsorption experiments were conducted in chromatography glass columns (1 cm inner diameter and 15 cm column). An amount of 0.5 g of glass beads (250–300 µm) was inserted at the bottom of the column for a homogeneous flow distribution through the column. The columns were packed with known quantities of adsorbents: 3 g of sewage-sludge biochar and 4 g of iron-oxide-coated sand.

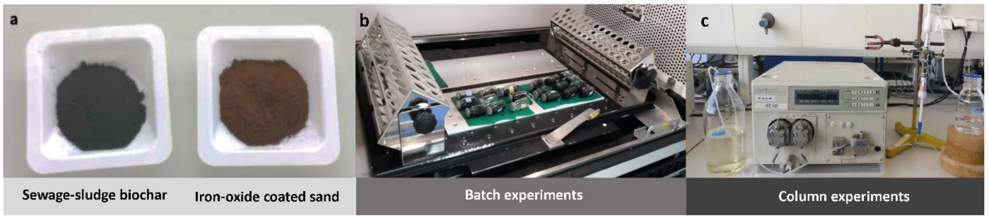

Figure 7.2: From waste by-products to DNA adsorbents at the root of circular water economy. **(a)** Macroscopic visualization of sewage-sludge biochar prepared by pyrolysis at 600°C of dewatered surplus activated sludge from a wastewater treatment plant and of used iron-oxide-coated sand reclaimed from a drinking water treatment plant. Batch **(b)** and continuous-flow column **(c)** setups used to characterize the DNA adsorption isotherms, characteristics, and efficiencies of the two reclaimed adsorbent materials.

Hydraulic residence time in the packed column

Hydraulic residence time distributions in the up-flow columns packed with either sewage-sludge biochar or iron-oxide-coated sand were recorded using a NaCl salt tracer (**Figure S.2**). The columns were filled with the sorbents at a bed height of 10 cm and fed with a saline solution at a flow rate of 1 mL min^{-1}. A concentration of 60 mmol L^{-1} NaCl salt solution (i.e., 3.5 g L^{-1}) was pulse-dosed at the column foot by using an HPLC liquid chromatography pump (Shimadzu LC-8A, USA). The concentration changes in the effluent were measured by electrical conductivity using a PRIMO 5 Microprocessor Conductivity Meter (Hanna instruments, USA), as a function of time by taking liquid samples of 0.5 mL from the column outlet.

Breakthrough of salmon sperm DNA in the up-flow packed column

The packed columns were fed up-flow with aqueous standard solutions of salmon sperm DNA of known concentrations using an HPLC liquid chromatography pump (Shimadzu LC-8A, USA). Adsorption breakthrough curves were recorded (i) with

inlet DNA concentrations of 0.1, 0.3 and 0.5 mg DNA L^{-1} at a fixed flow rate of 0.1 mL min^{-1} and (ii) with flow rates of 0.1, 0.3 and 0.5 mL min^{-1} at a fixed inlet DNA concentration of 0.3 mg DNA L^{-1}. Samples of 200 µL were collected at the column outlet in intervals of 15 min. The DNA concentration was measured spectrophotometrically until the ratio of C_t/C_o reached a constant value: C_o and C_t are the DNA concentrations at the column inlet and outlet, respectively. A C_t/C_o ratio close to 1 indicates saturation of the column with DNA (i.e., full adsorption capacity reached).

Data analysis of DNA breakthrough curves and maximum adsorption capacities in column

The performance of a fixed bed column can be explained by the breakthrough curves. The amount of time needed for breakthrough and the shape of the curve inform on the dynamic behavior of the column. Breakthrough curves are expressed as C_t/C_o versus time [47, 48]. The breakthrough point is usually defined as the point when the ratio between influent concentration, C_0 (mg L^{-1}) and outlet concentration, Ct (mg L^{-1}) becomes 0.05 to 0.90 [49]. The total capacity of the column (q_{total} in mg) gives the maximum amount of DNA that can be adsorbed and is calculated by integrating the area under the breakthrough curve given by Eq. 7.4 [47, 48, 50].

$$q_{total} = \frac{Q}{1000} \int_0^t C_{ad}\, \mathrm{d}t \tag{7.4}$$

where Q is the flow rate (mL min^{-1}); "t = total" is the total flow time (min); C_{ad} is the adsorbed DNA concentration (C_o – C_t) (mg L^{-1}).

The equilibrium DNA uptake or maximum adsorption capacity of the column q_{eq}(exp) (mg g^{-1}) is calculated by Eq. 7.5:

$$q_{eq(exp)} = \frac{q_{total}}{m} \tag{7.5}$$

where m is the dry weight of the adsorbent in the column (g).

Modelling DNA adsorption in the fixed-bed column

The column data were fitted with Thomas and Yoon-Nelson models for column modelling as in Chatterjee et al. [51]. In order to design an adsorption column, predicting the breakthrough curve and adsorbent capacity for the adsorbate under certain conditions is required. Data obtained from the experiments can be used for designing a prospective full-scale column operation.

The Thomas model (Eq. 7.6) was used to estimate the absorptive capacity of the adsorbent in the column.

$$\frac{C_t}{C_0} = \frac{1}{1 + exp(\frac{K_{TH} q_e x}{Q}) - K_{TH} C_0 t} \tag{7.6}$$

where k_{TH} (mL min^{-1} mg^{-1}) is the Thomas model constant; q_e(mg g^{-1}) is the predicted adsorption capacity; x is the mass of adsorbent (g); Q is the flow rate (mL min^{-1}); C_o is the inlet DNA concentration (mg L^{-1}); C_t is the outlet DNA concentration at time t (mg L^{-1}).

The Yoon-Nelson model (Eq. 7.7) was used to predict the run time before regeneration or replacement of the column becomes necessary. It is a very simple model to represent the breakthrough curve: it does not require any data about the characteristics of the system and the physical properties of the adsorbent [48]

$$\frac{C_t}{C_o - C_t} = exp(K_{YN} t - \tau K_{YN}). \tag{7.7}$$

where K_{YN} (min^{-1}) is the rate constant; τ (min) is the time required for 50% adsorbate breakthrough.

Removal of ARGs and ARB from filtered and unfiltered WWTP effluents in up-flow columns

After the detailed characterization of DNA adsorption properties with synthetic solutions of salmon sperm DNA, the column experiments were performed by feeding a real effluent water from WWTP Harnashpolder to the packed columns.

Experiments with filtered and unfiltered real WWTP effluent

Two sets of experiments were run with filtered (0.2 µm) and unfiltered WWTP effluent water to characterize the removal of free-floating exDNA and of total environmental DNA (i.e., both intracellular and extracellular DNA), respectively, and their related ARG/MGE content. The experiments were performed in triplicates. Volumes of 1 L of filtered/unfiltered WWTP effluent were passed through the columns at up-flow feeding flowrate of 0.3 mL min^{-1}. The removals of ARGs and ARB were measured by comparing their levels in the free-floating exDNA fraction and total environmental DNA of the inlet and outlet of the packed column. The extractions and purification procedures of free-floating exDNA and total environmental were described in details elsewhere [15] and given in short hereafter (**Figure 7.3**).

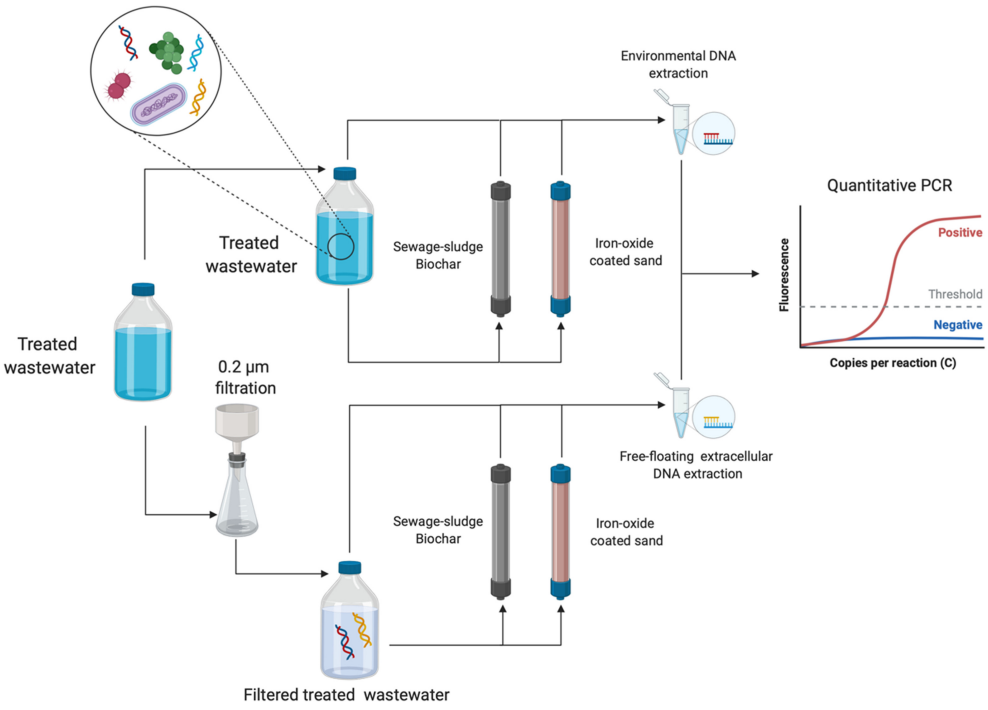

Figure 7.3: Schematic representation of the experimental adsorption column setup used and the quantitative PCR as analytical procedure applied. The aim was to study the adsorption and removal of antibiotic resistance bacteria, antibiotic resistance genes and mobile genetic elements by using sewage- sludge biochar and iron oxide-coated sand from treated effluent wastewater. Detail of material and setup used can be found in Figure 7.2.

Isolation of free-floating extracellular DNA from WWTP effluent matrices

To extract the free-floating exDNA, sample volumes of 1 L were filtered sequentially through 0.44 µm and 0.22 µm polyvinylidene fluoride (PVDF) membranes (Pall Corporation, USA) prior to isolation by ion exchange. The DEAE ion-exchange column was prepared and processed according to manufacturer's instructions. Buffers and solutions used for equilibrating, eluting, regenerating, cleaning and storing the DEAE ion-exchange column are the following. The equilibration buffer consisted of 50 mmol L^{-1} Tris, 10 mmol L^{-1} EDTA at pH 7.2. The elution buffer consisted of 50 mmol L^{-1} Tris, 10 mmol L^{-1} EDTA, 1.5 mol L^{-1} NaCl at pH 7.2. The regeneration buffer consisted of 50 mmol L^{-1} Tris, 10 mmol L^{-1} EDTA, 2 mol L^{-1} NaCl, pH 7.2. The cleaning solution consisted of 1 mol L^{-1} NaOH and 2 mol L^{-1} NaCl. The storage solution consisted of 20% ethanol in ultrapure water.

The full volume (1 L) of the pre-filtered sample containing the free-floating exDNA was loaded in a positively charged 1-mL diethylaminoethyl cellulose (DEAE)

ion-exchange column (BIA Separations, Slovenia) at a speed of 0.6 mL min^{-1} after equilibration in order to keep the pressure below the maximum limit of 1.8 MPa. After chromatographic retention, the exDNA was eluted at a flowrate of 1 mL min^{-1} with elution buffer and tracked over time with an HPLC photodiode array detector (Waters Corporation, USA) recording the UV-VIS absorption of DNA at 260 nm. The recovered raw free-floating exDNA was precipitated from the eluate with ethanol [52]. The residual proteins bound to the exDNA were digested by 2-h incubation with 0.85 g L^{-1} proteinase K (Sigma-Aldrich, UK); the enzymatic reaction was stopped at 50°C for 10 min. The protein-digested raw free-floating exDNA sample was finally purified using GeneJET NGS Cleanup Kit (Thermo Scientific, USA). The purified free-floating exDNA isolates were stored at 20°C pending analysis.

Extraction of total environmental DNA from WWTP effluent matrices

The total environmental DNA (i.e., intracellular and extracellular DNA) was extracted from the unfiltered water sample before loading the column and the effluent using the DNeasy Power Water kit (Qiagen, The Netherlands) following manufacturer's instructions. All DNA extracts were quantified by fluorometry using Qubit® (Thermo Fisher Scientific, USA).

Quantification of ARGs and MGE by quantitative polymerase chain reaction

The *16S rRNA* gene was selected as a proxy to quantify total bacteria. The genes analyzed by qPCR (**Table** S.1) were chosen from a selection panel of ARGs previously used for wastewater survey [18]. These ARGs confer resistance to antibiotics with the highest consumption in The Netherlands: erythromycin macrolides (*ermB*), sulfonamides (*sul1* and *sul2*), quinolones (*qnrS*) and extended-spectrum -lactamase (bla_{CTXM}). The class 1 integron-integrase gene (*intI1*) – a jumping gene driving horizontal gene transfer [53] – was included to assess the fate of MGEs. Standards for qPCR were generated from a curated antimicrobial resistance genes database (ResFinder). Standards, primers, and reaction conditions are listed in **Tables S.2 and S.3**.

7.3. Results and discussion

The preliminary screening of adsorbents revealed the interesting DNA adsorption characteristics of sewage-sludge biochar close to powdered activated carbon (**Figure 7.4**). Depending on concentrations of salmon sperm DNA standard and its ratio to adsorbent mass (20–140 µg DNA mL^{-1} for 40 mg of adsorbent material in 1 mL working volumes in Eppendorf tubes), and on water conditions from ultrapure water to tap water to filtered WWTP effluent, the sewage-sludge biochar and used iron-oxide-coated sand displayed superior adsorption potential than granular activated carbon and mineral wool.

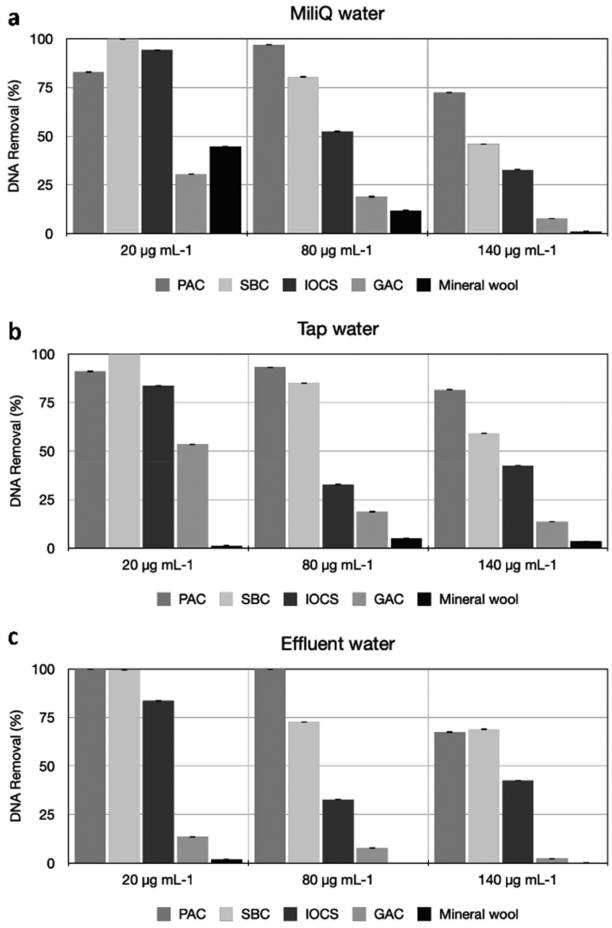

Figure 7.4: Removal of salmon sperm DNA standard by powdered activated carbon (PAC), sewage-based biochar (SBC), iron oxide coated sands (IOCS), granular activated carbon (GAC) and mineral wool in **(a)** ultrapure water, **(b)** tap water, and **(c)** effluent wastewater.

Powdered activated carbon is industrially manufactured and forms a definite solution to remove potentially problematic environmental DNA on top of chemical

micropollutants. Sewage-sludge biochar and used iron-oxide coated sand are reclaimed from WWTP and drinking WTP wastes, rendering these adsorbents as interesting low-cost mitigation solutions in the context of the circular water economy. A detailed examination of the physical-chemical properties of DNA adsorption onto these two circular products is elaborated in this study.

Physical-chemical characteristics of sewage-sludge biochar and iron-oxide-coated sand are suited for DNA adsorption and microbial retention

The surface morphologies of the sewage-sludge biochar processed by pyrolysis (600°C) of surplus activated sludge from the WWTP (**Figure 7.5a-b)** and of reclaimed iron-oxide-coated sand obtained from the drinking WTP (**Figure 7.5c-d)** were characterized by SEM. The surface morphologies of both by-products were highly heterogeneous and structurally complex, with many pores of different diameters. No fibers nor debris structures were observed in any of the materials.

The specific surface areas measured according to Brunauer-Emmett-Teller (BET) are provided in **Table 7.1**. The surface area of sewage-sludge biochar (32.4 m^2 g^{-1}) was lower than iron-oxide-coated sand (164.9 m^2 g^{-1}). Ash filling, which blocks access to the biochar micropores, could explain this difference [54]. Méndez et al. [55] got similar BET surface area values (37.18 m^2 g^{-1}) and pore diameter (9.46 nm) for sewage-sludge biochar pyrolyzed at same temperature.

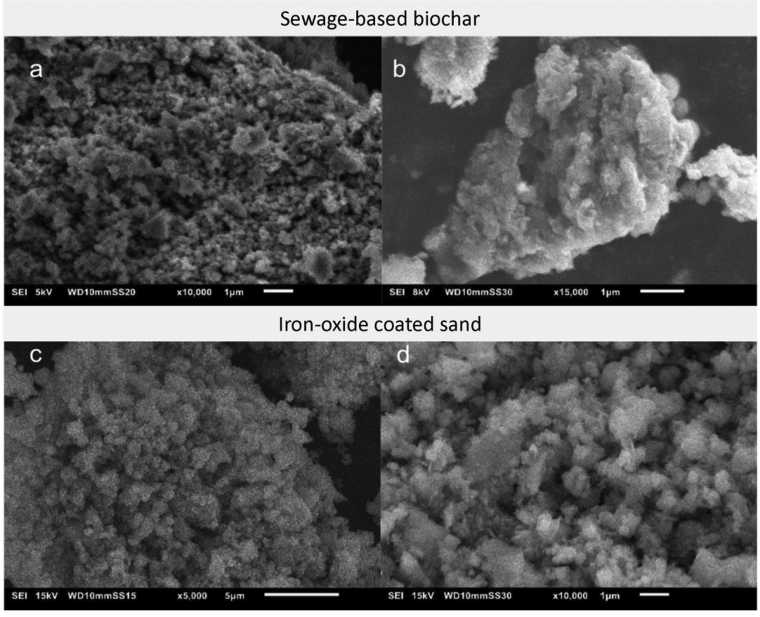

Figure 7.5: Scanning electron microscopy images of sewage-sludge biochar at magnifications of **(a)** 10.000× and **(b)** 15.000× and iron-oxide-coated sand at **(c)** 5.000× and **(d)** 10.000×.

Sharma [56] described the specific surface area of iron-oxide-coated sand from 12 different Dutch drinking WTP in the range of 5.4 to 201 $m^2\ g^{-1}$. They suggested that the BET surface area of iron-oxide-coated sand could mainly depend on their residence time (from months to years) in the drinking WTP.

The relatively low yield of sewage-sludge biochar production of 0.39 g dried sewage-sludge biochar g^{-1} dried sewage sludge matches other studies [57, 58]. The biochar production yield has a direct implication on its industrial applicability. It highly varies on the pyrolysis temperature used [59] since directly linked to amounts of volatile matter released [60]. For practice, other pyrolysis temperatures and seasonal biomass samples could be tested to address variations in the biochar production yield and its DNA adsorption capacity. Biochar-based systems form an important low-cost component to sustain sanitation in low- and middle-income countries. Sunlight-based processes are currently investigated to concentrate energy in solar furnaces to drive photothermal processes across a temperature range from 80 to more than 1000°C, thus perfectly suited for biochar production [61] from any kind of biomasses locally available.

The chemical properties of the adsorbent materials are presented in **Table 7.1**. The sewage-sludge biochar was mainly composed of oxygen, sulphur and carbon with traces of other elements like phosphorus, magnesium or calcium bioaccumulated during wastewater treatment. Iron-oxide-coated sands mainly comprised iron, oxygen and silica. The valence state of iron in the iron-oxide-coated sand was determined by Mössbauer spectroscopy, resulting in mainly ferrihydrite (III) particles (**Figure S.1**; **Table S.1**).

The porous morphologies and chemical characteristics of sewage-based biochar and iron-oxide-coated sand exhibit interesting properties for exDNA removal by entrapment and adsorption.

Table 7.1: Physicochemical properties and elemental compositions of sewage-sludge biochar prepared by pyrolysis at 600 °C of surplus activated sludge obtained from a WWTP and of iron-oxide-coated sand reclaimed from a drinking WTP.

Parameter	Sewage-sludge biochar	Iron-oxide-coated sand
Physicochemical properties		
Production yield (%)	38.6	–
Moisture content initial (%)	78.9	–
Moisture content final (%)	6.1	
Volatile matter (%)	68.1	–
Surface area (m_2g^{-1})	32.4	164.9
Pore diameter (nm)	10.1	6.2
pH (-)	8.0	8.2
Elemental composition (%)		
C	14.1	2.1
H	1.7	3.3
O	37.4[a]	43.7[a]
N	1.9	0.01
S	19.5	–
P	7.7	–
Ca	4.3	–
Mg	5.6	–
Fe	3.9	27.3
Si	3.2	23.6
Al	1.3	–

[a] Oxygen content estimation

Adsorption of nucleic acids by sewage-sludge biochar and iron-oxide-coated sand is governed by a multilayer Freundlich isotherm

From the batch tests performed in apothecary glass bottles of 25 mL with 5 mL working volumes, initial salmon sperm DNA concentrations of 100 µg DNA mL^{-1} and increasing amounts of adsorbents from 0 to 100 mg mL^{-1}, sewage-sludge biochar rapidly and efficiently removed the DNA present in the supernatant after 2 h equilibrium time onto 40–100 mg adsorbent mL^{-1} (**Figure 7.6a-b**). Reclaimed iron-oxide-coated sand displayed lower DNA adsorption capacity with a minimum of 80 mg adsorbent mL^{-1} needed to fully remove the DNA after an equilibrium time of at least 5 h. One may raise the question on whether the DNA removal occurred via adsorption or degradation. DNA did not show any degradation after 24 h of suspension in treated wastewater without any sewage-sludge biochar (**Figure 7.6a**). Recent studies have shown that the presence of biochar provided protection to exDNA against degradation by DNase I [38]. In addition, cross-verification methods like DNA fluorescence staining and microscopy could be used to consolidate adsorption results.

Both Langmuir and Freundlich isotherm models were used to analyze the DNA adsorption patterns on the two adsorbents (**Figure 7.6c-d**, **Table 7.2**). The Freundlich isotherm model was better describing the DNA adsorption profiles (R^2 = 0.99 and 0.93 for sewage-sludge biochar and iron-oxide-coated sand, respectively, on filtered WWTP effluent water) than the Langmuir monolayer isotherm model (R^2 = 0.92 and 0.89, respectively). This suggested a multilayer adsorption of DNA with heterogeneous distribution of active adsorption sites, agreeing with already published literature [38].

Table 7.2: Parameters derived from Freundlich (Eq. 7.2) and Langmuir (Eq. 7.3) isotherm models calibrated to the DNA adsorption profiles onto sewage-sludge biochar and iron-oxide-coated sand materials in ultrapure water and filtered (0.2 µm) WWTP effluent water.

Adsorbent	Type of water	Freundlich multilayer isotherm model				Langmuir monolayer Isotherm model		
		R^2 ()	K_F (mg DNA g^{-1})	1/n ()	n ()	R^2()	q_{max} (mg DNA g^{-1})	K_L (L mg^{-1} DNA)
Sewage-sludge biochar	Ultrapure water	0.95	1.4	0.13	7.87	0.89	2.2	1.81
	Filtered WWTP effluent	0.99	1.0	0.19	5.16	0.92	2.0	0.61
Iron-oxide-coated sand	Ultrapure water	0.81	0.3	0.31	3.20	0.78	1.7	0.06
	Filtered WWTP effluent	0.93	0.21	0.61	1.63	0.89	5.8	0.01

Table 7.2 compares the calibrated parameters of both adsorption models onto both adsorbent materials in ultrapure water and in filtered WWTP effluent water. Sewage-sludge biochar revealed a higher Freundlich constant KF (1 mg DNA g^{-1} adsorbent on effluent water) than iron-oxide-coated sand (0.21 mg DNA g^{-1} adsorbent). For a thermodynamically favorable adsorption, the exponent constant n for a given adsorbate and adsorbent at a particular temperature should lie between 1 and 10 [62]. This was the case for both adsorbents.

Sewage-sludge biochar was a more effective DNA adsorbent with higher affinity towards nucleic acids than iron-oxide-coated sand. It is important to highlight that the binding mechanisms differ between the two types of materials: hydrophobic forces rule adsorption on sewage-sludge biochar while the phosphate groups of DNA binds to iron of the iron-oxide-coated sand.

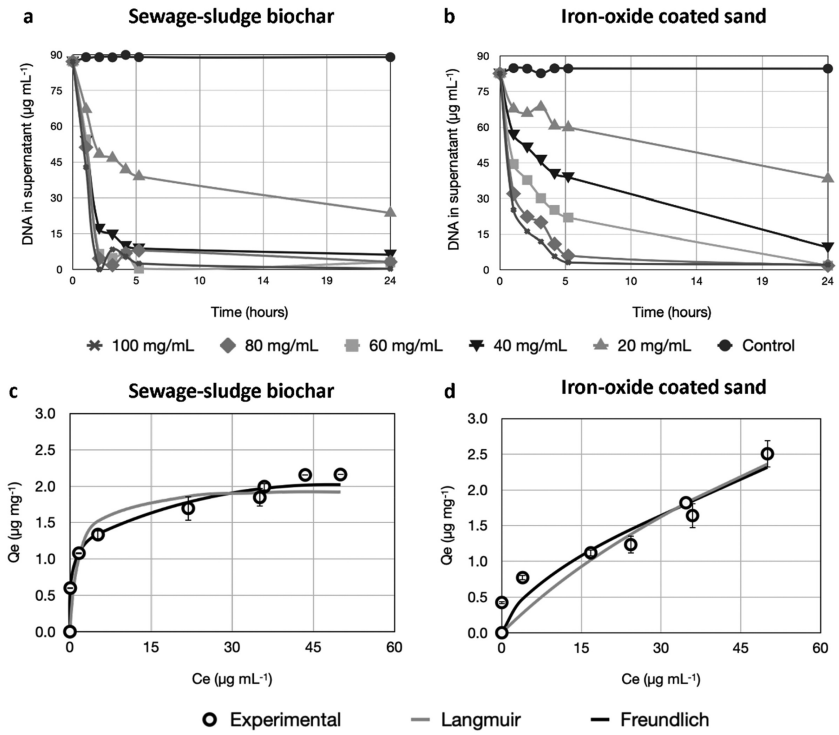

Figure 7.6: Equilibrium time of salmon sperm DNA on treated wastewater for **(a)** sewage sludge biochar and **(b)** iron oxide coated sands. An initial DNA concentration of 100 µg mL^{-1} was used with the adsorbent ranging from 0 to 100 mg mL^{-1}. Freundlich and Langmuir isotherms models were fitted from experimental data in ultrapure water on **(c)** sewage-sludge biochar and **(d)** iron-oxide-coated sand. The equilibrium salmon sperm DNA concentration (C_e; **a**–**b**) and the amount of salmon sperm DNA adsorbed per unit of adsorbent (Q_e; **c-d**) are displayed on the graphs.

No effect of pH and coexisting anions was observed on DNA adsorptions

The influence of pH on DNA adsorption was analyzed in Tris-HCl buffer medium at initial salmon sperm DNA concentrations of 20 and 100 mg DNA L^{-1} (**Figure 2.7a-b**), but not significant effect of pH was observed on DNA adsorption capacity onto the tested materials.

Organic clays, montmorillonite and biochar can adsorb more DNA under acidic (pH < 5) than alkaline (pH > 9) conditions [63, 64]. Biochar surfaces display an increased negative charge from pH 3 to 7 [65]. The isoelectric point of DNA is about pH 5 [66]. Phosphate groups confer a negative charge to DNA macromolecules when pH is above the isoelectric point. At low pH < 2, DNA mostly presents neutral electrical properties. In order to avoid electrostatic repulsion, sewage-sludge biochar and DNA should not be negatively charged simultaneously. At pH below 4, both biochar surfaces and DNA phosphate groups are protonated, decreasing

repulsion between them and increasing the DNA adsorption capacity. However, these theoretical principles do not align with our experimental results. Wang et al. [67] have similarly observed that pH shifts did not impact the adsorption of nucleic acids on willow-wood biochar. We conclude that DNA is mostly adsorbed via hydrophobic interactions rather than electrostatic ones.

Adsorption of ortho-phosphate onto iron-oxide-coated sand increase as the pH decreases, following an anionic adsorption behavior [68]. In our case, pH shifts did not show any significant effect on DNA adsorption by the phosphate groups.

Figure 7.7c presents the influence of ionic conditions on salmon sperm DNA adsorption at pH 7, initial concentration of 100 mg DNA L^{-1}. Na+ and Ca^{2+} addition at 1–60 mmol ion L^{-1} had no significant effect ($p > 0.05$) on DNA adsorption onto sewage-sludge biochar and iron-oxide-coated sand (**Table S.2**). Only the addition of 60 mmol Mg^{2+} L^{-1} in the test with sewage-sludge biochar displayed a significant increase of 33% ($p < 0.05$) in DNA adsorption capacity (0.89 mg DNA g^{-1} adsorbent).

Ion bridges and charge neutralization are the supposed main mechanisms increasing DNA adsorption by cations addition [69, 70]. However, DNA adsorption onto these materials did not seem to be driven by electrostatic interactions. For this reason, it is hypothesized that hydrophobic interactions or iron-phosphate interactions can play a role in the DNA adsorption onto the sewage-sludge biochar and iron-oxide-coated sand, respectively. Higher pyrolysis temperatures (>600°C) significantly increase the DNA adsorption efficiency by enhancing the surface area and hydrophobicity of the biochar [71].

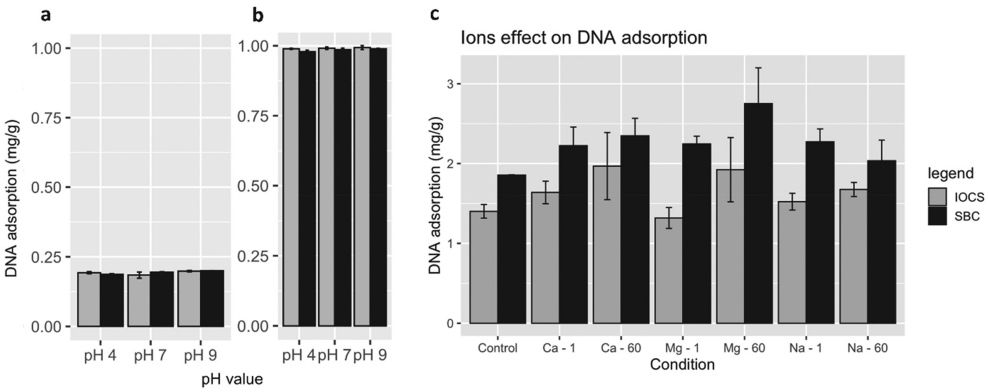

Figure 7.7: The influence of pH on DNA adsorption (mg DNA g material^{-1}) by sewage-sludge biochar (SBC) and iron-oxide-coated sands (IOCS). The initial concentration of DNA was 20 mg L^{-1} **(a)** and 100 mg L^{-1} **(b)**, respectively. No significant difference ($p < 0.05$) among treatments was observed. **(c)** The influence of Ca^{2+}, Mg^{2+} and Na^{+} on adsorption of DNA (100 mg L^{-1}) on sewage-sludge biochar (SBC) and iron-oxide-coated sands (IOCS). DNA adsorption stands for mg of DNA per g of adsorbent added. The concentrations of the ions were set at 1 and 60 mmol L^{-1}. Significant difference is defined by (*) when $p < 0.05$.

Sewage-sludge biochar is an efficient adsorbent for DNA removal in up-flow column systems

Two bench up-flow 15 × 1 cm chromatography glass columns equipped with 0.5 g of glass beads (250–300 µm) surmounted by 3 g of sewage-sludge biochar or 4 g of iron-oxide-coated sand particles filling were evaluated for the continuous-flow adsorption of salmon sperm DNA standard out of ultrapure water and of filtered WWTP effluent water.

The hydraulic residence time distributions (RTDs) measured by spiking NaCl at 60 mmol L^{-1} in the water flow displayed plug-flow patterns with axial dispersion in these column systems (**Figure S.2**). Iron-oxide-coated sand displayed a sharper peak but with long tailing. The RTD with sewage-sludge biochar was more equilibrated with a Gaussian shape. Both RTDs harbored a peak maximum (mode) at 10 min at a flow-rate of 1 mL min^{-1}.

The DNA breakthrough curves are depicted in **Figure 7.8**. In agreement with batch results, sewage-sludge biochar was more effectively adsorbing DNA than iron-oxide-coated sand from these water matrices. In ultrapure water, the effect of the adsorbent material on the breakthrough point was remarkable, i.e.,10.4 ± 1.9 times (depending on initial DNA concentrations of 0.1–0.5 mg DNA mL^{-1}) and 4.3 ± 0.9 times (depending on flow rates of 0.1–0.5 mL min^{-1}) higher (more time needed to get saturated) on sewage-sludge biochar than iron-oxide-coated sand. With filtered WWTP effluent water, the breakthrough point of sewage-sludge biochar was 4.2 ± 1.8 times (depending on initial DNA concentrations) and 4.6 ± 1.3 times (depending on flow rates) higher than iron-oxide-coated sand. The details on breakthrough points are delivered in (**Table S.3**) in Supplementary information.

The Thomas and Yoon-Nelson mathematical models were used to evaluate the effect of process variables on the efficiency of DNA adsorption in the packed-bed columns (**Table S.4**). The two models are mathematically equivalent [72]. The only difference between the model is the definition of their variables. Thomas model is used to estimate the absorptive capacity of the adsorbent while the Yoon-Nelson is used to predict the run time before regeneration or replacement of the column is needed.

The Thomas model was used to analyze the DNA breakthrough curves on sewage-sludge biochar and iron-oxide-coated sand on different water qualities. The Thomas model constant K_{TH} increased with the flow rate for both materials and both water qualities. The adsorption capacity at equilibrium qe was close to experimental results (q_e (exp)), especially on ultrapure water. Thomas model adequately described the experimental breakthrough data. This indicates that external and internal diffusions are not the only rate-limiting steps in the DNA adsorption process.

The Yoon-Nelson model was applied to determine how much time could the adsorbents be used for DNA removal. According to the interpolation of the model plot, the Yoon-Nelson model constant K_{YN} increased with the inlet DNA

concentration. The breakthrough time τ decreased with increasing flow rate and initial DNA concentration: the column saturated faster because of less contact time and higher number of DNA molecules to be adsorbed. The small differences between experimental and predicted τ values indicated that Yoon-Nelson model gave an appropriate fit to the experimental column data on continuous DNA adsorption.

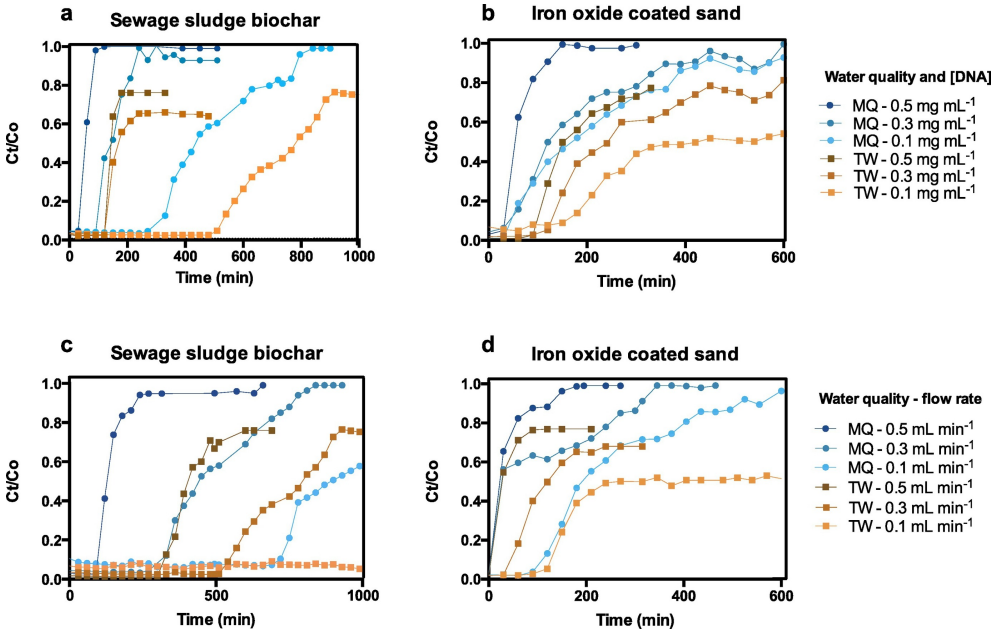

Figure 7.8: Experimental breakthrough curves for the continuous-flow adsorption of salmon sperm DNA in up-flow packed-bed columns filled with sewage-sludge biochar **(a, c)** and iron-oxide-coated sand **(b, d)** adsorbents. The effect of the initial DNA concentration (0.1–0.5 mg DNA mL^{-1}) was tested at a flow rate of 0.1 mL min^{-1} of either ultrapure water (MilliQ, MQ; blue curves) or filtered WWTP effluent water (treated wastewater, TW; brown curves). The effect of the flow rate (0.1–0.5 mL min^{-1}) was tested at an initial DNA concentration of 0.3 mg DNA mL^{-1}.

Humic acids interfere on DNA adsorption with effluent water matrices

With ultrapure water, both sewage-sludge biochar and iron-oxide-coated sand were fully saturated by salmon sperm DNA (ratio $C_t/C_o \approx 1$) in column studies. This exhaustion point could not be achieved with filtered WWTP effluent water (**Figure 7.8**). The effect of water qualities was explained by the interaction/adsorption of DNA on organic components of the filtered WWTP effluent water like humic acids (HAs) that are absent in ultrapure water. If DNA added in the inlet binds to organic components such as humic acids and adsorbs onto biochar, the detection of the DNA concentration that was supposed to be in the eluent will be compromised.

HAs are important components of soils and natural waters, that are formed during humification of organic matter by microorganisms and that bind metal ions in these environmental systems [73]. We incubated salmon sperm DNA and the adsorbents with a range of HAs concentrations (0 to 100 mg HAs L^{-1}) to assess their influence on DNA adsorption in batches.

Increasing HAs concentrations resulted in a significant decrease in the DNA adsorption capacity of the sewage-sludge biochar (Δ0.5 mg DNA g HA^{-1}, 90.5% decrease) and iron-oxide-coated sand (Δ0.12 mg DNA g HA^{-1}, 17% decrease) (**Figure 7.9**). When only HAs were supplied, DNA adsorbed onto them (0.42 mg g^{-1}). Saeki et al. [74] showed a similar effect when DNA molecules were exposed to HAs, suggesting that HAs can adsorb and fix DNA. HAs can also directly adsorb onto biochar [75], thus enhancing the DNA binding capacity of the biochar. This can explain why the DNA concentration in the column outlet never reached the inlet DNA concentration when the adsorbents in the columns were DNA-saturated.

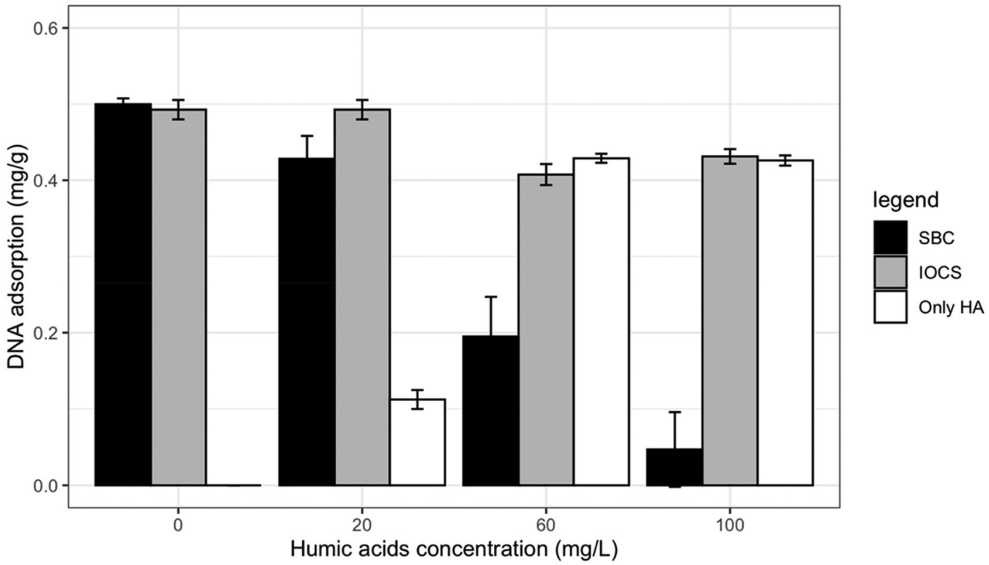

Figure 7.9: Influence of humic acids (HAs) on DNA adsorption on sewage-sludge biochar (SBC), iron-oxide-coated sands (IOCS) and only HAs. Salmon sperm DNA was used as a DNA template at a concentration of 20 µg mL^{-1}. DNA adsorption stands for mg of DNA per g of adsorbent added.

More than 95% of ARGs and MGEs present in the environmental DNA were removed by sewage-sludge biochar in up-flow column

The removal of ARGs and MGEs from 1 L of WWTP effluent water was assessed in the two up-flow packed-bed columns filled with biochar and iron oxide coated sand.

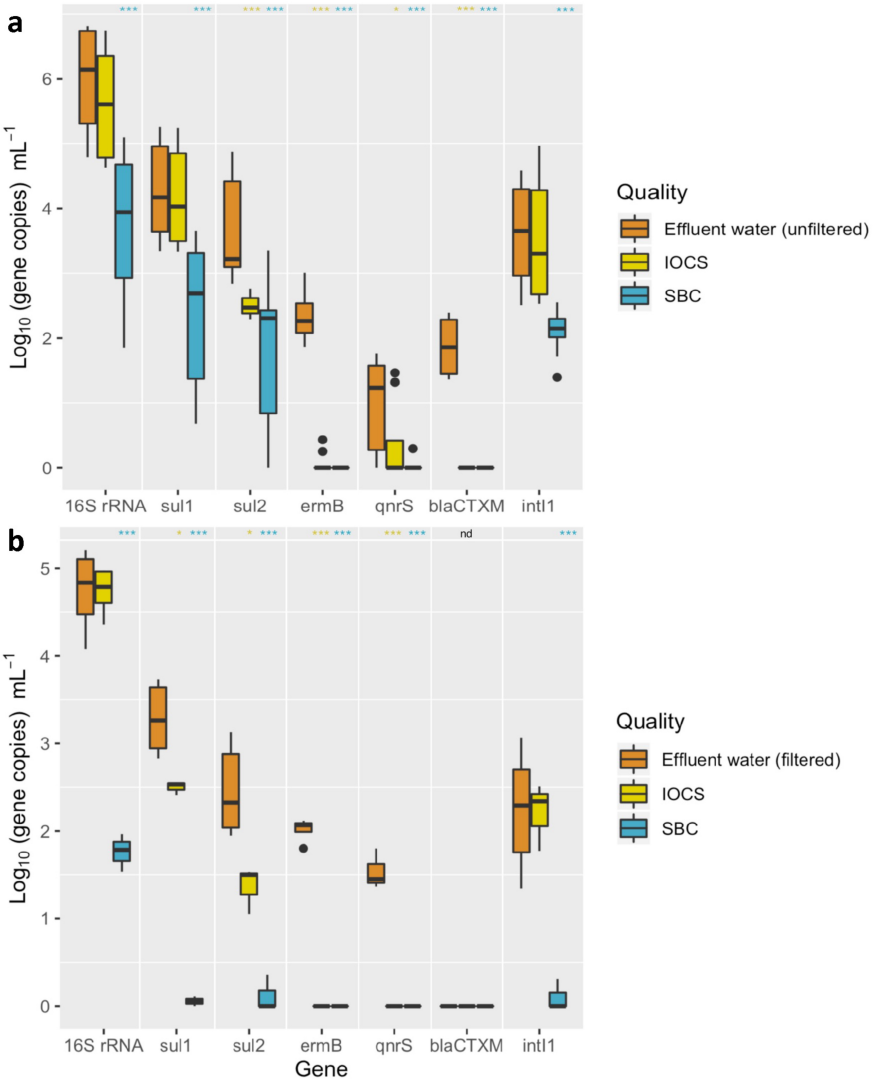

Figure 7.10: Quantitative PCR results assessing differences in the concentrations of ARGs and MGE in the unfiltered **(a)** and filtered **(b)** WWTP effluent and in the outlet stream of the adsorption columns filled with either iron-oxide-coated sand (IOCS) orsewage-sludge biochar (SBC). **(a)** Comparison was done with unfiltered effluent water samples assessing the removal of environmental DNA (i.e., including both free-floating exDNA and antibiotic resistantant bacteria). **(b)** Comparison was done with filtered effluent water samples assessing the free-floating exDNA removal (i.e., in absence of microorganisms). Values are shown on Log10 gene copies mL^{-1} from a panel of 16S rRNA gene, selected ARGs (*sul1*, *sul2*, *ermB*, *qnrS* and bla_{CTXM}) and one MGE (*intI1*). Statistical significance: $p < 0.05$(*), $p < 0.005$ (**), $p < 0.0005$ (***). Note: "nd" stands for "non-detected". Black dots represent data outliers.

Experiments were conducted both with raw (i.e., unfiltered) and 0.2-µm filtered WWTP effluent water in order to differentiate between the removals of the xenogenetic elements from the total environmental DNA (i.e., sum of free-floating extracellular DNA and microorganisms with their intracellular DNA) and the free-floating exDNA fraction. qPCR was used to quantify the concentrations of ARG and MGE copies from a representative panel of genes for the Netherlands.

With unfiltered WWTP effluent water (**Figure 7.10a**, **Table 7.3**), it was observed that all the tested genes in the sewage-sludge biochar eluent were significantly reduced ($p < 0.0005$) when compared with their inlet concentration (log_{10} gene copies mL^{-1}). Regarding the iron-oxide coated sands eluent, only *sul2*, *ermB*, and bla_{CTXM} was significantly reduced ($p < 0.0005$) and *qnrS* ($p < 0.05$) when compared from their inlet concentrations.

Table 7.3: Quantitative PCR results assessing the *16S rRNA* gene, a panel of antibiotic resistance genes, and the integrase I class 1 as a mobile genetic element. Values represent the log10 gene copies differences between the inlet (unfiltered or filtered effluent water) and outlet of the adsorption columns tested with either iron-oxide-coated sand or sewage-sludge biochar.

		ΔGene (log_{10} gene copies differences inlet-outlet						
Type of water	Material	*16S rRNA*	*sul1*	*sul2*	*ermB*	*qnrS*	bla_{CTXM}	*intI1*
Unfiltered effluent water	IOCS	0.34 ± 1.1	0.1 ± 1.0	1.2 ± 0.8	2.3 ± 0.4	0.7 ± 0.8	1.9 ± 0.4	0.1 ± 1.2
	SBC	2.3 ± 1.4	1.9 ± 1.3	1.8 ± 1.3	2.4 ± 0.4	1.0 ± 0.7	1.9 ± 0.4	1.5 ± 0.8
Filtered effluent water	IOCS	0.003 ± 0.5	0.8 ± 0.4	1.1 ± 0.5	2.1 ± 0.02	1.4 ± 0.04	0	0.03 ± 0.7
	SBC	3.0 ± 0.5	3.2 ± 0.4	2.3 ± 0.5	2.1 ± 0.03	1.4 ± 0.05	0	2.1 ± 0.6

With filtered WWTP effluent water (**Figure 7.10b**, **Table 7.3**), all the tested genes in the sewage-sludge biochar eluent were significantly reduced when compared with the inlet filtered treated wastewater ($p < 0.0005$), especially *qnrS*, *ermB* and bla_{ctxm} that were no longer detected in the column eluent. Regarding iron-oxide coated sands, only *sul1* and *sul2* ($p < 0.05$) and *ermB* and *qnrS* ($p < 0.0005$) were significantly reduced in the eluent when compared with the column inlet concentrations.

Overall, 97% and 66% of the targeted genes present in the total environmental DNA of the raw WWTP effluent water decreased from the inlet to the outlet of the sewage-sludge biochar and iron-oxide-coated sand columns, respectively. During experiments conducted with filtered WWTP effluent water, the genes were removed at 85% and 54% by retention of the free-floating exDNA in the sewage-sludge biochar and iron-oxide-coated sand columns, respectively.

Outlook

We highlighted that materials reclaimed from wastes of water engineering facilities, namely WWTP and drinking WTP, can become effective adsorbents to remove

ARGs and MGEs from WWTP effluents. We involved a detailed examination of both the free-floating exDNA fraction and the total environmental DNA.

Sewage-sludge biochar produced by pyrolysis of surplus sewage sludge is an attractive, reclaimed and low-cost alternative to manufactured powdered activated carbon for the removal of xenogenetic elements from wastewater by adsorption. Adsorption capacity similar to activated carbon was obtained with sewage-sludge biochar in batch tests. We acknowledge that biochar can be more variable in composition and properties than activated carbon due to the type of sludge and pyrolysis conditions. Before going for full-scale operation, the variability of adsorption properties of biochar needs to be checked depending on biomasses and conditions used for production. Further studies can be conducted to investigate this important aspect using multifactorial experimental design. Biochar is widely used worldwide for sanitation. Numerous studies have highlighted biochar as a very effective material to remove antibiotics, heavy metals, and resistance [39, 76, 77]. Besides high-grade technological solutions for industrialized countries, we need to bring science into low-cost scalable and implementable solutions for regions with less access to expensive technologies.

Sewage sludge surplus in WWTPs gradually increase with the rising world population and the needs for sanitation and installation of new WWTPs thereof. At European level, sludge production reaches 13 million tons by 2020 [78]. The treatment and discarding of sewage sludge (e.g., landfilling, agriculture and incineration) is an expensive and ecological burden. The European directive 86/278/EEC on agricultural use of sewage sludge set stringent regulations because of the presence of high concentrations of heavy metals and pathogens. Incineration is carried out in most of EU-15 countries, like the Netherlands [36, 78]. Large-scale incineration requires high investment and operating costs together with extensive cleaning and gas purification.

Pyrolysis can become an interesting alternative to reduce sludge volumes, remove pathogens, and simultaneously convert the sludge organic matter into biofuel or biochar [79]. In contrast to incineration, pyrolysis requires less or no oxygen and eventually reduces the generation of flue and acid gases to be cleaned [80]. Pyrolysis can also be interestingly driven in solar furnaces [61], minimizing energetic costs. Biochar produced out of dewatered sewage-sludge can efficiently remove chemical pollutants from wastewater [81] like agrichemicals, pharmaceuticals, personal care products or endocrine disrupting compounds [82]. The here-demonstrated ability of sewage-sludge biochar to remove nucleic acids and their problematic xenogenetic contents is an asset, besides promoting circularity in water resource factories.

Finally, exDNA free-floats in typical concentrations of 5.6 $\pm$ 2.9 µg L^1 in effluent wastewater [15]. The here-sampled WWTP treats 200000 m^3 day^{-1}, corresponding to a discharge of 1 kg exDNA day^{-1}. Since removing up to more than 85% of the free-floating genes, a sewage-sludge biochar solution can prevent the discharge of 310 kg exDNA $year^{-1}$ on top of problematic microorganisms within the environmental DNA released from the catchment area of this largest WWTP of the Netherlands.

7.4. Conclusion

We showed the potential of waste materials from WWTPs and drinking WTPs like surplus activated sludge and used iron-oxide-coated sand to get revalorized to remove free-floating exDNA and total environmental DNA containing ARGs and MGEs from treated wastewater. The main conclusions of this work are:

- Sewage-sludge biochar displayed physical-chemical characteristics and DNA adsorption efficiencies similar to powdered activated carbon. Sewage-sludge biochar can be efficiently implemented in batches or continuous-flow packed-bed systems. Further multifactorial studies should address the variability in product characteristics and adsorption capacities of biochars.
- The removal of ARGs and MGEs was remarkable, notably with sewage-sludge biochar. From the total environmental DNA (i.e., composed of both intracellular and extracellular DNAs), 97% of the evaluated genes were adsorbed and removed from raw unfiltered WWTP effluent water in continuous-flow packed-bed columns filled with sewage-sludge biochar while a 66% removal was achieved with iron-oxide-coated sand. From the free-floating exDNA fraction, 85% of ARGs and MGEs were retained with this exDNA fraction in the sewage-sludge biochar column; 54% with iron-oxide-coated sand.
- Recycling surplus sludge and other waste biomasses into a low-cost, scalable and implementable solution can help remove the load of AMR released in aquatic environments.

By aligning to UN SDGs for clean water sanitation and responsible consumption production, we provide here a solution to mitigate the emission of problematic xenogenetic elements from sewage into surface waters. Both end-of-pipe but also decentralized technologies can be developed from this science-based evidence to remove AMR from used water streams at low cost.

7.5. Supplementary material

Mössbauer spectra and fitted parameters for characterization of iron-oxide coated sand

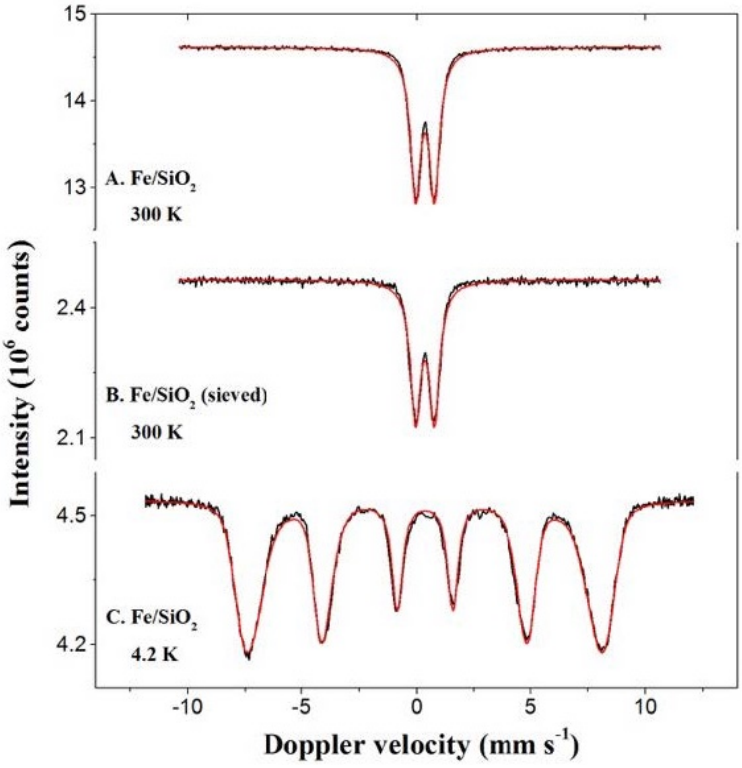

Figure S.1: Mössbauer spectra obtained at 300 and 4.2 K with the Fe/SiO_2 samples.

Table S.1: The Mössbauer fitted parameters of the Fe/SiO_2 samples.Experimental uncertainties:Isomer shift: I.S. ± 0.01 mm s^{-1}; Quadrupole splitting: Q.S. ± 0.01 mm s^{-1}; Line width: Γ ± 0.01 mm s^{-1}; Hyperfine field: ± 0.1 T; Spectral contribution: ± 3%; *Average magnetic field.

Sample	T (K)	IS (mm · s^{-1})	QS (mm · s^{-1})	Hyperfine field (T)	Γ (mm · s^{-1})	Phase	Spectral contribution(%)
Fe/SiO_2	300	0.36	0.82	- -	0.53	Fe^{3+}	100
Fe/SiO_2 (sieved)	300	0.36	0.82	- -	0.53	Fe^{3+}	100
Fe/SiO_2	4.2	0.35	-0.02	47.4*	0.48	Fe^{3+} (Ferrihydrite)	100

Batch and column studies

Table S.2: Statistical significance from the comparisons done between the control condition (ultrapure water.) and different ions concentrations (1 – 60 mM)

Material	Comparison	Difference	Lower	Upped	p.adj value
SBC	Control - Ca - 1 mM	-0.37	-1.04	0.30	0.52
SBC	Control - Ca - 60 mM	-0.49	-1.16	0.18	0.23
SBC	Control - Mg - 1 mM	0.39	-0.28	1.06	0.46
SBC	Control - Mg - 60 mM	0.90	0.23	1.57	0.01
SBC	Control - Na - 1 mM	0.42	-0.25	1.09	0.39
SBC	Control - Na - 60 mM	0.18	-0.49	0.85	0.96
IOCS	Control - Ca - 1 mM	-0.23	-0.91	0.43	0.88
IOCS	Control - Ca - 60 mM	-0.57	-1.24	0.10	0.12
IOCS	Control - Mg - 1 mM	-0.08	-0.75	0.59	0.99
IOCS	Control - Mg - 60 mM	0.52	-0.15	1.19	0.18
IOCS	Control - Na - 1 mM	0.12	-0.55	0.79	0.99
IOCS	Control - Na - 60 mM	0.27	-0.39	0.94	0.79

Table S.3: Adsorbents breakthrough points depending on the flow rate and DNA concentration.

Water quality	Adsorbent	Flow rate (mL min^{-1})	DNA concentration (mg L^{-1})	Breakthrough point (min)
Treated wastewater	Biochar	0.1	0.3	510
		0.3		120
		0.5		105
	IOCS	0.1	0.3	120
		0.3		45
		0.5		15
	Biochar	0.1	0.1	>2000
			0.3	540
			0.5	315
	IOCS	0.1	0.1	150
			0.3	120
			0.5	105
Ultrapure water	Biochar	0.1	0.3	315
		0.3		105
		0.5		45
	IOCS	0.1	0.3	105
		0.3		20
		0.5		10
	Biochar	0.1	0.1	570
			0.3	315
			0.5	120
	IOCS	0.1	0.1	45
			0.3	30
			0.5	15

Table S.4: Parameters obtained from the Thomas and Yoon-Nelson models describing the DNA adsorption and saturation behavior onto the tested materials in the column experiments. **n.s.**: not saturated.

Operation parameters				Thomas model				Yoon-Nelson model			
Material	**Water quality**	**C0** ($mgDNA\ L^{-1}$)	**Q** ($mL\ min^{-1}$)	K_{TH} (10^{-3}) (**L** $min^{-1}\ mg^{-1}$ **DNA**)	q_e ($mgDNA\ g^{-1}$ **adsorbent**)	q_e **(exp)** ($mgDNA\ g^{-1}$ **adsorbent**)	R^2 **(-)**	K_{YN} (10^{-3}) **(L min-1)**	τ **(min)**	τ**exp (min)**	R^2 **(-)**
Sewage-sludge biochar	Ultrapure	100	0.1	0.05	3.7	3.7	0.93	32	786	570	0.98
		300	0.1	0.05	3.6	3.7	0.93	29.5	399	315	0.92
		500	0.1	0.12	1.8	1.9	0.98	139.8	129	120	0.99
		300	0.3	0.13	3.5	3.7	0.98	20.9	132	105	0.94
		300	0.5	0.29	3.2	3.5	0.98	151.7	65	45	0.94
	Filtered effluent	100	0.1	n.s.	n.s.	n.s.	n.s.	3.2	2321	2000	0.98
		300	0.1	0.03	6.8	3.4	0.98	17.4	670	540	0.92
		500	0.1	0.04	6.9	4.1	0.92	35.1	342	315	0.93
		300	0.3	0.14	4.6	4.1	0.92	80.2	158	120	0.86
		300	0.5	0.36	6.9	5.2	0.99	64.1	148	105	0.87
Iron-oxide-coated sand	Ultrapure	100	0.1	0.07	0.1	0.5	0.93	5.6	334	45	0.98
		300	0.1	0.08	1.2	1.2	0.95	33.1	121	30	0.99
		500	0.1	0.18	0.7	0.7	0.98	27.7	38	15	0.99
		300	0.3	0.03	2.2	2.7	0.84	6.9	46	20	0.91
		300	0.5	0.31	1.6	2.0	0.94	17	22	10	0.93
	Filtered effluent	100	0.1	0.02	1.4	0.9	0.87	13.7	307	150	0.95
		300	0.1	0.03	3.0	2.6	0.79	47.2	177	120	0.98
		500	0.1	0.05	1.7	1.7	0.91	59.3	145	105	0.92
		300	0.3	0.12	2.3	2.3	0.99	8.4	135	45	0.90
		300	0.5	0.06	2.2	1.3	0.63	8.8	21	15	0.82

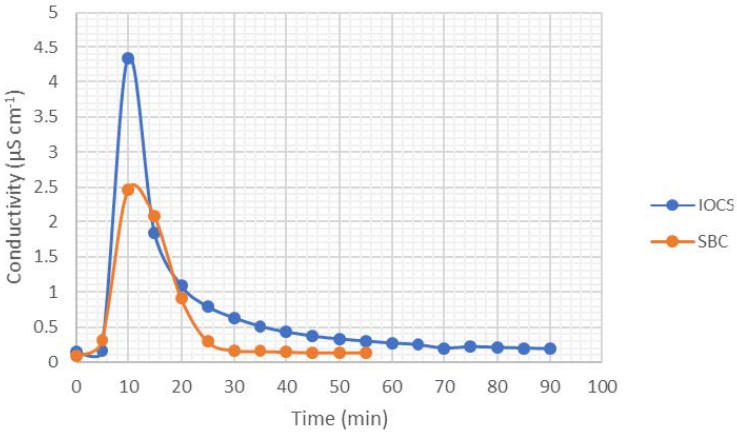

Figure S.2: Hydraulic residence time distributions of a 60 mmol L^{-1} NaCl solution fed at 1 mL min^{-1} in the columns packed with sewage-sludge biochar (SBC) and iron-oxide-coated sand (IOCS).

Bibliography

[1] UNICEF, WHO, and JMP. *Progress on household drinking water, sanitation and hygiene 2000-2017*. 2019, p. 140. ISBN: 978-92-806-5036-5. URL: https://washdata.org/sites/default/files/documents/reports/2019-07/jmp-2019-wash-households.pdf.

[2] M. A. Shannon, P. W. Bohn, M. Elimelech, J. G. Georgiadis, B. J. Marĩas, and A. M. Mayes. "Science and technology for water purification in the coming decades". In: *Nature* 452.7185 (2008), pp. 301–310. ISSN: 14764687. DOI: 10.1038/nature06599.

[3] A. D. McEachran, M. L. Hedgespeth, S. R. Newton, R. McMahen, M. Strynar, D. Shea, and E. G. Nichols. "Comparison of emerging contaminants in receiving waters downstream of a conventional wastewater treatment plant and a forest-water reuse system". In: *Environmental Science and Pollution Research* 25.13 (2018), pp. 12451–12463. ISSN: 16147499. DOI: 10.1007/s11356-018-1505-5.

[4] R. I. Eggen, J. Hollender, A. Joss, M. Schärer, and C. Stamm. "Reducing the discharge of micropollutants in the aquatic environment: The benefits of upgrading wastewater treatment plants". In: *Environmental Science and Technology* 48.14 (2014), pp. 7683–7689. ISSN: 15205851. DOI: 10.1021/es500907n.

[5] D. Weissbrodt, L. Kovalova, C. Ort, V. Pazhepurackel, R. Moser, J. Hollender, H. Siegrist, and C. S. Mcardell. "Mass flows of x-ray contrast media and cytostatics in hospital wastewater". In: *Environmental Science and Technology* 43.13 (2009), pp. 4810–4817. ISSN: 0013936X. DOI: 10.1021/es8036725.

[6] D. Cacace, D. Fatta-Kassinos, C. M. Manaia, E. Cytryn, N. Kreuzinger, L. Rizzo, P. Karaolia, T. Schwartz, J. Alexander, C. Merlin, H. Garelick, H. Schmitt, D. de Vries, C. U. Schwermer, S. Meric, C. B. Ozkal, M. N. Pons, D. Kneis, and T. U. Berendonk. "Antibiotic resistance genes in treated wastewater and in the receiving water bodies: A pan-European survey of urban settings". In: *Water Research* 162 (2019), pp. 320–330. ISSN: 18792448. DOI: 10.1016/j.watres.2019.06.039. URL: https://doi.org/10.1016/j.watres.2019.06.039.

[7] L. Rizzo, R. Krätke, J. Linders, M. Scott, M. Vighi, and P. de Voogt. *Proposed EU minimum quality requirements for water reuse in agricultural irrigation and aquifer recharge: SCHEER scientific advice*. Apr. 2018. DOI: 10.1016/j.coesh.2017.12.004.

[8] A. Pruden, R. Pei, H. Storteboom, and K. H. Carlson. "Antibiotic resistance genes as emerging contaminants: Studies in northern Colorado". In: *Environmental Science and Technology* 40.23 (2006), pp. 7445–7450. ISSN: 0013936X. DOI: 10.1021/es0604131.

[9] V. Tripathi and P. Tripathi. *Antibiotic resistance genes: An emerging environmental pollutant*. 9783319462479. 2017, pp. 183–201. ISBN: 9783319462479. DOI: 10.1007/978-3-319-46248-6{_}9.

[10] M. C. Lee Ventola. "Antibiotic Resistance Crisis". In: *P&T: a peer-reviewed journal for formulary management* 40.4 (2015), pp. 277–83. URL: https://www.ncbi.nlm.nih.gov/pmc/articles/PMC4378521/.

[11] I. M. Gould, A. M. Bal, I. M. Gould, and A. M. Bal. "New antibiotic agents in the pipeline and how they can help overcome microbial resistance New antibiotic agents in the pipeline and how they can help overcome microbial resistance". In: 5594.December (2015), pp. 185–191. DOI: 10.4161/viru.22507.

[12] M. R. Gillings, M. Westoby, and T. M. Ghaly. "Pollutants That Replicate: Xenogenetic DNAs". In: *Trends in Microbiology* 26.12 (2018), pp. 975–977. ISSN: 18784380. DOI: 10.1016/j.tim.2018.08.003. URL: http://dx.doi.org/10.1016/j.tim.2018.08.003.

[13] A. Karkman, T. A. Johnson, C. Lyra, R. D. Stedtfeld, M. Tamminen, J. M. Tiedje, and M. Virta. "High-throughput quantification of antibiotic resistance genes from an urban wastewater treatment plant". In: *FEMS Microbiology Ecology* 92.3 (2016), pp. 1–7. ISSN: 15746941. DOI: 10.1093/femsec/fiw014.

[14] D. Calderón-Franco, Q. Lin, M. C. M. van Loosdrecht, B. Abbas, and D. G. Weissbrodt. "Anticipating Xenogenic Pollution at the Source : Impact of Sterilizations on DNA Release From Microbial Cultures". In: *Frontiers in Bioengineering and Biotechnology* 8.March (2020), pp. 1–13. DOI: 10.3389/fbioe.2020.00171.

[15] D. Calderón-Franco, M. van Loosdrecht, T. Abeel, and D. Weissbrodt. "Free-floating extracellular DNA: Systematic profiling of mobile genetic elements and antibiotic resistance from wastewater". In: *Water Research* 189.116592 (2021), pp. 1–13. DOI: 10.1101/2020.05.01.072397.

[16] X. Lu, X. X. Zhang, Z. Wang, K. Huang, Y. Wang, W. Liang, Y. Tan, B. Liu, and J. Tang. "Bacterial pathogens and community composition in advanced sewage treatment systems revealed by metagenomics analysis based on high-throughput sequencing". In: *PLoS ONE* 10.5 (2015), pp. 1–15. ISSN: 19326203. DOI: 10.1371/journal.pone.0125549.

[17] C. J. H. von Wintersdorff, J. Penders, J. M. van Niekerk, N. D. Mills, S. Majumder, L. B. van Alphen, P. H. M. Savelkoul, and P. F. G. Wolffs. "Dissemination of Antimicrobial Resistance in Microbial Ecosystems through Horizontal Gene Transfer." In: *Frontiers in microbiology* 7 (2016), p. 173. ISSN: 1664-302X. DOI: 10.3389/fmicb.2016.00173. URL: www.frontiersin.org%20http://www.ncbi.nlm.nih.gov/pubmed/26925045%0Ahttp://www.pubmedcentral.nih.gov/articlerender.fcgi?artid=PMC4759269.

[18] R. Pallares-Vega, H. Blaak, R. van der Plaats, A. M. de Roda Husman, L. Hernandez Leal, M. C. van Loosdrecht, D. G. Weissbrodt, and H. Schmitt. "Determinants of presence and removal of antibiotic resistance genes during WWTP treatment: A cross-sectional study". In: *Water Research* 161 (2019), pp. 319–328. ISSN: 18792448. DOI: 10.1016/j.watres.2019.05.100. URL: https://doi.org/10.1016/j.watres.2019.05.100.

[19] N. Czekalski, T. Berthold, S. Caucci, A. Egli, and H. Bürgmann. "Increased levels of multiresistant bacteria and resistance genes after wastewater treatment and their dissemination into Lake Geneva, Switzerland". In: *Frontiers in Microbiology* 3.MAR (2012), pp. 1–18. ISSN: 1664302X. DOI: 10.3389/fmicb.2012.00106.

[20] M. Pazda, J. Kumirska, P. Stepnowski, and E. Mulkiewicz. *Antibiotic resistance genes identified in wastewater treatment plant systems – A review*. 2019. DOI: 10.1016/j.scitotenv.2019.134023. URL: https://doi.org/10.1016/j.scitotenv.2019.134023.

[21] R. Destiani and M. R. Templeton. "Chlorination and ultraviolet disinfection of antibiotic-resistant bacteria and antibiotic resistance genes in drinking water". In: *AIMS Environmental Science* 6.3 (2019), pp. 222–241. ISSN: 23720352. DOI: 10.3934/environsci.2019.3.222.

[22] M. S. Wu and X. Xu. "Inactivation of antibiotic-resistant bacteria by chlorine dioxide in soil and shifts in community composition". In: *RSC Advances* 9.12 (2019), pp. 6526–6532. ISSN: 20462069. DOI: 10.1039/c8ra07997h.

[23] Q. B. Yuan, M. T. Guo, and J. Yang. "Fate of antibiotic resistant bacteria and genes during wastewater chlorination: Implication for antibiotic resistance control". In: *PLoS ONE* 10.3 (2015), pp. 1–11. ISSN: 19326203. DOI: 10.1371/journal.pone.0119403.

[24] Y. Yang, B. Li, S. Zou, H. H. Fang, and T. Zhang. "Fate of antibiotic resistance genes in sewage treatment plant revealed by metagenomic approach". In: *Water Research* 62 (2014), pp. 97–106. ISSN: 18792448. DOI: 10.1016/j.watres.2014.05.019. URL: http://dx.doi.org/10.1016/j.watres.2014.05.019.

[25] D. Mao, Y. Luo, J. Mathieu, Q. Wang, L. Feng, Q. Mu, C. Feng, and P. J. J. Alvarez. "Persistence of extracellular DNA in river sediment facilitates antibiotic resistance gene propagation". In: *Environmental Science and Technology* 48.1 (2014), pp. 71–78. ISSN: 15205851. DOI: 10.1021/es404280v.

[26] A. Torti, M. A. Lever, and B. B. Jørgensen. "Origin, dynamics, and implications of extracellular DNA pools in marine sediments". In: *Marine Genomics* 24 (2015), pp. 185–196. ISSN: 18747787. DOI: 10.1016/j.margen.2015.08.007. URL: http://dx.doi.org/10.1016/j.margen.2015.08.007.

[27] Y. Zhang, A. Li, T. Dai, F. Li, H. Xie, L. Chen, and D. Wen. "Cell-free DNA: A Neglected Source for Antibiotic Resistance Genes Spreading from WWTPs". In: *Environmental Science and Technology* 52.1 (2018), pp. 248–257. ISSN: 15205851. DOI: 10.1021/acs.est.7b04283.

[28] A. D. Kappell, L. K. Kimbell, M. D. Seib, D. E. Carey, M. J. Choi, T. Kalayil, M. Fujimoto, D. H. Zitomer, and P. J. McNamara. "Removal of antibiotic resistance genes in an anaerobic

membrane bioreactor treating primary clarifier effluent at 20 °C". In: *Environmental Science: Water Research and Technology* 4.11 (2018), pp. 1783–1793. ISSN: 20531419. DOI: 10.1039/c8ew00270c.

[29] M. V. Riquelme Breazeal, J. T. Novak, P. J. Vikesland, and A. Pruden. "Effect of wastewater colloids on membrane removal of antibiotic resistance genes". In: *Water Research* 47.1 (2013), pp. 130–140. ISSN: 18792448. DOI: 10.1016/j.watres.2012.09.044. URL: http://dx.doi.org/10.1016/j.watres.2012.09.044.

[30] B. W. Grehs, A. R. Lopes, N. F. Moreira, T. Fernandes, M. A. Linton, A. M. Silva, C. M. Manaia, E. Carissimi, and O. C. Nunes. "Removal of microorganisms and antibiotic resistance genes from treated urban wastewater: A comparison between aluminium sulphate and tannin coagulants". In: *Water Research* 166 (2019). ISSN: 18792448. DOI: 10.1016/j.watres.2019.115056.

[31] N. Li, G. P. Sheng, Y. Z. Lu, R. J. Zeng, and H. Q. Yu. "Removal of antibiotic resistance genes from wastewater treatment plant effluent by coagulation". In: *Water Research* 111 (Mar. 2017), pp. 204–212. ISSN: 18792448. DOI: 10.1016/j.watres.2017.01.010. URL: https://linkinghub.elsevier.com/retrieve/pii/S0043135417300106.

[32] C. Stange, J. P. Sidhu, S. Toze, and A. Tiehm. "Comparative removal of antibiotic resistance genes during chlorination, ozonation, and UV treatment". In: *International Journal of Hygiene and Environmental Health* 222.3 (2019), pp. 541–548. ISSN: 1618131X. DOI: 10.1016/j.ijheh.2019.02.002. URL: https://doi.org/10.1016/j.ijheh.2019.02.002.

[33] C. S. Zhou, J. W. Wu, L. L. Dong, B. F. Liu, D. F. Xing, S. S. Yang, X. K. Wu, Q. Wang, J. N. Fan, L. P. Feng, and G. L. Cao. "Removal of antibiotic resistant bacteria and antibiotic resistance genes in wastewater effluent by UV-activated persulfate". In: *Journal of Hazardous Materials* 388.October 2019 (2020), p. 122070. ISSN: 18733336. DOI: 10.1016/j.jhazmat.2020.122070. URL: https://doi.org/10.1016/j.jhazmat.2020.122070.

[34] X. Cheng, H. M. Delanka-Pedige, S. P. Munasinghe-Arachchige, I. S. Abeysiriwardana-Arachchige, G. B. Smith, N. Nirmalakhandan, and Y. Zhang. "Removal of antibiotic resistance genes in an algal-based wastewater treatment system employing Galdieria sulphuraria: A comparative study". In: *Science of the Total Environment* 711 (2020), p. 134435. ISSN: 18791026. DOI: 10.1016/j.scitotenv.2019.134435. URL: https://doi.org/10.1016/j.scitotenv.2019.134435.

[35] J. P. Van Der Hoek, H. De Fooij, and A. Struker. "Wastewater as a resource: Strategies to recover resources from Amsterdam's wastewater". In: *Resources, Conservation and Recycling* 113 (2016), pp. 53–64. ISSN: 18790658. DOI: 10.1016/j.resconrec.2016.05.012. URL: http://dx.doi.org/10.1016/j.resconrec.2016.05.012.

[36] E. Agrafioti, G. Bouras, D. Kalderis, and E. Diamadopoulos. "Biochar production by sewage sludge pyrolysis". In: *Journal of Analytical and Applied Pyrolysis* 101 (2013), pp. 72–78. ISSN: 01652370. DOI: 10.1016/j.jaap.2013.02.010. URL: http://dx.doi.org/10.1016/j.jaap.2013.02.010.

[37] P. Krzemiński and M. Popowska. *Treatment Technologies for Removal of Antibiotics, Antibiotic Resistance Bacteria and Antibiotic-Resistant Genes*. Springer, Cham, 2020, pp. 215–224. ISBN: 9789811315770. DOI: 10.1007/978-981-13-1577-0{_}11. URL: https://doi.org/10.1007/978-3-030-40422-2_19.

[38] J. Fang, L. Jin, Q. Meng, D. Wang, and D. Lin. "Interactions of extracellular DNA with aromatized biochar and protection against degradation by DNase I". In: *Journal of Environmental Sciences (China)* 101 (2021), pp. 205–216. ISSN: 18787320. DOI: 10.1016/j.jes.2020.08.017. URL: https://doi.org/10.1016/j.jes.2020.08.017.

[39] Y. Fu, F. Wang, H. Sheng, F. Hu, Z. Wang, M. Xu, Y. Bian, X. Jiang, and J. M. Tiedje. "Removal of extracellular antibiotic resistance genes using magnetic biochar/quaternary phosphonium salt in aquatic environments: A mechanistic study". In: *Journal of Hazardous Materials* 411 (2021), p. 125048. ISSN: 0304-3894. DOI: 10.1016/j.jhazmat.2021.125048. URL: http://dx.doi.org/10.1016/j.jhazmat.2021.125048.

[40] A. N. Ngigi, Y. S. Ok, and S. Thiele-Bruhn. "Biochar affects the dissipation of antibiotics and abundance of antibiotic resistance genes in pig manure". In: *Bioresource Technology*

315.June (2020), p. 123782. ISSN: 18732976. DOI: 10.1016/j.biortech.2020.123782. URL: https://doi.org/10.1016/j.biortech.2020.123782.

[41] G. Zhou, X. Qiu, X. Wu, and S. Lu. "Horizontal gene transfer is a key determinant of antibiotic resistance genes profiles during chicken manure composting with the addition of biochar and zeolite". In: *Journal of Hazardous Materials* 408.October 2020 (2021), p. 124883. ISSN: 18733336. DOI: 10.1016/j.jhazmat.2020.124883. URL: https://doi.org/10.1016/j.jhazmat.2020.124883.

[42] A. W. Vermeer and L. K. Koopal. "Adsorption of humic acids to mineral particles. 2. polydispersity effects with polyelectrolyte adsorption". In: *Langmuir* 14.15 (1998), pp. 4210–4216. ISSN: 07437463. DOI: 10.1021/la970836o.

[43] A. W. Vermeer, W. H. Van Riemsdijk, and L. K. Koopal. "Adsorption of humic acid to mineral particles. 1. Specific and electrostatic interactions". In: *Langmuir* 14.10 (1998), pp. 2810–2815. ISSN: 07437463. DOI: 10.1021/la970624r.

[44] M. Naderi. "Surface Area: Brunauer-Emmett-Teller (BET)". In: *Progress in Filtration and Separation* (2015), pp. 585–608. DOI: 10.1016/B978-0-12-384746-1.00014-8.

[45] J. Villarroel-Rocha, D. Barrera, and K. Sapag. "Introducing a self-consistent test and the corresponding modification in the Barrett, Joyner and Halenda method for pore-size determination". In: *Microporous and Mesoporous Materials* 200 (2014), pp. 68–78. ISSN: 13871811. DOI: 10.1016/j.micromeso.2014.08.017. URL: http://dx.doi.org/10.1016/j.micromeso.2014.08.017.

[46] D. C. Leite, F. C. Balieiro, C. A. Pires, B. E. Madari, A. S. Rosado, H. L. Coutinho, and R. S. Peixoto. "Comparison of DNA extraction protocols for microbial communities from soil treated with biochar". In: *Brazilian Journal of Microbiology* 45.1 (2014), pp. 175–183. ISSN: 16784405. DOI: 10.1590/S1517-83822014000100023.

[47] R. Han, Y. Wang, X. Zhao, Y. Wang, F. Xie, J. Cheng, and M. Tang. "Adsorption of methylene blue by phoenix tree leaf powder in a fixed-bed column: experiments and prediction of breakthrough curves". In: *Desalination* 245.1-3 (2009), pp. 284–297. ISSN: 00119164. DOI: 10.1016/j.desal.2008.07.013. URL: http://dx.doi.org/10.1016/j.desal.2008.07.013.

[48] S. Rouf and M. Nagapadma. "Modeling of Fixed Bed Column Studies for Adsorption of Azo Dye on Chitosan Impregnated with a Cationic Surfactant". In: *International Journal of Scientific & Engineering Research* 6.2 (2015), pp. 538–544. ISSN: 2229-5518. DOI: 10.14299/ijser.2015.02.006.

[49] Z. Z. Chowdhury, S. B. Abd Hamid, and S. M. Zain. "Evaluating design parameters for breakthrough curve analysis and kinetics of fixed bed columns for Cu(II) cations using lignocellulosic wastes". In: *BioResources* 10.1 (2015), pp. 732–749. ISSN: 19302126. DOI: 10.15376/biores.10.1.732-749.

[50] S. Chen, Q. Yue, B. Gao, Q. Li, X. Xu, and K. Fu. "Bioresource Technology Adsorption of hexavalent chromium from aqueous solution by modified corn stalk : A fixed-bed column study". In: *Bioresource Technology* 113 (2012), pp. 114–120. ISSN: 0960-8524. DOI: 10.1016/j.biortech.2011.11.110. URL: http://dx.doi.org/10.1016/j.biortech.2011.11.110.

[51] S. Chatterjee, S. Mondal, and S. De. "Design and scaling up of fixed bed adsorption columns for lead removal by treated laterite". In: *Journal of Cleaner Production* 177 (2018), pp. 760–774. ISSN: 09596526. DOI: 10.1016/j.jclepro.2017.12.249. URL: https://doi.org/10.1016/j.jclepro.2017.12.249.

[52] D. Moore and D. Dowhan. "Purification and Concentration of DNA". In: *Current Protocols in Molecular Biology* (2002).

[53] L. Ma, B. Li, X. T. Jiang, Y. L. Wang, Y. Xia, A. D. Li, and T. Zhang. "Catalogue of antibiotic resistome and host-tracking in drinking water deciphered by a large scale survey". In: *Microbiome* 5.1 (2017), p. 154. ISSN: 20492618. DOI: 10.1186/s40168-017-0369-0. URL: https://www.ncbi.nlm.nih.gov/pmc/articles/PMC5704573/pdf/40168_2017_Article_369.pdf.

[54] W. Song and M. Guo. "Quality variations of poultry litter biochar generated at different pyrolysis temperatures". In: *Journal of Analytical and Applied Pyrolysis* 94 (2012), pp. 138–145. ISSN: 01652370. DOI: 10.1016/j.jaap.2011.11.018. URL: http://dx.doi.org/10.1016/j.jaap.2011.11.018.

[55] A. Méndez, M. Terradillos, and G. Gascó. "Physicochemical and agronomic properties of biochar from sewage sludge pyrolysed at different temperatures". In: *Journal of Analytical and Applied Pyrolysis* 102 (2013), pp. 124–130. ISSN: 01652370. DOI: 10.1016/j.jaap.2013.03.006. URL: http://dx.doi.org/10.1016/j.jaap.2013.03.006.

[56] S. K. Sharma. "Adsorptive iron removal from groundwater". In: *Intemational Institute for Infrastructural, Hydraulic and Environmental Engineering* Master the (2001), pp. 39–41.

[57] D. A. Roberts, A. J. Cole, A. Whelan, R. de Nys, and N. A. Paul. "Slow pyrolysis enhances the recovery and reuse of phosphorus and reduces metal leaching from biosolids". In: *Waste Management* 64 (2017), pp. 133–139. ISSN: 18792456. DOI: 10.1016/j.wasman.2017.03.012. URL: http://dx.doi.org/10.1016/j.wasman.2017.03.012.

[58] L. A. Tarelho, T. Hauschild, A. C. Vilas-Boas, D. F. Silva, and M. A. Matos. "Biochar from pyrolysis of biological sludge from wastewater treatment". In: *Energy Reports* xxxx (2019), pp. 22–25. ISSN: 23524847. DOI: 10.1016/j.egyr.2019.09.063. URL: https://doi.org/10.1016/j.egyr.2019.09.063.

[59] A. G. Daful and M. R Chandraratne. *Biochar Production From Biomass Waste-Derived Material*. Elsevier Ltd., 2018, pp. 1–9. ISBN: 9780128035818. DOI: 10.1016/b978-0-12-803581-8.11249-4. URL: http://dx.doi.org/10.1016/B978-0-12-803581-8.11249-4.

[60] I. F. Titiladunayo, A. G. McDonald, and O. P. Fapetu. "Effect of temperature on biochar product yield from selected lignocellulosic biomass in a pyrolysis process". In: *Waste and Biomass Valorization* 3.3 (2012), pp. 311–318. ISSN: 18772641. DOI: 10.1007/s12649-012-9118-6.

[61] A. Ayala-Cortés, C. A. Arancibia-Bulnes, H. I. Villafán-Vidales, D. R. Lobato-Peralta, D. C. Martínez-Casillas, and A. K. Cuentas-Gallegos. "Solar pyrolysis of agave and tomato pruning wastes: Insights of the effect of pyrolysis operation parameters on the physicochemical properties of biochar". In: *AIP Conference Proceedings* 2126 (2019). ISSN: 15517616. DOI: 10.1063/1.5117681.

[62] M. B. Desta. "Batch sorption experiments: Langmuir and freundlich isotherm studies for the adsorption of textile metal ions onto teff straw (eragrostis tef) agricultural waste". In: *Journal of Thermodynamics* 1.1 (2013). ISSN: 16879244. DOI: 10.1155/2013/375830.

[63] P. Cai, Q. Huang, X. Zhang, and H. Chen. "Adsorption of DNA on clay minerals and various colloidal particles from an Alfisol". In: *Soil Biology and Biochemistry* 38.3 (2006), pp. 471–476. ISSN: 00380717. DOI: 10.1016/j.soilbio.2005.05.019.

[64] K. Saeki and T. Kunito. "Adsorptions of DNA molecules by soils and variable-charged soil constituents GMOs". In: *Applied Microbiology* 1 (2010), pp. 188–195.

[65] J. H. Yuan, R. K. Xu, and H. Zhang. "The forms of alkalis in the biochar produced from crop residues at different temperatures". In: *Bioresource Technology* 102.3 (2011), pp. 3488–3497. ISSN: 09608524. DOI: 10.1016/j.biortech.2010.11.018. URL: http://dx.doi.org/10.1016/j.biortech.2010.11.018.

[66] P. Cai, Q. Huang, D. Jiang, X. Rong, and W. Liang. "Microcalorimetric studies on the adsorption of DNA by soil colloidal particles". In: *Colloids and Surfaces B: Biointerfaces* 49.1 (2006), pp. 49–54. ISSN: 09277765. DOI: 10.1016/j.colsurfb.2006.02.011.

[67] C. Wang, T. Wang, W. Li, J. Yan, Z. Li, R. Ahmad, S. K. Herath, and N. Zhu. "Adsorption of deoxyribonucleic acid (DNA) by willow wood biochars produced at different pyrolysis temperatures". In: *Biology and Fertility of Soils* 50.1 (2014), pp. 87–94. ISSN: 01782762. DOI: 10.1007/s00374-013-0836-0.

[68] Y. Huang, J. K. Yang, and A. A. Keller. "Removal of arsenic and phosphate from aqueous solution by metal (hydr-)oxide coated sand". In: *ACS Sustainable Chemistry and Engineering* 2.5 (2014), pp. 1128–1138. ISSN: 21680485. DOI: 10.1021/sc400484s.

[69] P. Cai, Q.-Y. Huang, and X.-W. Zhang. "Interactions of DNA with clay minerals and soil colloidal particles and protection against degradation by DNase". In: *Environmental Science and Technology* 40.9 (2006), pp. 2971–2976. ISSN: 0013936X. DOI: 10.1021/es0522985.

[70] T. H. Nguyen and K. L. Chen. "Role of divalent cations in plasmid DNA adsorption to natural organic matter-coated silica surface". In: *Environmental Science and Technology* 41.15 (2007), pp. 5370–5375. ISSN: 0013936X. DOI: 10.1021/es070425m.

[71] Z. Dai, T. M. Webster, A. Enders, K. L. Hanley, J. Xu, J. E. Thies, and J. Lehmann. "DNA extraction efficiency from soil as affected by pyrolysis temperature and extractable organic carbon of high-ash biochar". In: *Soil Biology and Biochemistry* 115 (2017), pp. 129–136.

ISSN: 00380717. DOI: 10.1016/j.soilbio.2017.08.016. URL: https://doi.org/10.1016/j.soilbio.2017.08.016.

[72] K. H. Chu. "Breakthrough curve analysis by simplistic models of fixed bed adsorption: In defense of the century-old Bohart-Adams model". In: *Chemical Engineering Journal* 380.June 2019 (2020), p. 122513. ISSN: 13858947. DOI: 10.1016/j.cej.2019.122513. URL: https://doi.org/10.1016/j.cej.2019.122513.

[73] J. Kochany and W. Smith. "Application of humic substances in environmental remediation". In: *Application of humic substances in environmental remediation* 1 (2001). URL: https://www.researchgate.net/publication/228760064.

[74] K. Saeki, Y. Ihyo, M. Sakai, and T. Kunito. "Strong adsorption of DNA molecules on humic acids". In: *Environmental Chemistry Letters* 9.4 (2011), pp. 505–509. ISSN: 16103653. DOI: 10.1007/s10311-011-0310-x.

[75] H. J. Feng, L. F. Hu, Q. Mahmood, Y. Long, and D. S. Shen. "Study on biosorption of humic acid by activated sludge". In: *Biochemical Engineering Journal* 39.3 (2008), pp. 478–485. ISSN: 1369703X. DOI: 10.1016/j.bej.2007.11.004.

[76] H. M. Aly. "Short communication: Biochar and its importance in adsorption of antibiotic and heavy metals from aqueous solutions". In: *Ecological Questions* 24.1993 (2016), pp. 75–78. ISSN: 20835469. DOI: 10.12775/EQ.2016.014.

[77] R. Tian, C. Li, S. Xie, F. You, Z. Cao, Z. Xu, G. Yu, and Y. Wang. "Preparation of biochar via pyrolysis at laboratory and pilot scales to remove antibiotics and immobilize heavy metals in livestock feces". In: *Journal of Soils and Sediments* 19.7 (2019), pp. 2891–2902. ISSN: 16147480. DOI: 10.1007/s11368-019-02350-2.

[78] A. G. Capodaglio and A. Callegari. "Feedstock and process influence on biodiesel produced from waste sewage sludge". In: *Journal of Environmental Management* 216.2018 (2018), pp. 176–182. ISSN: 10958630. DOI: 10.1016/j.jenvman.2017.03.089. URL: https://doi.org/10.1016/j.jenvman.2017.03.089.

[79] M. Inguanzo, A. Domınguez, J. Menéndez, C. Blanco, and J. Pis. "On the pyrolysis of sewage sludge: the influence of pyrolysis conditions on solid, liquid and gas fractions". In: *Journal of Analytical and Applied Pyrolysis* 63.1 (Mar. 2002), pp. 209–222. ISSN: 01652370. DOI: 10.1016/S0165-2370(01)00155-3.

[80] I. H. Hwang, Y. Ouchi, and T. Matsuto. "Characteristics of leachate from pyrolysis residue of sewage sludge". In: *Chemosphere* 68.10 (2007), pp. 1913–1919. ISSN: 00456535. DOI: 10.1016/j.chemosphere.2007.02.060.

[81] H. Fathi Dokht, S. A. Movahedi Naeini, E. Dordipour, L. W. De Jong, and E. Hezarjaribi. "Effects of sewage sludge and its biochar on soybean yield in fine-textured loess soil". In: *Environmental Health Engineering and Management* 4.2 (2017), pp. 81–91. ISSN: 2423-3765. DOI: 10.15171/ehem.2017.12.

[82] K. A. Thompson, K. K. Shimabuku, J. P. Kearns, D. R. Knappe, R. S. Summers, and S. M. Cook. "Environmental Comparison of Biochar and Activated Carbon for Tertiary Wastewater Treatment". In: *Environmental Science and Technology* 50.20 (2016), pp. 11253–11262. ISSN: 15205851. DOI: 10.1021/acs.est.6b03239.

8

General discussion and outlook

This thesis aimed to explore the fate of resistance determinants in urban water systems. The main focus addressed the nature of the floating genetic materials as a potential source of antibiotic resistance via natural transformation as a horizontal gene transfer phenomenon.

When this Ph.D. project started, I usually got asked, "How many people will die from this?", "Are these antibiotic resistance gene concentrations dangerous?" or "Shall we add more stringent control measures?". Such public questions do not have easy answers, mainly when seeking to translate environmental indicators into direct impact on human health. There are no shortcuts or dichotomic answers. The last twenty years have uncovered the issue, highlighted where to look at it, and proposed potential solutions. However, the reality is that scientists and joint actions with governments and organizations are still in the phase, where knowledge gaps are stated and technical advances are being developed.

Scientific elucidation of microbial processes that transfer antibiotic resistance in complex microbial communities of wastewater and drinking water environments is needed.

8.1. The general issue in antimicrobial resistance studies

A general issue in antimicrobial resistance studies is the impossibility of analyzing everything, everywhere, all at once. Therefore, the whole problem must be split into multiple research questions. It is usually difficult to grasp the key variables and translate them into measures independently, but very valuable when systematically combined. The central knowledge gap is where and which are the primary sources of antibiotics and antibiotic resistance genes (ARGs). It seems an easy question to answer, but the potential compartments involved in resistance development and transfer are many and widespread: human population, anthropogenic barriers, sewage, industrial pollution, animal agriculture, aquaculture, and a long list following up. These are only some locations where antibiotics are highly used. Once the potential hotspots have been selected, which data to collect, and how to quantify and present it appropriately is essential to categorize and rank risks. Something as basic as how to quantify ARGs to evaluate their load in the different compartments should still to be harmonized. Joint efforts on interlaboratory studies to validate and recommend methodologies for qPCR quantification in WWTP samples are being made, e.g., within the EU H2020 Twinning Project (REPARES) that bridged to this thesis.

Another key knowledge gap involves the role of the environment affected by anthropogenic inputs on the development and evolution of antibiotic resistance. This is mainly due to the complexity added in studies with bacterial communities, where exposure-effect relationships, such as antibiotic exposure and selection for resistance communities, are challenging to establish due to the time needed for them to emerge. Antibiotics could modulate interactions in microbial communities

(i.e., by quorum sensing or by selecting for resistant bacteria). Adequate methods are one of the main limitations when gene transfer and persistence in microbial communities want to be studied [1].

Then, the most critical question remains: how does exposure to antibiotic-resistant bacteria (ARB) affect human health when originating from this multiverse of environmental routes? Again, quantitative data on environmental exposure is essential and scarce to answer this. This would link disease burden to specific exposure routes such as food or water consumption. To do so, quantitative microbial risk assessment could be put in place, which involves a similar thinking process as the one done for (e.g.) genetically modified organisms (**Table** 8.1). Information on how bacteria, genes, and selective antibiotic concentrations reach the environment and how bacteria evolve in specific systems and time-frames is not enough evidence to deduce environmental transmission routes. More research on how to quantitatively attribute antibiotic resistance to specific transmission routes in different settings and geographical regions by expanding sampling plans and integrating the separate environmental compartments, time points, and other selection pressures such nutrient limitation and influent flow rates would give hints on gene flows.

In the antibiotic resistance field, little events do not necessarily mean better or less dangerous as one event in environmental settings can lead to severe consequences in later stages. When horizontal gene transfer rates are evaluated, even the less common transfer mechanisms, such as transformation or transduction in comparison to conjugation, must be considered: genetic transfer only needs to happen once at the right time and place (or host) to become a serious outcome.

Overall, this thesis did not aim at solving the antibiotic resistance problem at once, but to add some grains to the bricks used to construct a new section of this difficult building. If we had to fit this thesis into the quantitative microbial risk assessment (QMRA) framework, it would be embedded in between "hazard identification" and "exposure assessment". This new section wanted to discuss the role of free-floating genetic composition in aquatic and anthropogenic barriers environments and the antibiotic-resistance development that, until now, were unnoticed.

Table 8.1: Comparison of QMRA approach for GMOs and AMRs

	GMOs	AMRs
Main guidelines available	Directive 2009/41/EC [2]	Codex Alimentarius (CAC/GL 77-2011) [3]
	Directive 2001/18/EC [4]	[5]
	EFSA guidance on GMOs for food and feed [6]	[7]
Focus	Food, agriculture and medicine	Food, agriculture, medicine and veterinary
Hazard identification	Information of the GMM and parental strain	Characteristics of the microorganism
	Characteristics of inserted sequence(s)	Information related to the specific antibiotic resistance(s)
	Description of the genetic modification	Potential adverse effects
	Spectrum of potential adverse effects	
Exposure assessment	Routes of exposure	Concentration of antibiotics and ARBs
	Population size and frequency of exposure	Routes of exposure
	Exposure parameters	AMR transfer mechanisms
	Dose equation	Predictive dose model
Hazard characterisation	Dose-response model	Minimum inhibitory concentrations
	Magnitude estimation of consequences	Dose-response model
Risk Characterisation	Risk estimation as disease metrics	Risk estimation as disease metrics
	Limitations, uncertainty and variability	Limitations, uncertainty and variability

8.2. The free-floating genetic journey in aquatic environments

Water is the media that connects all the compartments under the One Health umbrella. Therefore, it is the logical path through which genetic information travels. If we set ourselves in a biotechnology department in a research facility, most probably there is work carried out on microorganisms: some of them on mixed culture fermentation and others on biocatalysis or microorganisms' metabolic engineering. When the experiments conclude, these microbial broths need to be discharged, but even if the microorganisms are "generally recognized as safe (GRAS)", sterilization procedures are usually in place. Then, *what happens with the DNA released from microbial cultures?* This could be the hypothetical beginning of our story.

Sterilization procedures do not entirely compromise extracellular DNA integrity

In **Chapter 2**, I investigated the effect of autoclaving, disinfection with glutaraldehyde, and microwaving to inactivate microbial broths, healthcare equipment, and GMOs produced at biofoundries. The results showed that current sterilization methods are effective on microorganism inactivation but do not safeguard an aqueous residue exempt from biologically reusable xenogenic material, being standard autoclaving the most severe DNA-affecting method. Therefore, stable DNA is released from microbial cultures and ends up in sewage streams with genetic information from microorganisms originating from human and animal discharges. Across the whole EU, about 90% of urban wastewaters are collected and treated according to the EU Waste Water Treatment Directive. Then, whatever genetic discharge would end up being treated in urban wastewater treatment plants, entering into contact with microbial communities responsible for the biological treatment. This chapter raised the follow-up question: *what is the composition of this free-floating extracellular DNA, and does it have the potential to be transformed by mixed cultures?*

Free-floating extracellular DNA can be extracted from complex water matrixes and is mainly composed of mobile genetic elements

In **Chapter 3**, we developed a method using anion-exchange chromatography to isolate and enrich free-floating extracellular DNA without causing cell lysis from complex wastewater matrices like influent (an amount of 9 g exDNA was obtained out of 1 L), activated sludge (5.6 g out of 1 L), and treated effluent (4.3 g out of 1 L). Antibiotic resistance genes and mobile genetic elements were metagenomically profiled for both intracellular and extracellular DNA fractions. The metagenome highlighted that exDNA mainly comprises mobile genetic elements (65%). The prevalence of mobile genetic elements in the extracellular fraction can indirectly promote antibiotic resistance development mainly via natural transformation. However, before evaluating potential factors inducing DNA uptake, another

question arose: *What are the dynamics of these MGEs and ARGs in full-scale wastewater and drinking water treatment plants?*

Anthropogenic barriers, such as wastewater and drinking water treatment plants, efficiently decrease the resistance determinants load in their effluents

In **Chapters 4** and **5**, the transfer of ARGs and MGEs and their removal capacity in a full-scale Nereda® reactor removing nutrients with aerobic granular sludge and in chlorine-free drinking water treatment plants were evaluated.

In the Nereda® reactor (**Chapter 4**), we tracked the composition and fate of the intracellular DNA and free-floating exDNA pools of influent, sludge, and effluent samples. Metagenomics was used to profile the microbiome, resistome, and mobilome signatures from both DNA extracts. *Pseudomonas*, *Acinetobacter*, *Aeromonas*, *Acidovorax*, *Rhodoferax*, and *Streptomyces* populations were the main potential hosts of ARGs in the sludge. In the effluent, 89% of the resistance determinants were from exDNA fraction, potentially released by cell lysis during aeration in the reactor. MGEs and multiple ARGs were co-localized on the same extracellular genetic contigs. Total intracellular ARGs decreased up to 42% due to wastewater treatment. However, some ARGs increased by 1-2 log gene copies mL^{-1}, in the exDNA pool from influent to effluent. Then, we concluded that the exDNA fractions are usually overlooked, especially in high microbial cell density settings, where communication and DNA exchange may occur.

Drinking water treatment plants (DWTPs, **Chapter 5**) are the last anthropogenic barrier before reaching tap water for human consumption. They are not designed to remove antibiotic resistance determinants, but to eliminate physical, chemical, and biological contaminants from the water before consumption. The effect of biological unit operations and chlorine-free full-scale DWTPs on resistance determinants has been largely overlooked, and especially on the risk of promoting the selection of ARB across the process chain. They reduced the load of ARGs and MGEs in the water by about 2.5 log gene copies mL^{-1}, despite their increase in the UV disinfection systems. The total microbial load was also reduced, and none of the DWTPs were enriched for ARB. This highlights the function of chlorine-free DWTPs for the supply of safe drinking water, while in addition reducing the load of antibiotic resistance determinants. Special attention must, however, be paid to disinfection processes for their propensity to amplify antimicrobial resistance.

Then, we know that antibiotic resistance and mobile genetic information reaching wastewater and DWTPs decrease their load after treatment, at least when inside active bacterial cells. It is less clear when it comes to exDNA, since the process per se involves cell decay and lysis that releases DNA into the environment.

One can wonder what would happen if this released DNA into the environment or human gut encountered specific selection pressures, such as the presence of antibiotics when people are being treated for an infection, or if the water

containing this DNA ended up in swine or poultry farms where antibiotics are used as growth promoters? The resulting question would address: *What is the effect of increasing antibiotic concentrations on DNA uptake in complex systems?*

Environmental antibiotic concentrations do not seem to promote transformation events, while lab-selection and industrial-discharge concentrations do

Microorganisms in complex systems have constantly evolved under various environmental stressors using different adaptive horizontal gene transfer mechanisms. These benefit from transferring genetic information like antibiotic resistance via mobile genetic elements such as plasmids. In **Chapter 6**, we showed the feasibility of distantly-related microorganisms for DNA uptake when strong environmental pressures were applied. Two chemostats (one control and one test) were inoculated with activated sludge and used to study the transformation capacity of a rolling-circle plasmid encoding GFP and kanamycin resistance genes at increasing concentrations of kanamycin. Plasmid DNA was daily spiked in the test chemostat. Potential natural transformant microorganisms were analyzed by Hi-C sequencing at the reactor steady-state uneder applications of environmental (2.5 mg L^{-1}) and lab-selection kanamycin concentrations (50 mg L^{-1}). We showed that the plasmid successfully transformed inside different bacteria such as *Bosea sp.*, *Runella sp.*, and *Microbacterium sp.* under lab selection antibiotic concentrations.

This opens the door for discussion if bacteria can only uptake DNA via the acquisition of the canonical competence state or if there are other mechanisms that, under certain circumstances, can promote DNA transformation. The second would be very interesting for future research as only a dozen bacterial species have been described as naturally competent.

Suppose free-floating extracellular DNA in the form of a plasmid and other mobile genetic elements can transform into distantly-related bacteria when strong selection pressures are applied. *Is there any technology available to remediate such DNA fraction and antibiotic-resistant bacteria?*

Residues from Wastewater and drinking water treatment plants are attractive as low-cost adsorbents to minimize the spread of antimicrobial resistances in the aquatic environment

In **Chapter 7**, we showed how byproducts from wastewater and drinking water treatment plants, such as sewage-sludge biochar and iron-oxide coated sands, were effective at removing antibiotic-resistant bacteria and free-floating extracellular DNA from effluent waters. By aligning to UN Sustainable Development Goals for clean water sanitation and responsible consumption and production, we provide a solution to mitigate the emission of problematic xenogenetic elements from sewage into surface waters. The remaining question is whether and where to introduce such control and remediation points. It would be unfeasible (economically and

logistically) to control all the treated water end-of-pipe. At the same time, decentralized technologies in antimicrobial resistance hotspots, where smaller flows are present, would be an option to be researched.

8.3. Perspectives and self-reflection

This thesis has demonstrated that free-floating extracellular DNA exists ubiquitously in aquatic environments before and after water treatment and sanitation. We now have a method (not the fastest, I must admit) to isolate extracellular DNA at a substantial amount enabling its sequencing at high-resolution: the exDNA contains genetic information for multiple mobile genetic elements and associated antibiotic resistance genes. We can now fill one important knowledge gap.

Then, should we stop here? If this is science, the logical answer would be "no, never.". Before closing this small delicate piece of easy-to-digest informative pages, I wanted to highlight what I learned and add some suggestions. Expanding the approach of some experiments would surely answer specific research questions better and with fewer sacrifices.

The complexity conundrum

High complexity is often linked to unpredictability and difficulty in drawing cause-effect connections. This thesis dealt with numerous metagenomic datasets collected from complex systems: wastewater samples, different-sized biomass samples, drinking water samples, enrichment cultures, among others. There are simply too many interactions going on between microorganisms and between them and the environment. This can easily lead to inconsistent and contradictory results towards better capturing mechanisms and processes.

The 'snapshot' approach, where the microbiome or resistome is analyzed at a single point in time, poses certain limitations. In this thesis, as time and resources allowed, we tried to assess the natural variability during different time points (**Chapters 4** and **6**) to check the effect of external factors such as the change in antibiotic concentrations.

Taking two steps backward could be beneficial for making sense of the data. Sometimes "Simple is Better." Initially, it was the intention of this thesis to assess which were the environmental selection pressures triggering extracellular DNA transformation into which bacteria from complex communities. It soon became apparent that that was not a simple task; not only for having to work in Biosafety level II installations but also for the number of variables that needed to be taken into account and sorted out when reproducing at lab-scale what could eventually occur in biological wastewater biological treatment systems.

Therefore, if the intention is to quantify the effect environmental factors on inducing transformation, I would start with a bottom-up approach (most

straightforward to most complex) and then integrate *in vitro*, *in vivo*, and *in situ* quantification experiments. It would begin with *in vitro* experiments in pure cultures (model Gram-negative to Gram-positive microorganisms) to quantify transformation rates in highly controlled bench-scale conditions under a factorial design of experiments. This would allow the generation of a mathematical model on gene transfer rates under different environmental conditions. The variables would follow a similar approach as in Pallares-Vega et al. [8], including different environmentally relevant temperatures, different nutrients availability such as rich *vs.* minimal media with all or lacking some essential chemicals such as phosphorus or specific trace elements, and the exposure to various chemicals concentration (antibiotics, chemicals, and other drugs found in receiving waters). Moreover, the nature of the exogenous DNA would be critical to be analyzed when transformation is assessed. For example, by evaluating transformation rates of double-stranded DNA versus single-stranded DNA, linear versus circular DNA, and methylation patterns presence. Some preliminary results [9] on this topic showed that DNA topology impacts natural transformation. There are significant differences in transformation frequencies when linear DNA (70-100%) is provided in *E. coli* K12 pure cultures in comparison to plasmid DNA (20-30%) (containing kanamycin resistance gene), especially when cells are encountered with bacteriostatic kanamycin concentrations (10 µg mL^{-1}) (**Figure 8.1**). The following experiments would involve *in vivo* quantification to confirm the results obtained *in vitro* using a synthetic known mock community with representative activated sludge bacteria. The factors selected from the combination of *in vitro* and *in vivo* experiments would be the perfect basis for *in situ* transformation quantification, which would be an adapted and targeted version of **Chapter 6** that addressed the effect of antibiotic concentrations on transformation events in mixed cultures.

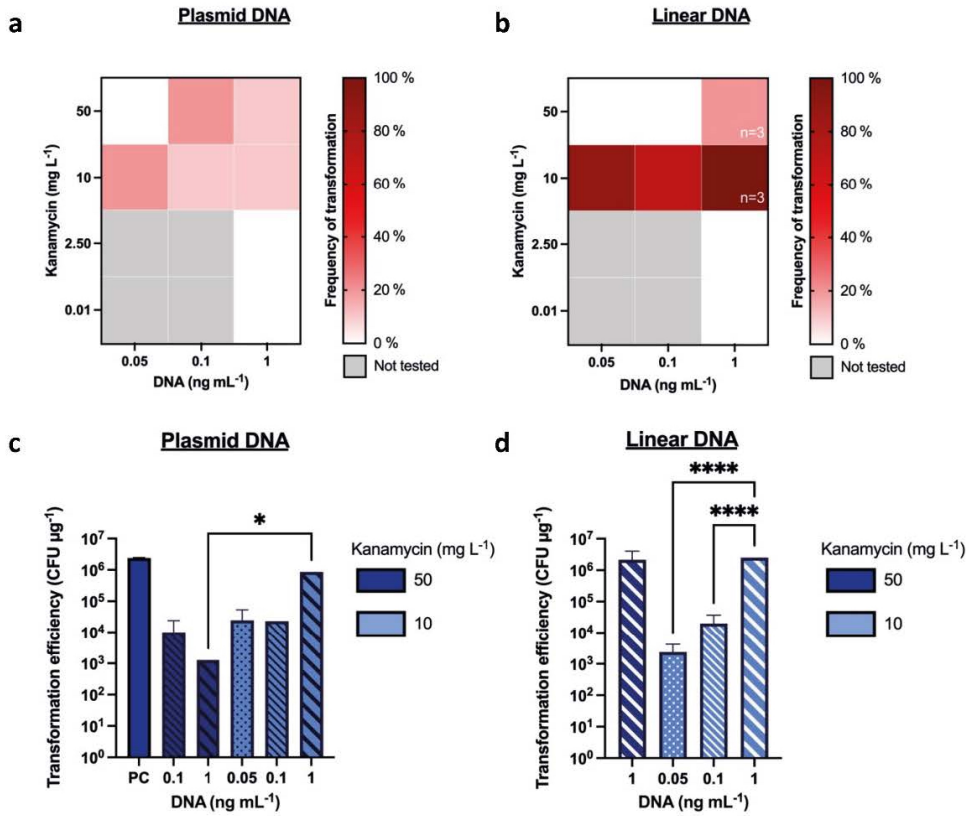

Figure 8.1: Heatmap of natural transformation frequency of *E. coli* K12 at 37C in M9 minimal media with 0.4% glucose and 0.6% tryptophan after 24h. Heat map of natural transformation frequency at 0.01, 2.5, 10, 50 mg L^{-1} kanamycin and 0.05, 0.1, 1 g mL^{-1} unmethylated **a** plasmid DNA, **b** linear DNA. For each conditions n = 10, unless stated. For those conditions that naturally transformed in a and b, natural transformation efficiency for **c** plasmid DNA and **d** linear DNA was plotted together with PC of artificially transformed *E. coli* K12 with pBAV1K-T5-gfp. Statistical analysis was performed by one-way ANOVA followed by Sidak's test (* P0.05, **** P0.0001).

The floating mobilome peculiarity

Intracellular DNA of prokaryotic and eukaryotic cells was released and maintained some of its integrity after different sterilization procedures (**Chapter 2**). Free-floating extracellular could be isolated from water matrixes and characterized as an enriched DNA fraction containing mobile genetic elements (**Chapter 3** and **4**). In Chapter 6, it was proven that, high antibiotic concentrations could induce cell survival mode by which they could transform plasmid DNA conferring resistance against specific antibiotics. The logical next step from here would be to characterize the extracellular mobilome at high-resolution: to identify specific plasmids, which are extrachromosomal and can be transferred between bacterial hosts. This would identify, at last, what is the transferability potential of such

genetic pool found floating in (waste)water environments. Preliminary results from this thesis have shown that the combination of the isolation method developed in **Chapter 3** plus long-read sequencing (e.g., Oxford Nanopore) have the potential to recover full circular genetic fragments from wastewater environments (**Figure 8.2**). Such circular closed genetic fragments range from 1000 bp up to more than 300 kb. This is interesting as such genetic fraction could contain information about plasmids with average length 30-200 kb but also viral nucleic acids which can go from 1-2.5 Mb average length. Further profiling would give an information of the host-range of such mobile genetic elements as well as their antimicrobial resistances cargo. Hybrid approaches combining short and long-read sequencing could be a promising alternative to recover MGEs for better functional characterization and host origin and association.

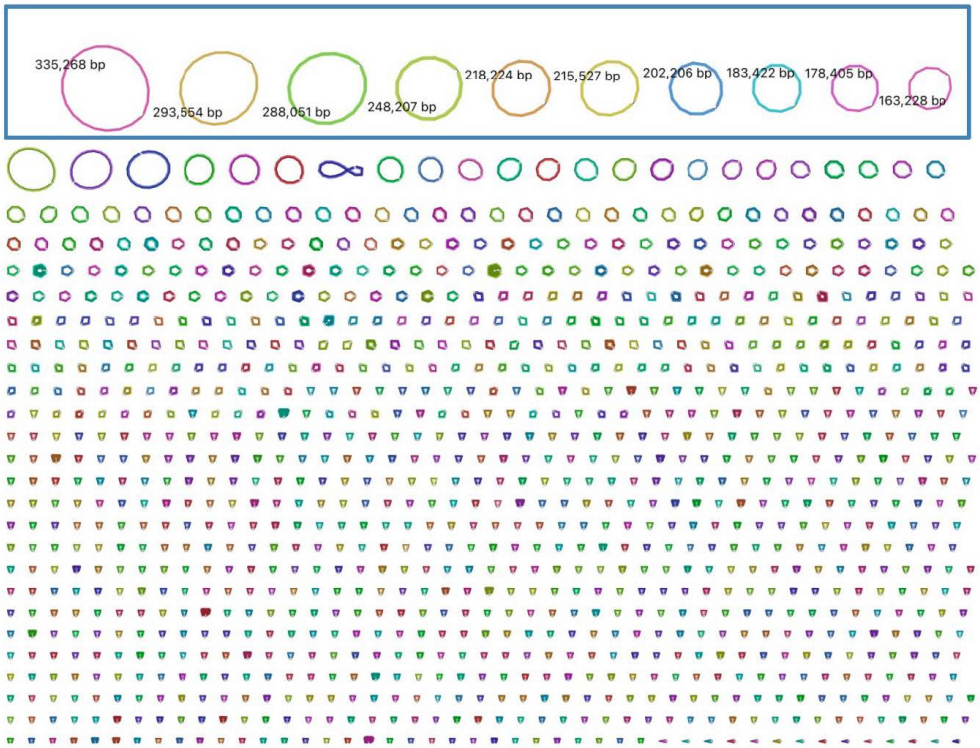

Figure 8.2: Bandage visualization of circular contigs obtained from long-read sequencing (ONT) using free-floating extracellular DNA from activated sludge samples.

The multiomics paradox

Do not get spellbound by the glowing, magical multiomics paraphernalia. That would be one of my warnings. No scandals, please. Let me explain.

A paradox comes from Latin paradoxa, meaning 'opposite to the common opinion.'

When we, enlightened scientists, start working in biotechnology, we always want to use the last advances to answer our research questions. In my Bachelor's and Master's degrees, I remember how they presented all the different -omic technologies as the saviors of current and future-to-be science. Somehow, they are. Big biological data has become a central part of biomedical research, industrial biotechnology, environmental sciences, and many other fields, advancing and establishing the biotech area where it belongs.

Therefore, we could say that the 'common opinion' is that -omics are good and can give us answers to multiple problems: which is not entirely a lie. However, it is easy to sink into the humongous amount of data multiomics generates. Metagenomics, metatranscriptomics, metaproteomics, and metabolomics can produce a large amount of data in a short time. However, a significant challenge is exploiting and interpreting these data to develp scientific theories and concepts that can be used to assist risk managers and engineering practitioners in the water safety and quality decisions [10].

Having a clear research question and anticipating and setting the tools to be used during the bioinformatic analysis will simplify the study and convey messages and outcomes. The massive amount of tools, datasets, databases, and pipelines available in the literature and online repositories can overwhelm new and experienced researchers in the field [11].

The data expedition

Reducing sequencing costs, advances in sequencing technologies and increased computational power have facilitated an overwhelming number of mobilome, resistome, and microbiome studies. Then, a multi-study meta-analysis would infer better relationships than' snapshot' experiments to evaluate the effect of different conditions such as seasonal variations, wastewater treatment configurations, and other particularities on the metagenomes. A meta-analysis is the examination of data from several independent studies of the same subject to determine overall trends. Examples of those are the recent meta-analysis on the activated sludge [12], drinking water [13], and gut microbiome [14]. This way, it is possible to generate results with greater statistical power than individual analyses [15].

Gene signatures, biomarkers, and pathways that provide new insights into a phenotype of interest have been identified by analyzing large-scale datasets in several fields of science. However, despite all the efforts, a standardized regulation to report large-scale data and identify the molecular targets and signaling networks are still lacking. Integrative analyses serve as complement (adding quantitative data like qPCR results) for meta-analysis methodologies to generate novel hypotheses.

The collaboration amalgamation

Coming back to the questions I was being asked by different stakeholders during my whole Ph.D. project, I would now say that I could give them an answer (a hint) if the human resources for such a quest were bigger and included an amalgam of different expertise. This would consist of not only scientists (wet and dry-lab) as interventions are not only of a technical nature but also of social and governmental nature. These stakeholders include the health-, water- and agriculture sectors, regulatory agencies, experts in risk assessment, pharma companies, trade associations, NGOs, (social) media, WHO, FAO, OiE (World Organization for Animal Health), EU, and the different government's [16, 17]. The aim of this joint venture would be "the development of acceptable emission levels and environmental quality standards for selective agents and resistant bacteria, as well as methodology to define such levels and standards" [1].

Bibliography

[1] D. G. Larsson, A. Andremont, J. Bengtsson-Palme, K. K. Brandt, A. M. de Roda Husman, P. Fagerstedt, J. Fick, C. F. Flach, W. H. Gaze, M. Kuroda, K. Kvint, R. Laxminarayan, C. M. Manaia, K. M. Nielsen, L. Plant, M. C. Ploy, C. Segovia, P. Simonet, K. Smalla, J. Snape, E. Topp, A. J. van Hengel, D. W. Verner-Jeffreys, M. P. Virta, E. M. Wellington, and A. S. Wernersson. *Critical knowledge gaps and research needs related to the environmental dimensions of antibiotic resistance*. 2018. DOI: 10.1016/j.envint.2018.04.041.

[2] European Parliament and European Council. *Directive 2009/41/EC of the European Parliament and of the Council of 6 May 2009 on the contained use of genetically modified microorganisms*. 2009.

[3] Codex Alimentarius. *Guidelines for risk analysis of foodborne antimicrobial resistance (CAC/GL 77-2011)*. Rome, 2001.

[4] European Parliament and European Council. *Directive 2001/18/EC of the European Parliament and of the Council of 12 March 2001 on the deliberate release into the environment of genetically modified organisms and repealing Council Directive 90/220/EEC*. 2001.

[5] N. J. Ashbolt, A. Amézquita, T. Backhaus, P. Borriello, K. K. Brandt, P. Collignon, A. Coors, R. Finley, W. H. Gaze, T. Heberer, J. R. Lawrence, D. J. Larsson, S. A. McEwen, J. J. Ryan, J. Schönfeld, P. Silley, J. R. Snape, C. Van den Eede, and E. Topp. "Human Health Risk Assessment (HHRA) for Environmental Development and Transfer of Antibiotic Resistance". In: *Environmental Health Perspectives* 121.9 (Sept. 2013), pp. 993–1001. ISSN: 0091-6765. DOI: 10.1289/ehp.1206316.

[6] EFSA Panel on Genetically Modified Organisms. "Guidance on the risk assessment of genetically modified microorganisms and their products intended for food and feed use". In: *EFSA Journal* 9.6 (June 2011), p. 2193. ISSN: 18314732. DOI: 10.2903/j.efsa.2011.2193.

[7] Y. Ben, C. Fu, M. Hu, L. Liu, M. H. Wong, and C. Zheng. "Human health risk assessment of antibiotic resistance associated with antibiotic residues in the environment: A review". In: *Environmental Research* 169 (Feb. 2019), pp. 483–493. ISSN: 00139351. DOI: 10.1016/j.envres.2018.11.040.

[8] R. Pallares-Vega, G. Macedo, M. S. Brouwer, L. Hernandez Leal, P. van der Maas, M. C. van Loosdrecht, D. G. Weissbrodt, D. Heederik, D. Mevius, and H. Schmitt. "Temperature and Nutrient Limitations Decrease Transfer of Conjugative IncP-1 Plasmid pKJK5 to Wild Escherichia coli Strains". In: *Frontiers in Microbiology* 12.July (2021). ISSN: 1664302X. DOI: 10.3389/fmicb.2021.656250.

[9] R. Kuriki. "Natural transformation of antibiotic resistance genes carried by mobile genetic elements in bacterial pure cultures and environmental enrichments". In: *TU Delft Repository* (2022).

[10] L. Cocolin, M. Mataragas, F. Bourdichon, A. Doulgeraki, M. F. Pilet, B. Jagadeesan, K. Rantsiou, and T. Phister. "Next generation microbiological risk assessment meta-omics: The next need for integration". In: *International Journal of Food Microbiology* 287.October 2017 (2018), pp. 10–17. ISSN: 18793460. DOI: 10.1016/j.ijfoodmicro.2017.11.008. URL: https://doi.org/10.1016/j.ijfoodmicro.2017.11.008.

[11] M. Krassowski, V. Das, S. K. Sahu, and B. B. Misra. "State of the Field in Multi-Omics Research: From Computational Needs to Data Mining and Sharing". In: *Frontiers in Genetics* 11.December (2020), pp. 1–17. ISSN: 16648021. DOI: 10.3389/fgene.2020.610798.

[12] V. Palanisamy, V. Gajendiran, and K. Mani. "Meta-analysis to identify the core microbiome in diverse wastewater". In: *International Journal of Environmental Science and Technology* 19.6 (2022), pp. 5079–5096. ISSN: 17352630. DOI: 10.1007/s13762-021-03349-4. URL: https://doi.org/10.1007/s13762-021-03349-4.

[13] C. Thom, C. J. Smith, G. Moore, P. Weir, and U. Z. Ijaz. "Microbiomes in drinking water treatment and distribution: A meta-analysis from source to tap". In: *Water Research* 212.January (2022), p. 118106. ISSN: 18792448. DOI: 10.1016/j.watres.2022.118106. URL: https://doi.org/10.1016/j.watres.2022.118106.

[14] C. Duvallet, S. M. Gibbons, T. Gurry, R. A. Irizarry, and E. J. Alm. "Meta-analysis of gut microbiome studies identifies disease-specific and shared responses". In: *Nature Communications* 8.1 (2017). ISSN: 20411723. DOI: 10.1038/s41467-017-01973-8.

[15] K. Cervantes-Gracia, R. Chahwan, and H. Husi. "Integrative OMICS Data-Driven Procedure Using a Derivatized Meta-Analysis Approach". In: *Frontiers in Genetics* 13.February (2022), pp. 1–17. ISSN: 16648021. DOI: 10.3389/fgene.2022.828786.

[16] R. Laxminarayan, A. Duse, C. Wattal, A. K. Zaidi, H. F. Wertheim, N. Sumpradit, E. Vlieghe, G. L. Hara, I. M. Gould, H. Goossens, C. Greko, A. D. So, M. Bigdeli, G. Tomson, W. Woodhouse, E. Ombaka, A. Q. Peralta, F. N. Qamar, F. Mir, S. Kariuki, Z. A. Bhutta, A. Coates, R. Bergstrom, G. D. Wright, E. D. Brown, and O. Cars. "Antibiotic resistance-the need for global solutions". In: *The Lancet Infectious Diseases* 13.12 (2013), pp. 1057–1098. ISSN: 14733099. DOI: 10.1016/S1473-3099(13)70318-9.

[17] R. Laxminarayan, C. F. Amábile-Cuevas, O. Cars, T. Evans, D. L. Heymann, S. Hoffman, A. Holmes, M. Mendelson, D. Sridhar, M. Woolhouse, and J. A. Røttingen. "UN High-Level Meeting on antimicrobials—what do we need?" In: *The Lancet* 388.10041 (2016), pp. 218–220. ISSN: 1474547X. DOI: 10.1016/S0140-6736(16)31079-0.

[18] D. Calderón-Franco, M. C. M. van Loosdrecht, T. Abeel, and D. G. Weissbrodt. "Catch me if you can : Capturing extracellular DNA transformation in mixed cultures via Hi-C sequencing". In: *bioRxiv* (2022), pp. 1–38. DOI: https://doi.org/10.1101/2022.09.16.508255.

[19] D. Calderón-Franco, R. Sarelse, S. Christou, M. Pronk, M. C. M. van Loosdrecht, T. Abeel, and D. G. Weissbrodt. "Metagenomic profiling and transfer dynamics of antibiotic resistance determinants in a full-scale granular sludge wastewater treatment plant". In: *Water Research* (2022). DOI: 10.1016/j.watres.2022.118571.

[20] D. Calderón-Franco, L. Orschler, S. Lackner, S. Agrawal, and D. G. Weissbrodt. "Monitoring SARS-CoV-2 in sewage: Toward sentinels with analytical accuracy". In: *Science of the Total Environment* 804 (2022). ISSN: 18791026. DOI: 10.1016/j.scitotenv.2021.150244.

[21] A. Miłobedzka, C. Ferreira, I. Vaz-Moreira, D. Calderón-Franco, A. Gorecki, S. Purkrtova, Jan Bartacek, L. Dziewit, C. M. Singleton, P. H. Nielsen, D. G. Weissbrodt, and C. M. Manaia. "Monitoring antibiotic resistance genes in wastewater environments: The challenges of filling a gap in the One-Health cycle". In: *Journal of Hazardous Materials* 424 (2022). ISSN: 18733336. DOI: 10.1016/j.jhazmat.2021.127407.

[22] D. Calderón-Franco, S. Apoorva, G. Medema, M. C. van Loosdrecht, and D. G. Weissbrodt. "Upgrading residues from wastewater and drinking water treatment plants as low-cost adsorbents to remove extracellular DNA and microorganisms carrying antibiotic resistance genes from treated effluents". In: *Science of the Total Environment* 778 (2021), p. 146364. ISSN: 18791026. DOI: 10.1016/j.scitotenv.2021.146364.

[23] D. Calderón-Franco, M. van Loosdrecht, T. Abeel, and D. Weissbrodt. "Free-floating extracellular DNA: Systematic profiling of mobile genetic elements and antibiotic resistance from wastewater". In: *Water Research* 189.116592 (2021), pp. 1–13. DOI: 10.1101/2020.05.01.072397.

[24] D. Calderón-Franco, Q. Lin, M. C. M. van Loosdrecht, B. Abbas, and D. G. Weissbrodt. "Anticipating Xenogenic Pollution at the Source : Impact of Sterilizations on DNA Release From Microbial Cultures". In: *Frontiers in Bioengineering and Biotechnology* 8.March (2020), pp. 1–13. DOI: 10.3389/fbioe.2020.00171.

Epilogue

In the last two weeks of my Ph.D., I had the pleasure to attend the International Symposium on the Environmental Dimension of Antibiotic Resistance in Gothenburg, Sweden. During Prof. Tong Zhang's keynote presentation, he shared the following ancient Chinese story to highlight the differences in the attention received between prevention and remedy approaches regarding antimicrobial resistance in water environments. I think it is a good way to close this thesis.

The story of Bian Que's brothers

The Duke asked the great physician "of your three brothers, which is the best physician?" The physician answered "The eldest is the best, then the second, and I am the least worthy of the three." the Duke said, "Might I hear about this?" The physician replied, "My eldest brother, in dealing with diseases, is attentive to the spirit. Before any symptoms have formed, he has already got rid of it. Thus his fame has never reached beyond our own clan. My next brother treats disease when its signs are most subtle, so his name is unknown beyond our own village. As for myself, I use stone needles on the blood vessels, prescribe strong drugs, and fortify the skin and the flesh. Thus my name has become known all over the country.".

Acknowledgements

Ph.D is often described as a journey, an adventure, a path to grow up both personally and professionally and many other cheesy metaphors. And it is somehow true. However, to me, these last four years have been the perfect excuse to expand my culinary skills and tasting abilities. What does food and eating have to do with this, you may wonder? Well, everything. Keep reading. Taking into account that we need to nurture ourselves from two to five times every day (this is an intermittent fasting-friendly section), we better enjoy the process, don't you think so?

This is exactly what has helped me the most finishing this Ph.D. I have enjoyed and shared time, a lot of time, cooking and sharing meals, coffees and table with many people. This section is for you.

First of all, I would like to thank my promotor and copromotors for their supervision these last four years. **David**, thank you for giving me the chance to show that the unknown and risky option is not necessarily a bad one. **Thomas**, thank you for introducing me to the big data analysis world and more importantly, for believing that I could do it. Without your technical insights, this thesis would have never happened. **Mark**, your vision is one of a kind. Thank you for making EBT a fun and comfortable place to work and be yourself.

I would like to highlight that this thesis would not be what it is without the contribution and hard work of many great students: **Elien, Sushanth, Apoorva, Roel, Stella, Aïsha, Marcos,** and **Riko**. Thanks to all of you for deciding this thesis was interesting enough to pursue your projects. I learned the most from all of you.

Some of the projects have been extensively boostered by the technical support EBT and BT has: Big shoutout to **Zita, Pilar, Marinka, Ben** and **Dirk** as well as **Apilena, Jannie** and **Astrid** for their flexibility and well receiving of some crazy projects we tend to put together. Thank you very much.

Two people I have shared plenty of meals are my paranymphs **Alexandra** and **Sergio**. I am not extremely good with words, but if someone has *genuinely* taught me a bunch of them, this is **Alexandra**. Thank you very much for picking me up when I first arrived to Delft. You still don't know the strength you gave me. I know the struggles, and for that I appreciate even more when you smile. Your dark outfits cannot hide the light you are able to bring to a room. I wish we could be neighbours forever. Romanian gastronomy is not a black box for me anymore but please, more sarmale. I would highly appreciate that.

Sergio, eres la persona más pesada que conozco, de verdad. Pero cuánto te voy a echar de menos cuando no podamos compartir tiempo y espacio juntos. Me has hecho sentir como en casa, siendo el trozo de España que necesitaba aquí, en todo momento. Our B2.190 office is the best and funniest and you are one of the main reasons. There's no doubt you are the best cultural ambassador and so it's your paella valenciana. Just add a bit more of salt, we are still young.

Marta, as my flatmate for three years, you are definitely the one I have shared more meals with. We have been through a Ph.D and a pandemic together. This must bind. I am already missing our talks with the virgin mary blanket, your sugar rushes, our endless discussions and the dinners at 11 at night. You have been a strong support and for that, thank you. What a journey, prima. I am going to pick one of your recipes but believe me, there could have been plenty more. A tavola with your tiramisù!

If I think of kindness, there are always two names coming to my mind: **Ingrid** and **Florence**. **Ingrid**, you were the first person I met when I arrived to EBT, being the chosen one for sitting next to me, you are welcome. I am glad you upgraded me from colleague to friend. Your competitiveness is contagious as it is your laugh. Thanks for bringing positiveness when I was in my lowest, sometimes listening is all we need. You have strongly introduced me into the vegetarian world (not fully converted though) but if I have to choose one of your french spécialités, is gonna be your crêpes. Don't worry, I won't share your secret to its taste.

I tend to go a bit accelerated in life. Can't fight it. However, every time I meet **Flo**, I automatically put myself in pause. You always comment how noisy I am and that I like to complain, as your little sister does. This is because I consider you part of my family here. Thanks for always making me feel welcome. Your hotpots are the closest I have felt to a spanish Sunday late lunch here: Filling and relaxing.

Georg, **Daniel** and **Fabio**. You guys have been like the "older" brothers I have never had. You taught me how to improve some of my soft skills. Your calm and unworried spirit towards friendship is, in my opinion, very valuable. You could build a Restaurant and I would be there for breakfast, lunch and dinner. From the german side I do select the amazing Schwarzwälder Kirschtorte, from the colombian side the tastiest empanadas and from the italian side the original pasta carbonara.

While interviewing me for this position, I asked Mark and David if they could describe me the EBT environment. This was top priority for me. They said it was a great place to interact while doing science. After four years here, I can say I took the perfect decision. Thank you **EBT members** for all the lunches together, Botanical gardens, Friday beers, parties, events, coffee breaks and nice discussions. Thanks for the laughs. Namely, **Danny, Marissa, Simon, Jules, Ana María, Laura, Felipe, Morez, Diana, Hugo, Karel, Michele** and my **Maria Paula** Liquid Chromatography.

The new EBT batch have made me feel very old...I mean very wise. You were all "Too hot to handle". Thank you for dealing with my not-so-always-popular "no

science talk while having lunch" rule. We managed to create an open space where we could be and laugh at ourselves. Our real masterchef **Maxim**, the rapper **Sam** de Man, **Chris** as co-sailor of this experience, my entertainment successor **Timmy**, that bright mind called **Nina**, the karaoke lover and relaxing **Stefan**, our spicy **Ali**, **Gonçalo** the wise, and the best mom **Samarpita**. Thank you guys, I am already missing you.

Francesc, Kiko, has sido un gran re-descubrimiento. Tu positivismo, tu energía, tu carácter, que lo tienes, y tu entusiasmo por la vida hace que siempre tengamos ganas de tenerte alrededor. Aprender a aceptar cumplidos mientras discutimos sobre la vida se ha convertido en uno de mis pasatiempos favoritos. Catalans are very well represented with you as the panellets we baked.

Lemin, you had to stand me in my best and worst time: during the last year of PhD. I loved sharing office with you and I'll miss your brightness and pragmatism. You, little Melinda, are a gem. Your dumplings are from another world.

Rodoula & Angelito, you mean home and comfort. Yes, you are the best hosts (I admit it) and I am so glad I could share time, trips and of course, amazing meals with you. Rodofeta, it is impossible to choose only a meal of yours but you conquered my stomach with your spanakopita and from there to the moon.

Apart from EBT, there's amazing people in other BT groups. **Marina**, my PhD companion. Prima, your resilience is inspiring. Big thanks for the "adoption" by the BPE section: **Oriol**, un placer reencontrarme contigo, **Tiago, Raquel, Song, Joan, Marijn, Roxana, and Daphne**. Also thanks for the nonsense conversations **Hugo B.** in BOC, its always fun to have you around.

This PhD was embedded in a bigger project with Leiden University with whom I have had many interesting User Committee meetings. Special thanks to **Renée** for being such a positive spirit during these tough last four years. I felt very understood during this journey.

In parallel, I also participated in the REPARES consortia where I had the chance to meet amazing scientists from all around Europe on the fight of antibiotic resistance spread through wastewater environment. **Rebeca**, qué alegría tenerte ahí y en general por toda tu ayuda y predisposición. Has sido un punto importante de referencia y un ejemplo de cómo hacer ciencia crítica para mí. Muchas gracias. Thanks to **Joana and Jacqueline** from Porto, **Lukasz** and **Przemyslaw** from Warsaw and **Dana** and **Sabina** from Prague for such nice interactions.

Los que me han visto nacer profesionalmente han sido mis amigos de la UAB. Mis biotecs de toda la vida, en la facultad de Biociencias empezó todo. Qué alegría poder decir que seguís aquí! A las duras y a las maduras. **Marina**, mi siempre compañera de batallas, contigo me voy a cualquier lado. **Ana G.**, cántame, háblame y estate cerquita. Tu sensibilidad es arrolladora. **Ana D.**, mi humorista particular. Aquí me quedo, firmado: tu mejor público. **Irene**, ai mare, tan iguales y diferentes a la vez. Decir las cosas claras nunca tuvieron una persona tan bien asociada. **Carlos**, Dr. López, mi primer compañero de lab, no todos pueden decir eso. Una

mente envidiable. **Cristina**, que el buen rollo que transmites no se vaya nunca y **Nando**, capaz de hacerme reir y reflexionar a la vez. Entre todos sois capaces de hacerme callar, con vosotros he aprendido a escuchar y sin vosotros no me río igual. Indivualmente sois fantásticos pero en conjunto, sois la dinámica con la que todo grupo desearía moverse.

Me tengo que poner ya sentimental porque llega la parte de agradecimientos a los que han estado ahí siempre cuando vuelvo a Martorell. The Montserratins, sois mi casa, mi juventud y a los que vuelvo cuando pierdo un poco el norte. **Pepe, Cristina, Martí, Helena, Ángel, Ana, Irene, Carlos, Esther y Albert**. Por los que estamos y los que ya no. Que podamos celebrar todo lo bueno que la vida nos depara. Os quiero cerca aunque estemos todos tan lejos.

Si alguien ha estado siempre presente sin pedir nada a cambio, es mi familia. Mis abuelas **Maruja** y **Presen**, mis tíos **Rosamari** y **Goyo** y sobretodo mis padres **Olga y Ramón**. De vosotros he aprendido que nada viene dado. Que si algo quieres, algo te cuesta y que el esfuerzo y sacrificio siempre tiene recompensa. Que si tienes 10, guardes 5 y que la honestidad y claridad te hacen auténtico. Siempre nos quedará la duda de si es el mundo que va muy despacio o nosotros con demasiada prisa. Somos así. Impacientes, cabezones y unos fuera risas. Soy quien soy gracias a vosotros. Gracias por todo. If you ever have the chance to come to my parents place, you should try my father's Arroz con cosas or my mother's Codfish Croquetas. It's an experience.

Por último, **Mariana**, a pessoa que me atura todos os dias, o que não é pouca coisa. Ter-te a meu lado traz-me paz. Ajuda-me a seguir em frente. És e tens sido o meu refúgio durante estes últimos anos de doutoramento. Obrigado pela excitação que trazes à minha vida. Que tudo o que temos vivido seja apenas o trailer de uma das tuas séries favoritas. Ainda temos todas as temporadas para ver. Te quiero. I am going to be obvious here and highlight your top chef Pastéis de Nata recipe. Love them.

[1]

[1] If you put all the underlined words together, believe me, you will have the tastiest international menu, which is at the end, what all of this is about, or not? You are welcome.

Curriculum vitæ

David Calderón Franco was born in Barcelona, Spain on February 21^{st} 1993. In 2011 he started his BSc. in Biotechnology at Universitat Autònoma de Barcelona. As part of his Biotechnology studies, he performed a 6-month $Erasmus^{+}$ in Technische Universität Hamburg-Harburg , where he took Bioprocess Engineering courses. His fascination for which solutions microorganisms can offer to a more sustainable future brought him to pursue a MSc. in Bioengineering at the Institut Químic de Sarrià, Ramon Llull University (Barcelona). During his $Erasmus^{+}$ master thesis in The Novo Nordisk Foundation Center for Biosustainability - Denmark Technical University, he studied how to metabolically engineer yeast strains for producing dicarboxylic acids.

After finishing his MSc., David moved to Basel to work in the start-up FGen, where he took part of a European collaboration project on engineering yeast strains and growth conditions for the production of vitamins. While working, he understood the need to integrate big data with biological relevance. Therefore, he started his second joint MSc. in Bioinformatics and Biostatistics between Barcelona University and the Open University of Catalonia, finishing his master's thesis on pipeline development to link antibiotic resistance genes to specific bacteria using Hi-C sequencing data.

Moved by his need to learn more and due to his experience with genetically modified organisms, David was granted a Ph.D. position on the Transmission of Antimicrobial Resistance Genes and Engineered DNA from Transgenic Biosystems in Nature research project. David's project has focused on determining the origin, fate, persistence, and removal of Antibiotic Resistance Genes and Mobile Genetic Elements through urban water systems. David has focused his research on evaluating the role of extracellular free DNA in spreading antibiotic resistance determinants in wastewater environments. The results of his research are presented in this thesis.

Since 2021, David has participated in EU project REPARES on behalf of TU Delft, working to foster the cooperation of academic institutions and stakeholders to tackle the antimicrobial resistance issue in wastewater and developing standardized methods to quantify ARGs in wastewater. Currently, he continues his career trying to bring knowledge gained during his Ph.D. into business as an entrepreneur in Hologenomix Life Sciences.

List of publications

10. D. Calderón-Franco, F. Corbera-Rubio, M. Cuesta-Sanz, B. Pieterse, D. de Ridder, M.C.M. van Loosdrecht, D. van Halem, M. Laureni and D.G. Weissbrodt. "Microbiome, resistome and mobilome of chlorine-free drinking water treatment systems". In: *Water Research* (2022), (submitted).

9. D. Calderón-Franco, M. C. M. van Loosdrecht, T. Abeel, and D. G. Weissbrodt. "Catch me if you can : Capturing extracellular DNA transformation in mixed cultures via Hi-C sequencing". In: *bioRxiv* (2022), pp. 1–38. DOI: https://doi.org/10.1101/2022.09.16.508255, (submitted).

8. M. Martínez-Quintela, D. Calderón-Franco, M.C.M. van Loosdrecht, S. Suárez, F. Omil and D.G. Weissbrodt. "Antibiotic resistance response to sulfamethoxazole from the intracellular and extracellular DNA fractions of activated sludge". In: *Water Research* (2022), (submitted).

7. S. Pillay, D. Calderón-Franco, A. Urhan, and T. Abeel. "Metagenomic-based surveillance systems for antibiotic resistance in non-clinical settings". In: *Frontiers in Microbiology. Evolutionary and Genomic Microbiology* (2022), DOI: https://doi.org/10.3389/fmicb.2022.106699.

6. D. Calderón-Franco, R. Sarelse, S. Christou, M. Pronk, M. C. M. van Loosdrecht, T. Abeel, and D. G. Weissbrodt. "Metagenomic profiling and transfer dynamics of antibiotic resistance determinants in a full-scale granular sludge wastewater treatment plant". In: *Water Research* (2022). DOI: 10.1016/j.watres.2022.118571

5. D. Calderón-Franco, L. Orschler, S. Lackner, S. Agrawal, and D. G. Weissbrodt. "Monitoring SARS-CoV-2 in sewage: Toward sentinels with analytical accuracy". In: *Science of the Total Environment* 804 (2022). ISSN: 18791026. DOI: 10.1016/j.scitotenv.2021.150244

4. A. Miłobedzka, C. Ferreira, I. Vaz-Moreira, D. Calderón-Franco, A. Gorecki, S. Purkrtova, Jan Bartacek, L. Dziewit, C. M. Singleton, P. H. Nielsen, D. G. Weissbrodt, and C. M. Manaia. "Monitoring antibiotic resistance genes in wastewater environments: The challenges of filling a gap in the One-Health cycle". In: *Journal of Hazardous Materials* 424 (2022). ISSN: 18733336. DOI: 10.1016/j.jhazmat.2021.127407

3. D. Calderón-Franco, S. Apoorva, G. Medema, M. C. van Loosdrecht, and D. G. Weissbrodt. "Upgrading residues from wastewater and drinking water treatment plants as low-cost adsorbents to remove extracellular DNA and microorganisms carrying antibiotic resistance genes from treated effluents". In: *Science of the Total Environment* 778 (2021), p. 146364. ISSN: 18791026. DOI: 10.1016/j.scitotenv.2021.146364

2. D. Calderón-Franco, M. van Loosdrecht, T. Abeel, and D. Weissbrodt. "Free-floating extracellular DNA: Systematic profiling of mobile genetic elements and antibiotic resistance from wastewater". In: *Water Research* 189.116592 (2021), pp. 1–13. DOI: 10.1101/2020.05.01.072397

1. D. Calderón-Franco, Q. Lin, M. C. M. van Loosdrecht, B. Abbas, and D. G. Weissbrodt. "Anticipating Xenogenic Pollution at the Source : Impact of Sterilizations on DNA Release From Microbial Cultures". In: *Frontiers in Bioengineering and Biotechnology* 8.March (2020), pp. 1–13. DOI: 10.3389/fbioe.2020.00171

Conference contributions

Presenting author is underlined.

8. Calderón-Franco, D., van Loosdrecht, M. C. M., Abeel, T. Weissbrodt, D., *Catch me if you can: Capturing extracellular DNA transformation in mixed cultures by Hi-C sequencing*, **International Symposium on the Environmental Dimension of Antibiotic Resistance**, Gothenburg, Sweden (September 2022). Oral presentation.

7. Calderón-Franco D., van Loosdrecht M.C.M., Abeel T., Weissbrodt D.G. *Antibiotic resistance determinants carried by free DNA across waterways.* **European Water Technology Week**, Wetsus, Leeuwarden, The Netherlands (September 2022). Oral presentation.

6. Calderón-Franco, D., van Loosdrecht, M. C. M., Abeel, T. Weissbrodt, D., *Catch me if you can: Capturing extracellular DNA transformation in mixed cultures by Hi-C sequencing*, **International Symposium on Microbial Ecology (ISME18) Conference**, Lausanne, Switzerland (August 2022). Poster.

5. Calderón-Franco, D., Sarelse R., Christou S., Pronk, M., van Loosdrecht, M. C. M., Abeel, T. Weissbrodt, D., *Transfer dynamics of resistance determinants: microbiome, resistome and mobilome of a full-scale aerobic granular sludge wastewater treatment plant*, **IWA Microbial Ecology and Water Engineering (MEWE21) Conference**, Delft, The Netherlands (hybrid) (October 2021). Oral presentation.

4. Calderón-Franco, D., Sarelse R., Christou S., Pronk, M., van Loosdrecht, M. C. M., Abeel, T. Weissbrodt, D., *Intracellular vs. Extracellular DNA: Microbiome, resistome and mobilome profiling of a full-scale granular sludge wastewater treatment plant*, **IWA Biofilms Virtual Conference – Emerging Trends and Developments in Biofilm Processes Conference**, Notre Dame, USA (virtual) (December 2020). Oral presentation.

3. Weissbrodt D.G., Calderón-Franco D., Guo B., Pallarés-Vega R. *Biotechnology and safety to manage antimicrobial resistance from urban to space water cycles.* **European Space Agency – Fully Virtual MELiSSA Conference "Current and Future Ways to Closed Life Support Systems"**, Ghent University, Belgium (virtual) (2022).

2. Calderón-Franco, D., van Loosdrecht, M. C. M., Abeel, T. Weissbrodt, D., *Free-floating extracellular DNA: systematic profiling of mobile genetic elements and antibiotic resistance from wastewater*, **EFB Microbial Stress: From systems to molecules and back Conference**, Roma, Italy (virtual) (November 2020). Oral presentation.

1. Calderón-Franco, D., Lin, Q., van Loosdrecht, M. C. M., Abbas, B. Weissbrodt, D., *Impact of sterilization procedures on release of xenogenic elements into urban waterways*, **IWA Microbial Ecology and Water Engineering (MEWE19) Conference**, Hiroshima, Japan (November 2019). Poster.

Invited talks

2. Weissbrodt D.G. and Calderón-Franco D. *Biotechnology and safety to manage xenogenetic elements and antimicrobial resistance in urban water systems.* **One Health European Joint Program FED-AMR: The role of free extracellular DNA in dissemination of antimicrobial resistance over ecosystem boundaries along the food/feed chain.** Austrian Agency for Health and Food Safety, Austria (2020). (virtual)

1. Calderón-Franco D. and Weissbrodt D.G. *Monitoring SARS-CoV-2 in sewage: toward sentinels with analytical accuracy.* **Online Conference on Monitoring of SARS-CoV-2 in the Sewage System, Technologieland Hessen**, Hessen, Germany (2021). (virtual)